RILEM Bookseries

Karen Scrivener
Aurélie Favier *Editors*

Calcined Clays for Sustainable Concrete

Proceedings of the 1st International Conference on Calcined Clays for Sustainable Concrete

Springer

Calcined Clays for Sustainable Concrete

RILEM BOOKSERIES

Volume 10

RILEM, The International Union of Laboratories and Experts in Construction Materials, Systems and Structures, founded in 1947, is a non-governmental scientific association whose goal is to contribute to progress in the construction sciences, techniques and industries, essentially by means of the communication it fosters between research and practice. RILEM's focus is on construction materials and their use in building and civil engineering structures, covering all phases of the building process from manufacture to use and recycling of materials. More information on RILEM and its previous publications can be found on www.RILEM.net.

More information about this series at http://www.springer.com/series/8781

Karen Scrivener · Aurélie Favier
Editors

Calcined Clays for Sustainable Concrete

Proceedings of the 1st International Conference on Calcined Clays for Sustainable Concrete

Springer

Editors
Karen Scrivener
EPFL/STI/IMX/LMC
Lausanne
Switzerland

Aurélie Favier
EPFL/STI/IMX/LMC
Lausanne
Switzerland

ISSN 2211-0844 ISSN 2211-0852 (electronic)
RILEM Bookseries
ISBN 978-94-017-9938-6 ISBN 978-94-017-9939-3 (eBook)
DOI 10.1007/978-94-017-9939-3

Library of Congress Control Number: 2015937380

Springer Dordrecht Heidelberg New York London

Printed on acid-free paper

Springer Science+Business Media B.V. Dordrecht is part of Springer Science+Business Media (www.springer.com)

Preface

The most promising route to improving the sustainability of cement and concrete is to blend Portland cement clinker with substitution materials often referred to as supplementary cementitious materials (SCMs). However, supplies of the most common SCMs, which are slag and fly ash, are quiet limited compared to the worldwide production of cement. Calcined clays are the most promising source of additional SCMs which can make a substantial contribution to lowering further the environmental impact of cement and concrete.

The book of proceedings of the international conference on the calcined clay for sustainable concrete contains papers written by practitioners and researchers from all continents. They brought together the advanced studies on the use of calcined clays in concrete. The topics covered are clays geology, hydration of blended cement, performance, alkali-activated binders, economical and ecological impacts and field applications.

The Editors would like to thank the authors for the outstanding contributions which reflect the scientific character of their work.

All papers were published without selection process to permit a full and truly international nature of these proceedings.

Finally, the Editors would like to thank the various organisations for their contribution and help in making these proceedings and conference a success.

Karen Scrivener
Aurélie Favier

Contents

Part I
Full Papers

Sulphate and ASR Resistance of Concrete Made with Calcined Clay Blended Cements

André Trümer and Horst-Michael Ludwig

Abstract This paper presents the results of several investigations concerning the durability of mortar and concrete with higher proportion of calcined clays in the cement part. For this purpose, different clays based on kaolinite, montmorillonite and illite were fired at optimum temperatures according to the strength contribution in cement. The raw materials were analyzed chemically (XRF) and mineralogically (XRD). The pore size distribution of the mortars was measured by mercury intrusion porosimetry. Cement pastes were produced in order to calculate the phase composition by XRD/Rietveld and to estimate the microstructure with SEM. The performance tests comprised investigations of the long-term behaviour in case of sulphate attack and alkali silica reaction respectively. The results show that the addition of the calcined clays are able to improve the concrete resistance against these exposures or at least doesn't affect it negatively compared to the control. It can be followed that the application of cements with higher percentage of calcined clays substituting clinker is not restricted to only slightly loaded concrete constructions.

1 Introduction

A lot of work has been spent on the activation of raw clays by means of firing. Several authors could show that this treatment is suitable for producing supplementary cementicious materials (SCM) [1–6], which are intended to substitute bigger amounts of clinker in cement in order to save energy, CO_2 and finally costs. These studies predominantly focus on the pozzolanic activities of the fired clays in the binding material resulting in an optimum strength of the composite cement. But only little effort has been spent to investigate the effects on the concrete durability. Concerning this aspect, only data for highly reactive metakaolin exist [7–10], which is not a suitable material for normal concrete due to its price. In most applications, the

A. Trümer (✉) · H.-M. Ludwig
Bauhaus-University Weimar, Weimar, Germany
e-mail: andre.truemer@uni-weimar.de

K. Scrivener and A. Favier (eds.), *Calcined Clays for Sustainable Concrete*,
RILEM Bookseries 10, DOI 10.1007/978-94-017-9939-3_1

concrete properties including its durability needn't to exceed normal requirements facilitating the use of less active calcined clays as part of the binder. Nevertheless, it is worthwhile to know the performance of such systems under severe environmental conditions. In order to improve this knowledge, the authors performed several investigations helping to assess the influence of calcined clay blended cements on special durability aspects of the concrete.

2 Experiments

Three different clays have been used for the experiments. Their compositions are shown in the Tables 1 and 2 revealing the different clay mineral bases kaolinite, montmorillonite and illite respectively, indicated by the capital letters K, M and I, and a relatively low amount of accessory constituents each. The chemical analysis was performed with an energy dispersive micro X-ray fluorescence (XRF) spectrometer Orbis_PC by EDAX/AMATEK. The mineralogical composition was measured by means of X-ray diffraction (XRD) of powders with a Siemens D5000 using CuKα radiation. The clays were fired in a muffle kiln by heating up with 10 °C/min, maintaining the maximum temperature for 1 h and cooling down on air. After a short milling the pozzolanic activity of the calcined clays has been assessed by testing the compressive strength of blended cements with 30 % clinker substitution according to DIN EN 196-1. The therefore used ordinary Portland cement (OPC) was an CEM I 42.4 R with an alkali content of Na_2O_{eq} = 1.03 %. The results of the strength tests of each clay calcined at optimum temperature can be seen in Fig. 1a. These materials were used in all following investigations.

The hardened mortars from the 91d strength tests were afterwards used to determine the pore size distribution by means of mercury intrusion porosimetry (MIP). Hardened cement pastes with an age of 91 days were produced in order to calculate the phase composition with XRD/Rietveld using ZnO as internal standard

Table 1 Chemical composition of the investigated clays

[%]	SiO_2	Al_2O_3	Fe_2O_3	CaO	MgO	TiO_2	K_2O	Na_2O	LOI	Total
K	53.5	32.1	0.3	0.1	0.2	0.12	0.23	0.01	14.17	100.73
M	50.7	15.7	5.5	5.7	3.3	0.30	2.26	0.40	16.21	100.07
I	62.8	14.8	5.7	1.7	2.4	0.72	4.11	1.63	5.6	99.46

Table 2 Phase composition of the investigated clays

[%]	Kaolinite	Montmor.	Illite	Muscovite	Quartz	Feldspar	Others
K	86				14		
M	5	62		10	14	3	6
I			47	7	27	15	4

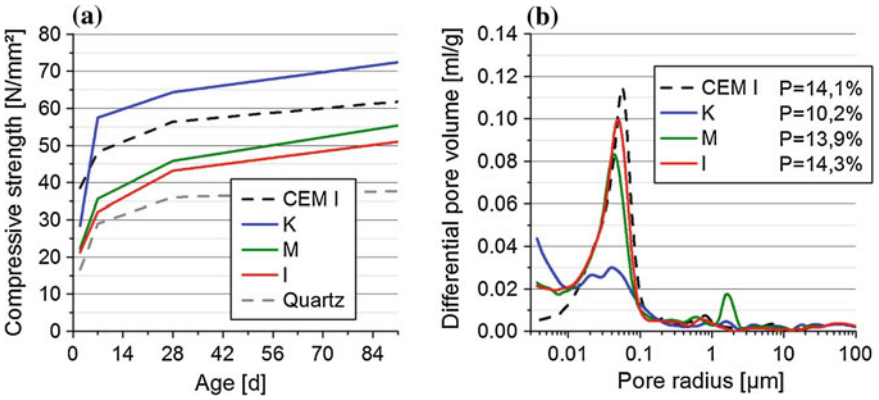

Fig. 1 Compressive strength development (**a**), and pore size distributions (**b**), of the regarded composite cements compared to OPC

and the software Autoquan. Moreover, microscope images were taken from the pastes by means of a Nova NanoSEM 230 from FEI.

To assess the performance of the mortars under severe environmental conditions, two different testing methods have been passed. The first is the determination of the sulphate resistance following the recommendation of the German Institute for Building Technique (DIBT). Therefore, mortars were produced like before and, this time, moulded to flat prisms of 1 cm thickness. After two days, the prisms were demoulded and then cured in saturated lime solution for 12 days. Afterwards, the samples were stored in 0.44 % Na_2SO_4 solution (=3000 mg/l SO_4^{2-}) at 5 and 20 °C respectively. The assessment of the sulphate resistance was fulfilled by measuring the expansion of the prisms until a half year of storing.

The second method used in this work is a quick test to assess the resistance against a harmful alkali silica reaction (ASR) [11]. Here, mortars were produced with a testing cement (CEM I 32.5 R, Na_2O_{eq} = 0.94 %), again blended with 30 % calcined clay, with reactive aggregates and with alkaline water leading to a total sodium equivalent of the system of 2.5 %. The mortars were moulded to standard prisms, which were stored, after one day of curing, in water at 70 °C and measured, like before, with respect to their expansion until an age of 28 days.

3 Results

3.1 Compressive Strength

The optimal firing temperatures for the kaolinitic (K), the montmorillonitic (M) and the illitic (I) clay are found to be 800, 800 and 900 °C respectively. Figure 1a shows that all of the this way burned clays give a distinctly higher strength contribution

than the inert quartz powder indicating a certain pozzolanic activity in the order I ≤ M < K. Surprisingly, the calcined illitic clay performs quite good, which contradicts to the findings of other authors [2, 3, 5], who declared this kind of material as non-reactive. As expected, the metakaolin gives the best strength contribution leading to relative values of 119 % compared to the OPC.

3.2 Microstructure

The pore size distributions and the total porosity of the mortars after 91 days are given in Fig. 1b. In comparison to the OPC, the calcined clay blended cements have equal porosities or, in case of the metakaolin, even a lower one. From the distributions, it can be seen that for all samples most of the pore volume is located between 10 and 100 nm. In the range below, the blended cements show higher values indicating a pore refinement due to the pozzolanic reaction.

The best indicator for the pozzolanic reaction is the amount of consumed portlandite (CH) in the hardened pastes. The XRD/Rietveld analysis gave a CH content of 18 % for the OPC. The percentages in the composite cements normalized to the OPC amount were K = 5 %, M = 14 % and I = 15 %, which partly agrees with [3] but, again, indicates a higher reactivity of the fired illitic clay then found by these authors. The difference in the portlandite content relative to the control is transformed into additional CSH and CAH phases explaining the low porosity of the metakaolin mortar.

The denser structure of the respective cement stone can be observed with the help of SEM techniques. Depicting the metakaolin cement, Fig. 2a shows a close network of hydration products with only small residues of CH. On the other hand, one can see big aggregates of layered portlandite crystals in Fig. 2b, which is an

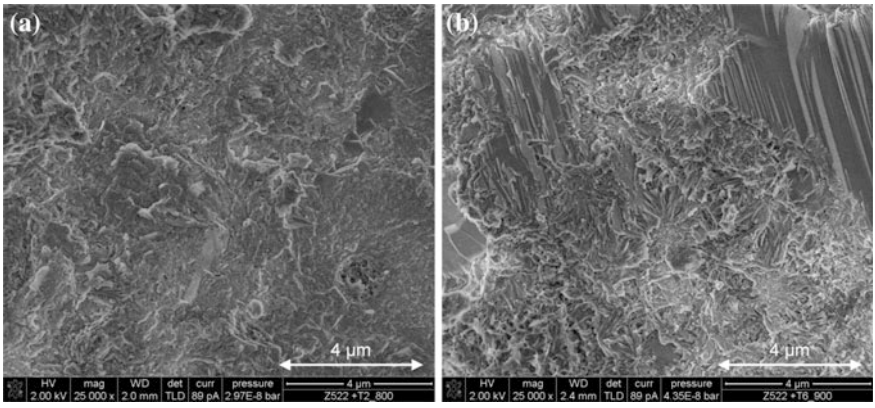

Fig. 2 SEM images of the hardened cement pastes blended with calcined kaolinitic (**a**), and illitic clay (**b**), respectively

image of the hydrated meta-illite blend. Simultaneously, the needle or, in some cases, foil shape of the CSH phases are well recognizable indicating a more open structure compared to Fig. 2a.

3.3 Durability Tests

The results of the performance tests concerning the sulphate and the ASR resistance are given in Figs. 3 and 4 respectively.

The graphs in Fig. 3 show a time dependent rise of the sulphate caused expansions for the OPC and the composite cement mortars with calcined montmorillonite and illite. Compared to the control, the two latter perform similar or, in case of the 20 °C test, even better.

The beneficial effect of the calcined clay addition can be explained by both the finer pore size distribution and the partly consumption of CH, which is essential for the formation of strain causing phases like gypsum and ettringite. As expected, the most marked impact on the material behaviour is caused by the metakaolin. It leads to hardly any expansions of the respective mortar due to the fine porosity and the low CH content of the hydrated cement. However, the calcined clay performance is expected to depend on the clinker basis meaning the lower the pH-value of the pore solution the lower the rate of the pozzolanic reaction. Since a lower excitation of the active phases results in a lower sulphate resistance, which can be seen from the deterioration at 5 °C due to the temperature effect, tests with low-alkali cements are planned to be performed in the nearer future.

The sulphate test is ongoing until one year of storing.

Figure 4 shows the results for the mortar bar tests. This method is usually executed to assess the sensitivity of aggregates concerning a possible alkali-silica-reaction (ASR). In the given case, a very reactive aggregate was chosen to show the

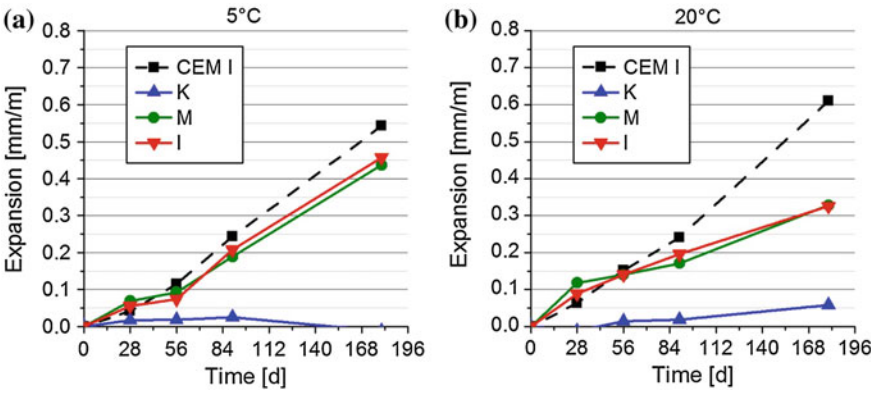

Fig. 3 Results of the sulphate resistance test run at different temperatures

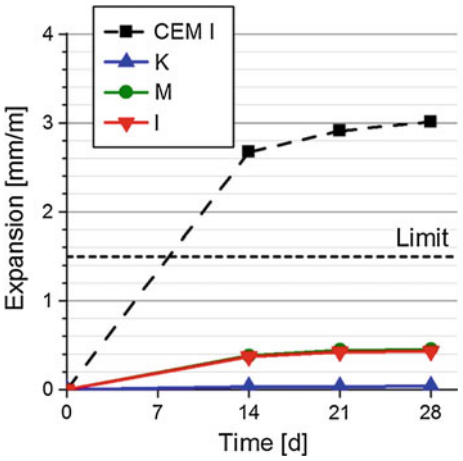

Fig. 4 Results of the mortar bar test for the ASR evaluation

influence of the binding material. The control illustrates the bad performance of the mortar when such kind of crushed sand is combined with high-alkali cement. The maximum expansion of 1.5 mm/m required for harmless aggregates is distinctly failed. However, by partly substituting the cement by the calcined clays the mortars behave completely uncritical. And once again, the performance order of the three kinds of fired clays can be confirmed indicating the calcined montmorillonite and illite to be comparable and the metakaolin as the most active material. The reduction of ASR risk by using calcined clay blended cements results from a finer porosity inhibiting ion transport, a decreased provision of calcium being a main constituent of expanding ASR gel [12] and the incorporation of alkali ions in the CSH phases due to lower C/S ratios [13].

4 Conclusions

- The following conclusions can be deduced from the represented results:
- The activity of the three investigated calcined clays increases in the order $I \leq M < K$.
- When optimally fired, illitic clays can be assessed as pozzolanic materials.
- Like other pozzolanic materials, calcined clays effect a depletion of portlandite promoting the formation of additional CSH phases in the hydrated cement.
- This causes a pore refinement and therefore a denser microstructure.
- Partly substitution of alkali-rich Portland cements by calcined clays strengthens the resistance of the respective concrete against sulphate attack and harmful ASR.
- It can be concluded that calcined clays are useful pozzolans regardless of the clay mineral base. The good performance of the respective composite cements proves the suitability of these materials even for extraordinary concrete

applications. However, for a final positive evaluation of the effect on concrete durability, the cements have to pass other tests concerning freeze-thaw-resistance, chloride penetration and carbonation.

References

1. Ambroise, J., Murat, M., Péra, J.: Hydration reaction and hardening of calcined clays and related minerals V. Extension of the research and general conclusions. Cem. Concr. Res. **15** (2), 261–268 (1985)
2. He, C., Osbaeck, B., Makovicky, E.: Pozzolanic reactions of six principal clay minerals: Activation, reactivity assessments and technological effects. Cem. Concr. Res. **25**(8), 1691–1702 (1995)
3. Fernandez, R., Martirena, F., Scrivener, K.L.: The origin of the pozzolanic activity of calcined clay minerals: A comparison between kaolinite, illite and montmorillonite. Cem. Concr. Res. **41**(1), 113–122 (2011)
4. Tironi, A., Trezza, M.A., Scian, A.N., Irassar, E.F.: Assessment of pozzolanic activity of different calcined clays. Cem. Concr. Compos. **37**, 319–327 (2013)
5. Danner, T.: Reactivity of Calcined Clays. Dissertation, Trondheim (2013)
6. Trümer, A., Ludwig, H.-M., Rohloff, K.: Investigations into the application of calcined clays as composite material in cement. ZKG Int. **9**, 52–57 (2014)
7. Kostuch, J.A., Walters, G.V., Jones, T.R.: High performance concretes incorporating metakaolin—A Review, Paper presented at concrete 2000, University of Dundee (1993)
8. Caldarone, M.A., Gruber, K.A., Burg, R.G.: High-reactivity metakaolin: A new generation mineral admixture. Concr. Int. **16**(11), 37–40 (1994)
9. Zhang, M.H., Malhotra, V.M.: Characteristics of a thermally activated alumino-silicate pozzolanic material and its use in concrete. Cem. Concr. Res. **25**(8), 1713–1725 (1995)
10. Gruber, K.A., Ramlochan, T., Boddy, A., Hooton, R.D., Thomas, M.D.A.: Increasing concrete durability with high-reactivity metakaolin. Cem. Concr. Compos. **23**(6), 479–484 (2001)
11. Stark, J., Erfurt, D.: Alkali-Kieselsäure-Reaktion. Schriftenreihe des F.-A.-Finger-Instituts für Baustoffkunde. Univ.-Verl., Weimar (2008)
12. Stark, J., Freyburg, E., Seyfarth, K., Giebson, C., Erfurt, D.: 70 years of ASR with no end in sight? (Part 1). ZKG Int. **4**, 86–95 (2010)
13. Lothenbach, B., Scrivener, K., Hooton, R.D.: Supplementary cementitious materials. Cem. Concr. Res. **41**(12), 1244–1256 (2011)

The Influence of Metakaolin on Limestone Reactivity in Cementitious Materials

Guillermo Puerta-Falla, Magdalena Balonis, Gwenn Le Saout, Narayanan Neithalath and Gaurav Sant

Abstract Recent studies have demonstrated that in the presence of limestone ($CaCO_3$), carbonate-AFm phases (i.e., hemi- and/or mono-carboaluminate) may be stabilized at the expense of sulfate-AFm, which is more commonly found in cement systems. This suggests that enhancing AFm phase formation may be a novel way of incorporating increased quantities of limestone as a reactive component in cement-based systems. Often, in an ordinary portland cement (OPC), the quantity of the AFm hydrates formed is limited by the availability of aluminum. Therefore, as means of enhancing AFm phase formation, this paper evaluates metakaolin addition to determine how it affects limestone reactions and carbonate-AFm formation in the OPC systems. The results of a multi-method study including: X-ray diffraction with Rietveld refinement (QXRD), strength measurements, thermogravimetric analysis, and thermodynamic calculations are used to quantify solid phase constitutions, and the extent of limestone that has been consumed in reaction. Obtained results suggest that pozzolanic reactions which occur when metakaolin is used as an aluminous source are observed to be beneficial in offsetting the dilutive effects of OPC replacement noted in blended cement formulations.

G. Puerta-Falla · G. Sant (✉)
Department of Civil and Environmental Engineering, University of California, Los Angeles, CA, USA
e-mail: gsant@ucla.edu

M. Balonis
Department of Materials Science and Engineering, University of California, Los Angeles, CA, USA

M. Balonis
Institute for Technology Advancement, University of California, Los Angeles, CA, USA

G. Le Saout
Centre des Matériaux de Grande Diffusion (CMGD), École des Mines d'Alès, Alès cedex, France

N. Neithalath
School of Sustainable Engineering and the Built Environment, Arizona State University, Tempe, AZ, USA

K. Scrivener and A. Favier (eds.), *Calcined Clays for Sustainable Concrete*, RILEM Bookseries 10, DOI 10.1007/978-94-017-9939-3_2

1 Introduction

CO_2 pressures facing the construction industry are providing an increasing impetus to reduce the use of ordinary portland cement (OPC) as the primary binder phase in concrete [1]. Towards reducing OPC use, emphasis has been placed on replacing OPC with supplementary cementitious materials (SCMs) in the form of: fly ash, blast furnace slags, silica fume, etc. [2, 3]. While capable of providing suitable properties, quantities of common SCMs available to replace OPC, are often, especially at local scales, inadequate to satiate the desired OPC replacement demand [4]. Due to concerns of the limited/localized availability of SCMs, there is interest in using limestone ($CaCO_3$), an abundant mineral, to reduce the clinker factors of OPC, and thus OPC use in concrete. The replacement of OPC by limestone induces a variety of effects ranging from: (a) dilution and strength reduction [5, 6], to (b) accelerated hydration at early ages that results from the so-called filler effects [7]. Of these effects, dilution, i.e., the reduction in strength that accompanies OPC replacement is a considerable issue, as technologically this is the most significant limitation which has ensured that, in practice, OPC replacement by $CaCO_3$ remains limited [8]. OPC is comprised of four main phases tricalcium silicate (C_3S), dicalcium silicate (C_2S), tricalcium aluminate (C_3A) and the ferrite (C_4AF) phases, wherein the kinetics of hydration of each phase differs from the others[1] [9]. Hydration of the C_3A in the presence of sulfate ions, provided by gypsum ($C\overline{S}H_2$), forms ettringite ($C_6A\overline{S}_3H_{32}$, AFt) at early ages and the monosulfoaluminate ($C_4A\overline{S}H_{12}$, SO_4-AFm, Ms), at later ages when gypsum is exhausted. However, in cases where carbonate ions may be present, e.g. as provisioned by the dissolution of limestone, C_3A reacts with such species to form the CO_3-AFm phases instead of SO_4-AFm and ettringite is stabilized to accommodate sulfate ions [10–12]. In general, monocarboaluminate ($C_4A\overline{C}H_{11}$, Mc) forms when there is an abundance of the (calcium) carbonate source present, and hemicarboaluminate ($C_4A\overline{C}_{0.5}H_{12}$, Hc) forms in the case of carbonate-deficient conditions [12]. In typical OPCs, the aluminate (mainly C_3A) phase content is regulated by governing standards [10]. This ensures that the extent of $CaCO_3$ that can react in a typical OPC is quite small and in the range of 2–5 % (by mass) [12]. As such, if it is desirable to increase $CaCO_3$ reactivity and thus OPC replacement levels, it is necessary to enhance the quantity of aluminous phases that can provide sufficient Al $(OH)_4^-$ (aluminate) species, which under conditions of portlandite saturation would react with $CaCO_3$ to produce the CO_3-AFm phases. In this work metakaolin (MET) is evaluated as aluminous agent which can extend the limestone reactivity in portland cement systems.

[1]Standard cement chemistry notation is used: C = CaO, S = SiO_2, A = Al_2O_3, F = Fe_2O_3, H = H_2O, $\overline{S} = SO_3$ and $\overline{C} = CO_2$.

Table 1 The oxide composition of materials utilized in this study as determined by X-ray fluorescence (XRF)

Oxide (%)	Type I/II OPC	MET
SiO_2	20.54	51.36
Al_2O_3	4.97	47.60
Fe_2O_3	3.10	0.39
CaO	65.75	0.02
MgO	2.43	0.09
SO_3	2.75	0.08
Na_2O	0.18	0.28
K_2O	0.29	0.18

2 Materials and Methods

An ASTM C150 compliant Type I/II ordinary portland cement (OPC) and commercially available limestone (nominally pure: >95 % $CaCO_3$, d_{50} = 3 μm) were used. The oxide compositions of the OPC and metakaolin (MET) are presented in Table 1. A series of cementitious mixtures were prepared using de-ionized (DI) water at a fixed water-to-solids ratio (*w/s* = 0.45) as described in ASTM C305. The series of mixtures produced comprised of: (a) plain OPC, pastes in which: (b) 30 % of the OPC is replaced by limestone[2] (c) 5-to-15 % of the OPC is replaced in 5 % increments by MET (d) 5-to-15 % of the OPC is replaced in 5 % increments by MET and an additional 30 % of the OPC is then replaced by limestone.

Compressive strength measurements were carried out at 90 days using cubic specimens (50 mm × 50 mm × 50 mm) cured at 25 ± 1 °C in lime water as described in ASTM C109 [8].

For thermal analysis (TG/DTG) a Perkin Elmer STA 6000 thermal analyzer with a Pyris data acquisition interface was used to determine solid phase quantities in cementitious mixtures.

To arrest hydration, solvent exchange was as described by Zhang and Scherer [13]. Quantitative X-ray diffraction analyses were carried out on powdered cementitious mixtures at desired ages using a Bruker D8 Advance diffractometer using Cu-Kα (λ = 1.54 Å) radiation. Care was taken to minimize preferred orientation errors by texturing the sample surface, and using a rotating sample stage. X-ray structure information for the relevant anhydrous and hydrated crystalline phases was sourced from standard databases or from the literature [14, 15]. Rietveld analysis was carried out using the X'Pert HighScorePlus© [16].

Thermodynamic calculations were carried out using a geochemical speciation code, GEMS-PSI: version 2.3.1 [17]. Thermodynamic data of solid and aqueous

[2]All replacements in this study are performed on a mass basis; some pastes were prepared with quartz instead of limestone to enable comparison of compression strength for blends containing reactive component (limestone) versus inert filler (quartz).

species are sourced from the GEMS-PSI database, and amended with additional information relevant to cementitious systems [12]. Calculations were performed under conditions of 1 bar, 25 °C and CO_2-free air.

3 Results and Discussion

As showed on Fig. 1, the replacement of OPC by metakaolin results in improved strength. Such beneficial effects of metakaolin addition, have also been highlighted by Vance et al. [18, 19] and Antoni et al. [20] and attributed to the pozzolanic character of metakaolin, and the formation of the Hc/Mc phases. This is significant in that in spite of very substantial reductions in the cement factor (CF), mechanical properties near equivalent to the pure OPC mixtures can be achieved. Figure 2 shows representative DTG traces at 90 days, and the portlandite content normalized by the cement factor (CF) for metakaolin containing mixtures. It is noted that portlandite contents of a given mixture decrease with increasing OPC replacement by metakaolin, even when dilution is accounted for. This is indeed expected due to the pozzolanic nature of metakaolin, which would consume lime to form a low(er) Ca/Si (and potentially higher Al-substituted) C-S-H phase which ensures that metakaolin containing mixtures show reduced decreases in compressive strength, in spite of the substantial OPC replacement. Figure 3 shows XRD patterns for the metakaolin containing mixtures after 90 days of hydration. It is noted that the portlandite content of a given mixture, in both limestone deficient/excess cases, reduces with increasing metakaolin content. Mc exists as the dominant phase, only when excess limestone is added to the system.

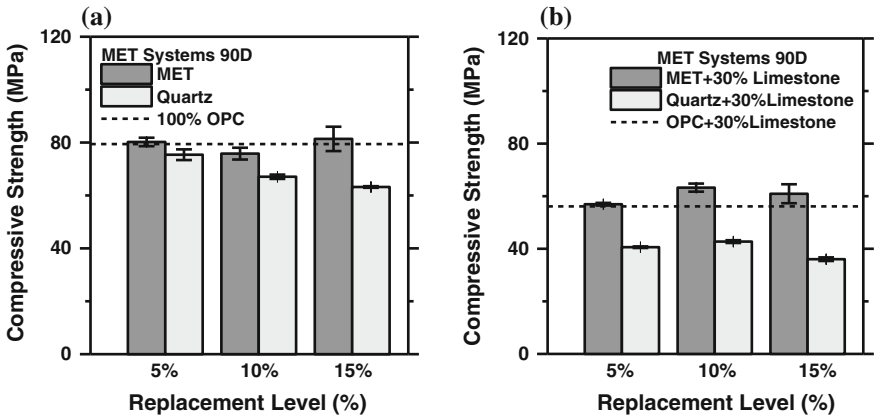

Fig. 1 Compressive strength at 90 Days for: **a** OPC systems **b** OPC + 30 % Limestone systems, at different levels of replacement by metakaolin (*MET*); results compared against quartz which is not reactive and acts as inert filler

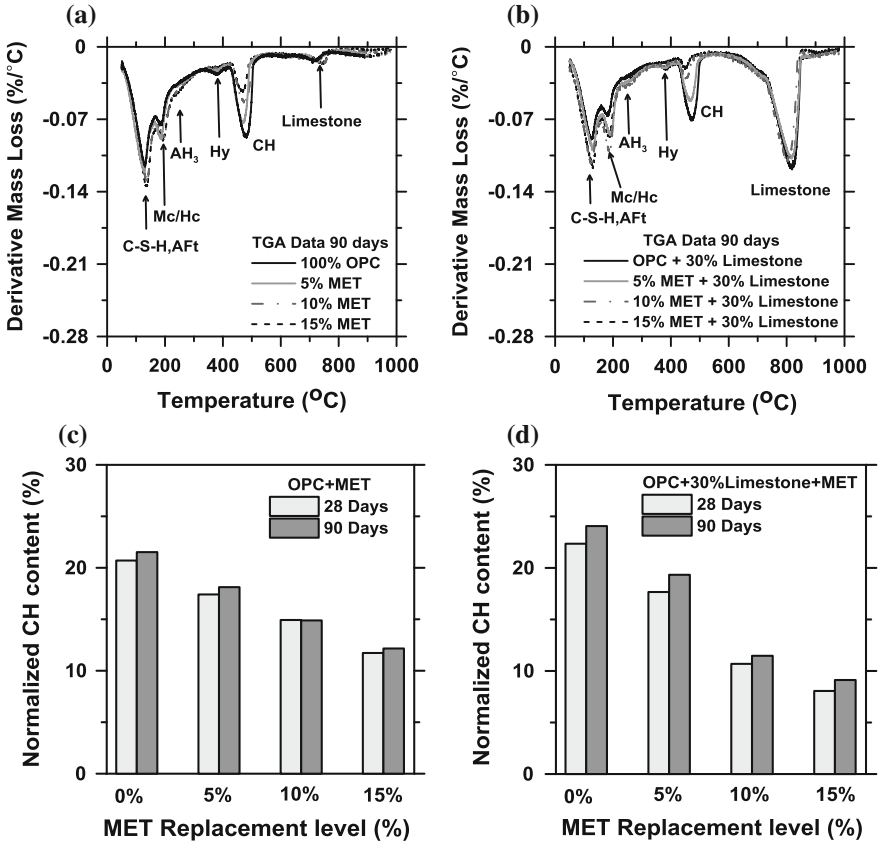

Fig. 2 Representative DTG curves for OPC mixtures for: **a** 0-to-15 % MET replacement, **b** 0-to-15 % MET replacement with additional 30 % of limestone dosed by OPC replacement. The normalized (by CF) portlandite contents for OPC mixtures for: **c** 0-to-15 % MET replacement, **d** 0-to-15 % MET replacement with additional 30 % of limestone dosed by OPC replacement. The portlandite contents were determined by thermal analysis (TGA/DTG)

When only limestone intrinsic to the OPC (limestone deficient system) is present, Mc is stabilized only when no metakaolin is added. However, when OPC is replaced by metakaolin, in increasing proportion, Hc is stabilized as stable and dominant phase. This is in line with the observations made by Antoni et al. [20] and Vance et al. [18, 19]. Contents of the CO_3-AFm (i.e., Hc/Mc) phases, reflect trends in limestone consumption. More CO_3-AFm phases form with increasing metakaolin content, and when excess limestone is present. It should be noted that while these trends follow evolutions in the equivalent CO_2/Al_2O_3 ratio, limestone reaction is limited, likely on account of its low dissolution rate. In spite of the near consumption of portlandite, e.g., in the 15 % metakaolin mixture containing excess limestone, strätlingite is not observed in the XRD patterns. It was noted that

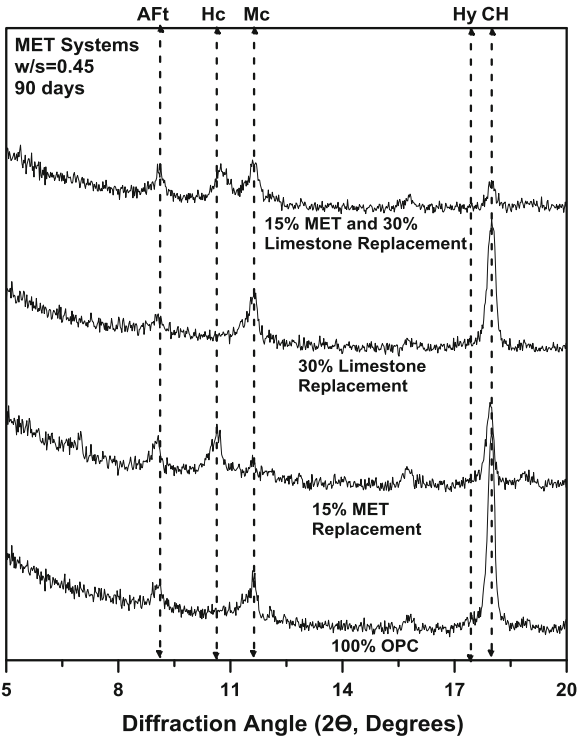

Fig. 3 XRD patterns for the plain (100 % OPC), limestone enriched (30 % OPC replacement by limestone) and MET enriched mixtures composed for limestone deficient and excess conditions. Hemicarboaluminate (*Hc*), monocarboaluminate (*Mc*), portlandite (*CH*), ettringite (*AFt*) and hydrogrossular (*Hy*)

ettringite is present in both the deficient and excess limestone cases, wherein the release of sulfate ions, due to preferred CO_3^{2-} ion uptake into the AFm phase, stabilizes ettringite in these systems. Figure 4 shows volumetric phase assemblages, calculated using GEMS, for 15 % OPC replacement by metakaolin in either limestone deficient or excess conditions. The systems presented show (determined by the portlandite match-point from TGA data) a degree of metakaolin reaction of 37 and 31 %, in limestone deficient and excess scenarios respectively.

Due to pozzolanic reaction, metakaolin ensures consumption of lime and increased formation of C-S-H formed, albeit, of a lower Ca/Si ratio and potentially also higher Al substitution. In agreement with XRD data, both C_2ASH_8 and Hydrogrossular phases are not predicted to form for relevant levels of metakaolin reaction. In contrast to the observations herein, XRD data of Antoni et al. [20] showed the presence of C_2ASH_8 and portlandite in coexistence with each other. While this is in violation of thermodynamic phase relations established by Damidot et al. [21], it may be on account of the somewhat higher metakaolin contents used in their study, or inhomogeneous reaction zones. This discrepancy could however, also be on account of uncertainties in determination of solubility data, small variations in which could alter stability fields dramatically. For example, as noted in the simulations shown herein (Fig. 4), strätlingite is predicted to form only when portlandite is consumed. When only limestone intrinsic to the OPC is present (see

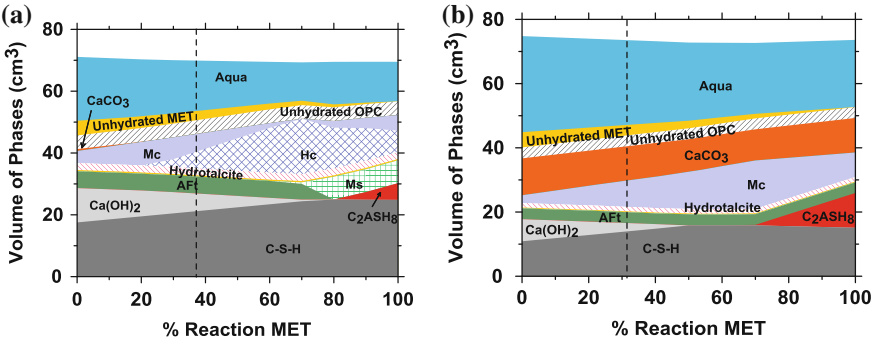

Fig. 4 Phase assemblages calculated using GEMS by incremental reaction of MET for **a** 15 % MET and **b** 15 % MET and additional 30 % limestone replacement of OPC. Monosulfoaluminate (*Ms*), ettringite (*AFt*), monocarboaluminate (*Mc*), hemicarboaluminate (*Hc*), strätlingite (C_2ASH_8), and hydrotalcite (M_4AH_{10}) are denoted. The *dashed lines* locate the estimated phase assemblage and MET degree of hydration, after 90 days

Fig. 4a), at low levels of metakaolin reaction, Mc is stabilized. With the passage of time and increase in metakaolin reaction the phase relation changes and Hc becomes dominant with Mc existing as the minor CO_3-AFm phase. For the degree of metakaolin reaction ascertained herein, Mc and Hc appear to exist in equivalent volumetric quantities, though on a mass basis this would translate to a larger quantity of Mc (the denser CO_3-AFm phase), in contrast to the XRD data shown in Fig. 3. While this may indicate that the ascertained degree of metakaolin reaction is lower than reality, it may also suggest kinetic restraint in the formation of Hc, from the Mc, Ms and portlandite (or vice versa depending on the chemical environment).

When excess limestone is present, Mc is predicted to be the dominant AFm phase (Fig. 4b). This is once again in contrast to the XRD observations in Fig. 3, where even under limestone excess conditions, when (15 %) metakaolin is present, Hc and Mc are noted to coexist; the reasoning for which is discussed above. It is seen that, at any degree of metakaolin reaction, a large quantity of limestone remains unreacted, ensuring modest levels of Hc/Mc formation. This leads to the idea that the compensation in mechanical properties (see Fig. 1), produced by the combined replacement of OPC, by limestone and metakaolin, is dominantly on account of the pozzolanic nature of metakaolin and less due to the formation of CO_3-AFm phases.

4 Conclusions

Metakaolin was evaluated in blended binder formulations in terms of its ability to enhance the reaction of limestone in cementitious systems. Such enhancements in limestone reaction are provoked by systematic manipulation of the binder

chemistry, e.g., in terms of the SO_3/Al_2O_3 and CO_2/Al_2O_3 ratios of the binder. It is noted that in spite of the provision of sufficient aluminium, calcium and water, the extent of limestone reacted is limited, mostly on account of its low reactivity (i.e., dissolution rate, and solubility). Due to reasonable (reactive) aluminum content metakaolin has shown to increase limestone reactivity and resulting formation of the CO_3-AFm (hemi- and/or mono-carboaluminate). On the account of its pozzolanic nature, it is also effective at ensuring strength equivalence, or improvement (in spite of reductions in the OPC content) as compared to the pure OPC formulations.

Acknowledgments Authors acknowledge full financial support provisioned by the NSF (CMMI: 1066583).

References

1. Concrete for the Environment.: Published on behalf of the nordic network concrete for environment by SP Swedish national testing and research institute. Boras, June 2003
2. Lothenbach, B., Scrivener, K.L., Hooton, R.D.: Supplementary cementitious materials. Cem. Concr. Res. **41**, 1244–1256 (2011)
3. Fernandez, R., Martirena, F., Scrivener, K.L.: The origin of the pozzolanic activity of calcined clay minerals: A comparison between kaolinite, illite and montmorillonite. Cem. Concr. Res. **41**, 113–122 (2011)
4. Schneider, M., Romer, M., Tschudin, M., Bolio, H.: Sustainable cement production—present and future. Cem. Concr. Res. **41**, 642–650 (2011)
5. Sato, T., Beaudoin, J.J.: Effect of nano-CaCO3 on hydration of cement containing supplementary cementitious materials. Adv. Cem. Res. **23**, 1–29 (2010)
6. Kumar, A., Oey, T., Kim, S., Thomas, D., Badran, S., Li, J., Fernandes, F., Neithalath, N., Sant, G.: Simple methods to estimate the influence of limestone fillers on reaction and property evolution in cementitious materials. Cem. Concr. Compos. **42**, 20–29 (2013)
7. Oey, T., Kumar, A., Bullard, J.W., Neithalath, N., Sant, G.: The filler effect: the influence of filler content and surface area on cementitious reaction rates. J. Am. Ceram. Soc. **96**, 1978–1990 (2013)
8. Annual book of ASTM standards.: American Society for Testing & Materials (2004)
9. Taylor, H.F.W.: Cement chemistry. Thomas Telford, London (1997)
10. Matschei, T., Lothenbach, B., Glasser, F.P.: The role of calcium carbonate in cement hydration. Cem. Concr. Res. **37**, 551–558 (2007)
11. Lothenbach, B., Le Saout, G., Gallucci, E., Scrivener, K.L.: Influence of limestone on the hydration of Portland cements. Cem. Concr. Res. **38**, 848–860 (2008)
12. Matschei, T., Lothenbach, B., Glasser, F.P.: Thermodynamic properties of Portland cement hydrates in the system CaO–Al2O3–SiO2–CaSO4–CaCO3–H2O. Cem. Concr. Res. **37**, 1379–1410 (2007)
13. Zhang, J., Scherer, G.W.: Comparison of methods for arresting hydration of cement. Cem. Concr. Res. **41**, 1024–1036 (2011)
14. American Mineralogist Crystal Structure Database. Available at: http://rruff.geo.arizona.edu/AMS/amcsd.php
15. Integrated Database of Raman Spectra.: X-ray diffraction and chemistry data for minerals. Available at: http://rruff.info/
16. Le Saout, G., Kocaba, V., Scrivener, K.L.: Application of the Rietveld method to the analysis of anhydrous cement. Cem. Concr. Res. **41**, 133–148 (2011)

17. Kulik, D.A., Wagner, T., Dmytrieva, S.V., Kosakowski, G., Hingerl, F.F., Chudnenko, K.V., Berner, U.R.: GEM-selektor geochemical modeling package: Revised algorithm and GEMS3K numerical kernel for coupled simulation codes. Comput. Geosci. **17**, 1–24 (2013)
18. Vance, K., Kumar, A., Sant, G., Neithalath, N.: The rheological properties of ternary binders containing Portland cement, limestone, and metakaolin or fly ash. Cem. Concr. Res. **52**, 196–207 (2013)
19. Vance, K., Aguayo, M., Oey, T., Sant, G., Neithalath, N.: Hydration and strength development in ternary Portland cement blends containing limestone and fly ash or metakaolin. Cem. Concr. Comp. **39**, 93–103 (2013)
20. Antoni, M., Rossen, J., Martirena, F., Scrivener, K.: Cement substitution by a combination of metakaolin and limestone. Cem. Concr. Res. **12**, 1579–1589 (2012)
21. Damidot, D., Glasser, F.P.: Investigation of the CaO-Al2O3-SiO2-H2O system at 25 °C by thermodynamic calculations. Cem. Concr. Res. **25**, 22–28 (1995)

Sustainable Secondary Resources from Brazilian Kaolin Deposits for the Production of Calcined Clays

H. Pöllmann, M.L. Da Costa and R. Angelica

Abstract An almost complete reuse of industrial residues coming from kaolin industry seems to be possible by producing different new types of carbon dioxide reduced cement types. Mainly the production of new cement types like calciumsulfoaluminate cement (CSA), calciumsulfoaluminate—(Belite)–(Ferrite) CSFA) cements seem to be possible. The landfill of these materials therefore has not to be taken into account. Especially the reuse of industrial residues as secondary cementitious materials is possible. Different clay mineral based industrial residues were investigated as potential pozzolanic materials and for reuse as a base raw material for CSA-production. Under this aspect not only composite cements can be of interest, but also these materials were used to burn different CO_2-reduced cement types. The geological surrounding of these huge amounts of clay mineral deposits in the Amazon area are investigated but also the not necessary landfill-technology for these residues is taken into account. Three main topics are under investigation: occurrence of secondary resources, availability and reuse of secondary cementitious materials and application of developed CO_2-reduced cement types. In this paper the occurrence and potential use of Brazilian waste kaolinites as secondary cementitious material is described.

1 Introduction

The potential of clay resources in Brazil/State Pará, is tremendous due to its relationship to the overall lateritic surroundings. After processing of the primary kaolin to paper kaolinite, the occurring rests from the kaolin deposits are excellent secondary raw materials for calcined clay production. Also the different qualities of

H. Pöllmann (✉)
University of Halle/Saale, Halle(Saale), Germany
e-mail: herbert.poellmann@geo.uni-halle.de

M.L. Da Costa · R. Angelica
Universidade Federal do, Belém, Pará, Brazil

K. Scrivener and A. Favier (eds.), *Calcined Clays for Sustainable Concrete*,
RILEM Bookseries 10, DOI 10.1007/978-94-017-9939-3_3

Fig. 1 Occurrence of kaolin deposits in northern Brazil. Occurrence of kaolins in the Brazilian Amazon region: State of Pará (*rectangle above* working area)

kaolins from the occurences are included. The geological abundance [1, 2] of these clays in the amazon region can be described by Fig. 1.

In the deposits it can be clearly distinguished between the different layers of different qualities of kaolins. In the geological profile in Fig. 2 the different kaolin-containing layers can be seen and the used two main layers, soft and hard kaolinites can be easily distinguished. The reddish colour comes from the different contents of iron-oxyhydroxide minerals.

For the use of these kaolinic materials as calcined clay resources for application in building material industry the following steps of investigation were performed:

1. Characterization of different qualities of china clay coming from waste kaolins and different qualities from different levels in the geological profile
2. Processing steps and optimization
3. Available amounts from varying regions and sources
4. Mixtures to produce supplementary cementitious materials

The different qualities of these kaolins were tested also for application in zeolite syntheses, pigments and ceramic industry and other minor applications [3–5]. Despite, it seems, that there is high potential for use of these kaolins in the field of thermally activated metakaolins as additives and as primary source for raw meal compositions [6, 7].

Fig. 2 Kaolinite deposit and kaolinite profile in Para/Brazil. III. Yellow clay cover—no use yet (*on the top*), II. Reduced quality (flint) *middle*, I. Best white quality kaolin soft (*on the bottom*)

2 Results

2.1 Description of Kaolins

The different kaolins for primary use and the not yet used waste kaolinites were analyzed for chemical and mineralogical properties. Table 1 gives an overview for their chemical composition.

It can be seen, that the chemical composition of the waste kaolins is slightly reduced in the silicon and aluminum contents in comparison to the theoretical value of kaolinite. Despite it is a highly valuable and rather close to the theoretical composition of kaolinite. From the geological profile the soft and the hard kaolinite can be distinguished. The two kaolins also show differencies in their mineralogical composition.

The mineralogical analysis profs the existence of the following accompanying minerals: Anatase, Rutile, Goethite, Hematite, Ilmenite, Crandallites.

The kaolinites in the different layers of the profile differ in their crystallinity (Hinckley Index: soft kaolinite: HI = 0.73, hard kaolinite: HI = 0.33) and therefore also in their properties due to dehydration and reactivity. The accompanying minerals are enriched in the less pure parts of the profile. The thermal activation of the kaolinites with different crystallinity depends on the temperature profile used (Fig. 3).

Table 1 Chemical composition of used kaolinite in comparison to waste kaolinite and theoretical composition of the mineral kaolinite

	Kaolinite	Waste	Kaolinite (theoret.)
SiO_2	44.64	41.82	46.54
Al_2O_3	38.12	35.63	39.50
H_2O	13.52	13.35	13.96
Fe_2O_3	2.35	2.20	–
TiO_2	2.25	1.30	–
Na_2O	–	1.83	–
K_2O	0.02	1.25	–

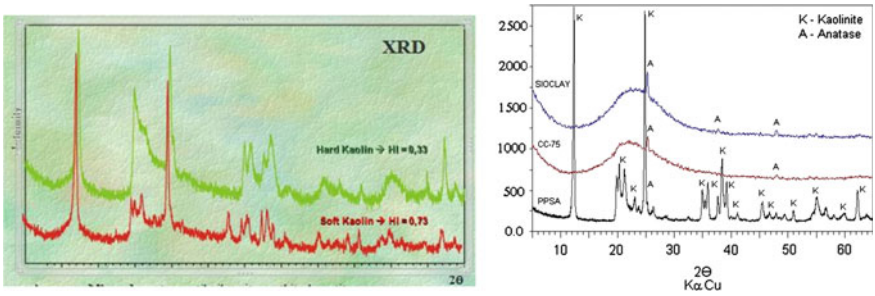

Fig. 3 XRD diagrams of hard and soft kaolin and the dehydration of kaolinitic clay from Amazon region

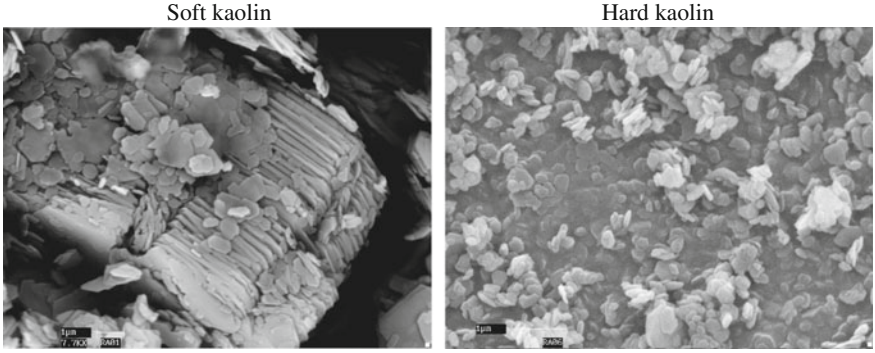

Fig. 4 SEM figures of soft and hard kaolin from Amazon region

The different kaolins also can be distinguished by SEM—analysis, due to their microstructure. Thermal activation of these kaolins was studied by [7] and their different properties described (Fig. 4).

2.2 Application

Besides the use of activated clays as an additive to cement mixtures also the use as a basic material for the production of CSA-Belite cements was investigated using different other waste materials as primary source. The different qualities of the used kaolinites from different Brazilian occurrences and the used conditions influence their hydration behaviour. In the following Table 2 mixtures of calcined clays with different other materials and their ratios for the production of CSAB-cements are summarized. In these mixtures, the differences of the mineralogical compositions of the raw kaolinites are of less importance. The ratios of the different raw materials

Table 2 Mixtures of basic materials for the production of CSAB-cements

Limestone (%)	Bauxite (%)	Anhydrite (%)	Kaolin/Metakaoline (%)
30–40	20–40	5–15	15–35

used for cements can be optimized using experimental planning programs to get maximum formation of hydraulic minerals in the final mixes [8].

Besides the calcined kaolin materials also some other raw materials are necessary to calculate the composition of the raw meals for the relevant cements of the type CSAB and CSABF. The sintering temperature ranges between 1000 and 1250 °C (Fig. 5).

Using the different raw meal mixtures the following new formed minerals can be identified in different quantities in the produced clinkers depending on the composition (Table 3):

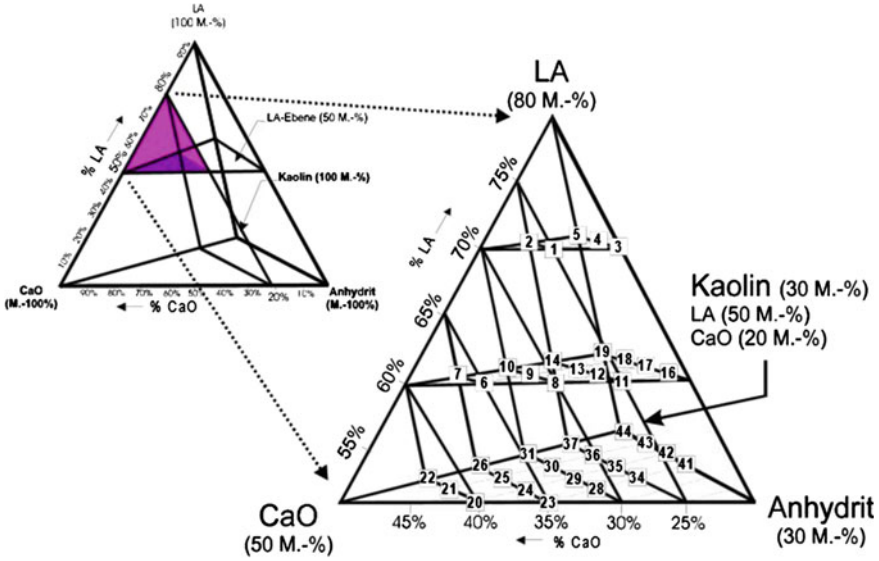

Fig. 5 Different mixtures of components for production of cementitious materials [6]

Table 3 Main phases in the sintered raw meal mixtures

Yeelimite	Larnite	Ternesite	Brownmillerite
Perovskite	Gehlenite	Amorphous phase	(Wollstonite, free lime, Ti—minerals)

3 Conclusions

The high amounts of different qualities of Brazilian kaolins make the Amazon region to one of the leading resources for kaolin in the world. Especially the qualities of kaolin, not used in paper and ceramic industry, are of high potential for use as activated clay materials in cement industry or as base material for raw meals of special cements.

References

1. Costa, M.L., Souza, D.J.L., Angélica, R.S.: The contribution of lateritization processes to the formation of the kaolin deposits from eastern Amazon. J. S. Am. Earth Sci. **27**, 219–234 (2009)
2. Barata, M.S., Angelica, R.S., Poellmann, H., Costa, M.L.: The use of wastes derived from kaolinite processing industries as a pozzolanic material for high-performance mortar and concretes. Eur. J. Min. **17**(1), 10 (2005)
3. Costa, M.L., Moraes, E.L.: Mineralogy, geochemistry and genesis of kaolins from the Amazon region. Miner. Deposita **33**, 283–297 (1998)
4. Kakali, G., Perraki, T., Tsivilis, S., Badogiannis, E.: Thermal treatment of kaolin: the effect of mineralogy on the pozzolanic activity. Appl. Clay Sci. **20**, 73–80 (2001)
5. Maia, A. A. B., Angelica, R. S., Freitas Neves, R. de., Pöllmann, H., Straub, C., Saalwächter, K.: Use of 29 Si and 27 Al MAS NMR to study thermal activation of kaolinites from Brazilian Amazon kaolin wastes. Appl. Clay Sci. 189–196 (2013)
6. Maia, A.A.B., Saldanha, E., Angélica, R.S., Souza, C.A.G., Neves, R.F.: Utilização de rejeito de caulim da Amazônia na síntese da zeólita A. Cerâmica **53**, 319–324 (2007)
7. Maia, A.A.B., Angélica, R.S., Neves, R.F.: Estabilidade Térmica da Zeólita A Sintetizada a partir de um Rejeito de Caulim da Amazônia. Cerâmica **54**, 345–350 (2008)
8. Korndörfer, J., Pöllmann, H., Costa, M. L., Angelica, R.: Mine tailings from the lateritic gold mine Igarape Bahia (Carajas region)—a basis for active hydraulic binders. Econ. Geol. ZAG SH1, 187–192 (2000)
9. Gallucio, S., Pöllmann, H.: Usage of secondary raw materials (residual bauxite, laterite and residual kaolin) for the synthesis of CSA-based cements. DMG-Tagung, Jena (2014)

Carbonation of Blended Binders Containing Metakaolin

R. Bucher, M. Cyr and G. Escadeillas

Abstract The pozzolanic materials are often recommended for their very good durability in aggressive environment. Unfortunately, this is not always true and particularly in the case of carbonation by the atmospheric CO_2. Although cement replacement by pozzolanic materials causes a decrease in pore size, the pozzolanic reaction consumes portlandite and decreases the protection potential against CO_2 ingress. This is the case for most pozzolanic materials, including metakaolin. The aim of this study is first to confirm the literature results of carbonation by using flash metakaolin in partial replacement of cements (CEM I, CEM II A-LL and CEM II A-V). Then the concretes with a metakaolin are compared with concretes based on standardized cement in order to assess the carbonation depth of metakaolin-based concretes and concretes used today in the building construction. Even though the cement replacement of CEM I and CEM II A-V by metakaolin increases the carbonation depth, results are not the same with the CEM II A-LL cement. The interaction of metakaolin with the cement limestone filler can explain this better performance, certainly because the hemicarboaluminate allows slowing down the CO_2 propagation through the matrix.

1 Introduction

The carbonation of concrete is usually slowed down by the reaction of CO_2 with Portlandite. It means that supplementary cementing materials (SCM) that consume the Portlandite could lead to an increase in the carbonation depth, especially if the permeability of the concrete is not reduced by the pozzolanic reaction. Results from the literature showed that a replacement of 25 % of Portland cement by metakaolin (MK) could lead to a carbonation depth of 9 mm instead of 2 mm after 28 days of accelerated test (50 % CO_2, 20 °C and 65 % RH) [1]. These results can be correlated with those of Kim et al. [2], who showed that accelerated carbonation

R. Bucher (✉) · M. Cyr · G. Escadeillas
LMDC, UPS—INSA Toulouse, Toulouse, France
e-mail: bucher.raph@gmail.com

K. Scrivener and A. Favier (eds.), *Calcined Clays for Sustainable Concrete*,
RILEM Bookseries 10, DOI 10.1007/978-94-017-9939-3_4

(5 % CO_2, 30 °C and 60 % RH) led to an increase of 56d-carbonation depth by 40–70 % when 5–10 % of MK was used in replacement of the cement. The carbonation depth could even be increased by 370 % for replacement rate of 20 %. Similar results were found by McPolin et al. [3] for replacement rates of 10 % (5 % CO_2, 20 °C and 65 % RH).

The aim of this paper is:

- To assess the effect of MK against CO_2 ingress, in comparison with commercial cements with and without SCM. Commercial blended cements (conform to EN 197-1) are actually accepted in the industry for all exposure classes, including for corrosion due to carbonation. It could be thus interesting to situate the combination CEM I—MK with cements containing mixtures of clinker and SCM such as slag and/or fly ash.
- To evaluate the consequence of the increase in the carbonation depth in terms of lifespan time.

2 Materials and Methods

2.1 Materials

Two reference cements without SCM were used (>95 % clinker): one normal CEM I and one low-C_3A CEM I (named PM-ES in France). In order to compare the behavior of matrices containing MK with those of commercial blended cements, several other cements conform to EN 197-1 [4] were used: one CEM II/A-LL (16 % of limestone filler), one CEM II/B-LL (22 % of limestone filler), one CEM II/A-V (15 % of fly ash), one CEM III/A (62 % of GGBS) and one CEM V/A (22 % of fly ash and 22 % of GGBS). The MK used in this study came from a flash-calcination process [5], i.e. that dehydroxylation (at around 700 °C) of powdered kaolinite clay was made within a few tenths of a second. The purity of the MK was around 50 %, the main impurity being quartz. More characteristics of this MK can be found elsewhere [1]. MK was used in replacement of fractions of the following cements: CEM I, CEM II/A-LL and CEM II/A-V. The mixtures assessed in this study are summarized in Table 1.

2.2 Methods

Compressive strength was measured at 28 days on three replicate 10 cm cubes. Carbonation depth after 28 days of curing was highlighted with a pH indicator (phenolphthalein) on split 7*7*28 cm prisms. Three replicate samples and 10 measurements per sample were made for each concrete formulation. Natural

Table 1 Mixture proportions of concrete

Materials (kg/m^3)	Cement	MK	Fine aggregates	Coarse aggregates	Water	W/B	HRWRA (%)	Air (%)	Slump (cm)	Compressive strength (MPa)
CEM I	280	0	738	1149	167	0.60	0.6	2.3	17.5	49.0
CEM I PMES	280	0	738	1149	167	0.60	0.5	1.8	18.5	–
CEM II/A-LL	280	0	738	1149	147	0.53	1.5	1.3	16.0	53.7
CEM II/A-V	280	0	738	1149	147	0.53	1.5	1.6	18.0	51.4
CEM II/B-LL	368	0	738	1149	170	0.46	0.6	2.1	19.0	44.0
CEM III/A	280	0	738	1149	167	0.60	0.5	1.7	17.0	48.2
CEM V/A	280	0	738	1149	147	0.53	1.5	1.6	18.0	48.3
CEM I 15	238	42	738	1149	167	0.60	1.0	1.9	17.0	47.4
CEM I 20	224	56	738	1149	167	0.60	1.3	2.0	18.0	52.9
CEM I 25	210	70	738	1149	167	0.60	1.3	1.9	17.5	49.1
CEM II/A-LL 15	238	42	738	1149	147	0.53	2.5	1.7	15.0	64.7
CEM II/A-V 15	238	42	738	1149	147	0.53	2.5	1.6	14.5	47.3

Fresh and hardened properties

carbonation was measured after 2 years and accelerated carbonation testing was performed according to XP P18-458 [6], i.e. exposition of the concrete for 70 days in a chamber (4 % CO_2, 20 °C, 50 % RH) after a pretreatment of 14 days at 20 °C and 50 % RH.

3 Results

Figure 1 presents the carbonation depth results for all the concretes in accelerated (a) and natural (b) conditions. The graphs include the main reference cements (black bars: CEM I, CEM II/A-LL and CEM II/A-V), the same cements with MK (grey bars), and the other reference blended cements (hollow bars). The shaded zones stand for the carbonation depths between the best and worst commercial cements in terms of carbonation. It can be seen that the CEM I always led to the lower carbonation, while the CEM V gave the higher carbonation depth, both in accelerated and natural conditions. It seemed obvious here that the pozzolanic reaction involved in the CEM V hydration was unfavorable to the carbonation of the concrete.

As expected, the use of MK as replacement of CEM I systematically led to an increase in the carbonation depth, but the values remained in the same order of magnitude than other commercial blended cements (hollow bars). If these increases are accepted in the case of commercially available blended cements, they probably should also been acceptable for blended mixtures made of CEM I or CEM II with MK.

Similar results were obtained when MK replaced a fraction of CEM II/A-V (fly ash cement), probably due to a higher consumption of the Portlandite by MK (decrease of the lime reserve). Only the replacement of 15 % of CEM II/A-LL by MK led to a slight decrease of the carbonation depth when compared to the reference. The compressive strength of this mixture was higher than the other concretes. Moreover, it can be noted that the good compatibility between MK and limestone filler in ternary blended binders has already been reported by Antoni et al. [7], who highlighted the formation of hemicarboaluminates in such matrices. These

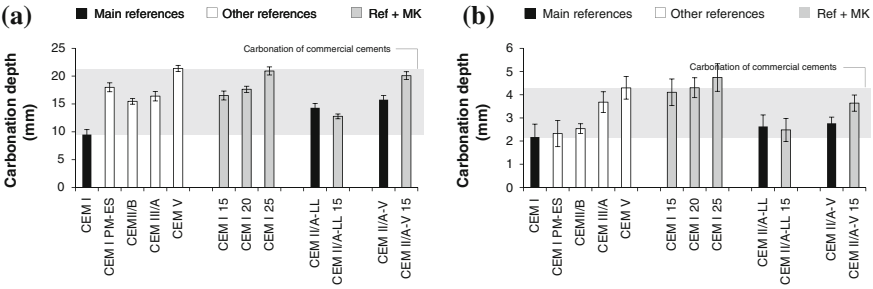

Fig. 1 Carbonation depth of concretes cured 28 days, after **a** 70 days of accelerated carbonation, and **b** 2 years in natural conditions

hydrates tend to be transformed into calcite when the CO_2 concentration increases [8], meaning that they could play the role (as Portlandite) of CO_2 pump in clinker-limestone filler-MK mixtures. This could help reducing the CO_2 ingress in this ternary blended matrix.

4 Lifetime Span Regarding Carbonation

In order to compare the effect of MK on the rate of CO_2 ingress in the concrete, a predictive carbonation model (Eq. 1) was used [9]. This model allowed us to calculate the carbonation depth as a function of time (a given time corresponding to the service life of a structure), and thus to compare the carbonation state of the different cements (blended or not) studied in the precedent section. This model was fitted on the experimental points from natural carbonation.

$$x_c(t) = \sqrt{\frac{2 \cdot D^0_{CO_2} \cdot P_0 \cdot t}{R \cdot T \cdot \left(1 + \beta \cdot C2 \cdot \left(\frac{P_0}{P_{atm}}\right)^n\right) \cdot \left(\frac{\varphi_p \cdot C2}{n+1} \cdot \left(\frac{P_0}{P_{atm}}\right)^n + Q1\right)}} \quad (1)$$

with:

- $\boldsymbol{P_0}$ pressure of CO_2 at the concrete surface (Pa)
- $\boldsymbol{R}$ universal gas constant (J/mol/K),
- $\boldsymbol{T}$ temperature (K)
- $\boldsymbol{\beta}$ fitting parameter independent of the material
- $\boldsymbol{C_2}$ number of moles of calcium in C-S-H for the material considered (mol/l of cement paste) (calculated with chemical data of cement and the C/S ratio of the C-S-H)
- $\boldsymbol{x_c(t)}$ carbonation depth (m)
- $\boldsymbol{t}$ time (s)
- $\boldsymbol{P_{atm}}$ atmospheric pressure at the concrete surface (Pa)
- $\boldsymbol{\varphi_p}$ fraction of paste in the concrete (liter of cement paste per liter of concrete or mortar)
- $\boldsymbol{n}$ fitting parameter independent of the material
- $\boldsymbol{Q1}$ number of moles of calcium initially contained in portlandite, Aft and Afm (mol/l of cement paste) (calculated with chemical data of cement and stoichiometric formulas)
- $D^0_{CO_2}$ coefficient of CO_2 diffusion in carbonated zones (m^2/s) (fitted)

The results of the calculations are given on Fig. 2, up to an age of 50 years of natural exposure to CO_2. This age corresponds to a normal lifespan of an ordinary structure [10]. The increase in the MK content (15–25 % in replacement of CEM I) could lead to +9 to +14 mm more carbonation when compared to the CEM I reference. However:

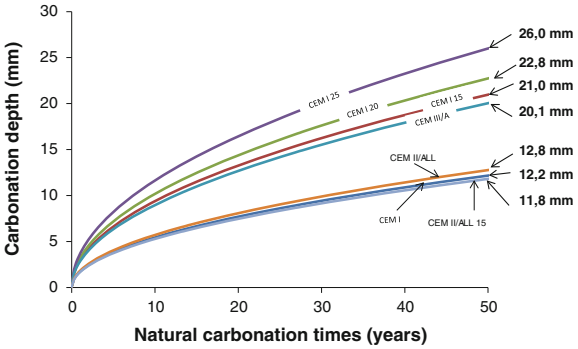

Fig. 2 Application of the model of natural carbonation for mixtures based on CEM I, CEM I + MK, CEM II/A, CEM II/A-LL + MK, and CEM III

- The carbonation depths should be around the ones of commercially blended cements (e.g. CEM III/A and CEM V/A). It could be noted that interesting results are obtained for ternary blended cements (clinker + filler + MK), since the carbonation could be as low as the CEM I.
- The maximum depth after 50 years should be much lower than the 50 mm usually requested to protect the steel rebars in real structures [1]. Moreover, this model calculated only the time of CO_2 ingress, without taking into account the time necessary for the corrosion to begin, or the time needed for the structure to be ruined due to the corrosion. It means that SCM (including MK) should protect the steel bars at least for the lifespan of the structure.

5 Conclusions

The following conclusions can be drawn from this study:

- The replacement of CEM I and CEM II/A-V (based on fly ash) by metakaolin leads to an increase in the carbonation depth of concrete.
- The carbonation depths of MK concretes are in the same order of magnitude than the ones of commercially available blended cements.
- The combination CEM II/A-LL + MK (i.e. ternary mixture composed of clinker, limestone filler and metakaolin) seems to be beneficial to the reduction of carbonation (both accelerated and natural).
- The calculation of the carbonation depth after 50 years of natural exposition shows that all SCM concretes (including MK) are still acceptable in terms of carbonation, especially when considering the concrete cover protecting the steel bars.

References

1. San Nicolas, R.: Approche performantielle des bétons avec métakaolins obtenus par calcination flash, Thesis in french (Toulouse, 2011)
2. Kim, H.S., Lee, S.H., Moon, H.Y.: Strength properties and durability aspects of high strength concrete using Korean metakaolin. Constr. Build. Mater. **21**, 1229–1237 (2007)
3. McPolin, D.O., Basheer, P.A.M., Long, A.E., Grattant, K.T.V., Sun, T.: New test method to obtain pH profiles due to the carbonation of concretes containing supplementary cementitious materials. J. Mater. Civ. Eng. **19**, 936–946 (2007)
4. EN 197-1, 'Cement-Part 1: composition, specifications and conformity criteria for common cements' (2001)
5. Salvador, S.: Pozzolanic properties of flash-calcined kaolinite: a comparative study with soak-calcined products. Cem. Concr. Res. **25**, 102–112 (1995)
6. XP P18-458.: Tests for hardened concrete-Accelerated carbonation test-Measurement of the thickness of carbonated concrete (2008)
7. Antoni, M., Rossen, J., Martirena, F., Scrivener, K.: Cement substitution by a combination of metakaolin and limestone. Cem. Concr. Res. **42**, 1579–1589 (2012)
8. Damidot, D., Stronach, S., Kindness, A., Atkins, M., Glasser, F.P.: Thermodynamic investigation of the CaO-Al_2O_3-$CaCO_3$-H_2O closed system at 25 °C and the influence of NaO. Cem. Concr. Res. **24**, 563–572 (1994)
9. Hyvert, N., Sellier, A., Duprat, F., Rougeau, P., Francisco, P.: Dependency of C-S-H carbonation rate on CO_2 pressure to explain transition from accelerated tests to natural carbonation. Cem. Concr. Res. **40**, 1582–1589 (2010)
10. Karimpour, M., Belusko, M., Xing, K., Bruno, F.: Minimising the life cycle energy of buildings: review and analysis. Build. Environ. **73**, 106–114 (2014)

Service Life and Environmental Impact Due to Repairs by Metakaolin Concrete After Chloride Attack

Aruz Petcherdchoo

Abstract A Crank-Nicolson based finite difference approach is developed for numerical assessment of chloride diffusion in concrete structures with repairs. The repair by cover concrete replacement is applied at a critical time which the chloride content at a threshold depth reaches its critical value for initiation of rebar corrosion. This aims at corrosion-free condition of concrete structures. The critical time is defined as the repair time, which the CO_2 due to repair concrete production and replacement processing occurs. From the study, it is found that increasing the amount of metakaolin in repair concrete by 4 % not only leads to longer service life extension after repairs and fewer repairs but also reduces the amount of CO_2 by 50 %.

1 Introduction

The deterioration of concrete structures under the chloride attack can be classified into three main forms; rebar corrosion, concrete cracking, and a combination of them. The rebar corrosion occurs prior to the others. The corrosion leads to the loss of the cross-sectional area of rebar, and consequently reduces the strength of concrete structures. This consequently shortens the service life of concrete structures. However, this can be remedied by using two main approaches to extend the service life; use of high-quality concrete and application of concrete repairs [1]. For the first approach, pozzolanic materials, such as fly ash, metakaolin, etc., are being widely used [1–4]. For the second approach, there are many repair methods, such as cover concrete replacement, silane treatment, cathodic protection, and etc. [5].

In addition to the service life extension, the environmental impact is nowadays considered as an important issue. This leads to not only the concept of sustainable development introduced in the Brundtland report published by the United Nation World Commission on Environment and Development [6] but also the Kyoto

A. Petcherdchoo (✉)
1518 Pracharat 1 Road, Wongsawang, Bangsue, Bangkok 10800, Thailand
e-mail: aruzp@kmutnb.ac.th

K. Scrivener and A. Favier (eds.), *Calcined Clays for Sustainable Concrete*,
RILEM Bookseries 10, DOI 10.1007/978-94-017-9939-3_5

protocol [7] which focused on the reduction of CO_2 emission. Subsequnetly, Heath et al. [8] referred to IPCC which stated that substituting concrete binders with geopolymers was found to be a realistic option for reducing the CO_2 emission. Moreover, Petcherdchoo [9] stated that concrete repairs not only helped extend the service life of concrete structures but also reduced the environmental impacts due to the reduction of concrete production in structure reconstruction.

In this study, two aforementioned remedial approaches are combined aiming at not only extending the service life of concrete structures but also reducing the CO_2 emission. Metakaolin concrete is chosen as a repair material due to insufficient production of other pozzolanic materials, such as fly ash, to satisfy the current needs [8]. For this, A Crank-Nicolson based finite difference approach combined with a CO_2 emission model is developed.

2 Chloride Diffusion in Concrete with Cover Replacement

The deterioration of concrete structures by chloride attack can be governed by chloride diffusion. The one-dimensional partial differential equation for chloride diffusion through concrete [10] and its Crank-Nicolson based finite difference formulation can be written as:

$$\begin{aligned}\frac{\partial C}{\partial t} &= \frac{\partial}{\partial x} D(t) \frac{\partial C}{\partial x} \Rightarrow \frac{c_{i,j+1} - c_{i,j}}{\Delta t} \\ &= \frac{1}{2}\left(\frac{[D(c_{i+1} - 2c_i + c_{i-1})]_{,j+1}}{(\Delta x)^2} + \frac{[D(c_{i+1} - 2c_i + c_{i-1})]_{,j}}{(\Delta x)^2} \right)\end{aligned} \tag{1}$$

where C is the chloride content as a function of position x and time after exposure t (in years), and D(t) is the time-dependent chloride diffusion coefficient [11]. Moreover, $c_{i,j}$ and D_j, in a general form, are the chloride content at the space i and time j, and the diffusion coefficient at time j, respectively. And, Δt and Δx are the incremental time step (1 week) and the mesh point size (1 mm), respectively. For numerical assessment, the boundary condition or surface chloride $C_S(t)$ and the material property or diffusion coefficient D(t) [12] can be obtained as:

$$C_S(t) = C_0 + kt \text{ and } D(t) = D_{28}\left(\frac{28}{365t}\right)^m \tag{2}$$

where

$$C_0 = [0.0042 + 0.038(W/B)]\,[\%MK] - [1.375(W/B) - 0.952] \tag{3}$$

$$k = [0.067 - 0.223(W/B)]\,[\%MK] + [2.64(W/B) - 0.7891] \tag{4}$$

$$D_{28} = [29.63 - 148.03(W/B)]\,[\%MK] + [2517.245(W/B) - 531.64] \quad (5)$$

$$m = [0.047 - 0.104(W/B)]\,[\%MK] + [1.557(W/B) - 0.201] \quad (6)$$

Using Eqs. (2) to (6), the space-dependent chloride profiles for concrete having W/B of 0.4 and 0 %MK (C40) is shown in Fig. 1a. The chloride content at concrete surface increases with time due to time-dependent surface chloride, and the rate of chloride diffusion is slower with increasing time due to time-dependent diffusion coefficient (see Eq. (2)). In year 26B (B: Before repair), the chloride profile at the threshold depth of 80 mm [13] reaches the critical value ($Cl_{crit,\%MK}$) of 0.4 % wt. of binder for rebar corrosion initiation [14] as calculated by:

$$Cl_{crit,\%MK} = 0.4[1 - 0.01(\%MK)] \quad (7)$$

For the first repair, the cover concrete is replaced by the metakaolin concrete having W/B of 0.4 and 4 % MK (C44) causing removal of chloride ions in cover concrete. Immediately after that, the chloride profile become the profile at year 26A (A: After repair) as shown in Fig. 3b. And, the diffusion coefficient is space-dependent due to two different diffusion coefficient, i.e., D_R (shaded area) and D_0 (white area). Hence, Eq. (1) becomes [15, 16]:

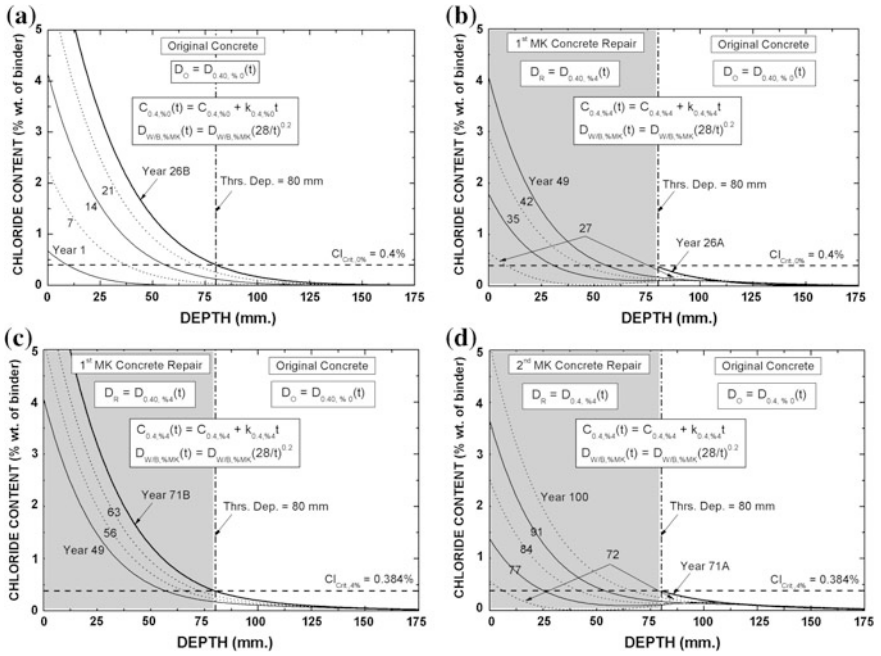

Fig. 1 Space-dependent chloride profile for C40 repaired with C44. **a** Years 1 to 26B. **b** Years 26A to 49. **c** Years 49 to 71B. **d** Years 71A to 100

$$\frac{\partial C}{\partial t} = \frac{\partial}{\partial x} D(t,x) \frac{\partial C}{\partial x} \tag{8a}$$

$$\frac{c_{i,j+1} - c_{i,j}}{\Delta t} = \frac{1}{2} \left(\frac{\left[D_{i+1/2}(c_{i+1} - c_i) - D_{i-1/2}(c_i - c_{i-1}) \right]_{,j+1}}{(\Delta x)^2} + \frac{\left[D_{i+1/2}(c_{i+1} - c_i) - D_{i-1/2}(c_{i,} - c_{i-1,}) \right]_{,j}}{(\Delta x)^2} \right) \tag{8b}$$

It is noted that the numerical computation by the Crank-Nicolson based formulation in Eq. (8b) is used, because a close-formed solution for Eq. (8a) is so complex to solve.

In computation using Eq. (8b), the chloride content in the replacement zone (shaded area) in Fig. 3b is updated as zero. In the year 26A, the chloride ions are about to redistribute from the original concrete through the repair concrete due to differential chloride content between two concrete materials (shaded and white area). So, at year 27, there are two parts of chloride ions, i.e., those redistributed near the threshold depth (right-handed) and those newly penetrated from concrete surface (left-handed). When the chloride profile reaches the critical value of 0.384 % in the year 71B in Fig. 1c, the same repair cycle as the first one is repeated as shown in Fig. 1d. It is noted that the critical value for the first and second repairs (Fig. 1a, c, respectively) is different due to different %MK in concrete at each repair time.

The time-dependent chloride profiles without and with cover replacement by C44 is compared in Fig. 2a. The chloride content is assessed at the fixed threshold depth of 80 mm. Without repair, the chloride content increases with time. If the time which the chloride profile reaches the critical value of 0.4 % is defined as the service life of the structure, the service life is approximately equal to 26 years. If C44 is applied over the repair depth of 80 mm in year 26, the service life can be prolonged. Immediately after the repair, the chloride profile decreases to zero due to removing the chloride ions together with the taken-off concrete. However, the chloride content suddenly increases due to immediate redistribution of chloride ions from the original concrete. By the effect of the first repair, the service life is prolonged by approximately 45 years. At the year 71, the chloride profile reaches the critical value of 0.384 %, the same kind as the first repair is reapplied. This results in prolonging the service life of the structure over the design service life of 100 years [17]. It is noted that only two repairs are necessary within the design service life. But if the normal concrete of C40 is applied, the number of repairs will be four as shown in Fig. 2b. So, if lower quality of repair materials (lower amount of metakaolin replacement) is used, the number of repairs will be more due to shorter service life extension after repairs. It is also noted that all the repairs are applied whenever the chloride content at the threshold depth reaches its critical value, hence, the repaired concrete structure is free of corrosion over the design service life.

3 Assessment of Co_2 Emission

In this study, whenever cover concrete replacement is applied, the environmental impacts in terms of CO_2 corresponding to concrete production CO_2^{PD} and replacement processing CO_2^{PC} are assumed to occur at the same time. The amount of CO_2 emission for these can be predicted from a CO_2 emission model in a functional unit of eq. kg/m^2 [12] as

$$\begin{aligned} CO_2 &= CO_2^{PD} \cdot x_p + CO_2^{PC} \\ &= \{[3.09(W/B) - 2.77][\%MK] - [650(W/B) - 625.6] + [1968]\} \cdot x_p + 23.4 \end{aligned} \quad (9)$$

where x_p is defined as the depth of replacement. It is noted that CO_2^{PD} was calculated based on concrete compositions, while CO_2^{PC} was calculated based on five processes; repair material transportation, hydrojetting for old concrete removal, application of shotcrete, and cleaning and coating rebars. Using Eq. (9), the cumulative amount of CO_2 emission for cover concrete replacement by C44 and C40 can be compared as shown in Fig. 3. Within 100 years, the cover replacement by better materials (higher amount of metakaolin replacement) causes lower cumulative CO_2 emission because of not only lower number of applications (see also Fig. 2) but also lower amount of CO_2 emission in each application of repairs (see also Fig. 2). It is also observed that the increase of the amount of metakaolin in repair concrete by 4 % leads to the reduction of the amount of CO_2 emission by about 50 %.

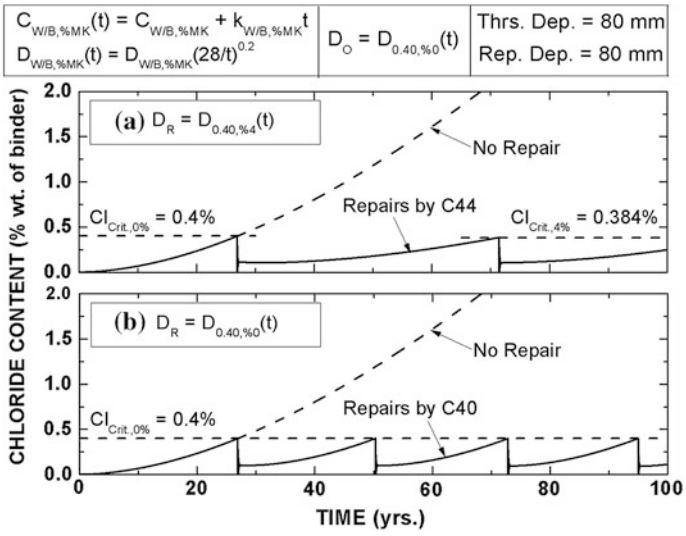

Fig. 2 Time-dependent chloride profile for C40 repaired with C44 and C40

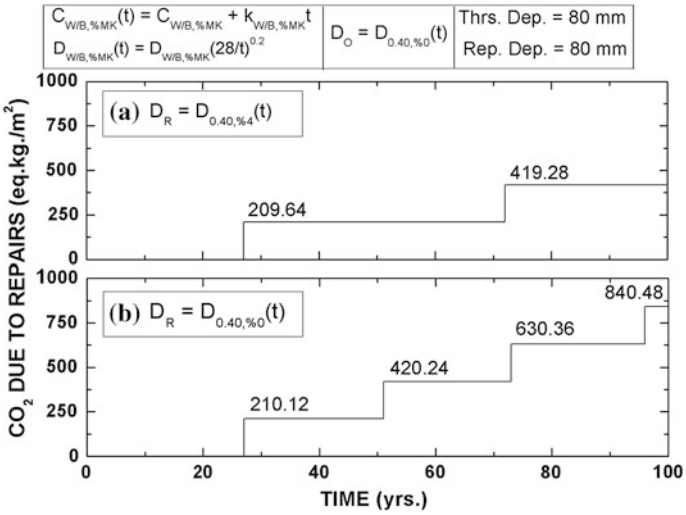

Fig. 3 CO_2 emission for concrete structure of C40 with C44 and C40

4 Conclusions

The numerical assessment of repairs by metakaolin concrete to extend corrosion-free service life of chloride attacked concrete structures considering environmental impacts in terms of CO_2 emission is studied. It is found that increasing the amount of metakaolin replacement in repair concrete by 4 % not only leads to longer service life extension after repairs and fewer repairs but also reduces the amount of CO_2 emission by about 50 %.

Acknowledgment This research was funded by the board of higher education and King Mongkut's University of Technology North Bangkok under the contract no. KMUTNB-GEN-58-22.

References

1. Petcherdchoo, A.: Time dependent models of apparent diffusion coefficient and surface chloride for chloride transport in fly ash concrete. Constr. Build. Mater. **38**, 497–507 (2013)
2. Bai, J., Wild, S., Sabir, B.: Chloride ingress and strength loss in concrete with different PC-PFA-MK binder compositions exposed to synthetic seawater. Cem. Conc. Res. **33**(3), 353–362 (2013)
3. Shekarchi, M., Rafiee, A., Layssi, H.: Long-term chloride diffusion in silica fume concrete in harsh marine climates. Cem. Concr. Compos. **31**(10), 769–775 (2009)
4. Nai-qian, F., Hsia-ming, Y., Li-Hong, Z.: The strength effect of mineral admixture on cement concrete. Cem. Concr. Res. **18**(3), 464–472 (1988)
5. Petcherdchoo, A.: Maintaining condition and safety of deteriorating bridges by probabilistic models and optimization. Ph.D. thesis, University of Colorado, Boulder, USA (2004)

6. WCED (The World Commission on Environment and Development): Our Common Future. Oxford University Press, Oxford (1987)
7. Sakai, K.: Environmental design for concrete structures. J. Adv. Concr. Technol. **3**(1), 17–28 (2005)
8. Heath, A., Paine, K., McManus, M.: Minimising the global warming potential of clay based geopolymers. J. Cleaner Prod. **78**, 75–83 (2014)
9. Petcherdchoo, A.: Service life cycle assessment of chloride attacked concrete structures with silane treatment considering environmental impacts. In: 10th International Symposium. on New Technologies for Urban Safety on Mega Cities in Asia, Thailand (2011)
10. Crank, J.: The Mathematics of Diffusion, 2nd edn. Clarendon, Oxford (1975)
11. Thomas, M.D.A., Bentz, E.C.: Life-365 Manual. Master Builders (2000)
12. Petcherdchoo, A.: Service Life and Environmental Impacts due to Repairs on Concrete Structures under Chloride Attack. Report KMUTNB, Bangkok (2015) (in Thai)
13. JSCE: Standard Specification for Durability of Concrete. Concrete Library (2002) (in Japanese)
14. FIB (CEB-FIP): Design of durable concrete structures. In: Structural Concrete Textbook on Behaviour, Design and Performance, 2nd edn., vol. 3. Sprint-Digital-Druck, Stuttgart (2009)
15. von Rosenberg, D.U.: Methods for the Numerical Solution of Partial Differential Equations. Elsevier, Amsterdam (1969)
16. Press, W.H., Teukolsky, S.A., Vetterling, W.T., Flannery, B.P.: Numerical Recipes in C: the Art of Scientific Computing, 2nd edn. Cambridge University Press, Cambridge (1996)
17. FIB (CEB-FIP): Model Code for Service Life Design. Task Group 5.6. Sprint-Digital-Druck, Stuttgart (2006)

Properties of Calcined Lias Delta Clay—Technological Effects, Physical Characteristics and Reactivity in Cement

N. Beuntner and K.Ch. Thienel

Abstract The investigation reveals chances for calcined clay comprising a mixture of different clay minerals as supplementary cementitious material. There is ample supply in southern Germany of the source material with its quartzous clay combined with a high content of mica and other clay minerals. Its content of kaolinite is less than 25 % by mass. The calcinations were done following two different procedures. On laboratory scale the raw clay was dried initially, crushed to a maximum particle size of less than 4 mm and subsequently calcined in small quantities of 50 g in a muffle furnace. On an industrial scale the raw clay was crushed coarse to a maximum particle size of 100 mm and subsequently fed in campaigns of 180 tons each into a tripartite rotary kiln normally used for the production of expanded clay. The resulting calcined clay particles had a maximum size up to 40 mm. Characteristic chemo-mineralogical properties and physical parameters (e.g. mineral composition and amorphous content, lime-retention, ion solubility in alkaline medium and BET-surface) of the calcined clays were measured. The comparison of the clays calcined in the laboratory and those calcined on industrial scale revealed a broader optimum temperature range for the latter accompanied by a partially reduced pozzolanic reactivity when used in combination with cement.

1 Introduction

Calcined clay containing a mixture of different clay minerals is suitable for cement substitution as a pozzolanic material in order to reduce CO_2 emissions. Because of worldwide availability and low carbon content, these calcined clays provide a forward-looking opportunity for producing sustainable concrete. The most popular calcined clay metakaolin is well known and widely discussed in literature for its pozzolanic properties [1]. The degree of pozzolanic reaction depends on the kaolinite (and to a lesser extend the mica and illite) content in clays, the structural

N. Beuntner (✉) · K.Ch. Thienel
University of the Federal Armed Forces, Munich, Germany
e-mail: nancy.beuntner@unibw.de

K. Scrivener and A. Favier (eds.), *Calcined Clays for Sustainable Concrete*,
RILEM Bookseries 10, DOI 10.1007/978-94-017-9939-3_6

order and physical factors [2, 4]. In addition, process parameters, e.g. temperature of heat treatment, rate of heating and calciner atmosphere affect the properties of thermally activated (calcined) clays [3]. Pozzolanic activity describes the reaction of dissolved Al- and Si-Ions (from calcined clay) with calcium hydroxide yielding hydrated compounds of Ca-Al-Si. Thereby, the solubility depends on degree of dehydroxylation. This is characterized by amorphous SiO_2 and related to the change of the coordination of Al^{3+} from octahedral to tetrahedral [2–4].

This paper deals with the properties Lias Delta clay with low kaolinite content calcined at laboratory scale compared to industrial scale. Results were compared to determinate the optimal calcination temperatures which will lead to the best pozzolanic activity with and additional focus on the influence of the grain size.

2 Experimental Procedure

2.1 Characterization of Raw Material

Lias Delta clay (Pliensbachian Lower Jurassic) was the source material for the tests. There is ample supply in southern Germany of such quartzous clay with its high content of mica and other clay minerals. The raw clay was characterized by means of X-ray diffraction (XRD), Infra-Red (IR) spectroscopy and its chemical composition by inductively coupled plasma optical emission spectrometry (ICP-OES). Specially, the mineralogical composition of the raw clay was calculated using a combined IR-XRD method proposed by Gehlken [5]. The characteristics of raw-material are described in Table 1.

Table 1 Characteristics of raw material

Chemical composition [%]		Mineralogical composition [%][a]		Physical properties	
		Clay Minerals			
SiO_2	52 ± 2	Kaolinite	25	Density [g/cm^3]	2.72
Al_2O_3	21 ± 1	Mica, dioctahedral	30	S_{BET} [m^2/g]	27.5
CaO	3 ± 1	Illite	11		
Fe_2O_3	8 ± 1	Chlorite	6		
Na_2O	0.4 ± 0.1	Quartz	18		
K_2O	3 ± 1	Feldspar	5		
TiO_2	1 ± 0.5	Calcite	3		
MgO	2 ± 0.5	Gypsum	1		
SO_3	1 ± 0.5	Pyrite	1		

[a]Relative error by 10 %

2.2 Calcination on Laboratory Scale

On laboratory scale the raw clay was dried first, crushed to a maximum particle size of less than 4 mm and subsequently calcined in small quantities of 50 g in a muffle furnace. The raw clay was calcined at different temperatures (T = 600, 720, 770, 820, 1000 °C) with residence time of 60 min. Finally, calcined samples were ground in a porcelain mortar. The calcined clay is referred to as *LCT_temperature.*

2.3 Calcination on Industrial Scale

On the industrial scale the raw clay was crushed coarse to a maximum particle size of 100 mm and subsequently fed in campaigns of 180 tons each into tripartite rotary kiln normally used for the production of expanded clay. The resulting calcined clay particles had a maximum size up to 40 mm. This calcined clay is referred to as *GCT_temperature.*

3 Results and Discussion

3.1 Characteristic Chemo-Mineralogical Properties

The most interesting XRD patterns of the raw and the calcined clay on laboratory scale and industrial scale are shown in Fig. 1. Mineralogical phases Chlorite, Kaolinite and Muscovite disappear depending on the thermal treatment. Chlorite is not detectable at 650 °C, Kaolinite vanishes at 700 °C. Mica is represented by Muscovite and Paragonite. Since Muscovite is undetectable at 500 °C, Paragonite is verifiable until 900 °C and finally Illite disappears at 900 °C. Starting with this temperature quartz becomes partially solvent. At 1000 °C, secondary silicates (especially ringwoodite, wollastonite and mullite) form. The investigations exhibited an accelerating dehydroxylation process for calcined at laboratory scale compared to industrial scale.

Particle size of clay has a considerable impact on mineralogical phases because of the temperature gradient and the sintered skin. Table 2 shows the mineralogical composition calculated for effective grain size 0–4 mm, 4–8 mm, 8–20 mm, more than 20 mm and furthermore the final industrial product GCT_750 and the laboratory product LCT_720.

Regardless of particle size the mineralogical composition confirmed the absence of kaolinite and chlorite peaks after thermal treatment at 720 °C. The presence of Fe-oxides, detectable at smaller sizes, results from sintered skin and missing oxygen transfer. Carbonates are detected in particles with a maximum size up to 8 mm. The amorphous content correlates with particle size and changing mineral content.

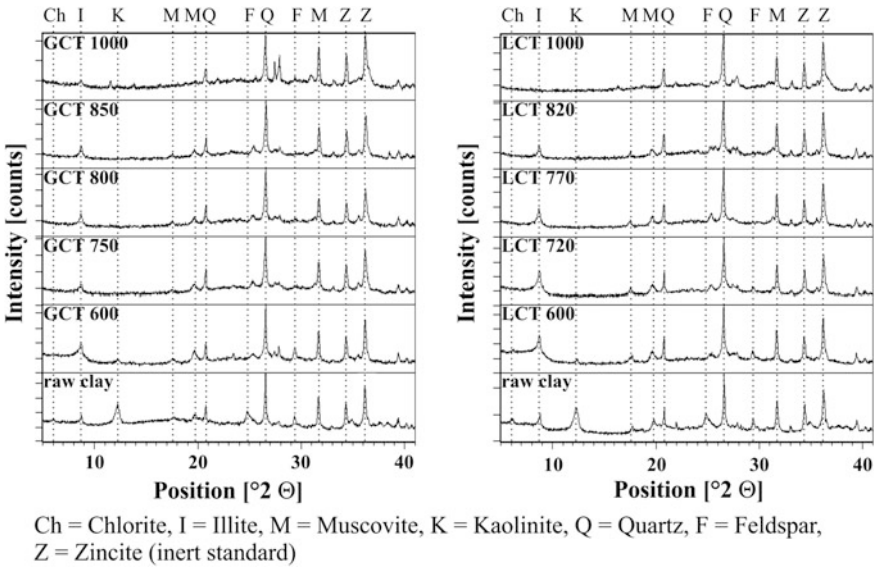

Fig. 1 XRD patterns of industrially calcined clay (*left*) and clay calcined on laboratory scale (*right*)

Table 2 Mineralogical composition according to particle size

Mineralogical composition	GCT_750	GCT_750	GCT_750	GCT_750	GCT_750	LCT_720
[w.-%]	0–4 mm	4–8 mm	8–20 mm	>20 mm	Final industrial product	Laboratory product
Carbonate	0.3	0.4	1.2	2.8	0.4	0.5
Quartz	16.9	18.8	18.3	18.2	18.3	18.5
Mica	4.9	4.0	4.7	5.5	3.8	5.3
Illite	4.5	4.4	4.7	5.0	4.4	4.1
Kaolinite	0	0	0	0	0	0
Chlorite	0	0	0	0	0	0
Feldspar	3.4	5.0	4.6	7.1	7.9	3.3
Secondary Silicates	0	0	0	0	3.4	1.2
Fe-oxide	0.8	0.4	0.2	0	0.6	0.4
Ore	1.3	1.2	1.8	1.6	0.8	0.4
Sulfate	1.5	0.8	0.5	0.8	1.1	0.6
Amorphous	66.4	65.0	64.0	59.0	59.3	65.7
Σ All Phases	100	100	100	100	100	100

In the IR-spectra (Figs. 2 and 3) the absorption bands of raw clay and calcined clay can be identified. The characteristic bands of the OH-group (3700, 3650 and 3620 cm^{-1}) are well defined for raw clay. Because of the missing OH-band at

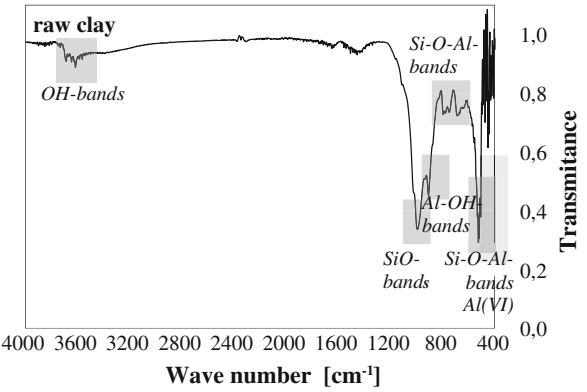

Fig. 2 IR-spectra of raw clay

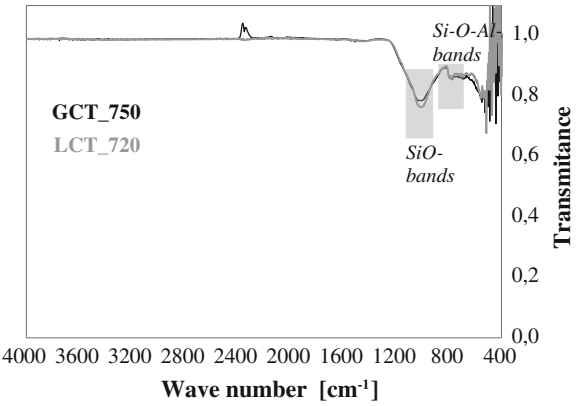

Fig. 3 IR-spectra of GCT_750 and LCT_720

3670 cm^{-1} the structure of raw clay is considered disordered and thus easier to dehydrate. Furthermore, the uncalcined clay shows the following characteristic bands: Al-OH at 912 cm^{-1}, Si-O at 1026 and 999 cm^{-1} and Si-O-Al^{VI} at 524 cm^{-1}. For calcined clays (with heat treatment at 750 °C), the typical OH-bands, Al-OH-bands and Si-O-Al^{VI} -bands disappears in the IR-spectra. Instead a new band at 800 cm^{-1} can be detected which is typical for a changed octahedral coordination of Al^{3+} to tetrahedral coordination [2, 4].

3.2 Physical Parameters

The physical parameters (density and BET specific surface) of raw and calcined clays can assist in characterizing thermal treatment, the degree of dehydroxylation and the initiation of the sintering process. Results are shown in Figs. 4 and 5. The specific surface and density are decreasing drastically in the temperature range 600–750 °C due to dehydroxylation of the dioctahedral minerals kaolinite and

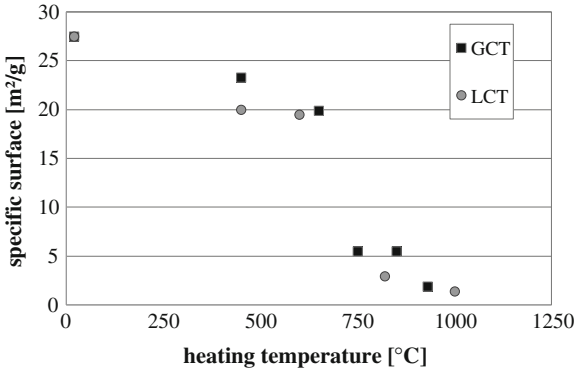

Fig. 4 Specific surface according to heating temperature

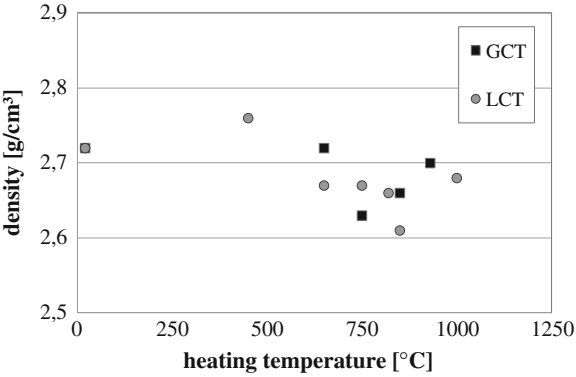

Fig. 5 Density according to heating temperature

muscovite. At 900 °C the specific surface of calcined clay is reduced to approximately 1 m^2/g because of the onset of the sintering process which goes along with increasing density. According to [3], lower densities tend to be associated with higher degrees of dehydroxylation.

3.3 Pozzolanic Activity

The thermally activated clays were characterized by their ion solubility in alkaline medium (Fig. 6). According to earlier results, maximum solubility was determined between 700 and 800 °C calciner temperature. The comparison of the clays produced in the laboratory and those calcined on industrial scale revealed for the latter a broader optimum temperature range for maximum solubility. Both calcined clays exhibited a significant reactivity in combination with cement. Mortar according to DIN EN 196 was made replacing 20 mass% of portland cement by calcined clay. The activity index at 28 days is shown in Fig. 7. The index exceeds 1.0 for an optimum calcination temperature in the range between 700 and 800 °C.

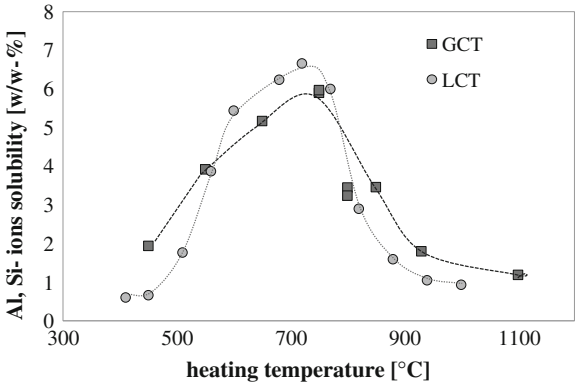

Fig. 6 Ion solubility depending on the heating temperature

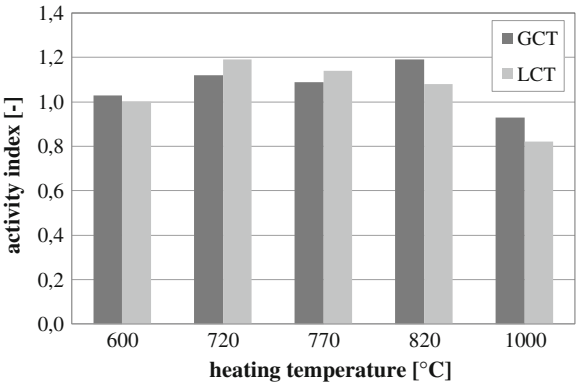

Fig. 7 Activity index at 28 days as a function of the heating temperature

For the optimal calcination temperature pozzolanic activity was ranging between 450–550 mg $Ca(OH)_2$ when determined using the Chapelle test [6]. Unfortunately, The Chapelle test is not sensitive enough to distinguish between the different thermal treatments used.

4 Conclusions

The investigation reveals chances for calcined clay composed of a mixture of different clay minerals as a supplementary cementitious material:

- Thermal activation is possible for clays with kaolin content by 25 mass%.
- Comparison of physical and chemico-mineralogical effects of clay calcined on laboratory scale or industrial scale shows that the latter process leads to a less amorphous and less reactive binder.

- The calcined clays with lowest density are those which are most dehydroxylated resulting in the highest reaction potential.
- The comparison of the clays produced on the laboratory and those calcined on industrial scale revealed a broader optimum temperature range for the latter, but it goes along with a somewhat reduced reactivity in combination with cement.

References

1. Sabir, B.B., Wild, S., Bai, J.: Metakaolin and calcined clays as pozzolans for concrete: a review. Cem. Concr. Compos. **23**, 441–454 (2001)
2. Tironi, A., Trezza, M.A., Scian, A.N., Irassar, E.F.: Kaolinitic calcined clays: Factors affecting its performance as pozzolans. Constr. Build. Mater. **28**, 276–281 (2012)
3. Slade, R.C.T., Jones, D.J.: Flash calcines of kaolinite: effect of process variables on physical characteristics. J. Mater. Sci. **27**, 2490–2500 (1992)
4. Bich, Ch., Ambroise, J.P.: Influence of degree of dehydroxylation on the pozzolanic activity of metakaolin. Appl. Clay Sci. **44**, 194–200 (2009)
5. Gehlken, P.-L.: Quantitative Phasenanalyse sedimentärer Minerale unter Berücksichtigung ihrer kristallchemischen Zusammensetzung. In: Quantitative Tonmineralanalyse. Beiträge zur Jahrestagung, vol. 5, pp. 14–23, Trier, September, 1997 (Berichte d. Dt. Ton- und Tonmineralgruppe e.V.)
6. French norm NF-P 18-513, Chapelle test modified (Annexe A) (2009)

Alternative Binders Based on Lime and Calcined Clay

Harald Justnes and Tone A. Østnor

Abstract Alternative binders are in this study defined as binders without Portland cement. In this particular project it will be based on calcined clay or fly ash as a source of reactive silica and alumina in combination with lime and calcium sulphate (e.g. gypsum) and/or calcium carbonate to stabilize special calcium aluminate phases like ettringite and/or calcium monocarboaluminate hydrate, respectively. Gaining strength is all about maximizing the transformation of liquid water to hydrates with hydraulic properties as fast as possible. Hence, admixtures speeding up the reaction kinetics can be part of the formulations as well. Two synergy principles have been described for making improved binders based on slaked lime and pozzolanic SCMs. One showing how neutral salts may accelerate by forming strong alkaline solutions in situ and another one how calcium carbonate can play a role when alumina containing SCMs are used by leading to an even higher conversion of liquid water into solid hydrates leading to lower porosity and higher strength. Calcined marl may substitute for calcined clay, but then the calcium carbonate content should be reduced in accordance with the remaining calcium carbonate content after calcination.

1 Introduction

Lime mortars were used already by the Romans who also discovered that these mortars became stronger when blended with supplementary cementing materials (SCMs) like volcanic ash, diatomaceous earth or even crushed, ground ceramic. In terms of today's demand of sustainability with minimized CO_2 emissions these binders are even worse than Portland cement (unless totally re-carbonated), and the present alternative binder concept is trying to minimize the required lime content

H. Justnes (✉) · T.A. Østnor
SINTEF Building and Infrastructure, Trondheim, Norway
e-mail: harald.justnes@sintef.no

K. Scrivener and A. Favier (eds.), *Calcined Clays for Sustainable Concrete*,
RILEM Bookseries 10, DOI 10.1007/978-94-017-9939-3_7

relative to SCMs. However, with the requirement of fast construction of the modern world, accelerators are crucial for fast hardening. The alternative is curing at elevated temperatures for prefabricated elements.

1.1 Principles of Accelerator Synergy

To speed up pozzolanic reactions between lime and SCMs, highly alkaline solutions are usually effective and work merely as catalysts as sketched for the reaction loop of lime-silica fume by Justnes [1]:

$$\begin{array}{ccccc} \mathrm{S(s)} & + & \mathrm{(N,K)H\ (aq)} & \rightarrow & \mathrm{(N,K)SH(aq)} \\ \uparrow & & + & & \\ \mathrm{CSH(s)} & + & \mathrm{(N,K)H(aq)} & \leftarrow & \mathrm{CH\ (aq\ or\ s)} \end{array} \quad (1)$$

Leading to the well-known overall pozzolanic reaction;

$$\mathrm{S + CH = CSH} \quad (2)$$

Alkalis are very important, as blending pure lime (CH) and pure silica fume (S) will take months to harden, while using simulated pore water of pH 13.5 gives decent 3 day strength [1] as shown in Fig. 1.

However, for the sake of the work-environment, strong alkalis present a hazard to handle. It is much safer to handle neutral, soluble salts that will form alkali hydroxides *in situe* when reacting with calcium hydroxide. This is the first synergy principle, and the only requirement of the neutral alkali salt is that its anion will form insoluble calcium salts;

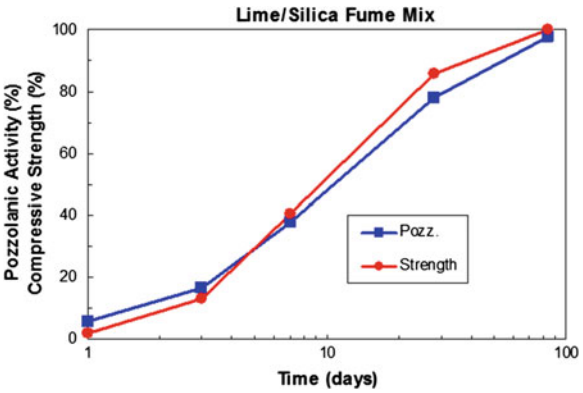

Fig. 1 Comparison of compressive strength (relative to 63.9 MPa at 84 days = 100 %) development of mortar with reactivity of silica fume in the cementitious material lime/SF with C/S = 1.11 and water-to-solid ratio 0.70 [1]

$$xCa(OH)_2 + 2(Na,K)_xA = Ca_xA_2(s) + 2x\ (Na,K)OH \quad (3)$$

Such possible salts are listed in Table 1 together with the solubility product (K_{sp}) of their corresponding calcium compounds and the equilibrium concentration of calcium. The lower the $[Ca^{2+}]$ for salts relative to $Ca(OH)_2$, the more reaction (3) is expected to be shifted to the right, and the more effective the accelerator is expected to be. Figure 2 shows strength development for lime/silica fume mortars with different accelerators capable of giving pH 14.2 in pore water if Eq. 3 was shifted all the way to the right. In terms of 1 and 3 days compressive strength, the order of efficiency is $Na_3PO_4 > NaF > Na_2CO_3 > K_2CO_3 > 2K_2CO_3 + Na_2CO_3 > KF > Na_2SO_4$. It is not known why potassium salts does not perform as well as corresponding sodium salts, but potassium is thought to have higher affinity to be bound by the CSH gel than sodium, which can be the reason. It is important to note that the common sodium sulphate does not perform very well, while sodium carbonate does due to much less soluble calcium carbonate than gypsum.

Table 1 The solubility product (K_{sp}) and equilibrium concentration of calcium for salts of general composition Ca_xA_2 (A = anion)

x	A	K_{sp}	$[Ca^{2+}]$ (mM)
1	OH^-	$5.5 \cdot 10^{-6}$	11.1
1	F^-	$5.3 \cdot 10^{-9}$	1.1
2	CO_3^{2-}	$2.8 \cdot 10^{-9}$	0.053
2	SO_4^{2-}	$9.1 \cdot 10^{-6}$	3.0
3	PO_4^{3-}	$2.0 \cdot 10^{-29}$	0.019

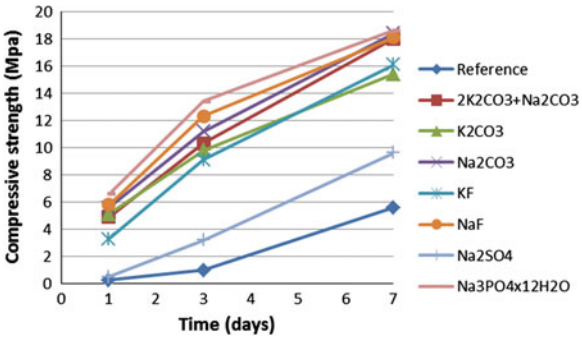

Fig. 2 The compressive strength evolution of silica fume/lime mortars [2] with equimolar dosage of different accelerators (i.e. capable of forming same amount of OH^-)

1.2 Principles of Binder Synergy

Silica fume is the simplest SCM chemically, while aluminosilicates like fly ash and calcined clays are much more complex. In addition to producing amorphous CSH in their reaction with lime, they can also form a wide range of crystalline calcium aluminate hydrates (CAH), including mixed products (CASH) like strätlingite, C_2ASH_8.

The CAH formation opens up for another principle of synergy to convert even more liquid water into solid hydrates, and hence reduce porosity and increase strength. Let us for simplicity assume the CAH to be calcium aluminate hexahydrate (C_3AH_6) that will react with limestone to form calcium carboaluminate hydrate as shown in Eq. 4. According to Eq. 4, 100 g calcium carbonate (1 mol) would then bind 90 g (5 mol) extra water. The total increase in volume of solids according to Eq. 4 is then (2.618−(0.375+1.500))·100 vol%/(0.375+1.500) = 40 vol%. So with a lot of CAH_6 produced, this will matter.

$$\underline{C}\underline{C} + C_3AH_6 + 5H = C_4A\underline{C}H_{11} \tag{4}$$

m = 1.00 g	3.78	0.90	5.68
M = 100.09 g/mol	378.29	18.02	568.50
n = 9.99 mmol	9.99	49.95	9.99
ρ = 2.67 g/ml	2.52	0.998	2.17
V = 0.375 ml	1.500	0.902	2.618

The above synergy principle has been studied for fly ash blended cement with limestone, and it has been shown that the blended cement containing limestone resulted in higher compressive strength than without [3–6].

2 Experimental

Natural clay dominated by kaolin was calcined in a rotary kiln at about 800 °C and used for these initial experiments. The content of slaked lime, $Ca(OH)_2$, and calcium carbonate, $CaCO_3$, in the total powder mix was selected according to the principle of having a Ca/Si = 1 + Ca/Al = 3 for calcium hydroxide and Ca/Al = 1 for calcium carbonate following the binder synergy principle.

A mortar containing 200 g calcined marl, 140 g slaked lime, 40 g limestone, 1050 g DIN sand and 240 g water was made. 11 g Na_2CO_3 was dissolved in the mixing water that according to the accelerator synergy principle would give an initial minimum pH close to 14 if no water was bound.

The compressive and flexural strength of the mortar were measured on three 40×40×160 mm prisms at 1, 3, 28 and 90 days of curing according to NS-EN 196-1.

The capillary suction technique was performed on four parallel 20 mm slices sawn from cast cylinders from each mortar mixture that were dried at 105 °C. The discs are placed on a grating 1 mm below the water surface in a covered box and the increase in weight as specimen suck water is monitored for 4 days and plotted versus square root of time. The method consist of 6 subsequent weighing steps from which one can calculate initial moisture content, total porosity (ε_{tot}), capillary porosity (ε_{cap}), entrained air volume (ε_{air}), average density of mortar solids (ρ_s) and dry density of mortar (ρ_d) as described by Justnes et al. [7].

Binder paste of the same composition was characterized by X-ray diffraction using Cu K_α radiation and thermal analysis (DTA/TG) under flowing N_2-gas.

3 Results and Discussion

The strength evolution of the mortar up to 90 days age is given in Table 2. The data extracted from the capillary suction profile of the mortar are listed in Table 3.

A segment (7-15° 2θ) of the X-ray diffractogram of binder hardened for 28 days are shown in Fig. 3. Next to the peak of an illite contamination is the major peak of calcium monocarboaluminate hydrate confirming the predicted reaction pattern.

Table 2 Strength evolution of mortar

Strength type	Average strength ± standard deviation [MPa] at ages [days]			
	1 day	3 day	28 day	90 day
Compressive	3.1 ± 0.1	14.2 ± 0.7	24.2 ± 0.4	26.5 ± 1.1
Flexural	1.3 ± 0.0	4.0 ± 0.2	6.1 ± 0.2	5.9 ± 0.1

Table 3 Mortar properties extracted from the capillary suction experiments of two individual parallel mixes

Parallel (6 discs each)	Capillary porosity ε_{cap} [vol. %]	Air content ε_{air} [vol.%]	Average density of solids, ρ_s [kg/m^3]	Dry density ρ_d [kg/m^3]
1	25.4 ± 0.2	3.5 ± 3.5	2619 ± 0	1865 ± 2
2	25.2 ± 0.5	3.8 ± 5.0	2613 ± 6	1857 ± 5

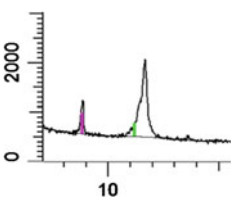

Fig. 3 XRD segment showing illite peak to the left and calcium monocarboaluminate hydrate to the right

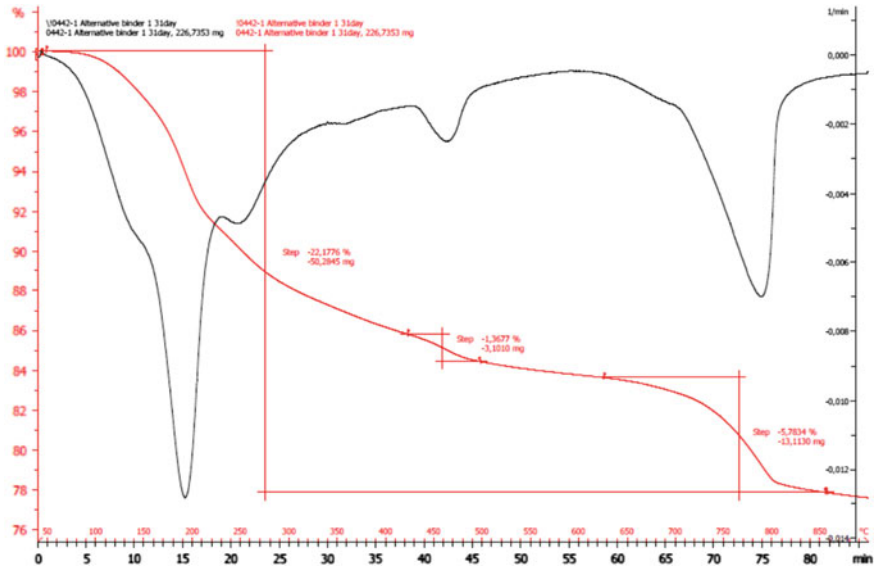

Fig. 4 The TG and DTG curved of the binder just after mixing (*upper graph*) and after 28 days curing (*lower graph*)

The thermogravimetry (TG) curves and the derivative (DTG) of the binder after 28 days curing are showed in Fig. 4.

The total mass losses after 0 and 28 days are 15.1 and 22.2 %, respectively, showing the amount of water bound. The mass loss due to calcium hydroxide seems considerably reduced in the period, indicating that too little was added, and may be the direct reason for the modest strength increase from 28 to 90 days for the mortar (see Table 2). The reason might be that the formed CSH had a higher C/S than 1 as assumed in the formulation.

4 Conclusions

Two synergy principles have been described for making improved binders based on slaked lime and pozzolanic SCMs. One showing how neutral salts may accelerate by forming strong alkaline solutions in situ. Another on how calcium carbonate can play a role when alumina containing SCMs are used by leading to an even higher conversion of liquid water into solid hydrates leading to lower porosity and higher strength.

An example have been showed for a binder consisting of calcined clay, slaked lime and calcium carbonate on how mortars can achieve a 28 days compressive strength of about 25 MPa and 3 day strength exceeding 10 MPa when cured at 20 °C. The strength may have been improved further by having a slightly higher ratio of calcium hydroxide.

Acknowledgment The paper is based on the work performed in COIN—Concrete Innovation Centre (www.coinweb.no) - which is a Centre for research-based Innovation, initiated by the Research Council of Norway (RCN) in 2006.

References

1. Justnes, H.: Kinetics of reaction in cementitious pastes containing silica fume as studied by ^{29}Si MAS NMR. In: Colombet, P., Grimmer, A.-R., Zanni, H., Sozzani, P. (eds.) Nuclear Magnetic Resonance Spectroscopy of Cement-Based Materials, pp. 245–268. Springer, Berlin (1998)
2. Justnes, H.: Accelerated hardening of mortars with hydraulic binders of silica fume/lime. Nord. Concr. Res. Publ. **17**(2), 30–41 (1995)
3. De Weerdt, K., Justnes, H.: Microstructure of Binder from the Pozzolanic Reaction between Lime and Siliceous Fly Ash, and the Effect of Limestone Addition. In: Proceedings of 1st International Conference on Microstructure Related Durability of Cementitious Composites, pp. 107–116, Nanjing, China, RILEM Proceeding PRO 61, 13–15 October 2008
4. De Weerdt, K., Kjellsen, K.O., Sellevold, E.J., Justnes, H.: Synergy between fly ash and limestone powder in ternary cements. Cem. Concr. Compos. **33**(1), 30–38 (2011)
5. De Weerdt, K., Ben Ha-Ha, M., Le Saout, G., Kjellsen, K.O., Justnes, H., Lothenbach, B.: Hydration mechanism of ternary Portland cements containing limestone powder and fly ash. Cem. Concr. Res. **41**(3), 279–291 (2011)
6. De Weerdt, K., Sellevold, E., Kjellsen, K.O., Justnes, H.: Fly ash–limestone ternary cements–effect of component fineness. Adv. Cem. Res. **23**(4), 203–214 (2011)
7. Justnes, H., Thys, A., Vanparijs, F and Van Gemert, D.: Porosity and diffusivity of concrete with long-term compressive strength increase due to addition of the set accelerator calcium nitrate. Proceedings of the 9th International Conference on Durability of Building Materials and Components, Brisbane, Australia, 17–20 March 2002

Optimization of Cements with Calcined Clays as Supplementary Cementitious Materials

Roland Pierkes, Simone E. Schulze and Joerg Rickert

Abstract Cements consisting of different types of Portland cement clinker and calcined clays were produced by mixing in laboratory scale. The clinkers differed regarding their contents of Al_2O_3 and alkalis as well as their phase composition. The used kaolinitic, illitic and chloritic clays show low ceramic qualities and represent typical clays of cement plant quarries. The produced cements contained 20 and 40 mass % of the calcined clays, respectively. On selective cements the influence of the sulphate dosage was investigated by measuring the compressive strength development according to EN 196-1 and characterising the hydration products by means of X-Ray Diffraction analyses (XRD) and thermal analysis (DSC). These investigations were planned using DOE (design of experiments). It could be shown that there is some potential for increasing the performance of the pozzolanic cement by a chemical-mineralogical adjustment of the calcined clay, the clinker and the sulphate agent.

1 Introduction

For use of calcined clays as a main constituent in cement in accordance with EN 197-1 a content of reactive SiO_2 of at least 25,0 mass % is required. Although suitable raw material resources exist in Europe, calcined clays have rarely been used in cements up to now. The influence of the chemical and mineralogical composition of clays on their suitability as a main constituent in cement has been successfully investigated in the recent past. In a forerun research program VDZ investigated a couple of different kaolinitic, illitic and chloritic clays, partially of low ceramic quality [1]. For each type of clay it was possible to reach the required 25 mass % reactive SiO_2 applying appropriate calcination conditions. At laboratory scale pozzolanic cements were mixed using these calcined clays as main constituent in portions of 20 or 40 mass % respectively. The cements performed well in crucial

R. Pierkes · S.E. Schulze (✉) · J. Rickert
VDZ gGmbH, Research Institute of the Cement Industry, Duesseldorf, Germany
e-mail: simone.schulze@vdz-online.de

K. Scrivener and A. Favier (eds.), *Calcined Clays for Sustainable Concrete*,
RILEM Bookseries 10, DOI 10.1007/978-94-017-9939-3_8

cement properties like workability and strength development. In a further research project the potential of cement optimisation by adjusting the clinker and calcined clay components with respect to their chemical composition was investigated. Furthermore it was tested if an additional amount of anhydrite could enhance the pozzolanic reaction of the calcined clays.

2 Materials

In continuation of the forerunning research program three clays already tested in [1] were calcined at different temperatures. The mineralogical characterisation of the clays is given in Table 1. After the calcination the clays were tested acc. their pozzolanic properties (Table 2).

At laboratory scale pozzolanic cements with 20 and 40 mass % of calcined clay (CEM II/A-Q and CEM IV/B (Q)) were produced by mixing the clays with four different Portland cements (Z1 – Z4). The CEM I's mainly varied in the C_3A and the alkali content, which are given in Table 3. Z4 was a sulphate resistant (-SR) cement acc. EN 197-1. The differences in C_3A influence the ratio of fast reactive alumina from the clinker to lower reactive alumina and silica from the calcined clay minerals and may also have effects on the kinetics of the reactions. Different alkali

Table 1 Mineralogical characterisation of clays (XRD)

Mineral group	**T7 – illitic**	**T10 – kaolinitic**	**T11 – chloritic**
Quartz	+++	+++	+++
Kaolinite	++	+++	++
Illite/Muscovite	+++	+++	+++
Chlorite	–	–	++
Feldspar	+	+	(+)
Calcite	(+)	(+)	+

+++ / ++ = main constituent + = minor constituent (+) = trace

Table 2 Chemical characterisation of calcined clays (e.g. T11-800 = T11, calcined at 800 °C)

Calcined clay	**Reactive SiO_2 acc. EN 197-1**	**Si acc. Surana**	**Al acc. Surana**
	mass %	**ppm**	**ppm**
T7-1000	20.9	50,014	13,453
T7-1200	28.4	24,868	2532
T10-800	24.7	65,320	51,284
T10-1000	34.3	65,999	13,055
T11-800	29.1	12,445	8654
T11-950	27.6	28,958	12,926
T11-1200	23.7	16,895	4209

Table 3 Specific parameters of CEM I used for pozzolanic cements

Parameter	Unit	Z1	Z2	Z3	Z4
		CEM I 42,5 R			CEM I 42,5 R-SR
C_3S	mass %	55	56	61	58
C_3A		13.4	11.4	9.5	2.4
Na_2O eq. acc. EN 196-2		0.77	0.71	1.13	0.61
compressive strength	MPa	35.6	30.0	29.8	28.0
- 2 days		55.3	46.3	53.2	48.9
- 7 days acc. EN 196-1		65.6	58.0	58.8	62.1
- 28 days					

contents of the CEM I's might influence the solubility and thus the pozzolanic reactivity of the calcined clays.

For tests on the variation of the sulphates a natural anhydrite, containing a low content of gypsum (< 10 mass %) and few trace minerals like quartz or calcite, was added to the pozzolanic cements. It was added in a finely ground state (about 8500 cm^2/g acc. Blaine) as well as less ground with a portion of 30 mass % grains coarser than 15 µm.

3 Methods

The chemical composition of the clays and cements was determined by means of XRF (Bruker S8). XRD measurements were carried out by means of PANalytical X'Pert Pro using Cu Kα radiation, and evaluated with the TOPAS® Rietveld Software.

According to [1] the clay samples were calcined under oxidising burning conditions, heated up to 800 to 1200 °C with a heating rate of about 300 K/h, followed by a passive cooling to less than 100 °C (8 to 12 hours). The calcined samples were examined by means of XRD, their amount of reactive compounds was determined acc. to EN 197-1 and Surana [2].

CEM II/A-Q with 20 mass % and CEM IV/B (Q) with 40 mass % of the respective clay components were produced by intensively mixing the respective ground calcined clay with the respective CEM I. Some cements were supplemented by ground anhydrite (2 or 4 mass % related to the calcined clay content). To reduce the sample matrix for these tests DOE (design of experiments, with the statistical tool MINITAB®) was used.

The compressive strength of cements was determined on 40 × 40 × 160 mm^3 mortar prisms with water/cement ratios of 0.50 according to EN 196-1. The cements with variation of the sulphate carrier were tested using 15 × 15 × 60 mm^3 prisms, so that the results should not be compared directly. Analyses on some hydrated cement samples were carried out by means of XRD and of DSC821 (Mettler 821) with a heating rate of 30 K/min from 30 °C to 600 °C.

4 Results

Figure 1 shows the compressive strength development acc. EN 196-1 of cements with Z1 or Z4 as CEM I component and 20 mass % of various calcined clays.

At early ages the strength development of the CEM I component dominated the compressive strength results of the pozzolanice cements. Between 7 and 28 days the strength contribution of the calcined clays increased. In Z4/T10-800/20 the exceptional high availability of alumina from the kaolinitic clay T10 may compensate the low alumina content of the SR-cement (Z4) and led to the highest compressive strength of all cements tested at 28 days. On the other hand, T11 calcined at 800 °C had only a poor pozzolanicity and led to the lowest strength values in combination with all types of CEM I.

Figure 2 depicts the compressive strength data of cements, consisting of Z1, Z2, Z3 or Z4 as CEM I component and 20 or 40 mass % of T10/800 respectively. As expected the strength values for the cements containing 40 mass % of calcined clay are lower than those from cements with 20 mass %. This effect is quite low for the combination with Z2 so that there might be a positive interaction of these compounds.

Considering all tests results it was possible to derive regression models pointing out the cement and calcined clay parameters which influence the compressive strength significantly. Table 4 shows the significant parameters for different testing times of compressive strength.

Beside the C_3A and C_3S contents which are significant in principle, also the soluble alumina and silica according to Surana play important roles for early age strength. At later ages typical parameters influencing the pozzolanic reaction, like the Na_2O equivalent of the cement or especially each kind of soluble silica of the calcined clays are of higher importance.

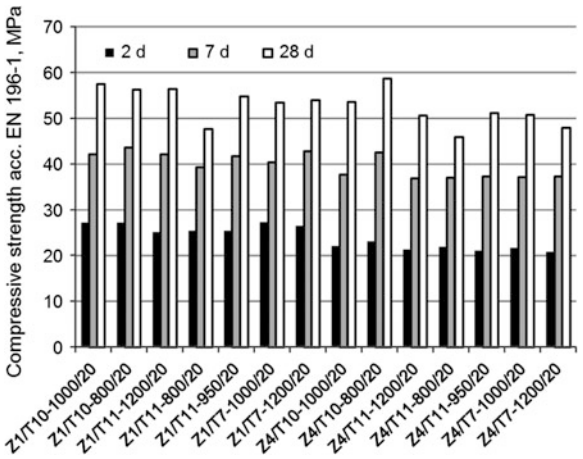

Fig. 1 Compressive strength of cements (acc. EN 196-1), consisting of component Z1 or Z4 and 20 mass % of variously calcined clays

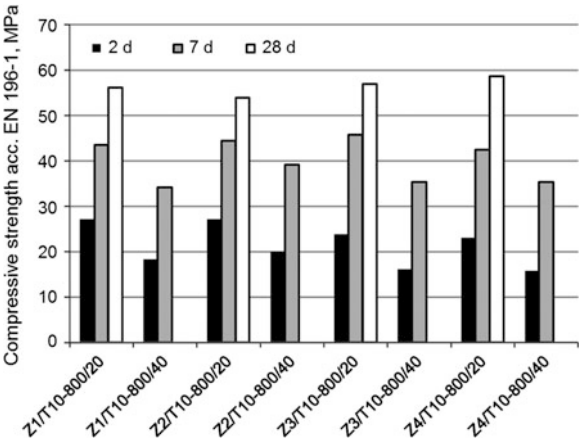

Fig. 2 Compressive strength of cements (acc. EN 196-1), consisting of different CEM I and 20 or 40 mass % of T10/800

Table 4 Factors influencing the compressive strength acc. EN 196-1 of cements with 20 mass % calcined clay

		Testing time		
		2 d	7 d	28 d
Factors caused by CEM I	Na_2O eq.		x	x
	C_3A	x	x	x
	C_3S	x	x	x
Factors caused by calcined clay	Si acc. Surana	x	x^2	x^2
	Al acc. Surana	x	x	x^2
	Reactive SiO_2		x^2	x^2
Regression coefficient		0.92	0.90	0.92

The number of samples tested with varying sulphatisation was determined by using DOE. The parameters, which influence the compressive strength at early ages, as described in Table 4 led to the choice of Z1 and Z4 with differing C_3A contents as CEM I components. To cover strongly differing values of soluble alumina T10 was chosen in its two calcination temperature steps. The other variables were a higher and a lower amount of anhydrite addition (2 and 4 mass %, related to the clay content), and the fineness of the added anhydrite (G = coarse, F = fine). The results of the experiments show that the 2 days compressive strength of these cements was influenced positively by C_3A, and also by an increasing anhydrite content and increasing anhydrite fineness. The effect of the content of alumina acc. Surana on the compressive strength is depending on the cement component. So a negative influence on the strength of the high-C_3A cement at each testing time was determined. Nevertheless the SR-cement (low C_3A) got a benefit from high alumina contents at the age of 7 days. Afterwards the effect of the anhydrite content on the compressive strength of the analysed cements was lowered and that of anhydrite fineness was neglectable for the CEM I-SR, but both factors keep their positive influences on the high-C_3A cement.

The hydration process of the anhydrite containing samples was observed by XRD and DTA analyses. Figure 3 presents the amounts of hydration products in various pozzolanic cements after 3 hours of hydration. Very low portlandite contents in Z4-cements indicated a slow reaction. In Z1-cements with anhydrite the gypsum contents were slightly higher than in the cement without addition. This might be an indication for a secondary gypsum precipitation, so that these cements were slightly super-sulphatisated. The ettringite content of the hydrated Z1-cements was increased by adding anhydrite, in opposite to the Z4-cements.

Figure 4 shows XRD pattern of the pozzolanic cements Z1/T10-800/20 and Z4/T10-800/20, added with various amounts of anhydrite of variable fineness, and hydrated for two days. The phase assemblage of hydration products is mainly depending on the clinker mineralogy. Z1-cements (high C_3A) show a distinctive peak of hemicarbonate beside ettringite and port-landite. Z4-cements (low C_3A, SR) only show ettringite as aluminous hydration product. With the selected amounts of additional anhydrite there seemed to be no effect on the hydration mineralogy.

5 Conclusions

It can be stated that all tested pozzolanic cements fulfilled the requirements of strength class 32,5 R acc. EN 197-1. With some CEM II/A-Q even strength classes up to 52,5 N can be attained.

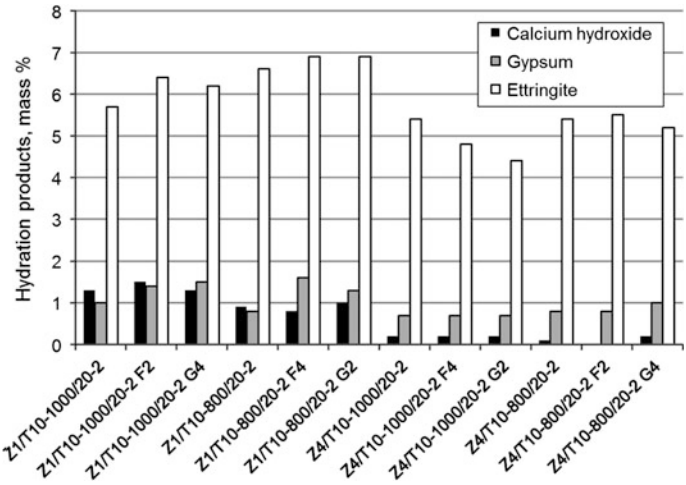

Fig. 3 Hydration products of various cements, hydrated for 3 h (DSC), (F2 = 2 mass % of fine anhydrite; G4 = 4 mass % of coarse anhydrite)

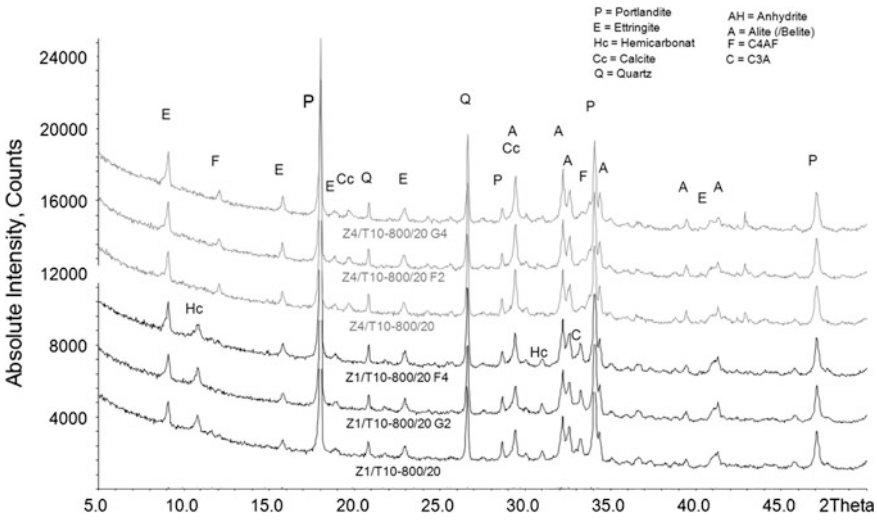

Fig. 4 XRD pattern of cements (Z1 and Z4 with 20 mass % of T10-800, added with 2 or 4 mass % of coarse or fine grained anhydrite), hydrated for 2 days

As expected, the compressive strength of the pozzolanic cements decreases with increasing amounts of calcined clays in the cements. The mineralogy and the calcination conditions of the clays strongly influence the availability of silica and alumina for pozzolanic reactions.

The hydration reactions of the pozzolanic cements and their strength development were partially related to a complex interaction of clinker and calcined clay properties. Especially in the very beginning of the hydration process the reactive alumina of the calcined clays compensated low soluble alumina contents in the clinker compound and enhanced the formation of hydration products like ettringite. These reactions could further be influenced by addition of an optimised sulphate agent. Later on the typical pozzolanic reactions became more important, related to parameters like the alkali content of the clinker and the reactive silica content of the calcined clay.

It could be shown that there is some potential for increasing the compressive strength of pozzolanic cements by a chemical-mineralogical adjustment of the calcined clay, the clinker and the sulphate agent.

Acknowledgments The Industrial Collective Research (IGF) project no. 17930 N of Verein Deutscher Zementwerke e.V., Research Institute of the German Cement Industry, is founded by the German Federation of Industrial Research Associations (AiF) within the framework of IGF of the Federal Ministry of Economics and Technology (BMWi) based on an enactment of the German Bundestag.

References

1. Schulze, S.E., Rickert, J.: Pozzolanic activity of calcined clays. In: 12th international conference of recent advances in concrete technology and sustainability issues (Prag 2012), American Concrete Institute 2012 (ACI Publication SP-289), Farmington Hills, pp. 277–287
2. Surana, M., Joshi, S.: Spectrophotometric method for estimating the reactivity of pozzolanic materials. Adv. Cem. Res. **1**, 238–241 (1988)

Feasibility of Calcined Marl as an Alternative Pozzolanic Material

Tobias Danner, Harald Justnes, Geir Norden and Tone Østnor

Abstract Calcareous clay rich in smectite was calcined at temperatures of 600–1000 °C using a pilot- and industrial scale rotary kiln. Compressive strength of mortars was tested between 1–365 days, when 20–65 % of OPC was replaced by calcined clay at equal w/c-ratios. With respect to reactivity as a pozzolan, the optimum calcination temperature was around 800 °C. With a replacement level of 50 % the 1-day strength was reduced but high enough for demoulding concrete infield practice, while after 28 days almost the same strength as with no replacement could be obtained. The raw and reactive calcined state of the clay was characterised using different methods like XRD, TG/DTG, SEM, FTIR, Al^{27}-NMR and Mössbauer Spectroscopy. At the optimum calcination temperature calcium carbonate from the clay is only partly decomposed. The main calcium carbonate source is coccoliths which enabled the formation of a reactive Ca enriched glass phase together with the decomposing clay minerals. Oxidation of Fe^{2+} to Fe^{3+} resulted in a structural disordering increasing the reactivity of the calcined clay. Pozzolanic activity was tested in pastes of calcined clay and calcium hydroxide.

1 Introduction

The manufacturing of cement is amongst the largest CO_2 emitters within the mineral processing industry, contributing about 5 % to the global CO_2 emissions annually [1, 2]. Due to the decomposition of limestone, the main raw material for cement production, and the fuel used for burning the clinker the global average

T. Danner (✉) · H. Justnes
NTNU—Norwegian University of Science and Technology, Trondheim, Norway
e-mail: tobdann@web.de

H. Justnes · T. Østnor
SINTEF Building and Infrastructure, Trondheim, Norway

G. Norden
Saint-Gobain Weber, Lillestrøm, Norway

K. Scrivener and A. Favier (eds.), *Calcined Clays for Sustainable Concrete*,
RILEM Bookseries 10, DOI 10.1007/978-94-017-9939-3_9

gross CO_2 emissions per ton of clinker was 866 kg CO_2 in 2006 [3]. The World Business Council for Sustainable Development provides ideas and approaches to reduce this level of CO_2 emissions up to 50 % by 2050. The four main points are improvement of energy efficiency, replacing high-carbon fuels with low-carbon fuels, CO_2 capture technologies and the use of blended cements [2, 4]. The last alternative is the most effective way to reduce the emissions and recent research is mainly concentrating on finding potential supplementary cementitious materials to reduce the clinker content in new cement formulations. The most popular cement replacing materials are Fly Ash and Slag which are already taken up in standard cements in many countries e.g. the Norwegian standard fly ash cement with up to 20 % siliceous fly ash and Embra's "Miljøsement" with about 30 % ground blast furnace slag [5]. To continue the reduction of the clinker content in the long run the right choice of materials is mainly a question of availability. Most Fly Ash and slag produced is already in use and will become scarce in many areas. Calcined clays may be the only alternative to serve the huge cement industry for a sustainable future. Raw clays are abundant and wide spread in most parts of the world. However, clay mineralogy and chemistry is very complex and not all clays are equally reactive in combination with cement. This study investigates the potential of calcareous smectite rich clay from marine origin to replace cement in cementitious based binders.

2 Materials and Methods

2.1 Constituent Materials

The constituent materials for calcium hydroxide consumption and hydration experiments on blended cements were laboratory grade Calcium hydroxide (Merck, Germany), a standard OPC CEM I 42.5 R (Norcem, Brevik, Norway) and calcined marl. The raw marl (or rather calcareous clay) is a tertiary sediment that was deposited in a marine environment. It consists of about 70 % clay minerals and about 20–25 % calcium carbonate deriving mainly from coccoliths. Calcination of the marl for pozzolanicity tests was done at IBU-Tec in Germany, in a small rotary kiln (7 m length) to simulate industrial conditions. For strength and durability tests with higher replacement levels marl was calcined on industrial scale in a rotary kiln usually used for Leca production. Grinding of the calcined materials to $d_{50} < 10$ µm was performed at UVR-FIA GmbH, Freiberg, Germany (Table 1).

Table 1 Chemical composition of OPC and calcined marl

	SiO_2	Al_2O_3	Fe_2O_3	CaO	K_2O	Na_2O	MgO	TiO_2	SO_3
OPC	19.9	4.8	3.3	61.9	1.0	0.5	2.7		3.3
Marl	49.6	18.1	10.6	14.1	2.4	0.7	2.9	1.0	

2.2 Experimental Methods

The mixing procedure and testing of the mortars was performed according to the Norwegian Standard NS-EN 196-1.

Marl-Lime (CH) pastes were mixed in a 1:1 ratio (by weight) with a water-to-powder ratio of 0.8 using an alkaline mixing water (pH 13.2, and KOH/NaOH = 2:1). All pastes were mixed by hand for 90 s. Pastes were cured for 28 days and 6 months at 20 and 38 °C and hydration was stopped with alcohol subsequently.

TG/DTG was performed with a Mettler Toledo apparatus (TGA/SDTA 851) under N_2-atmosphere in the temperature range from 40 °C to 1100 °C with a heating rate of 10 °C/min.

A Bruker AXS D8 Focus (θ-2θ configuration with Bragg-Brentano geometry), equipped with a LynxEye detector and a CuKα source (λ = 1.54 Å) was used for XRD measurements.

FT-IR spectra in the middle-IR (MIR) region were taken in transmittance mode using the KBr pellets technique. Measurements were performed on a Bruker IFS 66v FTIR spectrometer equipped with an IR source, KBr beam splitter, and DTGS KBr detector.

For backscattered electron images (BSE) a JEOL JXA-8500F Electron Probe Micro analyzer (EPMA) was used. Images were taken with an accelerating voltage of 15 kV.

The Al-MAS-NMR spectra have been recorded at 14.1 T, using a 4 mm CP/MAS NMR probe, a spinning speed of vR = 13.0 kHz, a 0.5 μs excitation pulse, a 2 s relaxation delay, 1 H decoupling during acquisition, and in between 6560 and 50,300 scans.

Mössbauer measurements were carried out at room temperature on a spectrometer with a constant acceleration type of vibrator and a 57CoRh source. The samples were ground and mixed with BN and spread out to form absorbers.

3 Results

3.1 Compressive Strength of Mortars

Mortars were prepared with 0, 20, 35, 50 and 65 % volume replacement of OPC by calcined marl. Compressive strength was tested after curing for 1, 3, 7, 28, 90 and 365 days at 20 °C. The strength evolution for all mortars is plotted as a function of time on a logarithmic scale in Fig. 1.

At early ages (1 & 3 days) the compressive strength of the mortars is reduced the higher the replacement level of OPC. Nevertheless the strength of the mortar with 50 % replacement by calcined marl is with about 10 MPa high enough for removing formwork of concrete in practice. Compressive strength of mortars with 20 and

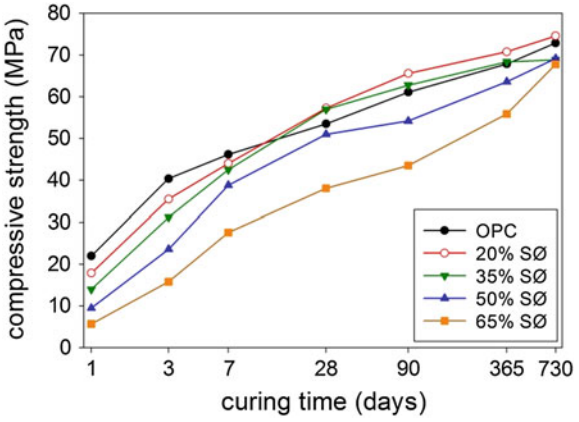

Fig. 1 Compressive strength development up to 1 year of mortars containing between 20–65 % marl calcined at 800 °C as cement replacement

35 % replacement is very close to the strength of the reference mortar with no replacement at already 7 days and higher than the reference at 28 days. Compressive strength with 50 % replacement is almost equal to the reference at 28 days. After 90 and 365 days of curing the mortars with 20 % replacement have a higher compressive strength than the reference mortar while 35 % replacement are about equal to the reference with 100 % OPC. Even with 50 % replacement of cement the compressive strength is very close to that of the reference after 365 days of curing. With 65 % replacement of cement by calcined marl the strength of mortars is constantly below that of the reference. However it is peculiar that the strength gain from 90 to 365 days, as well as from 1 to 2 years, is greater for mortar with the higher cement replacements. Different hypotheses to explain this are given by Justnes and Østnor [6].

The calcium hydroxide consumption in marl/lime pastes hydrated for 28 days and 6 month was 0.52 and 0.60 g lime/g marl respectively.

3.2 Phase Changes and Structural Modifications upon Calcination

From XRD data (Fig. 2 left) it can be seen that upon calcination the minor amounts of kaolinite in the marl are dehydroxylated and converted to metakaolin already at 650 °C. However the smectite (and illite) appear to retain some of their crystallinity up to a calcination temperature of 800 °C. Although, it was found with FT-IR spectroscopy (Fig. 2 right) that all clay minerals are completely dehydroxylated. This shows in the disappearing peaks between 3700 and 3400 cm^{-1} and 911 cm^{-1}. The higher background in the XRD diffractogram at 800 °C reflects an increased amount of amorphous phase content in the calcined marl. This is confirmed in the widening of the FT-IR peak at 1031 cm^{-1} usually describing the presence of amorphous silica [7]. Besides the dehydroxylation of the clay minerals, calcite is

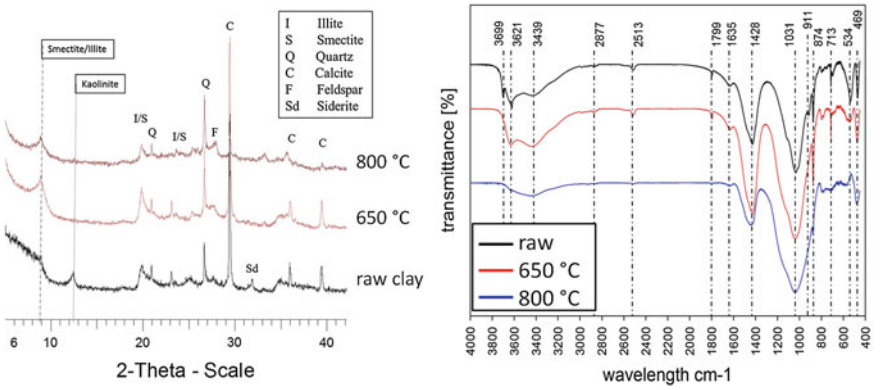

Fig. 2 XRD (*left*) and FT-IR (*right*) of the dried raw marl and marl calcined at 650–800 °C

not completely decomposed at 800 °C as visible in the presence of XRD peaks and the FT-IR peak at 1428 cm^{-1}. With TG a remaining calcite content of about 5 % was measured in the marl calcined at 800 °C. FT-IR absorbance at 534 and 469 cm^{-1} is typical for all clay minerals and assigned to Al-O-Si and Si-O-Si deformation bands respectively. The broadening and decreasing intensity of the Si-O-Si deformation band confirms a decrease in crystalline structure and distortions in the tetrahedral sheet. The slight shift of the peak to a higher wavenumber could also imply a change in bond length. The completely disappearing Al-O-Si deformation band might reflect a disconnection or modified bonding between octahedral and tetrahedral sheet in the metaclay (calcined marl) structure. It can also be a sign of decreased amount of octahedral cations [7]. This was confirmed by supplementary ^{27}Al-MAS-NMR spectra that showed that almost all octahedrally coordinated Al was converted to tetrahedrally coordinated Al upon calcination.

Mössbauer spectroscopy was performed on the raw and calcined marl to study the effect of iron upon calcination. It was suspected that a possible oxidation of iron could induce stresses in the calcined clay mineral structure thus leading to a higher reactivity. The averaged mössbauer results are given in Table 2.

The recorded isomer shifts and quadrupole splittings in the raw clay are characteristic for clay minerals [8]. The isomer shifts indicate that both Fe^{2+} and Fe^{3+} are in octahedral coordination [9]. Both iron species are substituted for Al^{3+} or Mg^{2+} in the octahedral layer of the clay minerals. All changes upon calcination recorded

Table 2 Isomer shifts (δ in mm/s) quadrupole splitting (Δ in mm/s) values percent of ferric and ferrous iron measured in the raw and calcined marl

Sample	Fe^{3+}			Fe^{2+}		
	δ	Δ	%	δ	Δ	%
Raw clay	0.39	0.52	77	1.12	2.20	23
800 °C	0.33	1.21	93	0.95	1.90	7

for iron are therefore representative for any change in the octahedral layer of the clay structure. The increased quadrupole splitting of Fe^{3+} with calcination indicates a change in coordination towards 5 and 6. While the decreased isomer shifts and quadrupole splitting of Fe^{2+} in the calcined marl indicates a change in coordination towards 4 [8]. The measured changes from the raw to calcined state can be interpreted as the result of strong distortions in the octahedral layer of the clay minerals. Also it can be seen from Table 2 that almost all the iron is present in oxidized form in the calcined marl. Regarding a simple oxidation reaction of Fe^{2+} it must be noted that this oxidation not only affects the iron atom but would also lead to the inclusion of an extra oxygen atom somewhere in the structure for every second iron oxidized. This will lead to further distortions and stress the structure.

From BSE images taken of the raw and calcined marl we can see clear changes in the microstructure of the clay matrix (Fig. 3).

In Fig. 3a coccoliths are visible with the typical radial symmetry embedded in the fine grey clay mineral matrix. These calcite bio-minerals or calcareous microfossils are the main $CaCO_3$ source of the raw marl. In marl calcined at 650 °C (Fig. 3b) no significant changes occur. But it seems that the dense matrix is starting to widen up separating different phases slightly from each other. When calcined at 800 °C the coccoliths are completely decomposed while the surrounding clay matrix appears to be more vitreous. The whole matrix seems to fuse together leading to a sponge like morphology. In addition all over the clay bigger glassy phases formed (Fig. 3d). This is typical for the firing of calcite bearing clays. The chemical composition of this phase was similar to that of the original clay material. Natural calcite minerals were found in some places stable in the clay matrix indicating that it is the decomposing coccoliths and clay minerals forming this new reactive glass enriched in Ca.

For the pozzolanic reactivity of the calcined marl the remaining inorganic calcium carbonate seems to play an important role. Carboaluminate hydrate phases were the main crystalline hydration products detected in calcined marl/lime pastes. Substitution of Fe deriving from the clay for Al in the AFm phases was observed with XRD. Besides that the formation of CSH phases and minor amounts of katoite were found with TG/DTG. ^{27}Al-MAS-NMR results showed the presence of 5-fold aluminum in the CSH phase.

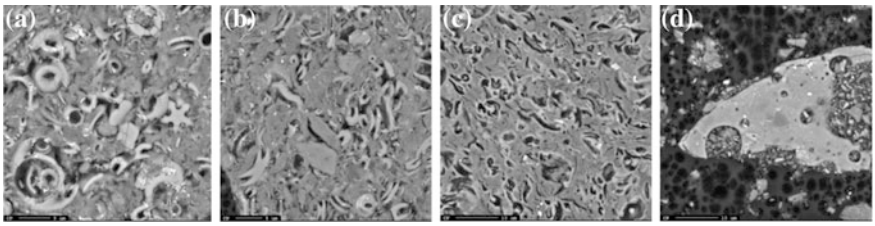

Fig. 3 BSE images of raw marl (**a**), marl calcined at 650 °C (**b**), and marl calcined at 800 °C (**c**–**d**)

4 Conclusions

Compressive Strength of mortars showed that the used calcined marl has high potential to be used as a pozzolan in cementitious based binders. After 28 days the compressive strength of mortars with 50 % OPC replacement was alsmost equal to the reference mortar with 100 % OPC. Calcination of the marl induced significant structural changes in the tetrahedral and octahedral layer of the clay minerals as detected with FT-IR and NMR-spectroscopy. The oxidation of iron in the octahedral layer of the clay mineral structure introduced further stresses increasing the reactivity. Besides the dehydroxylation of the clay minerals some amount of calcite was left stable in the calcined marl (XRD, TG, FT-IR, SEM). However the main calcite source of the marl, the coccoliths were completely decomposed forming a Ca-enriched reactive glass phase together with the decomposing clay minerals. Carboaluminate hydrate phases with a certain degree of Fe substitution for Al were the main crystalline hydration products detected in calcined marl/lime pastes.

References

1. Mehta, P.K.: Concrete technology for sustainable development. Concr. Int. **21**(11), 47–53 (1999)
2. Worrel, E., et al.: Carbon dioxide emissions from the global cement industry. Ann. Rev. Energy Environ. **26**, 303–329 (2001)
3. World Business Council for Sustainable Development (WBCSD): The cement sustainability initiative. Cement Industry Energy and CO_2 Performance Getting the Numbers Right (2011)
4. World Business Council for Sustainable Development (WBCSD): Carbon emissions reduction up to 2050. Cement Technology Roadmap (2009)
5. Justnes, H.: Making cements with less clinker content. SINTEF, Trondheim (2007)
6. Justnes, H., Østnor, T.,: Durability and Microstructure of Mortar with Calcined Mark as Supplementary Cementitious Cementing Material. XIII DBMC, Sao Paulo (2014)
7. Madejova, J., Komadel, P.: Baseline studies of clay minerals society clays: infrared methods. Clays Clay Miner. **49**(5), 410–432 (2001)
8. Murad, E., Cashion, J.: Mössbauer Spectroscopy of Environmental Materials. Kluwer Academic Press, New York (2004)
9. Takeda, M., Kawakami, O., Tominaga, T.: ^{57}Fe mössbauer spectroscopic studies of structural changes of montmorillonite on heating in reduced atmosphere. J. Phys. Colloque C2 supplément au nr. **3**(3), C2-472 (1979)

From Ancient to Modern Sustainable Concrete

A. Tagnit-Hamou, M.T. Tognonvi, T. Davidenko and D.Z. Belkacemi

Abstract The purpose of this paper is to show what ancient structures are made of and what can be done with today's materials to produce more sustainable modern concrete. Some samples of mortars collected from the Tipasa archaeological site and the Forbidden City site were submitted to XRD and SEM analysis. The samples from Tipasa were predominately calcined clay and/or lime. The samples from the Forbidden site consisted of wood, clay, and dolomite. The main binder in both cases was a type of C-A-S-H gel occasionally containing Mg, K, and/or Cl. Most of today's structures are based on portland cement. Achieving sustainable-development goals generally includes replacing part of the cement in concrete with industrial waste or calcined clay, especially metakaolin. More recently, wastepaper sludge ash (WSA) from the pulp and paper industry (possibly containing a certain quantity of metakaolin as well as some C_3A and C_2S) has been used in concrete. A microstructural study of hardened cement paste containing 40 % WSA revealed the formation of hydrated products such as a type of C-A-S-H gel, ettringite, and calcium carboaluminate.

1 Introduction

The use of clays in construction materials probably dates back to around 2000 BC. Burning lime with clays produces hydraulic lime, which, when mixed with water, becomes a waterproof binder that allowed the Romans, Greeks, Indians, and Egyptians to build with concrete. Some of these ancient structures that have withstood the ravages of weathering (Bronze Age archaeological site in Greece, Pantheon in Rome, etc.) can still be seen today, attesting to the durability of these materials.

A. Tagnit-Hamou (✉) · M.T. Tognonvi · T. Davidenko
Department of Civil Engineering, University of Sherbrooke, Sherbrooke, Canada
e-mail: a.tagnit@usherbrooke.ca

D.Z. Belkacemi
Tipasa Sites and Museums and University of Tipasa, Archeology Section, Tipasa, Algeria

K. Scrivener and A. Favier (eds.), *Calcined Clays for Sustainable Concrete*,
RILEM Bookseries 10, DOI 10.1007/978-94-017-9939-3_10

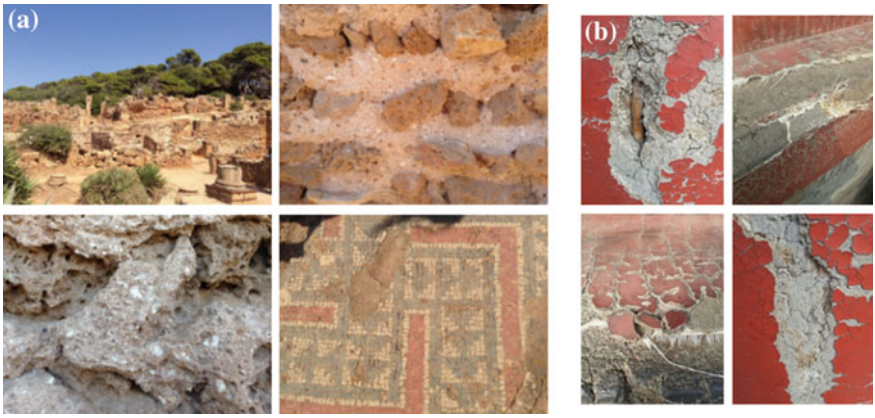

Fig. 1 Archaeological sites of **a** Tipasa and **b** the Forbidden City

The Tipasa archaeological site, located 70 km from Algiers on the shores of the Mediterranean (Fig. 1a), constitutes one of the most extraordinary archaeological complexes in the Maghreb. Archaeological excavation conducted in this region certified it as a human settlement dating back 40,000 years [1]. It was built with recognized ancestral know-how, consisting of various ancient building techniques (such as opus africanum, caementicum opus, opus quadratum, and opus mixtum) with various local materials (carved stones from local sandstone, rubble, binders, ceramics, clay bricks, pebbles, lime, etc.) [2]. The discovery of lime kilns [3] suggests that binders mainly composed of lime were calcined. In addition, a study of some of the mortars collected revealed the presence of lime with different rates of calcination and grinding [4]. It was also observed that materials such as crushed brick and ceramics collected from certain old buildings and walls were reused for new construction [4], pointing to a sort of recycling.

Moreover, in Asia, the Forbidden City is one of the archeological site worldwide recognized (Fig. 1b). It was more recent than Tipasa site. Located in the heart of Beijing and built between 1406 and 1420 by the Ming emperor Zhu Di, it was the former imperial palace, the home to 24 Chinese emperors over 491 years from 1420 to 1911 [5]. The Forbidden City is now known as the Palace Museum. Its construction materials include whole logs of precious Phoebe zhennan wood and large blocks of marble from quarries near Beijing. The floors of major halls were paved with "golden bricks," specially baked paving bricks [6].

Most of today's structures are based on portland cement. The availability of large amounts of industrial waste can be used to replace some of the cement content in concrete, depending on waste physicochemical properties. In general, silicate- and aluminosilicate-based wastes are used. In this study, special attention was paid to a wastepaper sludge ash-based binder. The pulp and paper industry generates a significant amount of waste in the form of a deinking sludge that contains a certain quantity of kaolinite clay. To minimize the negative environmental impact and costs related to disposed of the waste by landfilling, some plants use a fluidized-bed

boiler (BFB) to produce a part of the energy needed to operate the paper plant by using its own sludge as a raw fuel. After combustion under high pressure at around 850 °C, followed by quenching at about 200 °C [7], the resulting ash may contain metakaolin, which has proven to be a very good pozzolanic material. In addition, this wastepaper sludge ash contains a large amount of free lime (~10 wt%) and some cementitious phases, such as C_3A and C_2S, making them both pozzolanic and hydraulic materials. Consequently, they can be used to replace up to 40 % of cement content in concrete [7].

This paper aims at gaining understanding about some properties of mortars from ancient concrete and at exploring what can be done with new materials in today's context.

2 Characterization of Samples

Five samples collected from the Tipasa site and three from the Forbidden City site (Fig. 2) were submitted to XRD and SEM analysis.

Hardened pastes containing 40 % of three types of WSA (WSA1, WSA2 and WSA3) as cement replacement were characterized after 1 and 91 days of reaction. Pastes with a water-to-binder ratio (w/b) of 0.5 were prepared according to ASTM C 305; 100 % ordinary portland-cement paste was used as reference. WSA looks like sulfo-calcic Class C fly ash (with 45 % < CaO < 51 %, 20 % < SiO_2 < 25 %, 10 % < Al_2O_3 < 14 %, ~2 % Fe_2O_3, 4 < LOI < 13) and seems to be more hydraulic than pozzolanic [7, 8] due to the presence of some hydraulic components, such as anhydrite, free lime, calcium aluminate (C_3A), mayenite ($C_{12}A_7$), and calcium silicate (C_2S) (larnite). An amorphous metakaolin may, however, be present because of kaolin in the raw sludge. Depending on the rate of decomposition of the calcium carbonate, the free lime content can be greater or less than 10 % [7].

XRD analysis was performed on powder obtained after grinding the hardened samples. The microstructure of the polished surface of ancient samples was characterized using a scanning electron microscopy coupled with energy dispersive X-ray microanalysis (SEM/EDS). For the WSA-based hardened paste, SEM analysis was performed on a fresh fracture to reveal the morphology of the hydrated products at the very early stage, i.e., after 1 day of reaction.

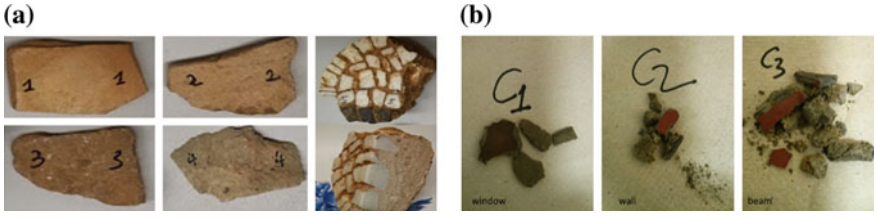

Fig. 2 Samples collected from the **a** Tipasa site and **b** Forbidden City site

3 Results

3.1 Tipasa Samples

Figure 3 displays results from XRD analysis of samples 1, 2, 3, 4, and 5. Samples 1, 2, and 3 show the same crystalline phases, unlike samples 4 and 5, which are totally different. Therefore, the first three samples could be made up of the same raw materials or collected in the same place. Crystalline phases such as quartz, calcite, and anorthite are present in all of the samples. Diopside, which is a magnesium source, is present in samples 1, 2, 3, and 4.

Sample 3 also contains other phases, such as serendibite, microcline, and sodium calcium iron. Sample 5 is mainly composed of calcite and quartz, suggesting that this material was built with an aerial lime-based mortar blended with quartz sand. The presence of NaCl in some part of the samples is probably due to the site's proximity to the sea. Since XRD is not suitable for determining amorphous phases, it isn't very useful in detecting the presence of gel-type hydrated products.

According to XRD analysis, samples 1, 2, and 3 could be the same, so only the microstructures of samples 3, 4, and 5 are shown (Fig. 4). The main elements forming the matrix of these samples are quartz, calcite and C-A-S-H type gel. It is important to note that the matrix also contains a clay-like material. Therefore, it seems that these materials are composed mainly of clay, lime, and sand.

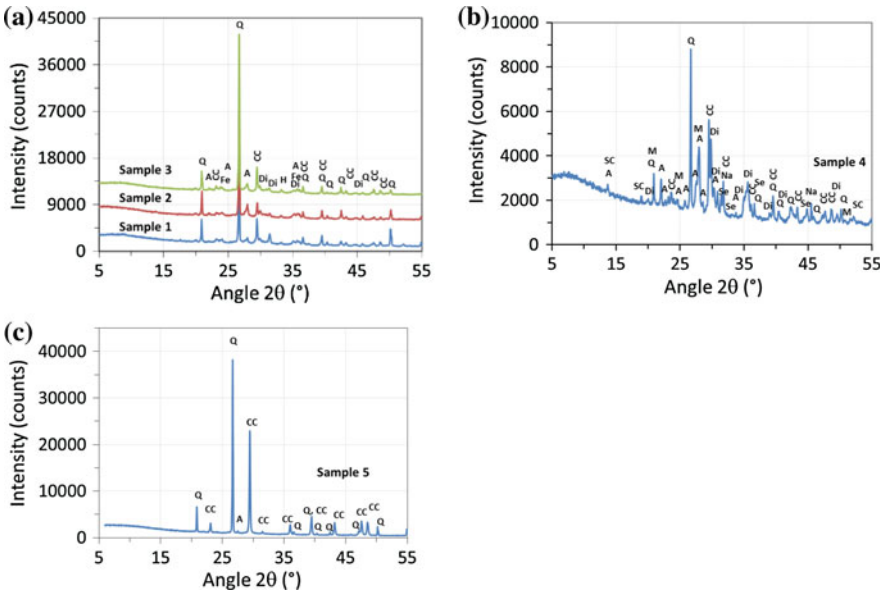

Fig. 3 XRD analysis of Tipasa samples: **a** samples 1, 2, and 3 and **b** sample 4. Q = quartz (SiO_2), CC = calcite ($CaCO_3$), Fe = hematite (Fe_2O_3), Di = diopside ($CaMgSiO_6$), A = snorthite ($Ca(Al_2Si_2O_8)$), SC = sodium calcium iron silicate ($Na_{0.20}Ca_{0.8}Fe_2SiO_8$), M = microcline ($K(AlSi_3O_8)$), Se = seremdibite ($CaMg_3O(Si_3O_9)$), Na = NaCl

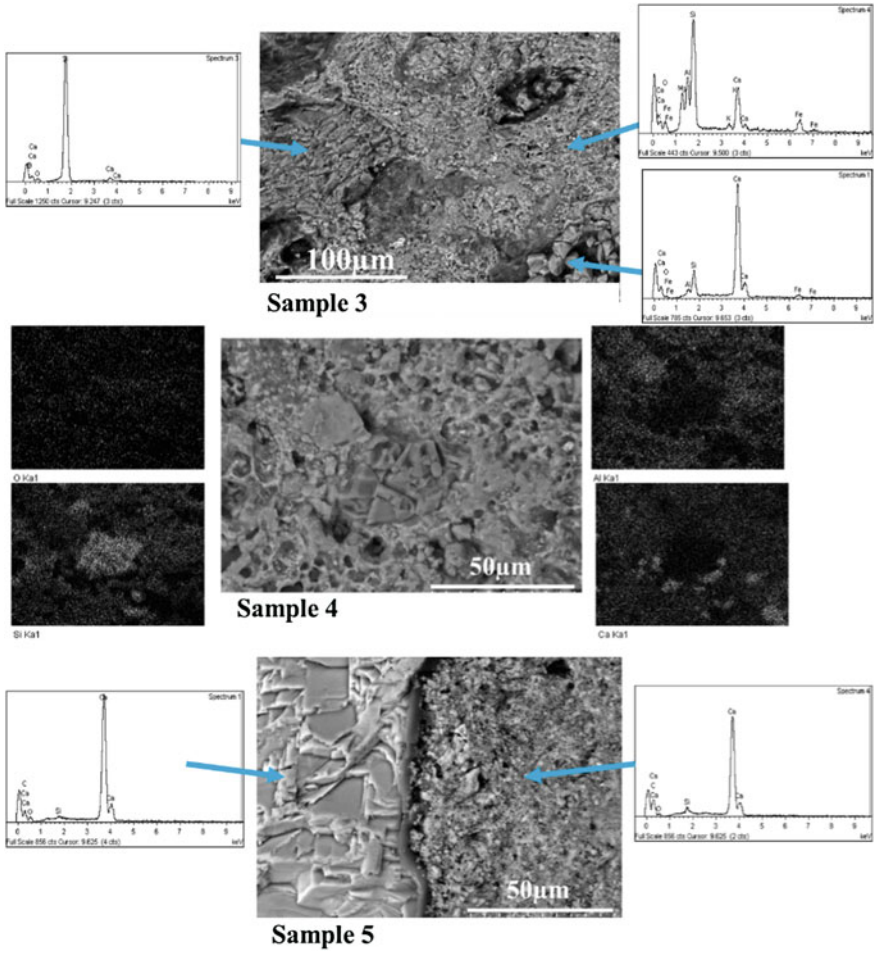

Fig. 4 SEM/EDS analysis of samples 3, 4, and 5 from the Tipasa site

3.2 Forbidden City Site

XRD analysis of the three samples (C1, C2, and C3) collected in the Forbidden City reveals the presence of quartz, dolomite, illite, anorthite, feldspar, and muscovite. The three samples appear to be the same (Fig. 5). These mortars do not contain any calcite, suggesting that lime was not used as a raw material. According to these results, it can be assumed that the constituent materials were mainly composed of clay and dolomite, probably marble as mentioned by Yang et al., who supposed that the materials used included wood and large blocks of marble [6].

Figure 6 provides the microstructure of samples C1 and C3. Both samples show almost the same elements, specifically, quartz and aluminosilicate-based materials

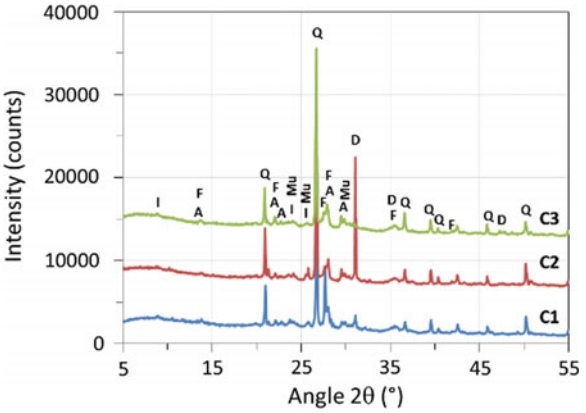

Fig. 5 XRD analysis of the Forbidden City samples: Q = quartz (SiO_2), D = dolomite ($CaMgCO_3)_2$, A = anorthite ($CaAl_2Si_2O_8$), F = feldspar ($K_{0.5}Na_{0.5}AlSi_3O_8$), I = illite $(K,H_3O)Al_2Si_3O_{10}(OH)_2$, Mu = muscovite $(K(Al,Fe)_2AlSi_3O_{10}(OH)_2$

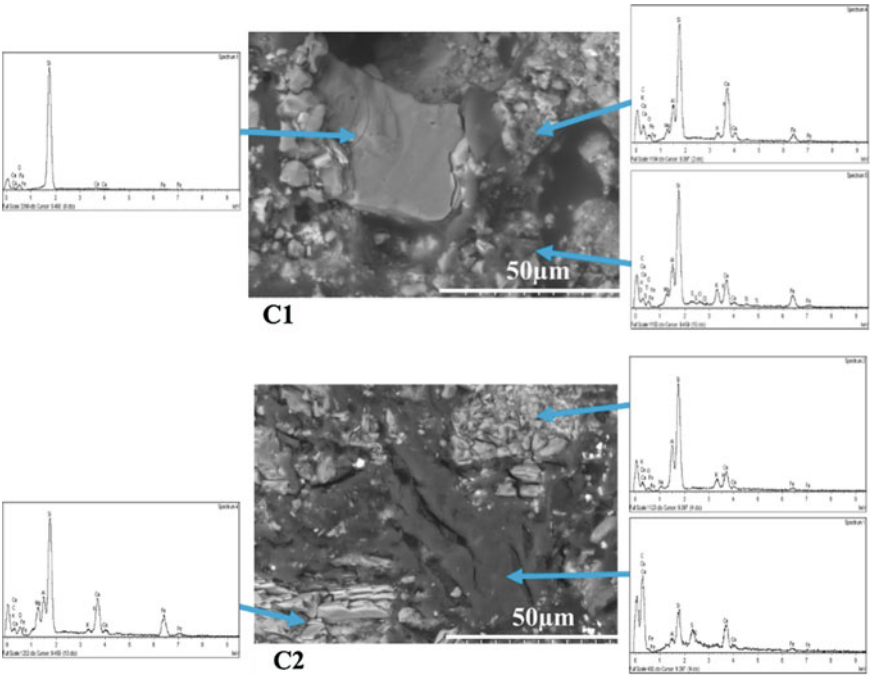

Fig. 6 SEM/EDS analysis of samples C1 and C2 from the Forbidden City

containing Mg and Ca due to the dolomite content. The presence of carbon and sulfur is probably from the wood used.

The gel responsible for the hardening of the ancient structures studied is C-A-S-H binder. It was demonstrated that the specific way the aluminum substitutes for silicon in C-A-S-H may be the key to the cohesion and durability of such concretes [9].

3.3 WSA-Based Pastes

Figure 7 shows the hydrated products of hardened cement pastes containing 0 % and 40 % WSA after 1 and 91 days of reaction. The hydrated products are the common products formed during cement hydration, in particular, ettringite, portlandite and C-S-H, even if C-S-H cannot be accurately identified by XRD due to its semi-crystalline nature. In the case of pastes containing 40 % WSA, calcium hemicarboaluminate (Hc) and calcium monocarboaluminate (Mc) as formed. Calcium carboaluminate hydrates are formed by the reaction of CO_2 with C_3A remaining after the depletion of sulfate ions [10]. Therefore, the formation of hemi- and monocarboaluminate depends on the sulfate, carbonate, and aluminate content in the system [11].

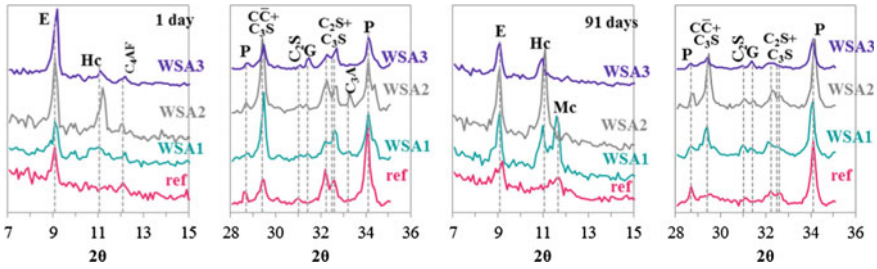

Fig. 7 XRD patterns of cement pastes containing 0 % and 40 % WSA as replacement after 1 and 91 days of hydration: C$\overline{C}$ = calcite; E = ettringite; G = gehlenite; Mc = monocarboaluminate; Hc = hemicarboaluminate; P = portlandite

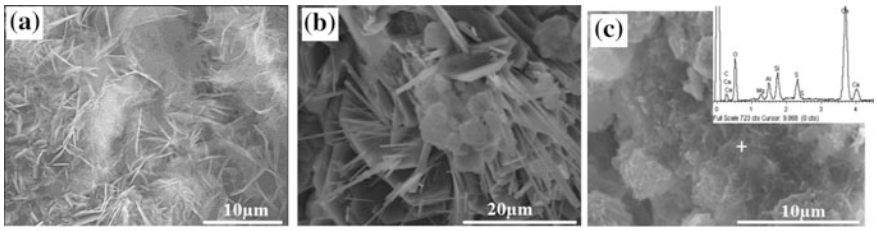

Fig. 8 SEM/EDS analysis of hydrated product of hardened paste containing 40 % WSA2 after 1 day of hydration: **a** calcium carboaluminate, **b** ettringite, and **c** calcium silicate hydrate (C-A-S-H)

The very early hydration stage (after 1 day of hydration) of the paste containing 40 % WSA2 was analyzed by SEM/EDS in order to identify the nature of the hydrated products. Figure 8 presents the morphology of the three main hydrated products—calcium carboaluminate, ettringite, and calcium (aluminate) silicate hydrate (C-A-S-H)—confirming the XRD results.

4 Conclusions

This investigation shows that the binder responsible for the resistance of ancient structures and the WSA-based paste studied is a type of C-A-S-H gel with more or less aluminum content. This gel is different from the C-S-H resulting from OPC hydration. It is probably the incorporation of aluminum in silicon replacement that makes C-A-S-H an exceptionally stable binder. The specific way the aluminum substitutes for silicon in the C-A-S-H may be the key to the cohesion and durability of such concretes.

References

1. Mourad, B., Farid, C., Chafia, Y.: Le Mousterien et l'Aterien d'Afrique du nord, d'autres formes de relations, le site de Sidi Saïd (Tipasa, Algerie). CNRPH. Colloque international sur la préhistoire maghrebine, Alger (2007)
2. Cintas, P.: Fouilles puniques à Tipasa, Alger. Imprimerie la Typolitho et J. Carbonel réunies (1949)
3. Lassus, J.: L'archeologie Algérienne. Lybica (Archéologie-Épigraphie) **VI**(2), 269–274 (1957)
4. Baradez, J.: La Maison des fresques et les voies la limitant. Lybica (Archéologie-Épigraphie) **IX**(1), 49–52 (1961)
5. How many rooms in the Forbidden City, Singtao Net. 2006-09-27, Retrieved 2015-02-12
6. Yang, X., Li, S., Chen, H.: The Invisible Palace. Foreign Language Press, Beijing. ISBN 7-119-03432-4, p. 15 (2003)
7. Davidenko, T., Xie, A., Mikanovic, N., Tagnit-Hamou, A.: Effect of wastepaper sludge ash on cement blends properties. In: Proceeding of the 12th International Conference on Recent Advances in Concrete Technology and Sustainability issues, pp. 709–727. Prague October 30–November 2 2012
8. Aitcin, P.C.: Comparative study of the cementitious properties of different fly ashes. In: Proceedings of the Second International Conference on Fly Ash, Silica Fume, Slag and Natural Pozzolans in Concrete, pp. 91–114. Madrid, (1986)
9. Jackson, M.D., Moon, J., Gotti, E., Taylor, R., Emwas, A., Meral, C., Guttmann, P., Levitz, P., Wenk, H.-R., Monteiro, P.J.M.: Material and elastic properties of Al-tobermorite in ancient Roman seawater concrete. J. Am. Ceram. Soc. **96**(8), 2598–2606 (2013)
10. Kuzel, H.-J.: Initial hydration reactions and mechanisms of delayed ettringite formation in Portland cements. Cem. Concr. Compos. **18**, 195–203 (1996)
11. Matschei, T., Lothenbach, B., Glasser, F.P.: The role of calcium carbonate in cement hydration. Cem. Concr. Res. **37**, 551–558 (2007)

Pozzolanicity of Calcined Clay

Anjan K Chatterjee

Abstract Out of the three major clay mineral groups, viz, kaolin, smectite and palygorskite – attapulgite, the cement science primarily focuses on the first group to be used on calcination as a pozzolanic admixture. The general understanding is that the dehydroxylation of dehydrated kaolinite in the temperature range of 550 – 650 °C apparently yields an x-ray amorphous alumino-silicate phase which provides the pozzolanic property to clay. There is not much of information on how the highly crystalline kaolinite loses its long-range order in the lattice on account of dehydroxylation. Little data are available on the effect of cation exchange capacity on pozzolanicity. Further, in EN-197-1 the usability of a calcined clay as a pozzolana has been linked with the presence of minimum 25 per cent reactive silica in it. The test methods for determining the pozzolanic property of calcined clays are still in the realm of arbitrariness. The present paper is a brief crystallo-chemical disquisition of the above issues, based on the characterization of six different Indian clay samples.

1 Introduction

Although there are three distinctly different groups of clay materials, viz., kaolin, smectite and palygorskite of industrial significance, the construction industry in general and the cement industry in particular mostly make use of kaolin in raw and processed forms. Specifically for use as a supplementary cementitious material in blended cement or concrete, thermal treatment of kaolinitic clays to a temperature beyond dehydroxylation is taken recourse to in order to activate their pozzolanic properties. The reactivities of dehydroxylated kaolinite with lime as determined through a standard test procedure is taken as its pozzolanic capacity. Through actual

A.K. Chatterjee (✉)
Conmat Technologies Private Limited, Kolkata, India
e-mail: anjan.k.chatterjee@gmail.com

K. Scrivener and A. Favier (eds.), *Calcined Clays for Sustainable Concrete*,
RILEM Bookseries 10, DOI 10.1007/978-94-017-9939-3_11

practice it has been established beyond doubt that the dehydroxylated kaolin (also called metakaolin) is x-ray amorphous in nature and releases alumina and silica in the course of cement hydration to form calcium alumino-silicate hydrate phases that enhance the strength and durability of concrete.

Similar reactions and effects are not observed with smectite and palygorskite groups of clay minerals upon dehydroxylation. It is also known that these groups of clay minerals often occur as associate minerals in kaolinitic clay, causing alteration in its pozzolanic behaviour and capacity. Although the published literature on clay minerals is profuse, it is not very clear how crystalline kaolinitic phase loses its crystallinity on account of dehydroxylation and make the anhydrous alumino-silicate phase soluble and reactive. The dissimilar behaviour of the other two major clay mineral groups under similar circumstances also awaits an explanation.

Another issue that has cropped up in the context of EN-197-1 is the validity of specifying the content of minimum 25 per cent reactive silica in a calcined clay to qualify as a pozzolana.

This paper is intended to address the above issues in a concise manner based on characterization features of some diverse clay minerals.

2 Distinctive Features of the Major Clay Mineral Groups

It is well known that the clay minerals are part of a larger family of phyllosilicates and are characterized by interlinked tetrahedral and octahedral sheets. The structural configuration of clay minerals has been dealt with in fair detail by Grim [1, 2], Brindley and Brown [3], Velde [4] and others [5], a summary of which is presented in Table 1.

As a result of constitutional diversity, the technical assessment of clays is rather complex. In broad terms the property controlling factors are the following:

- clay mineral species present
- occurrence of non-clay minerals
- presence of organic substances
- exchangeable ions
- particle characteristics (shape, size, orientation, etc.)
- structural assembly of 1 : 1 or 2 : 1 linkage of tetrahedral and octahedral sheets as well as neutralization of excess layer charge by various interlayer materials.

Calcination of clays and their thermochemical reactivity have been dealt with in [6–9].

Table 1 Structure and properties of the major clay mineral groups

Structural grouping	Major mineral phase	Broad composition	Structural features	Cation exchange capacity meq/100 g
2-layer kaolin group	Kaolinite	$(OH)_8Si_4Al_4O_{10}SiO_2$46.54 %	1:1 layer type (001) = 7.21 A	3–15
		Al_2O_3 39.50 %	B = 8.99 A	
		H_2O 13.96 %	Flaky habit	
3-layer smectite group	Montmorillonite (Expanding lattice)	$(OH_2)_4Si_8$ $Al_4O_{20}.nH_2O$	2:1 layer.	80–150
		Composition without interlayer material :	Equidimensional extremely thin flakes	
		SiO_2 66.7 %		
		Al_2O_3 28.3 %		
		H_2O 5.0 %		
		Some substitution of Si by Al in tetrahydral layer and of Al in octahedral layer by Mg, Fe, Zn, Ni, Li, etc. Lattice always unbalanced		
	Illite (Non-expanding lattice)	Muscovite – like dioctahedral $(OH)_4K_2$ (Si_6Al_2) Al_4O_{20} Biotite type is trioctahedral with incorporation of Mg and Fe. Illites differ from mica in having less replacement of Al for Si, less K and less randomness of silicate layers	Structural characterization same as micas, 2 : 1 layer type. Small poorly defined flake commonly grouped in irregular aggregates	10–40
Chain-structure palygorskite group	Palygorskite – Attapulgite - Sepiolite	Composition of the balanced ideal cell of Attapulgite $(OH_2)_4(OH)_2$ $Mg_5Si_8O.4H_2O$ Sepiolite and palygorskite show variations in the composition of Al, Mg and Si	2:1 inverted ribbons. Generally seem as bundles of lath-shape units	20–50

3 Characterization of Some Clay Samples and Their Pozzolanic Capacity

In the backdrop of what has been discussed above six Indian clay samples were randomly chosen and characterized. The oxide composition of these clays is given in Table 2. The corresponding phase analyses of the same samples are also shown in the same table.

The XRD patterns showed that on calcining of samples 1, 2 and 3 in a muffle furnace at 900 °C for 30 min the kaolinite phase could be totally dehydroxylated and made x-ray amorphous, while for sample No. 4 having goethite as an associate phase and sample No. 5, which was a mixture of kaolinite and illite, the total breakdown of the clay minerals could not be achieved. So far as the montmorillonitic clay is concerned, this phase was almost broken down on calcination at 900 °C but the hematite phase appeared to have recrystallized.

The above six samples were also subjected to thermal analysis and the weight loss values for all the six samples against temperature are summarised in Table 3.

In further characterization of the clay samples the Reactive Silica contents and their Cation Exchange Capacities were determined. In parallel the Lime reactivities of the calcined clays were also tested [10]. These results are presented in Table 4.

Data presented in Table 4 do not show any trend of conformity of the kaolonite contents, CEC values, presence of reactive silica and lime reactivity results. Thus, adoption of any one indirect index to evaluate the pozzolanic capability of a clay on calcination still remains quite arbitrary. Cara et al., based on their evaluation work of calcined kaolinitic clay of an Italian mine, came to the conclusion that the only

Table 2 Chemical and mineral composition of the clay samples

Oxides	[1]	[2]	[3]	[4]	[5]	[6]
LOI	13.72	13.48	11.06	7.76	9.96	9.63
SiO_2	46.02	45.95	60.41	53.60	56.98	52.55
Al_2O_3	35.90	36.05	26.24	16.68	27.10	24.01
Fe_2O_3	1.18	1.95	0.62	12.01	2.07	8.05
CaO	0.33	0.44	0.96	0.78	0.21	0.30
MgO	0.16	0.16	0.10	4.68	0.06	0.40
Na_2O	0.07	0.08	0.03	1.20	0.03	2.25
K_2O	0.02	0.10	0.15	0.69	1.26	0.10
TiO_2	1.86	1.68	0.22	2.02	2.21	2.20
Total	99.28	99.89	99.79	99.42	99.88	99.51
Phase analysis						
Minerals present	Kaolinite Anatase	Kaolinite Quartz Anatase	Kaolinite Quartz Muscovite	Kaolinite Quartz Anatase Goethite Hematite Anorthoclase	Quartz Kaolinite Illite Anatase	Montmori-llonite Hematite Quartz Cristobalite Anatase

Table 3 Weight losses of the clay samples as obtained from TGA curves

Sample No.	Temperature range, 0 °C	Wt. loss %	Remarks
1	Up to 350	1.20	Moisture loss
	350 – 650	13.34	Dehydroxylation of kaolinite
2	Up to 350	1.40	Moisture loss
	350 – 650	12.14	Dehydroxylation of kaolinite
3	Up to 250	0.42	Moisture loss
	250 – 750	10.05	Dehydroxylation of kaolinite
4	Up to 200	8.65	Moisture loss
	200 – 350	1.03	Breakdown of goethite
	350 – 750	4.36	Dehydroxylation of kaolinite
5	Up to 400	1.30	Moisture loss from illite
	400 – 550	5.70	Incomplete dehydroxylation of kaolinite
	500 – 1000	4.00	Prolonged breakdown of clay minerals
6	Up to 100	12.00	Moisture loss
	100 – 700	7.00	Dehydroxylation of kaolinite

Table 4 Indirect indices of pozzolanic capacity of the clay sample

Sample No.	Major clay minerals	Cation Exchange Capacity meq/100 g	Reactive Silica %	Lime Reactivity, N/mn^2
1	90 % kaolinite	3.5	36.2	9.2 at 900 °C
2	80 % kaolinite	3.1	31.5	8.6 at 900 °C
3	70 % kaolinite	12.8	27.4	7.6 at 900 °C
4	40 % kaolinite	19.4	18.7	3.9 at 900 °C
5	50 % kaolinite + 14 % illite	13.2	27.6	12.4 at 600 °C
6	6 % kaolinite + 80 % montmorillonite	86.5	49.8	5.1 at 700 °C

investigation that could shed light upon the pozzolanic properties are those based on the determination of the effective calcium hydroxide consumption [11]. Their data, however, indicated that the total consumption of lime by the calcined kaolinitic clays in pastes took 180 days for most of the samples and the residual values of lime at all prior ages were quite random and erratic. A fairly similar study carried out by Fabbri et al. [12] also indicated that the pozzolanic activity of metakaolin should be evaluated after at least seven days of reaction with calcium hydroxide and the authors suggested that an average value from the 7, 14 and 28 days of curing might be used to indirectly evaluate the pozzolanic potential of a given clay sample.

The thermal analysis of kaolinite has been extensively studied by Chakraborty [13]. The broad findings were that a poorly crystallized kaolinite showed a comparatively lower temperature endothermic and exothermic peaks than the

Table 5 Reactive silica contents of samples 5 and 6

Constituents	Sample no. 5			Sample no. 6		
	200 °C	700 °C	900 °C	200 °C	600 °C	900 °C
LOI (%)	9.53	1.68	0.3	9.63	2.35	0.24
Total SiO_2 (%)	57.7	61.93	63.39	52.55	55.68	57.22
Reactive SiO_2 (%)	27.58	38.59	34.19	49.81	44.80	34.19
Reactive SiO_2 as percentage of total SiO_2 on LFB	48	62	54	94	80	60

well-crystallized variety but its ultimate effect on the pozzolanic potential has not been dealt with. It appears that the pozzolanic potential of a dehydroxylated kaolinite depends on the completeness of the dehydroxylation process, the specific surface area generated, the absence of recrystallization and agglomeration and the presence of associated clay and non-clay minerals. The significant presence of illite and predominance of montmorillonite in the clay composition alter the dehydroxylation behaviour of calcined clays and their resultant pozzolanic potential.

The factors influencing the acid/alkali solubility of the x-ray amorphous alumino-silicate phase are still not very evident. The content of reactive silica, which is a fairly reliable index of the pozzolanic potential of glassy fly ash, does not seem to be an effective indicator of pozzolanic capacity of metakaolinitic materials. In the sample Nos. 5 and 6 the reactive silica contents at different temperatures of calcination were found to be quite high (Table 5). It is interesting to note from Table 5 that the reactive silica percentages in Sample Nos. 5 and 6 were apparently high in uncalcined state but on calcination Sample No. 5 showed a maximum at 700 °C, while sample No. 6 showed progressive reduction with temperature. Further, the trend of reactive silica contents for both the samples did not conform with the Lime Reactivity values.

Finally, the CEC values (see Table 4) seem to behave more like a tool to identify the clay minerals present in an argillaceous substance, based on their structural configurations. The layers in kaolinite are held together by fairly weak bonds, whereas there is strong bonding in illite and montmorillonite because of the presence of positively charged metal ions – potassium in the case of illite and sodium in the case of montmorillonite. These crystallochemical differences are reflected in the CEC values.

4 Conclusions

Calcined clay is an important pozzolanic substance in making blended cement and concrete. Since all clays do not display comparable pozzolanic potential, a more in-depth study of the crystal chemistry of the clay minerals is necessary for precise prognosis of their pozzolanic behaviour. In the present study involving three clay samples of varying kaolinite content with some non-clay minerals, one clay sample

with associated goethite and hematite, another clay having a mix of kaolinite and illite and the sixth clay sample which is predominantly montmorillonite in composition, the following observations could be made :

i. The first three kaolinite clays with kaolinite contents ranging from 70 to 90 per cent showed an increasing trend of lime reactivity and reactive silica contents but CEC values do not conform to this trend.
ii. The other three clay samples containing goethite, illite and montmorillonite show significantly different values of lime reactivity, reactive silica and CEC.
iii. The CEC results seem to provide good indication of clay mineral types and can perhaps be developed into an indirect measure of pozzolanicity, the work on which is progressing in the author's laboratory.
iv. The reactive silica content did not appear to be a reliable indicator as anomalous values were obtained, particularly for impure kaolin and smectite groups of clays.

References

1. Grim, R.E.: Applied Clay Mineralogy, p. 422. McGraw Hill Book Co., New York (1962)
2. Grim, R.E.: Clay Minerals, 2nd edn, p. 596. McGraw Hill Book Co., New York (1968)
3. Brindley, G.W., Brown, G.: Crystal Structures of Clay Minerals and Their X-ray Identification, p. 495. Mineralogical Society, London (1980)
4. Velde, B.: Introduction to Clay Minereals Chemistry, Origins, Uses and Environmental Significance, p. 198. Chapman & Hall, London (1992)
5. Murray, H.H.: Applied Clay Mineralogy, p. 180. Elsevier, Oxford & Amsterdam (2007)
6. Jones, Tom R.: Metakaolin as a pozzolanic addition to concrete. In: Bensted, J., Barnes, P. (eds.) Structure and Performance of Cements, pp. 372–398. Spon Press, London & New York (2002)
7. Fernandez, Rodrigo, Martinera, Fernando, Serivener, Karen: The origin of pozzolanic activity of calcined clay minerals : a comparison between kaolinite, illite and montmorillonite. Cem. Concr. Res. **41**(1), 113–122 (2011)
8. Salvador, S.: Pozzolanic properties of flash calcined kaolinite : a comparative study with soak-calcined products. Cem. Concr. Res. **25**(1), 102–112 (1995)
9. Teklay, Abraham, Yin, Chungen, Rosendahl, Lasse, Bojer, Martin: Calcination of kaolinite clay particles for cement production : a modeling study. Cem. Concr. Res. **61–62**, 11–29 (2014)
10. Katyal, N.K., Sharma, J.M., Dhawan, A.K., Ali, M.M., Mohan, K.: Development of a rapid method for the estimation of reactive silica in fly ash. Cem. Concr. Res. **38**, 104–106 (2008)
11. Cara, Stefano, Carcargui, Gianfranco, Massida, Luigi, Meloni, Paola, Sanna, Ulrico, Tomanini, Massimo: Assessment of pozzolanic potential in lime-water systems of raw and calcined clay from the Donnogazza Mine (Sardinia – Italy). Appl. Clay Sci. **33**, 66–72 (2006)
12. Fabbri, B., Guattieri, S., Leonardi, C.: Modifications induced by the thermal treatment of kaolin and determination of reactivity of metakaolin. Appl. Clay Sci. **73**, 2–10 (2013)
13. Chakraborty, A.K.: Phase Transformation of Kaolinite Clay, p. 342. Springer, New Delhi (2014)

Research on Properties of MK–CFBCA Mineral Admixtures

Guiming Wang, Ming Bao, Tao Sun, Shuxuan Xing and Kun Li

Abstract The main characteristic of CFBCA-MK mineral admixtures (MCMAs) is discussed in this paper. Compressive strength, fluidity and volume deformation test are measured for fresh and hardened concrete properties. With 15 % usage of MCMAs, compressive strength of concrete increases 19.13 % and 24.14 % from 3 days to 28 days, respectively, and it can reduce shrinkage of concrete. The results of XRD, TG and IR analysis indicated that circulating fluidized bed combustion desulfurization ash (CFBCA) can provide SO_4^{2-}, and metakaolin (MK) mainly provides active Al_2O_3 and SiO_2, which provides conditions for the formation of ettringite (AFt) and C-S-H gel. When the proportion of CFBCA and MK is 3:7, it can generate more AFt and C-S-H gel in the early hydration. It indicates that MCMAs can endow concrete with good early mechanical properties and micro-expansion properties.

1 Introduction

The combustion of solid fuels will be the main source of energy for the production of electricity at least for the few next decades. The circulating fluidized bed (CFB) has maintained an important position in the market in recent years [1]. CFBC desulphurization ash (CFBCA) is one by-product of CFBC boiler with the optimized desulphurization temperature usually controlled at 850–900 °C [2]. Due to their high SO_3 content, it has a big difference with the ordinary fly ash. A large number of CFBCA emissions not only occupy the land resources, but also causes

G. Wang (✉) · M. Bao · T. Sun
State Key Laboratory of Silicate Materials for Architectures, Wuhan University of Technology, Wuhan, China
e-mail: guimingw@hotmail.com

S. Xing
China United Concrete Beijing Xinhang Co., Ltd, Beijing, China

K. Li
Maoming Kaolin Science and Technology Company, Maoming, China

K. Scrivener and A. Favier (eds.), *Calcined Clays for Sustainable Concrete*,
RILEM Bookseries 10, DOI 10.1007/978-94-017-9939-3_12

serious pollution on soil and water nearby, therefore, how to effectively utilize it become imperative.

So far, many methods have been devised and used to utilize the CFBCA. However, the effective disposal or utilization of it has not been established in China. Some mechanically-treat methods of CFBCA were investigated, and modified CFBCA can be utilized as an admixture in cement or concrete [3–5]. Many studies show that it can also be used as road material, such as roadbed material and pavement bricks. Xia [6] used the CFBCA as main raw materials to develop the non-autoclaved aerated concrete. Chi [7] found that CFBCA can be used to replace fine aggregate to make roller compacted concrete. Dung [8] indicated that slag and CFBCA can be mixed to produce cement. Chen [9] pointed out that CFBCA can be utilized for the preparation of foam concrete due to its later volume expansion. Moreover, it would results in a higher length change in mortar when adding over 30 %.

Previous investigations have indicated that CFBCA can be used to make concrete. However, its effect is not ideal. And the use of MK as mineral addition for concrete has received considerable interest in recent years [10–15]. CFBCA has become restricted use due to its high SO_3 and high f-CaO, Metakaolin (MK), which is fine treated calcined clays and active cementitious component, makes a substantial contribution to lowering further the environmental impact of mortar and concrete. CFBCA is richer in anhydrite, free lime, relatively low SiO_2 and Al_2O_3 contents, and MK contains abundant SiO_2 and Al_2O_3, which can provide conditions for the formation of AFt and C-S-H gel. Therefore, combination of MK and CFBCA may provide concrete with good mechanical properties and volume stability. However, there are only a few investigations of the use of CFBCA and MK in concretes as an admixture to make high performance concrete. Consequently, in order to fully utilize the characteristic of CFBCA in concretes, it is very important to investigate MCMAs and their effects on the properties of concretes.

The objective of this study is to investigate the influence of MCMAs on mechanical and micro-expansion properties of concretes. Cementitious mechanism of MCMAs is also studied by XRD, FT-IR and TG. The results may be provided a useful way for further applying CFBCA and MK in concrete.

2 Materials and Methods

2.1 Materials

CFBCA was from Guangdong baolihua electric power Co., Ltd. in China. OPC was supplied by the Huaxin Cement Co., Ltd. Table 1 shows the chemical compositions of CFBCA, MK and Portland cement.

Sand used in the mortar experiment is ISO standard sand. The natural river sand (fineness modulus:2.5) and gravel sizing of 5–19 mm are used as aggregates.

Table 1 Chemical composition of CFBCA, MK and OPC (% by mass)

	SiO_2	Al_2O_3	Fe_2O_3	CaO	MgO	K_2O	Na_2O	TiO_2	SO_3	P_2O_5	Cl	loss
CFBCA	36.2	17.65	6.18	12.34	0.87	2.23	0.36	0.62	6.01	0.16	0.035	16.98
cement	21.5	5.86	2.85	59.81	2.23	0.67	0.2	–	2.06	–	–	3.7
MK	54.46	39.86	1.98	–	–	0.43	–	–	0.18	0.05	–	2.01

A polycarboxylate based superplasticizer with a solid content of 40 %, is used to achieve the fluidity of the mixtures. Ordinary drinking water is used for all the mortar and concrete mixes. Quartz powder is fine quartz sand, over 0.075 mm sieve selected as experimental material.

2.2 Test Methods

Cement paste fluidity of specimens was measured according to Chinese standard GB/T 8077-2000. Mortar strength test was carried out based on GB/T17671-1999. Slump test was carried out based on GB/T 50080-2002. The compressive strength of all samples was measured according to GB/T 50081-2002. The fresh concretes were formed in 100 × 100 × 515 mm^3 steel mould, then using non-contact shrinkage of concrete deformation apparatus to measure its early age autogenous shrinkage.

3 Results and Discussion

3.1 Properties of Mortar

Compressive strength of mortars containing CFBCA is showed by Fig. 1. As shown in Fig. 1, Compressive strength of mortar increases at first and then descends with CFBCA content increasing. The higher $CaSO_4$ and The particles of CFBCA which is irregular and loose textured result in the higher water requirement ratio, which brings in higher compressive strength in low CFBCA content but harmful in high content. Consequently, the utilizations of CFBCA on cement are limited.

Compressive strength of mortar containing MCMAs are showed by Fig. 2. MCMAs replaces 10 % cement, and the proportion of MK and CFBCA follows by 1:9 to 9:1. Compared with CFBCA, the compressive strength of mortars with MCMAs is increased by 21.4 % to 40.7 % in 28 days. Moreover, an optimal combination of MK and CFBCA is attained by 7:3. Thus, the ratio of MK and CFBCA in MCMAs is chosen by 7:3 for next study.

Mortar properties with MCMAs or quartz powder are showed in Figs. 3 and 4. When MCMAs content is below 20 %, compressive strength of mortars is

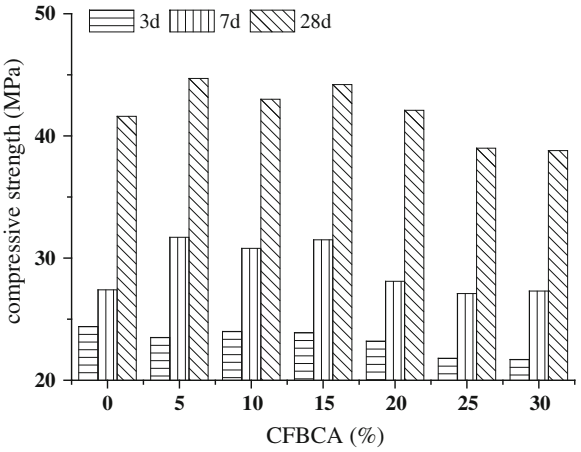

Fig. 1 Compressive strength of mortar with CFBCA

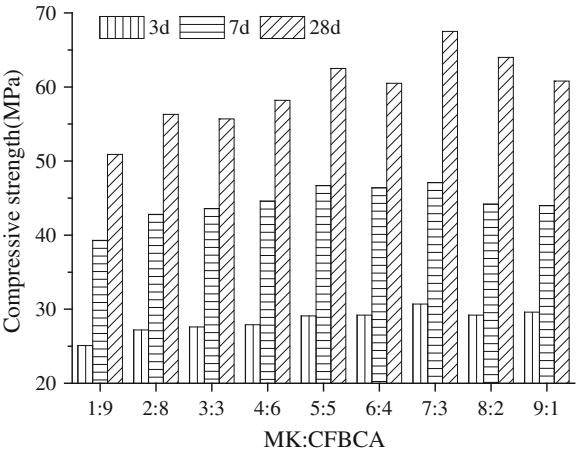

Fig. 2 Compressive strength of the mortars with MCMAs

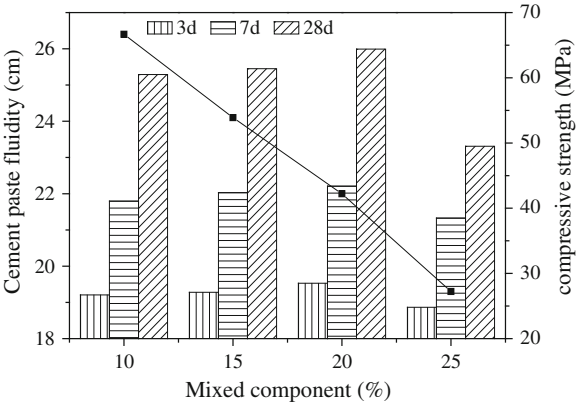

Fig. 3 Different dosage of MCMAs on the properties of mortar

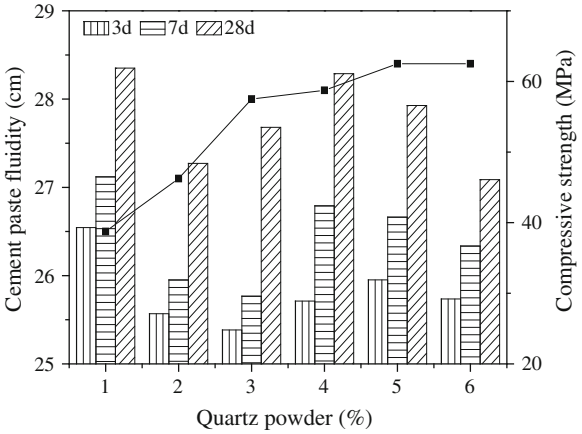

Fig. 4 Different dosage of quartz powder on the properties of mortar

increased. Beyond 20 %, it causes difficulty of molding due to low fluidity. This is mainly due to MCMAs excessive water demand, making the cementitious system flow decreased. However, as shown in Fig. 4, after incorporation with quartz powder, the fluidity of the cement pastes is increase. Though compressive strength of mortars is reduced in 3 days, quartz powder can reduce the heat of hydration, while still providing strength development in 28 days.

3.2 MCMAs on Concrete Properties

The composition of concrete mixes is listed in Table 2. Concrete properties containing MCMAs are showed in Figs. 5 and 6. Compared to A0 sample, compressive strength of A1 is increased 19.13 % and 24.14 % from 3 days to 28 days, respectively, but slump is dropped 30 mm. However, after adding quartz powder, slump of flesh concrete is increased, and strength is still increased in 28 days. As shown in Fig. 6, the volume changes mainly occur in 3 days, which is period of ettringite (AFt) formation. Comparison with the A0 sample, MCMAs can improve ettringite formation to compensate concrete shrinkage. By contrast A2 and A3 displacement curves can be found that quartz powder play an inhibitory effect on the shrinkage of concrete. This is mainly due to reduction of hydration heat and

Table 2 Mix proportion of concrete experiment (kg/m^3)

Number	Cementitious materials				Superplasticizers	Mixing water	Fine aggregate	Coarse aggregate
	Cement	MK	CFBCA	Quartz powder				
A0	550	–	–	–	6.6	137.5	605	1075
A1	467.5	57.75	24.75	–	6.6	137.5	605	1075
A2	440	57.75	24.75	27.5	6.6	137.5	605	1075

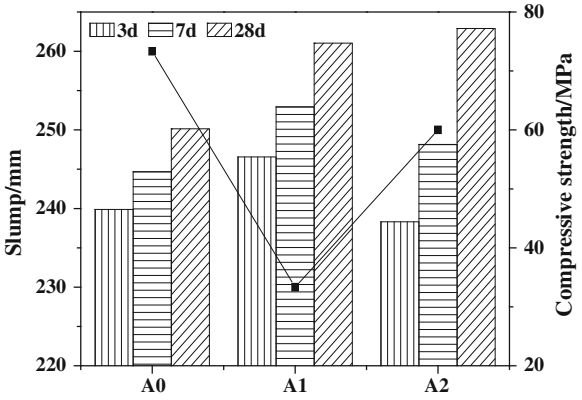

Fig. 5 MCMAs on concrete performance

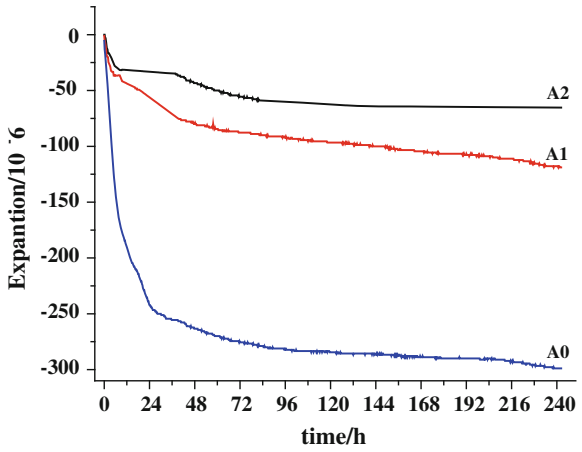

Fig. 6 Volume change of concrete with MCMAs

cement autogenous shrinkage. After quartz powder replaced cement, it reduces hydration heat and prevents AFt decomposition. Therefore, relatively high early strength and high-performance micro-expansion concrete can be prepared by MCMAs mixtures.

3.3 Effect of MCMAs on Cement Hydration

The XRD results of the hydrated pastes are shown in Fig. 7. It can be seen that main hydration products at 1 days are portlandite, ettringite (AFt) and C-S-H. Furthermore, the AFt peaks of samples with MCMAs are higher than the blank sample, and the portlandite are the exact contrary, which may due to acceleration of reaction between active Al_2O_3 and SO_4^{2-}. Therefore, it is contribute to early strength and reduce autogenous shrinkage of cement.

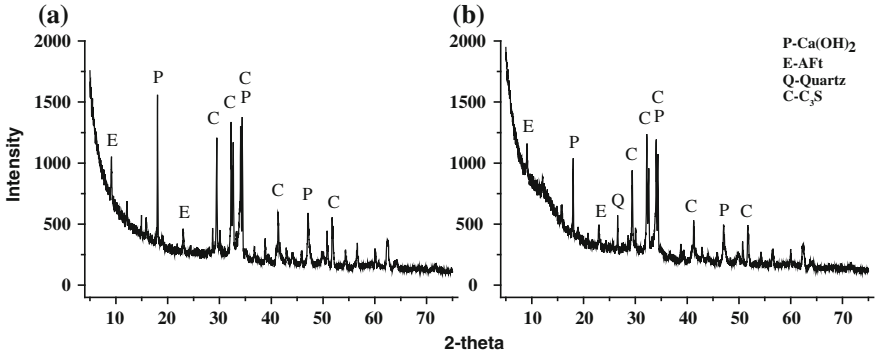

Fig. 7 XRD patterns of the hydrated samples at 1 days. **a** without mineral admixtures, **b** with mineral admixtures

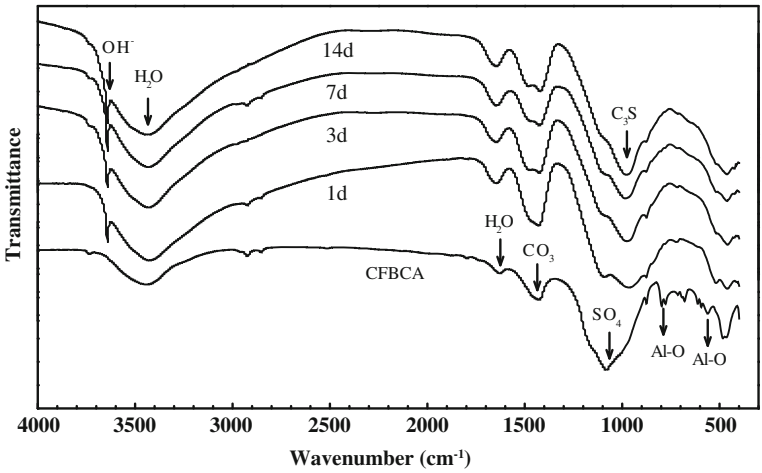

Fig. 8 FT-IR spectra of CFBCA and hydrated MCMAs at different curing ages

FT-IR spectra of CFBCA and hydrated pastes with MCMAs at different curing ages are presented in Fig. 8. The vibrations in the region 1600-3700 cm^{-1} are assigned to the presence of the H_2O and O-H. The isolated OH stretching (3690 cm^{-1}) is attributed to interaction of the water hydroxyl with the cations, associated to the $Ca(OH)_2$ molecules, which means the presence of $Ca(OH)_2$. The vibrations in are (1060 cm^{-1}) assigned to the presence of the SO_4^{2-} in CFBCA, which means the presence of $CaSO_4$ in CFBCA. Moreover, compared with the CFBCA, band of SO_4^{2-} have a slight displacement to around 1115 cm^{-1} in hydrated pastes and the band of SO_4^{2-}(1060 cm^{-1}) disappear at 14 days, which are attributed to the formation of AFt. The FI-IR and XRD results indicate that the CFBCA provide SO_4^{2-} to hydration cementitious systems, and MK mainly provides active Al_2O_3 and SiO_2, which generate AFt and C-S-H gel.

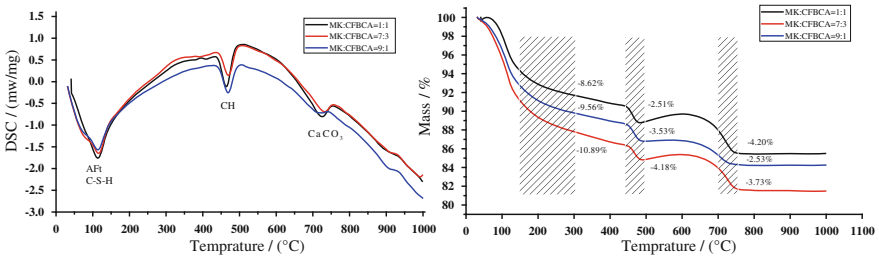

Fig. 9 Thermal analysis observations of the hydrated pastes

Thermal analysis observations of the three kinds of mix type of MCMAs pastes at 3 days are shown in Fig. 9. The TG results indicate that when the proportion of CFBCA and MK is 3:7, it can generate more AFt and C-S-H gel in the early hydration, which are in agreement with results of mortar compressive strength test. It is indicated that proportion of CFBCA and MK can alter the ratio of SO_4^{2-} and active Al_2O_3 and SiO_2, thus impact forming of AFt and C-S-H.

4 Conclusions

- Higher compressive strength is observed in MCMAs than comparable mortars with CFBCA. The mixtures with various combinations of MK and CFBCA are attained by optimal ratio of 7:3.
- Incorporated with MCMAs, the high strength micro-expansive concrete can be made.
- The main hydration products of the MCMAs samples are C-S-H, ettringite and some protlandite. CFBCA can provide SO_4^{2-} and MK mainly provides active Al_2O_3 and SiO_2, which can promote the growth of AFt and C-S-H gel.

Acknowledgments This research is financially supported by Yang Fan Innovative & Entrepreneurial Research Team Project (No.201312C12) and self-determined and innovative research funds of WUT (No.155201012).

References

1. Armesto, L.: Characterization of some coal combustion solid residues. Fuel **78**(5), 613–618 (1999)
2. Havlica, J., Brandstetr, J., Odler, I.: Possibilities of utilizing solid residues from pressured fluidized bed coal combustion (PFBC) for the production of blended cements. Cem. Concr. Res. **28**(2), 299–307 (1998)
3. Fu, X., Li, Q., Zhai, J., et al.: The physical–chemical characterization of mechanically-treated CFBC fly ash. Cem. Concr. Compos. **30**(3), 220–226 (2008)

4. Li, X., Chen, Q., Ma, B., et al.: Utilization of modified CFBC desulfurization ash as an admixture in blended cements: physico-mechanical and hydration characteristics. Fuel **102**, 674–680 (2012)
5. Li, X., Chen, Q., Huang, K., et al.: Cementitious properties and hydration mechanism of circulating fluidized bed combustion (CFBC) desulfurization ashes. Constr. Build. Mater. **36**, 182–187 (2012)
6. Xia, Y., Yan, Y., Hu, Z.: Utilization of circulating fluidized bed fly ash in preparing non-autoclaved aerated concrete production. Constr. Build. Mater. **47**, 1461–1467 (2013)
7. Chi, M., Huang, R.: Effect of circulating fluidized bed combustion ash on the properties of roller compacted concrete. Cem. Concr. Compos. **45**, 148–156 (2014)
8. Dung, N.T., Chang, T., Chen, C.: Engineering and sulfate resistance properties of slag-CFBC fly ash paste and mortar. Constr. Build. Mater. **63**, 40–48 (2014)
9. Chen, X., Yan, Y., Liu, Y., et al.: Utilization of circulating fluidized bed fly ash for the preparation of foam concrete. Constr. Build. Mater. **54**, 137–146 (2014)
10. Kannan, V., Ganesan, K.: Chloride and chemical resistance of self compacting concrete containing rice husk ash and metakaolin. Constr. Build. Mater. **51**, 225–234 (2014)
11. Sfikas, I.P., Badogiannis, E.G., Trezos, K.G.: Rheology and mechanical characteristics of self-compacting concrete mixtures containing metakaolin. Constr. Build. Mater. **64**, 121–129 (2014)
12. Perlot, C., Rougeau, P., Dehaudt, S.: Slurry of metakaolin combined with limestone addition for self-compacted concrete. Application for precast industry. Cem. Concr. Compos. **44**, 50–57 (2013)
13. Hassan, A.A.A., Lachemi, M., Hossain, K.M.A.: Effect of metakaolin and silica fume on the durability of self-consolidating concrete. Cem. Concr. Compos. **34**(6), 801–807 (2012)
14. Kim, H.K., Hwang, E.A., Lee, H.K.: Impacts of metakaolin on lightweight concrete by type of fine aggregate. Constr. Build. Mater. **36**, 719–726 (2012)
15. Madandoust, R., Mousavi, S.Y.: Fresh and hardened properties of self-compacting concrete containing metakaolin. Constr. Build. Mater. **35**, 752–760 (2012)

Optimization of Alkali Activated Portland Cement—Calcined Clay Blends Based on Phase Assemblage in the $Na_2O–CaO–Al_2O_3–SiO_2–H_2O$ System

Erika Vigna and Jørgen Skibsted

Abstract In the development of low-CO_2 emission binders, the inclusion of small amounts of alkali activators in hybrid Portland cement systems may be used to increase the Portland cement replacement level above that in common Portland cement – SCM systems. The co-precipitation of C-S-H and N-A-S-H-type hydration products in these systems has been investigated by studying the influence of Ca^{2+} and Na^+ ions on the formation and compatibility of C-A-S-H and N-A-S-H phases, prepared from alumino-silicate materials with fixed Si/Al ratios and sodium concentrations but variable calcium contents. The structural characterization, by means of solid-state MAS NMR, thermal analysis and powder X-ray diffraction, shows that C-A-S-H and N-A-S-H phases can coexist in the low-Ca part of the CaO-Al_2O_3-SiO_2 system, as seen by the presence of zeolitic phases by XRD and C-A-S-H phases by NMR. The formation of N-A-S-H phases seems to be less dependent on the Si/Al ratio, at least for the studied molar ratios of Si/Al = 1.0 and 2.0. For high fractions of calcium, C-A-S-H phases and strätlingite are the main hydration products. The results from the studies of the synthetic samples in the Na_2O – CaO – Al_2O_3 – SiO_2 – H_2O system have been used to propose optimum compositions for hybrid cement blends based on Portland cement, metakaolin (as SCM) and small amounts of an alkali salt.

1 Introduction

The cement industry is responsible for roughly 5-7 % of the global anthropogenic CO_2 emission [1] and society's demand for cement in construction applications is continuously increasing, especially in the developing countries, and it is expected to double by 2050. An innovative approach to reduce CO_2 emission may be the development of hybrid cements, where the inclusion of alkali activators enables the

E. Vigna (✉) · J. Skibsted
Department of Chemistry and Interdisciplinary Nanoscience Center (INANO), Aarhus University, Langelandsgade 140, DK-8000, Aarhus C, Denmark
e-mail: evigna@chem.au.dk

K. Scrivener and A. Favier (eds.), *Calcined Clays for Sustainable Concrete*, RILEM Bookseries 10, DOI 10.1007/978-94-017-9939-3_13

production of cements with a higher fraction of supplementary cementitious materials (SCM's) and comparable mechanical performance as compared to traditional Portland – SCM systems.

The principal hydration product from Portland cement hydration is a calcium alumino-silicate hydrate (C-A-S-H) phase whereas alkali-activation (with Na^+ ions) of alumina-silicate rich SCM's generally results in the formation of condensed sodium alumino-silicate hydrate (N-A-S-H) phases. These two hydration products exhibit only a low degree of structural order and their compatibility has important implications on the design of hybrid Portland cement – alkali activated alumina-silicate systems in which both phases may be present. Insight into the underlying chemistry may be achieved by studying the uptake of a fourth element (such as Na_2O) in the $CaO - Al_2O_3 - SiO_2 - H_2O$ system [2, 3].

The aim of this work is to investigate the influence of Ca^{2+} and Na^+ ions on the formation and compatibility of synthesized C-A-S-H and N-A-S-H phases, prepared from alumino-silicate materials (metakaolin and silica) with two fixed Si/Al ratios and three fixed sodium concentrations but variable calcium contents. This information will subsequently be used in the design of Portland cement – SCM – alkali salt blends, targeting Portland cement replacement levels of 75–90 wt%.

2 Experimental

Hydrated samples in the $Na_2O - CaO - Al_2O_3 - SiO_2 - H_2O$ (N-C-A-S-H) system have been prepared from analytically pure $Ca(OH)_2$ (Sigma-Aldrich), silica (SiO_2, Bie & Berntsen A/S), and metakaolin, the latter produced from thermal treatment of kaolinite (Fluka) at 600 °C for 20 h. Two different series have been prepared, corresponding to initial molar ratios of $SiO_2/Al_2O_3 = 2.0$ (*i.e.*, Si/Al = 1.0, samples 1-6) and $SiO_2/Al_2O_3 = 4.0$ (*i.e.*, Si/Al = 2.0, samples 7 - 12) and different CaO contents. The specific compositions of the samples are shown as projections onto the $CaO - SiO_2 - Al_2O_3$ phase diagram in Fig. 1b.

For each series, three groups of samples have been made, using (a) demineralized water and solutions of (b) 1.0 M NaOH, and (c) 5.0 M NaOH. For each synthesis, 2 g of solids was mixed with either water or the NaOH solutions, using a total volume of 25 mL, and subsequently cured in airtight glass-tubes at 40 °C, employing continuous stirring with a magnet stirrer. After two weeks, the suspensions were filtered and the precipitate gently washed with demineralized water before it was dried in a desiccator over silica gel at room temperature.

The phase assemblages for the individual samples have been investigated by powder X-ray diffraction, thermal analysis as well as ^{27}Al and ^{29}Si MAS NMR experiments, including ^{27}Al MQMAS spectra for selected samples.

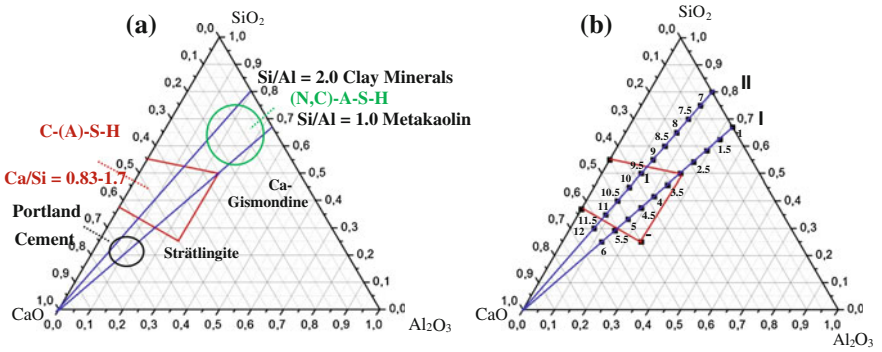

Fig. 1 Ternary CaO – Al_2O_3 – SiO_2 phase diagram (mol%), illustrating **a** the typical regions for formation of C-A-S-H and N-A-S-H phases and **b** the CaO – Al_2O_3 – SiO_2 compositions of the synthesized samples studied in this work

3 Results and Discussion

The individual samples of the two series with fixed molar ratios of Si/Al = 1.0 and 2.0, cured in water and in 1.0 and 5.0 M NaOH solutions, have all been characterized by ^{27}Al and ^{29}Si MAS NMR. The degree of reaction for the anhydrous materials in the individual samples is conveniently evaluated by ^{29}Si MAS NMR which probes crystalline and amorphous phases in an equal manner. Generally, these spectra show that the degree of reaction increases by increasing the alkalinity of the samples. For the samples cured in water, almost no reaction is observed for the lowest Ca contents (*i.e.*, samples 1a, 2a and 7a, 8a, *c.f.*, Fig. 1b). However, for higher Ca contents, nearly all metakaolin has reacted and formed a C-A-S-H phase, strätlingite, and potentially also minor amounts of a hydroxy-AFm phase, as revealed by ^{29}Si and ^{27}Al MAS NMR. The 5.0 M NaOH samples show all a full degree of reaction, where zeolitic N-A-S-H phases dominate at low Ca contents. Increasing the Ca content for these samples results in a reduction of the amount of zeolitic N-A-S-H phase as well as formation of cancrinite (Na_6Ca_2-$[Al_6Si_6O_{24}](CO_3)_2{\cdot}2H_2O$) and katoite $Ca_3Al_2(SiO_4)_{3-x}(OH)_{4x}$; x = 1.5 - 3.0 [4], and generally hydration products with a higher degree of structural order as compared to those observed at lower NaOH concentration.

The present paper focusses on the samples synthesized in 1.0 M NaOH for which the ^{29}Si MAS NMR spectra are shown in Fig. 2. A low degree of reaction is observed in the absence of Ca^{2+} ions (samples 1 and 7) whereas a N-A-S-H phase is the dominating component for small concentrations of Ca^{2+} ions, at least for the Al/Si = 1.0 series (*i.e.*, samples 1.5, 2 and 7). This is seen by the ^{29}Si resonance at -89.6 ppm, assigned to a $Q^4(4Al)$ site and in accordance with the identification of Na-zeolite A by powder XRD (Fig. 3). For the Si/Al = 1.0 series, the $Q^4(Al)$ site is observed for samples 1.5 – 3, corresponding to molar CaO fractions of 6.3 – 18.8, where its intensity decreases with increasing Ca^{2+} content. The corresponding ^{27}Al

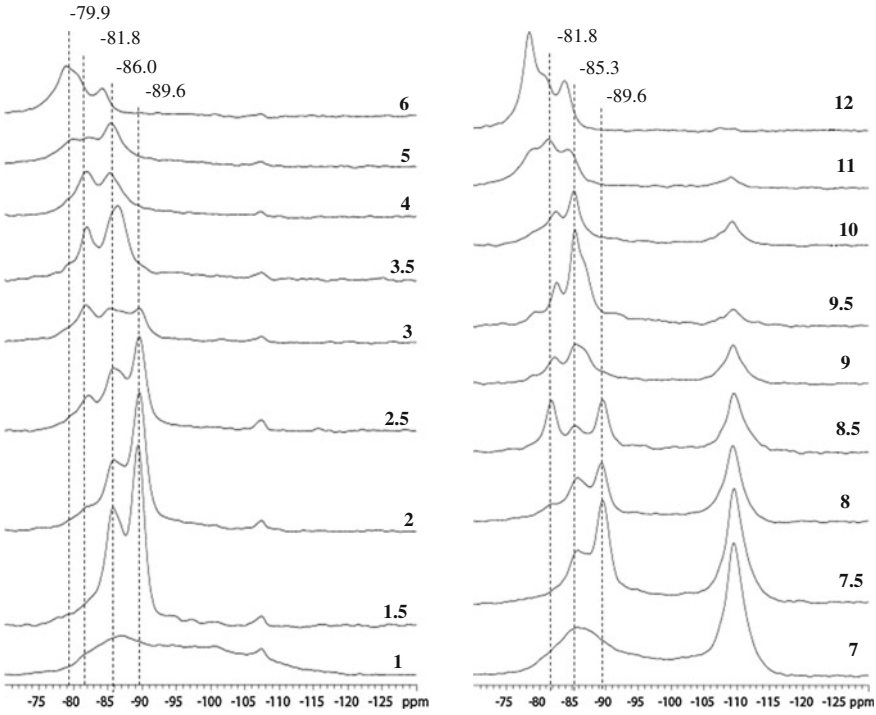

Fig. 2 ^{29}Si MAS NMR spectra (7.1 T, ν_R = 6.0 kHz) of the synthesized samples with Al/Si = 1.0 (*left*) and Al/Si = 2.0 (*right*) cured in 1.0 NaOH solution and corresponding to the CaO –Al_2O_3 – SiO_2 compositions given in Fig. 1b

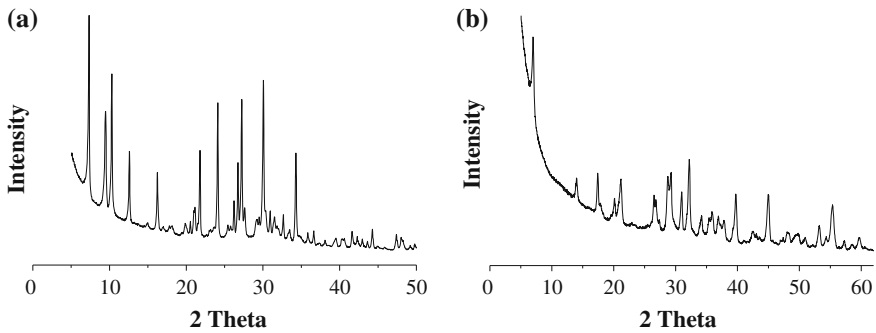

Fig. 3 Powder X-ray diffraction patterns for samples 1.5 (**a**) and 5 (**b**), both synthesized in a 1.0 M NaOH solution. Reflexions from Na-zeolite A, Na-zeolite 5A, and katoite are identified by A 5A, and K, respectively

resonance from $Al(OSi)_4$ units is observed at 59.2 ppm in the ^{27}Al NMR spectra (not shown), in agreement with the ^{27}Al chemical shift reported Na-zeolite A [5, 6]. The resonance at -86 ppm is assigned to a low-Ca C-S-H phase, which mainly

includes Q^2 sites. The intensity for the Q^2 site decreases with increasing Ca content and a resonance at -81.8 ppm becomes more prominent, which is ascribed to the Q^2(1Al) site of the C-A-S-H phase. Thus, the decrease in Q^2 intensity reflects that the bridging sites of the silicate chains are replaced by AlO_4 tetrahedra, and thereby that the Al/Si ratio of the C-A-S-H phase increases. For the samples with high Ca contents, where Na zeolite A is not observed (*i.e.*, samples 3.5–6), the C-A-S-H phase is the dominating hydration product along with strätlingite (samples 3.5–5) and katoite (samples 5 and 6). Strätlingite is identified by ^{27}Al MAS NMR (Al(4) resonance at 62 ppm) whereas katoite is seen by the ^{29}Si resonance at -79.9 ppm. The ^{29}Si MAS NMR spectra of the Si/Al = 2.0 series reveal that a significant part of the silica, used in the synthesis ($\delta(^{29}Si)$ = -110 ppm), has not reacted for the low Ca contents. However, the amount of reacted silica increases with increasing Ca content. Na-zeolite A is identified as a main component for the 7.5–8.5 samples, where sample 8.5 in addition contains well-defined peaks at -82.3 ppm and -85.3 ppm. Strätlingite is detected by ^{27}Al MAS NMR in samples 9 – 11, whereas the peaks observed by ^{29}Si NMR for samples 11 and 12 bear a clear resemblance to those observed for aluminate-rich C-A-S-H phases with a clear identification of the Q^2(1Al) peak at -81.8 ppm.

All the samples have been analyzed by powder XRD and two typical diffractograms are shown in Fig. 3 for samples 1.5 and 5 of the Al/Si = 1.0 series cured in 1.0 M NaOH. Generally, the XRD patterns show that the alkalinity of the system and the fraction CaO in the system have a major influence on the crystalline phases formed. Samples with low Ca content show Na zeolite A as the main product whereas katoite appears to be the principal crystalline phase at high Ca contents (*c.f.*, Figure 3). For the samples cured in water, zeolitic N-A-S-H phases are not observed by XRD but only strätlingite for samples 2-4 and 8-9 and katoite for samples 5-6 and 11-12. The 5.0 M NaOH samples show zeolitic structures at low Ca contents (Na zeolite A for samples 1.5 and 7.5-9). For higher amounts of calcium, cancrinite is detected (samples 2–4) and for the highest Ca contents only katoite has been identified by XRD (samples 5-6 and 10-12). The 1.0 M NaOH samples show the co-existence of different types of zeolites in the low-Ca part of the phase diagram. In sample 1.5, zeolite A and 5A have been detected (Fig. 3) as well as in samples 7.5-9, where zeolite P has also been observed. Katoite is identified for the Ca-rich samples (5-6 and 10-12) as shown in Fig. 3 for sample 5.

For the samples cured in 1.0 M NaOH, the ^{27}Al and ^{29}Si MAS NMR spectra indicate the presence of both N-A-S-H (Na zeolite A) and C-A-S-H phases for low fractions of CaO (*i.e.*, samples 1.5 - 3 and 7.5-8.5). Additional evidence for this observation is obtained by ^{27}Al MQMAS NMR, where improved resolution in the ^{27}Al MAS NMR spectra is achieved by removal of the second-order quadrupolar broadening in one dimension of MQMAS spectrum.

This is illustrated in Fig. 4 for sample 3 cured in 1.0 M NaOH where three distinct AlO_4 peaks are clearly observed at 73, 62 and 59 ppm, originating from tetrahedral Al in the C-A-S-H phase, in strätlingite, and in the N-A-S-H phase, respectively.

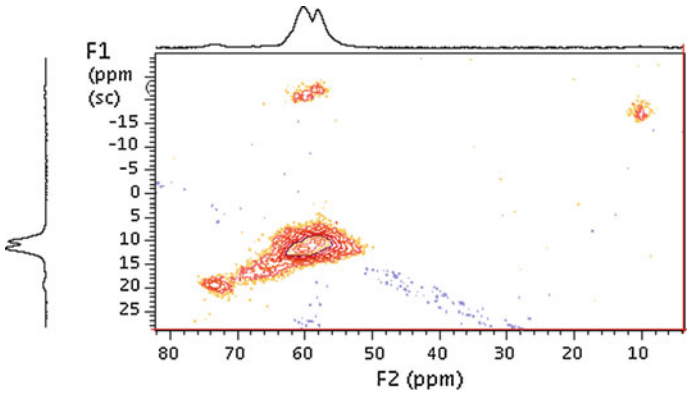

Fig. 4 ^{27}Al MQMAS NMR spectrum (14.1 T, ν_R = 13 kHz) of sample 3 synthesized in a 1.0 M NaOH solution, obtained with the three-pulse *z*-filter pulse sequence using ^{1}H decoupling (TPPM) in both the t_1 and t_2 evolution periods. The F1 dimension is scaled relative to the transmitter frequency at 41.3 ppm

The mutual presence of N-A-S-H and C-A-S-H phases is observed for both the Si/Al = 1.0 and 2.0 series cured in 1.0 M NaOH for molar fractions of CaO of 6 – 19 %, corresponding to 5 – 15wt% CaO in the CaO–Al_2O_3–SiO_2 system. For a Portland cement with a bulk content of 68 wt% CaO, 22 wt% SiO_2 and 4 wt% Al_2O_3 similar compositions can roughly be obtained for binary blends containing 10–25 wt % Portland cement and 75–90 wt% calcined alumino-silicate clay (metakaolin). As the next part of this project, such blends, including a sodium salt as an activator, will be prepared and their physical performance, microstructure and hydrate phase assemblages will be characterized and compared with the results from the present study of the model compounds in the Na_2O – CaO – Al_2O_3 – SiO_2 – H_2O system.

4 Conclusions

Alkali- and water-activated samples in the CaO – Al_2O_3 – SiO_2 system have been prepared for two fixed Si/Al molar ratios of 1.0 and 2.0 and different CaO contents, ranging from 0–65 mol% CaO, and characterized by ^{27}Al and ^{29}Si MAS NMR as well as powder X-ray diffraction. For the samples cured in water the reaction products are a C-A-S-H phase, strätlingite, and katoite. Zeolitic N-A-S-H phases (*e.g.*, Na zeolite A) are formed in both alkali-activated systems (1.0 and 5.0 M NaOH) for molar CaO contents in the range 6 – 19 % and their formation appears to be less sensitive to the Si/Al ratio, at least for ratios in the range 1.0–2.0. The N-A-S-H phases are found to co-exist with a C-A-S-H phase and strätlingite, although thermodynamic equilibrium may not be achieved for the hydrated system cured for two weeks at 40 °C. The mutual presence of these phases for specific compositions in

the Na_2O – CaO – Al_2O_3 – SiO_2 system may form the basis for the design of new hybrid Portland cement – SCM blends, employing small amounts of a sodium salt for alkali-activation, and targeting high cement substitution levels of 75–90 wt%.

Acknowledgments The Danish Council for Strategic Research is acknowledged for financial support to the LowE-CEM project.

References

1. Damtoft, J.S., Lukasik, J., Herfort, D., Sorrentino, D., Gartner, E.M.: Sustainable development and climate change initiatives. Cem. Concr. Res. **38**, 115–127 (2008)
2. Lodeiro, I.G., Fernández-Jiménez, A., Palomo, A., Macphee, D.E.: Compatibility studies between N-A-S-H and C-A-S-H gels. Study in the ternary diagram Na_2O-CaO-Al_2O_3-SiO_2-H_2O. Cem. Concr. Res. **40**, 27 (2010)
3. Garciá-Lodeiro, I., Fernández-Jiménez, A., Palomo, A., MacPhee, D.E.: Effect of Calcium additions on N-A-S-H cementitious gels. J. Am. Ceram. Soc. **93**, 1934–1940 (2010)
4. Fernández-Jiménez, A., Vásquez, T.: Effect of Sodium Silicate on Calcium Aluminate cement hydration in highly alkaline media: a microstructural characterization. J. Am. Ceram. Soc. **94**, 1297–1303 (2011)
5. Engelhardt, G., Michel, D. (ed.): High-Resolution Solid-State NMR of Silicates and Zeolites. Wiley, London (Great Britain, 1987)
6. Grutzeck, M.W., Kwan, S., Dicola, M.: Zeolite formation in alkali-activated cementitious systems. Cem. Concr. Res. **34**, 949–955 (2004)

Phase Assemblages in Hydrated Portland Cement, Calcined Clay and Limestone Blends From Solid-State ^{27}Al and ^{29}Si MAS NMR, XRD, and Thermodynamic Modeling

Zhuo Dai, Wolfgang Kunther, Sergio Ferreiro, Duncan Herfort and Jørgen Skibsted

Abstract The use of calcined clays as SCM's provides a valuable contribution to the reduction in CO_2 emission associated with cement production since they can be produced at significantly lower temperatures and do not involve a calcination reaction. Moreover, it is well known that binary blends of Portland cement and small amounts of limestone powder can increase the strength of the resulting concrete. In this study we have investigated the substitution of cement by metakaolin and limestone as well as blends of cement, metakaolin, silica fume and limestone, in all cases with a 35 wt% replacement level of Portland cement. The phase assemblages of the hydrated blends are characterized by XRD, ^{27}Al and ^{29}Si MAS NMR spectroscopy, and thermodynamic modelling. The X-ray diffractograms show that larger amounts of the AFm phases are formed for the samples containing both limestone and calcined clay whereas ^{29}Si MAS NMR studies of the hydrated pastes provide information about the uptake of Al in the C–S–H phase and structural details about the resulting C–A–S–H phases. ^{27}Al MAS NMR is used to follow the formation of the hydrated aluminate species, in particular the formation of strätlingite. The results from XRD and NMR after prolonged hydration are compared with the phase assemblages predicted from thermodynamic modelling. Overall, good agreements are observed between the experiments and the modeled predictions.

Z. Dai (✉) · W. Kunther · J. Skibsted
Department of Chemistry and Interdisciplinary Nanoscience, Center (INANO), Aarhus University, Langelandsgade 140, DK-8000, Aarhus C, Denmark
e-mail: zhuodai@inano.au.dk

S. Ferreiro · D. Herfort
Aalborg Portland a/S, Cementir Holding, 9100 Aalborg, Denmark

K. Scrivener and A. Favier (eds.), *Calcined Clays for Sustainable Concrete*, RILEM Bookseries 10, DOI 10.1007/978-94-017-9939-3_14

1 Introduction

Supplementary cementitious materials (SCM's) used in cement and concrete receive at the moment great interest due to economic and ecological aspects [1]. However, the use of SCMs is currently limited as a result of the reduction in mechanical strength at early ages. The addition of limestone (LS) has been investigated extensively and it is widely used nowadays in small amounts in binary cement blends. It is generally accepted that addition of up to 5 wt% of limestone improves the physical properties of the binary system [2] whereas larger substitutions of cement with limestone lead to reduced mechanical properties [3]. The positive effect of limestone is mainly the concomitant stabilization of the voluminous ettringite and monocarbonate phases instead of monosulfate formation [2]. The combination of limestone and SCM substitution in cement systems has also been highlighted in recent years [4–6], for which synergetic effects can occur as a result of the reaction between the alumina from the SCM and limestone, forming additional amounts of AFm phases and stabilizing ettringite [5, 6]. Recently, we have investigated white Portland cement (wPc)–metakaolin (MK) blends, with different substitution levels, and demonstrated that increasing MK contents result in an increasing amount of aluminum incorporated in the C–S–H phase and a decreasing Ca/Si ratio of the C–S–H [7]. In the present work, ternary wPc–MK–LS blends are investigated as well as blends that in addition include silica fume (SF). The MK–SF ratio in the latter blends is adjusted to match the Si:Al ratio found in a montmorillonite 2:1 clays.

2 Materials and Methods

An overall cement substitution level of 35 wt% was used according to the European cement standard, EN 197-1. Seven different SCM/(SCM + LS) ratios of $x = 0$, 0.17, 0.34, 0.5, 0.67, 0.75 and 0.94 are studied (for simplicity, samples in the wPc–MK–LS system are denoted as *x*MK, while samples from the wPc–MK–SF–LS blends are denoted as *x*MKSF). For each blend, the compressive strength has been determined on mortars bars whereas the hydration products have been identified for corresponding paste samples by XRD and NMR. The main chemical and mineralogical compositions of the used materials are summarized in Table 1. The ferrite phase in the white Portland cement is not considered since only a small bulk amount of Fe_2O_3 (0.2 wt%) is present in the wPc.

Solid-state ^{27}Al and ^{29}Si MAS NMR was employed to follow the hydration of the Portland cement–SCM blends in a semi-quantitative manner. ^{29}Si MAS NMR provides information about the hydration kinetics of the alite and belite phases of the wPc and of MK and SF whereas ^{27}Al MAS NMR detects different aluminate phases present in the hydrating systems. XRD was also applied to identify the hydrate phase assemblages in the cement–SCMs blends. The hydration kinetics

Table 1 Bulk oxide and mineralogical compositions (wt%) for the sources of white Portland cement (wPc), metakaolin (MK), silica fume (SF) and limestone (LS) used in this work

	SiO_2	Al_2O_3	Fe_2O_3	CaO	MgO	L.o.I.	Calcite	C_3S	C_2S	C_3A
wPc	21.8	3.6	0.2	66.1	1.1	2.6	3.1	64.9	16.9	7.9
Limestone	3.9	0.3	0.1	53.7	1.1	41.8	94.0	–	–	–
Metakaolin	54.8	39.5	1.4	0.22	0.5	3.6	–	–	–	–
Silica fume	90.4	0.3	0.03	1.4	0.9	3.4	–	–	–	–

data from NMR were implemented into thermodynamic modelling. A detailed description of the experimental [8] and modeling methods [9] will be given elsewhere.

3 Results and Discussion

3.1 ^{29}Si and ^{27}Al MAS NMR

The hydration of alite, belite, metakaolin, and silica fume has been studied by ^{29}Si MAS NMR using computer deconvolution methods, as described elsewhere [7]. The ^{29}Si MAS NMR spectra are separated into sub spectra for alite, belite, metakaolin, silica fume and three different SiO_4 sites of the C–S–H phase (denoted as Q^1, Q^2(1Al) and Q^2). The degree of reaction (H) for the silicate phases is calculated as, $H(t) = [1 - I(t)/I(t_0)]$, where $I(t_0)$ and $I(t)$ are the relative intensities from the deconvolutions of the ^{29}Si MAS NMR spectra before (t_0) and after hydration (t). The deconvolved intensities also allow calculation of the Al/Si ratio for the C–S–H phase from the relation: $Al/Si = Q^2(1Al)/\{2[Q^1 + Q^2(1Al) + Q^2]\}$. As an example, Fig. 1 shows the ^{29}Si MAS spectra obtained for the 0.94MKSF sample before hydration and after hydration for one and 182 days. Similar ^{29}Si MAS NMR spectra have been obtained for the other blends and analyzed in terms of degree of hydration and incorporation of Al in the C–S–H phase. These results show that the hydration of the alite and belite phases is accelerated by the substitution of the wPc with MK, SF and LS. This is attributed to the presence of a large number nucleation sites provided by LS and the SCM's as well as the pozzolanic reactions for the SCM's. For the C–S–H phases of the individual blends, it is observed that the Al/Si ratio only varies marginally with the hydration time but increases with MK content in the systems studied. This is apparent from the plot of Al/Si ratios, averaged over time, as a function of the metakaolin contents (Fig. 1), which shows nearly linear relationships for both the systems with and without silica fume. The different slopes reflect the different compositions of the two series of blends and different degrees of reaction for the individual constituents.

The variation in the incorporation of Al in the C–S–H is further supported by ^{27}Al MAS NMR studies. In these spectra, the quantification of the ^{27}Al intensities is

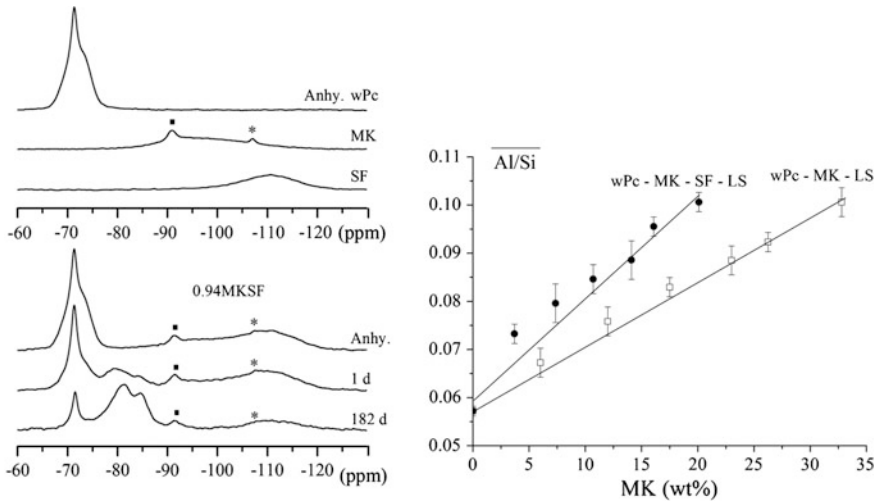

Fig. 1 *Left* ^{29}Si MAS NMR spectra (9.39 T, ν_R = 6.0 kHz) of anhydrous wPc, MK, SF and of anhydrous 0.94MKSF and the blend hydrated for one day and for 182 days, respectively. The asterisks indicate the resonance from a small impurity of quartz in MK and the solid squares the presence of a minor amount of non-dehydroxylated kaolinite. *Right* Plot of the Al/Si ratios, averaged over hydration time, for the individual blends of the two binder systems as a function of MK content

complicated by quadrupolar coupling effects, which result in non-symmetric lineshapes for the ^{27}Al central transition. Nevertheless, spectral integration over the distinct chemical shift regions for the tetrahedral (Al(4)), fivefold (Al(5)) and octahedral (Al(6)) sites can provide an estimate of the relative fraction of these species. The broad peak from Al(4) at high SCM replacements contains resonances for Al incorporated in the C-A-S-H phase as well as the tetrahedral Al sites in strätlingite. This spectral region can be deconvolved using sub spectra for Al(4) incorporated in the C–S–H and for the tetrahedral Al in strätlingite, following our recent studies of binary wPc–MK blends [7]. The normalized intensities for the distinct chemical shift regions for tetrahedral, five-fold, and octahedrally coordinated Al are shown in Fig. 2 as a function of the SCM content and based on the analyses of ^{27}Al MAS NMR spectra for all samples after 182 days of hydration. These plots clearly demonstrate that a major part of the aluminate species released from MK form AFm and AFt phases which both only include Al in octahedral coordination. The intensities for the octahedral sites increase with increasing SCM content in both systems. The maximum amount of Al(6) in the wPc–MK–LS system is found for the 0.75MK blend, while the intensities are comparable for 0.67MKSF and 0.75MKSF in the wPc–MK–SF–LS system. This observation correlates well with the compressive strength values for both systems after 182 days of hydration [8], indicating that highest compressive strength for these systems is related to an increased amount of AFt/AFm phases. In addition, the ^{27}Al MAS

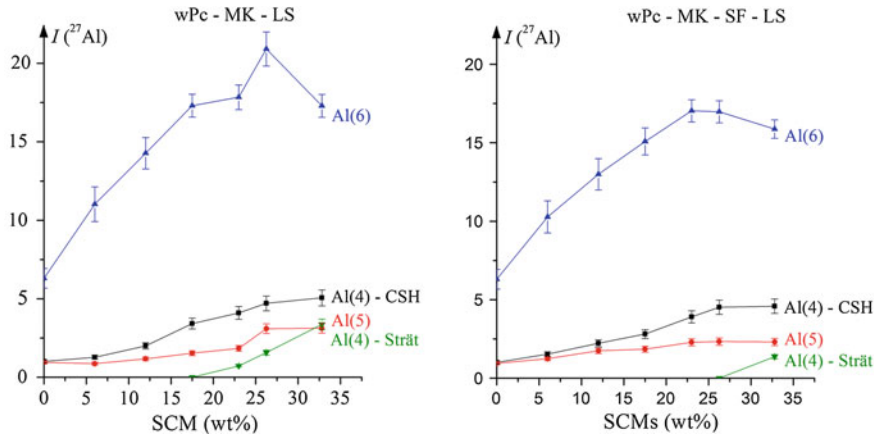

Fig. 2 Normalized ^{27}Al MAS NMR intensities for the ^{27}Al central transitions for the two different binder systems hydrated for 182 days as a function of the SCM replacement level, the maximum replacement corresponding to SCM/(SCM + LS) = 0.94. Note that the intensities for Al(4) are divided into contributions from Al(4) in the C–S–H and Al(4) in strätlingite

NMR data show a nearly linear increase of the intensity for Al(4) incorporated in the C–S–H with increasing SCM content, which agrees well with the results from ^{29}Si NMR (Fig. 1). An increase in five-fold coordinated Al is also observed, which is assigned to a larger fraction of AlO_5 sites in the interlayer of the C–S–H phase, obtained by replacement for seven-fold coordinated interlayer Ca^{2+} sites. This implies that these units may contribute to the charge-balance of the Al^{3+} sites in the silicate chain structure, as observed for wPc–MK blends [7].

3.2 Phase Assemblages and Thermodynamic Modelling

Phase assemblages determined experimentally by X-ray diffraction and ^{29}Si, ^{27}Al MAS NMR are compared with those calculated from thermodynamic modeling. The thermo-dynamic modeling includes the hydration kinetics for the alite, belite, MK and SF phases, employing the degrees of hydration from ^{29}Si MAS NMR, whereas the hydration of C_3A is calculated by the Parrott and Killoh model [10].

Thermodynamic modelling predicts the presence of monocarbonate and ettringite and the absence of monosulphate for all samples, which is in good agreement with the results from XRD. Moreover, the total volume of monocarbonate and ettringite reaches its maximum for the samples with SCM/(SCM + LS) ratios of 0.66 and 0.75, in agreement with the maxima of Al(6) intensity observed by ^{27}Al MAS NMR (c.f., Fig. 2). Inclusion of the kinetic data results in a good prediction of the porosity which agrees well with the observed variations in compressive strength [8]. However, there are some discrepancies between the modeling and the

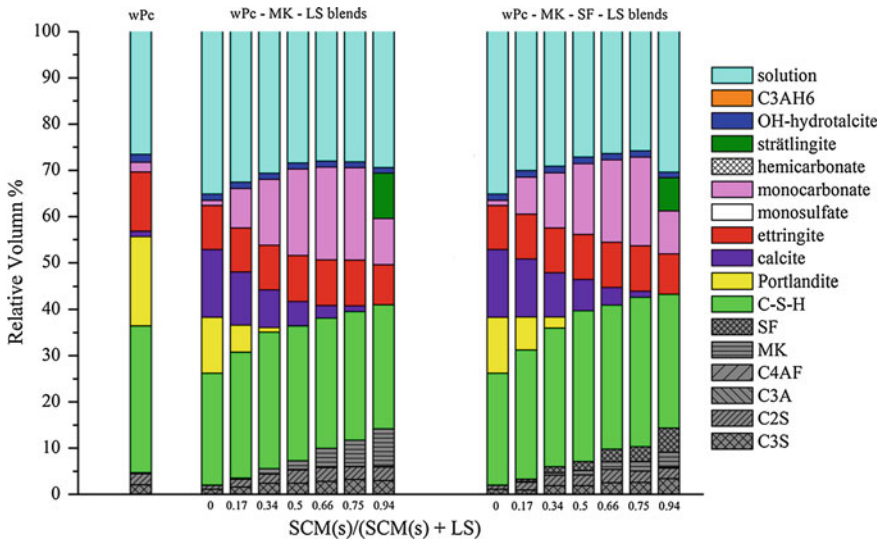

Fig. 3 Phase assemblages for the two series of blended samples after 182 days based on thermodynamic modeling

experimental data. For example, the formation of strätlingite is not predicted for the 0.66MK and 0.75MK blends of the wPc–MK–LS system, whereas ^{27}Al MAS NMR clearly reveals the presence of strätlingite in these samples. In addition, the presence of portlandite is observed by XRD in all the paste samples while it is not predicted by thermodynamic modeling at high SCM replacements. This may reflect the fact that thermodynamic modelling assumes a system in homogeneous equilibrium, which may only be fulfilled locally in heterogeneous cement–SCMs blends. A more detailed discussion on the thermodynamic modeling results will be given in related publications [8, 9] (Fig. 3).

4 Conclusions

The principal conclusions about the two studied systems with a fixed Portland cement replacement level of 35 wt% (wPc– MK–LS and wPc–MK–SF–LS) are as follows.

– The replacement of wPc by SCM and limestone has a significant impact on the formed hydrate phase assemblages, which includes C-A-S-H, portlandite, calcite, mono-carbonate, ettringite, strätlingite and other AFm phases depending on the quantity of MK used.
– The formation of monocarbonate and the stabilization of ettringite correlates well with compressive strength measurements.

- The Al/Si ratio of the C–S–H increases with the MK content, but is almost independent of the hydration time.
- ^{29}Si MAS NMR is found to be a valuable tool in estimating the degrees of reaction for the cement phases and SCM's, *i.e.*, alite, belite, metakaolin and silica fume.
- ^{27}Al MAS NMR is more sensitive for the detection of strätlingite (Al(4) resonance) than XRD, but cannot distinguish between different AFm phases.
- The predictions from thermodynamic modelling of the cement–SCM blends agree well with the experimental data when the degrees of hydration for the principal phases are taken into account.

Acknowledgments The Danish National Advanced Technology Foundation is acknowledged for financial support to the SCM project.

References

1. Lothenbach, B., Scrivener, K., Hooton, D.: Supplementary cementitious materials. Cem. Conc. Res. **41**, 1244–1256 (2011)
2. Hawkins, P., Tennis, P.D., Detwiler, R.J.: The Use of Limestone in Portland Cement: a State-of-the-art Review, EB227, p. 44. Portland Cement Association, Skokie (2003)
3. Tsivilis, S., Chaniotakis, E., Kakali, G., Batis, G.: An analysis of the properties of Portland limestone cements and concrete. Cem. Concr. Comp. **24**, 371–378 (2002)
4. De Weerdt, K., Kjellsen, K.O., Sellevold, E., Justnes, H.: Synergy between fly ash and limestone powder in ternary cements. Cem. Concr. Comp. **33**, 30–38 (2011)
5. Steenberg, M., Herfort, D., Poulsen, S.L., Skibsted, J., Damtoft, J.S.: Composite cement based on Portland cement clinker, limestone and calcined clay. In: Proceedings of the XIII International Congress on the Chemistry of Cement, p. 97 (7 pages). Madrid, 3–8 July 2011
6. Antoni, M., Rossen, J., Martirena, F., Scrivener, K.: Cement substitution by a combination of metakaolin and limestone. Cem. Conc. Res. **42**, 1579–1589 (2012)
7. Dai, Z., Tran, T.T., Skibsted, J.: Aluminum incorporation in the C–S–H Phase of white Portland cement-metakaolin blends studied by 27Al and 29Si MAS NMR spectroscopy. J. Am. Ceram. Soc. **97**, 2662–2671 (2014)
8. Dai, Z., Kunther, W., Garzón, S. F., Herfort, D., Skibsted, J.: Investigation of blended systems of supplementary cementitious materials with white Portland cement and limestone, (in preparation)
9. Kunther, W., Dai, Z., Skibsted, J.: Modeling the hydration of metakaolin blended cements based on hydration kinetics obtained by ^{29}Si MAS NMR spectroscopy, (in preparation)
10. Parrot, L., Killoh, D., 'Prediction of cement hydration', *Proc. Brit. Ceram. Soc.* (1984) 41–53

Heated Montmorillonite: Structure, Reactivity, and Dissolution

Nishant Garg and Jørgen Skibsted

Abstract The dehydroxylated form of the principal 1:1 clay, kaolinite, known as metakaolin, has been widely studied in terms of its structure and reactivity. However, detailed information on the dehydroxylation of the abundant 2:1 clay, montmorillonite, is lacking in this respect. Three montmorillonites, calcined at various temperatures have been characterized by solid-state ^{29}Si MAS NMR. The dehydroxylation (600 – 800 °C) results in progressive distortion of the SiO_4 tetrahedra, followed by crystallization of inert, stable phases at higher temperatures. The dissolution kinetics of a structurally pure montmorillonite, SAz-2, calcined at two different temperatures are found to be in good agreement with its pozzolanic reactivity established in an earlier study. It is also found that SAz-2, calcined at its optimum calcination temperature of 800 °C, undergoes incongruent dissolution reaching a molar Si/Al ratio of 3.7 in a 0.1 M NaOH solution after one day of dissolution. It has been reaffirmed that both the degree of dehydroxylation and the type of structural phases (Q^3/Q^4) have a significant impact on the reactivity of the calcined montmorillonite. The clear identification of inert phases and reactive sites by solid-state NMR may have major implications in the utilization of not only montmorillonites but also other calcined clays.

1 Introduction

An evaluation of the full potential of calcined clays as viable supplementary cementitious materials (SCMs) [1] requires that we look beyond "metakaolin". Metakaolin, which is the highly reactive, metastable phase formed half-way during the kaolinite-mullite thermal transformation sequence, has been widely studied in terms of its structure and pozzolanic reactivity. However, in a direct contrast to this, expansive or 2:1 clays and their calcined versions have been less popular. This

N. Garg (✉) · J. Skibsted
Department of Chemistry and Interdisciplinary Nanoscience, Center (iNANO), Aarhus University, Langelandsgade 140, DK-8000 Aarhus C, Denmark
e-mail: ngarg@chem.au.dk

K. Scrivener and A. Favier (eds.), *Calcined Clays for Sustainable Concrete*, RILEM Bookseries 10, DOI 10.1007/978-94-017-9939-3_15

disinterest in calcination of clays other than kaolinite is primarily due to their intrinsic, low reactivity, – the inferior performance of such clays has been reported in past studies [2, 3]. For montmorillonite, an abundant 2:1 clay, understanding *how* does its structure transforms upon application of heat, *what* are the calcination-temperature ranges which result in optimum performance, and *whether* calcined mont-morillonites dissolve congruently or incongruently, are some of the questions that need to be answered in detail. The objective of the present paper is to provide a partial answer to these questions.

2:1 clay minerals are characterized by one octahedral sheet that is sandwiched between two tetrahedral sheets, as opposed to 1:1 clays where the octahedral and tetrahedral sheets alternate in a one to one manner. 2:1 clay minerals are further classified into families of clays based on the negative electrical charge of the layer which results from isomorphic substitution, and can vary between 0 (*e.g.* talc) to -2 (*e.g.* brittle mica). In 2:1 clays, "smectites" are a loosely defined group of clays whose layer charge is between -0.2 to -0.6 which is in return balanced by positively charged alkaline or alkaline-earth cations together with water molecules. Smectites can be further classified based on the nature and type of octahedral sites present in each mineral. Montmorillonite is a dioctahedral smectite with a dominant trivalent octahedral cation (Al^{3+}) along with significant amounts of magnesium in the octahedral sheet, having the general composition $(M_y^+ \cdot nH_2O)(Al_{2-y}^{3+}Mg_y^{2+})Si_4^{4+}O_{10}(OH)_2$, where M indicates the interlayer cation [4].

In this paper, we analyse the transformation of three montmorillonites (with varying amounts/types of impurities) upon calcination, primarily by solid-state NMR. Then, we bring our focus to the purest (impurity free) montmorillonite in this set and analyse its reactivity and dissolution behaviour after calcination. This structurally pure montmorillonite has recently been studied in detail as reported elsewhere [5]. Here, we build upon these recent findings and shed new light on previously obtained results. Specifically, the dissolution kinetics has been measured for the calcined montmorillonite in an attempt to understand the evolution of the liquid phase as well as the solid phase during a high-pH dissolution. A deeper understanding of water-clay interfacial chemistry is crucial for fully exploiting the potential of calcined clays.

2 Materials and Methods

Three standard montmorillonite clays (STx-1b, SWy-2, SAz-2) were purchased from the Source Clays Repository managed by the Clays Minerals Society (CMS), Purdue University (Indiana, USA). Table 1 shows the chemical composition of the clays. Each clay was finely ground before calcination, and $\sim$1.0 g of clay was placed in a furnace maintained at the desired temperature for two hours, following which the calcined clay was quenched to room temperature. Further details can be found elsewhere [5].

Table 1 Chemical properties of three montmorillonites from the Clay Minerals Society, Purdue, USA

Phase/Compound	SAz-2 (Arizona, USA)	SWy-2 (Wyoming, USA)	STx-1b (Texas, USA)
X-Ray Diffraction (Rietveld Analysis)			
montmorillonite	98 %	75 %	67 %
Others	a) quartz 1 %	a) feldspar: 16 %	a) opal-CT: 30 %
	b) others 1 %	b) quartz: 8 %	
		c) gypsum, mica, kaolinite 1 %	b) quartz, feldspar, kaolinite: 3 %
Elemental analysis (wt%)			
SiO_2	59.65	64.42	72.79
Al_2O_3	19.98	19.11	14.44
Fe_2O_3	1.77	3.88	1.09
MgO	6.73	2.57	2.85
CaO	3.15	1.58	1.82
Na_2O	0.06	1.50	0.26

The data is taken from reference [8] and parallel articles in the same issue

Single-pulse and cross-polarization (CP) ^{29}Si MAS NMR spectra for SAz-2 calcined at selected temperatures were recorded on a Varian INOVA-400 spectrometer (9.39 T), using a homebuilt CP/MAS NMR probe for 7 mm o.d. zirconia (PSZ) and thin-walled Si_3N_4 rotors and spinning speeds of ν_R = 4.0 to 6.0 kHz. An rf field strength of $\gamma B_1/2\pi$ = 42 kHz, a relaxation delay of 1-10 s, and typically 8000 scans were employed. A sample of β-Ca_2SiO_3 (δ_{iso} = –71.33 ppm) was used as a secondary reference sample for the ^{29}Si chemical shifts.

The dissolution experiments involved a home-made, closed batch-type dissolution reactor where the evolution of Al and Si concentrations were recorded as a function of time [6]. The liquid/solid ratio was kept at 4000 to avoid any precipitation and to simulate far-from-equilibrium dissolution conditions. The stirring rate was 300 rpm in a PTFE bottle maintained at 25 °C in an oil bath. The sieved fraction (20 – 100 μm) of the calcined clay was exposed to a 0.1 M NaOH solution for a period of 24 hours. Sample aliquots of 15 mL were collected at selected time intervals and replaced with fresh activating solution. The aliquots were filtered through a 0.2 μm syringe filter, nitrified and acidified with 1 % HNO_3 prior to their measurement by inductively coupled plasma – optical emission spectroscopy (ICP-OES). Matrix-matched standard solutions were used to calibrate the instrument prior to the measurements. Each sample was analysed thrice and the standard deviation was less than 1 %.

3 Results and Discussion

3.1 Structure

Most natural montmorillonites exhibit a single resonance around -93 ± 1 ppm in their ^{29}Si MAS NMR spectra which corresponds to a Q^3-type SiO_4 environment. In the Q^n terminology, n refers to the number of Si-O-Si type bonds (or the number of neighbouring silicons). In the case of these clays, the Q^3-type silicon is also coordinated to two octahedral sites in the octahedral sheet through a triple-coordinated oxygen.

SAz-2 has a single resonance at -93.3 ppm but since both STx-1b and SWy-2 contain silica polymorphs (quartz/cristobalite) as impurities, their overall centres of gravity are shifted slightly towards more negative chemical shifts (Fig. 1). Calcination of the clays up to 200 °C results in dehydration where the majority of the interlayer water is removed, resulting in a $\sim$1 ppm shift towards lower frequencies. However, major structural changes are not induced until 500 °C *i.e.*, until the onset of the dehydroxylation process.

When the montmorillonites are calcined at 600 °C and beyond, there is a radical change in their chemical shift. Likewise, the linewidths of the resonances get subsequently broader suggesting that a dehydroxylated, amorphous structure has begun to form. In the case of SAz-2 a reduction in the signal obtained from ^{29}Si $\{^1$H$\}$ CP/MAS NMR spectra correlated well to the ongoing dehydroxylation process, and by 800 °C all protons were removed from the system [5]. It is interesting to note that similar trends are observed for the other two montmorillonites upon calcination, suggesting that SAz-2 can be considered as a model compound or ideal sample for studying montmorillonites. Even though the dehydroxylation is complete around 800 °C for all three montmorillonites (based on thermogravimetric analysis, not shown here), their structure continues to transform upon calcination as

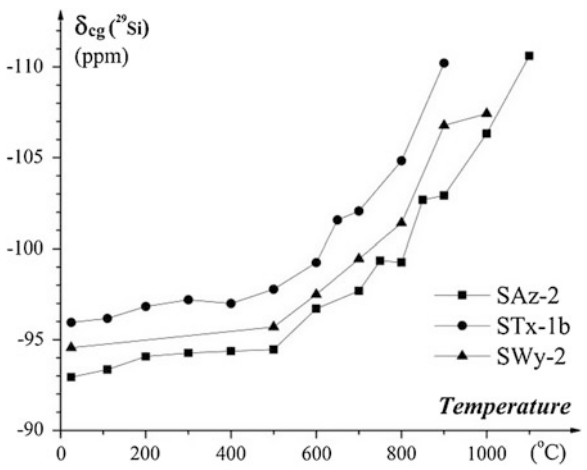

Fig. 1 ^{29}Si chemical shifts (centers of gravity, δ_{cg}(^{29}Si), 4.7 T, ν_R = 7 kHz)) for the three montmorillonites calcined at the listed temperatures for 2 hours

their chemical shifts move further towards lower values. At high temperatures stable Q^4 type condensed phases with chemical shifts in the vicinity of -105 ppm or lower values begin to crystallize in these montmorillonites.

Clear evidence of Q^4-type inert, condensed domains has been found for SAz-2 at temperatures beyond 900 °C [5], and considering that the other two montmorillonites (STx-1b and SWy-2) also follow similar trends as seen in Fig. 1, it can be assumed that their thermal transformation behaviour upon calcination is similar. Thus, it can be concluded that mont-morillonites, *i.e.*, silica rich 2:1 clays, undergo a general thermal decomposition sequence of dehydration, dehydroxylation, amorphization, and crystallization upon calcination.

3.2 Reactivity and Dissolution

In this section, we focus on the behaviour of the ideal montmorillonite, SAz-2, and assume that other montmorillonites will behave more or less similarly. In terms of pozzolanic reactivity, we have recently found that SAz-2 is most reactive at the calcination temperature of 800 °C where a complete dehydroxylation has occurred and no inert, condensed Q^4-type phases have formed [5]. The Q^4-type phases, which can be detected by exploiting the ^{29}Si spin-relaxation behaviour, are known to be highly inert and stable in nature. Here, we show further evidence for the detrimental effect of the Q^4-type phases on the calcined clays performance. If we consider pozzolanic reactivity as essentially a dissolution/precipitation process in an alkaline solution, then a highly dissolvable calcined clay will be desirable. Hence, we selected SAz-2 calcined at two temperatures, 800 °C and 900 °C, which have previously exhibited high and low reactivity, respectively [5]. In Fig. 2 it can be seen that the rate of dissolution of SAz-2 calcined at 800 °C is much higher than that of SAz-2 calcined at 900 °C. This is a clear evidence for the higher reactivity of SAz-2 heated at 800 °C, in agreement with our recent reactivity studies for this mineral [5]. Considering that calcined montmorillonites are essentially multi-oxide

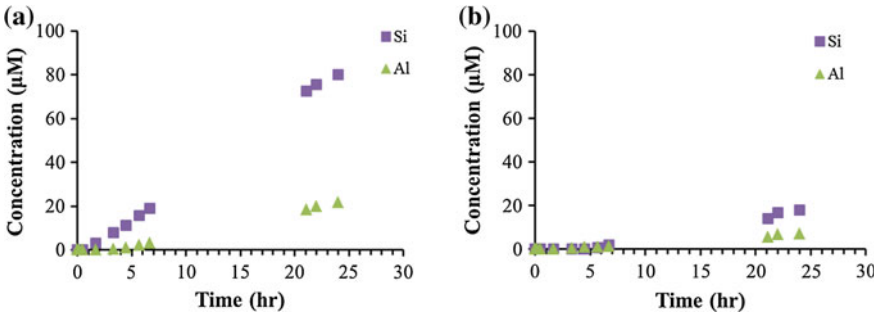

Fig. 2 The dissolution behaviour of SAz-2 calcined at **a** 800 °C and **b** 900 °C in a 0.1 M NaOH solution

glasses in terms of their structure, the highly depolymerized nature of SAz-2 calcined at 800 °C is more likely to undergo hydrolysis in comparison to the polymerized clay heated at 900 °C [7].

A congruent dissolution of SAz-2 should result in a Si/Al molar ratio of ~2.5 in solution based on its elemental composition. Interestingly, SAz-2 calcined at 900 °C seems to be undergoing apparently congruent dissolution (Si/Al = 2.5 at 24 hours) but on the other hand SAz-2 calcined at 800 °C undergoes incongruent dissolution (Si/Al = 3.7 at 24 hours) under the experimental conditions adopted here. At 800 °C, SAz-2 contains a high proportion of an amorphous aluminosilicate phase having weak Si-O-Si/Al bonds from which silicon readily dissolves from the structure and at a rate faster than that of aluminium, resulting in a high solution Si/Al ratio of 3.7. For the sample calcined at 900 °C, a fraction of silicon exists as a separate, inert Q^4-type phase and thereby the total amount of silicon that leaches from the amorphous aluminosilicate phase is significantly reduced. Also, we have seen previously that at 900 °C the aluminium sites are present in a more ordered form as compared to

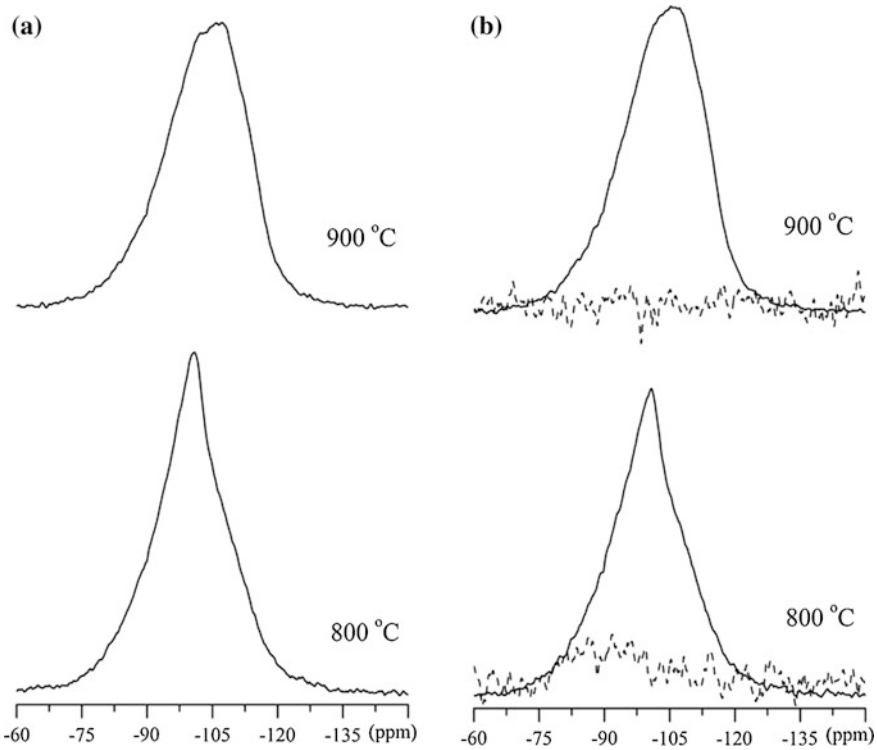

Fig. 3 ^{29}Si MAS NMR spectra (9.39 T, ν_R = 6 kHz) of SAz-2 calcined at 800 and 900 °C. The left-hand spectra (**a**) represent the samples before dissolution whereas the right-hand spectra (**b**) are acquired for samples after one day of dissolution in a 0.1 M NaOH solution. ^{29}Si{^{1}H} CP/MAS NMR spectra (9.39 T, ν_R = 4.0 kHz, τ_{CP} = 1.0 ms) of the samples shown in (**b**) are represented by *dotted lines*

800 °C [5] which supports the observation that lesser amount of aluminium is released from the SAz-2 calcined at 900 °C.

From the ^{29}Si MAS NMR spectra of SAz-2 calcined at 900 °C (Fig. 3), it is obvious that the broad resonance is further shifted to a more negative chemical shift, indicating a dominant presence of Q^4-type phases. No significant differences can be noted between the spectra of the calcined SAz-2 before and after the dissolution at both temperatures and this is probably because only less than 10 % (by weight) of the clay is dissolved in solution after one day.

However, the ^{29}Si{^{1}H} CP/MAS spectra (Fig. 3) offers insight into the silicon sites that were in contact with the excess of hydroxyl groups from the solution. In the ^{29}Si{^{1}H} CP/MAS NMR spectrum of SAz-2 calcined at 800 °C, a broad resonance between -80 to -100 ppm is observed which can be assigned to hydroxylated silanol sites on the external surface of the clay particles. Since the Q^4-type sites at lower chemical shifts form the bulk of the structure, they are far away from surface hydroxyl groups and are thus invisible in the cross-polarization spectra. This observation supports the fact that no signals are observed in the CP/MAS spectrum of SAz-2 calcined at 900 °C because this calcined clay is dominated by condensed, Q^4-type silica sites which influence its dissolution behaviour.

4 Conclusions

Montmorillonites undergo upon calcination a typical thermal transformation sequence of dehydration, dehydroxylation, amorphization, and then crystallization. This sequence has been followed by ^{29}Si MAS NMR for three different montmorillonites with varying amounts of impurities. For the pure montmorillonite, SAz-2, it is concluded that its high reactivity at 800 °C is a combination of factors including a high degree of dehydroxylation, increased disorder, as well as the absence of inert, condensed Q^4-type phases. The dissolution kinetics reported here for SAz-2 are in good agreement with its pozzolanic reactivity reported in a recent study [5]. The optimally calcined montmorillonite appears to undergo incongruent dis-solution – a finding which may have implications on thermodynamic modelling of such clays.

Acknowledgments The Danish National Advanced Technology Foundation is acknowledged for the financial support to the SCM project.

References

1. Lothenbach, B., Scrivener, K., Hooton, R.D.: Supplementary cementitious materials. Cem. Concr. Res. **41**(12), 1244–1256 (2011)

2. He, C., Osbaeck, B., Makovicky, E.: Pozzolanic reactions of six principal clay minerals: activation, reactivity assessments and technological effects. Cem. Concr. Res. **25**(8), 1691–1702 (1995)
3. Fernandez, R., Martirena, F., Scrivener, K.L.: The origin of the pozzolanic activity of calcined clay minerals: a comparison between kaolinite, illite and montmorillonite. Cem. Concr. Res. **41** (1), 113–122 (2011)
4. Bergaya, F., Theng, B.K.G., Lagaly, G.: Handbook of Clay Science. Elsevier, Amsterdam (2011)
5. Garg, N., Skibsted, J.: Thermal activation of a pure montmorillonite clay and its reactivity in cementitious systems. J. Phys. Chem. C **118**(21), 11464–11477 (2014)
6. Garg, N., Skibsted, J.: Manuscript in preparation, (2015)
7. Snellings, R.: Solution-controlled dissolution of supplementary cementitious material glasses at pH 13: the effect of solution composition on glass dissolution rates. J. Am. Ceram. Soc. **96**(8), 2467–2475 (2013)
8. Mermut, A., Cano, A.: Baseline studies of the clay minerals society source clays: chemical analyses of major elements. Clays Clay Miner. **49**(5), 381–386 (2001)

Reactivity of Heated Kaolinite from a Combination of Solid State NMR and Chemical Methods

Cristina Ruiz-Santaquiteria and Jørgen Skibsted

Abstract The effect of the heat-treatment temperature for kaolinite on the types of formed aluminum and silicon sites after dehydroxylation and the relation of these sites to the reactivity of the heated materials are investigated in this work. Kaolinite has been heated to temperatures in the range 500 – 1100 °C in intervals of 50 °C. The reactivity for each sample has been tested in acid media using HF (1 vol.%) and the residues have been stored and dried for further analysis. The heat-treated samples and their corresponding residues are analyzed by solid-state ^{29}Si and ^{27}Al MAS NMR, where comparison of the spectra for the heated clay and the residue provide information about the structurally reactive sites. The chemical methods indicate that kaolinite reaches its maximum reactivity at ~800 °C. The reactivity decreases at higher temperatures as a consequence of the formation of spinel-type and mullite phases, as deduced by ^{27}Al NMR and by the evolution with temperature of the Si/Al ratio for the dissolved phase, determined by ICP analysis. Comparison of normalized ^{29}Si and ^{27}Al NMR spectra for the heated samples and their residues provides the basis for a clear differentiation between different silicon and aluminum environments present in the samples. The ^{27}Al NMR spectra suggest the presence of different tetrahedral aluminum sites and that these sites are correlated with different silicon environments, suggesting that Q^3 and Q^4 silicon sites coexist in metakaolin.

1 Introduction

Kaolinite, $Si_2Al_2O_5(OH)_4$, is a 1:1 layer alumino-silicate clay that has been extensively studied due to its multiple industrial applications. Several applications require that the reactivity is enhanced and it is well-known that a significant increase in reactivity can be achieved when kaolinite is subjected to a heat-treatment process

C. Ruiz-Santaquiteria · J. Skibsted (✉)
Instrument Centre for Solid-State NMR Spectroscopy, Department of Chemistry and Interdisciplinary Nanoscience Center (iNANO), Aarhus University, Aarhus C, Denmark
e-mail: jskib@chem.au.dk

K. Scrivener and A. Favier (eds.), *Calcined Clays for Sustainable Concrete*,
RILEM Bookseries 10, DOI 10.1007/978-94-017-9939-3_16

where the layered structure is dehydrolylated. The dehydroxylation of kaolinite depends partly on the source of material, its particle size and its starts roughly at 450 - 500 °C, resulting in the formation of a metastable and amorphous phase, metakaolin [1]. The optimum thermal treatment is strongly dependent on the specific application and thus, improved knowledge about the structural transformations that kaolinite undergoes during the dehydroxylation process is of great interest. However, the lack of structural order in the heated material complicates structural studies and in this respect, solid-state ^{29}Si and ^{27}Al MAS NMR have proved to be valuable tools since they provide structural information about crystalline as well as amorphous components in composite materials. The structural transformations upon heat-treatment of kaolinite have been widely studied by solid-state NMR methods [2–4], although the characteristic, broad and featureless resonance, observed by ^{29}Si MAS NMR, does not allow a direct differentiation of specific Si sites in the material after dehydroxylation. Thus, identification of specific silicon sites in metakaolin has still not been achieved, partly as a result of the overlap of ^{29}Si chemical shifts for the different $Q^3(n\text{Al})$ and Q^4 (mAl) structural units.

In this study, reactivities of kaolinite samples heated up to 1100 °C are determined in acidic media and both the as-prepared samples and their corresponding residues are studied by means of ^{29}Si and ^{27}Al MAS NMR. Comparison of the normalized ^{29}Si and ^{27}Al NMR spectra for the heated samples and their residues makes it possible to differentiate more clearly between different silicon and aluminum environments that are present in the samples, providing an improved understanding of their evolution with temperature and their impact on reactivity. Moreover, ^{29}Si{^{1}H} CP/MAS NMR experiments have proven useful for selective observation of the hydroxylated sites in the residues after the chemical attack. In addition, ICP-AES experiments have been performed on the filtrates generated by the chemical attack experiments with the aim of determining the Si/Al ratios for the dissolved phases. The results from these analyses are directly correlated with the structural modifications of kaolinite that occur upon heat-treatment.

2 Experimental Procedure

Premium-grade kaolinite, containing a small impurity of quartz ($\sim$2.6 wt%), was obtained from Imerys Minerals, UK. This clay was heat-treated in an open furnace at temperatures between 500 and 1100 °C in intervals of 50 °C, following the same heat-treatment scheme (two hours at the target temperature). For each heated sample, one gram was subjected to chemical attack in 100.0 mL HF (1 vol.%) at room temperature under stirring for five hours. After this exposure, the liquid and residue were separated by filtration and the residue was rinsed with distilled water until a neutral pH was reached. The mass of the solubilized clay was calculated from the weight difference between the starting material and the dried residue. The Si/Al ratio of the dissolved phase was determined from the Si and Al contents in the filtrate, obtained with a Spectro Arcos ICP-AES instrument.

Single-pulse ^{29}Si MAS NMR spectra were recorded on a Varian INOVA-300 spectrometer using a homebuilt CP/MAS probe for 5 mm o.d. zirconia (PSZ) rotors, a spinning speed of ν_R = 10.0 kHz and a relaxation delay of 30 s. The ^{29}Si{^{1}H} CP/MAS NMR spectra were acquired with the same probe and rotor, using ν_R = 4.0 kHz and two different CP contact times of 1.0 and 5.0 ms. The ^{27}Al MAS NMR spectra were recorded on a Varian Direct-Drive VNMR-600 spectrometer, using a homebuilt CP/MAS probe for 4 mm o.d. zirconia rotors, a spinning speed of ν_R = 13.0 kHz, and a 2-s relaxation delay.

3 Results

The fraction of dissolved material for the heated kaolinite samples in the 1.0 vol.% HF solution is shown in Fig. 1a as a function of the heat-treatment temperature. Even a major part of untreated kaolinite is dissolved under these aggressive conditions. The percentage of dissolved material increases with temperature until 550 °C where a full dehydroxylation of kaolinite is expected to have occurred. Only minor variations are observed in the range 500 – 900 °C, in accordance with the presence of a metastable phase, metakaolin, in this temperature interval. The reactivity reaches a maximum at 800 °C and decreases from 900 – 1100 °C, the latter associated with the transformation of metakaolin into a spinel-type phase and mullite. The decrease in reactivity from 900 – 1100 °C is accompanied by an increase of the Si/Al molar ratio for the dissolved phase (Fig. 1b), which is ascribed to the formation of the aluminate-rich spinel-type and mullite phases at higher temperatures. These phases exhibit a higher degree of structural order than metakaolin and thus, the dissolution of aluminate species from these phases is expected to be lower. Kaolinite and metakaolin have a Si/Al molar ratio of 1.0 whereas slightly lower ratios are observed for the dissolved phase of kaolinite and the heated samples in the range 500 – 900 °C.

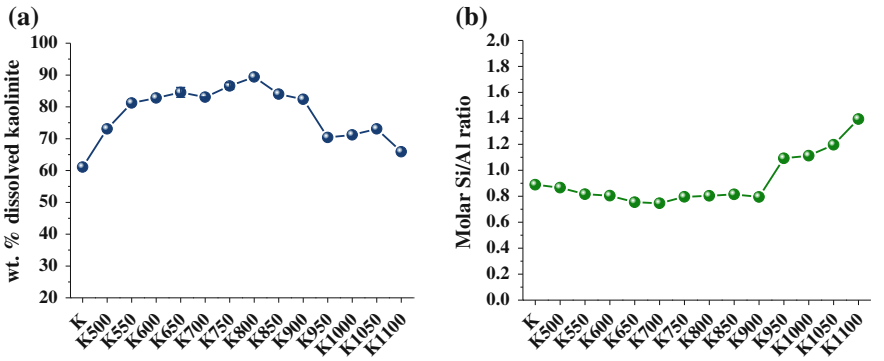

Fig. 1 **a** Fraction (wt%) of dissolved material in the 1.0 vol.% HF solution as a function of the heating temperature. **b** The Si/Al molar ratio of the dissolved phase determined by ICP-AES analyses of the filtrates

This indicates a preferential dissolution of aluminate species and thereby a slightly incongruent dissolution of silicon and aluminum.

^{29}Si MAS NMR spectra of selected heated kaolinite samples and their corresponding residues from the HF experiments are shown in Fig. 2. The deconvolutions of the individual spectra have been carried out using the same number of resonances and only minor variations of their chemical shifts and linewidths.

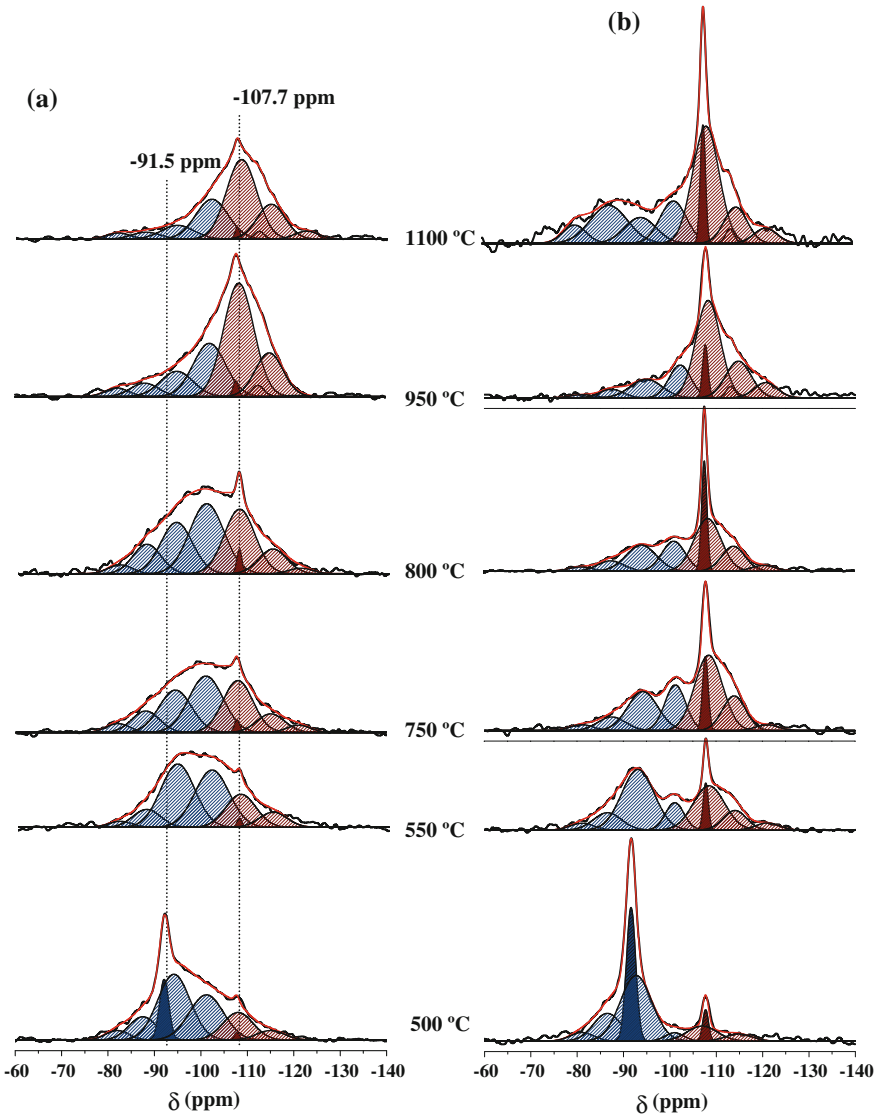

Fig. 2 ^{29}Si MAS NMR spectra (7.1 T, ν_R = 10.0 kHz) of **a** selected heat-treated kaolinite samples and **b** their corresponding residues from the acid attack experiments

Comparison of the spectra and deconvolutions for the heat-treated samples and their residues reveals that different silicon sites in the clay material exhibit different reactivities. The spectra of the residues include stronger signals from quartz (-107.7 ppm) than the heated samples, reflecting that quartz is not affected by the acid attack. Moreover, a small fraction of kaolinite (-91.5 ppm) is observed for the sample heated at 500 °C and a strong signal from kaolinite is also observed for the 500 °C residue, as a result of the lower reactivity of kaolinite compared to metakaolin. The contribution to the spectra from metakaolin is simulated by four resonances (dashed blue peaks in Fig. 2) located at -82 ppm, -84 ppm, -94.5 ppm and -101 ppm and by three resonances centered at lower chemical shifts than quartz (dashed red peaks) at -108 ppm, -115 ppm and -121 ppm. The chemical shifts of the latter three peaks strongly suggest that they originate from $Q^4(0Al)$ silicon sites, either as a part of the metakaolin structure or arising from an amorphous silica phase present in the samples. From the deconvolutions of the ^{29}Si MAS NMR spectra of the residues, it is apparent that the three $Q^4(0Al)$ peaks gives a major contribution to these spectra, demon-strating that these fully condensed SiO_4 units are less reactive than the other components of the metakaolin structure. The center of gravity for the overall peak from metakaolin is observed at -101 ppm for the samples heated in the temperature range 550 – 850 °C. From 900 to 1100 °C, the center of gravity shifts from -101 ppm to -108 ppm, reflecting the formation of the spinel-type and mullite phases along with silica. Moreover, for the samples heated at 950 °C and above, a narrow resonance around -112 ppm appears in the spectra which intensity increases when the heating temperature is raised. This peak reflects a partial crystallization of silica [5], and thereby the formation of a less-reactive phase, in agreement with the reactivity measurements in Fig. 1.

$^1H \rightarrow {}^{29}Si$ cross-polarization (CP) NMR spectra of the heated kaolinite samples and residues also provide useful information since they only contain resonances from silicon sites with H atoms in their near vicinity. For the samples heated above 500 °C, no resonances are observed by $^{29}Si\{^1H\}$ CP/MAS NMR (spectra not shown), in agreement with the absence of Si–OH bonds and thereby fully dehydroxylated samples. However, distinct resonances are observed at roughly -101 ppm and -108 ppm for the residues of the samples heated at 750 and 850 °C (Fig. 3). The peak at -101 ppm is strongly enhanced in the CP/MAS NMR spectra acquired with the short contact time (1.0 ms), indicating the presence of strong ^1H – ^{29}Si dipolar couplings for these sites. Highest intensity for the -108 ppm resonance is observed when a long contact time (5.0 ms) is employed, reflecting somewhat weaker dipolar couplings for these sites. Thus, the resonances at -101 and -108 ppm are assigned to $(SiO)_3Si^*$-OH and (SiO)Si*OSi-OH sites, respectively, where the latter peak reflects a fully condensed $Q^4(0Al)$ site with a Si-OH sites in its next-nearest coordination sphere. The two types of silicon sites are present at the surface of the metakaolin/silica phases. The absence of these peaks in the $^{29}Si\{^1H\}$ CP/MAS NMR spectrum of the residue of the sample heated at 950 °C demonstrates that a more ordered/crystalline silica phase has formed, which surface is not hydroxylated during exposure to the HF solution.

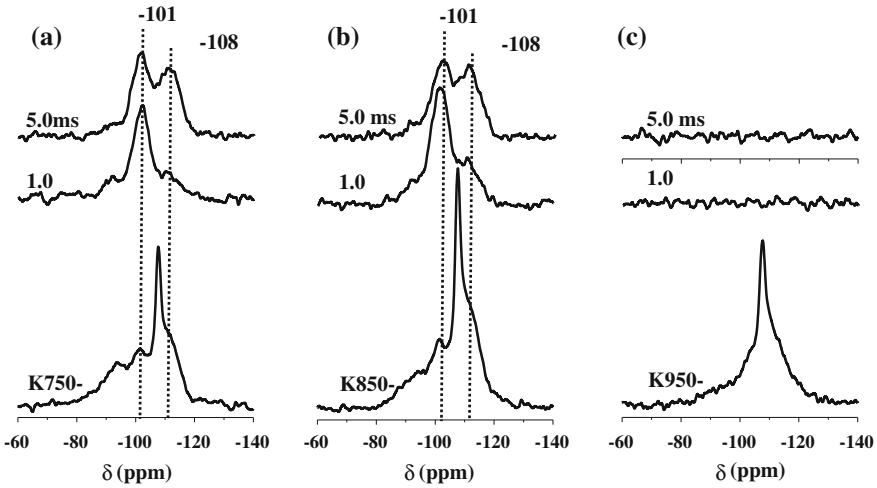

Fig. 3 $^{29}Si\{^{1}H\}$ CP/MAS NMR spectra of the residues of kaolinite heated at **a** 750 °C, **b** 850 °C, and **c** 950 °C acquired with CP contact times of 1.0 and 5.0 ms. The corresponding single-pulse ^{29}Si MAS NMR spectra of the residues are shown in the *bottom row*

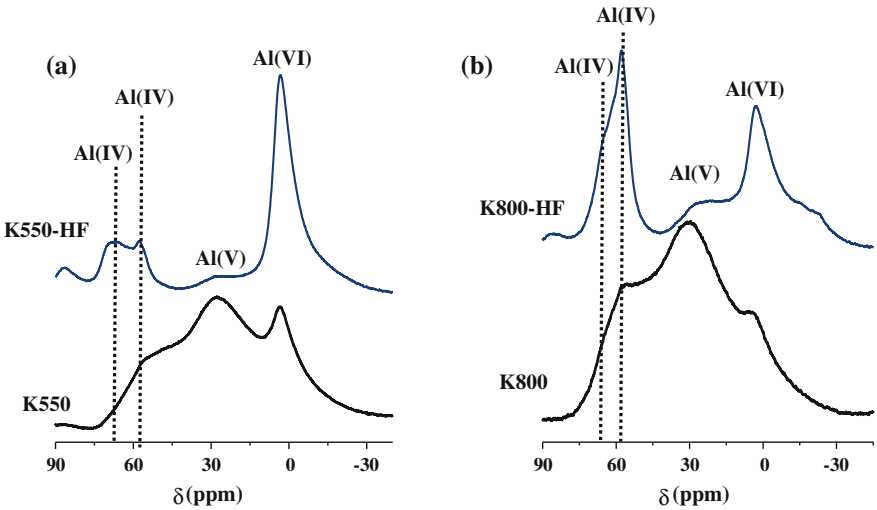

Fig. 4 ^{27}Al MAS NMR spectra (14.1 T, ν_R = 13.0 kHz) of kaolinite heated at **a** 550 °C and **b** 800 °C and of their corresponding residues from the HF solution (*upper row* spectra)

The ^{27}Al MAS NMR spectra of the heated samples reveal that for temperatures below ~900 °C, the samples include Al in tetrahedral, five-fold and octahedral coordination whose relative intensities vary with temperature. Figure 4 shows ^{27}Al NMR spectra of the samples heated at 550 and 800 °C and their residues from the

HF solutions. The spectra of the heated samples contain overlapping centerbands from the three different coordination states, which are affected by second-order quadrupolar effects, preventing a straightforward deconvolution analysis. However, the peak at 35 ppm originates from five-fold coordinated Al and it is clearly seen that this component has almost completely vanished in the spectra of the residues, demonstrating that the pentahedral Al sites are highly reactive. In addition, the residues contain at least two different AlO_4 sites, which may also be present in the samples before acid attack, and a rather narrow AlO_6 resonance which may arise from hydroxylated surface sites.

4 Conclusions

The combination of chemical procedures and solid-state MAS NMR represents a valuable approach to gain new information about the nanostructure and reactivity of heat-treated kaolinite samples. Comparison of the ^{29}Si NMR spectra for the heated clays and their residues allow identification of different silicate environments in metakaolin and characterization of the chemical reactivity for these silicate species. In addition to metakaolin, an amorphous silica phase is formed which becomes predominant at $\sim$900 °C and crystallizes out at higher heating temperatures. ^{29}Si $\{^1H\}$ CP/MAS NMR studies of the residues from acid attack have revealed that this phase is less reactive than metakaolin and almost inert in its ordered form at heating temperatures above 900 °C. These structural changes are also reflected in the reactivity measurements where a decrease is observed at 900 °C and above. Finally, ^{27}Al MAS NMR spectra of the heated samples and their residues have shown that the fivefold coordinated Al sites in metakaolin is the most reactive Al sites and that almost a full degree of reaction is observed for these sites in the chemical attack experiments.

Acknowledgments The Danish Council for Strategic Research is acknowledged for financial support to the LowE-CEM project.

References

1. Ramachandran, V.S., Paroli, R.M., Beaudoin, J.J, Delgado, A.H.: Handbook of Thermal Analysis of Construction Materials, 1st edn. Noyes publications (2002)
2. Meinhold, R.H., MacKenzie, K.J.D., Brown, I.W.M.: Thermal reactions of kaolinite studied by solid state ^{27}Al and ^{29}Si NMR. J. Mater. Sci. Lett. **4**, 163–166 (1985)
3. Rocha, J., Klinowski, J.: ^{29}Si and ^{27}Al magic-angle-spinning NMR studies of the thermal transformation of kaolinite. Phys. Chem. Miner. **17**, 179–186 (1990)

4. Sanz, J., Madani, A., Serratosa, J.M., Moya, J.S., Aza, S.: Aluminum-27 and Silicon-29 magic-angle spinning nuclear magnetic resonance study of the kaolinite-mullite transformations. J. Am. Ceram. Soc. **71**, 418–421 (1988)
5. Engelhardt, G., Michel, D.: High-Resolution Solid-State NMR of Silicates and Zeolites. Wiley, New York (1987)

Durability of Portland Cement Blends Including Calcined Clay and Limestone: Interactions with Sulfate, Chloride and Carbonate Ions

Zhenguo Shi, Mette R. Geiker, Klaartje De Weerdt, Barbara Lothenbach, Josef Kaufmann, Wolfgang Kunther, Sergio Ferreiro, Duncan Herfort and Jørgen Skibsted

Abstract The durability has been investigated for mortars made from a pure Portland cement (CEM I) and five Portland cement – SCM blends, using a cement replacement level of 35 wt% and the following SCM's: (*i*) pure limestone, (*ii*) pure metakaolin, (*iii*) metakaolin and limestone (3:1 w/w), (*iv*) metakaolin and silica fume, and (*v*) metakaolin, silica fume and limestone. The blends with metakaolin and silica fume employ a fixed ratio for these components which mimics the alumina-silicate composition of a 2:1 clay (*i.e.*, montmorillonite). All mortars were demoulded after hydration for one day and cured saturated in water at 20 °C for 90 days prior to exposure. Expansions induced by sulfate attack, chloride profiles, and carbonation depths were measured to investigate the durability performances of the mortars. Porosity and pore connectivity were analysed before exposure by mercury intrusion porosimetry. The results show that mortars incorporating metakaolin, independent of additional silica fume or limestone, all exhibit very high resistance towards sulfate attack and chloride ingress, but are vulnerable to carbonation. The binary Portland cement – limestone blend is most susceptible to all types of studied chemical attacks, as expected. The pure Portland cement exhibits poor resistance to sulfate attack and chloride ingress, but high resistance to

Z. Shi (✉) · W. Kunther · J. Skibsted
Department of Chemistry and Interdisciplinary Nanoscience, Center (iNANO), Aarhus University, Langelandsgade 140, 8000 Aarhus C, Denmark
e-mail: zshi@chem.au.dk

M.R. Geiker
Department of Structural Engineering, Norwegian University of Science and Technology, Trondheim, Norway

K. De Weerdt
SINTEF Building and Infrastructure, Trondheim, Norway

B. Lothenbach · J. Kaufmann
Laboratory for Concrete and Construction Chemistry, Empa, Dübendorf, Switzerland

S. Ferreiro · D. Herfort
Cementir Holding S.p.A, Aalborg Portland A/S, Aalborg, Denmark

K. Scrivener and A. Favier (eds.), *Calcined Clays for Sustainable Concrete*, RILEM Bookseries 10, DOI 10.1007/978-94-017-9939-3_17

carbonation. The observed performances for the different blends can be explained based on their microstructure and phase assemblages. For example, the presence of metakaolin increases the chloride-ion binding capacity and enhances chloride resistance by the low pore connectivity present in the hydrated blends with metakaolin.

1 Introduction

A major part of recent studies of calcined clays as supplementary cementitious materials (SCM's) in Portland cement blends has focused on the reactivity and the impact on physical performance (*e.g.*, compressive strength) of the calcined clays in cement blends. Less attention has been paid to durability studies of these new materials. However, these types of chemical and structural analyses are also required prior to an industrial realization. The durability of Portland cement – calcined clay blends, with and without additions of limestone, is investigated in the present work by studies of mortars interactions with sulfate and chloride solutions as well as CO_2, using standardized or specifically developed procedures for characterization of sulfate attack, chloride ingress and carbonation.

2 Experimental

2.1 Materials

The binders used in this study were white Portland cement (wPc, CEM I), limestone (LS), metakaolin (MK) and white silica fume (SF). The wPc itself included 3.1 wt% LS, 4.1 wt% gypsum and 2.7 % wt% free lime. The MK was produced in the laboratory by thermal treatment of kaolinite at 550 °C for 20 h. The chemical compositions of the starting materials, determined by X-ray fluorescence (XRF), are given in Table 1. To prepare the mortars a CEN reference sand (Normsand) was used, which has a silica content of at least 98 wt%. The workability of the mortars was adjusted to the same level by addition of small amounts of the superplasticizer (SP), Glenium 27.

Table 1 Bulk chemical compositions of the raw materials (wt%)

	SiO_2	Al_2O_3	Fe_2O_3	CaO	MgO	K_2O	Na_2O	SO_3	TiO_2	P_2O_5	LOI
wPc	21.81	3.56	0.24	66.13	1.10	0.43	0.041	3.371	0.309	0.042	2.57
LS	3.92	0.33	0.14	53.73	0.35	0.05	0.08	0.05	0.02	0.10	41.8
MK	52.84	39.49	1.42	0.22	0.483	0.998	0.05	0.061	0.88	0.105	3.55
SF	90.44	0.34	0.03	1.37	0.93	1.87	0.19	0.30	0	0.55	3.35

2.2 Binder Compositions and Mortar Preparations

The compositions of the blends (Table 2) targeted an incorporation of 35 wt% SCM for the white Portland clinker (wPc*). This results in a real binder composition of 31.9 wt% replacement of white Portland cement (wPc), considering the small amounts of LS and gypsum in the wPc. MK is a 1:1 clay with an ideal Si/Al = 1.0 molar ratio. However, the bulk ratio of Si/Al = 1.13 for the actual sample of MK accounts for a 2.0 wt% quartz impurity. The MS and MSL blends (Table 2) employ a combination of MK and SF in a ratio that mimics a 2:1 clay (molar ratio: Si/Al = 2.0). The used ratio of Si/Al = 2.36 is higher than the ideal ratio of 2.0 in order to account for the partial substitution of Al by Mg in the octahedral layers, which has been found in the real montmorillonite clays.

The designed blends were used to produce mortars with a constant water to binder ratio by weight (w/b = 0.5) and a constant binder to sand ratio by weight (b/s = 1:3). The dosage of SP was adjusted to the content of MK (SP/MK = 0.07) or of MK and SF (SP/(MK + SF) = 0.04), both ratios by weight.

Mortars were cast in different moulds depending on the type of durability test. After demoulding, the mortars were cured saturated in water at 20 °C for 91 days prior to the different exposure conditions. From the measured degrees of hydration for the principal phases in the mortars, using ^{27}Al and ^{29}Si MAS NMR analyses of similar paste samples, the mortars can be considered as nearly fully hydrated.

2.3 Methods

The physical properties of the mortars were characterized prior to the durability tests. Porosity and pore connectivity were analysed using mercury intrusion porosimetry (MIP).

Mortar prisms of 20 × 20 × 160 mm^3 were prepared for the sulfate resistance tests, which were performed with a concentration of 16 g/L (0.11 M) Na_2SO_4 at 20 °C. The solution was exchanged weekly during the early exposure to maintain a high and as far as possible constant sulfate concentration. The length and weight of

Table 2 Compositions of the Portland cement — SCM blends

Blend	Components	Ratio	wPc	MK	SF	LS	Si/Al
			(%)	(%)	(%)	(%)	(MK + SF)
P	White Portland cement	–	100	0	0	0	–
L	MK/(MK + LS)	0	68.1	0	0	31.9	–
ML	MK/(MK + LS)	0.75	68.1	25.5	0	6.4	1.13
M	MK/(MK + LS)	0.94	68.1	31.9	0	0	1.13
MSL	(MK + SF)/(MK + SF + LS)	0.75	68.1	15.6	9.88	6.4	2.36
MS	(MK + SF)/(MK + SF + LS)	0.94	68.1	19.5	12.4	0	2.36

the mortars were measured every week. Mortar cylinders with a diameter of 50 mm and a height of 35 mm, were prepared for the chloride resistance tests. One cut end-surface of the mortars was exposed to 700 mL of a 2.8 M NaCl solution for 35 days, followed by a grinding process where layers of increasing thickness (1 – 4 mm) were gradually removed for one exposed surface to collect powder for a chloride profile analysis. The total chloride concentration of the powder samples, collected for each layer, was measured by titration with 0.01 M $AgNO_3$. Mortar prisms for carbonation, 40 × 40 × 160 mm^3, were exposed to a controlled atmosphere with 1.0 vol.% CO_2 in an incubator at 20 °C. The relative humidity (RH) was set to target a value of 57 %, which matches the optimum RH in the range ∼40 – 70 % to maximize carbonation reactions [1].

3 Results

Porosity and pore connectivity of the mortars prior to the durability tests were analysed by MIP. Typical intrusion curves of the mortars after the first and second intrusions are shown in Figs. 1 and 2. It is observed that the incorporation of MK in the mortars results in a refined microstructure, as seen by the reduced pore connectivity as compared to the reference mortar (P), although their total intruded porosities are almost identical (Fig. 1). Furthermore, comparison of the first and second intrusion curves indicates that the mortars incorporating MK have a larger fraction of "ink-bottle pores" [2] as compared to the reference mortar (P). The MIP

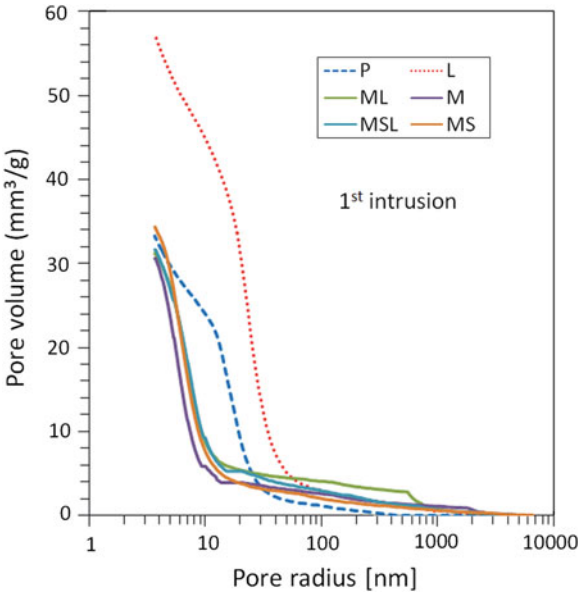

Fig. 1 Intrusion curves from the first MIP intrusion cycle for the six mortars

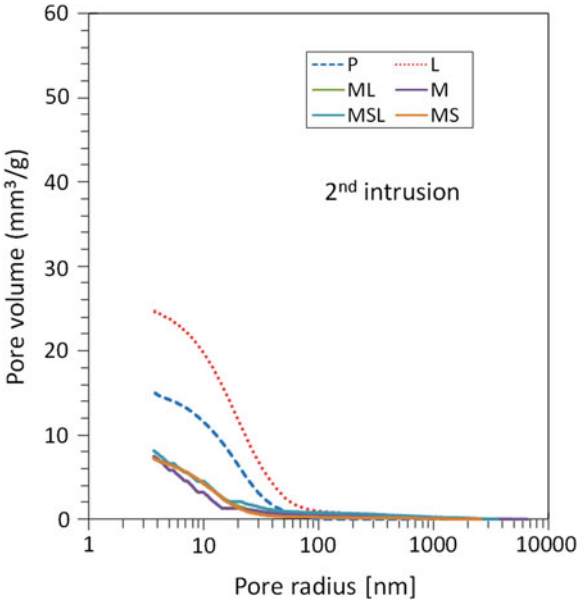

Fig. 2 Intrusion curves from the second MIP intrusion cycle for the six mortars

results also reveal that the binary wPc – LS blend has an increased total porosity and coarser threshold pore radii, as compared to the P mortar.

To illustrate the early-age performance of the mortars exposed to the sodium sulfate solution, the expansion of the mortars is plotted as function of the square root of time as in Fig. 3. The expansion of the P and L mortars increases significantly after two weeks of exposure. In general, the L mortar exhibits a higher expansion than the P mortar within the studied exposure for one year. However, the difference between the P and L mortars becomes smaller with time and has vanished after 400 days. Both mortars exhibit poor resistance against sulfate attack. The other four mortars including MK with and without SF or LS exhibit a very similar and a very high resistance to sulfate attack.

The mass change for the mortars is controlled by several factors such as ingress of sodium sulfate solution and leaching of cement hydrates. From the measured high degrees of hydration for the principal phases in the mortars, by ^{27}Al and ^{29}Si MAS NMR analyses of similar paste samples, phase changes should mainly be attributed to interactions between sulfate ions and the cement hydrates. Figure 4 shows the mass changes for the studied mortars where the values are normalized to the measurements after seven days of exposure. The results indicate that the relative mass of the L mortar increases with exposure time, which is supported by the observation of increased expansion. In contrast, the four mortars with MK demonstrate a decrease in mass where the decreasing rate becomes less pronounced during the later stage. It is apparent that the mass increase for the L mortar is attributed to the formation of sulfate-containing phases during the sulfate attack and that the decrease of mass for the MK mortars is attributed to leaching of the mortars.

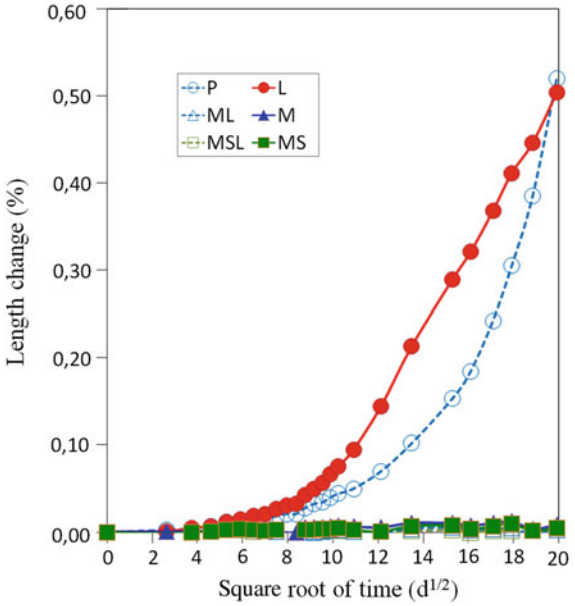

Fig. 3 Length changes for the mortar bars immersed in the Na_2SO_4 solution at 20 °C

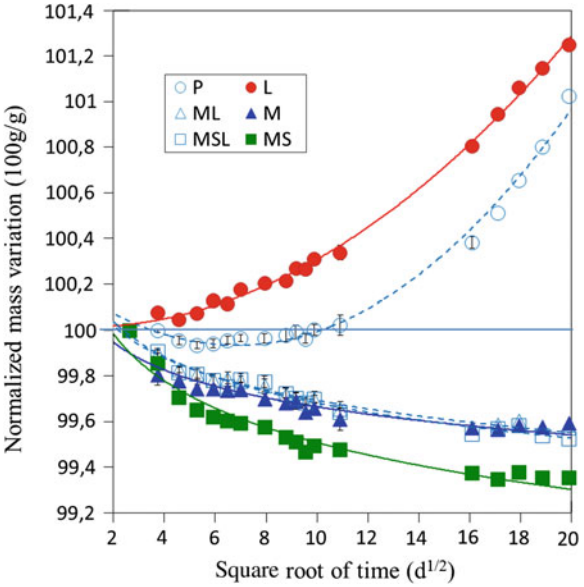

Fig. 4 Normalized mass variations for the mortar bars immersed in the Na_2SO_4 solution at 20 °C

It should be noticed that an initial decrease and then increase of the mass for the P mortar is observed. This clearly demonstrates the competition between leaching of hydrates and formation of sulfate-containing phases, which has also been reported in the literature [3].

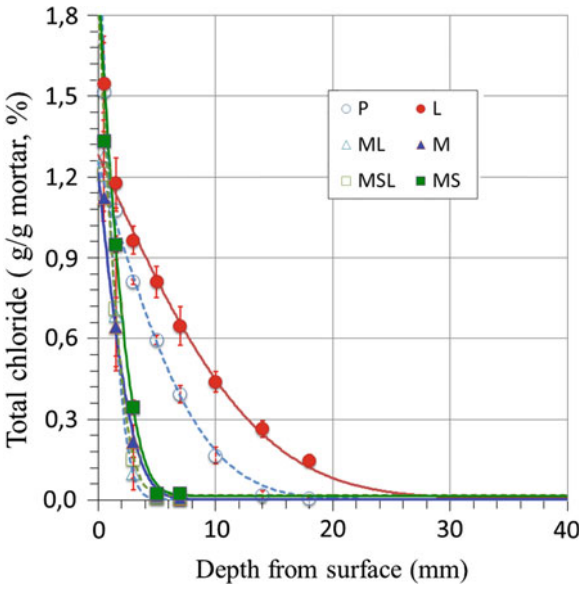

Fig. 5 Chloride profiles for the mortars exposed to the 2.8 M NaCl solution for 35 days

The total chloride profiles for all mortars exposed to a 2.8 M NaCl solution for 35 days are illustrated in Fig. 5 and show the typical decrease of total chloride content with increasing depth from the exposed surface. The P and L mortars exhibit higher total chloride contents than the four MK mortars. The L mortar contains a higher amount of chloride than the P mortar at any depth. The total chloride contents of the mortars including MK decrease more significantly than the contents for the P and L mortars. No differences in the total chloride profiles can be observed for the MK mortars. It should be noticed that the penetration depths of chloride ions in the MK mortars are below 5 mm from the exposed surface. Such shallow depths indicate a very high resistance to chloride ingress for these mortars.

The carbonation depths measured by the phenolphthalein spray method are plotted as a function of the square root of time in Fig. 6. The standard deviations reflect variations in the carbonation front indicated by phenolphthalein, which is influenced by air voids and larger sand particles. Since the mortars were kept saturated in demineralized water, no initial carbonation for any of the mortars was observed. A significant carbonation is observed for all SCM-containing mortars after 7 days of exposure to 1 vol.% CO_2, at 57 % RH, and the depths increase linearly as function of the square root of time. An exception is the P mortar which displays a very slow carbonation process. It is apparent that the L mortar is most vulnerable to carbonation and that highest resistance is observed for the P mortar.

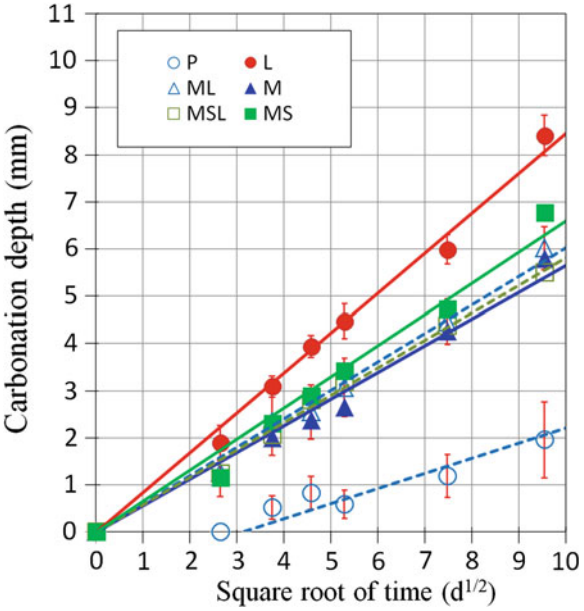

Fig. 6 Carbonation depths for the mortars exposed to 1 vol.% CO_2 at 57 % RH

4 Discussion

The performance of the different mortars exposed to Na_2SO_4 and NaCl solutions can be explained by the variations in porosity and pore connectivity. The L mortars have the largest total porosity and pore connectivity and thus, it is not surprising that the sulfate and chloride ions can easily enter the pores and react with the cement hydrates. Comparison of the four MK mortars with the reference (P) indicates that the MK binders exhibit a very high sulfate and chloride resistance, shown by the shallow chloride penetration depths (less than 5 mm) and the small mass changes during sulfate exposure for the MK mortars. This is related to their very fine pore networks. Schmidt et al. [4] have observed that the main impact of LS additions on the resistance to sulfate degradation is a physical effect, *e.g.*, changes of the porosity where a few percent of LS decreases the porosity and 25 % LS increases the porosity, resulting in a higher and lower resistance to sulfates, respectively. In the present work, it is demonstrated that the sulfate resistance of the prisms is not solely affected by the porosity, but also the pore connectivity, since the total porosities of the P and MK mortars are identical as shown in Fig. 1. In contrast, the carbonation performance is not dominated by porosity and pore connectivity, especially not for MK mortars. The carbonation is mainly dependent on the chemical composition, *i.e.*, the amount of portlandite.

5 Conclusions

The L mortar exhibits lowest performance in all the durability tests in this study. The P mortar shows poor resistance to sulfate attack and chloride ingress, but highest resistance to carbonation. The MK mortars have the highest chloride and sulfate resistance, but a poor resistance towards carbonation. The performance with respect to chloride ingress and sulfate attack can be described as a physical effect, where the pore connectivity is more important for the durability than the total porosity for MK mortars. The carbonation performance of the MK mortars cannot solely be explained by physical effects since the presence of portlandite has a major impact on the carbonation rate.

Acknowledgments The Danish Council for Strategic Research is acknowledged for financial support to the LowE-CEM project.

References

1. Morandeau, A., Mickaël, T., Patrick, D.: Investigation of the carbonation mechanism of CH and CSH in terms of kinetics, microstructure changes and moisture properties. Cem. Conc. Res. **56**, 153–170 (2014)
2. Kaufmann, J.: Pore space analysis of cement-based materials by combined nitrogen sorption–wood's metal impregnation and multi-cycle mercury intrusion. Cem. Concr. Comp. **32**, 514–522 (2010)
3. Rozière, E., Loukili, A., El Hachem, R., Grondin, F.: Durability of concrete exposed to leaching and external sulphate attacks. Cem. Conc. Res. **39**, 1188–1198 (2009)
4. Schmidt, T., Lothenbach, B., Romer, M., Neuenschwander, J., Scrivener, K.: Physical and microstructural aspects of sulfate attack on ordinary and limestone blended Portland cements. Cem. Conc. Res. **39**, 1111–1121 (2009)

Thermodynamic Modeling of Portland Cement—Metakaolin—Limestone Blends

Wolfgang Kunther, Zhuo Dai and Jørgen Skibsted

Abstract The partial replacement of Portland cement by different supplementary cementitious materials (SCM´s) has been investigated extensively in recent years with the aim of reducing the embodied CO_2 of blended Portland cements. In this work, we have utilized the maximum cement substitution of 35 wt%, according to the standard EN 197-1, and investigated the effect of changing the metakaolin/limestone ratio on the hydrating phase assemblages. Paste samples of the hydrated cement blends have been characterized by XRD, ^{27}Al and ^{29}Si MAS NMR spectroscopy and the results are compared with thermodynamic modeling. ^{29}Si MAS NMR is a very valuable technique for studies of hydrated cement blends, since it allows detection of amorphous and crystalline phases in an equal manner. The determined degrees of hydration have been implemented into thermodynamic modeling to improve the modeling approach and thereby the agreement between predicted and observed phase assemblages. A simple equation has been established for implementation of the hydration kinetics which employs only one mass and one dissolution-rate parameter to describe the hydration successfully. The agreement between the experimental and modeled phase assemblages improves significantly when the hydration kinetics for the anhydrous alite, belite, and amorphous MK phases are implemented. The phase assemblages of the hydrated blends change only for very high MK contents from a C(-A)-S-H, calcite, portlandite, monocarbonate and ettringite system to a phase assemblage that in addition contains strätlingite and other AFm phases.

W. Kunther (✉) · Z. Dai · J. Skibsted
Department of Chemistry and Interdisciplinary Nanoscience Center (iNANO), Aarhus University, Langelandsgade 140, 8000 Aarhus C, Denmark
e-mail: kunther@chem.au.dk

K. Scrivener and A. Favier (eds.), *Calcined Clays for Sustainable Concrete*, RILEM Bookseries 10, DOI 10.1007/978-94-017-9939-3_18

1 Introduction

Limestone (LS) is nowadays commonly used in commercial cements to reduce the embodied CO_2 of cements by diluting the clinker content. This substitution reduces some performance parameters, like the compressive strength, with increasing replacement levels [1, 2]. The partial replacement of Portland cement by different supplementary cementitious materials (SCM´s) has been investigated extensively in recent years with the aim of reducing the embodied CO_2 of blended Portland cements while maintaining its performance. Metakaolin (MK) is an ideal compound to model aluminosilicate-rich SCM´s in cement blends due to its high reactivity. For a few percent limestone additions, it has been shown that the combination of limestone with aluminosilicate-rich SCM´s increases the compressive strength of a binder beyond the expectations for the individual components [3, 4]. The observed strength increase was correlated to an increased formation of monocarbonate [4] and explained by a decrease in porosity as ettringite - a very voluminous hydrate phase - is stabilized [3, 5].

2 Materials and Methods

In this work we have utilized the maximum cement substitution level (35 wt%), according to the European cement standard EN 197-1, and investigated the effect of variations in the MK and LS ratio for the hydrating blends. Table 1 contains the most important chemical and mineralogical composition data for the materials used. Further experimental [6] and modeling details [7] will be described in related publications. XRD and ^{27}Al, ^{29}Si MAS NMR spectroscopy are used to characterize the hydration of the Portland cement – metakaolin – limestone blends and the resulting phase assemblages. XRD is used to specify and verify the phase assemblages in general with a focus on a distinction of the different AFm phases.

The ferrite clinker phase has not been considered since the minimal iron content in the wPc can completely be accommodated in alite and belite [8]. The degree of hydration for the calcium aluminate phase ($Ca_3Al_2O_6$, C_3A) has not been considered, since the ^{27}Al MAS NMR spectra reveal that this phase reacted completely after a few days of hydration. Thus, a full degree of reaction for the C_3A phase is employed for all hydration times.

Table 1 Oxide composition and mineralogy for the white Portland cement (wPc), limestone (LS) and metakaolin (MK)

	SiO_2	Al_2O_3	Fe_2O_3	CaO	L.o.I.	calcite	C_3S	C_2S	C_3A
wPc (wt%)	21.8	3.6	0.2	66.1	2.6	3.1	64.9	16.9	7.9
LS (wt%)	3.9	0.3	0.1	53.7	41.8	94.0	–	–	–
MK (wt%)	54.8	39.5	1.4	0.22	3.6	–	–	–	–

3 Results and Discussion

3.1 Approach of the Investigation

Hydration kinetics is mediated by the pore solution, but this aspect is not sufficiently understood to be implemented directly in thermodynamic modeling. Empirical approaches, for example the Parrott and Killoh model [9], assume independent hydration reactions for the individual clinker phases and utilize experimental hydration kinetics data for the individual phases to model the hydration of cement. In this work, we have determined the degree of hydration for alite, belite, and metakaolin by ^{29}Si MAS NMR. In addition, ^{27}Al MAS NMR of the hydrated blends reveals that all C_3A has reacted after a few days of hydration ^{29}Si MAS NMR allows quantification of amorphous as well as crystalline hydrate phase and provides measures of the degree of reaction for the siliceous, anhydrous phases in this investigation. The degrees of reaction for alite, belite, and metakaolin are implemented as input in the thermodynamic modeling with a specifically developed empirical equation, to model the time dependent hydration of the investigated blends.

3.2 Observed Phase Assemblages

Generally, the phase assemblages of the blends after prolonged hydration consist of C(-A)-S-H phases, calcite, portlandite, monocarbonate and ettringite. The phase assemblages for the highest metakaolin content (33 wt% of the blend) change mainly in the distribution of anions between the AFm phases, which leads to the unique situation where strätlingite is observed along with monosulfate, hemicarbonate, and monocarbonate.

1. The blends are identified by the MK content (wt%). Thus, the LS content of the blends corresponds to the difference: 35 wt% – MK (wt%). n.d. = not detected.
2. ^{27}Al MAS NMR (= NMR in the table) cannot distinguish between different AFm phases under the present experimental conditions.
3. Weak intensities.

3.3 Thermodynamic Modeling

Thermodynamic modeling of the hydrate phase assemblages with and without consideration of the hydration kinetics is compared in this section. The calculations without constraints provide the phase assemblage corresponding to full reaction for all phases. Limitations on the amounts of hydrated alite, belite, and metakaolin

during hydration, caused by their non-complete reaction, are implemented in the hydration kinetics approach. The hydrated amounts are implemented with a simple, exponential equation in the modeling. The degrees of hydration for alite, belite, and metakaolin have been were determined experimen-tally by ^{29}Si MAS NMR.

Figure 1 compares the phase assemblages for full hydration (*i.e.*, thermodynamic equilibrium) and the predicted phase assemblage after 182 days of hydration, considering the degrees of reaction for the principal phases for the different blends. For full hydration, the phase assemblages consist of C-S-H, portlandite, ettringite, monocarbonate and calcite up to the addition of 20 wt% MK. C-S-H phases are predicted employedhere as a result of the current lack of thermodynamic data for C-A-S-H phases. However, the aluminum uptake in C-S-H phases is observed in the ^{27}Al and ^{29}Si MAS NMR experiments. For higher MK contents, the predicted quantity of monocarbonate decreases and it is replaced by increasing amounts of strätlingite. The calcite content decreases as the cement replacement level is constant (35 wt%). The modeled phase assemblages do not describe the experimentally observed phase assemblages well (Table 2). Only the highest MK substitution level leads to the clear observation of strätlingite by XRD and ^{27}Al MAS NMR.

It is clear that the assumption of full hydration for all phases is not suitable for the prediction of the phase changes observed for the blends containing limestone. In the absence of limestone, hydration kinetics may be neglected, since the predicted phase assemblages are rather close to those observed experimentally after 182 days of hydration [7].

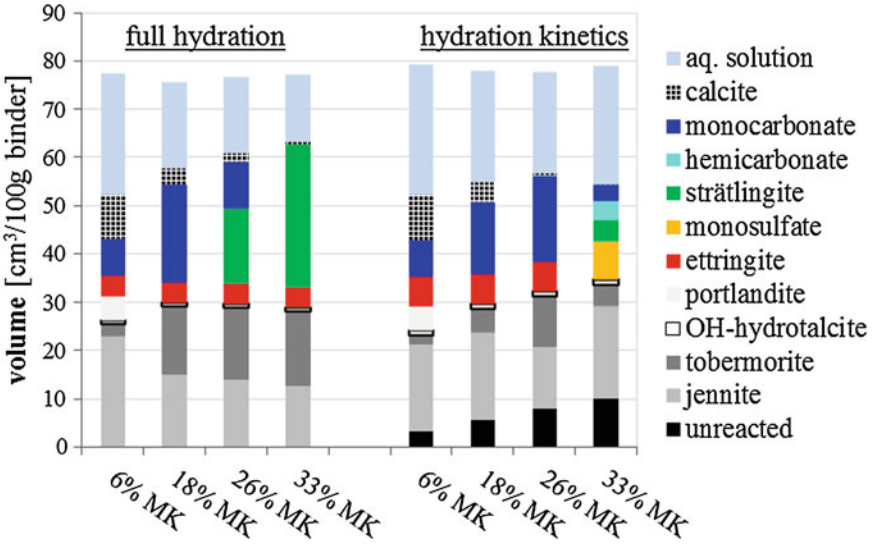

Fig. 1 Comparison of the predicted phase assemblages calculated assuming full hydration of all SCM´s and clinker phases (*left*) and after 182 days of hydration taking into account the hydration kinetics obtained from ^{29}Si MAS NMR (*right*)

Table 2 Detected phases in the different wPc – MK – LS blends after 182 days of hydration.[a]

	6 % MK	18 % MK	26 % MK	33 % MK
Calcite	XRD	XRD	XRD	XRD
Monocarbonate[b]	XRD	XRD	XRD	XRD[c]
Hemicarbonate[b]	n. d.	XRD	XRD	XRD
Strätlingite	n. d.	n. d.	NMR[c]	XRD + NMR
Monosulfate[b]	n. d.	n. d.	n. d.	XRD[c]
Ettringite	XRD + NMR	XRD + NMR	XRD + NMR	XRD + NMR
Portlandite	XRD	XRD	XRD	XRD

To improve the modeling, we have implemented a mathematical expression for the hydration of alite, belite, and metakaolin. This equation is inspired by empirical equations used to describe dissolution processes in other fields and it is optimized for the specific application by minimizing the number of variable parameters. All variable parameters should be related to observable parameters to avoid additional fitting parameters. The resulting equation is:

$$Q(t) = k \exp(-n/t) \tag{1}$$

where $Q(t)$ is the reacted amount of a phase as a function of time and k and n are variable parameters. The k parameter limits the quantity of the phase that reacts during the period of observation whereas the hydration rate, n, is parameterized together with the time (t) period under investigation. The equation describes a sigmoidal behavior (Fig. 2), with a short period of little material release, followed by a rapid increase that finally slows down and approaches k asymptotically.

The hydration kinetics, fitted and described by this equation for each phase (alite, belite, and metakaolin) are found to have a crucial impact on the predicted hydrated phases as evidenced by the modeled data in Fig. 1 (right-hand side) which employ Eq. (1) for the siliceous, anhydrous phases. The predicted phase assemblages fit well with the experimentally observed phases listed in Table 2.

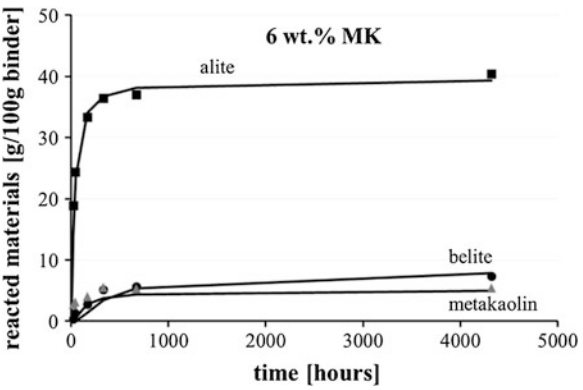

Fig. 2 Comparison of the predicted quantities of alite, belite, and MK (*lines*) and the experimental data (*symbols*) for the wPc blend containing 6 wt% MK and 29 wt% LS

3.4 Discussion

The comparison of the predicted and observed phase assemblages shows that the influence of limestone is significant and that it cannot be neglected for binders made from white Portland cement – metakaolin – limestone blends. The predicted pore volume development, in terms of quantities of pore water, is observed to scale well with the compressive strength development determined for corresponding mortars [6], despite that the modeling approach does not account for the quantities of gel water, whose distribution is affected by the micro-structures formed.

A few minor discrepancies are observed between the modeling and the experimental data. Ettringite is not predicted to form in the blend with 33 wt% MK although this phase is observed experimentally. Monosulfate is detected in relatively small quantities. This can be explained by small modeling artifacts. The quantity of aluminum released during hydration determines the amounts of AFm and AFt phases. The quantity of anions available (hydroxyl, sulfate and carbonate ions) will determine the distribution of phases between AFt and the different AFm phases. This is also highlighted by the experimental observation of hemi-carbonate for high MK contents (Table 2), which is not predicted by the modeling and related to an overestimation of calcite reactivity during hydration. Additionally, these aspects are exaggerated by the lack of thermodynamic data for aluminum uptake in C-S-H. The amount of Al in the C-S-H will reduce the amount of AFm phases and thus stabilize ettringite. The formation of C-A-S-H phases is experimentally confirmed [6] and the Al content in this phase increases with increasing MK contents [10]. It is quite common to observe portlandite by XRD in paste samples (Table 2), even when thermodynamic modeling predicts its absence. This can be explained by the heterogeneity of cementitious materials, which leads to several local equilibrium states that deviate slightly from the overall equilibrium state.

4 Conclusions

- Generally, our approach for including hydration kinetics has proved to be of high value, especially when limestone is used in the mix design, to model the observed phase assemblages compared to a full reaction (*i.e.*, thermodynamic equilibrium). The equilibrium calculations deviate especially from the experimental data for the quantities of AFm phases and strätlingite.
- ^{29}Si MAS NMR is capable to describe the hydration kinetics for the principal siliceous, phases, alite, belite, and metakaolin.
- The hydration kinetics has been implemented by an exponential function, specifically developed for this type of data, which considers the quantity of reacted material and a reaction rate that are fitted to the experimental data.
- The predicted phase assemblages change only for very high MK contents from a C-S-H, calcite, portlandite, monocarbonate and ettringite system to a phase

assemblage that in addition contains strätlingite and other AFm phases. To model these phase changes it is necessary to consider the hydration kinetics.
- The calculated phase changes predict a decrease in porosity with increasing MK contents, until all LS is consumed, which corresponds nicely with the higher compressive strengths observed for up to 26 wt% of MK [6].

Acknowledgment The Danish National Advanced Technology Foundation is acknowledged for financial support to the SCM project.

References

1. Nehdi, M., Mindess, S., Aïtcin, P.-C.: Optimization of high strength limestone filler cement mortars. Cem. Conc. Res. **26**, 883–893 (1996)
2. Tsivilis, S., Chaniotakis, E., Kakali, G., Batis, G.: An analysis of the properties of Portland limestone cements and concrete. Cem. Conc. Comp. **24**, 371–378 (2002)
3. De Weerdt, K., Ben Haha, M., Le Saout, G., Kjellsen, K.O., Justnes, H., Lothenbach, B.: Hydration mechanisms of ternary Portland cements containing limestone powder and fly ash. Cem. Conc. Res **41**, 279–291 (2001)
4. Steenberg, M., Herfort, D., Poulsen, S.L., Skibsted, J., Damtoft, J. S.: Composite cement based on Portland cement clinker, limestone and calcined clay. In: 13th International Congress of the Chemistry of Cement, p. 97 (7 pages) (Madrid, Spain) (2011)
5. Damidot, D., Lothenbach, B., Herfort, D., Glasser, F.P.: Thermodynamics and cement science. Cem. Conc. Res. **41**, 679–695 (2011)
6. Dai, Z., Kunther, W., Garzón, S. F., Herfort, D., Skibsted, J.: Investigation of blended systems of supplementary cementitious materials with white Portland cement and limestone (in preparation)
7. Kunther, W., Dai, Z., Skibsted, J.: Modeling the hydration of metakaolin blended cements based on hydration kinetics obtained by ^{29}Si MAS NMR spectroscopy (in preparation)
8. Taylor, H.F.W.: Cement Chemistry. Thomas Telford (1997)
9. Parrot, L., Killoh, D.: Prediction of cement hydration. In: Proceedings of British Ceramic Social pp 41–53(1984)
10. Dai, Z., Tran, T.T., Skibsted, J.: Aluminum Incorporation in the C-S–H phase of white Portland cement-metakaolin blends studied by 27Al and 29Si MAS NMR spectroscopy. J. Am. Ceram. Soc. **97**, 2662–2671 (2014)

Comparison of the Pozzolanic Reactivity for Flash and Soak Calcined Clays in Portland Cement Blends

Kasper E. Rasmussen, Mette Moesgaard, Lea L. Køhler, Thuan T. Tran and Jørgen Skibsted

Abstract The increased attention towards the use of calcined clays as supplementary cementitious materials (SCM's) has prompted several studies of calcined kaolinite (metakaolin) and to a lesser extent also of heat-treated montmorillonite. However, a major part of these studies does not pay specific attention to the calcination process itself. Furthermore, most studies have been performed on phase-pure clays and such clays are not economically viable for applications as SCM's at an industrial scale. In this work we investigate the reactivity of SCM's produced by flash calcination of a natural kaolinite sample and a natural mixed smectite/illite sample. Several key properties of the flash calcined materials are tested and compared to calcined clays obtained by a conventional soak-calcination method. The analyses include characterization of physical properties such as BET surface area, specific density and particle fineness and of the microstructure and degree of reaction by powder XRD as well as ^{29}Si and ^{27}Al MAS NMR. Moreover, the pozzolanic reactivity of the SCM's are investigated by a Chapelle-like test combined with NMR studies of Portland cement—SCM paste samples at different hydration times. Finally, the performance of mortar samples produced with a 35 wt% SCM substitution level is tested with respect to compressive strength and water requirement following the ASTM standard.

K.E. Rasmussen · J. Skibsted (✉)
Department of Chemistry and Interdisciplinary Nanoscience Center (iNANO), Aarhus University, 8000 Aarhus C, Denmark
e-mail: jskib@chem.au.dk

M. Moesgaard · L.L. Køhler
F.L. Smidth A/S, R & D Center Dania, 9550 Mariager, Denmark

T.T. Tran
Aalborg Portland A/S, Cementir Holding, 9100 Aalborg, Denmark

K. Scrivener and A. Favier (eds.), *Calcined Clays for Sustainable Concrete*, RILEM Bookseries 10, DOI 10.1007/978-94-017-9939-3_19

1 Introduction

The partial replacement of Portland cement by supplementary cementitious materials (SCM's) has been employed in the cement industry for the past couple of decades [1]. Currently, the use of SCM's is strongly motivated by a reduction in CO_2 emissions, obtained by a lower clinker content [2], although optimum SCM additions may also improve the properties of blended Portland cement – SCM systems in concrete applications. Traditionally, SCM's are industrial by-products such as granulated blast furnace slag, fly ashes and silica fume. However, with society's increasing demand for cement materials, the supplies of these by-products may not be sufficient to provide a sustainable solution to clinker replacement in Portland cement systems [2].

Conventional large-scale production of metakaolin involves either rotary kilns or fluidized bed reactors, which are inefficient from an energy-consumption perspective. The flash calcination process [3], which is well-known from the minerals sector [4], offers a much faster and economically viable alternative to soak calcination methods. The present work focuses on SCM's produced in a pilot-scale gas-suspension flash calciner, employing very short retention times (*i.e.*, less than one second). The optimum heat-treatments for two natural clay samples are investigated using several different calcination temperatures. The pozzolanic properties of the flash calcined samples are compared to SCM's prepared by a conventional soak-calcination procedure. Furthermore, it is shown that ^{29}Si and ^{27}Al MAS NMR allow for a thorough structural characterization which may improve our knowledge on the relationship between thermal activation and pozzolanic reactivity for clay minerals. Finally, the compressive strength performance of the SCM's is tested in ordinary Portland cement – SCM mortar samples prepared with a clinker replacement level of 35 wt%.

2 Materials and Experimental

A kaolinite clay containing 5 – 10 wt% quartz and a mixed illite/smectite (I/S) with impurities of roughly 10 wt% quartz and 10 wt% calcite, both obtained from large natural deposits, have been investigated. The soak calcinations were carried out in an electric furnace at temperatures in the range 600 – 1000 °C. The samples were placed in the pre-heated furnace and maintained at a constant temperature for 60 min. The flash calcination process was performed in a gas-suspension calciner at set temperatures ranging from 800 to 1100 °C. The theoretical gas retention time for the calcinations was 0.5 s.

Pozzolanic reactivities have been assessed using two different tests, the first test being a Chapelle-like procedure. Here, 1.000 g SCM and 2.500 g $Ca(OH)_2$ was mixed with 50 mL of three-times distilled water. The suspension was cured at 40 °C in a sealed conical flask for 48 h under continuous stirring, and the solid formed

was isolated by filtration followed by gently drying. Quantitative XRD was used to determine the remaining amount of crystalline $Ca(OH)_2$ whereas ^{29}Si MAS NMR was employed to characterize the structure of the reaction product. The second test involved preparation of Mini-RILEM prism mortars, following the EN-196-1 standard. The compressive strength of the mortars was determined after 1, 3, 7 and 28 days of hydration. An ordinary, grey Portland cement was used for the mortar experiments.

3 Results and Discussion

3.1 Characterization of the SCM's

A range of physical properties have been analysed for both the flash- and soak-calcined materials. This includes BET surface area, density (specific and bulk) and particle fineness. From these measurements, a clear trend is observed of decreasing BET surface areas and specific densities when the calcination temperature is increased. Furthermore, the as-prepared calcined materials have been studied by ^{27}Al and ^{29}Si NMR as well as with XRD. For the kaolinite-based SCM's, it is evident from ^{29}Si MAS NMR that the silicate species in the flash calcined samples experience an increased disorder compared to the soak calcined samples, as seen by larger line broadening of the resonances for the flash-calcined samples. For the I/S-based SCM's, the ^{27}Al MAS NMR spectra reveal that the flash-calcined clays contain a larger fraction of penta-coordinated aluminate units. Moreover, XRD reflections from spinel and feldspar-like phases are observed in the diffractograms for the soak-calcined I/S-SCM's. This is further supported by both ^{27}Al and ^{29}Si NMR which indicates the formation of fully condensed aluminosilicate framework phases in some of the soak-calcined SCM's.

3.2 SCM Reactivity in $Ca(OH)_2$ Solution

The cured SCM – $Ca(OH)_2$ samples have been studied by NMR and XRD experiments. From the XRD diffractograms (not shown), the amount of remaining crystalline $Ca(OH)_2$ in the solid residues can be determined by quantitative Rietveld refinements. The degree of $Ca(OH)_2$ consumption calculated from these values is shown in Fig. 1 for the SCM's as a function of the calcination temperature. The temperature for the flash-calcined samples is an average calcination temperature, estimated from measured values from four temperature sensors placed along the gas-suspension calciner. For the kaolinite-based SCM's, the flash-calcined samples consume significantly more $Ca(OH)_2$ than the soak-calcined kaolinites, indicating a

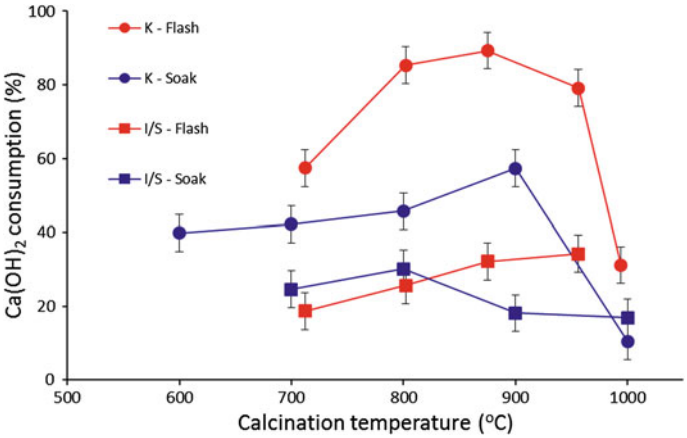

Fig. 1 Degree of $Ca(OH)_2$ consumption for cured SCM-$Ca(OH)_2$ samples as a function of the average calcination temperature for flash-calcined SCM's (*circles*) and soak-calcined samples (*squares*). The degree of consumption is determined as $\Delta_{CH} = [1 - m(t)/m(t_0)] \cdot 100$ %, where $m(t_0)$ and $m(t)$ are the amounts of crystalline $Ca(OH)_2$ before (t_0) and after curing (t), respectively, as determined by quantitative XRD

higher degree of reactivity. The optimum calcination temperature appears to be close to 900 °C for both heat-treatment methods. For the I/S-based SCM's, optimum heat-treatment is achieved roughly at 800 °C by the soak-calcination method, whereas the most reactive SCM's are obtained with an average temperature of 950 °C by flash calcination. In contrast to the kaolinite-based SCM's, there is only a small difference in reactivity for the optimum performing soak-calcined I/S-SCM (30 %) and flash-calcined I/S-SCM (34 %) materials. These results on the reactivities are supported by both ^{27}Al and ^{29}Si NMR data (not shown) for the cured samples. For all types of SCM's, there is a clear correspondence between the degree of consumption of Ca $(OH)_2$ and the amount of C-S-H-like phases, observed by ^{29}Si MAS NMR (*i.e.*, peaks assigned to Q^1, $Q^2(1Al)$ and Q^2 SiO_4 sites). Furthermore, the ^{29}Si NMR spectra of the solid residues for the SCM - $Ca(OH)_2$ samples with the most reactive SCM's show almost no signal intensity in the spectral region from -90 to -110 ppm, demonstrating that almost all of silicon in the calcined clay has reacted with Ca $(OH)_2$ in these samples. Similarly, the ^{27}Al MAS NMR spectra show a clear trend of more intense resonances from octahedrally coordinated aluminum present in calcium-aluminate hydrate phases for the most reactive SCM's. For the kaolinite-based SCM's, strätlingite is observed by NMR and XRD as a reaction product for most of the cured SCM - $Ca(OH)_2$ samples, which reflect the high amount of reactive aluminum species in these SCM's. The formation of high amounts of calcium-aluminate phases in the kaolinite – SCM's is in accordance with the highest fraction of $Ca(OH)_2$ being consumed in these blends.

3.3 Mortar Tests

Portland cement – SCM mortars (65:35) were cast with a water/binder ratio of 0.5 and a binder/sand ratio of 1:3 (all ratios by weight). The performances of the mortars were tested by their compressive strengths after 1, 3, 7 and 28 days of hydration, which are shown in Fig. 2 along with data for a 100 wt% OPC reference mortar. After hydration for one day all mortars of the blends exhibit a significantly lower performance than the reference mortar, and there is no significant difference in strength for the individual blends. For the kaolinite-based SCM's, the flash-calcined SCM's exhibit slightly higher compressive strengths than the soak-calcined SCM's after 3 and 7 days of hydration, in agreement with the $Ca(OH)_2$ reactivity tests. However, after 28 days of hydration, the best performing soak-calcined SCM produces similar strength values as the optimum flash-calcined SCM. This suggests that the flash-calcined SCM's react faster than the soak-calcined SCM's but that the overall degree of reaction is similar after prolonged hydration. This agrees well with the higher degree of structural disorder, observed by ^{29}Si NMR for the flash-calcined samples. It is also interesting to note that four of the kaolinite-based SCM systems perform better than the OPC reference mortar after 28 days of hydration. This situation is not observed for any of the I/S-based SCM mortars, where the two best performing flash-calcined SCM's result in mortars with 96 % of the strength for the reference after 28 days. This may reflect that the I/S clay contains roughly 40 wt% illite, since calcined illite is reported to have poor pozzolanic properties [5]. In contrast to the kaolinite-based SCM's, there is a clear distinction in performance for

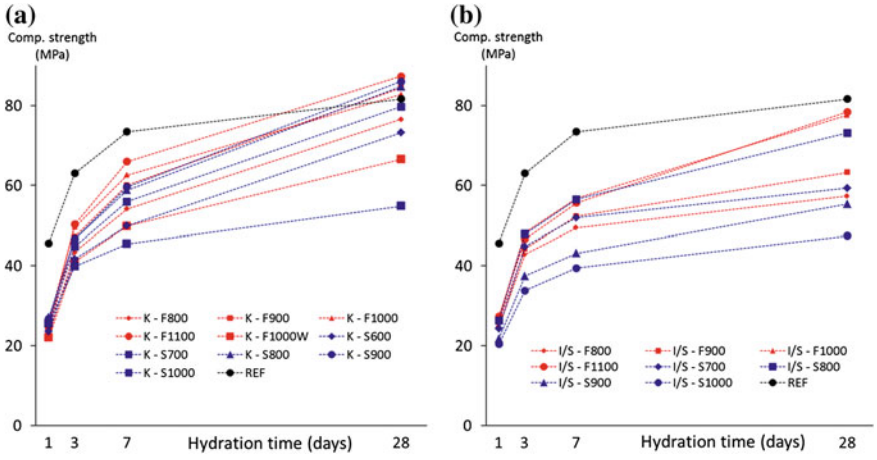

Fig. 2 Compressive strengths for Portland cement – SCM mortars using **a** kaolinite-based and **b** I/S-based SCM's after 1, 3, 7 and 28 days of hydration. The calcination method (Soak or Flash) and calcination set-temperatures are indicated for the individual blends. The shown data are average values of three measurements. Error bars have been omitted from the figure as the standard deviations do not exceed 3 % for any of the values

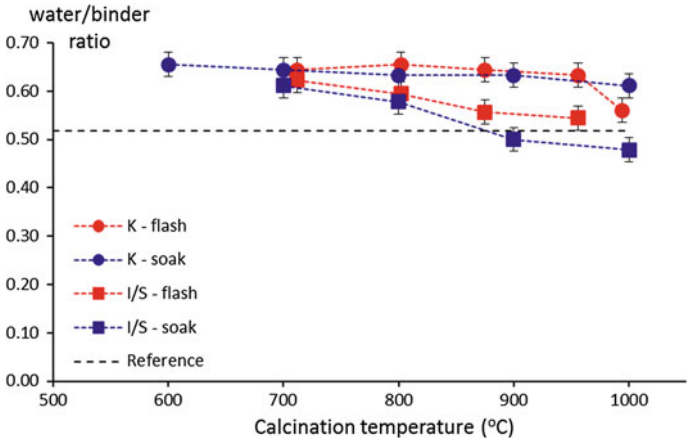

Fig. 3 Water/binder ratios required to achieve a normal flow for the 65:35 OPC – SCM mortars. The reference OPC mortar required a water/binder ratio of 0.517 (*dashed line*)

the different I/S-based SCM systems. These differences can be related to the structural properties obtained from ^{27}Al and ^{29}Si MAS NMR experiments, which indicate that condensed alumina-silicate phases form to a higher extent in the SCM's prepared by the soak-calcination method. These phases are less reactive under the actual experimental conditions, resulting in lower amounts of Si and Al species available to form hydrate phases that contribute to the strength.

The water requirement for normal consistency has been measured according to the procedure of the ASTM C1437 standard, however, using mortar mix proportions corresponding to EN mortar mixes. The results are shown for the individual blends in Fig. 3 as the water/binder ratio needed to obtain a normal flow. Overall, there is a trend of decreasing water requirement with increased calcination temperature, which is also expected from the associated decrease in BET surface areas for the calcined materials. Interestingly, the flash-calcined MK samples do not have an increased water requirement, as reported in earlier studies [6], and all samples seem to follow the same trend line.

4 Conclusions

The results of this work indicate that a flash-calcination process can produce high-quality SCM's for both 1:1 and 2:1 clays from natural deposits. For the 1:1 clays (*i.e.*, kaolinite) the rapid heating by flash calcination induces a larger degree of disorder in the structure of the calcined materials, as compared to observations for similar SCM's prepared by a traditional soak-calcination method. The larger disorder results in more reactive/soluble SCM materials, which exhibit increased pozzolanic reactivities, as revealed by the $Ca(OH)_2$ reactivity experiments

performed in this work. For the 2:1 clay, the present results suggest that the rapid heating suppresses melting and recrystallization of unreactive, fully condensed alumina-silicate phases, such as feldspar and spinel. This leads to higher amounts of reactive Si and Al species in the flash calcined SCM's compared to the soak calcined SCMs, as seen by the higher compressive strengths and higher amounts of $Ca(OH)_2$ consumption for these samples.

Acknowledgement The Danish National Advanced Technology Foundation is acknowledged for financial support to the SCM project.

References

1. Lothenbach, B., Scrivener, K., Hooton, D.: Supplementary cementitious materials. Cem. Concr. Res. **41**, 1244–1256 (2011)
2. Damtoft, J.S., Lukasik, J., Herfort, D., Sorrentino, D., Gartner, E.M.: Sustainable development and climate initiatives. Cem. Concr. Res. **38**, 115–127 (2011)
3. Meinhold, R.H., Atakul, H., Davies, T.W., Slade, R.C.T.: Flash calcination of kaolinite studied by dsc, TG and MAS NMR. J. Therm. Anal. **38**, 2053–2065 (1992)
4. Esahan, H., Ekmekyapar, A., Sevin, F.: Flash calcination of a magnesite ore in a free-fall reactor and leaching of magnesia. Int. J. Miner. Process. **42**, 121–136 (1994)
5. He, C., Makovicky, E., Osbæck, B.: Pozzolanic reactions of six principal clay minerals: activation, reactivity assessments and technological effects. Cem. Concr. Res. **25**, 1691–1702 (1995)
6. Salvador, S.: Pozzolanic properties of flash-calcined kaolinite: a comparative study with soak-calcined products. Cem. Concr. Res. **25**, 102–112 (1995)

The Impact of VMA on the Rheology, Thixotropy and Robustness of Self-compacting Mortars

Farid Van Der Vurst, Steffen Grünewald and Geert De Schutter

Abstract Due to the higher sensitivity of fresh self-compacting concrete (SCC) to small variations in the mix proportions – also referred to as a lower robustness – applications with SCC are still limited. Because viscosity modifying admixtures (VMAs) are often reported to increase the robustness of SCC, the relationship between robustness, rheological characteristics, and thixotropic build-up of self-compacting mortars is examined whit an experimental program. The robustness with regard to small variations in the water dosage is measured together with the rheological and thixotropic properties of mortars made with various admixtures (purified attapulgite clay, diutan gum, corn starch, and propylene carbonate). Based on those results, the possible connections between the rheology, thixotropy and robustness of self-compacting mortar were evaluated.

1 Introduction

Self-compacting concrete (SCC) is a concrete, which does not need any external vibration to ensure proper consolidation and casting of the concrete. Considering the higher requirements and more difficult mix design of SCC, its robustness is in general lower compared to vibrated concrete (VC) [1]. The rheological characteristics of a good SCC are within a more narrow range, which has to be limited to prevent segregation, bleeding, blocking during the flow, and too sticky behaviour. Because SCC contains in general a larger number of constituents, they can cause more variations in the fluid behaviour [2] or incompatibilities with the cement, fillers, superplasticizer, VMA, retarder, or other possible ingredients [3, 4]. Moreover, the use of superplasticizer(s) increases the impact of variations of different cement deliveries [5, 6]. Some superplasticizers and VMAs are reported to

F. Van Der Vurst (✉) · S. Grünewald · G. De Schutter
Magnel Laboratory for Concrete Research, Ghent University, Ghent, Belgium
e-mail: farid.vandervurst@ugent.be

S. Grünewald
Concrete Structures Group, Delft University of Technology, Delft, The Netherlands

K. Scrivener and A. Favier (eds.), *Calcined Clays for Sustainable Concrete*,
RILEM Bookseries 10, DOI 10.1007/978-94-017-9939-3_20

increase the robustness of SCC [7–9]. Because some authors considered the possibility of a link between thixotropy and robustness of SCC [1, 10], the impact on the robustness of several products with a strong influence on the rheology and thixotropy of concrete was studied in this experimental program.

2 Experimental Setup

Because variations in the water content have a larger impact on the rheology of concrete compared to other variations [11], this experimental program focusses on the robustness with regard to small changes in the water content (±6.95 l/m^3 in the water content, corresponding with a variation of ±5 l/m^3 water in the equivalent concrete). The mortar mixes were produced with Rhine sand, Portland cement CEM I 52.5 N with a Blaine index of 370 m^2/kg, limestone filler, and a polycarboxylate superplasticiser with a solid concentration of 35%.

The influence of purified attapulgite clay, diutan gum, corn starch, and propylene carbonate (properties summarized in Table 1) on the robustness of mortars is evaluated by measuring the variations in flow spread, V-funnel flow time, and Bingham parameters. The influence on the thixotropy was evaluated by adding a structural build-up step to the rheological test and by measuring the breakdown speed during the pre-shear step of the rheological test. A fixed specific mix procedure with timing of the tests was applied to avoid changes in the shear history during the experimental tests. For each mixture, the VMA dosage was based on the manufacturers recommended dosage or literature and the superplasticizer dosage was adjusted to reach a flow spread of 240 – 260 mm. Table 2 summarizes the compositions of all reference mixes.

The rheological tests were performed with an Anton Paar MCR 102 coaxial cylinder rheometer with an inner cylinder with sanded surface, radius of 20 mm and height of 60 mm rotating in an ribbed outer cylinder with a radius of 35 mm. The shear rate profile applied during the rheological test is shown in Fig. 1. The measured torque profile (Fig. 2) based on the last 5 s of each rotational velocity step was used to calculate the Bingham constants (Eq. 1) of the mortars using the Reiner-Rivlin equations. τ_0 is the yield stress and μ is the plastic viscosity. A plug flow correction at the lowest rotational velocities was needed for most of the mortars [24]. Since the torque – rotational velocity diagram was linear and no segregation occurred during the tests, the Bingham model was applicable. The exponential decrease in torque measured during the pre-shear and the exponential increase in torque measured during the last step at 5 rpm were used to calculate the breakdown and build-up speed ($\alpha_{breakdown}$ and $\alpha_{build\text{-}up}$) fitting the curves to Eqs. 2 and 3.

$$\tau = \tau_0 + \mu \cdot \dot{\gamma} \tag{1}$$

Table 1 Properties of the applied VMA's

	Attapulgite clay	Diutan gum	Starch	Propylene carbonate (PPC)
Description	Small clay needles with negative charges along its main axis and the pH-dependent charges at the ends [12]	High molecular weight microbial polysaccharide compatible with cement hydration products [13]	Natural polysaccharide. In this experimental program, corn starch is used	When added to water, it dissolves to propylene glycol and carbonate anion [14]
Effect in concrete	A strong increase of the floc strength [15, 16]	Hydrogen bonds fix part of the water and increases the yield stress and plastic viscosity [17]. Polymer chains entangle at rest and align with the flow when sheared	Increases the yield stress, but has only a small effect on the plastic viscosity [10]. Superplasticizer should be added before the starch to prevent adsorption onto cement particles [18]	The propylene glycol develops water bonds, inducing a network structure [14]. The carbonate anions might affect the cement hydratation process
Effect robustness	Combined with a reduction of the amount of filler, it should improve the robustness	Reported to enhance the robustness of SCC mixes [13]	Reported to enhance the robustness of SCC mixes [8, 19–22]	Unknown
Application	- Stabilizing mineral suspensions - Slipform pavement SCC [23]	- Stabilizer in SCC	- Stabilizer in SCC	- Aprotic solvent - Thixotropy-enhancing admixture in SCC [14]

Table 2 Mix proportions of all reference mixes

Component	No VMA	Diutan gum	Corn starch	Attapulgite clay	Propylene carbonate
Sand [kg/m^3]	1140	1140	1140	1140	1140
Cement [kg/m^3]	487	487	487	487	487
Limestone filler [kg/m^3]	348	348	348	348	348
Water [kg/m^3]	243	243	243	243	243
Superplasticizer [l/m^3]	4.00	5.08	4.15	4.23	4.00
VMA [kg/m^3]	–	0.12	2.43	0.75	1.22

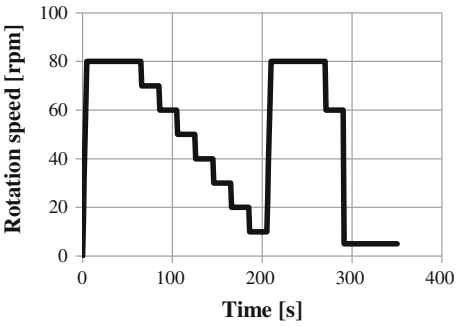

Fig. 1 The shear rate profile of the rheological test

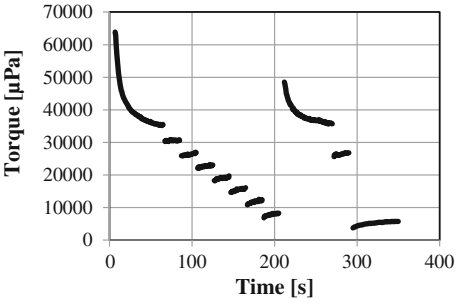

Fig. 2 The measured torque during the rheological test of the mixture without VMA

$$\tau_{80rpm} = C_1 + C_2 \cdot \exp(-\alpha_{breakdown} \cdot \dot{\gamma} \cdot t) \tag{2}$$

$$\tau_{5rpm} = C_3 - C_4 \cdot \exp\left(-\alpha_{build-up} \cdot \dot{\gamma} \cdot t\right) \tag{3}$$

3 Results and Dicussion

Table 3 summarizes the measured workability and rheology parameters for all mixtures with the reference water dosage together with their robustness. For each workability test, the result of the reference test (e.g. S), the difference between the maximum and the minimum values (e.g. ΔS), this difference divided by the water variation (e.g. ΔS/10 l/m^3), and the difference divided by the test result of the reference mixture (e.g. $\Delta S/S_{ref}$) are listed.

Table 3 Discussion of robustness for all tests (*)

	No VMA	Diutan gum	Corn Starch	Attapulgite clay	Propylene carbonate
Flow spread S [mm]	248	240	243	250	250
ΔS	86	35	69	57	70
$\Delta S/10\ l/m^3$	8.6	3.5	6.9	5.7	7.0
$\Delta S/S_{ref}$	0.35	0.15	0.28	0.23	0.28
V-funnel time VF [s]	10.4	10.9	7.4	7.8	11.7
ΔVF	4.1	6.5	3.5	3.0	16.3
$\Delta VF/10\ l/m^3$	0.41	0.65	0.35	0.30	1.63
$\Delta VF/VF_{ref}$	0.40	0.60	0.47	0.38	1.39
Yield stress YS [Pa]	17	26	14	12	11
ΔYS	12	20	24	14	17
$\Delta YS/10\ l/m^3$	1.2	2.0	2.4	1.4	1.7
$\Delta YS/YS_{ref}$	0.69	0.76	1.76	1.17	1.50
Plastic viscosity PV [Pa.s]	8	13	8	7	10
ΔPV	7	6	6	5	5
$\Delta PV/10\ l/m^3$	0.7	0.6	0.6	0.5	0.5
$\Delta PV/PV_{ref}$	0.84	0.46	0.76	0.73	0.50
Thixotropic breakdown speed $\alpha_{breakdown}$ [-]	0.0043	0.0051	0.0039	0.0041	0.0039
Thixotropic build-up speed $\alpha_{build-up}$ [-]	0.017	0.012	0.015	0.023	0.021

(*) The underlined values were used as a measure for the robustness of this experimental program

3.1 Flow Spread and V-Funnel Time

Since all reference mixtures have about the same flow spread, the difference divided by the water variation $\Delta S/10\ l/m^3$ and the difference divided by the test result of the reference mixture $\Delta S/S_{ref}$ are both indicating of the robustness of the mortars, with high values referring to low robustness. Diutan gum provides a significantly larger robustness than attapulgite clay, being more robust than propylene carbonate and corn starch. The mixture without VMA had the least robust flow spread.

The addition of diutan gum did not affect the V-funnel time in comparison to the reference mix without VMA; corn starch and attapulgite clay decreased the V-funnel time; and propylene carbonate increased the V-funnel time. Because the variation in the V-funnel time depends on the V-funnel time of the reference mixture, the robustness of the V-funnel time of a mortar should be evaluated using the ratio of the differences in V-funnel time to the reference V-funnel time. Based on this parameter, the robustness of the mixture with attapulgite clay, corn starch, and no VMA are more robust than the mixture with diutan gum. Propylene carbonate caused the largest decrease in robustness.

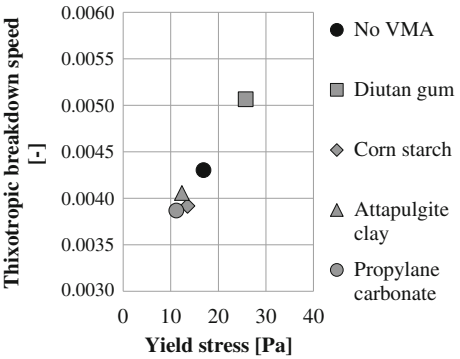

Fig. 3 The relation between the thixotropic breakdown speed and the yield stress

3.2 Yield Stress

Although the flow spread of all mixtures was about the same, large differences were observed in the yield stress. Diutan gum increased the yield stress with 53% while all other VMA's resulted in a decrease of the yield stress (17 to 35%). The origin of these differences might be found in the strength of the thixotropic network build during the three minutes rest in between the mixing and performing the flow spread test. As is illustrated in Fig. 3, the mixtures with higher yield stresses also reached more rapidly its equilibrium state during the pre-shear step of the rheology test and therefore probably were able to reach the same flow spread as a mixture with half the yield stress.

The mixtures without VMA and with attapulgite clay had the most robust yield stress, followed by the mixtures with propylene carbonate, diutan gum and corn starch. Although the yield stress of the mixtures with a VMA became less robust, all mortars showed a more robust flow spread behaviour. Changes in the build-up and breakdown speed of the thixotropic network alone cannot explain the observed ranking of robustness in this test program. The large dependency of the thixotropic build-up to variations in the water content makes the final behaviour more complicated.

3.3 Plastic Viscosity

Diutan gum caused the largest increase in plastic viscosity; propylene carbonate slightly increased it; and attapulgite clay and corn starch had no influence on the plastic viscosity. The plastic viscosity is somehow correlated with the V-funnel time, but it is not the only parameter determining the V-funnel time of a mixture. For example the addition of diutan gum resulted in a similar V-funnel time, although the plastic viscosity doubled.

The impact of admixtures on the robustness of mortars depends on the used definition. In absolute values, the differences in plastic viscosity of all mixtures were about 6 Pa.s, but divided by the reference plastic viscosity of each mixture, the mixtures with diutan gum and propylene carbonate were significantly more robust than mixtures with attapulgite clay and corn starch, which were more robust compared to the mixture without VMA.

The robustness of the V-funnel time decreased as the plastic viscosity of the mixture increased by the addition of diutan gum or propylene carbonate. When corn starch or attapulgite clay were added, the plastic viscosity itself remained about the same, but both the robustness of the V-funnel time and the plastic viscosity increased. Probably, the sensitivity of the V-funnel time increases more than proportional for mixtures with a higher plastic viscosity. Both diutan gum and propylene carbonate are reported to mainly affect the free water in the mixtures while attapulgite clay and starch most probably interact with the cement particles [14–18].

4 Conclusions

Because VMAs are reported to have a positive impact on the robustness of SCC, four VMAs were selected for a preliminary study on mortar: attapulgite clay, diutan gum, corn starch, and propylene carbonate. The superplasticizer dosage was adjusted in order to keep the slump flow in a range of 240 – 260 mm.

Adding a VMA to the reference mixture increased the robustness of the flow spread test, decreased the robustness of the yield stress, and increased the robustness of the plastic viscosity. The robustness of the V-funnel increased when corn starch or attapulgite clay was added, but decreased when diutan gum or propylene carbonate was added. The robustness of the V-funnel test decreased as the plastic viscosity increased.

Based on these experimental results, it can be concluded that the thixotropic breakdown speed of self-compacting mortars affects the relation between the yield stress and the flow spread test, but has no clear influence on the robustness of the flow spread test. The working mechanism of the VMA affects the robustness of the plastic viscosity of the self-compacting mortars.

References

1. Bonen, D., Deshpande, Y., Olek, J., Shen, L., Struble, L., Lange, D.A., et al.: Robustness of SCC. In: Lange, D.A. (ed.) Self-consolidating Concrete. The Center for Advanced Cement Based Materials (ACBM), Urbana (2007)
2. Nunes, S., Oliveira, P.M., Coutinho, J.S., Figueiras, J.: Rheological characterization of SCC mortars and pastes with changes induced by cement delivery. Cem. Concr. Compos. **33**(1), 103–115 (2011)

3. Hanehara, S., Yamada, K.: Interaction between cement and chemical admixture from the point of cement hydration, absorption behaviour of admixture, and paste rheology. Cem. Concr. Res. **29**(8), 1159–1165 (1999)
4. Chen, C.-T., Struble, L.: Cement-dispersant incompatibility due to ettringite bridging. J. Am. Ceram. Soc. **94**(1), 200–208 (2011)
5. Kubens, S.: Interaction of cement and admixtures and its effect on rheological properties. Doctoral thesis, Bauhaus-Universität Weimar, Götingen (2010)
6. Kubens, S., Wallevik, O.: Interaction of cement and admixtures—the influence of cement deliveries on rheological properties. In: Fisher, H.-B. (ed.) Ibausil—Internationale Baustofftagung, pp. 679–686. FA Finger—Institut für Baustoffkunde, Weimar (2006)
7. Haldenwang, R., Fester, VG.: The influence of different superplasticisers on the flowability and reproducibility of a SCC mix. In: Wallevik, O., Khrapko, M. (eds.) 9th International Symposium on High Performance Concrete. New Zealand Concrete Society, Rotorua (2011)
8. Grünewald, S., Walraven, JC.: Robust flowable concrete with viscosity agents. In: Mechtcherine, V., Schroefl, C. (eds.) International RILEM Conference on Application of superabsorbent polymers and other new admixtures in concrete construction, pp. 385–394. RILEM Publications, Dresden (2014)
9. Billberg, P.H.: Influence of powder type and VMA combination on certain key fresh properties of SCC. In: Wallevik, O., Khrapko, M. (eds.) 9th International Symposium on High Performance Concrete. New Zealand Concrete Society, Rotorua (2011)
10. Bouras, R., Chaouche, M., Kaci, S.: Influence of viscosity-modifying admixtures on the thixotropic behaviour of cement pastes. Appl. Rheol. **18**(4), 45604-1–45604-8 (2008)
11. Rigueira, J.W., García-Taengua, E., Serna-Ros, P.: Self-consolidating concrete robustness in continuous production regarding fresh and hardened state properties. ACI Mater. J. **106**(3), 301–307 (2009)
12. Quanji, Z., Wang, K., Lomboy, GR., Shah, SP.: Influence of nano-clay addition and clay replacement on thixotropic behavior of fresh cement paste. In: Roussel, N., Bessaies, H. (eds.) 7th International RILEM Symposium on Self-Compacting Concrete, p. 8. RILEM Publications SARL, Paris (2013)
13. Sakata, N., Yanai, S., Yoshizaki, M., Phyfferoen, A., Monty, H.: Evaluation of S-657 Biopolymer as a new viscosity-modifying admixture for self-compacting concrete. In: Ozawa, K., Ouchi, M. (eds.) Second International Symposium on Self-Compacting Concrete, pp. 229–236. Tokyo (2001)
14. Khayat, K.H., Assaad, J.: Use of thixotropy-enhancing agent to reduce formwork pressure axerted by self-consolidating concrete. ACI Mater. J. **105**(1), 88–96 (2008)
15. Tregger, N.A., Pakula, M.E., Shah, S.P.: Influence of clays on the rheology of cement pastes. Cem. Concr. Res. **40**(3), 384–391 (2010)
16. Kawashima, S., Chaouche, M., Corr, D.J., Shah, S.P.: Rate of thixotropic rebuilding of cement pastes modified with highly purified attapulgite clays. Cem. Concr. Res. **53**, 112–118 (2013)
17. Schmidt, W., Brouwers, J., Kühne, H.-C., Meng, B.: Effects of superplasticizer and viscosity-modifying agent on fresh concrete performance of SCC at varied ambient temperatures. In: Khayat, K.H., Feys, D. (eds.) Design, Production and Placement of Self-Consolidating Concrete, pp. 65–77. RILEM, Springer, Montreal (2010)
18. Palacios, M., Flatt, R.J., Puertas, F., Sanchez-Herencia, A.: Compatibility between polycarboxylate and viscosity-modifying admixtures in cement pastes. ACI Special Publication **288**, 29–42 (2012)
19. Naji, S., Hwang, S.-D., Khayat, K.H.: Robustness of self-consolidating concrete incorperating different viscosity-enhancing admixtures. ACI Mater. J. **108**(4), 432–438 (2011)
20. Leemann, A., Winnefeld, F.: The effect of viscosity modifying agents on mortar and concrete. Cem. Concr. Compos. **29**(5), 341–349 (2007)

21. Phan, T.H.: Thixotropic behaviour of self-compacting pastes (in french). XXIVèmes Rencontres Universitaires de Génie Civil 2006 (2006)
22. Grünewald, S., Walraven, JC.: The effect of viscosity agents on the characteristics of self-compacting concrete. In: Shah SP. (ed.) Second North American Conference on the Design and Use of Self-consolidating Concrete/4th International RILEM Symposium on Self-Compacting Concrete, pp. 9–15. Hanley Wood, Addison (2005)
23. Voigt, T., Mbele, J.-J., Wang, K., Shah, S.P.: Using fly ash, clay and fibres for simultaneous improvement of concrete green strength and consolidatability for slip-form pavement. J. Mater. Civ. Eng. **22**(2), 196–206 (2010)
24. Wallevik, J.E.: Rheology of particle suspensions—fresh concrete, mortar and cement paste with various types of lignosulfonates. Doctoral thesis, Department of Structural Engineering, The Norwegian University of Science and Technology (NTNU), Trondheim (2003)

Calcined Coal Gangue and Clay Shale for Cementitious Materials Without Clinker

Huiwen Wan and Zhifei Gao

Abstract Coal gangue and clay shale usually contain more than 70 % SiO_2 and Al_2O_3, which have potential pozzolanic activity when calcined at suitable temperature. In this study, the feasibility of utilizing calcined coal gangue and clay shale in the production of multiple cementitious materials was assessed under the condition of no cement clinker. The minerals and chemical composition of coal gangue and clay shale were characterized by analytical techniques such as X-ray diffraction (XRD) and X-ray fluorescence analysis (XRF). The optimal calcining temperature of coal gangue and clay shale was obtained through differential thermal analysis (DTA), and the activity evaluation method was conducted to get the optimal calcining procedure. The results showed that, the optimal calcining procedure for coal gangue and clay shale to obtain the best pozzolanic activity is as following: coal gangue and clay shale under the ratio of 7:3 were calcined at 780 °C for 2 h, and then quickly cooled in the air. The cementitious materials, which were prepared by calcining coal gangue, clay shale, slag, gypsum and CaO (as activator) under the ratio of 45:35:5:15, could reach the strength of class P.C. 32.5 of the Chinese standard GB175-2007.

1 Introduction

China is one of the largest coal-producing countries, and as the solid waste of coal-producing process, coal gangue has become one of China's largest solid industrial waste with the increasing amount of coal production. It has been reported [1] that approximately 0.15 ton of coal gangue is produced for every 1 ton of coal mined. At present, China's coal gangue has accumulated to over 3.8 billion tons, covered an area of 70 km^2, and are increasing with a rate of 150 million tons per year. Shale is clayey sediments whose main components are SiO_2 and Al_2O_3, and it is widely distributed with low level of utilization. Aluminosilicate minerals in shale are

H. Wan (✉) · Z. Gao
State Key Laboratory of Silicate Materials for Architectures,
Wuhan University of Technology, Wuhan 430070, China
e-mail: wanhw@whut.edu.cn

K. Scrivener and A. Favier (eds.), *Calcined Clays for Sustainable Concrete*,
RILEM Bookseries 10, DOI 10.1007/978-94-017-9939-3_21

crystalline with stable structure and no hydration activity. Numerous studies show that [2, 3] low-temperature calcined coal gangue and shale can be used as admixtures for cement production and mineral admixtures for concrete production. Moreover, the calcination temperature and the cooling technology have a significant effect on its potential activity [4, 5].

This paper selected the typical coal gangue and shale samples to investigate the effect of proportion and calcination temperature of coal gangue and shale on the pozzolanic activity, and calcined coal gangue-shale cementitious material without clinker was prepared by calcining coal gangue, clay shale, slag, gypsum and CaO at optimal proportion and calcining temperature.

2 Raw Materials and Test Methods

2.1 Experimental Raw Materials

The coal gangue, shale and slag powder used are resourced from Guangdong, China. The coal gangue and shale are bulk; while slag powder was ground to a specific surface area of 350 m^2/kg. The chemical composition of raw materials are shown in Table 1.

According to Table 1, chemical composition of coal gangue and shale are mainly SiO_2 and Al_2O_3, which is over 70 wt%.

The crystalline phases in coal gangue and shale were analyzed by XRD, shown in Figs. 1 and 2.

Figures 1 and 2 shows that the main minerals in coal gangue and shale are α-quartz and kaolinite, with small amounts of illite, montmorillonite and muscovite. The potential pozzolanic activity comes from the thermal decomposition of kaolinite and illiteinto amorphous SiO_2 and Al_2O_3.

2.2 Test Methods

2.2.1 Calcining Temperature and Processing of Coal Gangue and Shale

The lump of coal gangue and shale were crushed to particle size of approximately 5 mm, mixed in various proportions and then placed in the muffle furnace for

Table 1 Chemical composition of coal gangue, shale and slag powder (wt%)

	Loss	CaO	SiO_2	Al_2O_3	Fe_2O_3	MgO
Coal gangue	12.11	1.12	56.62	21.59	3.41	0.70
Shale	19.51	0.13	51.38	21.02	3.92	0.49
Slag powder	1.72	36.82	32.24	12.46	0.47	11.75

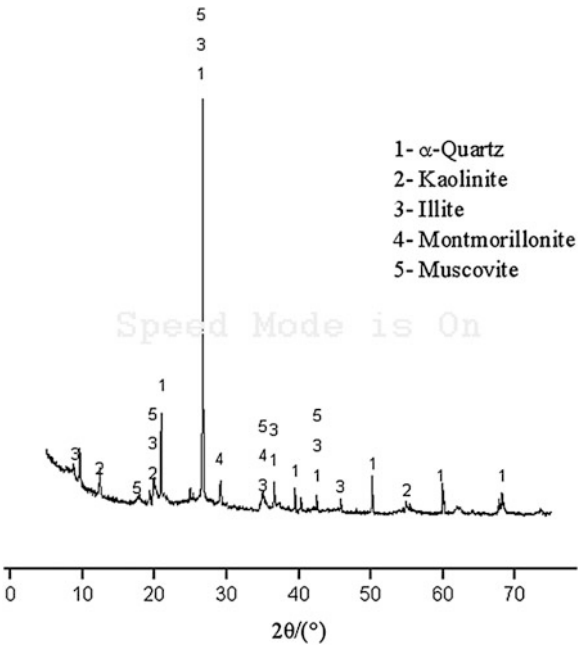

Fig. 1 XRD results of coal gangue

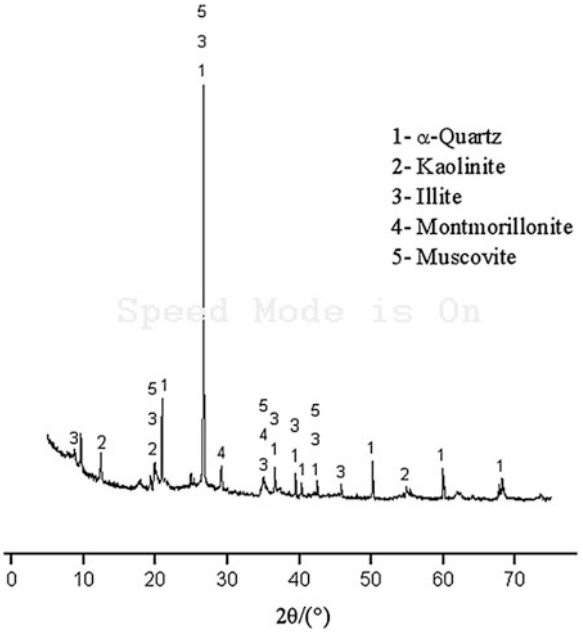

Fig. 2 XRD results of Shale

calcination. The calcination temperatures were set at 620, 700 and 780 °C. Samples incubated for 2 h at the above temperatures, and then cooled in air.

2.2.2 Pozzolanic Activity Test for Calcined Coal Gangue and Shale

The calcined samples were placed in a ball miller to grind to a fineness of 90 % of particles smaller than 80 μm. The test method of pozzolanic activity of the calcined sample is as follows. The reference sample was 100 % P.O. 42.5 cement, and the samples were 30 wt% calcined sample with 70 wt% P.O. 42.5 cement. Activity index is the strength percentage of the sample comparing to the reference sample. Mortar strength test was performed according to GB/T 17671-1999 "Cement mortar strength test method (ISO Act)".

3 Results and Discussion

3.1 Determination of Optimal Calcining Temperature of the Coal Gangue and Shale

DTA/TG curves of coal gangue and shale are shown in Figs. 3 and 4. TG curves of coal gangue and shale showed a weak endothermic peak around 85 °C with weight loss, indicating that free water in both was heated and evaporated. A strong

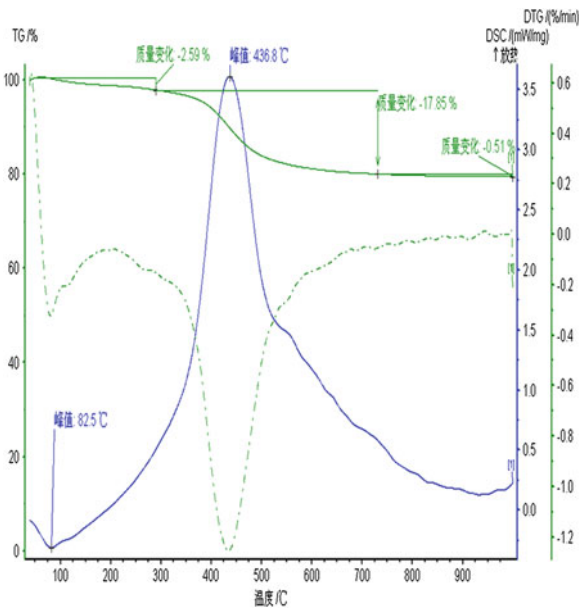

Fig. 3 DTA/T Gcurves of coal gangue

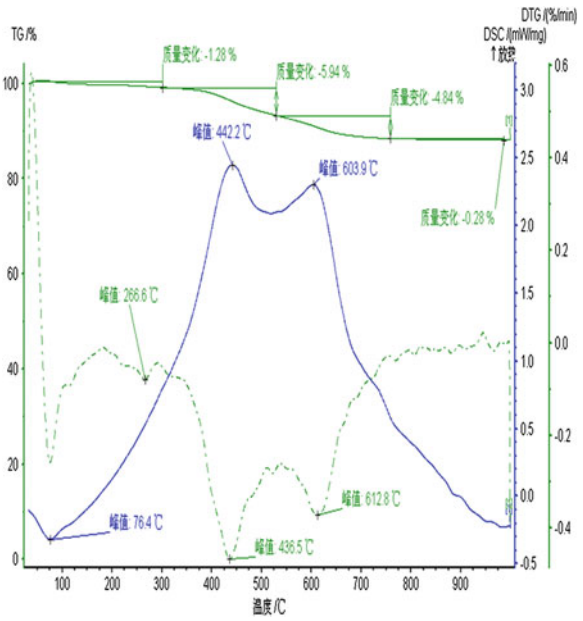

Fig. 4 DTA/T Gcurves of shale

endothermic peak at around 450 °C with more weight loss was attributed to the loss of chemically bond water of clay-based material during decomposition.

According to these curves [4], at 650 °C, the following reaction occurred in the clay minerals to form amorphous phases with pozzolanic activity.

$$Al_2O_3 \cdot 2SiO_2 \rightarrow Al_2O_3 + 2SiO_2$$

When the clay minerals were heated to 950 °C, amorphous SiO_2, Al_2O_3 and other active components react to form mullite and other crystalline phases, reducing the pozzolanic activity. The reaction is as follows.

$$3Al_2O_3 + 2SiO_2 \rightarrow 3Al_2O_3 \cdot 2SiO_2$$

Therefore, calcination temperature range of coal gangue and shale with better pozzolanic activity should be around 600–800 °C. And the calcination temperatures were set at 620, 700 and 780 °C in this study accordingly. The incubation duration is set to 2 h according to the literature [3]. In the case of too short incubation duration, neither the carbon-based substances are completely burnt nor the minerals are fully decomposed, resulting in the low pozzolanic activity. If the incubation duration is too long, the active components, which are amorphous SiO_2 and Al_2O_3, will crystallize again to form inactive mullite, resulting in the decrease of pozzolanic activity. Quench in the air allows the formation of small amount of glassy phases, which improves the activity and grinding properties of the sample.

Table 2 Activity of samples atvarious proportions and calcining temperatures

Serial number	Temperature/^{o}C	Coal gangue(M):shale(Y)	3d strength/MPa		28d strength /MPa		Activity index	
			Flexural	Compression	Flexural	Compression	3d	28d
1	620	M::Y = 3:7	5.7	28.7	6.8	38.2	80	76
2	620	M:Y = 5:5	5.6	21.7	7.2	34.4	60	68
3	620	M:Y = 7:3	6.0	27.3	7.2	40.8	76	81
4	620	M:Y = 10:0	5.4	25.8	7.2	32.5	72	64
5	700	M:Y = 3:7	6.0	26.7	7.7	42.7	74	84
6	700	M:Y = 5:5	6.4	25.5	8.2	40.6	71	81
7	700	M:Y = 7:3	6.8	26.6	7.7	39.5	74	78
8	700	M:Y = 10:0	6.4	25.5	6.4	32.4	71	64
9	**780**	**M:Y = 3:7**	**6.2**	**27.3**	**6.8**	**47.6**	**76**	**94**
10	780	M:Y = 5:5	6.3	26.9	6.3	44.9	74	89
11	780	M:Y = 7:3	7.4	29.0	6.8	45.7	81	91
12	780	M:Y = 10:0	6.4	27.8	5.5	42.8	77	85
14		100 % cement	6.3	36.0	8.9	50.4	100	100

3.2 *Effect of Proportions and Calcining Temperature on the Activity*

The activity indexes of coal gangue and shale samples at various proportions and calcining temperatures are shown in Table 2.

According to activity index in Table 2, the optimal calcining temperature of coal gangue and shale is 780 °C, and the coal gangue/shale ratio is 7:3, when the activity of the calcined sample is highest.

3.3 *Preparation of Calcined Coal Gangue-Shale Cementitious Material Without Clinker*

Several mixes of cementitious materials made from calcined minerals, slag powder, gypsum and lime are shown in Table 3. As the content of CaO in the calcined coal gangue and shale is too low, additional CaO was added in the above cementitious materials without clinker system as activator [6].

The mechanical properties of above cementitious materials at 3 and 28 days are shown in Table 4. According to these results, the standard consistency of each sample is 26–30 %, initial setting time is around 2 h, and final setting time is 4–6 h. However, the mechanical properties are different largely with various contents of slag powder and lime. Because the content of CaO in the calcined sample and slag powder is low, the alkalinity of the system is not high enough to stimulate pozzolanic reaction. When CaO was added to the system, the pozzolanic reaction was effectively activated, resulting in significantly increased mechanical properties of the system. When the amount of CaO reaches 15 %, the compressive strength of the system with 45 % calcined sample and 35 % slag powder reached 16.2 MPa and 35 MPa at 3 and 28 days respectively. Considering the standard consistency, setting time and mechanical properties of mixes, sample C1 met the performance requirements of 32.5 MPa strength grade cement.

Table 3 Mixes of cementitious material without clinker (wt%)

Serial number	Calcined sample	Slag powder	CaO	Gypsum	Sodium sulfate
A1	50	40	5	3	2
A2	55	35	5	3	2
B1	45	40	10	5	/
B2	50	35	10	5	/
B3	55	30	10	5	/
C1	**45**	**35**	**15**	**5**	**/**
C2	50	30	15	5	/
M	45	30	20	5	/

Table 4 Mechanical properties of cementitious materials without clinker

Serial number	Standard consistency %	Setting time, min		3d strength /MPa		28d strength /MPa	
		Initial setting	Final setting	Flexural	Compression	Flexural	Compression
A1	29.1	138	326	3.1	11.0	6.5	30.1
A2	29.3	150	340	3.0	10.7	5.8	30.3
B1	26.3	118	247	4.3	18.2	8.2	32.4
B2	27.6	130	285	5.1	19.2	9.0	31.0
B3	28.3	139	305	4.9	20.5	7.6	31.6
C1	**26.4**	**110**	**260**	**4.1**	**16.2**	**9.2**	**35.0**
C2	28.0	146	293	4.7	15.6	8.6	31.8
M	26.8	124	270	3.8	14.1	8.8	30.7

4 Conlusions

The effect of proportion and calcination temperature of coal gangue and shale on the pozzolanic activity was investigated, and calcined coal gangue-shale cementitious material without clinker was prepared by calcining coal gangue, clay shale, slag, gypsum and CaO at optimal proportion and calcining temperature. According to the results, the following conclusions can be drawn.

1) When the proportion of coal gangue and shale is 7:3 and the calcination temperature is controlled at 780 °C for 2 h with rapid cooling in the air, the pozzolanic activity of calcined coal gangue and shale reached the maximum.
2) The cementitious material without clinker can be prepared with calcined samples of 70 wt% coal gangue and 30 wt% shale. With the addition of 5 wt% gypsum and 15 wt% CaO, the 3d and 28d compressive strength of the cementitious materials system composed of 45 wt% calcined sample and 35 wt % slag powder reached 16.2 MPa and 35 MPa respectively. And the performance met the requirements of 32.5 MPa strength grade cement.

References

1. Jianjun, Cao, Yongjuan, Liu, Guangli, Guo: Comprehensive Utilization of coal gangue. Env. Pollut. Control Technol. Equip. **5**(1), 19–22 (2004)
2. Gang, Dong, Pengming, Wang, Qi, Feng: Experimental study on thermal activation of pozzolanic activity of coal gangue. Build. Gypsum Cementitious Mat. **10**, 9–11 (2004)
3. Chen, M., Chunhua, F., Li, X.: Shudy on burning shale as cement admixture. Portland Bull. **29** (6), 1397–1401 (2010)

4. Shvarzman, A., Kovler, K., Grader, G.S., et al.: The effect of dehydroxylation/amorphization degree on pozzolanic activity of kaolinite. Cem. Concr. Res. **33**(3), 405–416 (2003)
5. Changling, He: Thermal stability and pozzolanie activity of raw and calcined mixed layer mica/smectite. Appl. Clay Sci. **1**, 141–161 (2000)
6. Xianwei, Ma., Niu, Jishou: Discussion of coal gangue activation method. Utilization Min. Res. **2**, 41–45 (2008)

Red Ceramic Wastes: A Calcined Clay Pozzolan

Viviana Rahhal, Zbyšek Pavlík, Monica Trezza, Cristina Castellano, Alejandra Tironi, Tereza Kulovaná, Jaroslav Pokorný, Robert Černý and Edgardo F. Irassar

Abstract The properties and hydration of blended cements containing from 8 to 40 % by mass of ceramic waste (CW) from different countries (Argentine and Czech Republic) are investigated. The mini slump, the heat released rate up to 48 h, the pozzolanic activity and the compressive strength at 2, 7 and 28 are determined. Hydration process is characterized by XRD analysis and the pore size refinement is accessed by MIP. Results show that both CWs increase the water demand with increasing the cement replacement level, and they possess pozzolanic activity after 7 days. At early age, the heat released and the compressive strength are lower than that of the Portland cement (PC) for all replacement levels. At 28 days, the pozzolanic reaction significantly improves the compressive strength. From XRD analysis, it is evident that CW reacts to form AFm phases (hemicarboaluminate at 7-28 and later transformed to monocarboaluminate) depending on the replacement level and CW used. CH peak reduction due to the pozzolanic reaction appears at 28 days. The reduction of porosity up to 16-24 % of CW replacement is in accordance with the compressive strength results.

1 Introduction

Portland cement industry promotes the partial replacing of PC with natural materials, less embolied-energy materials, industrial wastes or by-products from different manufacturing processes having pozzolanic properties. Among these materials, the interest on the calcined clays and the industrial CW is renewed.

For use of CW as pozzolan, the composition fluctuations and raw materials change must be considered because not all of modern red bricks have pozzolanic

V. Rahhal · M. Trezza · C. Castellano · A. Tironi · E.F. Irassar (✉)
Facultad de Ingeniería, CIFICEN (CONICET-UNCPBA), Olavarría, Argentina
e-mail: firassar@fio.unicen.edu.ar

Z. Pavlík · T. Kulovaná · J. Pokorný · R. Černý
Faculty of Civil Engineering, Czech Technical University in Prague, Czech Republic
Czech Republic

K. Scrivener and A. Favier (eds.), *Calcined Clays for Sustainable Concrete*,
RILEM Bookseries 10, DOI 10.1007/978-94-017-9939-3_22

properties [1]. Then, the behavior of CW from different manufacturers with the same appearance may differ. Several researchers have proposed different alternatives to use the wastes of ceramic industry, in particular for production of roof tiles [2], bricks [3] and floor tiles [4]. Sabir et al. [5] found that the partial replacement of PC by ground red brick (GRB) reduces the early compressive strengths. But, the later strength of blended cement (up to 20 % GRB) is similar or greater than that of the PC. Brazilian researchers estimate that a 10 % reduction of CO_2 emissions can be attained using 20 % replacement of cement by CW produced in their country [6].

Since the benefits and potential of CWs application in the development of blended binder are evident, two PCs and two CWs are studied in the paper in order to identify proper materials for industrial application.

2 Materials and Testing Methods

Two CEM I cements (ArgPC, CzPC) and two ceramic wastes (ArgCW, CzCW) from Argentine Republic and Czech Republic were used to make the same test-plan. Table 1 reports the chemical composition determined by XRF of PCs. C_3A-content is low (~2.5 %) in ArgPC and medium (~6.5 %) in CzPC. Calcite is the minor component (<5 %) in both PCs. The physical characteristics of PC are also given in Table 1. The CzPC is finer than ArgPC and they are classified as CEM I 42.5R and CEM I 32.5, respectively.

The ArgCW consisted of the scrap discarded as waste in a local brick manufacturer (firing temp ~ 950-1050°C). The ArgCW was crushed and finely ground in laboratory ball grinding mill. The CzCW was a by-product originating from the brick producer during the grinding of highly precise cavity brick blocks previously fired at about 800-850 °C. The CzCW was used as collected in the factory. The chemical composition and the physical characteristics of CWs are reported in Table 1. PSD of CW was measured in wet dispersion (ethanol) by laser diffraction (Analysette 22 Micro Tec Plus- FRITSCH). The ArgCW is composed by a glassy phase with dome from 18 to 30° 2Θ deg, quartz, feldspars (mainly as anorthite) and low content of hematite. The composition of CzCW was glassy phase with a dome from 5 to 30° 2Θ deg and the crystalline compounds were quartz, feldspars (albite, microcline and orthoclase) and mica (muscovite and biotite). Using the Rietveld method, the amount of amorphous material was estimated as 37 % for ArgCW and 47 % for CzCw.

The CW was incorporated in blended binder in 8, 16, 24, 32 and 40 % of weight of cement. For all blended cements, the assessed properties were:

The initial **mini-slump test** and the loss of flow ability at 30, 60, 120 and 180 min were determined on paste (w/cm = 0.50) mixed in planetary laboratory machine and remixing every 15 min. Pozzolanic activity of blended cements was determined by **Frattini test**. The **rate of heat evolution** and the cumulative heat released during hydration of paste (w/cm = 0.50) were measured up to 48 h under isothermal conditions at 20 °C in conduction calorimeter. The **compressive**

Table 1 Chemical composition and physical properties of used materials

Chemical composition, %											
Materials		SiO_2	Al_2O_3	Fe_2O_3	CaO	MgO	SO_3	Na_2O	K_2O	TiO_2	LOI
Portland cement	ArgPC	21.5	3.8	3.8	64.3	0.8	2.6	0.1	1.1	-.-	2.1
	CzPC	18.9	4.2	3.8	62.4	1.0	2.3	0.02	1.1	0.8	1.5
Ceramic waste	ArgCW	64.6	17	5.6	2.5	1.5	-.-	4.2	2.9	0.7	0.6
	CzCW	51.3	20	6.0	11.5	4.5	1.0	1.3	3.2	0.8	1.1
Physical properties											
Materials		Density, kg/m^3		SS Blaine, m^2/kg		Particle size, μm					
						d_{90}		d_{50}		d_{10}	
Portland cement	ArgPC	3.15		315		63.5		19.0		2.7	
	CzPC	3.08		330		38.2		14.2		2.3	
Ceramic waste	ArgCW	2.68		590		64.7		30.2		6.0	
	CzCW	2.77		665		36.6		22.7		4.5	

strength was obtained on prims specimens (using a transversal section of 16 cm^2) cured during 24 h in molds and later in sealing condition until test age (2, 7 and 28 days). The reported value is the mean of four tests.

Pastes (*w/cm* = 0.50) sealed curing were used to determine the hydration products by XRD, the matrix density and the pore size distribution. At 2, 7 and 28 days, paste fragments were ground and **XRD analysis** was performed on Philips PW 3710 diffractometer (CuKα radiation, 40 kV and 20 mA). Other paste fragments were vacuum dried to measure the **matrix density** on Helium Pycnomatic ARC (Thermo Sc) and the pore size distribution on **mercury intrusion porosimetry (MIP)** using device Pascal 140 and Pascal 440 (Thermo Sc).

3 Results and Discussion

3.1 Mini slump Test

The spread diameter of cement pastes as a function of time is showed in Fig. 1. ArgPC paste (Fig. 1a) has an initial spread diameter (124 mm) higher than the corresponding to the CzPC (Fig. 1b - 84 mm). It is attributed to the mineralogical composition and the high specific surface of CzPC that increases the water demand. For both set of materials, the initial spread diameter of blended cement decreases (124 to 92 mm for Arg-set and 84 to 58 mm for Cz-set) with increasing the CW content. The trend of the mini-slump loss of plain and blended cements is similar for both set of materials.

3.2 Pozzolanic Activity of Blended Cements

Previous reported results of Frattini test [7] show that all PC-CW combinations have not pozzolanic activity at 2 days. At 7 days, blended cements with 8 and 16 %

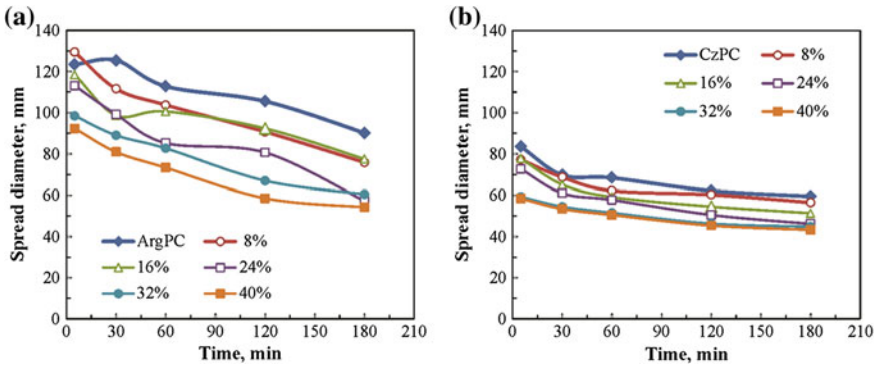

Fig. 1 Results of the mini-slump test **a** ArgCW-ArgPC; **b** CzCW-CzPC

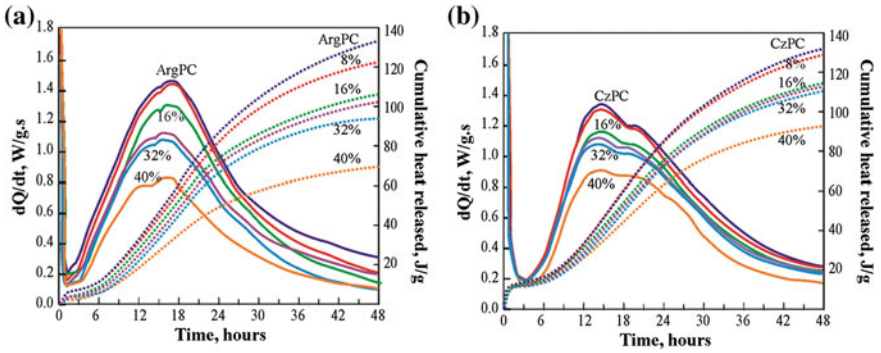

Fig. 2 Heat resealed rate and cumulative heat released **a** ArgPC-ArgCW; **b** CzPC-CzCW

CW have not pozzolanic activity, those with 24 % CW are located on to the calcium isotherm curve and those with 32 and 40 %CW are pozzolanic. At 28 days, all blended cements have pozzolanic activity. This test determines that both CW has pozzolanic activity between 7 and 28 days.

3.3 Heat Released

Figure 2 shows results of the rate of heat evolution and the cumulative heat released. Analyzing the dQ/dt curve, it shows that blended cements copy the shape of the curve corresponding to the parent cement without significant variation on the occurrence time for second and third peak and with a declined intensity of the heat signal when increases the replacement level of CW. This behavior revels that CW acts as filler during the early hydration of PC causing the filler and dilution effects. The cumulative heat is lower than the corresponding PC al all test age. For 40 % CW, the duration of dormant period is longer, and the heat released decays considerably.

3.4 Compressive Strength

Figure 3 shows the compressive strength (CS) at 2, 7 and 28 days as function of CW. The ArgPC can be replaced with ground ArgCW (up to 16 %) without impairing the CS after 28 days (Fig. 3a). Replacing 8 % of the ArgPC by CW even retain or increases the CS at all ages. At 28 days, the strength index measured as the ratio between compressive strength of blended cement and plain cement was from 0.97 to 0.77 for 8 to 40 % ArgCW. The CzPC pastes have high CS than the ArgPC and the incorporation of CzCw causes a proportional decrease of CS at 2, 7 and

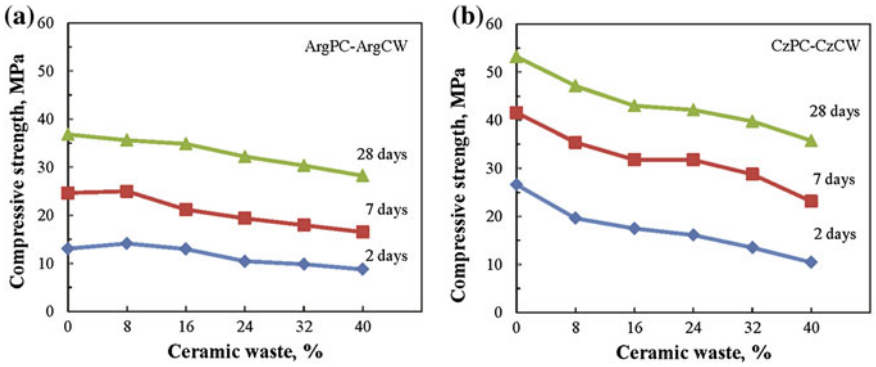

Fig. 3 Results of compressive strength **a** ArgPC-ArgCW; **b** CzPC-CzCW

28 days. However, the CS of CzPC-CzCWs was always greater than the corresponding to ArgPC-ArgCW. This observation indicates the great influence of parent cement on this parameter. For example, the strength index of CzPC with 24 % CzCW was 0.61, 0.76 and 0.79 at 2, 7 and 28 days, respectively. The strength index is higher than 0.75 indicating the progress of pozzolanic reaction after 7 days.

3.5 Mechanism and Kinetic of Hydration PC-CW

Table 2 summarizes the hydrated compounds and the intensity of main peak for all pastes, of XRD pattern previously reported [7]. At 2 days, the ArgPC and CzPC pastes show the presence of ettringite (E), calcium hydroxide (CH) and the unhydrated PC phases (C_4AF and C_2S). No assignable peaks to AFm phase were found. For all blended cements, similar hydrated compounds assemblage is occurred to the corresponding PCs. Quartz (Q) and feldspars (F), impurities in CW, are also identified. At 7 days, E and CH were accompanied by hemicarboaluminate (HC) in both PCs. The Frattini test show pozzolanic activity at 7 days for blended cements (Arg and Cz) with 32 and 40 % CW. The pozzolanic reaction of CW produces a cementing compound like C–S–H and some alumina hydrated phases that depend on the available CH and the CW reactivity. When CH is high and the reactive alumina in CW is high, the AFm phase obtained is C_4AH_{13}. The transformations to C_4AH_{13} first to HC and then to monocarboaluminate (MC) is due to the carbonate added as minor component in the PCs. According to the solubility products for C_4AH_{13}, HC and MC [8], the MC is the more stable AFm-phase. The AFm phase associated with the pozzolanic reaction at 7 days is the HC and its main peak intensity is greater for blended cements with 40 % CW. At 28 days, the insipient formation of MC coexists with the HC and their peak intensities are greater in the CzPC-CzCW. This is justified by the different CW reactivity.

Table 2 Hydrated compounds and peak intensity for cement pastes at 2, 7, and 28 days

Age, days		ArgPC-ArgCW						CzPC-CzCW					
		0	8	16	24	32	40	0	8	16	24	32	40
2	E	✓✓	✓✓	✓✓	✓✓	✓✓	✓	✓✓	✓✓	✓✓	✓✓	✓✓	✓✓
	CH	✓✓✓	✓✓✓	✓✓✓	✓✓✓	✓✓✓	✓✓	✓✓✓	✓✓✓	✓✓✓	✓✓✓	✓✓✓	✓✓
7	E	✓✓	✓✓	✓✓	✓✓	✓✓	✓	✓✓	✓✓	✓✓	✓✓	✓✓	✓✓
	HC	✓	✓	✓	✓	✓✓	✓✓	✓	✓	✓✓	✓✓	✓✓	✓✓✓
	CH	✓✓✓	✓✓✓	✓✓✓	✓✓✓	✓✓✓	✓✓	✓✓✓	✓✓✓	✓✓✓	✓✓✓	✓✓✓	✓✓
28	E	✓✓	✓✓	✓✓	✓✓	✓✓	✓✓	✓✓	✓✓	✓✓	✓✓	✓✓	✓✓
	HC		✓	✓	✓	✓	✓✓	✓	✓	✓	✓	✓✓	✓✓✓
	MC		✓	✓	✓	✓✓	✓✓	✓	✓	✓	✓✓	✓✓	✓✓
	CH	✓✓✓	✓✓✓	✓✓✓	✓✓✓	✓✓	✓✓	✓✓✓	✓✓✓	✓✓	✓✓	✓✓	✓✓

✓✓✓ very strong
✓✓ strong
✓ weak

Table 3 Matrix density, total cumulative volume and threshold pore diameter of pastes

Property	Age, days	ArgPC-ArgCW				CzPC-CzCW			
		0	8	24	40	0	8	24	40
Matrix density, kg/m^3	2	2528	2568	2538	2597	2509	2435	2432	2485
	7	2342	2423	2420	2437	2338	2297	2339	2407
	28	2321	2356	2395	2422	2308	2257	2319	2356
Total cumulative volume, cm^3/g	2	27.5	32.9	35.9	41.1	27.2	33.4	39.4	40.1
	7	23.7	28.9	34.2	37.1	23.8	28.4	36.0	36.6
	28	21.1	24.6	29.1	34.3	21.1	18.3	19.2	24.9
Threshold pore diameter, μm	2	1.13	1.48	1.72	2.64	0.91	0.92	1.05	1.13
	7	0.62	0.93	1.17	1.75	0.27	0.36	0.97	1.15
	28	0.19	0.67	0.75	1.20	0.19	0.16	0.18	0.15

3.6 Matrix Density and Porosity

Table 3 reports the matrix density of paste. This property depends on the assamblage of unhydrated and hydrated compounds and especially on the porosity. For all samples, the matrix density decreases when the hydration progress and blended cement with 8 % CW have the large reduction from 7 to 28 days. The CzPC and its blended cements have low density matrix at all ages due to a large volume of ettringite.

The total cumulative volume of intrusion and threshold pore widths for paste containing 0, 8, 24 and 40 % of CW at 2, 7 and 28 days are also reported in Table 3. As expected, the increased curing time reduces the total porosity and causes a smaller threshold pore widths for both systems due to the hydration progress. The incorporation of CW increased the total porosity of the blended cement pastes, whereas the both properties increased with an increase in the replacement level of CW. Well-defined threshold pore widths were defined from 1.72 to 0.91 μm at 2 days at early age.

4 Conclusions

Based on the results of this study, the following conclusions can be drawn:

- Ceramic waste originated in ceramic factory can be used as a pozzolanic material contributing to reduction of CO_2 emission in cement based materials.
- CW replacement decreases the initial mini slump, has little significance on the mini-slump loss and reduces the heat released during cement hydration up to 48 h without significant changes in the time of occurrence of main peaks.

- CW behaves as filler at early ages but when the hydration progress, its pozzolanic activity consumes the CH, produces AFm phases that depend on the ages and carbonate presence.
- Blended cements with CW had low compressive strength at early ages but comparable strength-class at later age. Blended cement pastes containing CW exhibited higher porosity than those of PC paste, but reduction in threshold value for more reactive CW.

Acknowledgments The authors gratefully acknowledge the financial supports received for this cooperation by the MINCyT of the Argentine Republic and the MEYS of the Czech Republic. The work was also partially supported by the Czech Science Foundation, under project No 14-04522S and by the ANPCyT under project PICT 0160-12.

References

1. Baronio, G., Binda, L.: Study of the pozzolanicity of some bricks and clays. Const. Build. Mat. **11**(1), 41–46 (1997)
2. Sánchez, M.I., Marin, F., Rivera, J., Frias, M.: Morphology and properties in blended cements with ceramic wastes as a pozzolanic material. J. Am. Cer. Soc. **89**(12), 3701–3705 (2006)
3. Naceri, A., Hamina, M.C.: Use of waste brick as a partial replacement of cement in mortar. Waste Man **29**(8), 2378–2384 (2009)
4. Ay, N., Unal, M.: The use of waste ceramic tile in cement production. Cem. Concr. Res. **30**(3), 497–499 (2000)
5. Sabir, B.B., Wild, S., Bai, J.: Metakaolin and calcined clays as pozzolans for concrete: a review. Cem. Concr. Compos. **23**, 441–454 (2001)
6. Toledo Filho, R.D., Gonçalves, J.P., Americano, B.B., Fairbairn, E.M.R.: Potential for use of crushed waste calcined-clay brick as a supplementary cementitious material in Brazil. Cem. Concr. Res. **37**, 1357–1365 (2007)
7. Irassar, E. F., Rahhal, V., Tironi, A., Trezza, M., Pavlík Z., Pavlíková, M., Jerman, M., Cerný; R.: Utilization of ceramic wastes as pozzolanics materials; in nanotechnology 2014: electronics, manufacturing, environment, energy & water. Washington, vol. 3, p. 230–233 (2014)
8. Matschei, T., Lothenbach, B., Glasser, F.P.: The AFm phase in Portland cement. Cem. Concr. Res. **37**, 118–130 (2007)

Assessment of Sustainability of Low Carbon Cement in Cuba. Cement Pilot Production and Prospective Case

Sofía Sánchez Berriel, Yudiesky Cancio Díaz, José Fernando Martirena Hernández and Guillaume Habert

Abstract This study combines two techniques for the assessment of sustainability in cement and concrete production: Life Cycle Analysis and Eco-efficiency. The first technique is used to assess the environmental impact of Low Carbon Cement (LC3) production from quarrying to the factory´s gate. The LCA is developed in order to compare three Cuban cements and its associated impacts: OPC, PPC and LC3. For that purpose, an inventory is developed using official statistics of the cement sector, calculated productive and economic indexes and emission factors. Global warming and energy use, are the main identified impacts. The second method is employed for the calculation of the improvement potential derived from the substitution of OPC by LC3 in a model house built with LC3 in Santa Clara city. A considerable improvement of 54 percent in the eco-efficiency indicator has been achieved as a result of using blended cement that is a proper combination of clinker, metakaolin, gypsum and limestone. The results become a challenge for Cuban construction sector in order to generalize the technology as a sustainable product from the economic, social and environmental point of view.

1 Introduction

Concrete, made with Portland cement, is second only to water in total volume produced and consumed annually by society [1]. Due to its large consumption, it has a significant environmental impact at global scale, mainly associated with cement production. Among all the solutions proposed to solve the negative impact

S.S. Berriel (✉) · Y.C. Díaz
Faculty of Economic Sciences, Central University of Las Villas, Santa Clara, Cuba
e-mail: ssanchez@uclv.edu.cu

J.F.M. Hernández
Center for the Research and Development of Structures and Materials (CIDem), Central University of Las Villas, Santa Clara, Cuba

G. Habert
Chair of Sustainable Construction, ETH Zurich, Zurich, Switzerland

K. Scrivener and A. Favier (eds.), *Calcined Clays for Sustainable Concrete*, RILEM Bookseries 10, DOI 10.1007/978-94-017-9939-3_23

of cement industry worldwide, clinker substitution is proven to be the most effective to reduce carbon emissions. The production of a new cement with a 0.50 clinker ratio, denominated Low Carbon Cement (LC3) it's presented as a good solution with attractive production costs and minimum capital investment. To prove that in 2013 an industrial trial was carried out in Cuba. This paper presents the assessment of sustainability in LC3 cement and concrete produced in the Cuban industrial trial, through two techniques: Life Cycle Analysis and Eco-efficiency. Both methodologies are widely use to assess environmental impacts of cements in literature [2–6].

In the first part, a description of LC3 production is given. Then, costs, energy and environmental impacts are evaluated using Life Cycle Assessment approach to compare with Portland cements traditionally produced in Cuba. Finally, the eco-efficiency of a house built with LC3 is assessed and compared with OPC use in the same structure. Combining both methods a complete study is made about the impact of LC3 production in Cuba, in order to generalize its production.

2 Production of a Low Carbon Cement in Cuba, Industrial Trial

An industrial trial was carried out in 2013 to produce a large amount of the new cement (LC3) under real conditions at cement factory *Siguaney*. After calcination, according with Vizcaino et al. [7] the reactivity of the material calcined in the rotatory kiln compared with the material calcined at the lab, indicates that the industrial calcination was successful. After grinding process, a production of 110 tons of Low Carbon Cement was obtained. Thus, of the remaining tonnes approximately 10 tons were pack in sacks for lab testing and the rest were stored in bulk in a silo. Table 1 presents the chemical composition of the cement obtained (LC3) and the used as reference for the impacts assessment.

The rest of the material was distributed among builders and building material manufacturers, whom (under strict supervision) focused on two main cement applications: (1) manufacture of hollow concrete blocks (500 x 200 x 150 mm) and (2) manufacture of 25 MPa precast concrete elements at a prefabrication plant [7].

Table 1 Composition of cements taken for impacts assessment

Cement Type	Cements composition (%)				
	CK	CC[1]	Gypsum	Ccl	Zeolite
OPC (P-35 in Cuba)	0.88	0.05	0.07	–	–
PPC (PP-25 in Cuba)	0.75	–	0.05	–	0.20
LC3(industrial trial)	0.50	0.14	0.09	0.27	–

[1]Calcium carbonate

3 Assessment of Case Study Production of LC3, Cuba

To assess LC3 production under industrial trial conditions, costs were calculated in two steps: 1) breakdown of calcined clay, clinker and other raw materials production costs; 2) breakdown of LC3, Ordinary Portland Cement (OPC) and Pozzolanic Portland Cement (PPC) production costs. Results show that, with LC3 production, as is shown in Fig. 1, it is possible to reduce costs of cement substituting a portion of clinker by limestone and calcined clay. Present substitution levels rises 13 % with PPC production and savings are around 10 % in this case. With LC3 savings are between 4-40 % in comparison with PPC costs depending on transport costs of kaolinite clay.

Energy balance was calculated in Mega Jules (MJ) using real consumption indexes of energy [8] and the average caloric power of Cuban crude oil which is the fuel used in Siguaney. As was expected clay calcination process uses less energy intensive. Higher reduction is presented in thermal energy for calcination process. There is observed a reduction of more than 1500 MJ per ton of cement produced.

To estimate CO_2 emissions was followed the methodology of the Intergovernmental Panel for Climate Change, 2006 (IPCC) [9], whereas clinker (CK) production is multiplied by an emission factor. The emissions caused by the chemical decomposition of $CaCO_3$ y $MgCO_3$ contained in raw materials (grey limestone and clays), were deduced through stoichiometry calculations with by calculating the differences in the CaO and MgO content of the raw materials before been introduced in the kiln and at the exit (CK or calcined clay) [10]. The CO_2 emissions in the phase of cement grinding, are associated with the electricity consumption in the ball mill. Other sources of emissions are considered negligible and thus discarded. The final calculation of CO_2 emissions is presented in Fig. 2.

The low carbon cement produced in non-optimized conditions during industrial trial, reduces approximately 360 kg CO_2/tonnes in relation to OPC (P-35), this is

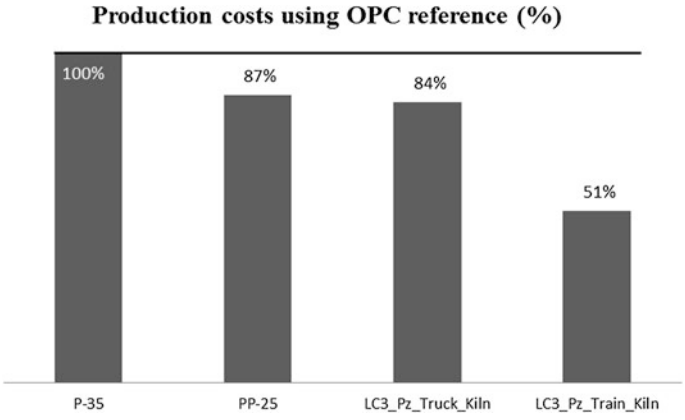

Fig. 1 Production costs of LC3 (%) compared with OPC and PPC reference

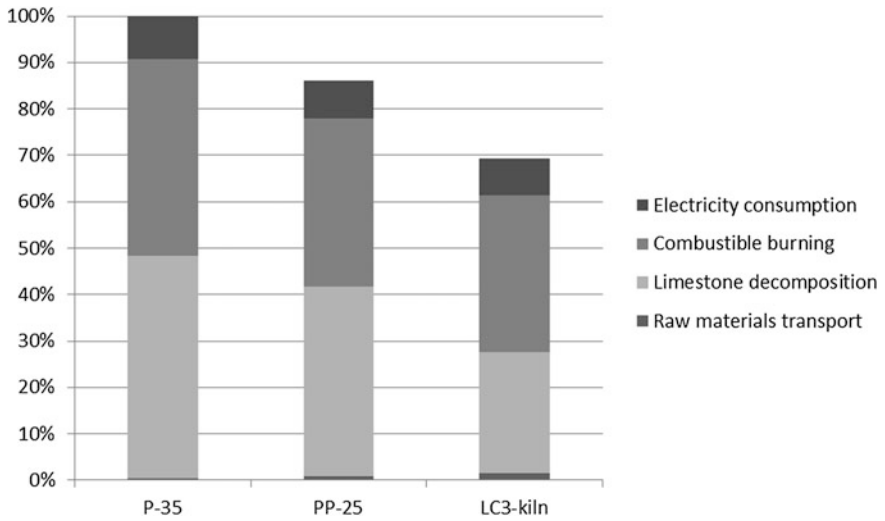

Fig. 2 CO_2 emissions associated to LC3 production with 45 % of SCM and compared to the reference cements P-35 and PP-25

approximately 31 %. Reduction in reference to traditional Cuban blended cement (PP-25) is in the range of 155 kg CO_2/tonne. A small increase is reported in transport emissions due to the amount of new raw material that needs to be carry, but this is negligible if we compare reductions generated during cement production process.

4 Eco-Efficiency Model House Built with LC3, Cuba

To assess the eco-efficiency of a model house built with LC3 in Santa Clara city (Picture 1a) having a square meter as functional unit (Picture 1b), a new eco-efficiency calculation method was developed by Cancio, 2014 [11]. Main steps of this methodology are: stablish the functional unit to analysis, design and analyze the supply chain, calculate eco-efficiency indicators, results comparison and evaluation.

In Cuban case, three scenarios were evaluated as is shown in Table 2. Results show that a house built entirely with LC3, or some components (Scenarios 3 and 2) presents higher eco-efficiency compared with the house built with OPC traditional cements (Scenario 1). That proves LC3 use in house construction is feasible with a reduction of CO_2 emissions and associated costs between 30 and 40 %.

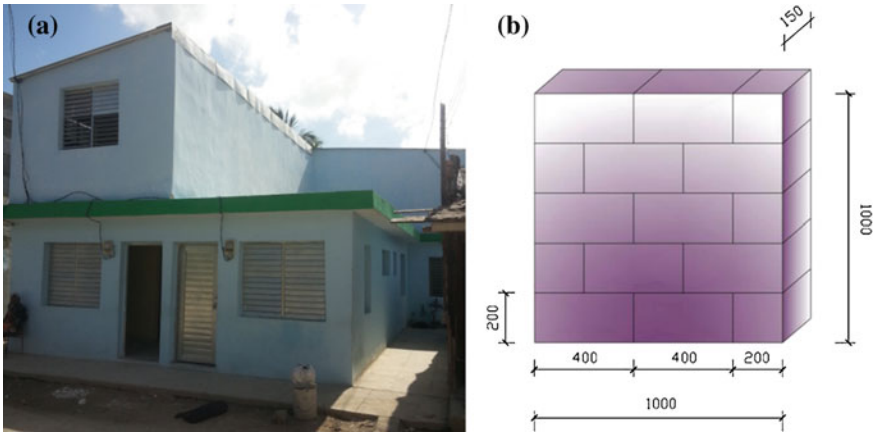

Picture. 1 **a** Model house built with LC3 in Santa Clara city, **b** Functional unit: m^2

Table 2 Eco-efficiency calculation results in different scenarios

Scenarios	Scenario definition	Emissions (kg co_2/m^2 wall)	Market price based-cost (usd/m^2 wall)	Value added (usd/m^2 wall)	Eco-efficiency indicator (usd/co_2/m^2 wall)
1	PPC Mortars/ OPC Blocks	24	5.2	495	20
2	LC3 Mortars/ OPC Blocks	22	3.7	496	22
3	LC3 Mortars/ LC3 Blocks	16	3.2	497	30

5 Conclusions

- LC3 production in Cuba will have positive economic and environmental impact, with a reduction of the production cost between 4 and 40 % and savings of CO_2 between 15 and 30 %. This will depend on the technology used to produce the calcined clay and also the kaolinite clay deposit select for its production.
- LC3 use to build houses increases the eco-efficiency of this activity with a significant reduction of carbon emissions and production costs along all the productive chain.

Acknowledgments The authors would like to acknowledge Siguaney cement factory for the technical and material support. The authors would like to thanks to the whole team of the "*Low Carbon Cement*" Project for all the advisory and technical help during this paper creation.

References

1. World Business Council for Sustainable Development and Cement Sustainability Initiative: (2008) Cement industry energy and CO_2 Performance: "getting the numbers right". Disponible en: http://www.wbcsdcement.org/
2. Boesh, M.E., S. Hellweg: Identifying improvement potentials in cement production with life cycle assessment. Environ. Sci. Technol. **44**(23) (2010)
3. Habert, G., Billard, C., Rossi, P., Chen, C. y N. Roussel (2010) Cement production technology improvement compared to factor 4 objectives in "Cement and concrete research". No. 40. Pgs 820–826. Disponible en: http://ees.elsevier.com/CEMCON/default.asp
4. Damineli, B., Kemeid, F., Aguiar, P. Vanderley, Y.J.: Measuring the eco-efficiency of cement use. Cement Concr. Compos. 32, 555–562 (2010). Disponible en: http://www.elsevier.com/locate/cemconcomp
5. ISO 14045:2012(E): Environmental management—ecoefficiency assessment of product systems—principles, requirements and guidelines
6. WBCSD: Eco-efficiency: creating more value with less impact (1999). http://www.wbcsd.org
7. Vizcaíno, L., Sánchez, S., Damas, S, Pérez, A., Scrivener, K., Martirena, F.: Industrial trial to produce a low clinker, low carbon cement. Materiales de Construccion. **65**(317) (2015), January–March 2015, e045. ISSN-L:0465-2746. doi: http://dx.doi.org/10.3989/mc.2015.00614
8. Siguaney Factory: Energy report—September. Work document in digital version (2014)
9. Eggleston, H.S., Buendia, L., Miwa, K., Ngara, T., Tanabe, K.: IPCC guidelines for national greenhouse gas inventories. In: National Greenhouse Gas Inventories Programme (2006) http://www.ipcc-nggip.iges.or.jp
10. WBCSD-CSI: The Cement CO_2 and Energy Protocol-Version 3.0. (2005). http://www.wbcsdcement.org/
11. Cancio, Y., Sánchez, I.R., Martirena, J.F.: Methodology to measure the eco-efficiency of a house built with LC3 in Santa Clara city. Cuba, Power point presentation (2014)

Ternary Blended Cement with Limestone Filler and Kaolinitic Calcined Clay

Alejandra Tironi, Alberto N. Scian and Edgardo F. Irassar

Abstract The use of calcined clays providing from low grade kaolinitic clays combined with the limestone filler in ternary blended cement formulation has received considerable attention in recent years. This paper describes the results of a research project to study the behavior of kaolinitic calcined clays (CC) in combination with limestone filler (F). Blended cements were obtaining replacing CC (0–30 %) and F (0–10 %) by mass by Portland cement (PC). The pozzolanicity of blended cement was assessed by the Frattini tests at 2, 7 and 28 days. The response of the system was evaluated in terms of flow, and the compressive strength at 2, 7 and 28 days. The hydration progress was determined by the type and amount of hydration compounds at 2, 7 and 28 days using the Rietveld method. The change in pore size distribution was determined by mercury intrusion porosimetry (MIP). Hydrated phases obtained correspond to the pozzolanic reaction (contribution CC) and phase stabilization (contribution F) modifying the pore structure and all factors contribute to develop acceptable mechanical properties with a large reduction of energy consumption and CO_2 emission.

1 Introduction

The use of calcined clays providing from low grade kaolinitic clays combined with the limestone filler in ternary blended cement formulation has received considerable attention in recent years [1]. The metakoalinite (MK) containing in calcined clays is the pozzolanic material [2], quartz is the main impurity of calcined clay [3] and the limestone filler provides the carbonate to form the AFm phases [4]. Calcium carbonate reacts with alumina from MK, forming additional AFm phases and stabilizing

A. Tironi (✉) · E.F. Irassar
Facultad de Ingeniería, CIFICEN (CONICET –UNCPBA), BJWI 7400, Olavarria, Argentina
e-mail: atironi@fio.unicen.edu.ar

A.N. Scian
Centro de Tecnología de Recursos Minerales Y Cerámica (CONICET – UNLP),
La Plata, Argentina

K. Scrivener and A. Favier (eds.), *Calcined Clays for Sustainable Concrete*,
RILEM Bookseries 10, DOI 10.1007/978-94-017-9939-3_24

ettringite [5]. The aim of this paper is to investigate the use of calcined clay providing from low grade kaolinitic clay in combination with limestone filler as partial cement replacement in binary and ternary cements.

2 Materials and Methods

2.1 Blended Cements

Blended cements (bc) were obtained replacing calcined clay (0 to 30 % by mass) and limestone filler (0 to 10 %) by Portland cement (PC). The PC used is a normal Portland cement with a Blaine fineness of 315 m^2/kg, and its Bogue´s potential composition is 60 % C_3S, 16.4 % C_2S, 3.8 % C_3A and 11.5 % C_4AF by mass. For this PC, limestone is added as minor component (<°3 %). Kaolinitic clay was calcined at 750 °C and during 4 h to produce calcined kaolinitic clay (CC) with 44 % of metakaolinite (MK). Quartz is the main impurity in CC and it could be considered as filler due to its small particle size. The CC has a Blaine fineness of 623 m^2/kg, and limestone filler (F) of 515 m^2/kg. Blended cements were denominated as 10F, 30CC, 5F15CC, and 10F30CC according to the level of replacement of each addition.

2.2 Pozzolanic Activity

The pozzolanicity of blended cements was assessed by the Frattini test at 2, 7 and 28 days. The water demand of ternary system was evaluated in terms of mortar flow and the mechanical performance in terms of compressive strength at 2, 7 and 28 days.

In Frattini test [6], 20 g of blended cement was mixed with 100 ml of boiled distilled water. After preparation, samples were left in a sealed plastic container at 40 °C. At test time, samples were vacuum filtered through paper and cooled at ambient temperature in sealed Buchner funnels. The filtrate was analyzed for [OH^-] by titration against dilute HCl with methyl orange indicator and for [Ca^{2+}] by pH adjustment to 13, followed by titration with 0.025 M EDTA solution using Murexide indicator. This test compares the [Ca^{2+}] and [OH^-] contained in an aqueous solution that covers the hydrated sample with the solubility curve for CH in an alkaline solution at the same temperature.

Flow and compressive strength tests were assessed on standard mortars (1:3 and w/bc = 0.50) made with standard European sand (EN 196-1). The mortar was mixed in planetary mixer, the specimens were cast and compacted by vibration and cured 24 h in the molds in a moist cabinet. Then, they were removed from the mold and immersed in lime-saturated water until test age at 20 ± 1°C. Compressive strength was measured on mortars cubes (25 x 25 x 25 mm) [3] and the report values correspond to the average of five specimens.

2.3 Hydration

The hydrated phases were studied in pastes prepared with w/bc of 0.50. At 2, 7 and 28 days the hydration was stopped using acetone, dried and ground. The crystalline phases were identified by X-ray diffraction (XRD) (Philips X'Pert PW 3710, CuKα radiation with graphite monochromator operating at 40 kV and 20 mA). To quantify the crystalline and amorphous phases the Rietveld method with internal standard (TiO_2) [7] and PANalytical HighScore Plus [8] software were used. These values were checked by thermogravimetric analysis (TG) at 7 days.

2.4 Porosity

The pore size distribution in dried pastes at 2 and 28 days was determined using a mercury intrusion porosimeter (MIP-ThermoFisher Sc PA440) for the pore size diameters from 7.3 to 14000 nm.

3 Results and Discussion

3.1 Pozzolanic Activity

Figure 1 shows the results of Frattini test for blended cements. At all ages, PC and 10F cements do not have pozzolanic activity and the points representing the results are above the saturation curve. At 2 days, the combined effect of dilution and pozzolanic reaction decreases the [CaO] in the supernatant solution of blended cement with 30 % of CC. After 7 days, all bc prepared with CC showed evidence of

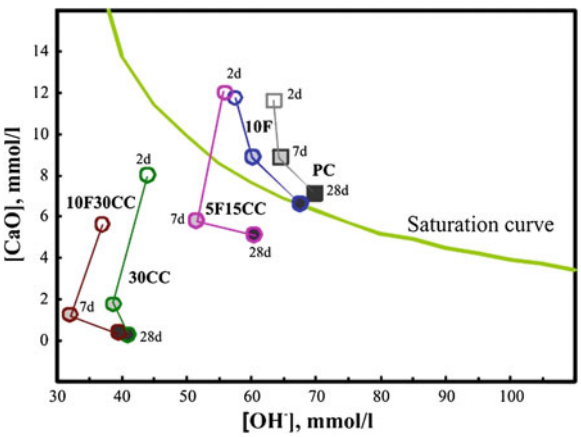

Fig. 1 Frattini test results at 2, 7 and 28 days

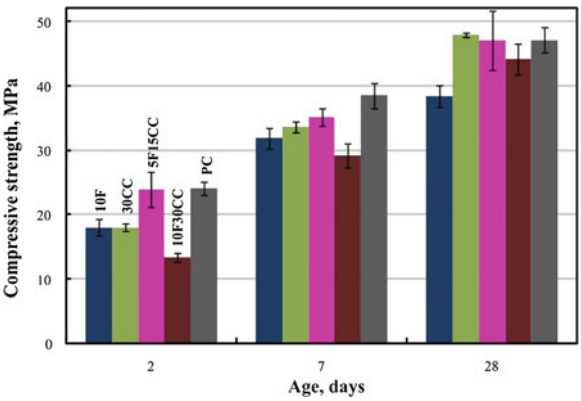

Fig. 2 Compressive strength of mortars at 2, 7 and 28 days

pozzolanic reaction. The [CaO] and [OH^-] reduction was greater when the CC replacement level increases. For 10F30CC and 5F15CC, the presence of limestone filler stimulates the pozzolanic reaction at 7 days, but it has less influence at advanced hydration ages (i.e., points of 10F30CC is overlapping the 30CC point).

The flow measured in standard mortars was 129, 129, 66, 150 and 68 % for PC, 10F, 30CC, 5F15CC and 10F30CC, respectively. Both additions have contrary effect on the workability: the CC decreases this property while the limestone filler improves it. The best result is obtained for 5F15CC cement.

Figure 2 shows the compressive strength (CS) at 2, 7 and 28 days. At 2 days, CS of 5F15CC (20 % of total addition) is comparable with that PC. The CS decreases when increasing the total replacement level (30CC and 10F30CC). For this case, the expected reduction of CS due to the dilution effect exceeds the contribution to the CS made by the proper pozzolanic reaction and/or the stimulation of PC hydration. At 7 days, 5F15CC remains as the highest CS blended cement, but the 30AC improves its contribution to CS compared with 2 days performance. At 28 days, the maximum value of CS was for 30CC showing the significant contribution of the pozzolanic reaction of calcined clay, this was followed by 5F15CC and then by 10F30CC. The last blended cement (10F30CC) with 40 % replacement of PC has CS greater than 40 MPa at 28 days, indicating an acceptable mechanical performance with a large reduction of gas emission by MPa obtained.

3.2 Hydration

Figure 3 shows the amount of CH determined from quantification by XRD analysis and Rietveld method in hydrated pastes at 2, 7 and 28 days. At 2 days, 10F contains the greatest amount of CH due to the stimulation caused by limestone filler. For bc with CC, the CH decrease in paste due to the dilution effect and the consumption by the pozzolanic reaction. In 5F15CC paste, the CH consumption was higher than expected by dilution and amount of reactive MK (6.6 % in 5F15CC and 13.2 % in

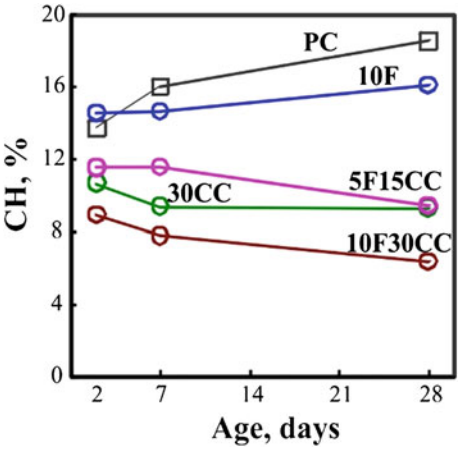

Fig. 3 CH content in hydrated pastes at 2, 7 and 28 days

30CC) showing the favorable stimulation caused by limestone filler. These results are in agreement with the CS-value at the same age (Fig. 2). At 7 days, the CH content in paste is reduced for all bc containing CC due to either dilution effect and pozzolanic reaction. Finally, the pastes made with ternary cement (5F15CC and 10F30CC) show a high CH consumption that expected by the replacement level.

Figure 4 shows the XRD patterns corresponding to hydrated pastes at 28 days. Two types of AFm phases are detected: hemicarboaluminate (HC) and

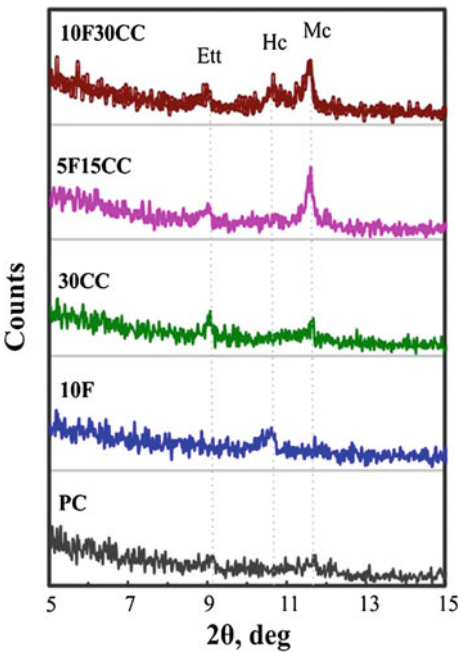

Fig. 4 XRD pattern for hydrated pastes at 28 days

Table 1 Pore size distribution of pastes at 2 and 28 days

Paste	Volume accumulated of pores, (mm^3/g)		Volume of pores between 10 to 50 nm, (mm^3/g)		Volume of pores diameters > 50 nm, (mm^3/g)	
	2 days	28 days	2 days	28 days	2 days	28 days
PC	194	112	55	41	133	62
10F	237	163	52	63	183	96
30CC	277	171	65	79	203	75
5F15CC	260	177	60	87	194	84
10F30CC	285	162	65	102	211	39

monocarboaluminate (MC). For ternary blended cements (5F15CC and 10F30CC), the intensity of peak assigned to MC increases considerably in accordance with previous results reported by Antoni et al. [5]. For blended cements with CC, the amount of CH decreases with time (Fig. 3) and the progress of pozzolanic reaction release a large amount of reactive alumina. In presence of limestone filler, the AFm phase is stabilized as MC and it could stimulate the pozzolanic reaction.

3.3 Porosity

Table 1 presents the cumulative pore volume of pastes.

From 2 to 28 days, there is a great reduction of the total porosity with great increases of volume of finer pores (10 to 50 nm) indicating the pore size refinement process of pozzolanic reaction (Table 1). For all hydrated blended cements, the volume of pores with diameter larger than 50 nm decreased from 2 to 7 days and the largest decrease was for 10F30CC cement. The volume of pores with diameter 10 to 50 nm decreases for the PC paste from 2 to 28 days (55 to 41 mm^3/g). However, it increases for some blended cements pastes, especially for 10F30CC where the filler fraction (quartz + limestone) is high.

4 Conclusions

- The blended cements containing 0–10 % of limestone filler (F) and 0–30 % of calcined clay (CC) develop compressive strength similar than that PC at 28 days, due to the interaction between these two components and the contribution of quartz filler. Compressive strength of blended cement 5F15CC is comparable with that PC since 2 days.
- Hydrated phases obtained correspond to the pozzolanic reaction (contribution kaolinitic calcined clay) and phase stabilization (contribution limestone filler) modifying the pore structure.

- The addition of kaolinitic calcined clay and limestone filler modify the pore system increasing the volume of pores with minor diameter.
- All factors contribute to develop acceptable mechanical properties with a large reduction of energy consumption and CO_2 emission: blended cement 10F30CC with 40 % replacement of PC has compressive strength greater than 40 MPa at 28 days.

References

1. Scrivener, K.L.: Options for the future of cement. Ind. Conc. J **88**(7), 11–21 (2014)
2. Murat, M.: Hydration reaction and hardening of calcined clays and related minerals. II. Influence of mineralogical properties of the raw-kaolinite on the reactivity of metakaolinite. Cem. Concr. Res. **13**, 511–518 (1983)
3. Tironi, A., Trezza, M.A., Scian, A.N., Irassar, E.F.: Kaolinitic calcined clays: factors affecting its performance as pozzolans. Con. Build. Mat **28**, 276–281 (2012)
4. Matschei, T., Lothenbach, B., Glasser, F.P.: The AFm phase in Portland cement. Cem. Concr. Res. **37**, 118–130 (2007)
5. Antoni, M., Roseen, J., Martirena, F., Scrivener, K.: Cement substitution by a combination of metakaolin and limestone. Cem. Concr. Res. **42**, 1579–1589 (2012)
6. EN 196-5 Standard: methods for testing cement. Part 5: pozzolanicity test for pozzolanic cements
7. Gómez-Zamorano, L.Y., Escalante, J.I.: Hidratación y microestructura de cemento Portland sustituido parcialmente con sílice ultrafina. Mater. Constr **59**, 5–16 (2009)
8. Kocaba, V.: Development and evaluation of methods to follow microstructural development of cementitious systems including slags, Thèse N° 4523, École polytechnique fédérale de lausanne, faculté sciences et techniques de l'ingénieur

Blended Cements with Kaolinitic Calcined Clays: Study of the Immobilization of Cr(VI)

Mónica A. Trezza, Alejandra Tironi, Edgardo F. Irassar and Alberto N. Scian

Abstract Numerous investigations on the immobilization of chromium in cement-based systems were carried out in the recent years. The aim of this study is to analyze the influence of the crystallinity of kaolinite used to make calcined kaolinitic clay when are used in pastes for immobilization of Cr(VI). In previous study, it was found that the reactivity of kaolinitic calcined clays used as partial replacement of Portland cement largely depends on the crystallinity of kaolinite in the raw clay. Calcined clays obtained from raw materials containing kaolinite with disordered structure presents a very high pozzolanic activity allowing high-percentage replacement (30 %) in blended cements. In this study, pastes of blended cement with 15 % and 30 % by mass of two kaolinitic calcined clays (order and disorder structure of kaolinite) were elaborated using a solution of 5000 ppm of $K_2Cr_2O_7$ and a solution-to-cementing material ratio of 0.50. The immobilization efficiency was measurement by lixiviation test and the modifications in the hydrated phases was studied by X-ray diffraction and SEM/EDS analysis. The results shown that kaolinitic calcined clay from ordered kaolinite was more efficient than disordered kaolinite to retention of Cr(VI), reaching values higher than that of PC-paste.

1 Introduction

Numerous investigations on the immobilization of chromium in cement based systems were carried out in the recent years [1–6]. Results indicate the incorporation of this metal at different hydrated phases of cement like Cr- Etringitte [7–9] and others in the gel as Cr-C-S-H [9], and others like new chromium compounds such

M.A. Trezza · A. Tironi (✉) · E.F. Irassar
Facultad de Ingeniería, CIFICEN (CONICET –UNCPBA), B7400jwi Olavarria, Argentina
e-mail: atironi@fio.unicen.edu.ar

A.N. Scian
Centro de Tecnología de Recursos Minerales y Cerámica CONICET La Plata—UNLP, La Plata, Argentina

K. Scrivener and A. Favier (eds.), *Calcined Clays for Sustainable Concrete*, RILEM Bookseries 10, DOI 10.1007/978-94-017-9939-3_25

$Ca_5(CrO_4)_3OH$ [4] or $CaCrO_4.2H_2O$ [10]. In the Cr-incorporation mechanisms, the cement composition plays an important role and the type of mineral addition, too.

Metakaolin (MK) is a pozzolanic material obtained by calcination of kaolinitic clays. Highly reactive pozzolanic materials, including calcined clays, can lead to help the sustainable cement production.

In previous studies, two kaolinitic clays with different cristalinity were characterized, calcined and analyzed as partial replacement of Portland cement at 15 % and 30 % by mass. Calcined clays obtained from kaolinite containing disordered structure present very high pozzolanic activity allowing high replacement levels (30 %) in blended cements [12].

The aim of this study is to analysis the influence of the crystallinity of kaolinite, in pastes elaborated with calcined kaolinitic clay, when are used for immobilization of Cr(VI). The immobilization efficiency was measurement by lixiviation test, and the modification in the hydrated phases was studied by X-ray diffraction (XRD) and SEM/EDS.

2 Materials and Methods

2.1 Blended Cements

In this study, blended cements (BC) were prepared with two kaolinitic calcined clay (MK1 and MK2) added as a partial replacement of Portland cement at levels of 15 % and 30 % by mass.

The cement used is a normal Portland cement (PC) with a Blaine fineness of 383 m^2/kg. The clinker composition reported by the cement factory was 53 % C_3S, 24 % C_2S, 9 % C_3A and 10 % C_4AF. For this cement, limestone is added as minor component (< 5 %).

Two Argentine kaolinitic clays were used: K1 with very high kaolinite content (94 %) and ordered structure, and K2 with high kaolinite content (76 %) and disordered structure. Complete details for these clays can be obtained elsewhere [12]. The clays were calcined to obtain metakaolinite (reactive amorphous phase), and then they ground until 80 % of mass passed through the 45 μm sieve (# 325), a typical goal for grinding process of blended cements. Both samples (denominated MK1 and MK2) have good pozzolanic activity, but MK2 from kaolinite with disordered structure (K2) is more reactive [12].

2.2 Pastes

Blended cement pastes were elaborated using a solution of 5000 ppm of $K_2Cr_2O_7$ and the water solution to blended cement ratio (ws/bc) was 0.50. Pastes were sealed

with plastic film and cured until 28 days at laboratory temperature. In order to compare the hydrated phases obtained in system with and without chromium; pastes mixed with distilled water were prepared.

2.3 Lixiviation Test

The leaching of Cr(VI) was evaluated at 28 days for hydrated pastes using the EPA Extraction Procedure Toxicity [13]. This test has been used by several authors in Portland cement pastes [5, 6, 14]. The samples were ground to a powder and leached in water, the extraction time was 18 h. The supernatant was analyzed for Cr (VI) according to IRAM 1514-revised standard [15]. For determining Cr(VI), the sample was reacted with diphenyl-carbazide in acid solution to produce a red complex. The absorbance of the solution was then measured at a wavelength of 540 nm by a spectrophotometer. The immobilization in pastes is determined as the difference between added and leaching chromium.

2.4 Hydration Phases

To study the hydration compounds in pastes with and without chromium at 28 days, paste fragments was immersed in acetone during 24 h to stop the hydration, dryed overnight in oven at 40 °C and then cooled in a desiccator.

The crystalline hydration phases were identified by XRD analyses on powdered paste samples (< 45 μm). Determination was performed on Philips PW 3710 diffractometer operating with CuKα radiation at 40 kV and 20 mA using carbon monochromator.

The morphological aspect and identification of elements in hydrated phases of pastes were performed by Scanning Electron Microscopy (SEM, Carl Zeiss EVO MA10) equipped with an energy dispersive spectrometer X-ray (EDS) Oxford brand, model INCA Energy, with software (INCA) for data processing. Small fragments of pastes were mounted on the holder and coated with gold films using a Denton Vacuum Desk II coater system.

3 Results and Discussion

3.1 Lixiviation Test

Table 1 summarizes the percentage of Cr(VI) retained in hydrated pastes at 28 days. The greatest Cr(VI) retention capacity is developed by the blended cement 15 % MK1 overpassing the PC retaining capacity in 5 %. For blended cement elaborated

Table 1 Cr(VI) % retained in hydrated pastes at 28 days

Paste	% retained
PC	86
15 %MK1	91
30 %MK1	88
15 %MK2	65
30 %MK2	63

with more reactive MK (15 and 30 % MK2), the retention capacity decreases according to the results reported by Pera et al. [1]. However, this capacity increases when pastes were elaborated with a slow but effective MK (15 and 30 %MK1). Tantawy et al. [3] determined that the additional formation of C-S-H due to the pozzolanic activity encapsulates the chromium, in agreement to the results reported here. Then, it can be pointed out that the time of formation of additional C-S-H is also an important variable to be considered in the retention capacity.

3.2 Hydration Phases

Figure 1 illustrates the XRD patterns for blended cement pastes with and without Cr (VI) at 28 days. In order to compare the hydrated phases, PC-pastes and blended cements with the highest (15 %MK1) and the lowest (30 %MK2) retention capacity of Cr(VI) were selected.

For portland cements (Fig. 1), XRD-pattern shows the presence of unhydrated PC phases (C_2S, C_3S and C_3A), and hydrated phases like ettringite (Ett) and CH, accompanied by low intensity of hemicarboaluminate (HC) and monocarboaluminate (MC). For blended cements with kaolinitic calcined clays, quartz (Q) was identified as a clay impurity with greater intensity in MK2 pastes. Also, it can be observed that the intensity of CH-peaks decreases due to pozzolanic reaction. In PC-paste, the chromium incorporation determines a decreased in the intensity of peak assigned to CH showing the well-known delay in the hydration caused by the Cr (VI). According to Wang [5], some part of Ca^{2+} reacted with CrO_4^{2} retarding the Portland cement hydration. The expected formation of $CaCrO_4$ ($2\theta = 32.3°$ and 35.2°) and $CaCrO_4.2H_2O$ [5, 10] could not be clearly detected due to the overlapping peaks with anhydrous Portland cement phases. It is also observed that the main peak of ettringite ($2\theta = 9.098^{o}$) shows a decrease in the intensity, shifting and splitting and it was assigned to the formation of Cr-ettringite [7–9]. The intensity of MC peak ($2\theta = 11.680^{o}$) also decreases. The same observation can be made for

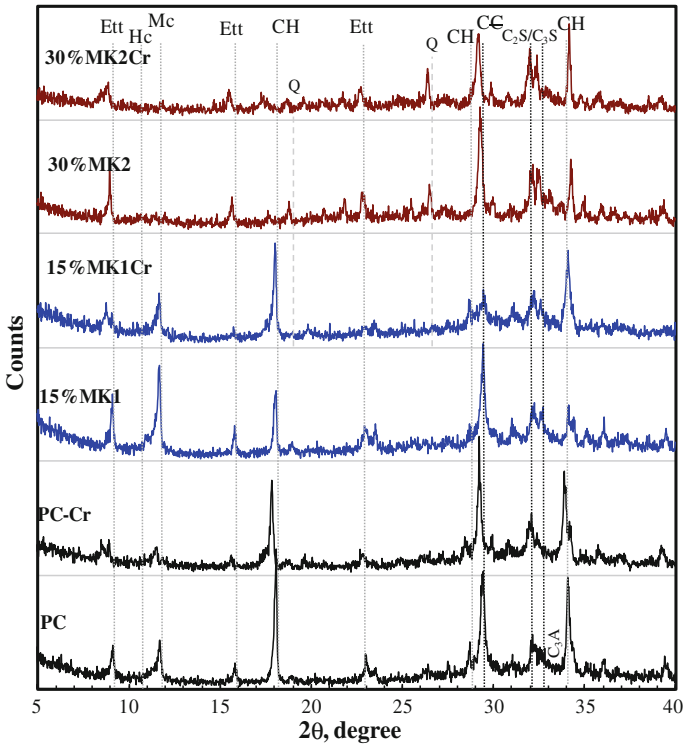

Fig. 1 XRD pattern for hydrated pastes with and without chromium at 28 days

MK1 and MK2 blended cements when they are compared with those hydrated in the presence of chromium. In MK2 pastes, the absence of CH was attributed to the pozzolanic reaction.

Figure 2 shows the SEM/EDS observations for pastes with chromium at 28 days. In PC-paste and MK1-pastes with different replacement levels (Fig. 2 a,b,d) the chromium was identified into the gel and like part of pseudo-crystals. In MK2-pastes, chromium was identified only in pseudo-crystals (Fig. 2 c,e). It is attributed to the highly efficient and rapid pozzolanic reaction generated by MK2. The slow formation of gel in PC and MK1 allows the Ca–Cr competition, leading to greater incorporation of chromium into the gel and consequently a greater retention capacity.

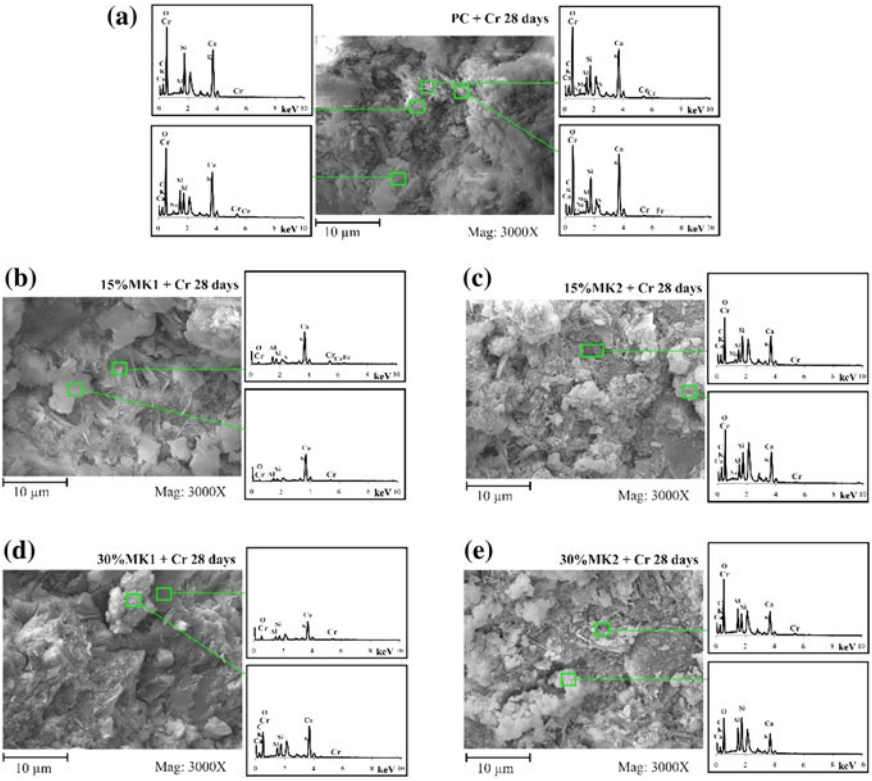

Fig. 2 SEM/EDS hidrated pastes at 28 days

4 Conclusions

- Leaching tests showed that all blended cement pastes achieved a high percentage of retention of Cr (VI), even with high replacements levels. Kaolinitic calcined clay from ordered kaolinite (MK1) was more efficient than disordered kaolinite (MK2), in the retention of Cr (VI), reaching values higher than PC-pastes.
- The presence of chromium in the system did not inhibit the pozzolanic reaction of kaolinitic calcined clays.
- The shifting and splitting of peaks observed by XRD, enables to infer the incorporation of Cr (VI) in ettringite phase.
- The results obtained by SEM /EDS allowed identified the presence of chromium like part of pseudo-crystals trapped in the gel and chromium in gel for PC-pastes and MK1-pastes. Absence of chromium in MK2-gel was attributed to rapid pozzolanic action caused by this addition and determined a lower percentage of retention.

References

1. Pera, J., Thevenin, G., Chabannet, M.: Desing of e novel system allowing the selection of an adequate binder for solidification/stabilization of waste. Cem. Concr. Res. **27**(10), 1533–1542 (1997)
2. Laforest, G., Duchesne, J.: Immobiliationof chromium (VI) evaluated by binding isotherms for ground granulated blast slag and ordinary Portland cement. Cem. Concr. Res. **35**(12), 2322–2332 (2005)
3. Tantawy, M.A., El-Roudi, A.M., Salem, A.A.: Immobilization of Cr(VI) in bagasse ash blended cement pastes. Con. Build. Mat **31**, 218–223 (2012)
4. Singyoung, S., Songsiriritthigul, P., Asavapisit, S., Kajitvichyanukul, P.: Chromium behavior during cement-production processes: a clinkerization, hydration and leaching study. J. Haz. Mat **191**, 296–305 (2011)
5. Wang, S., Vipulanandam, C.: Solidification/stabilization of Cr(VI) with cement: leachability and XRD analyses. Cem. Concr. Res. **30**(3), 385–389 (2000)
6. Trezza, M.A., Ferraiuelo, M.F.: Hydration study of limestone blended cement in the presence of hazardous wastes containing Cr(VI). Cem. Concr. Res. **33**(7), 1039–1045 (2003)
7. Bensted, J., Prakash Varma, S.: Studies of ettringite and its derivatives. Cem. Tech **2**(3), 73–77 (1971)
8. Bensted, J., Prakash Varma, S.: Studies of ettringite and its derivatives. Part II- chromate substitution. Silic. Ind. **37**(12), 315–318 (1972)
9. Perkins, R.B., Palmer, C.D.: Solubility of $Ca_6[Al(OH)_6]_2(CrO_4)_3.26H_2O$, the chromate analog of ettringite; 5–75 °C. Ap. Geochem. **15**, 1203–1218 (2000)
10. Lin, Ch-K, Chen, J.-N., Lin, Ch-Ch.: An NMR and XRD study of solidification/stabilization of chromium with Portland cement and β-C_2S. J. Haz. Mat **48**(1–3), 137–147 (1996)
11. Tironi, A., Castellano, C.C., Bonavetti, V.L., Trezza, M.A., Scian, A.N., Irassar, E.F.: Kaolinitic calcined clays—Portland cement system: hydration and properties. Con. Build. Mat **64**, 215–221 (2014)
12. Tironi, A., Trezza, M.A., Scian, A.N., Irassar, E.F.: Potential use of Argentine kaolinitic clays as pozzolanic material. Appl. Clay Sci. **101**, 468–476 (2014)
13. EPA Extraction Procedure (EP) Toxicity method and structural integrity test, method 1310A, revision 1 (1992)
14. Omotoso, O.E., Ivey, D.G., Mikula, R.: Quantitative X-Ray diffraction analysis of chromium (III) doped tricalcium silicate pastes. Cem. Concr. Res. **26**(9), 1369–1379 (1996)
15. Norma IRAM1514-1: Determinación del contenido de Cr(VI) soluble en agua (2012)

The Efficacy of Calcined Clays on Mitigating Alakli-Silica Reaction (ASR) in Mortar and Its Influence on Microstructure

Chang Li, Jason H. Ideker and Thanos Drimalas

Abstract Previous research has shown that using metakaolin is an effective strategy for mitigation of alkali-silica reaction (ASR). Metakaolin reduces the OH^-, K^+ and Na^+ concentrations in pore solution. The high aluminium content in metakaolin has also been shown to contribute to ASR reduction. However, the efficacy of calcined clays from different sources and qualities for ASR mitigation is still limited. This study investigated the mechanisms of ASR suppression by using one known highly reactive fine aggregate and four calcined clays from different sources. The optimum replacement for ASR mitigation was determined by replacing 5 %, 10 %, 15 % and 20 % of portland cement with the different calcined clays and then tested for expansion in the accelerated mortar bar test (AMBT). Results indicated the chemical composition and mineral phase of calcined clays had a significant influence on the efficacy of ASR mitigation. In addition, ASR gel was found in control mixture and the mixture with 10 % calcined clay 1 (CC1). ASR gel composition was investigated into the two mixtures by using energy-dispersive X-ray spectroscopy (EDS) in coupled with scanning electron microscopy (SEM), but no significant differences were found in gel composition between the two mixtures.

1 Introduction

Calcined clay has been used in mortar and concrete for many decades as an effective pozzolan due to its pozzolanic reactivity and high content of silica and alumina. Previous research also indicated that using clacined clays in mortar and concrete, as a replacement for portland cement, results in reducing CO_2 emission,

C. Li (✉) · J.H. Ideker
School of Civil and Construction Engineering, Oregon State University, Corvallis, USA
e-mail: licha@onid.oregonstate.edu

T. Drimalas
Department of Civil, Architecture and Environmental Engineering, The University of Texas, Austin, USA

K. Scrivener and A. Favier (eds.), *Calcined Clays for Sustainable Concrete*,
RILEM Bookseries 10, DOI 10.1007/978-94-017-9939-3_26

increases concrete durability and later age strength development [1, 2]. The benefits of concrete durability from calcined clays have been attributed to their pozzolanic reactivity, which depleted calcium hydroxide in concrete and converted it to C-S-H and C-A-S-H [3–7].

High quality calcined clay, e.g. metakaolin, has shown effectiveness in mitigating alkali-silica reaction (ASR). According to Ramlochan, 20 % metakaolin replacement was effective in reducing OH^-, K^+ and Na^+ concentration in pore solution [4]. Similarly, research conducted by Gruber showed that with 15 % to 20 % of metakaolin replacing OPC was effective in mitigating ASR in concrete [5]. Tests done by Walters and Jones showed that concrete with 10 % metakaolin or higher was effective in controlling ASR induced expansion [3]. In addition, the high alumina content of metakaolin has drawn attention of researchers. Al has been reported to have an influence on controlling ASR [8–10]. As a material with high content of Al, metakaolin may have the advantage of mitigating ASR in lower quantities compared to fly ash and/or slag, owing to its chemical composition. Possible assumptions include alteration of C-S-H structure, lower pH in pore solution and Al absorbed on the surface of reactive silica to slow down the dissolution rate [9]. Despite these findings on high quality calcined clays, limited study has been done on using calcined clays of different chemical composition for ASR mitigation. Thus, it was of great interest to investigate how calcined clays from different sources and quality affect the ASR expansion, microstructure of mortar and the composition of ASR gel.

2 Materials and Experiments

This study used four calcined clays from different sources: one was from Washington, USA (CC1), two were from Avelar, Portugal (CC2 and CC3) and the other was from Suriname (CC4). The chemical composition of four calcined clays is listed in (Table 1).

Cement used in the study is portland cement with high alkali content. Chemical composition of cement is listed in (Table 2).

Table 1 Chemical composition of calcined clays (%)

	SiO_2	Al_2O_3	Fe_2O_3	CaO	MgO	Na_2O	K_2O	TiO_2	MnO_2	P_2O_5	SrO	BaO	SO_3	LOI
CC1	51.93	42.18	1.43	0.40	0.12	0.05	0.23	1.99	–	0.17	0.04	0.11	0.05	1.32
CC2	54.11	39.94	1.26	0.25	0.20	0.15	1.38	0.63	0.01	0.12	0.02	0.04	0.05	1.87
CC3	60.17	27.00	3.05	0.40	0.53	0.90	3.22	0.39	0.02	0.16	0.02	0.04	0.35	3.73
CC4	50.12	43.62	0.69	0.05	0.02	0.00	0.10	1.76	0.01	0.02	0.01	0.02	0.02	3.57

Table 2 Chemical composition of cement (%)

SiO_2	Al_2O_3	Fe_2O_3	CaO	MgO	Na_2O	K_2O	Na_2O_{eq}	TiO_2	MnO_2	P_2O_5	SrO	BaO	SO_3	LOI
19.61	4.38	2.76	62.21	2.72	0.28	0.84	0.83	0.23	0.12	0.23	0.28	0.00	3.76	2.60

In this study, the mitigation of ASR was monitored by using accelerated mortar bar test (AMBT). A local fine siliceous reactive aggregate was used for the control mixture and the portland cement was replaced by CC1, CC2, CC3 and CC4 respectively at 5 %, 10 %, 15 % and 20 % to determine the effective mitigation level for each of used calcined clay. The water/cement ratio was fixed at 0.47. Expansion of all specimens was monitored and recorded up to 28 days.

Samples with size of 25.4 mm × 25.4 mm × 5 mm were taken from the mortar bars at the 14th day for SEM analysis. Then samples were submerged in isopropyl alcohol for 72 h to stop hydration. Isopropyl alcohol was replaced once after 24 h submerging. Afterwards, the samples were impregnated with a two-part epoxy. After impregnation in the epoxy, the samples were subsequently polished by using an automated Struers RotoPol-35 polishing machine. In addition oil based suspension fluid was used with diamond grits of different size. Diamond grits were re-applied to the polishing platen every hour for 8 h (9 µm: 4 h, 3 µm: 2 h and 1 µm: 2 h). All the samples were observed by FEI Quanta 600F environmental SEM. Energy-dispersive X-ray spectroscopy (EDS) with silicon drift detector was used for ASR gel composition analysis. Backscatter electron (BSE) images were acquired to EDS analysis on detecting and measuring characteristic X-rays.

3 Results and Discussion

Figure 1 shows the XRD results of different minerals in four investigated calcined clays. In general, CC1 has fewer (crystalline) minerals than other calcined clays, and the SiO_2 in CC1 mostly existed as quartz. Meanwhile, broad bands were

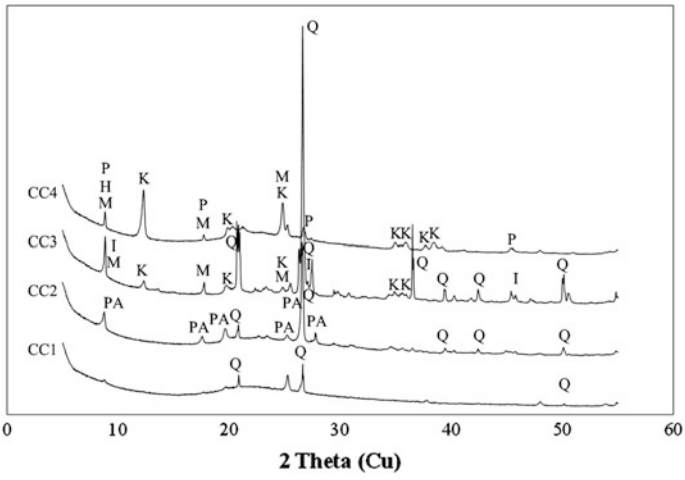

Fig. 1 XRD analysis on four investigated calcined clays (*I* Illite, *K* Kaolinite, *M* Muscovite, *P* Potassium manganese hydroxide; *PA* Potassium aluminum silicate; *Q* Quartz)

observed between 8.8 to 20.0 2θ degree as well as 21.0 to 24.8 2θ degree, which could be amorphous alumina in calcined clay. Compared with CC1, all other calcined clays showed higher degree of crystallinity.

Figure 2 shows the AMBT expansion results (14-day) of control group and groups with different calcined clays at different replacement levels.

Figure 2 shows the results of AMBT where portland cement was partially replaced by different calcined clays. When compared to the control mixture, mortar bars with different calcined clays all showed reduction in expansion. In the study, the control mixture with no calcined clay replacement showed an expansion of 0.66 % after 14 days submerged in 1 N NaOH. CC1 showed most effective in ASR expansion reduction and 5 % of CC1 reduced the expansion at 14 days by 36 % (0.66 % to 0.42 %). With 10 % CC1, ASR was able to be mitigated below the 0.10 % expansion limit and 14-day expansion to be reduced to 0.05 %. For CC2 and CC4, a replacement level at 15 % was effective to mitigate ASR. Additionally, CC3 was not able to mitigate ASR below the 0.10 % expansion limit until 20 % of CC3 were incorporated in the mixture. From these results calcined clays of varying composition and quality greatly influenced the efficacy of ASR mitigation.

By comparing the composition of calcined clays used in this study, it was found that four calcined clays had significant differences in the amount of SiO_2, Al_2O_3, Na_2O and K_2O. Among the investigated calcined clays, CC3 had the lowest alumina content (27.00 %), which was 15 % lower than that of other clays (39 % ~ 43 %). Previous research indicated alumina had a significant influence on mitigating ASR. With the presence of alumina, a hydration product C-S-A-H will be produced. By influencing the Ca/Si in the system, the ability of binding alkalis were hence improved [1, 11]. On the other hand, Chappex showed the dissolution rate of Si was slowed down due the existence of alumina [9]. In addition, a larger amount of Na_2O and K_2O were present in CC3 (0.90 % and 3.22 % respectively),

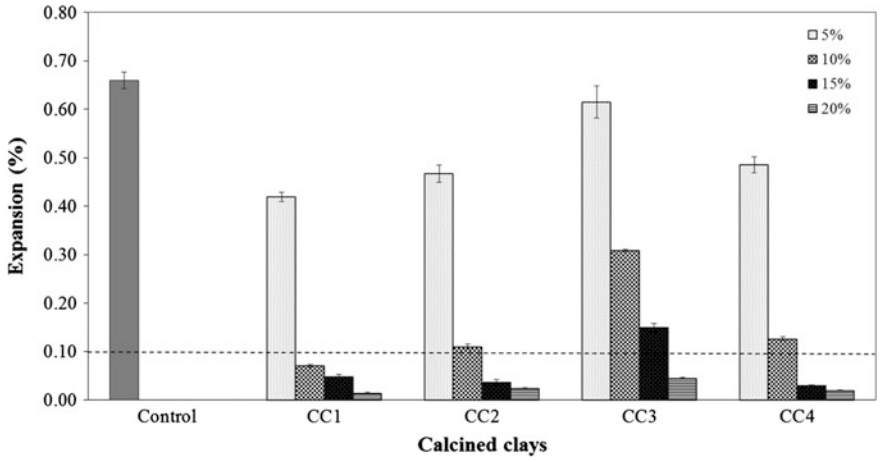

Fig. 2 Expansion results of mortar bars incorporated with calcined clays (14-day)

which may have contributed a higher amount of alkali, could hence influenced the mitigation efficacy of the clays. On the other hand, according to the XRD results (in Fig. 1), the complicated mineral phases in CC3 such illite and muscovite could have lower potential of pozzolanic reactivity [12].

SEM analysis was used to investigate how calcined clays influenced the formation of ASR gel and its composition. Control mixture, 10 % CC1, 10 % CC2 and 10 % CC3 mixtures were investigated. Samples with 10 % calcined clay level were chosen because 10 % replacement was a boundary showed that CC1 was able to mitigate ASR, while the others weren't. Figure 3 shows the backscattered images of mortar samples cured at 80°C under 1 N NaOH bath after 14 days.

In Fig. 3, it shows the ASR gel formed and filled within the cracks of siliceous aggregates. Plenty of gel was observed in the control samples. And ASR gel filling in the aggregates was also observed when 10 % CC3 were used for Portland cement replacement. In comparison very little ASR gel was observed in 10 % CC1 and 10 % CC2 mixtures. ASR gel could be dissolved or removed during sample preparation process. However, cracks within the aggregates were also observed in 10 % CC1 and 10 % CC2 mixture. Meanwhile, compared with control mixture and 10 % CC3 mixture, the overall number of cracks in 10 % CC1 and 10 % CC2 mixtures was much lower, which reflected the result obtained from AMBT test. The composition of the ASR gel formed in these two mixtures was also investigated in this study. Figure 4 shows the composition results of control mixture and mixture with 10 % CC3 replacement.

In Fig. 4, ASR gel composition of control mixture and 10 % CC3 mixture were shown. In the control mixture, Si/Al ratio varied from 2.66 to 3.39, while 2.32 to 3.34 was observed in 10 % CC3 mixture. On the other hand, the ratio of Si/(Na + K) in control mixture varied from 1.82 to 2.24, while a more fluctuating range (1.61 to 2.73) were observed in 10 % CC3 mixture. Based on results above,

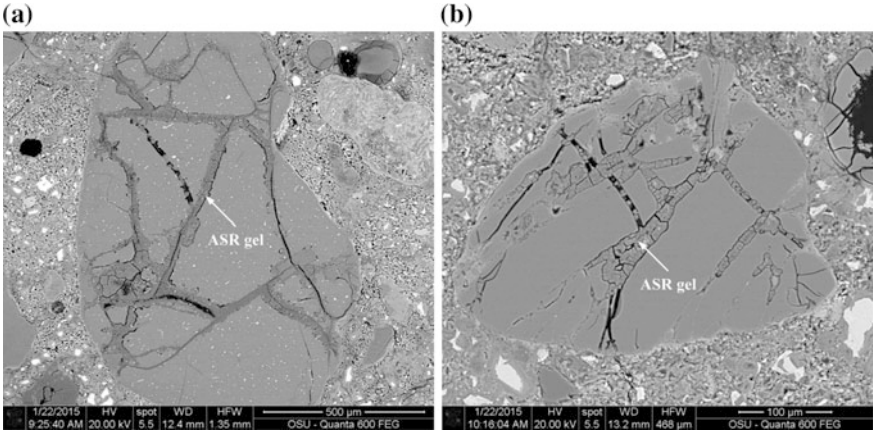

Fig. 3 Backscattered image of investigated mortar mixtures **a** Control mixture; **b** Mixture with 10 % CC3)

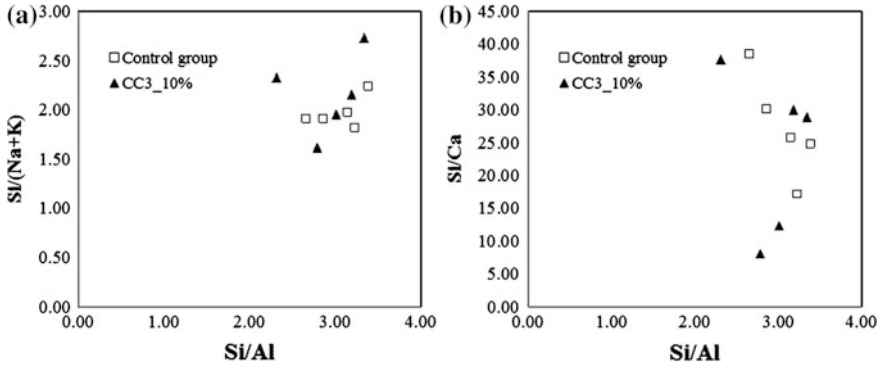

Fig. 4 ASR gel composition of investigated mixtures **a** Si/Al vs. Si/(Na + K); **b** Si/Al vs. Si/Ca)

no significant change on ASR gel composition was found when 10 % CC3 were incorporated into the mortar mixture. Additionally, Si/Ca varied in both mixtures, no trend of change in Si/Ca was observed when 10 % CC3 was incorporated, despite 10 % CC3 failed to mitigate ASR. However, it is important to note that the composition of ASR could also be affected by the variation of aggregate particles.

4 Conclusions

In this study, calcined clays of four different sources were investigated for their efficacy of ASR mitigation. Results indicated that the chemical composition and mineral phase of the calcined clays can significantly influence the efficacy of ASR mitigation. Different replacement levels were suggested for each of investigated calcined clay. Calcined clays with higher content of Al_2O_3 and lower content (Na_2O + K_2O) showed better effect in reducing expansion in mortar bars. Cracks were observed in the control mixture and all 10 % calcined clay mixtures since the aggregates used were highly reactive. ASR gel filled within cracks of aggregates was observed in control mixture and 10 % CC3 mixture. The influence of calcined clay on ASR gel composition was still not fully understood. Further study on synthetic ASR gel with different calcined clays incorporated and concrete prism test on a long-term run are recommended.

Acknowledgments We thank W. R. Grace & Co., Saint-Gobain Weber and Laboratory of Construction Materials at École polytechnique fédérale de Lausanne (LMC-EPFL) for providing the calcined clays.

References

1. Sabir, B.B., Wild, S., Bai, J.: Metakaolin and calcined clays as pozzolans for concrete: a review. Cement Concr. Compos. **23**, 441–454 (2001)
2. Wild, S., Khatib, J., Jones, A.: Relative strength, pozzolanic activity and cement hydration in superplasticised metakaolin concrete. Cem. Concr. Res. **26**(10), 1537–1544 (1996)
3. Walters, G.V., Jones, T.R.: Effect of metakaolin on alkali-silica reaction (ASR) in concrete manufactured with reactive aggregate, vol. 126. ACI Special Publication (1991)
4. Ramlochan, T., Thomas, M., Gruber, K.A.: The effect of metakaolin on alkali-silica reaction in concrete. Cem. Concr. Res. **30**(3), 339–344 (2000)
5. Gruber, K., et al.: Increasing concrete durability with high-reactivity metakaolin. Cement Concr. Compos. **23**(6), 479–484 (2001)
6. Coleman, N., Page, C.: Aspects of the pore solution chemistry of hydrated cement pastes containing metakaolin. Cem. Concr. Res. **27**(1), 147–154 (1997)
7. Wild, S., Khatib, J.: Portlandite consumption in metakaolin cement pastes and mortars. Cem. Concr. Res. **27**(1), 137–146 (1997)
8. Warner, S.J.: The role of alumina in the mitigation of alkali-silica reaction. Master Thesis of Oregon State University (2012)
9. Chappex, T.: The role of aluminium from supplementary cementitious. Thesis of Ecole Polytechnique Federale De Lausanne (2012)
10. Chappex, T., Scrivener, K.L.: The effect of aluminum in solution on the dissolution of amorphous silica and its relation to cementitious systems. J. Am. Ceram. Soc. **42**, 1–6 (2012)
11. Kostuch, J., Walters, V., Jones, T.: High performance concretes incorporating metakaolin: a review. Concrete **2000**(2), 1799–811 (1993)
12. Fernandez, R., Martirena, F., Scrivener, K.L.: The origin of the pozzolanic activity of calcined clay minerals: a comparison between kaolinite, illite and montmorillonite. Cem. Concr. Res. **41**(1), 113–122 (2011)

Influence of MK-Based Admixtures on the Early Hydration, Pore Structure and Compressive Strength of Steam Curing Mortars

Jinlong Han, Zhonghe Shui, Guiming Wang, Jiancong Shao and Yun Huang

Abstract Prestressed high-strength concrete (PHC) pipe piles are one of the most widely used concrete elements in building foundation construction. In this study, the effects of material composition on the compressive strength development, early hydration and pore structure of PHC were investigated by a series of analytical techniques. Supplementary cementitious materials, namely metakaolin (MK), granulated ground blast-furnace slag (GGBFS) and limestone powder (L.S) were used to prepare cement pastes and mortars under steam curing condition to improve early compressive strength. Finally the mortar containing 10 % MK and 10 % L.S was prepared, with the compressive strength up to 89 MPa at 1 day and 93 MPa at 7 days. The effects of the blended mineral admixtures on the early hydration and microstructure of steam cured pastes and mortars were investigated by XRD, TG-DTC and MIP. The results showed that the mineral admixtures could consume Ca $(OH)_2$ owing to pozzolanic reaction and promote concrete hydration, which led to the improvement of the properties of hydration products and optimization of pore structure and pore size distribution.

J. Han (✉) · Z. Shui · G. Wang · Y. Huang
State Key Laboratory of Silicate Materials for Architectures,
Wuhan University of Technology, Wuhan, China
e-mail: hhjjllhjl@163.com

J. Han · G. Wang
School of Materials Science and Technology, Wuhan University of Technology,
Wuhan, China

J. Shao
Maoming Kaolin Science and Technology Company, Maoming, China

K. Scrivener and A. Favier (eds.), *Calcined Clays for Sustainable Concrete*,
RILEM Bookseries 10, DOI 10.1007/978-94-017-9939-3_27

1 Introduction

Prestressed high-strength concrete (PHC) pipe piles are widely used in all kinds of engineering projects, such as industry and civil buildings, highway and railway, port and wharf constructions, due to the advantages of high strength, high density and high bearing capacity and reductions in building time. To improve economic efficiency, increasing the utilization efficiency of the moulds to improve production efficiency is a key way. Shortening the cycle of the mould application means the PHC pipe piles should gain a high strength as soon as possible especially at early age.

Without altering productive process, changing the composition binding material such as utilizing mineral admixtures as supplementary cementitious material to replace part of cement is a normal way to gain a high strength at early age [1–3]. Liu reported that the addition of UFA and ground slag can increase the compressive strengths of concrete containing supplementary cementing materials [1]. Metakaolin (MK), because of its high pozzolanic properties due to its amorphous structure and high surface area, has been used as a highly active and effective pozzolan for the partial replacement of cement in concrete. Unlike other pozzolans, it is a kind of primary products, not a by-product or secondary product. The capability of metakaolin used as a mineral addition to improve mechanical and durability properties of cement and concrete is well noted in concrete science, not only under normal maintenance [4–7] but also steam curing [8–10].

In this paper, firstly, the cement pastes and mortars under steam curing were prepared. Then its mechanical property was tested, the early hydration products were studied by X-ray diffraction (XRD) and thermal gravity and Differential Scanning Calorimeter (TG-DSC) analysis, the changes of porous characteristics were evaluated by mercury intrusion porosimeter (MIP) test. Finally, the relationship among mechanical property, hydration products and porous characteristics were discussed.

2 Experimental Procedure

2.1 Materials

The cement used was 52.5 type I Portland cement (PC) complying with Chinese National standard GB175-2007. Blast furnace slag (GGBS), metakaolin (MK) and

Table 1 Chemical composition of binders (%)

Chemical composition	SiO_2	Al_2O_3	CaO	Fe_2O_3	SO_3	MgO	Na_2O	K_2O	LOI
PC	19.37	3.92	68.3	3.69	0.81	1.61	0.13	0.59	1.09
MK	53.15	44.43	0.02	0.7	0.21	0.13	0.34	0.53	0.12
GGBFS	33.64	15.27	35.46	0.45	2.05	10.2	0.51	0.52	0.15
L.S	8.27	2.64	45.11	0.9	2.01	0.11	–	4.29	35.43

Table 2 Mix design of cement pastes and mortars/g

Blended	Mixes	PC	MK	GGBFS	L.S	Sand	Water	HRWRA
Cement pastes	P0	800	–	–	–	1350	200	8
	P1	720	80	–	–			
	P2	640	80	80	–			
	P3	640	80	–	80			
Mortars	M0	500	–	–	–	–	125	5
	M1	450	50	–	–			
	M2	400	50	50	–			
	M3	400	50	–	50			

limestone powder (L.S) were also used as mineral admixtures. The chemical composition and physical properties of PC, GGBS, MK and L.S were listed in Table 1. Natural sand with a fineness modulus of 2.8 was used as fine aggregates. A polycarboxylate type High-Range Water Reducer Admixture (HRWRA) with a solid content of 40 % was used to achieve the required workability for the mixtures.

2.2 Specimen Preparation and Steam Curing Regimes

The details of mix design are given in Table 2. After mixing and vibration, the mortar mixture was placed in 40 × 40 × 160 mm moulds for compressive strength test and MIP test, and the cement paste mixture was placed in 40 × 40 × 40 mm moulds for XRD, TG-DSC analysis.

2.3 Thermal Treatment

Immediately after moulding, the pastes and the mortars were exposed to a steam curing cycle with a total duration of 17 h. The cycle included 4 h of presetting at 25 °C, followed by 3 h of heating at 15 °C temperature increase per hour up to 70 °C, 7 h of exposure at 70 °C and a 3 h cooling down period. Then removed from their moulds and stored at 20 ± 2 °C for testing ages.

2.4 Methods

2.4.1 Mechanical Tests

The compressive strength test was carried out at the ages of 1 and 7 days using a 2000 kN capacity compression testing machine.

2.4.2 Mineralogical Analysis: XRD

The measuring instrument used for XRD worked with Co-Kα radiation ($\lambda_{K\alpha}$ = 1789) at 40 kV and 30 mA. The 2-Theta values ranged from −10° to 168° and were recorded in 0.04° steps with a counting time of 10 s per step. The measurement was carried out on powder passing through a 40 μm sieve. The XRD technique identifies crystallized hydrated and anhydrous phases in a paste.

2.4.3 Thermal Analysis: TG-DSC

Differential Scanning Calorimetry (DSC) and thermogravimetric analysis (TG) were used to qualitatively and quantitatively analyze the hydration reactions. DSC locates the temperature ranges corresponding to the thermal decomposition of different phases in a paste.

2.4.4 Porosity and Pore Size Distribution by MIP

Total pore volume and pore size distribution measurements were carried out by mercury intrusion porosimeter (MIP). High-pressure Porosimeter Micrometrics Auto Pore IV 9510 (with sufficiently large pressure range up to 414 MPa) was used to measure pores ranging from 3 nm to 400 μm. Before testing, the samples were immersed in alcohol immediately for 48 h, then dried up at 105 °C for 24 h in vacuum oven.

3 Results and Discussion

3.1 Mechanical Performance

The compressive strength test was conducted on 40 × 40 × 160 mm specimens immediately after steam curing at the ages of 1 and 7 days. The final strength was an average calculated from six measurements on half parts of the specimens. The results are presented in Fig. 1.

As shown in Fig. 1, the compressive strength of the mortars at 1 and 7 days are in the sequence of M3, M1, M2, and M0. The mortar M3 containing 10 % MK and 10 % L.S gains 89 MPa at 1 day and 93 MPa at 7 days, which are 17 % and 14 % higher than the control mortar M0 respectively.

The strength results of mortars show that using MK, GGBS or L.S to replace part of cement can lead to better performances at early and later ages when steam curing is adopted.

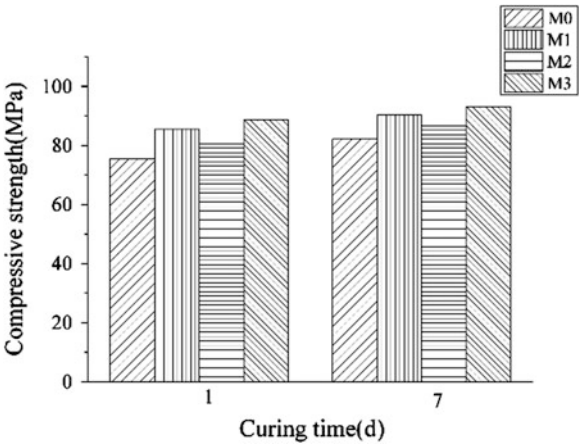

Fig. 1 Compressive strength *X-axis* 2θ (°) *Y-axis* intensity (arbitrary units) of mortars M0, M1, M2 and M3

The XRD technique identifies crystallized hydration products and unhydrated clinker. Figure 2 shows the X-ray diffraction patterns for the reference paste (P0) and the pastes incorporating MK (P1, P2 and P3) at 1 day.

Several observations and comments can be made according to the analysis of the XRD patterns. The main peaks in the patterns are $Ca(OH)_2$, ettringite and unhydrated C_3S. Observing the diffraction peaks at about 2θ = 18.1° (4.9 Å) and 2θ = 34.1° (2.63 Å), the peak height of $Ca(OH)_2$ decreased obviously for pastes P1, P2 and P3 relative to the reference paste P0. This issue is related to a reaction

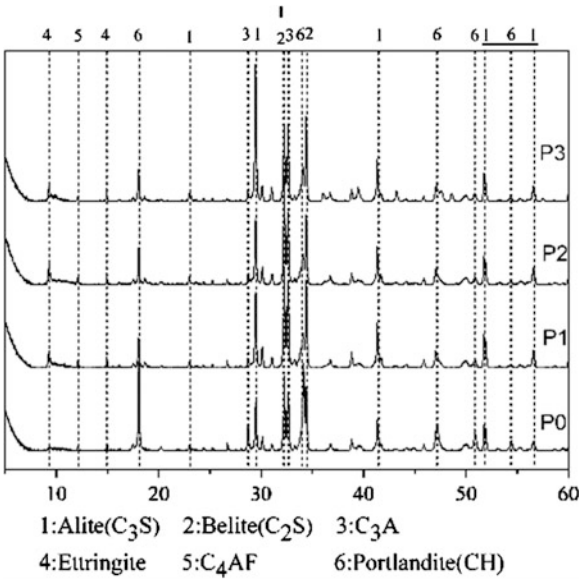

Fig. 2 XRD patterns for pastes P0, P1, P2 and P3 at 1 day 3.2. X-ray Diffraction (*XRD*) analysis

between active ingredients like activated alumina in MK and calcium hydroxide (CH), transforming calcium hydroxide (CH) into secondary C–S–H or C-A-H gel.

According to the diffraction peak at about 2θ = 9.1°, ettringite is visible for P1, P2 and P3, except for P0, indicating that MK, MK and GGBFS, MK and L.S all can promote the formation of ettringite.

3.2 Thermal Analysis

Figure 3 shows the DSC curves of steam cured reference cement pastes (P1) and paste incorporating MK (P1-10MK%, P2-10 %MK and 10 % GGBFS, P3-10 % MK and 10 % LS). Specific hydrated phases resulting from pozzolanic reaction could be distinguished by DSC analysis has been reported in several studies. The amount of C-S-H and CH are considerable concerned (Fig. 4).

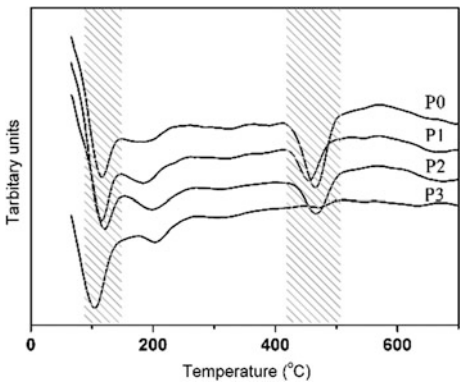

Fig. 3 DSC pattern for pastes P1, P2, P3 and P4 at 1 day of age

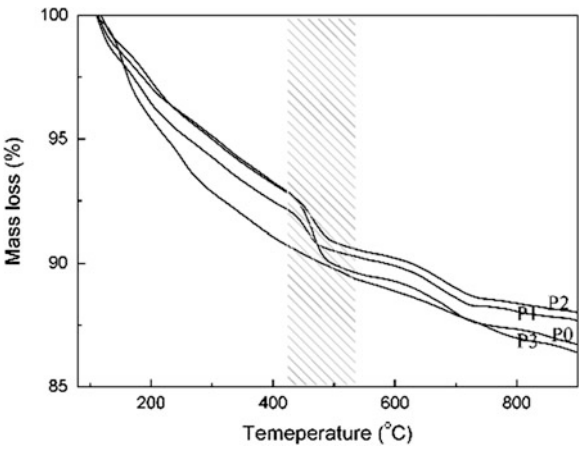

Fig. 4 TG pattern for pastes P1, P2, P3 and P4 at 1 day of age

The pozzolanic reaction can be observed by the decomposition of hydration products at about 100 °C. P3 presents a marked endothermic peak. This observation can be explained by the development of a large amount of C–S–H phases.

As expected from the XRD results, a smaller amount of CH is visible at the temperature about 450 °C in pastes with MK (P1, P2 and P3) than in reference pastes(P0), especially the amount of CH of P3 is smallest, indicating the consumption of CH by the pozzolanic reaction at the age of 1d.

3.3 Porosity and Pore Size Distribution by Mip

Effects of MK, GGBFS and L.S on pore structure of mortars are shown in Figs. 5 and 6 at 1 day under steam curing.

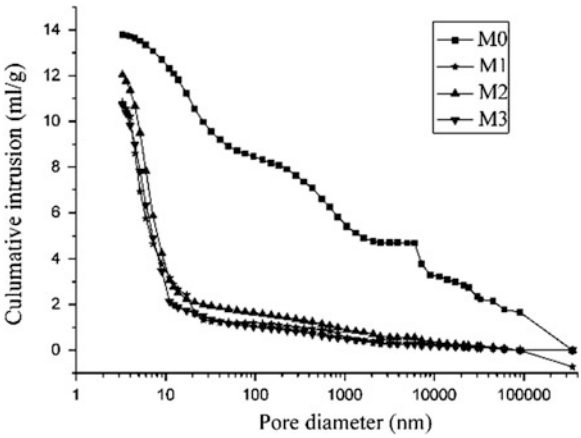

Fig. 5 Cumulative intrusion volume of mortars M0, M1, M2 and M3 at 1 day

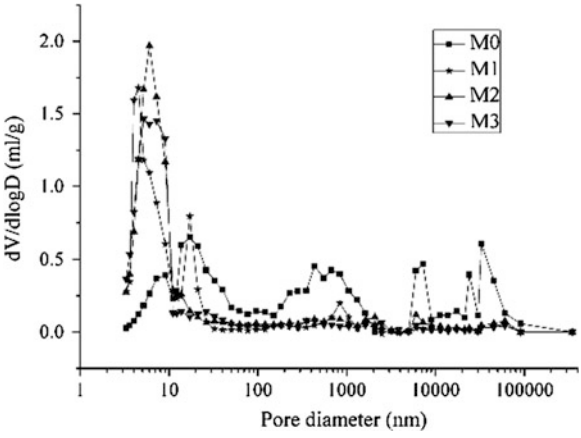

Fig. 6 Pore size distribution of Mortars M0, M1, M2 and M3 at 1 day

Due to micro aggregate filling and the pozzolanic effect of mineral admixtures, the total pore volume of mortar decreases significantly .Accumulative intrusion volume of mortar can be calculated in Fig. 5, 14.44 % for M0, which is higher than 11.27 % for M1, 12.46 % for M2, 10.97 % for M3. This is consistent with the strength test results of the mortars for the less total pore volume make mortar denser.

Figure 6 shows that pore size distribution shifts to the small pore diameter portion when MK, GGBFS and L.S replace part of cement due to its micro aggregate filling and the pozzolanic effect. It can be calculated that the content of micro pore that less than 10 nm of M0, M1, M2 and M3 account for 9.46 %, 70.8 %, 65.32 % and 80.07 % of the accumulative intrusion volume, respectively. The result is consistent with the strength test results of the mortars. C–S–H gels with higher strength were formed due to reactions between mineral admixtures and cement to optimize the microstructure of concrete.

4 Conclusions

- The compressive strength of mortar can be improved with the incorporation of MK, GGBS and L.S at early age and later age. The mortar M3 containing 10 % MK and 10 % L.S gains 89 MPa at 1 day and 93 MPa at 7 days under the steam curing.
- According to the results of XRD and thermal analysis, the amount of the hydration products (C-S-H and C-A-S-H) is increased with the incorporation of MK, while the amount of $Ca(OH)_2$ is decreased due to the pozzolanic reaction at the age of 1 day. The evolution of hydration observed is in agreement with the strength results on mortars.
- The MIP results show that pore size distribution shifts to the small pore diameter portion when MK, GGBFS and L.S replace part of cement and the total pore volume of mortar decreases significantly, which make the mortar denser and, the compressive strength increase.

Acknowledgments This research is financially supported by YangFan Innovative & Entrepreneurial Research Team Project (No.201312C12).

References

1. Liu, B., Xie, Y., Li, J.: Influence of steam curing on the compressive strength of concrete containing supplementary cementing materials. Cem. Concr. Res. **35**, 994–998 (2005)
2. Ho, D.W.S., Chua, C.W., Tam, C.T.: Steam-cured concrete incorporating mineral admixtures. Cem. Concr. Res. **33**, 595–601 (2003)

3. Baoju, L., Youjun, X., Shiqiong, Z., Jian, L.: Some factors affecting early compressive strength of steam-curing concrete with ultrafine fly ash. Cem. Concr. Res. **31**(2001), 1455–1458 (2001)
4. Frias, M., Cabrera, J.: Pore size distribution and degree of hydration of metakaolin cement pastes. Cem. Concr. Res. **30**(4), 561–569 (2000)
5. Fraire-Luna, P.E., Escalante-Garcia, J.I., Gorokhovsky, A.: Composite systems fluorgypsum blastfurnance slag metakaolin, strength and microstructures. Cem. Concr. Res. **36**, 1048–1055 (2006)
6. Janotka, I., Puertas, F.M., Palacios, M.: Metakaolin sand–blended-cement pastes: rheology, hydration process and mechanical properties. Constr. Build. Mater. **24**, 791–802 (2010)
7. Duan, P., Shui, Z., Chen, W., Shen, C.: Effects of metakaolin, silica fume and slag on pore structure, interfacial transition zone and compressive strength of concrete. Constr. Build. Mater. **44**, 1–6 (2013)
8. Cassagnabère, F., Mouret, M., Escadeillas, G.: Early hydration of clinker-slag-metakaolin combination in steam curing conditions. Cem. Concr. Res. **39**, 1164–1173 (2009)
9. Cassagnabère, F., Escadeillas, G., Mouret, M.: Study of the reactivity of cement/metakaolin binders at early age for specific use in steam cured precast concrete. Constr. Build. Mater. **23**, 775–784 (2009)
10. Ramezanianpour, A.M., Esmaeili, Kh, Ghahari, S.A., Ramezanianpour, A.A.: Influence of initial steam curing and different types of mineral additives on mechanical and durability properties of self-compacting concrete. Constr. Build. Mater. **73**, 187–194 (2014)

Design and Preparation of Metakaolin-Based Mineral Admixture and its Effects on the Durability of Concrete

Zhonghe Shui, Kai Yuan, Tao Sun, Qiu Li and Weineng Zeng

Abstract Many attempts have been made to find a highly-effective way to improve concrete durability. Metakaolin-based mineral admixtures were designed and produced for this purpose and their effects on concrete durability were investigated in this study. The design principles of the admixture were based on the match of the potential active ingredients, such as active SiO_2 and Al_2O_3, among the major active mineral materials including metakaolin (MK), fly ash (FA) and limestone powder (LSP). The proportions of MK, FA and LSP in the admixtures were determined by triangle phase diagram of CaO-SiO_2-Al_2O_3. Based on the above principle, three MK-based mineral admixtures were designed and applied in the concrete by substituting ordinary Portland cement, namely C1 (5 wt%MK + 2 wt%FA), C2 (7 wt%MK + 2 wt%FA + 2 wt%LSP) and C3 (9 wt%MK + 2 wt%FA + 2 wt% LSP). Finally, the effects of the admixtures on the durability of concrete were studied by a range of analytical techniques. The chloride permeability resistance of concrete was significantly improved with the addition of the admixtures. The chloride diffusion coefficient decreased by over 50 % at 56 days. The admixture significantly reduced the shrinkage strain of concrete, and further decrease occurred with the increase of limestone powder content and metakaolin content in admixtures. Improvement of concrete performance resulted from the increase of amount of hydration products, refinement of pore structure and densification of interfacial transition zone (ITZ) caused by the admixture.

Z. Shui · K. Yuan (✉) · T. Sun · Q. Li
State Key Laboratory of Silicate Materials for Architectures,
Wuhan University of Technology, Wuhan, China
e-mail: yuankai17@126.com

Z. Shui · K. Yuan
School of Materials Science and Technology, Wuhan University of Technology,
Wuhan, China

W. Zeng
Maoming Kaolin Science and Technology Company, Maoming, China

K. Scrivener and A. Favier (eds.), *Calcined Clays for Sustainable Concrete*,
RILEM Bookseries 10, DOI 10.1007/978-94-017-9939-3_28

1 Introduction

There are many studies [1, 2] in the literature focusing on the improvement of concrete by replacing Portland cement of mineral admixtures; such as fly ash, silica fume, blast-furnace slag, etc. Due to pozzolanic and filling effects of these certain mineral admixtures, they are capable of enhancing the durability through the pore refinement and the cement paste matrix [3]. Generally, appropriate mineral admixtures can improve concrete durability significantly and extend its service time which is good for economizing resources and energy and also can reduce environmental damage caused by waste concrete.

As a highly-active supplementary cementitious material, metakaolin (MK) has been extensive studied. MK is an ultrafine pozzolanic material, produced by calcining kaolin at 700 to 900 °C to remove the chemically bound water and deteriorate the crystalline structure [4]. Unlike the other industry byproducts pozzolanic materials, the component and purity of MK can be accuracy controlled. It has been demonstrated that incorporating MK leads to improvement of the concrete behaviour [5]. But as is known to all, the use of MK makes a decrease in workability. So the addition of MK into concrete through composite admixtures would be beneficial.

Amorphous silica and alumina are the main components in pozzolanic materials. The effectiveness of a pozzolanic material depends on its reactivity. The reactivity determined by two factors, one factor was the maximum amount of calcium hydroxide to ensure the pozzolanic reaction occurs, other factor as directly related with the material fineness [6]. The main object of this study is to design a composite admixture which consists of the appropriate proportion of metakaolin, fly ash and lime stone powder. The effects of composite admixture on chloride resistance and drying shrinkage were investigated.

2 Experiment

2.1 Materials

Commercial cement P.I 52.5 was used in this study, with a density of 3100 kg/m^3 and specific surface area of 376 m^2/kg. Limestone powder was sieved at 45 μm and remainder was 3.3 wt%. Water content of fly ash was 0.14 wt% and the density was 2300 kg/m^3. The chemical compositions of cement, metakaolin, fly ash and limestone powder are shown in Table 1.

Natural river sand was used as fine aggregate with a fineness modulus of 2.83, apparent density of 2635 kg/m^3, packing density of 1456 kg/m^3 and silt content of 0.39 %. Coarse aggregate was limestone with continuous gradation ranged from 4.75 to 26.5 mm, apparent density of 2840 kg/m^3, packing density of 1445 kg/m^3 and silt content of 0.35 %. The crushing value of coarse aggregate was 7.28 %.

2.2 Active Component Characterization

The content of active components of MK, FA and LSP were analysed for the admixture design. The insoluble method was employed for MK. The pozzolanic active component in MK is 74.57 wt%, which contains 20.98 wt% Al_2O_3 and 51.63 wt% SiO_2. For FA, the percentage of active Al_2O_3 and active SiO_2 was 6.27 wt% and 20.42 wt% respectively, which was calculated by mixing FA with saturated limewater for 48 h. The effect of LSP was mainly pore filling and Gibbs free energy reducing for C-S-H polymerisation. Approximately 2-5 wt% of LSP participated in hydration.

2.3 Admixture Design

The proportion of MK, FA and LSP in admixture was determined according to the active component in each raw material during the hydration of mineral admixture. Two principals were introduced: (1) the hydration of calcium-aluminium-silicon system favours the formation of C-S-H and C-A-S-H gels; (2) the hydration of active component in silicon aluminium materials such as MK and FA should be sufficient. Studies showed that C-S-H gel is the main binding phase which is the source of compressive strength of cement paste. In addition, CH with lamellar structure resulted in reduced mechanical strength. Improve of mechanical strength is feasible through generating more C-S-H in cement paste by modification of raw materials. Rodger studied the hydration products of Portland cements paste and FA composite cement paste and the results indicated that Ca/Si ratio in C-S-H gel ranged from 1.65 to 2.0 [7]. Harrison's studies indicated Ca/Si of C-S-H in Portland cement with admixtures was 1.89-2.0 [8]. Richardson suggested Ca/Si of C-S-H in Portland cement pastes ranged from 1.65 to 1.90 [9]. These studies indicated that Ca/Si ratio of C-S-H in Portland Cement-based cementitious materials system is in the range of 1.6-2.0. Considering Ca and Si consumed by other hydration products, increasing C-S-H content is feasible by controlling the Ca/Si ratio of the raw materials to match the Ca/Si ratio of C-S-H, which is of 1.6-2.0. Besides the Ca and Si consumed by C-S-H, Ca in $Ca(OH)_2$ should also be considered. The content of CaO can be obtained by analysis and calculation of hydration of P.I 52.5 cement

Table 1 Chemical composition of cement, MK, FA and LSP (wt%)

	Al_2O_3	SiO_2	Fe_2O_3	CaO	K_2O	TiO_2	SO_3	P_2O_5	Na_2O	MgO	LOI[a]
Cement	5.37	23.19	3.4	63.59	0.53	–	1.22	–	0.34	0.13	2.23
MK	44.58	53.27	0.7	0.02	0.53	0.29	0.22	0.39	0.34	0.13	–
FA	37.93	49.2	3.62	3.01	0.85	–	0.65	–	0.34	0.35	1.15
LSP	–	–	–	43	–	–	–	–	–	–	57

[a]*LOI* loss on ignition

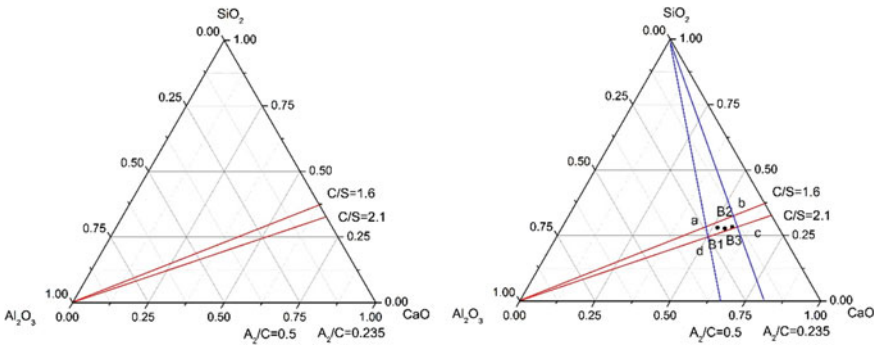

Fig. 1 Triangle phase diagram

paste under water/cement ratio of 0.3. The optimum proportion of CaO-SiO_2-Al_2O_3 in raw materials was calculated accordingly and presented in concentration triangle (Fig. 1).

The optimum content of aluminium phase in raw materials is determined according to the reaction between MK (AS_2), FA and CH. The reaction varies under different AS_2/CH ratios which were listed as follows:

$$AS_2/CH = 0.5, \quad AS_2 + 6CH + 9H \rightarrow C_4AH_{13} + 2C\text{-}S\text{-}H \tag{1}$$

$$AS_2/CH = 0.6, \quad AS_2 + 5CH + 3H \rightarrow C_3AH_6 + 2C\text{-}S\text{-}H \tag{2}$$

$$AS_2/CH = 1.0, \quad AS_2 + 3CH + 6H \rightarrow C_2ASH_8 + C\text{-}S\text{-}H \tag{3}$$

Above formula suggested that AS_2/CH ratio ranged from 0.5 to 1.0 for the reaction of metakaolin. Therefore the molar ratio of Al_2O_3/CaO was between 0.25:1 and 0.5:1.

The reaction of FA is as follows:

$$A/C = 0.99, \quad 1.1CH + S + 2.8H \rightarrow C_{1.1}SH_{3.9} \tag{4}$$

$$A/C = 0.25, \quad A + 4CH + 9H \rightarrow C_4AH_{13} \tag{5}$$

Molar ratio of SiO_2/Al_2O_3 is approximately 1.86 in FA pozzolanic materials, resulted in $AS_{1.86}$/CH of 0.47, indicating that the molar ratio of Al_2O_3/SiO_2 is 0.235:1.

The influence of LSP can be ignored due to the low activity. The optimum Al_2O_3/SiO_2 ratio ranged from 0.235 to 0.5 for active component to react with CH.

According to the above analysis, the optimum composition of admixture favours complete reaction with CH is shown in Fig. 2, which shows the area with four boundary point, namely a(0.471, 0.294, 0.235), b(0.539, 0.256, 0.205), c(0.585,

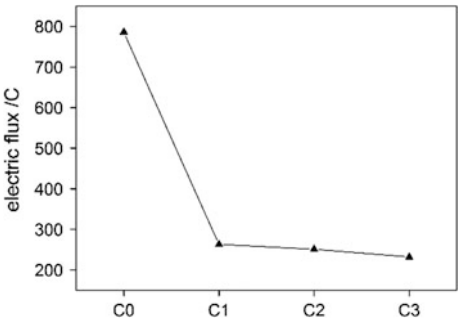

Fig. 2 Electric flux of concrete

Table 2 Cementitious materials mix (wt%)

Mix	Cement	MK	FA	LSP
B1	93.0	5.0	2.0	0
B2	89.0	7.0	2.0	2.0
B3	87.0	9.0	2.0	2.0

Table 3 Mix proportions of concrete (kg/m^3)

Mix	Cement	MK	FA	LSP	Fine aggregate	Coarse aggregate	Super plasticizer	Water
C0	450.00	0	0	0	715.0	1105.0	3.6	135.0
C1	395.25	21.25	8.50	0	715.0	1105.0	3.6	135.0
C2	378.25	29.75	8.50	8.50	715.0	1105.0	3.6	135.0
C3	369.75	38.25	8.50	8.50	715.0	1105.0	3.6	135.0

0.278, 0.137) and d(0.538, 0.336, 0.126). The point coordinate values represent proportion of CaO, SiO_2 and Al_2O_3, respectively.

The cementitious materials mixes were designed accordingly and were shown in Table 2. Concrete mixes were designed accordingly, as seen in Table 3 with control specimen C0.

2.4 Tests Methods

The water/binder ratio (w/b) of concrete is 0.3 and the proportions of three mineral admixtures were determined by analysis above.

Chloride permeability of concrete was assessed by two methods, according to ASTM C1202 and NT Build 492. In the former method, the cylindrical concrete samples with dimensions of $\phi 100 \times 200$ mm were prepared. After cured for 28 days, the samples were cut into size of $\phi 100 \times 50$ mm from middle and the circular surfaces were sealed. Tests were performed according to the standard

ASTM C1202. Chloride diffusion coefficient of specimens at 56 days was measured according to the standard NT Build 492.

Shrinkage deformation was assessed according to Chinese Standards GB/T 50082-2009. The non-contact shrinkage deformation test was performed to obtain shrinkage during 0 to 200 h. Scanning electron microscopy (SEM) was performed by FEI Quanta 450FEG Environmental SEM under the conditions of spot size 5, accelerating voltage 20 kV.

3 Results and Discussion

3.1 Chloride Permeability

The electric flux passed through concrete specimens during 6 h was shown in Fig. 2. The electric flux of specimens with mineral admixture was effectively reduced comparing with that of control specimen. According to Fig. 3, for the specimens containing mineral admixture, the chloride diffusion coefficient of C1, C2 and C3 at 56 days decreased by 51.61 %, 54.84 % and 56.99 % respectively, indicating that MK-based admixture greatly improved the chloride permeability resistance of concrete. The results can be attributed to refinement of pore structure in the concrete which in turn effectively reduced chloride transportation channel. Furthermore, the consumption of $Ca(OH)_2$ and formation of more C-S-H resulted in denser interfacial transition zone and improved the permeability resistance.

3.2 Shrinkage

The volume deformation of concrete was mainly caused by drying shrinkage and chemical shrinkage. According to Fig. 4, the shrinkage of concrete with MK-based mineral admixture decreased with the increase of MK content. Introducing LSP

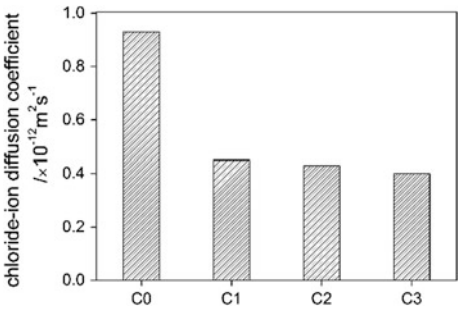

Fig. 3 Chloride diffusion coefficient of concrete

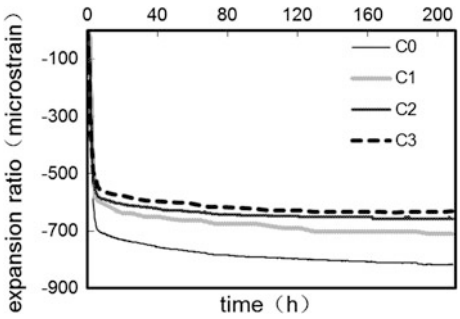

Fig. 4 Shrinkage of concrete specimens

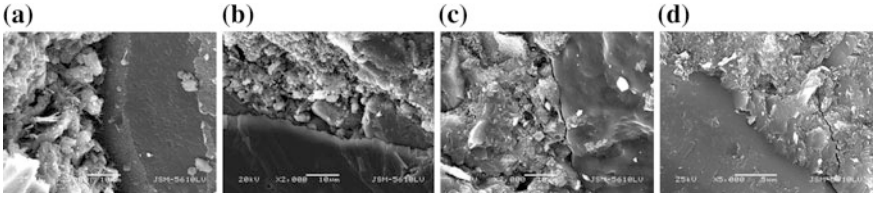

Fig. 5 Microstructure of concrete

further reduced the shrinkage of concrete up to 200 h by comparison of C1 and C2 specimens. The shrinkage of concrete incorporating MK-based mineral admixture was reduced by approximately 13-23 %.

3.3 Microstructure

The microstructures of concrete specimens cured for 28 days were shown in Fig. 5. Needle-like AFt, layered CH and C-S-H were identified in concrete specimens. The microstructures appeared denser in the specimens with mineral admixture addition comparing the control specimen. Moreover, the interfacial transition zone as denser as well and the interface between coarse aggregate and hydration products was better connected in specimens with mineral admixtures. The denser microstructure and interfacial transition zone favoured the higher chloride permeability resistance of concrete.

4 Conclusions

- Based on CaO-Al_2O_3-SiO_2 activity system and activity analysis, three mineral admixtures, namely B1 (5 wt%MK + 2 wt%FA), B2 (7 wt%MK + 2 wt% FA + 2 wt%LSP) and B3 (9 wt%MK + 2 wt%FA + 2 wt%LSP) was designed to archive the best Ca/Si ratio for C-S-H gel.
- MK-based mineral admixtures significantly reduced electric flux of concrete. The chloride diffusion coefficient decreased by 50-60 % comparing to the control specimen.
- Shrinkage of concrete containing MK-based mineral admixtures reduced by 13-23 % comparing to the control specimen. Moreover, shrinkage decreased with the increase of MK or LSP content.
- The durability of concrete was significantly improved by addition of composite admixture. The microstructure analysis of concrete confirmed that the effect was attributed to the refinement of the pore structure and improvement of interface transition zone.

Acknowledgments This research is financially supported by YangFan Innovative & Entrepreneurial Research Team Project (No. 201312C12).

References

1. Ambroise, J., Murat, M., Pera, J.: Hydration reaction and hardening of calcined clays and related minerals. Cem. Concr. Res. **15**, 261–268 (1985)
2. Ding, J., Li, Z.: Effects of metakaolin and silica fumeon properties of concrete. ACI Mater. J. **99** (4), 393–398 (2002)
3. Chindaprasirt, P., Homwuttiwong, S., Sirivivatnanon, V.: Influence of fly ash fineness on strength, drying shrinkage and sulfate resistance of blended cement mortar. Cem. Concr. Res. **34**, 1087–1092 (2004)
4. Khatib, J.M.: Wild S pore size distribution of metakaolin paste. Cem. Concr. Res. **26**(10), 1545–1553 (1996)
5. Paiva, H., Velosa, A., Cachim, P., Ferreira, V.M.: Effect of metakaolin dispersion on the fresh and hardened state properties of concrete. Cem. Concr. Res. **42**, 607–612 (2012)
6. Hewlett, P.C.: Chemistry of Cement and Concrete. Butterworth-Heinemann, Oxford (2001)
7. Rodger, S.A., Groves, G.W.: Electron microscopy study of an ordinary portland cement and ordinary portland cement-pulverized fuel ash blended pastes. J. Am. Ceram. Soc. **72**(6), 1037–1039 (1989)
8. Harrisson, A.M., Winter, N.B., Taylor, H.F.W.: An examination of some pure and composite portland cement pastes using scanning electron microscopy with X-ray analytical capabilities. In: 8th International Congress on the Chemistry of Cement, vol. IV, pp. 170–175. Rio de Janeiro (1986)
9. Richardson, I.G., Groves, G.W.: Microstructure and microanalysis of hardened ordinary cement paste. J. Mater. Sci. **28**, 265–277 (1993)

Reactivity and Microstructure of Calcined Marl as Supplementary Cementitious Material

Tone Østnor, Harald Justnes and Tobias Danner

Abstract The reactivity and microstructure of cement paste and mortar where cement is replaced by up to 65 vol.% calcined marl are discussed. It was found that the compressive strength evolution of mortar is following the same linear relation with amount of hydrate water at early ages for different cement replacements (35-65 vol.%), but that this deviates and give higher strength than predicted by the bound water at higher ages. Strength increases on a long term in spite of depleted calcium hydroxide at earlier ages and are discussed in terms of changes in CSH and CAH. XRD does not reveal any unusual crystalline products, but ettringite and hemi-/mono-carboaluminate hydrate. SEM with WDS in a 2 year old mortar found pure CAH in a pore with atomic Ca/Al = 1.6 and some Si that might be a hydrogarnet.

1 Introduction

Marl, or calcareous clay, is considered "bad" clay for production of burnt clay products (e.g. bricks and light weight aggregate) since it is clay contaminated with substantial amounts of calcium carbonate that will form CaO after burning. This can lead to "pop outs" when calcium oxide reacts with water to calcium hydroxide during service.

Calcined marl has been proven earlier by Justnes et al. [1] to be an effective pozzolan in cementitious products. Thus, marl can be a large SCM resource that is not yet exploited to make blended cements or as mortar/concrete additive. Marl with 10-20 % $CaCO_3$, or rather calcareous mudstone, was calcined at 800 °C leaving 20 % of the original $CaCO_3$ intact.

T. Østnor (✉) · H. Justnes
SINTEF Building and Infrastructure, Trondheim, Norway
e-mail: tone.ostnor@sintef.no

H. Justnes · T. Danner
NTNU—Norwegian University of Science and Technology, Trondheim, Norway

K. Scrivener and A. Favier (eds.), *Calcined Clays for Sustainable Concrete*,
RILEM Bookseries 10, DOI 10.1007/978-94-017-9939-3_29

Calcined marl can be considered "industrial pozzolan" within the European cement standard (EN 197-1), and it may be feasible to make a pozzolanic cement with up to 55 % clinker replacement (CEM IV/B) considering the 28 day strength and sufficient early strength documented in this paper for mortar where cement is replaced by calcined marl.

2 Materials and Experiments

2.1 Materials

The marl was provided by Saint Gobain Weber who calcined it in a rotary kiln close to industrial conditions. The calcined marl were ground to d_{50} = 7 μm. Normal Portland cement (CEM I 42.5R according to NS-EN 197-1) produced by Norcem Brevik, Norway, was used for all the mortar and paste mixes. The super plasticizer used was Dynamon SP 130 supplied by Mapei AS, Norway.

2.2 Mortar and Paste Mixes

The mortars were made with 0, 20, 35, 50 and 65 vol.% replacement of cement with calcined marl to secure a constant volume of binder. The consistency of fresh mortar was determined using a flow table. The water-to-binder ratio (w/b) was 0.5 in all the mortars while the flow was maintained within ±5 % of the reference by varying the amount of super plasticizer; 0.0, 0.2, 0.3, 0.5 and 0.9 % (of binder weight) for the mortars with 0, 20, 35, 50 and 65 vol.%, respectively. The mortar mixes were cast in 40 × 40 × 160 mm moulds. After 24 h the prisms were removed from the moulds and stored in a cabinet at 90 % RH and 23 ± 2 ºC.

In the paste mixes was OPC replaced with 35, 50 and 65 % calcined marl with a w/b ratio of 0.5 and cured for 1, 3, 7, 28, 90 and 365 days at 90 % RH and 23 ± 2 ºC.

3 Results

3.1 Compressive Strength

The average compressive strength and flexural strength for all mortars as a function of time are given in Table 1 together with standard deviations based on 5 and 3 parallels, respectively.

Table 1 Compressive (upper value) and flexural (lower value) strengths as a function of time for mortars where various amounts of cement have been replaced by calcined marl

Marl (vol.%)	Average strength ± standard deviation [MPa] at ages [days]						
	1 d	3 d	7 d	28 d	90 d	365 d	730 d
0	22.0 ± 0.3	40.4 ± 1.0	46.2 ± 1.0	53.5 ± 0.6	61.1 ± 1.6	67.9 ± 0.9	72.9 ± 2.4
	4.8 ± 0.1	6.7 ± 0.4	7.4 ± 1.0	7.8 ± 0.3	8.4 ± 0.4	8.8 ± 0.4	9.0 ± 0.5
20	17.9 ± 0.4	35.5 ± 0.5	44.0 ± 1.0	57.3 ± 1.3	65.6 ± 0.9	70.8 ± 1.3	74.6 ± 0.8
	3.8 ± 0.3	5.9 ± 0.2	7.2 ± 0.2	7.4 ± 0.2	7.7 ± 0.6	9.0 ± 0.5	9.1 ± 0.2
35	14.0 ± 0.1	31.2 ± 0.4	42.5 ± 0.6	57.0 ± 0.8	62.8 ± 1.6	68.4 ± 1.0	68.9 ± 2.9
	3.1 ± 0.1	5.4 ± 0.2	6.5 ± 0.2	7.6 ± 0.5	8.3 ± 0.2	7.9 ± 0.2	9.0 ± 0.5
50	9.5 ± 0.2	23.6 ± 0.3	38.8 ± 0.4	51.0 ± 1.2	54.2 ± 1.1	63.6 ± 1.3	69.2 ± 1.5
	2.2 ± 0.1	4.5 ± 0.2	5.9 ± 0.3	6.5 ± 0.3	6.8 ± 0.4	8.3 ± 0.9	9.4 ± 0.3
65	5.7 ± 0.1	15.8 ± 0.3	27.6 ± 0.1	38.1 ± 1.2	43.5 ± 1.0	55.9 ± 1.3	67.8 ± 0.7
	1.3 ± 0.1	3.2 ± 0.1	4.9 ± 0.2	5.2 ± 0.4	6.1 ± 0.3	6.8 ± 0.4	8.2 ± 0.4

3.2 Thermogravimetric Analysis (TGA)

The paste samples were analysed by thermogravimetric analysis and simultaneous differential thermal analyses (TGA/SDTA) with a Mettler Toledo TGA/SDTA 851. The frozen sample was weighed into aluminium oxide crucibles. Prior to the thermal analysis the samples were submitted to a drying step in order to avoid interference by the non-reacted free or adsorbed water. During the drying step the sample was kept at 40 °C and dried in the instrument by the purge gas, N_2, at a flow of 50 ml/min. This procedure lasted for 3 h. At that time the mass of the sample had become more or less constant. Immediately after the drying step, the thermal analysis was carried out. The sample was heated from 40 °C to 950 °C with a heating rate of 10 °C/min. The purge gas was nitrogen (N_2) with a flow of 50 ml/min.

The TG curves were divided into four main parts:

The steady weight loss up to about 450 °C is due to the dehydration of reaction products

The sharp weight loss step in the interval between 450 °C and 600 °C is caused by the dehydration of calcium hydroxide.

The weight loss in the higher temperature range, from about 600 °C to 950 °C, attributed to the decomposition of carbonates.

The weight loss from 105 °C to 950 °C was taken as the total mass loss, often taken as chemical bound water in spite of containing CO_2.

The compressive strength is compared to mass loss of hydrates as function of time in Fig. 1.

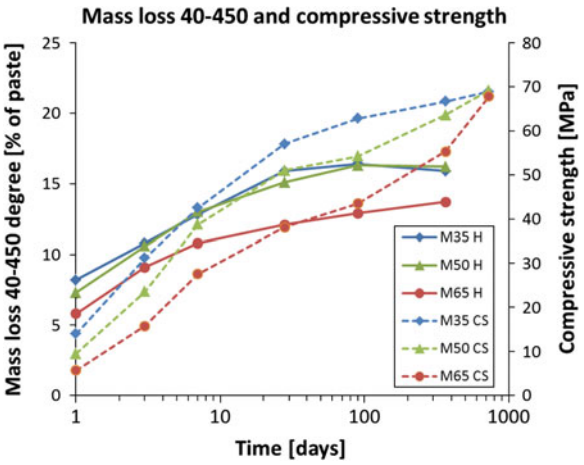

Fig. 1 Mass loss between 40-405 °C and compressive strength as function of curing time

3.3 X-ray Diffraction (XRD)

One sample of each paste mix, cured for 90 days and 1 year at 23 °C and 90 % RH, was analysed by AXS D8 focus X-ray diffractometer. Prior to XRD the samples were dried at 32 % RH. The dried powders were submitted to an angular scan between 5 and 75° 2θ with a step size of 0.06° and a step time of 1.0 s and the diffractograms are shown in Figs. 2 and 3.

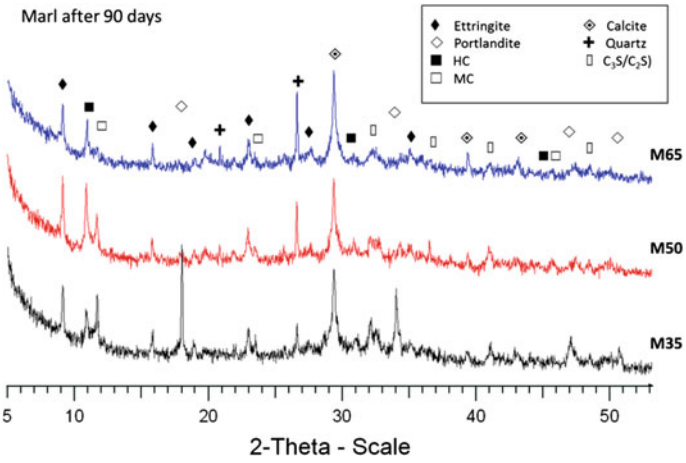

Fig. 2 XRD pattern of marl samples cured for 90 days

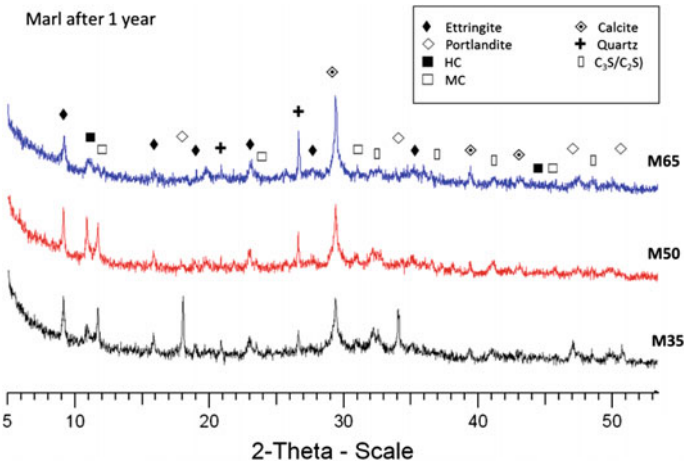

Fig. 3 XRD pattern of marl samples cured for 1 year

3.4 Scanning Electron Microscope (SEM)

One sample from all the mortar mixes cured for 90 days and 2 year were cast in epoxy resin, plane polished to achieve a cross-section of the material and sputtered with carbon. The instrument used in this study was JEOL JXA – 8500F Electron Probe Micro analyser. The samples were analysed in the BSE (back scattered electron) mode where dense compounds and/or compounds composed of heavy elements appear bright (e.g. unreacted C_4AF mineral in cement) and compounds of low density and/or composed of elements with low atomic number appears dark (e.g. CSH). Details of interest were first checked for elements by EDS (energy dispersive spectra) semi-quantitatively, while detailed analyses were performed by WDS (wave length dispersive spectra). Figure 4 shows BSE of mortar where 65 vol.% cement is replaced by calcined marl and the analysis point in a detail proven to be CAH by WDS giving 18.8 Ca, 11.5 Al, 2.8 Si and 1.3 Fe in atom% as the only elements >0.5 % (except O and H).

4 Discussion

The compressive strength at 28 days is about equal to or higher than reference for cement substitution of calcined marl up to 50 %. For higher substitution, the compressive strength is substantially lower probably because calcium hydroxide has been depleted and pozzolanic reaction halted. The faster strength gain of the reference from 28 to 90 days compared to mortar with ≥50 % replacement is an indication of this, but it is peculiar that the strength gain from 90 to 365 days, as

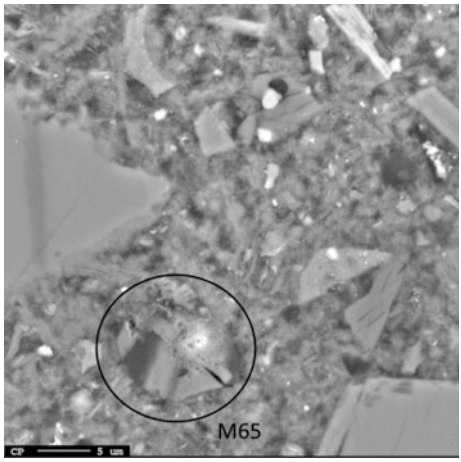

Fig. 4 BSE image of mortar sample where 65 vol.% of the cement is replaced with calcined marl after 2 year curing. The analysed CAH in the circle has Ca/Al = 1.6, close to C_3AH_6 with some Si (i.e. hydrogarnet)

well as from 1 to 2 years, is greater for mortar with the higher cement replacements with no calcium hydroxide present compared to the reference. There are four hypotheses that might explain the latter effect as also discussed by Justnes and Østnor [2]:

1. There are two types of CSH in the system. One with high C/S from hydration of cement and one with low C/S from the direct pozzolanic reaction between calcined marl and calcium hydroxide. The one with higher C/S has higher solubility of Ca^{2+} and is considered weaker mechanically than the one with lower C/S. Slowly the two different CSHs will equilibrate to an overall stronger CSH with intermediate C/S.
2. The solubility of Ca^{2+} from CSH with high C/S and pH is so high that one can have a direct further pozzolanic reaction with unreacted calcined marl.
3. The silicate anions of in particular CSH with low C/S will polymerize over time creating longer chain lengths of the CSH which may lead to even higher strength.

When calcined marl reacts, both silicate and aluminate is released forming CSH and CAH, as well as possibly intermediate products like C_2ASH_8. Crystalline CAH generally demands a higher atomic Ca/Al than amorphous CSH demand Ca/Si, and the CSH is more flexible in its Ca/Si. The craving for Ca by the aluminate could lead to the de-calcification lowering the Ca/Si of the overall CSH that will adapt to that by increased polymerization of silicates (i.e. point 3 above). Inclusion of aluminate in the CSH structure (i.e. bridging of dimers) will also contribute to higher degree of polymerization of CSH. In total this may lead to a higher strength binder.

The compressive strength of mortars is plotted against the mass loss of hydrates in corresponding pastes in Fig. 5 for 35, 50 and 65 % cement replacement by calcined marl. It is interesting that all 3 mixes follow about the *same straight line* in

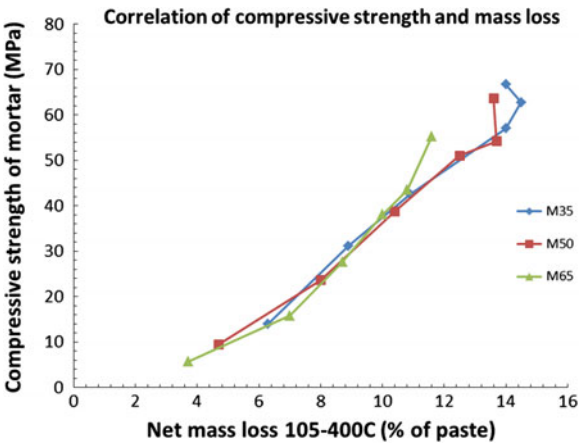

Fig. 5 Correlation of compressive strength and mass loss between 40 and 450 °C

the early ages before they break off at different points and give higher strength than expected from hydrate water supporting point 3 and 4 in the above discussion as CSH polymerization should give less bound water due to fewer –Si-OH end groups.

The XRDs in Figs. 2 and 3 are showing that ettringite is stabilised on the expense of monosulphate due to reaction with carbonate as explained by De Weerdt et al. [3], but another interesting feature is that higher cement replacement by calcined marl seems to stabilize calcium hemicarboaluminate hydrate over monocarboaluminate hydrate (or something else) with exact same peak position at about 11° 2θ. The SEM investigation revealed crystals of CAH with molar Ca/Al = 1.6 including some Si in a pore after 2 years curing corresponding more to hydrogarnet, but the main peak of this should be at around 33° 2θ. XRD also show that crystalline CH is depleted for 65 % as well as 50 % cement replacement after 90 days.

5 Conclusions

The compressive strength evolution of mortar follows the same linear relation with amount of hydrate water at early ages for 35-65 vol.% cement replacements, but shows higher strength than predicted by bound water at later ages. Strength increases on a long term in spite of depleted calcium hydroxide at earlier ages. This may be due to CSH polymerization. XRD only reveals ettringite and hemi-/monocarboaluminate hydrate products, while SEM found pure CAH in a pore with atomic Ca/Al = 1.6 and some Si that might be a hydrogarnet.

Acknowledgments The paper is based on the work performed in COIN, see www.coinweb.no for information.

References

1. Justnes, H., Østnor, T., Danner, T.: Calcined marl as effective pozzolana. In: Proceedings of the International RILEM Conference on Advances in Construction Materials through Science and Engineering, RILEM PRO 79, Hong Kong, China, 8 p. 5–7 September 2011
2. Justnes, H., Østnor, T.A.: Durability and microstructure of mortar with calcined marl as supplementary cementing material. In: Proceedings of the XIII conference on Durability of Building Materials and Components (DBMC), Sao Paulo, Brazil, pp. 771–780, 3–5 September 2014
3. De Weerdt, K., Sellevold, E., Kjellsen, K.O., Justnes, H.: Fly ash—limestone ternary cements—effect of component fineness. Adv. Cem. Res. **23**(4), 203–214 (2011)

Assessing the Synergistic Effect of Limestone and Metakaolin

D. Nied, C. Stabler and M. Zajac

Abstract The effect of simultaneous addition of limestone and metakaolin on the properties of blended cements after 2 and 28 d of curing were investigated using a multi method approach. Hardened properties after 2 d of hydration are largely independent from the limestone to metakaolin ratio. After 28 d of curing, a strong influence of the quality of metakaolin used as well as the ratio of metakaolin to limestone on the hardened properties is observed. High quality metakaolin leads to higher compressive strength values. In the present experimental matrix the highest compressive strength values are obtained with a limestone to metakaolin ratio between 1 and 0.33. A positive effect between limestone and metakaolin is found, which leads to a refinement of the pore microstructure and consequently to higher compressive strength values. The absence of limestone leads to the destabilisation of ettringite, which transforms into monosulphate, and the formation of significant amounts of strätlingite if high quality metakaolin is used.

1 Introduction

Supplementary cementitious materials (SCMs) are widely used in cement industry to reduce the CO_2 footprint. However, the knowledge about fundamental interaction between cement components and performance is limited. Hydration of the cement clinker and hydraulic/pozzolanic reaction of the SCMs occur simultaneously and may influence the reactivity of each other [1]. The aim of this study is to gain new insights into the mechanism of hydration of the calcined clay-limestone composite cements.

D. Nied (✉) · C. Stabler · M. Zajac
HeidelbergCement Technology Center, Leimen, Germany
e-mail: dominik.nied@htc-gmbh.com

K. Scrivener and A. Favier (eds.), *Calcined Clays for Sustainable Concrete*,
RILEM Bookseries 10, DOI 10.1007/978-94-017-9939-3_30

2 Experimental Procedure

The impacts of limestone addition to an OPC-metakaolin blend with a constant OPC content were investigated as well as the influence of the metakaolin quality. Therefore, metakaolin was subsequently replaced by limestone in 10 w% steps leading to the mixes listed in Fig. 1 (left) for the compressive strength testing. According to EN 197-1 most cement are classified regarding their early and late strength after 2 days (d) and 28 d, respectively. Consequently, the present study focuses on the assessment of cement paste and mortar properties at these stages of hydration. The hydration of four blends (L-M1, Q-M1, L-M2 and Q-M2) was investigated using a multi-method approach on cement paste samples with a w/b ratio of 0.5. The pozzolanic materials used within this study were commercially available metakaolin of two different qualities. Rietveld method revealed an X-ray amorphous content of 55 w% for low quality metakaolin M1 and >95 w% for high quality metakaolin M2. The main crystalline phases in case of M1 are quartz, muscovite, albite, andalusite and corundum. The used OPC came from one of HeidelbergCement´s plants. Rietveld gave the following phase distribution (w%): C_3S 57.8; C_2S 15.6; C_3A 6.1; C_4AF 10.7; CaO 1.7 and anhydrite 4.5. The particle size distribution of all raw materials is depicted in Fig. 1 (right). Compressive strength testing was performed in so called µ-mortar composed of sand (Θ < 1 mm), cement and water in mass ratio of 3:2:1.1, respectively. Water to binder ratio of 0.55 was used to ensure sufficient workability without using chemical admixtures at high metakaolin dosages. In case of the blend 4M2 calcium ligninsulphonate was dosed at 0.3 w% of cement to ensure sufficient workability. Silicon forms were filled with mortar and 2 × 2 × 2 cm^3 mortar cubes were produced using a standard vibration table. After 1 day, the samples were de-molded and stored at RH > 95 % and T: 20 °C. The compressive strength of 5 samples (cubes) was tested for one date in a standard mortar press with a loading rate of 0.4 kN/s. The portlandite

mix design [w%]

	OPC	M1 / M2	limestone	quartz
4L	60		40	
3L-1M*	60	10	30	
L-M*	60	20	20	
Q-M*	60	20		20
1L-3M*	60	30	10	
4M*	60	40		

* two different metakaolin qualities: M1 low and M2 high quality

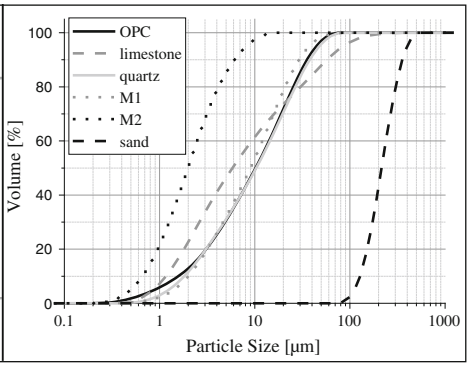

Fig. 1 Particle size distribution of the raw materials measured by laser granulometry (*left*) and mix design of the investigated blends (*right*)

content was quantified using the tangent method and the dehydration peak between 400 and 550 °C. The applied methods within this study are, if not stated separately, described elsewhere [2].

3 Results

3.1 Mechanical Properties

Compressive strength values for varying metakaolin to limestone ratios after 2 and 28 d of curing are depicted in Fig. 2 (left: low quality metakaolin M1; right: high quality metakaolin M2). In case of M1, the 2 d compressive strength is independent of the metakaolin to limestone ratio. For samples containing M2, the 2 d compressive strength values are slightly increasing with increasing M2 content. The 28 d strength, however, is strongly influenced by the amount and type of metakaolin. For the low quality metakaolin M1, the 28 d compressive strength linearly increases with the replacement of limestone by metakaolin until it reaches its maximum in the blend 1L-3M1. The blend with no limestone but only M1 shows a significantly lower late strength. The compressive strength values at 28 d obtained with M2 show a similar trend but at significantly higher strength values.

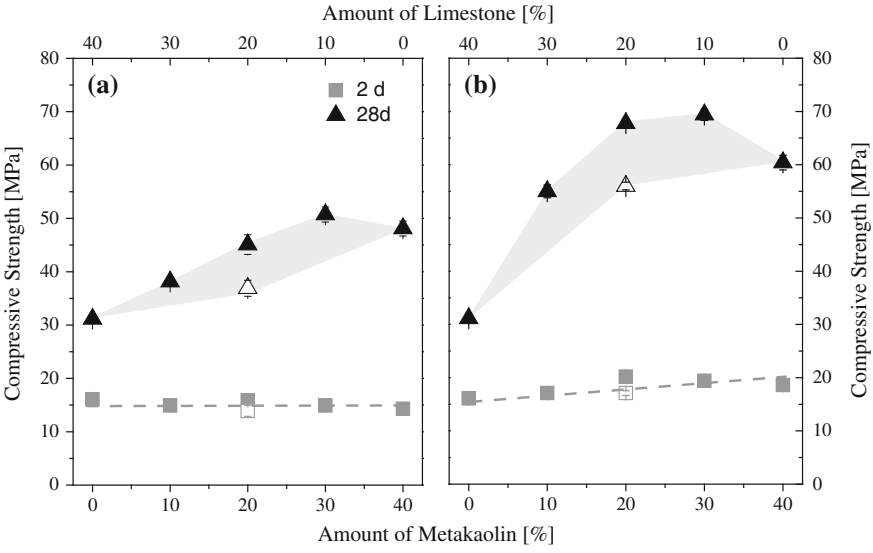

Fig. 2 Compressive strength values after 2 (*square*) and 28 d (*triangle*) of hydration. Mixes contain 60 % OPC and varying ratios of limestone and metakaolin (*left* M1; *right* M2). The hollow symbols are blends with quartz instead of limestone. The *grey* area shows the positive impact of limestone on performance

The hollow symbols shown in Fig. 2 represent the blends, in which the limestone is replaced by quartz (Q-M1 and Q-M2). When compared to their limestone counterparts, they show significantly lower strength values in case of both metakaolin qualities. This effect is significantly more pronounced at later ages.

3.2 Hydrate Assemblage at 2 Days

The hydrating blends containing metakaolin and limestone show, besides the presence of ettringite, the formation of hemicarbonate (see Fig. 3). A significant difference between the two metakaolin qualities is not visible after two days of hydration. The major difference between limestone and quartz containing samples is the absence of hemi- and monocarbonate. Additionally, the formation of monosulphate is detectable in both samples but more prominent in case of M2. After 2 d of hydration the portlandite content is significantly lower in the M2 containing samples when compared with M1 blends (see Fig. 3 right). This trend is not observed for the total water content, which is very similar when comparing the two metakaolin qualities. However, by comparing the limestone with the quartz blends a clear difference in the total bound water content is visible, with the lower values for the quartz mixes. One notes that the portlandite content is similar for the limestone and quartz containing samples. Results from mercury intrusion

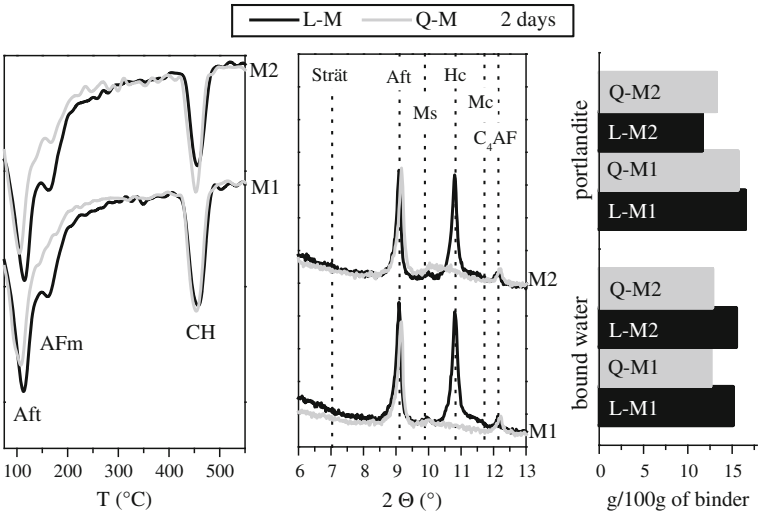

Fig. 3 DTG (*left*), XRD (*middle*) and total bound water and portlandite content (*right*) for blends with 1:1 ratio of metakaolin to limestone/quartz at 2 d of hydration for low (M1) and high (M2) quality metakaolin (Strät: strätlingite, Aft: ettringite, Ms: monosulphate, Hc: hemicarbonate, Mc: monocarbonate)

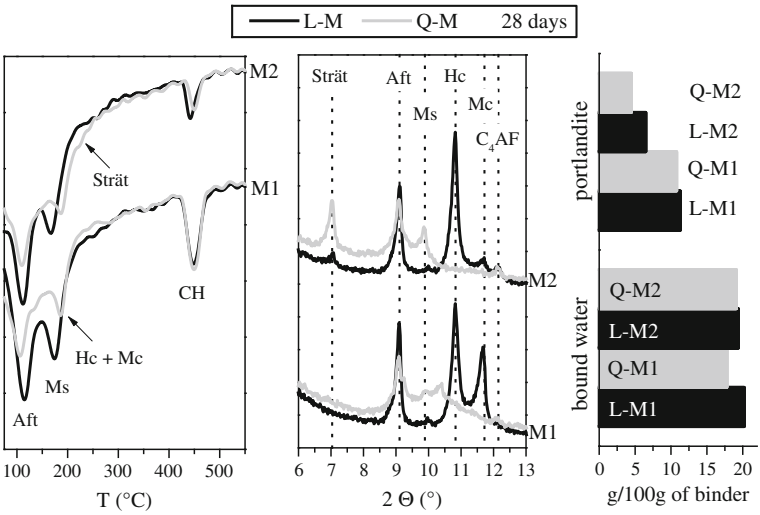

Fig. 4 DTG (*left*), XRD (*middle*) and total bound water and portlandite content (*right*) for blends with 1:1 ratio of metakaolin to limestone/quartz at 28 d of hydration for low (M1) and high (M2) quality metakaolin (Strät: strätlingite, Aft: ettringite, Ms: monosulphate, Hc: hemicarbonate, Mc: monocarbonate)

porosimetry (see Fig. 5 left) reveal a higher porosity in case of M1 samples. Furthermore, L-M samples show a refinement of the porosity when compared to Q-M blends (Fig. 4).

3.3 Characterisation of Hydrate Assemblage After 28 Days

After 28 days of hydration a clear difference between the two metakaolin qualities can be observed. In case of the low quality metakaolin M1, hemicarbonate starts to transform to monocarbonate. For the blend containing high quality metakaolin M2, this transformation is visible only in very small quantities. The persistence of metastable hemicarbonate in the presence of unreacted calcite was also observed in the study from Antoni et al. [3]. They further observed the formation of strätlingite in the investigated blends containing either 30 w% of pure metakaolin or a metakaolin limestone blend. This finding is supported within this study for blends containing high quality metakaolin M2. Strätlingite is detected in the blend L-M2 after 28 d of hydration. For the blends with quartz instead of limestone the presence of substantial amounts of monosulphate is visible for both metakaolin qualities. Additionally, in case of the high quality metakaolin M2, significant amounts of strätlingite are present, which further confirms the findings from Antoni et al. [3].

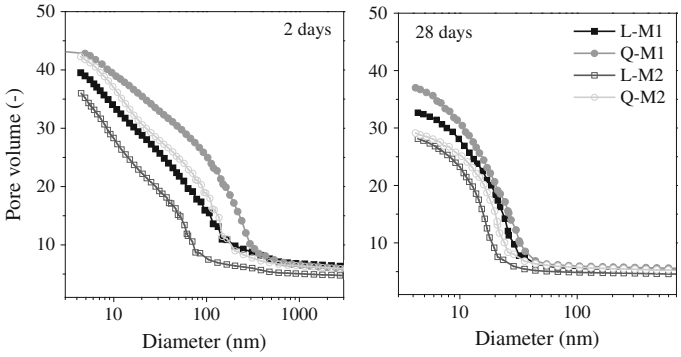

Fig. 5 Porosity determined from mercury intrusion porosimetry after 2 (*left*) and 28 d (*right*) of curing for blends with 1:1 ratio of metakaolin to limestone/quartz for low (M1) and high (M2) quality metakaolin

Although, the total bound water content is for all four samples similar, the sample Q-M1 shows the lowest value. In case of M1 there is no difference in the portlandite content. The M2 blends show significantly lower portlandite contents and the Q-M2 has less portlandite than the limestone counterpart.

The results from mercury intrusion porosity after 28 d of curing are shown in Fig. 5 (right). They are in good agreement with the obtained strength values. In case of the low quality metakaolin M1 the total porosity is higher than for the high quality metakaolin M2 containing blends. Additionally the M2 containing samples show a significant refinement of the porosity when compared to M1 blends. The limestone blends show also a refinement of the porosity when compared to their quartz counterparts.

4 Conclusions

- The present study shows that parts of metakaolin in OPC-metakaolin blends can be replaced by limestone to increase the compressive strength after 28 d and potentially the workability. The optimal ratio, however, depends on the metakaolin quality.
- The incorporation of limestone leads to the stabilisation of ettringite and to a refinement of the porosity when compared to quartz samples.
- The significant difference in monophases in limestone containing samples compared with quartz samples suggest that either the OPC and/or the metakaolin hydration are significantly altered in the presence of limestone at early times.

References

1. Lothenbach, B., Scrivener, K., Hooton, R.D.: Supplementary cementitious materials. Cem. Concr. Res. **41**, 1244–1256 (2011)
2. Zajac, M., Bremseth, S.K., Whitehead, M., Ben, M.: Haha, effect of CaMg(CO3)2 on hydrate assemblages and mechanical properties of hydrated cement pastes at 40 C and 60 C. Cem. Concr. Res. **65**, 21–29 (2014)
3. Antoni, M., Rossen, J., Martirena, F., Scrivener, K.: Cement substitution by a combination of metakaolin and limestone. Cem. Concr. Res. **42**, 1579–1589 (2012)

Study on Influence of Limestone Powder on the Fresh and Hardened Properties of Early Age Metakaolin Based Geopolymer

Jiang Qian and Mu Song

Abstract The objective of this study is to evaluate the effect of limestone powder as a filler material on the fresh and hardened properties of early-age geopolymer. The geopolymer was prepared by alkali activating metakaolin added with limestone filler from 10 % to 30 % by weight. It was found that the incorporation of limestone powder improved the fluidity and strength. 10 % addition of limestone powder increased 17.43 % and 14.36 % of the 7d compressive and flexural strength respectively, and the sample with 15 % addition improved the fluidity of fresh geopolymer distinctly. The mechanism of limestone powder as filler material on the enhancement of properties of geopolymer was investigated by using X-ray diffraction analysis and scanning electron microscopy. The delayed formation of amorphous products with an increased prominence of calcite and a more compacting structure were observed from the XRD and SEM results. Thus the rheology property and the strength development were both promoted due to a better particle size distribution as the extra LS was added.

1 Introduction

Geopolymer, as an inorganic polymer material, has showed a great potential of anticorrosion and low permeability [1]. A great many of researchers have studied the relationship between different alkali solutions, mineral admixtures, composition and properties of geopolymer [2]. The reaction mechanism of metakaolin based geopolymer is widely known as a formation process of Si-O-Al framework, which is similar to zeolite [3]. While some researchers found that in the presence of Ca^{2+},

J. Qian (✉) · M. Song
State Key Laboratory of High Performance Civil Engineering Materials, Jiangsu Research Institute of Building Science, Nanjing 210008, People's Republic of China
e-mail: jiangqian@cnjsjk.cn

J. Qian · M. Song
Jiangsu SOBUTE New Materials Co., Ltd., Nanjing 211103, People's Republic of China

K. Scrivener and A. Favier (eds.), *Calcined Clays for Sustainable Concrete*,
RILEM Bookseries 10, DOI 10.1007/978-94-017-9939-3_31

both N-A-S-H and C-A-S-H gels could be observed with the replacement of Al^{3+} by Ca^{2+} [4, 5]. Accordingly, incorporation of appropriate contents of cheap components rich in Ca, like limestone, could decrease the cost and energy consumption (calcination of metakaolin) of the preparation of geopolymer materials.

Therefore, the paper was focused on the properties and reinforcing mechanism of metakaolin-limestone-alkali geopolymer. The amount of limestone on the rheological property and mechanical property was investigated. Microstructural tests and theoretical analysis were also conducted to reveal the influence of limestone.

2 Materials and Methods

2.1 Materials

The raw materials used was all commercially available. The chemical composition of metakaolin (MK) determined by X-ray fluorescence (XRF) is shown in Table 1. The particle size distribution of MK and limestone (LS) is shown in Fig. 1.

The alkali-activated solution was made from potassium silicate (modulus: 2.0; wt%: 32.5 %) and potassium hydroxide (concentration: 12.5 mol/L).

2.2 Test Specimens and Testing Procedure

All paste mixes were prepared in a cement mixer under a certain procedure: First, powders and solutions were pre-mixed separately before they were added together. Then, the paste was rapidly casted into a steel mould (40 × 40 × 160 mm) after

Table 1 Chemical analysis of metakaolin

Chemical composition	SiO_2	Al_2O_3	Fe_2O_3	CaO	MgO	K_2O	Na_2O	SO_3
Mass percentage/%	60.85	34.51	0.95	0.5	0.39	0.19	0.34	1.82

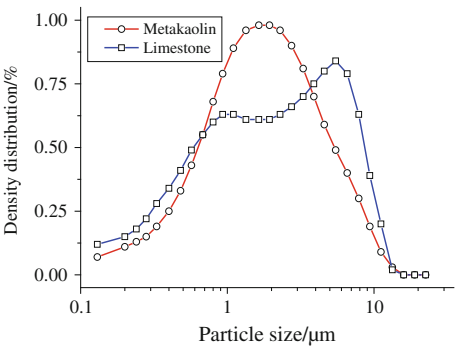

Fig. 1 Particle size distribution of MK and LS

Table 2 Mix compositions of pastes

Mix	MK/g	Potassium silicate solution/g	Potassium hydroxide solution/g	LS (wt%)
P1	1000	765	612	0
P2	1000	765	612	10
P3	1000	765	612	15
P4	1000	765	612	20
P5	1000	765	612	30

1 min low-speed agitation and 2 min high-speed agitation. All paste mixes were prepared under a constant temperature and humidity condition (20 , 65 %RH). After 24 h sealed curing, the specimens were removed from moulds and cured at 20 ± 2 °C, 95 %RH. The composition data of all the samples synthesized in this study is shown in Table 2.

The mini-slump test was carried out to evaluate the workability of geopolymer pastes. The middle point of the top surface was taken as the reference point to measure the spread. Mechanical test was performed as per Chinese Standard (GB/T 17671-1999) on an AEC-201 automatic compression machine (Wuxi, China). Average of three specimens were taken for the strength after 1 and 7 days.

Crystalline phases of geopolymer samples were analyzed by using X-ray diffraction analysis (XRD) from Thermo Fisher Scientific Inc, Waltham, MA/USA. A Cu Kα radiation and a scanning rate of 2°/min from 5° to 70° 2θ were selected. The specimens were prepared by mechanical grinding using a ring mill. Microstructural images of geopolymer samples were obtained using a Scanning Electron Microscope (SEM, FEI QUANTA 250).

3 Results and Discussion

3.1 Rheological Analysis

The rheological behavior is one of the most important properties of geopolymer, especially when it is used as a coating material. Several studies have shown the beneficial effects of limestone on the fresh properties of OPC systems [6, 7], while similar research in metakaolin-based geopolymer material was really rare.

The mini-slump spread results are showed in Fig. 2. Increasing the addition of limestone from 0-15 % in the paste could significantly increase the spread of paste. However, a sharp decrease of spread was noted when the addition is from 15-30 %. The results showed that limestone could improve the workability of metakaolin-based geopolymer within 20 % addition.

As LS was added in a certain content, more “free water” (free alkali-activated solution, to be exactly) could be released for the “filler effect” of LS. And the water film thickness, which is the most important factor governing the rheology of paste [8],

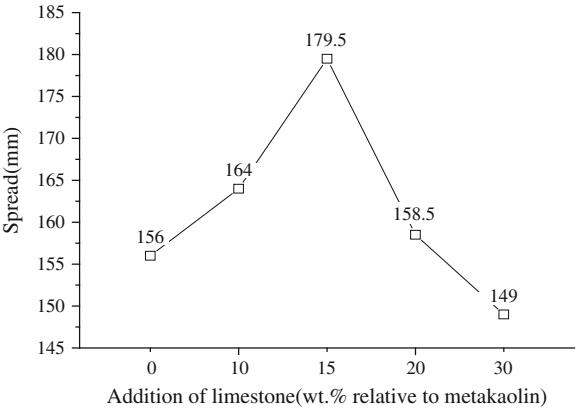

Fig. 2 Mini-slump spread and viscosity of geopolymer with limestone filler

was thus enlarged by this excess part of "free water". Likewise, the LS filler introduced between metakaolin particles might help to break the flocculation structure. Therefore, the flow ability of paste was improved though the solid content increased.

3.2 Mechanical Strength Analysis

The mechanical test results are showed in Fig. 3. The 1-day compressive strength appeared to decrease with the increasing addition of LS. The slight influence of LS addition on both compressive and flexural strength of 1-day paste could be recognized besides the reference sample. Moreover, the beneficial effect of LS to strength also showed after 7 days, which could be attributed to "filler effect" and the

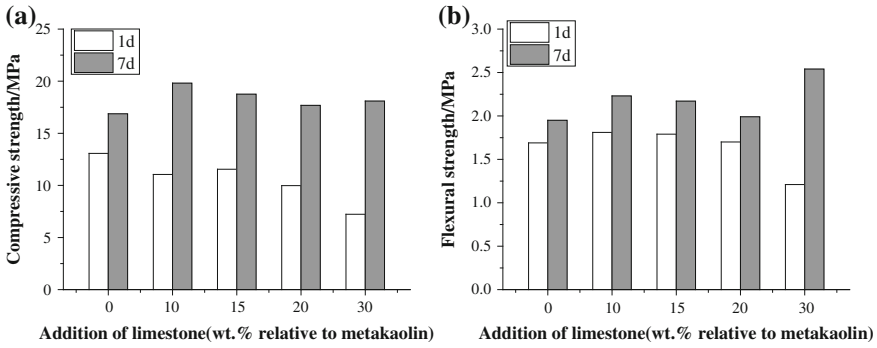

Fig. 3 Effect of LS addition on 1 and 7 day strength of geopolymers: **a** compressive strength; **b** flexural strength

nucleation sites created by LS. The influence of LS on compressive and flexural strength were similar, except an abnormal increase after 7 days and a relative low flexural strength were observed when LS addition was 30 %. Release of the adsorbed alkali solution by LS might help to promote the geopolymerization process, and the strength was thus increased "abnormally" after 7 days.

3.3 XRD Analysis

The X-ray patterns of each 1 day-old paste (reference, 10 % and 30 % LS addition) and pure metakaolin were showed in Fig. 4. The main crystalline phases found from the diffractograms were calcite, quartz and kaolinite. The metakaolin hump (15-32°2θ) was partially removed and a new hump (25 ∼ 35°2θ, often regarded as amorphous and semi-crystalline products) was formed after 1-day geopolymerization reaction. It appeared that the crystalline phases initially present had reacted, and no more significant crystalline phase could be detected after alkaline activation.

Comparing the X-ray patterns between geopolymer pastes with or without LS used, an increased prominence of calcite could be observed as more LS was added. However, the broad hump between 25 ∼ 35°2θ flattened obviously which could be attributed to the extra LS "diluted" the geopolymer content in the paste and delayed the geopolymerization process between metakaolin and alkali solution. The reduction of 1-day strength could also be explained by the phenomenon, especially

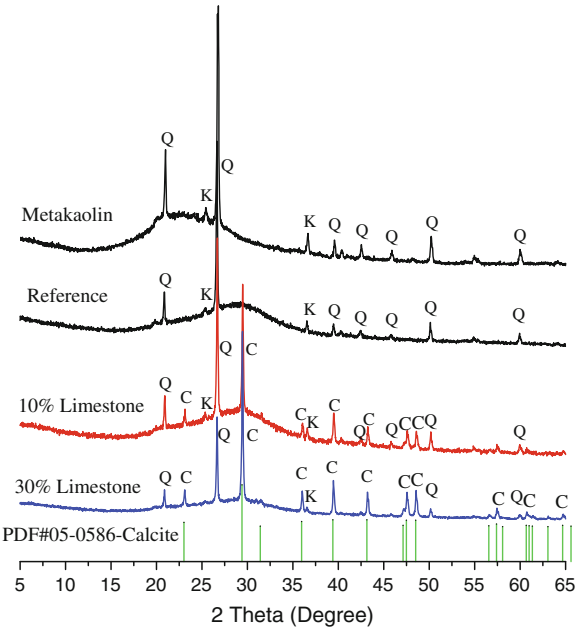

Fig. 4 X-ray patterns of 1 day-old paste with different LS addition. Phases identified are: C-calcite, Q-quartz, K-kaolinite

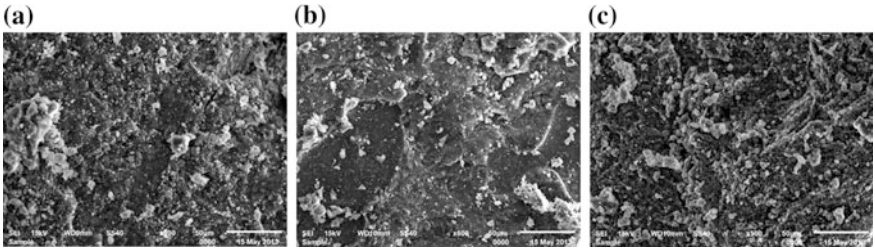

Fig. 5 Second electron images of 1 day-old pastes with different LS addition: **a** 0 % LS; **b** 10 % LS; **c** 30 % LS

when the LS addition was 30 %. No calcium-containing crystalline phases other than calcite were observed, thus the reaction between LS and geopolymer seemed to be really rare (Fig. 5).

3.4 SEM-EDX Analysis

The SE images of 1 day-old samples showed the paste consisted of a binder matrix with LS particles if added. The relatively high packing density of the pastes correlated with the high strength after 1-day curing well. As the LS addition increased, more separated particles among geopolymer matrix could be recognized. The side effect of extra LS became more significant as more liquid phase was adsorbed and the beneficial effect of increasing packing density gradually vanished when the addition came to 30 %. A certain amount around 10 % of LS maximize the beneficial effect to geopolymer paste. New phases with different morphologies and strong bond between LS and geopolymer matrix were hardly found, proving LS-including reaction rarely existed.

4 Conclusions

- LS could improve the workability of metakaolin-based geopolymer within 20 % addition. 15 % addition of LS maximized the mini-slump spread of paste.
- The influence of LS on compressive and flexural strength were similar. The beneficial effect of LS to strength showed after 7 days. 10 % addition of LS increased 17.43 % and 14.36 % of the 7d compressive and flexural strength respectively.
- An increased prominence of calcite and the delayed formation of amorphous products could be observed from the XRD results. From SEM results, a more compacting structure was found with the sample containing 10 % addition of LS.

Acknowledgments Authors appreciate the financial supports from the China Postdoctoral Science Foundation under the contract No. 2013M531296, and the Postdoctoral Science Foundation of Jiangsu Province under the contract No. 1301160C).

References

1. Zhang, Zuhua, Yao, Xiao, Zhu, Huajun: Potential application of geopolymers as protection coatings for marine concrete I. Basic properties. Appl. Clay Sci. **49**, 1–6 (2010)
2. Delair, Stéphanie: Élodie Prud'homme, Claire Peyratout, etc, 'Durability of inorganic foam in solution: the role of alkali elements in the geopolymer network'. Corros. Sci. **59**, 213–221 (2012)
3. Huang, Yi, Han, Minfang: The influence of α-Al_2O_3 addition on microstructure, mechanical and formaldehyde adsorption properties of fly ash-based geopolymer products. J. Hazard. Mater. **193**, 90–94 (2011)
4. García-Lodeiro, I., Palomo, A., Fernández-Jiménez, A., Macphee, D.E.: Compatibility studies between N-A–S–H and C–A–S–H gels. Study in the ternary diagram Na2O–CaO–Al2O3–SiO2–H2O. Cem. Concr. Res. **41**, 923–931 (2011)
5. Yip, C.K., Lukey, G.C., Provis, J.L., van Deventer, J.S.J.: Effect of calcium silicate sources on geopolymerisation. Cem. Concr. Res. **38**, 554–564 (2008)
6. De Weerdt, K., Kjellsen, K.O., Sellevold, E., Justnes, H.: Synergy between fly ash and limestone powder in ternary cements. Cem. Concr. Compos. **33**, 30–38 (2011)
7. Bentz, D., Irassar, E.F., Bucher, B., Weiss, W.J.: Limestone fillers conserve cement; part 2: durability issues and the effects of limestone fineness on mixtures. Concr. Int. **31**, 35–39 (2009)
8. Wong, H.H.C., Kwan, A.K.H.: Rheology of cement paste: role of excess water to solid surface area ratio. J. Mater. Civ. Eng. **20**(2), 189–197 (2008)

Evaluation of the Permeation Properties of Concrete Added with a Petrochemical Industry Waste

Nancy Torres Castellanos, Janneth Torres Agredo and Ruby Mejía de Gutiérrez

Abstract In this work, the evaluation of the performance of concrete added with a petrochemical industry waste called Fluid Catalytic Cracking Catalyst residue (FCC) from a Colombian petroleum company is presented. Results of this concrete are compared, with the results of concrete added with a pozzolan with similar characteristics such as the Metakaolin (MK). The analysis of the pozzolanic materials included the determination of the particle size, the pozzolanic activity, and the chemical and mineralogical composition. Different percentages of FCC were used as Portland cement replacement in proportions of 0, 10, 20 and 30 %; similarly concrete added with 20 % of MK as replacement was elaborated. The curing time was 28, 56, 90 and 180 days. These concretes were evaluated through the permeation properties such as: total absorption, porosity, surface absorption and capillary absorption. Results showed that concrete with FCC and MK had similar behavior, and slightly superior than the control sample. The total absorption and porosity were less than 3 % and 10 % respectively for the all of the samples; it means that these concretes had good quality and compactness. The results of surface absorption and capillary absorption showed that these concretes had low permeability too. This behavior is enhanced with the curing age.

N.T. Castellanos
Universidad Nacional de Colombia, Bogotá, Colombia
e-mail: nancy.torres@escuelaing.edu.co

J.T. Agredo (✉)
Universidad Nacional de Colombia, Palmira, Colombia
e-mail: jtorresa@unal.edu.co

R.M. de Gutiérrez
Universidad del Valle, Cali, Colombia
e-mail: ruby.mejia@correounivalle.edu.co

K. Scrivener and A. Favier (eds.), *Calcined Clays for Sustainable Concrete*,
RILEM Bookseries 10, DOI 10.1007/978-94-017-9939-3_32

1 Introduction

Water can be seen as the main cause of the degradation of building materials, especially concrete [1]. An excess of water expressed at high water/cement ratio used for concrete proportions can generate the phenomenon of exudation and increase the amount of capillary pores, especially those connected with the exterior [2, 3]. During the life service of concrete, the high porosity compromises the physical-mechanical properties of concrete and its permeability [4]. Therefore to assess the durability properties of concrete, it is necessary to study the transport mechanisms of fluids and substances from the outside and into the material by some tests such as permeability, porosity and absorption. To enhance the ability of concrete to withstand the different mechanisms of degradation, it has been necessary to involve supplementary cementitious materials, which partially replace the Portland cement. These are responsible for the pozzolanic reaction characterized by the consumption of calcium hydroxide $Ca(OH)_2$, allowing them to form calcium silicate hydrates (CSH) [5, 6]. The rising of this phase, promotes lower porosity, and an improvement in durability and resistance properties [7, 8].

Metakaolin (MK) is a type of calcined clay which is one of the most used and studied supplementary cementitious materials. It presents a high reactivity and excellent pozzolanic properties because of its chemical composition, amorphous structure and high specific surface [9–13]. It has been demonstrated that when MK is used as a partial replacement of cement, it accelerates the hydration of Portland cement and reduces the content of calcium hydroxide in the concrete mix, while it improves permeability and shows lower values of porosity, water absorption and sorptivity [9, 14, 15].

On the other hand, a residue of the petrochemical industry called spent fluid catalytic cracking catalyst (FCC), has been studied in the last few years. This material presents pozzolanic characteristics comparable to Metakaolin [16–20]. Given the similar characteristics of these two materials, a pilot program was developed in order to assess some properties that are influential in durability, including the total absorption, porosity, surface absorption and capillary absorption. Concrete mixes were developed with partial replacement of FCC in (0 %, 10 %, 20 % and 30 %) percentages of Portland Cement, and their behavior were compared with concrete mixes that were replaced in a 20 % of MK, at different curing ages.

2 Materials and Experimental Procedure

An ordinary Portland cement (OPC) was used for concrete preparation. Spent fluid catalytic cracking catalyst (FCC) and Metakaolin (MK) were used as supplementary materials. FCC was supplied by a Colombian petroleum company (Ecopetrol, Cartagena). The chemical and physical characteristics of these raw materials are shown in Table 1. As shown, the FCC is composed almost entirely of silica and

Table 1 Chemical and physical characteristics of the FCC, MK, and cement used

Characteristics	Cement (OPC)	MK	FCC
Chemical composition%			
SiO_2	19.43	53.38	43.97
AI_2O_3	4.00	43.18	45.48
Fe_2O_3	3.61	1.29	–
CaO	64.46	0.05	0.43
MgO	1.52	0.35	–
K_2O	0.39	1.11	0.15
TiO_2	0.34	0.59	0.69
Loss on ignition	2.58	0.52	2.19
Physical properties			
Density (g/cm^3)	3.13	2.50	2.63
Average particle size (pm)	16.07	7.53	18.00
Pozzolanic activity index, 28 days		92.90	97.40

alumina, with a composition similar to that of Metakaolin. The pozzolanic activity was determined according to ASTM C618 standards, it requires a minimum pozzolanic activity index of 75 % at 28 days of curing to consider a material as a pozzolan. All the supplementary materials used comply with that parameter.

Figure 1 shows two X-ray diffractograms (XRD) for FCC and MK. In this case a RX Rigaku RINT 2200 machine was used. In the case of the FCC, it's shown that it has both amorphous and crystalline material, identifying in greater scale a crystalline pattern similar to the faujasite zeolite (F) with formula $Na_2[Al_2Si_{10}O_{24}].nH_2O$ with peaks located in $2\theta = 6.19°$, 15.6°, 23.58°; also present kaolinite (K) and quartz (Q). In the case of MK, an amorphous material characteristics is shown, which is presented by the baseline survey in the region $2\theta = 20$ to 30°, and the disappearance of the peaks corresponding to kaolinite.

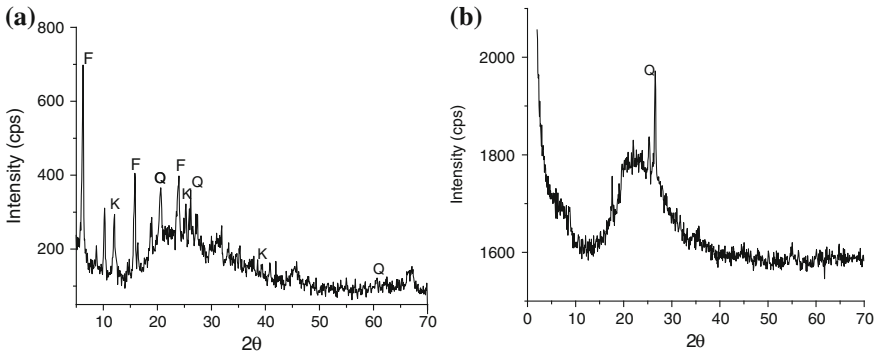

Fig. 1 X-ray diffractograms **a** FCC, **b** MK. (*F* faujasite, *Q* quartz, *K* kaolinite)

Table 2 Proportion of materials in mixtures

Mixture denomination	Cement and addition (kg/m^3)	w/C	Aggregates (kg/m)	
			Coarse	Sand
Control	380	0.50	950	777
10 % FCC	C: 342 FCC: 38	0.50	950	777
20 % FCC	C: 304 FCC: 76	0.50	950	777
30 % FCC	C: 266 FCC: 114	0.50	950	777
20 % MK	C: 304 MK: 76	0.50	950	777

3 Preparation of Concrete Mixes

A control concrete mixture¸ was made along with four concrete mixtures added with the proportions showed in Table 2. The coarse aggregate had maximum nominal size of 12.7 mm, nominal density of 2668 kg/m^3, unit weight of 1542 kg/m^3 and absorption of 3.0 %. Sand had nominal density of 2679 kg/m^3, unit weight of 1667 kg/m^3, absorption of 2.1 % and a fineness modulus of 2.84. A constant water-to-binder ratio (w/C) of 0.5 was used, therefore was necessary to incorporate a high efficiency superplasticizer. Specimens were cured in water saturated with $Ca(OH)_2$ at room temperature for periods up to 180 days.

To assess the absorption properties, the followed procedures were those determined by the ASTM C642 on samples of 75 mm diameter and 150 mm height, BS 1881-208 on samples of 150 mm diameter and 100 mm height and ASTM C1585, on samples of 100 mm diameter and 50 mm height.

4 Results and Discussion

In Fig. 2, the results of absorption and porosity obtained from the different studied mixes are presented. In general all the samples have a low absorption that decreases along different curing ages. A high decreasing trend is noticed in the control sample and the one with FCC added at a 20 %. All samples of concrete with 180 days of curing, except the ones with 30 % of FCC, have less than 1 % absorption and less than 2 % porosity; similar to those reported by results in [21]. A good behavior is present in samples that have an addition of FCC-10 %, similar to the ones reported by [22]. Reduced absorption and porosity for different samples in all test ages, could be attributed to the contribution of additions to the filling effect (thus modifying the concrete microstructure) [4] and the effect of curing, which improves hydration cement and pozzolanic reactions, creating a denser microstructure with less pore capillary volume, thereby reducing the permeability.

shows the data of the readings taken at 10 min, which allows the study of the initial surface absorption of concrete. The sample with 10 % FCC has similar

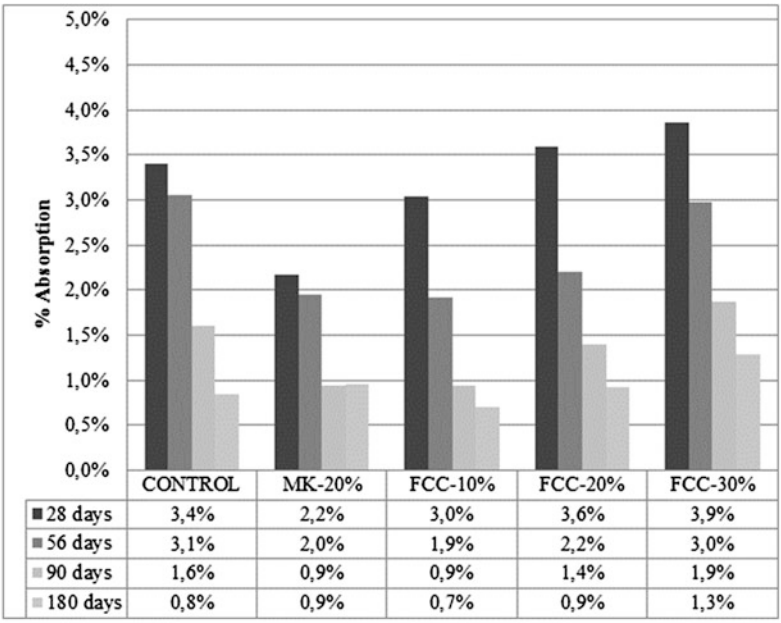

	CONTROL	MK-20%	FCC-10%	FCC-20%	FCC-30%
28 days	3,4%	2,2%	3,0%	3,6%	3,9%
56 days	3,1%	2,0%	1,9%	2,2%	3,0%
90 days	1,6%	0,9%	0,9%	1,4%	1,9%
180 days	0,8%	0,9%	0,7%	0,9%	1,3%

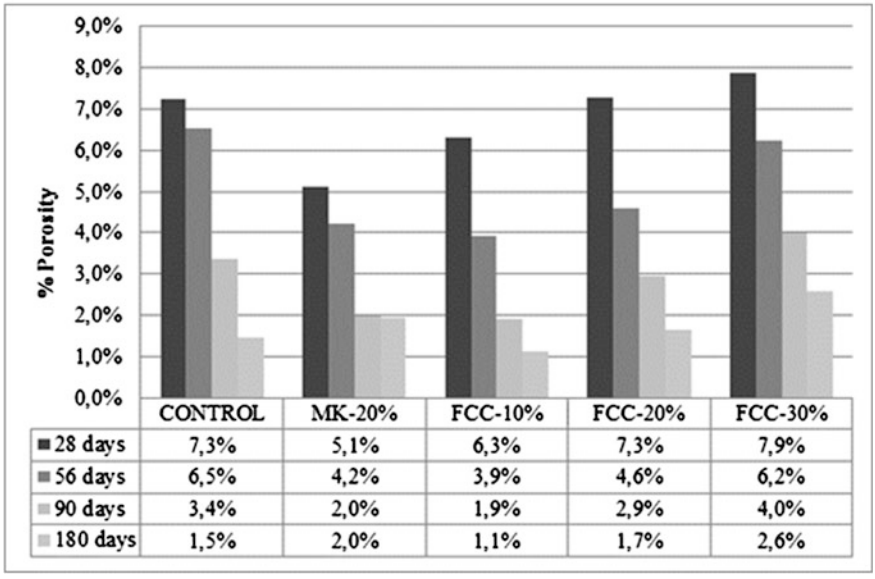

	CONTROL	MK-20%	FCC-10%	FCC-20%	FCC-30%
28 days	7,3%	5,1%	6,3%	7,3%	7,9%
56 days	6,5%	4,2%	3,9%	4,6%	6,2%
90 days	3,4%	2,0%	1,9%	2,9%	4,0%
180 days	1,5%	2,0%	1,1%	1,7%	2,6%

Fig. 2 Absorption and Porosity

permeability values like the ones found in control and MK samples at 180 days of curing. The samples added with MK and FCC-10 % (in this case) present the best behavior. These additions have a high alumina content, which modifies the structure

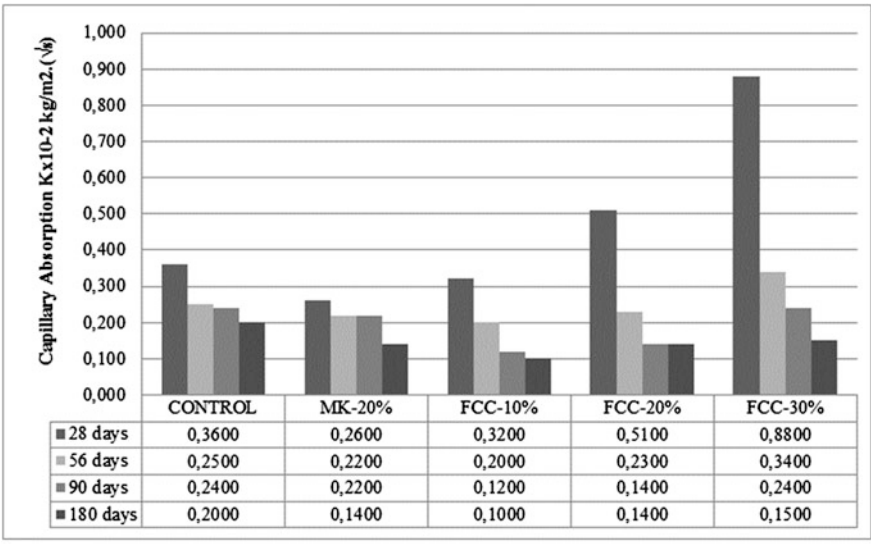

	CONTROL	MK-20%	FCC-10%	FCC-20%	FCC-30%
28 days	0,3600	0,2600	0,3200	0,5100	0,8800
56 days	0,2500	0,2200	0,2000	0,2300	0,3400
90 days	0,2400	0,2200	0,1200	0,1400	0,2400
180 days	0,2000	0,1400	0,1000	0,1400	0,1500

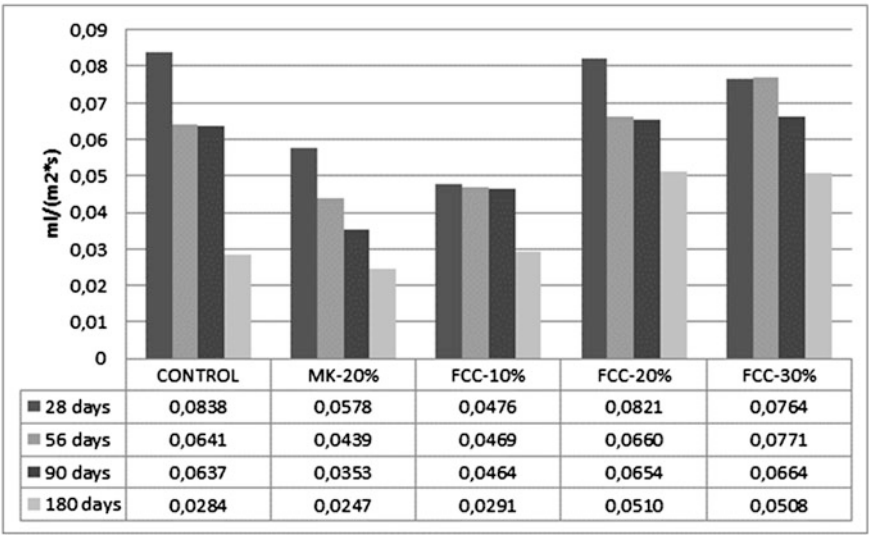

	CONTROL	MK-20%	FCC-10%	FCC-20%	FCC-30%
28 days	0,0838	0,0578	0,0476	0,0821	0,0764
56 days	0,0641	0,0439	0,0469	0,0660	0,0771
90 days	0,0637	0,0353	0,0464	0,0654	0,0664
180 days	0,0284	0,0247	0,0291	0,0510	0,0508

Fig. 3 Initial superficial absorption and Capillary absorption

of the CSH gel, forming a sheet structure that influences in the efficient pore filling, decreasing the permeability [23]. The samples with MK exhibit a good performance at 28 days, compared to the control sample. These results are consistent with those reported by [24].

Regarding the capillary absorption (Fig. 3), the sorptivity coefficient decreases for different curing ages, mainly in the MK-20 % and FCC 10 % samples compared to the control one, being the sample added with FCC-10 %, at 180 days of curing,

50 % lower than the value found at 28 days. The good performance of the added mixtures can be attributed to the higher densification obtained in the cementitious material because of the high fineness that have these additions; allowing plugging of capillary pores [24].

5 Conclusions

- The chemical and mineralogical composition of FCC are very similar to MK, thereby, the behavior of concrete added with these materials was comparable. The results of the test make evident a similar behavior of MK-20 % and FCC-10 % as an optimal replacement of cement, which results are better than the ones obtained with the control sample.
- The results presented show that the pozzolan evaluated, in partial replacement of cement is a good alternative to produce concrete with a good durability, considering water absorption was less than 5 % and the porosity percentage less than 10 %.
- In the study, the use of industrial residue demonstrates that the FCC, could have a potential use as a partial replacement to Portland cement. This results may have a positive impact from an environmental point of view.

Acknowledgments The authors are grateful towards the Universidad Nacional de Colombia, Escuela Colombiana de Ingeniería and Universidad del Valle, for the support given during the development of this research.

References

1. Fernández, A., Palomo, A.: Propiedades y aplicaciones de los cementos alcalinos. Revista Ingeniería de Construcción **24**, 15–213 (2009)
2. Delagrave, A.: Influence of chloride ions and pH level on the durability of high performance cement pastes (part II). Cem. Concr. Res. **26**, 749–760 (1996)
3. Mehta, K. and P. Monteiro, Concreto: Estructura, Propiedades y Materiales. Instituto Mexicano del Cemento y del Concreto A.C., México, D.F., **1**, 8–33 (1998)
4. Detwiler, R., Mehta, P.: Chemical and physical effects of silica fume on the mechanical behavior of concrete. ACI Mater. J. **86**, 609–614 (1989)
5. Schieltz, N.C.: The interpretation of X-ray patterns of pozzolans. Symp. UsePozz. Mater. Mort. Concr. ASTM Special Tech **99**, 4–127 (1950)
6. Talero, R.: Contribución al estudio analí y físico-químico del sistema: cementos puzolánicos-yeso-agua, in Ftad de C. Químicas. Universidad Complutense de Madrid, Madrid (1986)
7. Mehta, K., Monteiro, P.: Concrete, Microstructure, Properties, and Materials. ed. McGraw-Hill, United States (2006)
8. Taylor, H.F.W.: *Enciclopedia de la Química Industrial: La Química de los Cementos*. Ediciones URMO ed. Escuela de Ingenieros Industriales de Bilbao, Universidad de Deusto. Bilbao, España (1967)

9. Caldarone: High-reactivity metakaolin: a new generation mineral mixture. Concrete International: Design and Construction, pp. 37–41 (1994)
10. Balogh, A.: High reactivity metakaolin. Concr. Constr. **40**(7), 1–3 (1995)
11. Kakali, G., et al.: Thermal treatment of kaolin: the effect of mineralogy on the pozzolanic activity. Appl. Clay Sci. **20**(1–2), 73–80 (2001)
12. Razak, H.A., Wong, H.S.: Strength estimation model for high-strength concrete incorporating metakaolin and silica fume. Cem. Concr. Res. **35**(4), 688–695 (2005)
13. Torres, J., Mejía de Gutiérrez, R., Puertas, F.: Effect of Kaolin treatment temperature on mortar cloride permeability. Materiales de Construcción **57**(285), 9 (2007)
14. Mejía de Gutiérrez, R., et al.: Análisis del Proceso Térmico de producción de una puzolana. Materiales de Construcción **54**, 65–72 (2004)
15. Asbridge, A.H., Chadbourn, G.A., Page, C.L.: Effects of Metakaolin and the Interfacial Zone on the Diffusion on chloride ions through Cement Mortars. Cem. Concr. Res. **31**(11), 1567–1572 (2001)
16. Paya, J., Monzo, J., Borrachero, M.: Fluid Catalytic Cracking Residue (FC3R) as a New Pozzolanic Material: Thermal Analysis Monitoring of FC3R/Portland Cement Reactions, Seventh CANMET/ACI. In: International Conference on Fly Ash, Silica Fume Slag and Natural Pozzolans in Concrete, pp. 5–22 (2001)
17. Borrachero, M., et al.: El Catalizador Gastado de Craqueo Catalítico Adicionado al Cemento Pórtland: Las Primeras 48 Horas de Curado y la Evolución de la Resistencia Mecánica. In: VIII Congreso Nacional de Propiedades Mecánicas de Sólidos. Gandia (2002)
18. Soriano, M.L.: Nuevas Aportaciones en el Desarrollo de Materiales Cementantes con Residuo de Catalizador de Craqueo Catalítico (FCC). Universidad Politécnica de Valencia (2008)
19. Trochez, J., Torres, J., Mejía de Gutiérrez, R.: Estudio de la hidratación de pastas de cemento adicionadas con catalizador de craqueo catalıtico usado (FCC) de una refinería colombiana. Revista Facultad de Ingeniería Universidad de Antioquia **55**, 26–34 (2010)
20. Torres, N., Torres, J., Mejía de Gutiérrez, R.: Performance under sulfate attack of concrete additioned with fluid catalytic cracking catalyst residue (FCC) and metakaolin (MK). Revista Ingeniería e Investigación **33**(1), 18–22 (2013)
21. Mejia de Gutiérrez, R., et al.: Concreto adicionado con metacaolín: Comportamiento a carbonatación y cloruros. Revista Facultad de Ingeniería Universidad de Antioquia **48**, 55–64 (2009)
22. Pacewska, B., et al.: Modification of Properties of Concrete by a New Pozzolan a Waste Catalyst from the Catalytic Process in a Fluidized Bed. Cem. Concr. Res. **32**(1), 145–152 (2002)
23. Richardson, I.G.: The natura of CSH in hardened cements. Cem. Concr. Res. **29**, 1131–1147 (1999)
24. Dhir, R., Jones, M.R.: Use of the unfamiliar cement to ENV 197-1. In: Ravindra Dhir, M.R. J. (ed.) Concrete. London (2002)

Calcined Illitic Clays as Portland Cement Replacements

Roxana Lemma, Edgardo F. Irassar and Viviana Rahhal

Abstract Different illitic clays (Buenos Aires Province, Argentine) were selected to study their potential pozzolanic activity. Clays were characterized by X-ray diffraction (XRD), Fourier transformed infra-red spectroscopy (FTIR) and thermal analysis (TG). Clays are calcined at 300, 600 and 950 °C and ground until 85 % mass passed through a 45 μm sieve. The pozzolanic activity was evaluated by the Frattini test and the strength activity index (SAI) at 2, 7 and 28 days on blended cements containing 25 % by weight of calcined clay. Results indicates that calcined illitic clays are suitable as raw material to prepare calcined clay pozzolan when they are fired at 950 °C as revels the Frattini test and they have a SAI from 0.75 to 0.94 at 28 days depending the amount of clayed minerals in the raw shale-stone. Secondary clay minerals don't change significantly the pozzolanic behavior of illitic calcined clays.

1 Introduction

The search for alternative low cost, low emission and low emboiled energy materials in the cement production lead to analyze the available materials near to the factories. In this region, the utilization of common clays (especially, illitic shales) is on the focus.

The clayed minerals are classified in four main groups: smectite, illite, kaolinite and chlorite, and they can be activated to make a pozzolana. Depending on the clay minerals, the temperature range for thermal activation varies from 500 to 1000 °C. The temperature will be selected to produce the dehydroxylation of the clay mineral [1]. This metastable state is necessary to obtain a reactive pozzolana, but some calcined clay can produce large water demand limiting the percentage of addition.

Illite is one of the more abundant clayed minerals of the earth's crust and its chemical composition is $(K, H_3O)(Al, Mg, Fe)_2(Si, Al)_4O_{10}[(OH)_2, (H_2O)]$. It comes

R. Lemma · E.F. Irassar · V. Rahhal (✉)
Facultad de Ingeniería, CIFICEN (CONICET-UNCPBA), B7400JWI Olavarría, Argentina
e-mail: vrahhal@fio.unicen.edu.ar

K. Scrivener and A. Favier (eds.), *Calcined Clays for Sustainable Concrete*,
RILEM Bookseries 10, DOI 10.1007/978-94-017-9939-3_33

from the alteration of feldspars and micas of igneous, sedimentary or metamorphic rocks due to the weathering process. Several investigations [2–4] show that illite clays possess certain reactivity after a thermal activation at approximately 950 °C.

Illitic clay-stones generally consist of a mixture of different clay minerals (illite, kaolinites, montmorillonite and chlorite) and associated minerals (quartz, feldspar and anatase). In clay-stones, the identification and quantification of clay minerals is difficult and combinations of several analytical methods are required. The variability of nature and composition of secondary and associated minerals has a significant influence on the thermal activation process and the suitability of calcined clay as pozzolan.

The aim of this research is to understand the influence of raw materials (illict shale) on the thermal treatment and the potential reactivity as pozzolan for formulates blended cements.

2 Materials and Procedures

2.1 Clay-Stone Samples

Four different clay-stones obtained from quarries of cement producer are used. Two samples were obtained from Cerro Largo Fm and the others Cerro Negro Fm located at the SO of the Tandilia System near to Olavarría city, Buenos Aires Province, Argentine. In the Olavarría region, the igneous-metamorphic Buenos Aires Complex is partially covered by two sedimentary units: the Sierras Bayas Group (Villa Mónica, Colombo-Diamictite, Cerro Largo and Loma Negra units) and the Cerro Negro Fm as described by Cingolani [5]. The Villa Mónica Fm is composed of shallow-marine siliciclastic rocks and the upper member is characterized by dolostones and shales. In the Cerro Largo Fm, the quartz-arenites pass transitionally into siltstones and claystones (also called Olavarría Fm) with a maximum thickness of 37 m. These clay-stones are formed mainly by illitic shale with a fine grain and colored from beige to red. Cerro Largo Fm is the bed of Loma Negra unit constitute mainly by micritic limestones with a maximum thickness of 45 m. Superposed to Loma Negra units, the Cerro Negro Fm (100–400 m thick) is composed by shale, mudstones and sandstone.

The samples are called as IC01 and IC03 for clay-stones obtaining from the upper layer of limestone (Cerro Negro Fm) and, IC02 and IC04 for samples from the deeper layer (Cerro Largo Fm).

2.2 Characterization of Clay-Stones

The chemical composition of clay-stones was determined by XRF analysis. The mineralogical composition was studied by X-ray diffraction (XRD), Fourier

transformed infra-red spectroscopy (FTIR), and differential thermal analysis combined with thermal gravimetric analysis (DTA-TG). XRD was performed using a Philips PW 3710 diffractometer operating with CuKα radiation at 40 kV and 20 Ma. FTIR spectrums were obtained using a Nicolet Magna 500 spectrophotometer and the thermal analysis was carried on using a Seteram™LABSYS at 30–1000 °C and a heating rate of 13 °C/min.

2.3 Calcination and Grinding

The quarry samples were homogenized, dried in laboratory ambient and crushed to particle size lower than 4.75 mm sieve (#4). Samples were fired in a programmable laboratory furnace at heating rate of 13 °C/min up to 300, 600 and 950 °C, holding 30 min at this temperature and cooling in the oven to room temperature. The firing temperatures were fixed according to the thermal analysis results that are described later. Then, calcined clays were ground in laboratory ball mill until the retained on 45 μm sieve (# 325) is lower than 15 %. Finally, XRD analyses were made.

2.4 Pozzolanic Activity Test

The pozzolanic activity of calcined clays fired at different temperatures were determine by the Frattini test (EN 197-5) and the Strength Activity Index (SAI—EN 450-1) at 2, 7 and 28 days. Blended cement was prepared with a replacement of 25 % by mass of Portland cement by calcined clay. Complementary, the flow of blended cement mortars was determined in the flow-table test (EN 1015-3) as indication of water demand. For both tests, the Portland cement used (CEM I 42.5) has a mineralogical clinker composition of C_3S = 64 %, C_3A = 3 %, the alkalies (Na_2O_{eq}) = 0.75 % and calcite is the minor component.

3 Results and Discussion

3.1 Characterization

Table 1 shows the chemical composition of clay-stones. SiO_2 and Al_2O_3 are the predominant oxides and the high SiO_2/Al_2O_3 ratio indicates the presence of free silica. The high amounts of Fe_2O_3 and K_2O indicate the presence of illite. The Fe_2O_3 content is 6.9 to8.0 % and its proportion is high in both clays from Cerro Largo Fm (IC02 and IC04). The alkali components (K_2O and Na_2O) can act as fluxing agent decreasing the firing temperature.

Table 1 Chemical and mineralogical composition of claystones

Clay	Chemical composition, %									Clay minerals			
	SiO_2	Al_2O_3	$Fe2O_3$	CaO	MgO	Na_2O	K_2O	TiO_2	LOI	I	K	M	Ch
IC01	61.5	16.7	7.3	0.3	2.3	1.4	3.7	0.8	5.2	47	–	3	2
IC02	60.0	18.0	8.0	0.3	2.7	1.0	4.0	1.0	4.6	40	–	–	11
IC03	65.2	15.3	6.9	1.3	2.3	1.0	3.5	0.7	4.2	40	3	3	–
IC04	64.2	16.3	7.8	0.5	1.4	0.1	5.4	0.8	3.6	50	12	–	–

The XRD patterns of clay-stones are shown in Fig. 1. All samples contain illite as main clay mineral. Secondary clay minerals are: chlorite and montmorillonite in IC01; chlorite in IC02, kaolinite and montmorillonite in IC03 and kaolinite in IC04. Quartz (Q) was found in all samples as the crystalline form of free silica. Feldspars also appear as minor associated mineral, especially in IC01 and IC03. The approximately mineralogy composition estimated using the normative method is reported in Table 1:

Clay minerals were confirmed using the FTIR analysis: The broad OH-stretching band at 3625-3620 cm^{-1} coupled with the 829 cm^{-1}, 750 cm^{-1} doublet indicates illite in all samples. The broad OH-stretching band at 3624 cm^{-1} of montmorillonite (overlapping illite and inner OH groups of kaolinite) is much greater breadth, but the well-resolved OH deformation bands at 915 cm^{-1} (Al–Al-OH) and 843 cm^{-1} (Al-MgOH) revels its presence in IC01 and IC03. For IC01 and IC02, chlorite has the broad band at 3548 and 3424 cm^{-1}. Kaolinite in IC03 and IC04 is identified by the sharp band at 3696 cm^{-1} corresponding to the OH-stretching doublet and the OH-deformation bands situated at 938 and 913 cm^{-1}.

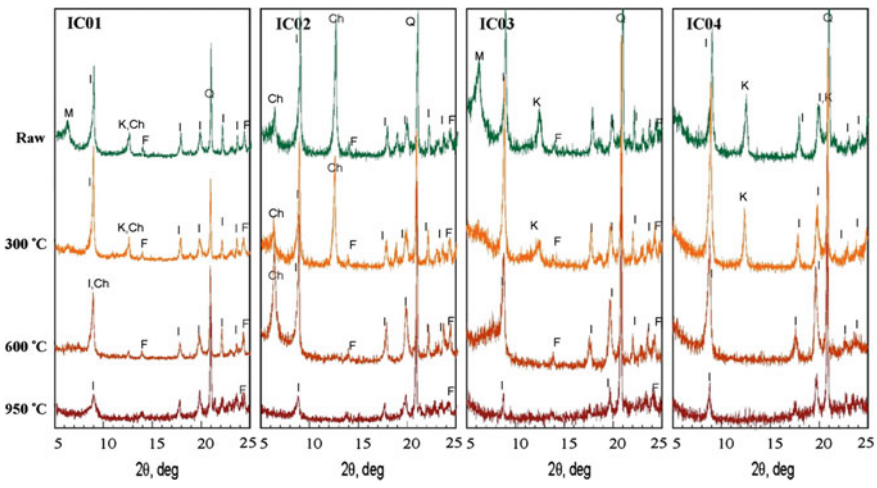

Fig. 1 XRD patterns for raw claystones and after firing at 300, 600 and 950 °C

TG analysis reveals that the temperature ranges of main changes correspond to loss of adsorbed water and molecular water between layers (300 °C), the dehydroxylation of kaolinite at 500–600 °C, chlorite at 450–750 °C and finally the illite/smectite at approximately 900 °C. Then, the recrystallization and formation of spinel occurs at high temperature. All process cause a loss mass of 3.1 to 5.6 %. As used clays are a mixture of clay minerals, the thermal reactions of individual's clays minerals cannot be completely distinguished by TG.

3.2 Heating Transformations

Figure 1 also shows the XRD after firing clay-stones at 300, 600 and 950 °C to assign the transformations in the mineral phases. At 300 °C, the montmorillonite peak collapsed (peak at 6.2° 2θ is replaced by a dome center at 7.8° 2θ) in IC01 and IC03 clays. At 600 °C, kaolinite is transformed to metakaolin and its peak at 12.4 ° 2θ disappears in IC03 and IC04 samples. Also, the dehydroxylation of the interlayer of chlorite occurs by the loss of half or more of the OH groups as H_2O resulting the "odified chlorite structure" [6]. For IC02, XRD pattern shows the increased intensity of peak at 6.4° 2θ and a general loss in intensity of higher order peaks (12.4° and 18.8° 2θ) at 600 °C. Finally, the chlorite peaks disappear at 950 °C. Illite peaks (8.9°, 17.8° and 18.9° 2θ) are reduced at 950 °C and they completely disappear at 1000 °C when a melting mass is obtained in the furnace. But, the spinel formation is detected at this temperature indicating that the upper temperature to make meta-clays is surpassed. The formation of hematite is detected at 600 °C and it increases at 950 °C developing the reddish color of these calcined clays.

3.3 Fratini Test

Figure 2 shows the results of Frattini test. Results indicate that all samples at the three firing temperatures do not present pozzolanic activity at 2 and 7 days. At 2 days, the [OH^-] and [CaO] of all blended cements are low compared with the PC cement and it can be due to adsorption/absorption phenomena. From 2 to 7 days, it can observed an increase of the [OH^-] (points displace to right) and it is attributed to alkalis released from the calcined clays. From 7 to 28 days, the [CaO] decreases in all blended cements, while the [OH^-] has a variable behavior with firing temperature. For clays fired at 300 and 600 °C, the [CaO] reduction occurs while [OH^-] remains approximately constant. For low temperature, three calcined clays (IC02, IC03 and IC04) have a point located bellow the isothermal curve (positive). IC02 and IC03 fired at 600 °C move its position on the isothermal curve (negative) while IC04 results remains under the curve (positive). The greatest drop of [CaO] occurs for four calcined clays fired at 950 °C and the [OH^-] has an increase for IC02, IC03

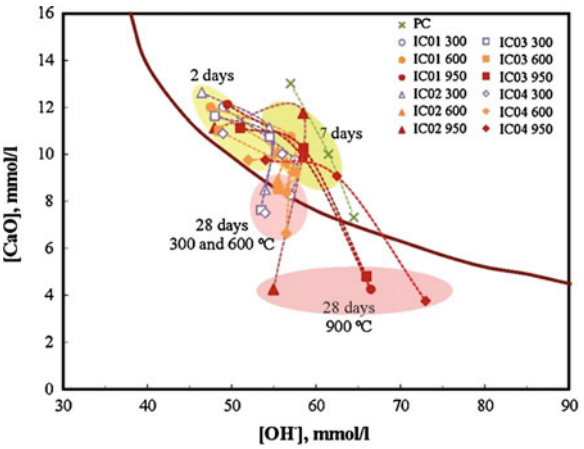

Fig. 2 Results of Frattini test for blended cements at 2, 7 and 28 days

and IC04, and no-significant variation for IC02 calcined clay. Four points are below the isothermal curve indicating a positive pozzolanic activity.

At 28 days, positive results obtained at low firing temperature can be attributed to ions interchange phenomenon between the calcined clays at 300 °C and solution, and to the reaction of meta-clays derived from dehydroxylation of secondary clay minerals present.

3.4 Strength Activity Index

Figure 3a shows the results of flow measured for standard mortar. All blended cements have a flow reduction when the added calcined clays were fired at 300 and 600 °C. This reduction was more significant (∼60 %) for IC04. When clay was fired at 950 °C, the flow of blended cements containing IC01 and IC02 is slightly

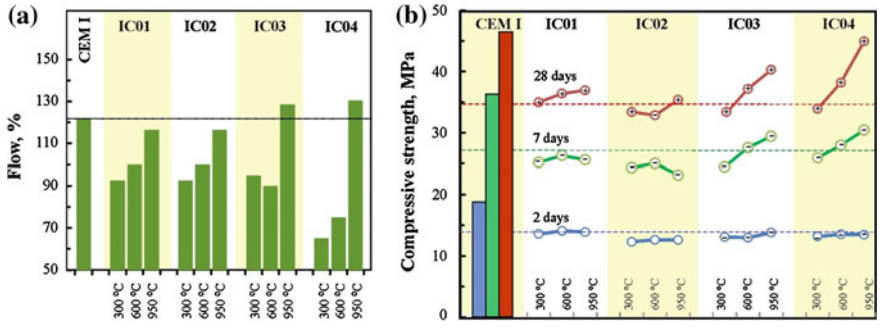

Fig. 3 **a** Flow of standard mortar and **b** Compressive strength of blended cements

lower (~6 %) compared with the PC-mortar flow and it is higher (~7 %) for blended cement with IC03 and IC04.

Figure 3b summarizes all results of compressive strength (CS). At the left, bars indicate the CS of PC at 2, 7 and 28 days, and the points indicate the CS for blended cements. The plus or minus sign into the bullet indicate the result of Frattini test. Dashed lines are the 75 % of CS of PC at 2, 7 and 28 days.

At 2 days, CS of blended cement is lower than the 75 % of that PC (SAI < 75 %). For 25 % by mass of replacement, the dilution effect cause an increase of the effective water-to-PC ratio (0.60) increasing the porosity of system that only can be compensated by the stimulation of PC hydration and the filler effect. As calcined clay is inactive, the results of the combination of these effects are the reduction of CS of blended cement instead of the different firing temperature.

At 7 days, the SAI of IC01 and IC02 was lower than 75 % for all fired temperature. These results are in accordance with the Frattini test. On the other hand, the SAI of IC03 and IC04 increases with the fired temperature and it is greater than 75 % for clays fired at 600 and 950 °C. But, the Frattini test indicates a negative pozzolanic activity for these samples. It can be attributed to the filler and stimulation effect caused by the calcined clays.

At 28 days, four calcined clays fired at 900 °C showed a SAI greater than 75 % in accordance with the positive results of Frattini test. For all calcined clays, the SAI at low fired temperature was lower. For IC01 and IC02, high fired temperature do not produces a significant change on the SAI (0.76 to 0.80 and 0.72 to 0.77), but it was very important for IC03 (0.71 to 0.84) and IC04 (0.74 to 0.97) when it increase from 300 to 950 °C. The SAI and Frattini-test results are in the same way for clays fired at 600 and 950 °C, but there is a disagreement for clays treated at 300 °C.

4 Conclusions

- Common clays containing illite as main clay mineral in its composition are suitable as raw material to prepare calcined clay pozzolan when they are fired at 950 °C causing the collapse of illite structure and preventing the formation of stable phases such as spinel.
- The presence of secondary clay minerals such as kaolin, chlorite and montmorillonite don't change significantly the pozzolanic behavior of illitic calcined clays. Low firing temperatures cause its dehydroxylation and the Frattini test results could be positive.
- The best performance according to SAI was attained for IC04-claystone containing the large proportions of clayed minerals

Acknowledgments The authors would like to thank Eng. Monica Trezza for their assistance in carrying out the FTIR analysis, the CIC for the student-fellowship for Roxana Lemma and the ANPCYT for providing funding for the work under the PICT 0160-12.

References

1. He, C., Osback, B., Makovicky, E.: Pozzolanic reactions of six principal clay minerals: activation, reactivity assessments and technological effects. Cem. Concr. Res. **25**(8), 1691–1702 (1995)
2. He, C., Osback, B., Makovicky, E.: Thermal stability and pozzolanic activity of calcined illite. App. Clay. Sci. **9**, 337–354 (1995)
3. Buchwald, M. Hohmann, K. Posern, E. Brendler: The suitability of thermally activated illite/smectite clay as raw material for geopolymer binders. App. Clay Sci. 46(2009), 300–304
4. Sabir, B.B., Wild, S., Bai, J.: Metakaolin and calcined clays as pozzolans for concrete: a review. Cem. Concr. Compos. **23**(6), 441–454 (2001)
5. Cingolani, C.A.: The Tandilia System of Argentina as a southern extension of the Río de la Plata craton: an overview. Int. J. Earth Sci. **100**(2–3), 221–242 (2011)
6. Wudi Zhan And Stephen Guggenheim: The dehydroxylation of chlorite and the formation of topotactic product phases. Clays and Clay Min. **43**(5), 622–629 (1995)

Low Carbon Cement: Durability Performance Assessment with Laboratory and Site Tests

Ernesto Díaz, Fernando Martirena, Adrian Alujas and Roberto Torrent

Abstract As part of the validation procedures for low carbon cement (LCC), with only 50 % clinker content, its durability performance will be established by exposing specimens and large scale elements to a natural marine environment in the N. coast of Cuba. Before subjecting the elements to the exposure site, it was decided to assess their potential durability by the non-destructive measurement of the coefficient of air-permeability kT (Swiss Standard SIA 262/1:2013) and cover depth. Preliminary trials were run on cast specimens and directly on precast elements industrially produced with mixes of equivalent strength, prepared with the LCC and a conventional OPC. Further, kT measurements were made after the elements have been at the exposure site for almost one year. The kT results are encouraging in terms of the potential durability of LCC concretes and confirm the importance of the quality of the execution on the performance of full scale elements as well as the need of in situ measurements.

1 Introduction

Cuba is facing the challenge of sustaining its construction development without increasing the demand of imported fuel needed for the concomitant production of cement. Thus, reducing the clinker factor (CF) in cement composition has been the

E. Díaz (✉)
Centro Técnico Para El Desarrollo de Materiales de Construcción, Havana, Cuba
e-mail: ernesto@ctdmc.co.cu

F. Martirena
CIDEM, Universidad Central de Las Villas, Santa Clara, Cuba

A. Alujas
CEQA, Universidad Central de Las Villas, Santa Clara, Cuba

R. Torrent
Materials Advanced Services Ltd, Buenos Aires, Argentina

K. Scrivener and A. Favier (eds.), *Calcined Clays for Sustainable Concrete*,
RILEM Bookseries 10, DOI 10.1007/978-94-017-9939-3_34

objective of continued research efforts. Since 2005 a collaborative effort between the Ecole Polytechnique Federal de Lausanne, EPFL in Switzerland and the Universidad Central de las Villas, in Cuba has ended up in a new cementitious system based on the synergy between calcined clays and limestone, which enables clinker substitution higher than 50 % [1].

The new cement, named LC3, consists of a combination of clinker with a 2:1 blend of low grade calcined clay and limestone. The cement can outperform Portland cement even at early ages, and it has proven to have a high resistant in aggressive conditions like chloride rich environments [2]. The Cuban cement industry undertook a full scale industrial trial for the manufacture of the new cement in 2013, and 300 tons of LC3 were produced and used in various applications [3].

To prove its real sustainability value it is necessary to compare the performance of concretes made with LC3 against equivalent concretes made with a reference Portland cement, in Cuba named P-35, with special focus on their durability performance.

With this purpose, massive concrete specimens were produced and placed at an exposure site built on the northern coast of Cuba (Fig. 1), where the elements are exposed to natural marine environment. The concrete elements were produced with mixes of equivalent strength, prepared with the LC3 and P-35 cements.

Before subjecting the elements to the exposure environment their potential durability will be assessed by means of the following NDTs: coefficient of air-permeability kT [4] and cover depth. Preliminary trials were run on cast specimens and directly on precast elements industrially produced prior to being placed at the exposure site and after a year of exposure. The tests were complemented with measurement of chloride migration and carbonation. This paper discusses the preliminary results obtained in the experimental program.

Fig. 1 Exposure site at the northern coast of Cuba

2 Description of the Preliminary Tests

Several types of precast elements, produced at two different precast plants were tested, as described in Table 1. The endings LC3 and OPC indicate that cements LC3 or P-35 were used, respectively, to prepare the concretes. The aggregates and water reducer used are those commonly in use at the precast plants. The reported compressive strength was measured on cylinders cast with the same mix and cured 28 days in water. The construction of the elements followed the conventional process applied in the precast plants.

The potential durability of concrete samples and precast elements was assessed by measuring (non-destructively) the coefficient of air-permeability kT with the *PermeaTORR* instrument. This test method, standardized in Switzerland [5], is based on creating vacuum with a pump in a measuring cell surrounded by a guard-ring that adhere to the surface (Fig. 2). Once the evacuation process in the cell is shut-off, its pressure gradually increases due to the air flowing from the concrete pores into the measuring cell. The flow is controlled by keeping at all times the pressure of the measuring cell and the guard-ring equal. The coefficient of air-permeability kT (10^{-16} m^2) is calculated as function of the increase in pressure recorded in the measuring chamber. The test duration ranges between 2 and 6 min. Limiting values of kT are defined (262/1:2913 2013) for structures exposed to carbonation- and chloride-induced corrosion.

The test was applied in the laboratory on 150 mm cubes cast with the concrete used for the construction of some of the precast elements, following the procedure indicated in [6]. Further, the test was applied to elements situated at the exposure site. To complement the tests, 50 × 200 mm cores were taken from the elements measured. Carbonation depth was measured in the outer part of the core aided by the phenolphthalein test. The remaining part was cut in two pieces and tested for compressive strength.

Table 1 Main characteristics of the precast elements cast and tested

						Strength Mpa			
Identif.	Strength design (Mpa)	Cement	w/c	Slump	Date manuf.	3d	7d	28d	Comments
M381	25	360	0.47	8	02/11/2013	–	21.00	31.40	Culvert 1 × 1 × 2-LCC, Element A (bridges)-LCC, LM 32-5 slab GP- LCC, **Foundation C-1-LCC**
M25	25	360	0.47	12	06/02/2014	–	18.50	30.77	Foundation with LC3
M30	20	330	0.47	11	08/02/2014	–	19.00	24.40	Foundation with LC3
M32	25	300	0.40	8	10/02/2014	17.40	–	27.90	Foundation with P35
M35	20	270	0.59	9	11/02/2014	15.10	–	26.80	Foundation with P35

Fig. 2 Measuring kT on one culvert (l.) and on one Block C1 (r.)

The air permeability test was applied in the field on the precast elements indicated in Table 2, following the standard procedure. Typically 6 tests were conducted on each element at an age between 3 to 4 months. As specified in (Swiss Standard SIA 262/1:2013), it was checked that the surface moisture did not exceed 5.5 %, measured with the CMExpert II electrical impedance-based instrument.

3 Test Results and Analysis

The results of air-permeability kT obtained on the precast elements are presented at Tables 2 and 3 compares values between real elements before setting them at the exposure site, the cylinders taken as samples and the measurements done at elements placed at the exposure site.

Table 2 Results of tests for air permeability performed at different times

Elements tested						2014-06-elements	2014-06-cylinders	2015-02 cores	
Description	ID sample	manuf date	3d	7d	28d	kT	kT	kT ms 1	kT ms 2
C-1-LCC	M381	25/10/2013	–	21.0	31.4	0.13	0.023	0.0011	0.001
C-1-LCC	M381	02/11/2013	–	21.3	31.4	0.16	0.023		
PC-3 panel LCC	M381	08/11/2013	_	21.0	31.4		0.023		
C1-D4-LCC	M25-LCC	06/02/2014	_	18.5	30.8		0.1	0.001	0.031
C1-D3-LCC	M30-LCC	08/02/2014	_	19.0	24.4		0.25	0.19	0.052
C1-D9-P35	M35-P35	11/02/2014	15.1	_	26.8		0.18		
C1-D11-P35	M32-P35	10/02/2014	17.4	–	27.9		0.34	0.0036	0.035

Table 3 Comparison of kT values versus compressive strength

	Str core/28d (%)	kT core/elem	kT elem/cyl (%)
M381-LC3	116	1 %	4.78
M25-LC3	89	NA	1.00
M30-LC3	61	NA	76.00
M32-P35	62	NA	1.06

The symbol indicates the geometric mean kT_{gm} of the individual measured values. For the cores, kT measurements were made exactly in the same element where they were taken. The size of the cores did not allow to perform air permeability measurements in them.

It can be seen that all the tested precast elements made with the LCC cement, show a lower permeability than the companions made with the OPC. This trend remains regardless the age of the cement and its content per m3. This could indicate a denser pore structure which lowers porosity of the elements; this has been reported in the literature for cementitious systems like the one proposed [2].

Further, some differences can be observed between kT measurements made in real elements at different ages and conditions with measurements carried out in cylinders, thus indicating that manufacturing conditions are worse than those where the cylinders were preserved. This latest is very important for the engineering part of it, for lab values made on the basis of testing cylinders can be misleading.

Preliminary carbonation tests carried out in 50 mm cores made with both LC3 and P35 did not show yet any sign of carbonation when phenolphthalein was applied, as presented in Fig. 3. This is yet too early to expect some degree of carbonation. The impermeable pore structure, as measured by air permeability, especially in the outer surface of the elements may have helped to achieve this result.

Fig. 3 Preliminary results of carbonation depth with phenolphthalein test

4 Conclusions

The results, that are just preliminary due to the limited amount of data collected so far, highlight the following facts:

- The air permeability kT of LCC concretes is considerably lower (1.3 to 6.3 times less) than that of the OPC concretes.
- The value of kT of the industrial elements is significantly higher (about 8 times) than that of the companion cast specimens.
- The values of kT measured in elements after some time of exposure are consistent with the ones measured before.
- Preliminary carbonation tests at elements show that carbonation has not started yet at one year.

The results of these tests are encouraging in terms of the potential durability of LCC concretes and confirm the importance of the quality of the execution on the performance of full scale elements as well as the need to measure it on site for a realistic durability appraisal.

References

1. Martirena, F., Scrivener, K.: Ecomaterials in low-cost housing. connecting cutting-edge science with the grassroots. In: Bolay, G. J.-C., Schmid, M., Tejada, E.H. (eds.) Technologies and Innovation for Development, pp. 101–111. Springer, Lausanne (2012)
2. Antoni, M., et al.: Cement substitution by a combination of metakaolin and limestone. Cem. Concr. Res. **42**(12), 1579–1589 (2012). Available at: http://linkinghub.elsevier.com/retrieve/pii/S0008884612002074. Accessed 18 Sept 2014
3. Vizcaíno-Andrés, L.M., Sánchez-Berriel, S., Damas-Carrera, S., Pérez-Hernández, A., Scrivener, K.L., Martirena-Hernández, J.F.: Industrial trial to produce a low clinker, low carbon cement. Materiales de Construcción **65**(317) (2015)
4. 262/1:2913, S.: Bauwesen Betonbau—Ergänzende Festlegungen (2013)
5. Jacobs, F., et al.: Specification and site control of the permeability of the cover concrete: the swiss approach dedicated to professor Dr. Bernhard Elsener on the occasion of his 60th birthday. Mater. Corros. **63**(12), 1127–1133 (2012)
6. Services, M.M.A.: Measures the Air meability of the Cover Concrete and other Porous Materials (2014)

Influence of the Manufacturing Process on the Performance of Low Clinker, Calcined Clay-Limestone Portland Cement

A. Perez, A. Favier, F. Martirena and K. Scrivener

Abstract This paper discusses influence of manufacture parameters of a new type of cement (low carbon cement, LC3) which can substitute up to 50 % of clinker by calcined clay and limestone. Limestone powder accelerates the early hydration and calcined clays and contributes to strength development at later ages due to its pozzolanic reaction. Further, it facilitates improving rheology of the fresh mix without compromising strength, possibly due to the synergetic interaction between calcined clays and limestone. Workability of this new system is strongly affected by the Particle Size Distribution (PSD) and PSD is affected by the grinding process, therefore, due to the different hardness and grindability between the materials forming this cement, new production parameters must be defined. This study compares the results obtain by separate grinding and intergrinding, especially the impact at rheology and early strength. The influence of clinker and limestone on both properties has been assessed, aided by microstructural studies using different techniques (XRD, TGA, IC, etc.) to determine the best fineness combination and analyze the effect of PSD of the new system in cement properties. Intergrinding seems to give reasonable good results in terms of rheology and early strength.

1 Introduction

The properties and performance of blended cements are affected by the proportions and the reactivity of the mineral additions but also to a large extend by the particle size distribution (PSD). The different components of the blended cement each need

A. Perez (✉)
CIDC, Havana, Cuba
e-mail: iogiove1@gmail.com

A. Favier · K. Scrivener
LMC, EPFL, Lausanne, Switzerland

F. Martirena
CIDEM, UCLV, Santa Clara, Las Villas, Cuba

K. Scrivener and A. Favier (eds.), *Calcined Clays for Sustainable Concrete*,
RILEM Bookseries 10, DOI 10.1007/978-94-017-9939-3_35

to obtain certain fineness in order to be hydraulically, latent hydraulically or pozzolanically effective [1]. The PSD of blended cements also plays an important role in optimizing the water demand and the workability of concrete. If particle diameters tend to be similar there is a larger volume between particles that needs to be filled with water in order to get a movable paste. On the other hand, if there is a good proportion of a fine and coarse particle the spaces between particles are lower and water requirement is lower.

Achieving a good PSD when clinker and mineral additions are ground together implies optimizing packing in order to minimize void space between the cement particles. Consequently the workability is improved for a given w/c ratio and alternatively the water demand required to produce a desired slump is reduced [2].

Isothermal calorimetry can be a good test to assess influence of PC fineness. Clinker fineness seems to be the most important parameter regarding the heat of hydration during the first 24 h [3]. Limestone PSD has also an effect in the development of strength, the finer the limestone, the greater is the effect. This has been attributed to its filler effect: the surface of the limestone particles serves as a nucleation and precipitation surface of the hydration products and the effective water to PC ratio increases when the water to binder ratio is kept constant [4]. Comparisons between inert filler with similar PSD than limestone prove that it not have the same beneficial impact on strength as limestone [3].

Blended cements can be ground in two ways: by intergrinding or by separate grinding. In the intergrinding process all components are ground together. In that way the cement is homogenized during the grinding, and only one silo is needed for storing. Because of interactions between the different cement components due to differences in grindability, the PSD of the blended cement and the different components is difficult to control [1, 5].

The second technology consists of separate grinding the components and mixing according to the desired proportions. PSD of each component and of the blended cement can be controlled and an appropriate grinding procedure can be used for each component according to its grindability. This could complicate grinding at industrial scale since more silos shall be needed and special grinders as well [6].

This paper discusses the impact of PSD of all the components on the rheology and early strength of the ternary blend, calcined clay-limestone cement (LC3). All the materials were ground separately and sieved in three different fractions (fine, medium, and coarse) to be able to design a specific PSD in order to evaluate it effect on the performance of the obtained cements.

2 Materials and Methods

The materials used for the cement blends were, Cuban Clinker (Cienfuegos), Cuban Calcined Clay (Pontezuela), Cuban Limestone, and Cuban Gypsum. Clinker was produced in the Cienfuegos Cement factory in Cuba, gypsum from the one

currently on industrial used in the manufacture of Portland cement and limestone from Cuban locations. Pontezuela calcined clay was produced by dehydroxylation of Pontezuela clay in a cement rotary kiln [7].

The chemical and mineralogical composition of all materials was characterized by X-ray Fluorescence. The calcium sulfate source used contained 97 % of $CaSO_4 \cdot 2H_2O$ and of quartz, feldspar and carbonates; the limestone used was 92 % of $CaCO_3$. The limestone used was 99 % of $CaCO_3$.

For separate grounded blends each raw material was grinded in a Bond mill and separated by sieving (except gypsum) in three different fractions and (less than 40 μm, between 40 and 63 μm and more than 63 μm) in order to be able to produce a well-known PSD materials. Three different PSD was designed and prepared for each material changing the amount of each fraction (finer, medium and coarse). The percentage of each fraction in the designed PSD are showed in Table 1.

Table 2 shows the composition of the nine different LC3 blends produced changing the designed PSD of clinker and limestone (the calcined clay PSD was the medium for all the blends) and a reference cement with clinker in the medium range of fineness.

For interground blends raw material was ground together in a Bond mill. Three different blends was prepared at three different grinding times (25, 45 and 65 min) PSD of all the fractions was determined by laser diffraction in order to determine the PSD of all the blends. Clinker was dispersed in isopropanol while calcined clay and limestone were dispersed in a 0.01 % PAA solution. For the intergrinding blends the PSD was measured by sieving in three fractions, less than 40 μm, between 40 and 63 μm and up to 60 μm.

Mortars prisms 4 × 4 × 16 mm were cast at 0.5 water/cement ratio according to the standard mortar procedure. Superplasticizer dosage was fixed in 1 % using a sulfonated poly naphthalene admixture. Compressive strength of all the mortars was tested at 3, 7 and 28 days. Rheology of mortars was tested before the casting by minislump test using a minicone with 10.5 cm of bottom diameter, 5.5 cm of upper

Table 1 Percentage of each fraction

Name	% 0–40 μm	% 40–63 μm	% 63–100 μm
Fine (F)	60	23	17
Medium (M)	40	23	37
Coarse (C)	17	23	60

Table 2 Blends composition

	1	2	3	4	5	6	7	8	9	10
Clinker	F	M	C	F	M	C	F	M	C	M
Calcined clay	M	M	M	M	M	M	M	M	M	
Limestone	F	F	F	M	M	M	C	C	C	

diameter and 15.5 cm high. The slump diameter was measured as rheological parameter [8]. The impact of each component on hydration was assessed aided by isothermal calorimetry. Pastes of significant blends were prepared and tested in a calorimeter at 20 °C. For the first study blends with different clinker fineness and the same limestone fineness (1, 2, and 3) were tested in order to access the influence of clinker fineness. In the second study the clinker fineness was kept constant while the limestone fineness was changed (series 2, 5 and 8).

3 Discussion

Results of minislump tests—considered in this paper to assess rheology—are presented in Fig. 3. The most influencing factor on rheology is clinker fineness, as expected. The finer the clinker, the blend is more workable. This could be caused by the higher specific surface area, which provides more area to interact with superplasticizer, and thus a higher deflocculation takes place. Limestone fineness also has an important impact on rheology; the best values are obtained in blends with medium limestone for finer and medium clinker. This could reflect the packing effect caused by the differences in PSD of each element. For the coarser blends, seem to be that because the poor packing and the low effect of the admixture produce a poor workability and the results are no conclusive (Figs. 1 and 2).

There are interesting results for interground blends, especially for the series ground 45 min, which attains a very good workability compared to the separate ground blend. The influence of limestone could be the reason behind this encouraging result, which could envision the possibility of using current grinding facilities at cement plants for the manufacture of multi-component cement blends. This study must however be concluded and expanded with more different materials.

Compressive strength of all series—separate ground and interground—is presented in Fig. 4. Early age strength is also heavily influence by the presence of limestone. 3 days compressive strength increases with increasing limestone fineness. The heat evolution curves shows that changing the fineness of limestone powder had little effect on the calorimetric curve but the reaction time not change. After 7 and 28 days only the finer limestone seems to have an effect in the strength.

Clinker fineness has definitely the highest impact on early strength. Increasing the clinker fineness increases the compressive strength for all the combinations at all ages. Clinker fineness appears to be the most important parameter regarding the heat of hydration during the first 24 h. The finer the clinker, the faster is the hydration, the higher is the maximum peak.

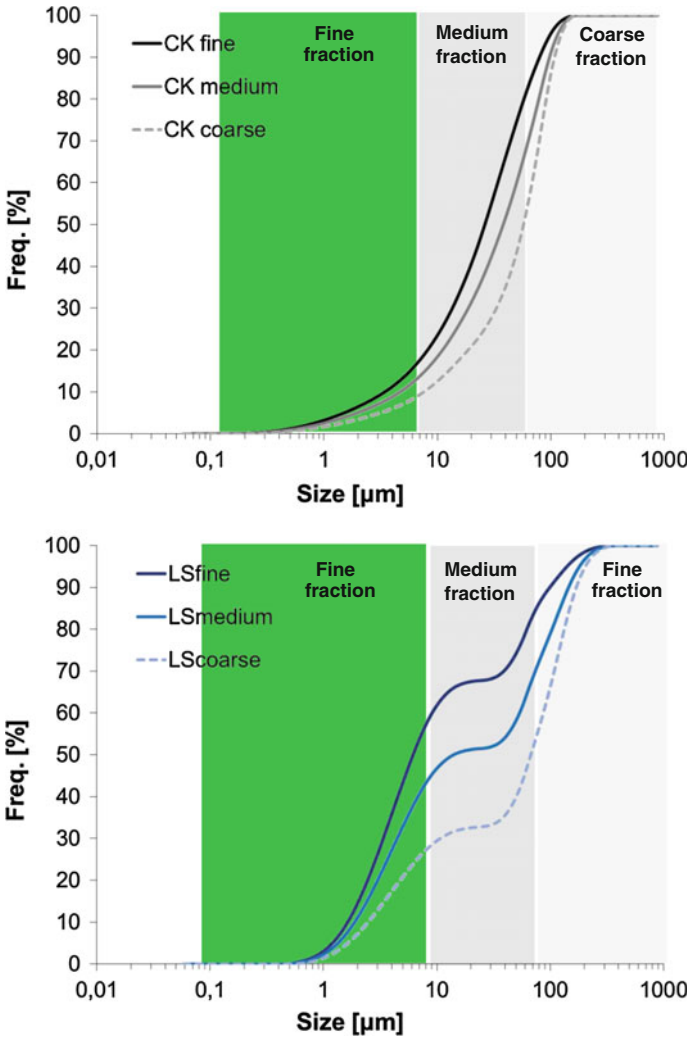

Fig. 1 Percentage of each material fraction, in order, clinker, limestone and calcined clay

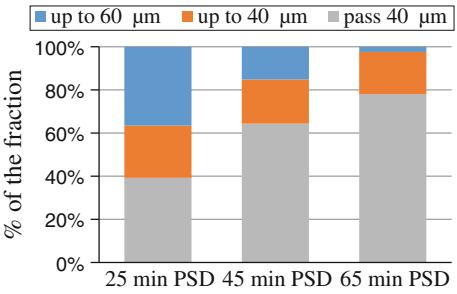

Fig. 2 Percentage of each fraction in the three intergrounded blends

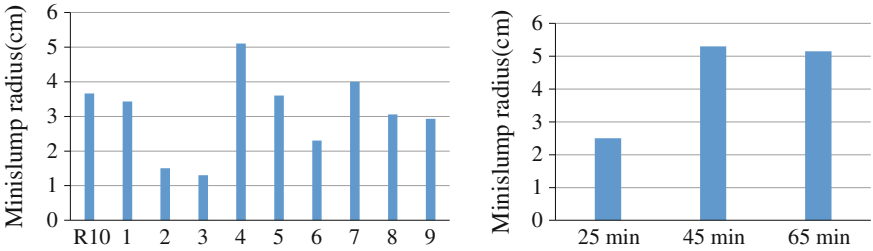

Fig. 3 Minislump radius for separate grinded blends and intergrinded blends

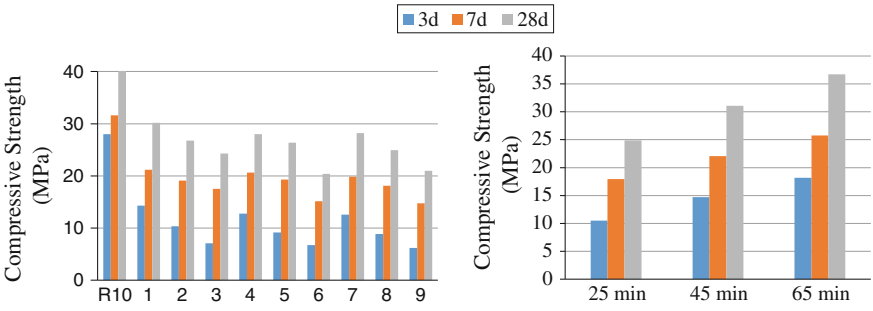

Fig. 4 Compressive strength at 3, 7 and 28 days for separate grinding and intergrinding blends

4 Conclusions

This preliminary study of the influence of grinding parameters on the manufacture of multi-component cements concludes that clinker fineness has the greatest importance in terms of rheology and early strength. Limestone can contribute to improve rheology for blends with very fine clinker, and if finely ground could also contribute to improve packing, which could reflect on better properties of the concrete matrix.

Intergrinding al components in the same chamber in a ball mill yields interesting results despite the high fineness of the resulting sample, even compared to those of separate grinding. This could be encouraging for cement manufacturers, which could mean that current grinding facilities could be useful for the production of the new cement.

References

1. Tsivilis, S., Tsimas, S., Moutsatsou, A.: Contribution to the problems arising grinding multicomponent cements. Cem. Concr. Res. **22**, 95–102 (1992)
2. Celik, I.B., Oner, M., Can, N.M.: The influence of grinding technique on the liberation of clinker minerals and cement properties. Cem. Concr. Res. **37**, 1334–1340 (2007)
3. De Weerdt, K., Sellevold, E.J., Kjellsen, K.O., Justnes, H.: Fly ash-limestone ternary cements: effect of component fineness. Adv. Cement Res. **23**(4), 203–214 (2011)
4. Vizcaíno-Andrés, L.M., Sánchez-Berriel, S., Damas-Carrera, S., Pérez-Hernández, A., Scrivener, K.L., Martirena-Hernández, J.F.: Industrial trial to produce a low clinker, low carbon cement. Materiales de Construcción, **65**(317) (2015)
5. Vizcaíno-Andrés, L.M., Mathieu, G., Martirena Hernández, J.F., Scrivener, K.L.: Effect of fineness in clinker-calcined clays-limestone cements. Adv. Cement Res. (2015) (submitted)
6. Justnes, H., De Weerdt, K.: Sintef Report, p. 30 (2007)
7. Alujas, A., Fernández, R., Quintana, R., Scrivener, K.L., Martirena, F.: Pozzolanic reactivity of low grade kaolinitic clays: influence of calcination temperature and impact of calcination products in OPC hydration. Appl. Clay Sci. **108**, 94–101 (2015)
8. Roussel, N.: Correlation between yield stress and slump: comparison between numerical simulations and concrete rheometers results. Mater. Struct. **39**, 501–509 (2006)

Development of Room Temperature Curing Geopolymer from Calcined Water-Treatment-Sludge and Rice Husk Ash

Anurat Poowancum, Ekkasit Nimwinya and Suksun Horpibulsuk

Abstract Geopolymer is an environmental friendly material, and is expected to use as the cement replacement materials. Because, the geopolymer production does not emit carbon dioxide gas, and is a low energy consuming process. Moreover, geopolymer can be synthesized from variety kinds of waste materials. The present work, the room temperature curing geopolymer has been developed by using the calcined water-treatment-sludge (WTS) and the rice husk ash (RHA) as the precursors. Mixture of sodium hydroxide solution and sodium silicate solution was used as an alkali activator solution. The results show that the RHA promotes strength of the WTS-geopolymer. By adding RHA 30 wt%, strength of geopolymer is close to the minimum required strength of the ordinary Portland cement (OPC). In addition, density of WTS-RHA geopolymer is 3 times lower than that of the OPC. Knowledge in the present work opens an opportunity to apply geopolymer for using in variety kinds of engineering applications, especially the lightweight construction materials.

1 Introduction

The ordinary Portland cement (OPC) is widely used for constructing work in civilization of human society. However, OPC is an environmental unfriendly material. Because, the producing process of OPC requires high energy consumption

A. Poowancum (✉)
School of Ceramic Engineering, Faculty of Engineering,
Suranaree University of Technology, Nakhon Ratchasima, Thailand
e-mail: anurat@sut.ac.th

E. Nimwinya
School of Agricultural Engineering, Faculty of Engineering,
Suranaree University of Technology, Nakhon Ratchasima, Thailand

S. Horpibulsuk
School of Civil Engineering, Faculty of Engineering, Suranaree University of Technology,
Nakhon Ratchasima, Thailand

K. Scrivener and A. Favier (eds.), *Calcined Clays for Sustainable Concrete*,
RILEM Bookseries 10, DOI 10.1007/978-94-017-9939-3_36

and emit high quantities of carbon dioxide gas [1]. The latter is cause of the global warming problem, and is the important reason that induces numerous researchers study on the geopolymer for using as the cement replacement materials [2].

Geopolymer is an inorganic polymer technology [3], and is synthesized by the aluminosilicate compound materials with alkali hydroxide and/or alkali silicate [4]. Nowadays, geopolymer has been the subject of intense study, because it is an environmental friendly material, does not emit carbon dioxide gas, low energy consumption, low toxicity, and stable at high temperature [5]. Moreover, geopolymer can be synthesized from variety kinds of waste materials.

Water treatment sludge (WTS) is a waste from the water treatment process in production of tap water and drinking water, is extracted from raw water by coagulation technique [6]. WTS is a problem of big city around the world [7]. Environmentalist proposes the effective way to solve the problem of WTS is reused or processed it to be the usable products [8]. The important chemical compositions of WTS are Al_2O_3 and SiO_2 [9], which are the essential components of the geopolymer structure. However, geopolymer is synthesized from WTS has low strength [10]. Khater et al. [11] reported that the strength development of geopolymer matrix depended on types of precursor and the SiO_2/Al_2O_3 ratio [11]. The strength of WTS-geopolymer can be improved by the modification of the SiO_2/Al_2O_3 ratio. Rice husk ash (RHA) is the waste from the biomass power generation and the rice drying process. It is a source of reactive silica, which is abundant in the rice producing countries, including Thailand. By using abundance wastes, i.e., WTS and RHS as the precursor, the sustainable materials for replacement cement can be obtained.

The aim of this work is to develop the room temperature curing geopolymer by using the calcined WTS and RHA as a sustainable precursor. Effect of WTS/RHA ratios on density, setting time, and compressive strength are examined.

2 Experimental Procedure

WTS was obtained from Bangkhen water treatment plant at Bangkok metropolis, Thailand. To remove impurities, WTS was washed by mixed with water at a WTS/water ratio of about 1.2 by mass, then passed through sieve number 325 mesh, and dried at 100 °C for 24 h. The dried WTS was milled by electric mortar and passed through sieve number 325 mesh, after that was calcined at 600 °C for 2 h to obtain the calcined WTS powder. RHA was obtained from Korat Yong-sa-nguan Company, Thailand. The RHA was wet milled by ball mill for 6 h, then dried at 100 °C for 24 h before being passed through sieve number 325 mesh. Sodium hydroxide (NaOH) pellets and distilled water were mixed to obtain a concentration of 10 M, then mixed with sodium silicate (Na_2SiO_3) solution to prepare alkali activator solution. Na_2SiO_3 consists of Na_2O = 8.0 %, SiO_2 = 27.0 % and H_2O = 65.0 %. The ratio of Na_2SiO_3 solution to NaOH solution was fixed at 1.5 by weight. The mixed solution was stored of 24 h prior to use. The calcined WTS

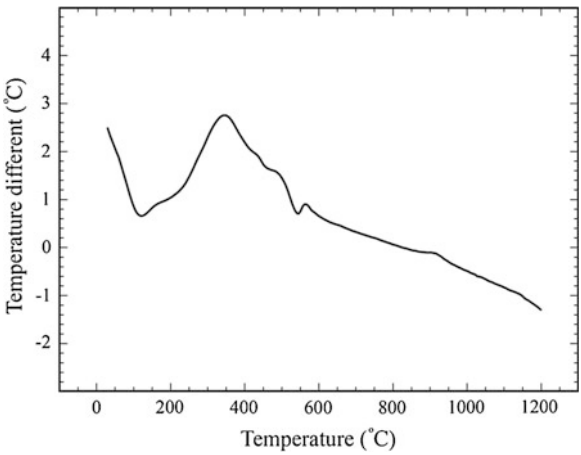

Fig. 1 The thermal behavior of WTS

powder and RHA powder were mixed at various WTS/RHA ratios of 100:0, 85:15, 70:30, 60:40 and 50:50 by weight. The mixed powder was then mixed with an alkali activator solution by a mortar at a solid to liquid ratio of 1.0. The geopolymer paste was poured into a 50 mm × 50 mm × 50 mm steel mold and compacted as described in ASTM C109 [12]. The molded samples were sealed with a film to prevent moisture evaporation during curing at room temperature (27–30 °C). Density and compressive strengths were measured after 7 days of curing. Chemical compositions of WTS and RHA was evaluated by X-ray fluorescence (XRF, HORIBA, XGT-5200). The thermal behavior of WTS was investigated by a differential thermal analysis (DTA, Perkin Elmer, DTA 7). The measurements were made with heating rate of 10 °C/min. The result of DTA in Fig. 1 presented that dehydroxylation occurred at approximately 550 °C. Therefore, WTS was calcined at 600 °C. Density of WTS and RHA was measured by a pycnometer following ASTM D854 [13]. Setting time of geopolymer pastes was examined according to ASTM C266 [14]. Density and compressive strength of the cured geopolymers were measured following to ASTM C138 [15] and ASTM C109 [12], respectively.

3 Results and Discussion

Chemical compositions of WTS and RHA are shown in Table 1. The main components of WTS is SiO_2 (58.99 wt%) and Al_2O_3 (24.64 wt%). RHA mainly consists of SiO_2 (89.17 wt%), Al_2O_3 does not be detected.

Initial and final setting times of geopolymer pastes are the parameters controlling the workability of the concrete geopolymer. Setting time of WTS-RHA geopolymer is increased with increasing of the RHA contents, as shown in Fig. 2. The initial setting time is 2.5 h for the WTS-geopolymer paste while it is 13.5 h for RHA replacement ratio of 50 wt%. It is clearly note that the initial setting time increases

Table 1 Chemical compositions and density of WTS and RHA

Raw materials	Chemical compositions (wt%)									Density (g/cm^3)
	Al_2O_3	SiO_2	K_2O	Na_2O	CaO	MgO	Fe_2O_3	TiO_2	Etc.	
WTS	24.64	58.99	1.54	4.08	0.69	1.14	6.63	0.88	1.41	2.61
RHA	0	89.17	1.12	7.29	0.61	1.22	0.41	0.03	0.15	2.15

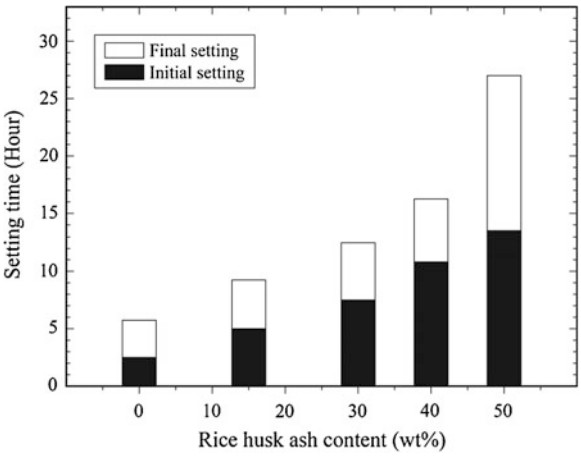

Fig. 2 Initial and final setting times of geopolymer after curing for 7 days

as the increasing in silica content. To understand the role of RHA on the setting time of WTS-RHA geopolymer, it is preferable to express in term of SiO_2/Al_2O_3 ratio as it has been proved as a prime factor [10]. Table 2 presents SiO_2/Al_2O_3 ratios for various RHA/WTS ratios, which was calculated from the chemical compositions in RHA and WTS (Table 1) as well as in Na_2SiO_3. The hardening of geopolymer is a result from the condensation of aluminate and silicate species during geopolymerization process [16]. The condensation rate between silicate and aluminate species is faster than that between silicate and silicate species [16]. As such, the increase of SiO_2/Al_2O_3 ratio caused by increasing of RHA content leads to the delay of setting time, which is in agreement with the previous studies [16].

Figure 3 shows the relationship between strength and RHA replacement. The strength of geopolymer paste is increased with increasing of RHA replacement up

Table 2 Calculation of SiO_2/Al_2O_3 ration in different replacement of RHA

Compositions (wt%)		SiO_2/Al_2O_3 ratio
RHA	WTS	
0	100	3.1
15	85	3.8
30	70	4.9
40	60	5.9
50	50	7.3

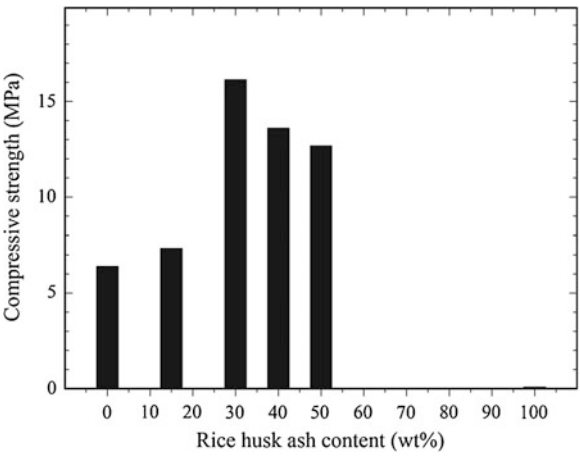

Fig. 3 Compressive strength of 7 days cured geopolymer

to 30 wt% which is regarded as the critical replacement. At the critical replacement of RHA, the maximum strength of geopolymer paste is 16 MPa, which is slightly lower than that of the minimum requirement of OPC (19 MPa) [17].

Beyond the critical replacement, the strength decreases and tends toward zero at 100 wt% RHA replacement. This indicates that only the silica rich material (no presence of Al_2O_3) is not suitable used as a geopolymer precursor. Silica and alumina ratio plays a significant role on the strength development of geopolymer paste. The maximum strength of WTS-RHA geopolymer found at the SiO_2/Al_2O_3 ratio of 4.9 (30 wt% RHA replacement). However, Silva et al. [16] showed that the optimum SiO_2/Al_2O_3 ratio was found at approximately 3.0-3.8. The difference in the optimum SiO_2/Al_2O_3 ratio is possibly due to different types of the precursor.

Density after 7 days of the cured geopolymer is remarkable lower than that of the OPC, as shown in Fig. 4. Density of the OPC is approximately 3.15 g/cm^3 [18],

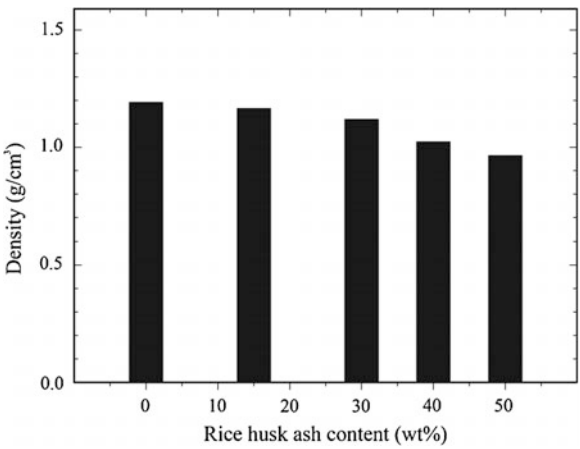

Fig. 4 Density of geopolymer after curing for 7 days

while density of geopolymer in the present work is in between 0.96 to 1.19 g/cm^3. The density tends to decreases with increasing RHA replacement due to the specific gravity of RHA is lower than that of WTS, as shown in Table 1. Compared to density of the OPC, the density of geopolymer paste is 3 times lower than that of OPC. The lower density is an advantage of the geopolymer binder over the OPC, which can be used for lightweight non-bearing and bearing structures.

4 Conclusions

In this work, the room temperature curing geopolymer has been developed. Geopolymers were synthesized by using the calcined water-treatment-sludge (WTS) as well as the rice-husk-ash (RHA) as the precursors, and the mixture of sodium hydroxide solution and sodium silicate solution as an alkali activator solution. The RHA promotes strength of WTS-geopolymer. By adding RHA 30 wt %, strength of geopolymer is significantly increased, and is close to the minimum requirement of the ordinary Portland cement (OPC). Setting times and strength of WTS-RHA geopolymer are strongly controlled by SiO_2/Al_2O_3 ratio. The higher SiO_2/Al_2O_3 ratio results in delay of setting times, because the condensation rate between silicate and aluminate species is faster than that between silicate and silicate species. The highest strength is obtained at the SiO_2/Al_2O_3 ratio of 4.9. The density of WTS-RHA geopolymer is 3 times lower than that of the OPC, which is useful as a binder to develop the lightweight structures.

Acknowledgments This research was supported by the Suranaree University of Technology and the Office of Higher Education Commission under NRU project of Thailand. The third author acknowledges the Thailand Research Fund under the TRF Senior Research Scholar program Grant No. RTA5680002.

References

1. Gartner, E.: Industrially interesting approaches to low-CO_2 cements. Cem. Concr. Res. **34**(9), 1489–1498 (2004)
2. Chindaprasirt, P., Chalee, W.: Effect of sodium hydroxide concentration on chloride penetration and steel corrosion of fly ash-based geopolymer concrete under marine site. Constr. Build. Mater. **63**, 303–310 (2014)
3. Lemougna, P.N., Chinje Melo, U.F., Delplancke, M.P., Rahier, H.: Influence of the activating solution composition on the stability and thermo-mechanical properties of inorganic polymers (geopolymers) from volcanic ash. Constr. Build. Mat. **48**:278–86 (2013)
4. Zhang, L.: Production of bricks from waste materials—a review. Constr. Build. Mater. **47**, 643–655 (2013)
5. Pacheco-Torgal, F., Abdollahnejad, Z., Miraldo, S., Baklouti, S., Ding, Y.: An overview on the potential of geopolymers for concrete infrastructure rehabilitation. Constr. Build. Mater. **36**, 1053–1058 (2012)

6. Keeley, J., Jarvis, P., Judd, S.J.: An economic assessment of coagulant recovery from waste treatment residuals. Desalination **287**, 132–137 (2012)
7. Husillos Rodriguez, N., Martinez Ramirez, S., Blanco Varela, M.T., Guillem, M., Puig, J., Larrotcha, E., Flores, J.: Re-use of drinking water treatment plant (DWTP) sludge: characterization and technological behaviour of cement mortars with atomized sludge additions. Cement concr. Res. **40,** 778–786 (2010)
8. Kyncl, M.: Opportunities for water treatment sludge re-use. Geoscience engineering **1**, 11–22 (2008)
9. Suksiripattanapong, C., Horpibulsuk, S., Chanprasert, P., Sukmak, P., Arulrajah, A.: Compressive strength development in geopolymer masonry units manufactured from water treatment sludge. Constr. Build. Mat. Submitted for publication (2014)
10. Naprarath, W., Suwimol, A., Kwannate, S.: Strength and microstructure of water treatment residue-based geopolymers containing heavy metals. Constr. Build. Mater. **50**, 486–491 (2014)
11. Khater, H.M., El-Sabbagh, B.A., Fanny, M., Ezzat, M., Lottfy, M.: Effect of nano-silica on alkali activated water cooled slag geopolymer. ARPN J. Eng. App. Sci. **2**(2), 170–176 (2012)
12. ASTM C109: Standard test method of compressive strength of hydraulic cement mortars (using 2-in. or [50 mm] cube specimens). Ann. Book ASTM Standard, vol. 04.01 (2002)
13. ASTM D854-14: Standard test methods for specific gravity of soil solids by water pycnometer. Ann. Book ASTM Standard, vol. 04.08 (2014)
14. ASTM C266: Standard test method for time of setting of hydraulic-cement paste by Gillmore needles. Ann. Book ASTM Standard, vol. 04.01 (2013)
15. ASTM C138: Standard test method for density (unit weight), yield, and air content (gravimetric) of concrete. Ann. Book ASTM Standard, vol. 04.02 (2011)
16. Silva, P.D., Sagoe-Crentsil, K.: The effect of Al_2O_3 and SiO_2 on setting and hardening of Na_2O-Al_2O_3-SiO_2-H_2O geopolymer systems. J. Aust. Ceram. Soc. **44**(1), 39–46 (2008)
17. ASTM C150/C150 M: Standard specification for Portland cement. Ann.l Book ASTM Standard, vol. 04.01 (2012)
18. ASTM C595/C595 M: Standard specification for blended hydraulic cements. Ann. Book ASTM Standard, vol. 04.02 (2013)

Characterising the Reaction of Metakaolin in an Alkaline Environment by XPS, and Time- and Spatially-Resolved FTIR Spectroscopy

John L. Provis, Syet Li Yong and Jannie S.J. van Deventer

Abstract The process of the dissolution of metakaolin in an alkaline environment remains incompletely understood; there are many mechanistic details which still require elucidation. Here, we apply X-ray photoelectron spectroscopy (XPS) and Fourier transform infrared spectroscopy (FTIR) to provide new information regarding the bonding environments in the altered layer on the surface of a metakaolin particle in contact with different alkali hydroxide solutions (Li, Na and K as alkali cations, and concentrations ranging from 1-8 mol/L). The use of photoacoustic infrared spectroscopy enables the collection of spectra as a function of depth into the particle, and these are compared with surface-sensitive attenuated total reflectance FTIR spectra. In parallel, chemical state plots derived from XPS spectra provide new insight into the evolution of bonding environments of the silicon and aluminium atoms comprising the altered layer on the metakaolin surface.

1 Introduction

Chemical reactions involving metakaolin (calcined kaolinite clay) interacting with an alkaline environment are central to the use of this material as a supplementary cementitious material in Portland cement blends [1], and as a precursor for alkali-activated aluminosilicate binders ('geopolymers') [2]. The process by which the

J.L. Provis (✉)
Department of Materials Science and Engineering, The University of Sheffield, Sir Robert Hadfield Building, Sheffield S1 3JD, UK
e-mail: j.provis@sheffield.ac.uk

S.L. Yong · J.S.J. van Deventer
Department of Chemical and Biomolecular Engineering, The University of Melbourne, Victoria 3010, Australia

J.S.J. van Deventer
Zeobond Pty Ltd, P.O. Box 23450, Docklands, VIC 8012, Australia

K. Scrivener and A. Favier (eds.), *Calcined Clays for Sustainable Concrete*, RILEM Bookseries 10, DOI 10.1007/978-94-017-9939-3_37

metakaolin particles lose their initial layered structure through dissolution reactions under alkaline conditions, releasing aluminate and silicate units, controls the development of cementitious binding phases which incorporate these aluminates and silicates, contributing strength and impermeability to the hardened material.

The structural details of the layering within metakaolin particles have been elucidated through combined computational and experimental approaches [3, 4], and the influence of this layering on the process of reaction of metakaolin to form a geopolymer binder has been simulated via a multi-scale density functional theory-coarse grained Monte Carlo methodology [5]. However, the direct experimental validation of this mechanism has to date proven elusive, although significant steps towards defining the nature of the initial gel phases have been taken recently [6, 7]. This paper contributes to the understanding of the initial stages of dissolution of metakaolin in alkaline environments, through the analysis of leached metakaolin samples by Fourier transform infrared (FTIR), Auger emission spectroscopy and X-ray photoelectron (XPS) spectroscopy.

2 Experimental Methodology

For each set of leaching experiments, 100 g of metakaolin was added to 800 mL of the specified alkali silicate or hydroxide solution. The solids were retained, washed with Milli-Q grade purified water then laboratory-grade ethanol, and stored in a dessicator for 24 h before XPS and FTIR analysis.

A Varian 7000 FT-Infrared Spectrometer equipped with a universal sampling accessory (utilised for variable specular reflectance) was used to collect infrared spectra. All spectra were obtained with a resolution of 2 cm^{-1}, and 128 scans per spectrum were taken. Depth profiling of the samples was achieved by acquiring a series of spectra at different infrared modulation frequencies via the use of a phase modulated step scan arrangement. Photoacoustic (PA) FTIR spectra were collected with a MTEC 100-PA detector attachment.

XPS and AES spectra were recorded using a VG310F instrument (Fisons Instruments) with non-monochromated Al Kα radiation. The instrument was operated in ultra-high vacuum (approximately 10^{-9} torr). The sample was mounted on a stainless steel holder using carbon tape, and spectra were corrected to C1 s at 285.0 eV.

3 Results and Discussion

3.1 Ftir

Figure 1 presents ATR-FTIR spectra of metakaolin leached with different concentrations of sodium hydroxide and sodium silicate in solutions. The metakaolin

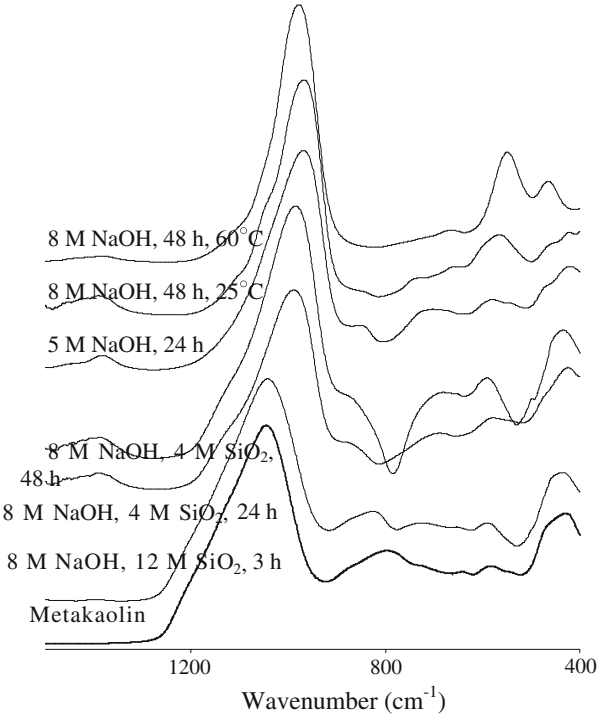

Fig. 1 FTIR spectra of metakaolin leached with different concentrations of alkali hydroxide and silicate solutions. All experiments conducted at 25 °C, except for the uppermost spectrum which relates to leaching at 60 °C

spectrum in Fig. 4.2 shows a broad peak at $\sim 1050\ cm^{-1}$ assigned to the stretching of tetrahedral Si-O-(Si,Al) bonds. The majority of the silicon sites are located within a discrete layer containing predominantly $Q^4(1Al)$ environments, so the predominant contribution to this peak is from the Si-O-Si bonds within the layer, in addition to the interlayer Si-O-Al bonds. For aluminosilicate materials, the participation of Al in the bonding network, as well as the generation of non-bridging oxygen sites, will reduce the wavenumber of this main Si-O-(Si,Al) peak [8]. The shift of this peak to lower wavenumber during the leaching of the metakaolin thus indicates a higher degree of participation of aluminium species in bonds involving silicates, and it is particularly interesting to note that this takes place even in the system with added SiO_2 in the leaching solution, although only after an initial 3 h period where this does not seem to be the case. This is indicating that the leaching process has progressed to the point, between 3 and 24 h of leaching, where the initially dissolved aluminate species are then being redeposited along with dissolved silicates onto the particle surfaces. This generates a layer of newly formed material which, although it may have a similar (or higher) bulk Si/Al ratio than the original metakaolin, contains a higher concentration of Si-O-Al bonds because it does not display the same layering in its structure.

When the metakaolin is leached in sodium hydroxide solutions, there is not the same scope for precipitation of silicate components from the solution environment,

and so the degree of reduction in the wavenumber of the main Si-O-(Si,Al) peak is greater. However, leaching in 8 M NaOH for 48 h at 60 °C actually shows less reduction in wavenumber than when the same conditions are applied at 25 °C. This indicates that there is also a contribution from the non-bridging oxygen sites to the wavenumber reduction at 25 °C, as the leaching process at elevated temperature is known to result in the partial hydrothermal conversion of the metakaolin to hydroxysodalite [9]. Hydroxysodalite has a fully $Q^4(4Al)$ structure, meaning that if a wavenumber lower than this is observed, there must be a contribution from non-bridging oxygen (Q^3) sites. This indicates that the leaching of metakaolin in NaOH at 25 °C is leading to a structure which is at least partially depolymerised. This may be because of Al extraction from the layered metakaolin structure, leaving the residual Q^3 silicate layers, or may be related to the deposition of a new partially-polymerised gel product on the metakaolin surface. To resolve this question, it is necessary to conduct depth-resolved analysis of the material.

3.2 Depth-Resolved FTIR

Figure 2 shows the photoacoustic FTIR spectra obtained at different phase modulation frequencies (effectively different depths) within a sodium silicate-metakaolin system with a liquid/solid ratio of 1.0, reacted for 8 days at 40 °C. This system hardened to form a geopolymer binder during the reaction process, and the analysis presented here was conducted on the results of this reaction. The surface (bottom spectrum in Fig. 2) corresponds to the surface of a metakaolin particle, which is terminated by a silicate layer. However, probing within the particle (increasing

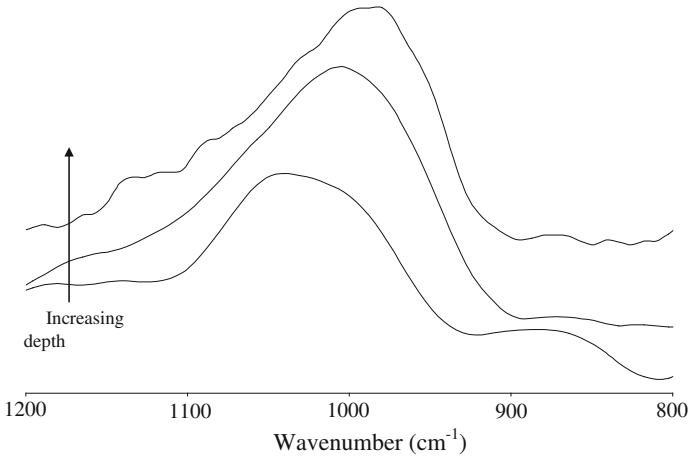

Fig. 2 Photoacoustic FTIR spectra of metakaolin reacted with 8 M NaOH & 2 M SiO_2 at a liquid/solid ratio of 1.0, after 8 days of reaction

depth; approximately a few hundred nm per step) shows that the main Si-O-(Si,Al) peak appears at a much lower wavenumber. This is consistent with simulations of the metakaolin-sodium silicate system which showed the formation of a geopolymer product within the boundaries of the original metakaolin particle [5]. This provides the first experimental confirmation for this effect, which is likely to take place as the aluminium released through the relatively rapid breakdown of the strained Al layers in the metakaolin structure interacts with silica, supplied both by the external solution entering the particle and by the start of breakdown of the silicate layers of the metakaolin. It is probable that this process also exfoliates the metakaolin particles, at least in part.

3.3 Xps

Figure 3 shows a Wagner (chemical state) plot for aluminium in metakaolin, and in the products of leaching the metakaolin with different alkali hydroxide solutions, at a concentration of 0.10 M, for 10 min. This shows that significant structural alteration can be induced at a much lower alkali concentration than was used in the FTIR experiments, and in a short period of interaction with the alkaline solution. The pH of the 0.10 M alkali hydroxide solutions is also not entirely dissimilar to the pore solution pH of Portland cement, which suggests that these results may be of relevance in understanding the reactions of metakaolin under that environment. As a supplementary cementitious material, it is often assumed that the chemical contributions of metakaolin are mainly taking place at later age, but the rapid chemical evolution of the Al environment under these conditions indicates that there could also be a significant early-age contribution from this material under appropriate

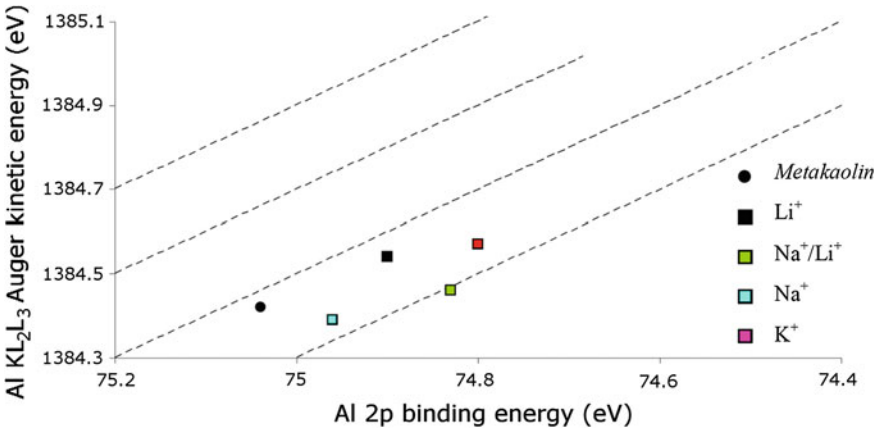

Fig. 3 Aluminium chemical state plot for metakaolin leached in 0.10 M solutions of different alkalis (as marked) for 10 min. The Na^+/Li^+ solution contained 0.08 M NaOH and 0.02 M LiOH

conditions. The decreased binding energy is indicating a more covalent character of the bonding environments around Al as a result of exposure to alkali hydroxide solutions.

4 Conclusions

The structure of metakaolin particles is significantly altered by exposure to alkaline environments, whether the environment is purely a hydroxide system or contains a significant content of dissolved silicates. The extraction of aluminate components from the distorted Al layers in the metakaolin can lead to the formation of aluminosilicate gels within the residual metakaolin particles. These results are important in understanding the reaction processes of metakaolin within alkali-activated geopolymer systems, and also when used as a supplementary cementitious material in Portland cement based binders.

Acknowledgments This study was sponsored by the Australian Research Council (ARC) through Discovery Project and Linkage Project Grants, including co-funding of the linkage project by Zeobond Pty Ltd.

References

1. Sabir, B.B., Wild, S., Bai, J.: Metakaolin and calcined clays as pozzolans for concrete: a review. Cem. Concr. Compos. **23**(6), 441–454 (2001)
2. Provis, J.L.: Geopolymers and other alkali activated materials—Why, how, and what? Mater. Struct. **47**(1), 11–25 (2014)
3. White, C.E., Provis, J.L., Proffen, T., Riley, D.P., van Deventer, J.S.J.: Combining density functional theory (DFT) and pair distribution function (PDF) analysis to solve the structure of metastable materials: the case of metakaolin. Phys. Chem. Chem. Phys. **12**(13), 3239–3245 (2010)
4. White, C.E., Provis, J.L., Proffen, T., Riley, D.P., van Deventer, J.S.J.: Density functional modeling of the local structure of kaolinite subjected to thermal dehydroxylation. J. Phys. Chem. A **114**(14), 4988–4996 (2010)
5. White, C.E., Provis, J.L., Proffen, T., van Deventer, J.S.J.: Molecular mechanisms responsible for the structural changes occurring during geopolymerization: Multiscale simulation. AIChE J. **58**(7), 2241–2253 (2012)
6. Favier, A., Habert, G., d'Espinose de Lacaillerie, J.B., Roussel, N.: Mechanical properties and compositional heterogeneities of fresh geopolymer pastes. Cem. Concr. Res. **48**, 9–16 (2013)
7. Steins, P., Poulesquen, A., Diat, O., Frizon, F.: Structural evolution during geopolymerization from an early age to consolidated material. Langmuir **28**(22), 8502–8510 (2012)
8. Chukanov, N.V.: Infrared spectra of mineral species: Extended library. Dordrecht: Springer, 1733 (2014)
9. Barrer, R.M., Mainwaring, D.E.: Chemistry of soil minerals. Part XIII. Reactions of metakaolinite with single and mixed bases. J. Chem. Soc. Dalton Trans. **22**, 2534–2546 (1972)

From a View of Alkali Solution: Alkali Concentration to Determine Hydration Process of Alkali Activating Metakaolin

Mu Song, Jiang Qian, Liu J. Zhong and Shi Liang

Abstract With increasing concerns on concept of sustainability from the world, alkali activating binder materials has gained lots of concerns from academy and industry. However, hydration mechanism of alkali activating metakaolin is still not clearly understood. As a key component of alkali activating binder material, role of alkali solution and its action mechanism on hydration of alkali activating metakaolin are reported rarely. The present research studied influence of alkali concentration on hydration process and microstructure formation of alkali activating metakaolin. Penetration resistance, setting time, compressive strength, hydration heat, and scanning electron microscope, were adopted to reveal the hydration process influenced by concentration of alkali solution. Results show that high concentration of alkali solution accelerated hydration process of metakaolin, but over high concentration was resulted in a decreasing trend of compressive strength in the entire age of 60 days.

1 Introduction

Alkali solution is a key component of alkali-activated metakaolin. On one hand, metakaolin is attacked by hydroxide ion to release silicate and aluminate ions which are main reactants of geopolymerization; on the other hand, alkali metal ion is useful to finish charge balance of geopolymer products, and silicate ion from alkali solution is active for the geopolymeriazation. Normally, alkali solution is composed of alkali metal hydroxide and water glass. As for as alkali metal hydroxide is concerned, concentration of the alkali solution has a clear influence on geopolymer property.

M. Song (✉) · J. Qian · L.J. Zhong · S. Liang
State Key Laboratory of High Performance Civil Engineering Materials, Jiangsu Research Institute of Building Science, Nanjing 210008, People's Republic of China
e-mail: musong@cnjsjk.cn

M. Song · J. Qian · L.J. Zhong · S. Liang
Jiangsu SOBUTE New Materials Co., Ltd, Nanjing 211103, People's Republic of China

K. Scrivener and A. Favier (eds.), *Calcined Clays for Sustainable Concrete*,
RILEM Bookseries 10, DOI 10.1007/978-94-017-9939-3_38

Importance of alkali solution has already gained some attentions in previous researches. Al Bakri et al. [1] found that the geopolymer paste with a combination of a Na_2SiO_3/NaOH ratio of 2.5 and a 12 M NaOH concentration produces a denser matrix and less unreacted FA which contributed to the maximum compressive. Gorhan et al. [2] observed that NaOH concentration had a clear effect on the properties of the fly ash-based geopolymer mortar cured at 85 degrees. Heah et al. [3] reported the optimal compressive strength of kaolin-based geopolymers was achieved at Al_2O_3/Na_2O of 1.09 and SiO_2/Na_2O molar ratios of 3.58. Heah et al. [4] found the increased Na_2O concentration enhanced the dissolution of kaolin as shown in X-ray diffraction (XRD) and Fourier transform infrared spectroscopy (FTIR) analyses. Tchakoute [5] thought the most convenient Al_2O_3/Na_2O molar ratio of fused volcanic ash to produce effective geopolymer mortars ranged between 0.13 and 0.18.

However, little attention has been devoted to the geopolymerization under a combined alkali solution of water glass and NaOH solution with different concentration. The present study investigated the effect of NaOH concentration on geopolymerization of alkali activating metakaolin under a constant ratio of water to solid and final modulus of water glass.

2 Experiment

2.1 Raw Materials

Metakaolin and alkali solution were used to prepare geopolymer. Metakaolin was purchased from local market, and the pink appearance was presented after calcination at 800 to 1000 °C. The total concentration of SiO_2 and Al_2O_3 accounts for about 94 %. As for the particle size distribution, 90 percentages of metakaolin has a particle size below 5.43 μm, and the average particle size is 1.73 μm. Alkali solution is prepared by sodium silicate and sodium hydroxide. In this study, modulus of sodium silicate was adjusted to 2 (42.5 % of solid content) by addition of sodium hydroxide and water. Solutions were stored for a minimum of 24 h prior to use to allow homogenization.

Different geopolymers were prepared and their recipes are listed in Table 1. According to our previous experience, ratio of water to solid and final modulus of water glass, were the most important factors to determine property of geopolymer. For the mixture of geopolymer, the present study used the both factors to replace molar ratio of SiO_2/Al_2O_3, K_2O/Al_2O_3 and H_2O/K_2O. Besides, concentration of NaOH changed under the fixed value of water to solid and final modulus of water glass. In order to prepare geopolymer, metakaolin and filler was dispersed by a mixer at a slow rate. Then alkali solution was added into mixer to stir moderately, until a homogeneous paste was attained.

Table 1 Recipe of geopolymers

Sample	Metakaolin (g)	Modulus of water glass	Sodium silicate (g)	Concentration of Sodium hydroxide (mol/L)	Sodium hydroxide (g)	Water/ Solid	Final modulus of water glass
C12.5	1000	2	902	12.5	722	1	0.82 ± 0.02
C15	1000	2	958	15	719	1	
C20	1000	2	1068	20	694	1	

2.2 Test Method

The penetration resistance and setting time was conducted in accordance with Chinese standard of JGJ/T 70-2009 "Standard for test method of performance on building mortar". The testing needle with an area of 30 mm^2, was used for the measurement of penetration resistance. The test was done when the resistance value surpassed 0.7 MPa, then setting time can be determined as the time of resistance reached at 0.5 MPa. Average of two repeated tests were taken for the value of resistance and setting time. All the specimens were kept at a constant temperature of 20 ± 2 °C with a relative humidity of 65 %. Average of three specimens, with a size of 20 mm × 20 mm × 20 mm, were taken for compressive strength after 3, 7, 28 and 60 days. All the specimens were kept at a constant temperature of 20 ± 2 °C with a relative humidity of 90 %.

In this study, the hydration heat of geopolymer was determined with a TAM AIR isothermal heat conduction calorimeter (TA instruments). The geopolymer sample was mixed by manual, and then within 5 min the sample ampoules were filled with 10 g paste, consisting of metakaolin and alkali solution. The microstructures of geopolymer paste were investigated by SEM Quanta 250 from FEI, USA.

3 Results

3.1 Penetration Resistance

Penetration resistance tester is a common method to determine setting time of mortar or concrete. In the present study, penetration resistance at different time was used to describe the setting process of inorganic polymer prepared by different alkali concentration. According to Fig. 1, increased alkali concentration decreased the time to reach the key value of penetration resistance which is defined as 0.5 MPa to represent setting time of mortar. Besides, C20 sample had a setting characteristic of earlier age than C12.5 and C20 samples. As expected, the penetration resistance increased rapidly from 0 MPa to 0.5 MPa after 20 min inorganic polymer had been casted into molds.

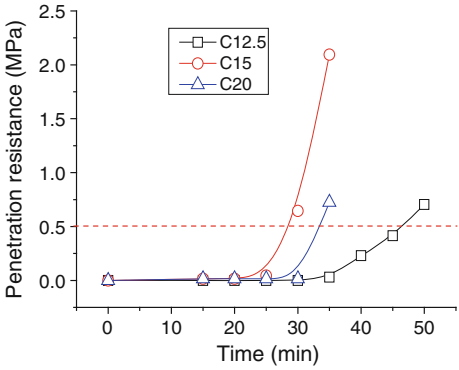

Fig. 1 Effect of alkali concentration on penetration resistance

Figure 2 shown the results of setting time of inorganic polymer prepared by different concentrations of alkali solution. As the concentration of alkali solution increased from 12.5 mol/L to 20 mol/L, the setting time decreased from 46 min to 33 min.

3.2 Hydration Heat

Exothermic reaction is a typical characteristic of polycondensation for inorganic polymer. Exothermic rate of geopolymerization is shown in Fig. 3. With increasing concentration of alkali solution, exothermic rate of alkali-activated metakaolin significantly increased. Particularly, the maximum exothermic rate of 20 mol/L of alkali solution was five times than 12.5 mol/L of alkali solution. In contrast with Portland cement PII 52.5, alkali-activated metakaolin has some characteristics of polycondensation as described follows: firstly, main peak of exothermic reaction in alkali-activated metakaolin has been observed in 25 min, but the peak in Portland

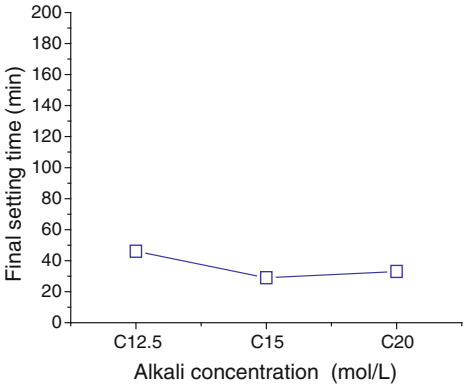

Fig. 2 Effect of alkali concentration on setting time

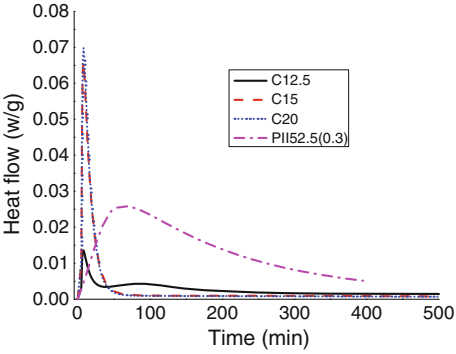

Fig. 3 Exothermic rate

cement PII 52.5 appeared in 50 min to 100 min; secondly, geopolymer prepared with 12.5 mol/L of alkali solution had a significantly lower exothermic rate than Portland cement PII 52.5, but 15 mol/L and 20 mol/L of alkali solution exhibited a three times of exothermic rate than Portland cement PII52.5; thirdly, 12.5 mol/L of alkali solution had a exothermic process with low heat flow after the main peak, however the heat flow of 15 mol/L and 20 mol/L of alkali solution almost reached 0 w/g.

3.3 Compressive Strength

Compressive strength at the age of 3 days to 60 days is shown in Fig. 4. With the increased concentration of NaOH, compressive strength exhibited a decreased trend and then recovered under a role of the high concentration in the entire age of 60 days. However, the recovered strength was still lower than the reference sample C12.5, which implied that over high concentration of alkali substance decreased the strength of geopolymer. As a matter of fact, the strength development is consistent

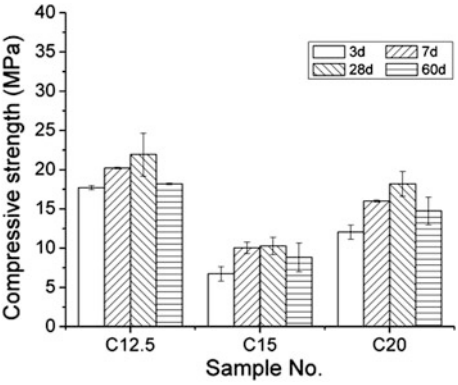

Fig. 4 Compressive strength

with the results of penetration resistance which has been found that C15 sample had the fastest process of geoplymer setting. Besides, decreased strength at late age has been observed for alkali-activated metakaolin.

3.4 SEM

Microstructural morphology of alkali-activated metakaolin was demonstrated in Figs. 5, 6, 7 and 8. According to Fig. 5, unreacted particles of sodium hydroxide have been found in the geopolymer at the age of 7 days, and some geopolymer products were formed in the shape of needle. However, particles of sodium hydroxide and needle shaped products disappeared in the microstructure of the geopolymer as the curing age increased from 7 days to 28 days (see Fig. 6). When

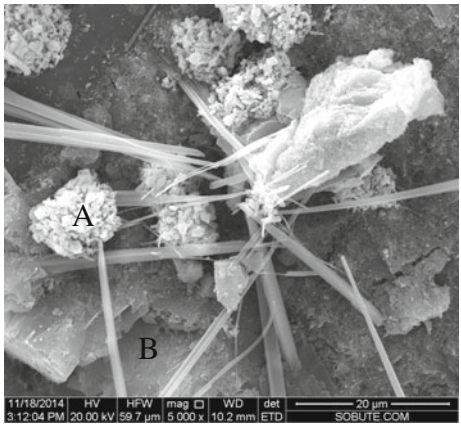

Fig. 5 C12.5-N-08-1 (7d) × 5000

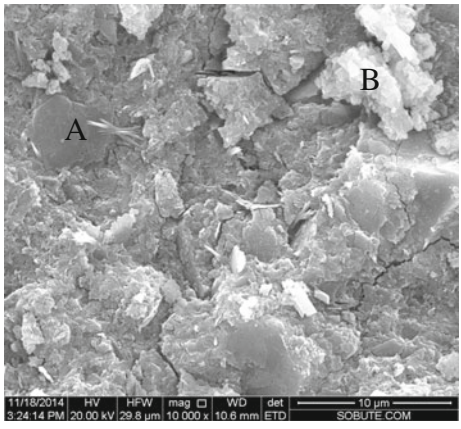

Fig. 6 C12.5-N-08-1 (28d) × 10000

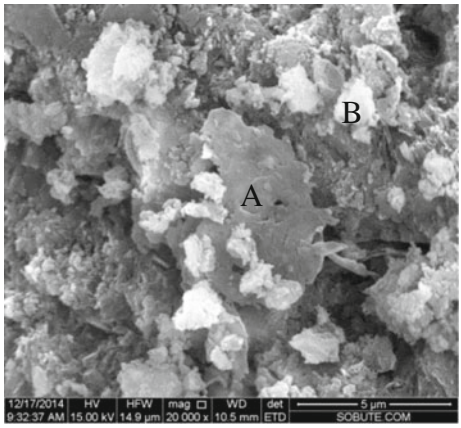

Fig. 7 C15-N-08-1 (28d) × 20000

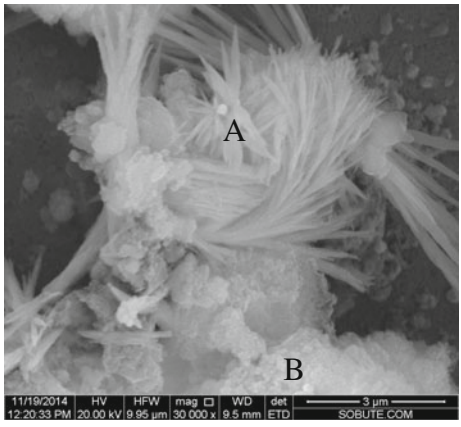

Fig. 8 C20-N-08-1 (28d) × 30000

the concentration of alkali solution increased from 12.5 mol/L to 20 mol/L, geopolymer products transformed from amorphous phase into crystalline phase with a shape of petals (see Fig. 8).

Table 2 listed chemical composition of selected points in the SEM patterns. With the increased concentration of alkali solution, atomic ratio of Si/Al decreased gradually from about 1.4 to 1.0 in the geopolymerization products, and meanwhile atomic ratio of Si/Na significantly decreased by about 40 %. The results indicated

Table 2 Chemical composition of selected points in geopolymer prepared by different concentrations of alkali solution

Atomic ratio	C12.5-N-08-1(28d)		C15-N-08-1 (28d)		C20-N-08-1 (28d)	
	A	B	A	B	A	B
Si/Al	1.45	1.40	1.51	1.27	0.93	1.14
Si/Na	1.89	1.35	3.78	1.71	0.48	0.81

that high concentration of alkali solution was resulted into Na^+ condensation in geopolymer system, and increased amount of Al^{3+}. Normally, increased ratio of Si/Al is helpful to improve strength of geopolymer. Therefore, higher concentration of alkali solution decreased the ratio of Si/Al and Si/Na so as to deteriorate the mechanic property. In addition, geopolymer product with a petal shape characterized by a low ratio of Si/Al and Si/Na, which represented a poor strength property.

4 Discussion

Proper concentration of alkali solution can be helpful for polycondensation process, but over high concentration of alkali solution deteriorated microstructure of geopolymer and increased its porosity at a late age so as to decrease the strength. Chindaprasirt [6] also found that the similar results of coarse high calcium fly ash geopolymer at 7 days age.

At the early age of geopolymerization process, increased concentration of alkali solution was resulted into high concentration of alkali metal ions and hydroxide ions, so that large amount of silicate and aluminate ions can be dissolved from metakaolin into the solution [7, 8] and the balanced charge can be rapidly reached to form polycondensation productions. Therefore, increased concentration of alkali solution accelerated the process of geopolymerization at an early age, and decreased the setting time and increased rate of exothermic reaction. From the point of view of microstructure, proper concentration of alkali solution improved the pore structure and morphology of geopolymer products. As the concentration increased to a critical value, large amount of alkali metal ions and hydroxide ions accelerated geopolymerization process and newly formed products hindered further polycondensation, and eventually the crystal products was disappeared. Heah [4] also found excess in alkali concentration was not beneficial for the strength development of kaolin geopolymers. However, the concentration higher than the critical value was contributed to further development of geopolymeriztion due to enough amout of alkali metal ions and hydroxide ions could diffusion into geopolymer products and reacted with metakaolin, hence the microstructure recovered from the poor condition to a dense structure, and large amount of petal-shaped products has been found.

5 Conclusions

- Proper concentration of alkali solution can be helpful for polycondensation process, but the over high concentration deteriorated the microstructure and decreased the strength;
- Increased alkali concentration, from 12.5 mol/L to 20 mol/L, accelerated the process of geopolymerization at an early age, and decreased the setting time and increased rate of exothermic reaction.

Acknowledgments Authors appreciate the financial supports from the China Postdoctoral Science Foundation under the contract No. 2013M531296, and the Postdoctoral Science Foundation of Jiangsu Province under the contract No. 1301160C.

References

1. Al Bakri, A.M.M., Kamarudin, H., et al.: Effect of Na_2SiO_3/NaOH ratios and NaOH molarities on compressive strength of fly-ash-based geopolymer. ACI Mater. J. **109**(5), 503–508 (2012)
2. Gorhan, G., Kurklu, G.: The influence of the NaOH solution on the properties of the fly ash-based geopolymer mortar cured at different temperatures. Compos. Part B-Eng. **58**, 371–377 (2014)
3. Heah, C.Y., Kamarudin, H., et al.: Study on solids-to-liquid and alkaline activator ratios on kaolin-based geopolymers. Constr. Build. Mater. **35**, 912–922 (2012)
4. Heah, C.Y., Kamarudin, H., et al.: Kaolin-based geopolymers with various NaOH concentrations. Int. J. Min. Metall. Mat. **20**(3), 313–322 (2013)
5. Tchakoute, H.K., Elimbi, A., et al.: Synthesis of geopolymers from volcanic ash via the alkaline fusion method: effect of Al_2O_3/Na_2O molar ratio of soda-volcanic ash. Ceram. Int. **39**(1), 269–276 (2013)
6. Chindaprasirt, P., Chareerat, T., Sirivivatnanon, V.: Workability and strength of coarse high calcium fly ash geopolymer. Cem. Concr. Compos. **29**(3), 224–229 (2007)
7. Xu, H., Van Deventer, J.S.J.: The geopolymerisation of alumino-silicate minerals. Int. J. Miner. Process. **59**(3), 247–266 (2000)
8. Phair, J.W., Van Deventer, J.S.J.: Effect of silicate activator pH on the leaching and material characteristics of waste-based inorganic polymers. Miner. Eng. **14**(3), 289–304 (2001)

What Happens to 5 Year Old Metakaolin Geopolymers' the Effect of Alkali Cation

Susan A. Bernal, Jannie S.J. van Deventer and John L. Provis

Abstract In this study we report X-ray diffraction and dilatometry results of metakaolin (MK) geopolymers produced with Na, K, Rb or Cs silicate solutions, and cured for 7 days and 5 years, with the aim of identifying variations in structure and performance (dimensional stability at elevated temperature) over an extended curing period at ambient temperature. All of the geopolymers studied are mainly X-ray amorphous after 5 years of curing; however, in Rb-based and Cs-based geopolymers formation of aluminosilicate crystalline phases was identified. As the alkali cation radius increases, so does the thermal stability of the MK-geopolymer, potentially as a consequence of the combined effect of the higher degree of ordering of the geopolymer itself, which might retard the dehydration of the geopolymers upon heating, and the reduced energy of hydration of larger alkali cations. The 7-day and 5-year cured samples produced with Rb and Cs silicate solutions do not exhibit significant dimensional changes above 300 °C, with a maximum shrinkage of <2 % after exposure to 1100 °C. This shows that increasing the radius of the alkali cation during geopolymerisation of MK has an effect on the thermal stability of these materials, and promotes the formation of a highly densified and rigid structure at advanced curing ages.

S.A. Bernal (✉) · J.L. Provis
Department of Materials Science and Engineering, The University of Sheffield, Sir Robert Hadfield Building, Sheffield S1 3JD, UK
e-mail: s.bernal@sheffield.ac.uk

J.S.J. van Deventer · J.L. Provis
Department of Chemical and Biomolecular Engineering, The University of Melbourne, Melbourne, VIC 3010, Australia

J.S.J. van Deventer
Zeobond Pty Ltd, P.O. Box 23450, Docklands, VIC 8012, Australia

K. Scrivener and A. Favier (eds.), *Calcined Clays for Sustainable Concrete*, RILEM Bookseries 10, DOI 10.1007/978-94-017-9939-3_39

1 Introduction

Metakaolin (MK), derived from dehydroxylation of kaolinite clays upon thermal treatment, is one of the main aluminosilicate precursors used in the production of geopolymers [1]. These materials are produced via a chemical reaction of a poorly crystalline aluminosilicate source and a highly concentrated alkaline solution, forming a hardened solid with a disordered pseudo-zeolite type structure [2]. MK-geopolymers have been extensively studied over the past 50 years, however, most studies have been focussed in the performance of these materials over a short period of curing (days to weeks), and limited attention has been paid to their longer-term structural evolution.

The kinetics of reaction and microstructural features of MK-geopolymers are strongly dependent on the characteristics of the MK used [3], along with the overall SiO_2/Al_2O_3 molar ratio of the system [4], and the type and concentration of the alkaline activator. Specifically, the alkali metal cation present in the activator influences the dissolution, polycondensation kinetics, and the consequent geopolymer gel and crystal formation processes. This is a consequence of the role of the alkali cations in the ordering of water and dissolved Al and Si complexes in solution, as well as their structural directing role in geopolymerisation.

The most widely used activators are solutions of sodium and/or potassium hydroxides and/or silicates [5]. Na^+ and K^+ have the same overall electric charge, but different charge densities as a result of their different radii, and so they have different effects in the geopolymerisation process and the microstructure of the material formed. This is associated with the different ionic sizes of these cations, which its affects charge density and hydration [6]. It has been identified [7] that potassium-based geopolymers have greater compressive strength compared with sodium-based geopolymers synthesised from alkali-feldspar/kaolinite matrices, as a consequence of a higher polymerising activity between silicate and aluminosilicate species when using K-based activators. In a NaOH solution compared with KOH, it is expected that Na^+ with a smaller cation size will be more active in inducing dissolution than K^+, resulting in a higher extent of reaction of silicate and aluminate precursors. However, it has been demonstrated [8] that there is also an ion pairing effect taking place in these systems. Metal cations with a smaller size and a higher positive charge favour ion pairing with smaller silicate oligomers such as monomers, dimers or trimers [8]. Therefore, Na^+ has a greater ability to stabilise silicate monomers, while the larger K^+ cation will stabilise silicate oligomers.

The effects of larger alkaline cations such as Cs and Rb on the structure of MK-geopolymers have attracted less attention than Na^+ and K^+, mainly due to the high cost of the hydroxide solutions containing these alkalis. However, MK-geopolymers have been identified as one of the most promising immobilisation matrices for alkali metal radionuclides such as ^{135}Cs and ^{137}Cs, which are highly leachable from Portland cement based wasteforms. Therefore, it is of great interest

to understand the role of Cs in these systems. The few reports on activation of MK with CsOH or Cs silicate demonstrate that the chemical binding of Cs to the geopolymer network is feasible, favouring the formation of crystalline phases including pollucite [9, 10]. On the other hand, no information is recorded in the literature regarding rubidium hydroxide activation of MK geopolymers.

In the contexts of nuclear waste disposal, cementitious matrices must retain performance for decades and even centuries, and therefore it is important to evaluate aged materials to understand the changes in phase assemblage and binder structure that can take place over a period of years after casting. In this study Na, K, Cs and Rb metakaolin geopolymers after 7 days and 5 years of curing were evaluated through X-ray diffraction and dilatometry.

2 Experimental Methodology

A commercial metakaolin (Metastar 402, Imerys UK) was used to produce geopolymers. The BET surface area of the metakaolin was 12.7 m^2/g, and the mean particle size (d_{50}) was 1.58 μm. Reagent-grade alkali hydroxides (NaOH, KOH, RbOH and CsOH) were purchased from Sigma-Aldrich (Australia), and alkaline silicate solutions with a molar ratio SiO_2/M_2O (M = Na, K, Cs or Rb) of 1.0 and H_2O/M_2O = 11 were prepared by dissolving fumed silica (Aerosil 200) in appropriate hydroxide solutions until clear. Solutions were stored for a minimum of 24 h before use. All geopolymer samples were formulated with an overall Al_2O_3/M_2O molar ratio of 1.0 and Si/Al = 1.5, considering the chemical composition of the MK and the alkaline solution used. The geopolymer pastes were produced by mechanically mixing the MK with the activator for 15 min, using a high shear mixer. Samples were transferred to polymeric moulds and vibrated for 15 min to remove entrained air. All samples were cured in a laboratory oven at 40 °C for 20 h, and then transferred into sealed containers for storage at ambient temperature (20–25 °C) until testing.

After 7 days and 5 years of curing, samples were crushed and sieved (<67 μm). A Philips PW 1800 diffractometer with Cu Kα radiation was used for studying 7-day cured samples, while 5-year cured samples were analysed using a Bruker D8 Advance instrument with Cu Kα radiation and a nickel filter. All data were collected with a step size of 0.020º, over a 2θ range of 5º to 70º. Dilatometry measurements were performed on a Perkin Elmer Diamond Thermomechanical Analyser (TMA), using cylindrical samples with 5 mm diameter and 10 mm height, at a constant heating rate of 10 °C/min, a constant load of 50 mN, and a nitrogen purge rate of 200 mL/min.

3 Results and Discussion

3.1 X-Ray Diffraction

All 7-day cured samples were X-ray amorphous, with the exception of remnant crystalline components in the commercial metakaolin (data not shown). In all 5-year old samples (Fig. 1) an amorphous hump between $18 < 2\theta < 45°$ is identified, consistent with the literature for metakaolin geopolymers. In the Na-based (Fig. 1a) and K-based (Fig. 1b) geopolymer the only crystalline phase present is kaolinite-1A ($Al_2Si_2O_5(OH)_4$; powder diffraction file, PDF, # 014-0164, marked Ka in Fig. 1a,b). Conversely, in the Rb-based geopolymer, the crystalline phases $RbAlSi_2O_6$ (marked Rb1 in Fig. 1c) (PDF#028-1077) and $RbAlSiO_4 \cdot H_2O$ (Rb2 in Fig. 1c) (PDF#030-1043) are present, while in the Cs-based geopolymers formation pollucite ($CsAlSi_2O_6$) (PDF#04-013-2101, L in Fig. 1d) is observed. These results elucidate that the use of activating solution with larger alkali cations promotes the formation of crystalline products in MK-geopolymers during an extended period of curing.

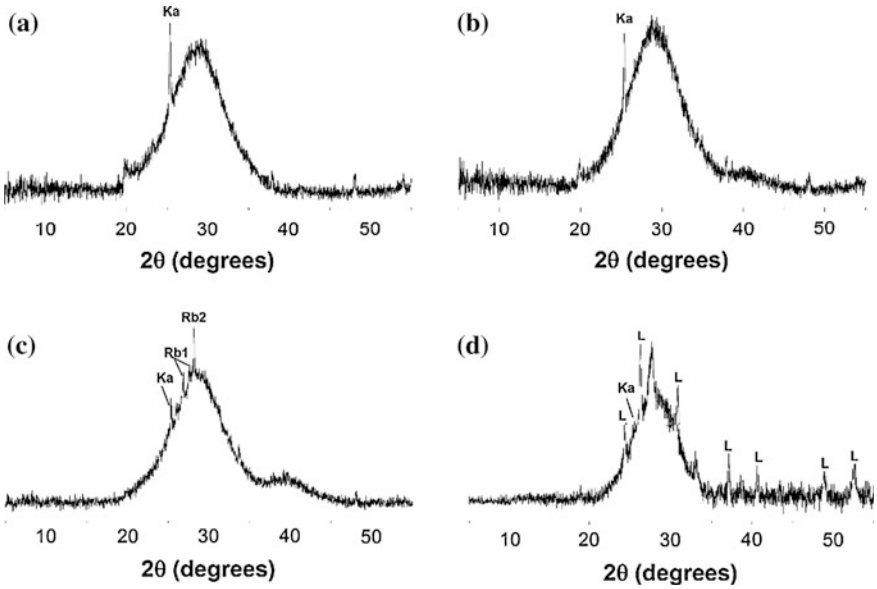

Fig. 1 X-ray diffractograms of 5-year cured MK geopolymers formulated with a Si/Al ratio of 1.5, activated with **a** Na, **b** K, **c** Rb and **d** Cs silicate solutions

3.2 Dilatometry

Consistent with previously studies [11–13], the 7 day cured Na-geopolymer shows (Fig. 2a) a slight shrinkage between approximately 100 and 300 °C, corresponding to the collapse of some of the pores as the pore water evaporates. This is followed by a period of slow and constant shrinkage from 300–700 °C corresponding to the physical contraction resulting from dehydroxylation, with condensation of silanol or aluminol groups on the surface of the geopolymeric gel leading to the release of water and the creation of Si-O-T (T: tetrahedral Si or Al) linkages [12, 14]. Thermal shrinkage then accelerates significantly at temperatures above 700 °C, via viscous sintering.

As the radius of the alkali cation increases, a significant reduction in the initial shrinkage (100–300 °C) is observed (Fig. 2a), so that Cs and Rb geopolymers show less than 2 % shrinkage in this temperature range. The onset of viscous sintering also shifts towards higher temperatures as the alkali radius increases, and it is not detected for Cs and Rb-containing geopolymers within the range of temperatures evaluated (up to 1000 °C). This demonstrates that early age Cs and Rb geopolymers are highly dimensionally stable at elevated temperatures. In aged samples, the Na-geopolymers (Fig. 2b) shrinks more at temperatures above 600 °C than is observed in specimens with 7 days of curing (Fig. 2a). This could be associated with changes in the pore structure, overall Si/Al ratio and fraction of remnant unreacted MK present, which modifies the viscous sintering process that is taking place in these samples. Both K and Rb aged geopolymers exhibit comparable shrinkage to that identified in 7-day cured samples, indicating that limited structural changes are occurring in these specimens with maturity, and that the physical and chemical distribution of hydroxyl sites in these samples are comparable.

The second derivatives of the dilatometry traces are reported in Fig. 3, and provide further clarity regarding the onset and nature of shrinkage phenomena. In Na based geopolymers (Fig. 3a), the onset temperature (~700 °C) remains similar between 7 days and 5 years of curing, but the rate of initial shrinkage is much more gradual in the more mature samples, which could be associated with the

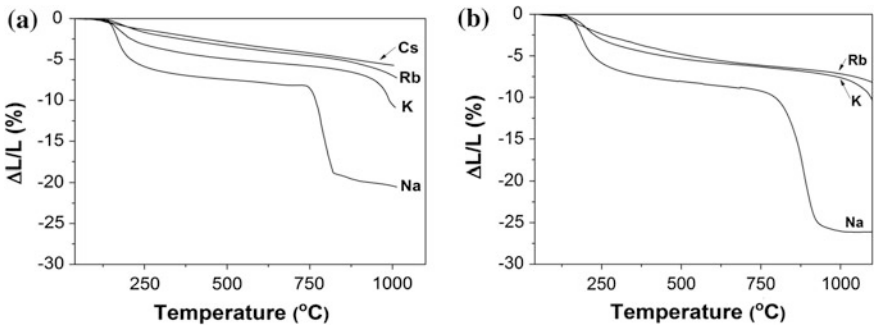

Fig. 2 Dilatometry curves of MK geopolymers formulated with a Si/Al ratio of 1.5, as a function of the alkali cation used, assessed after **a** 7 days and **b** 5 years of curing

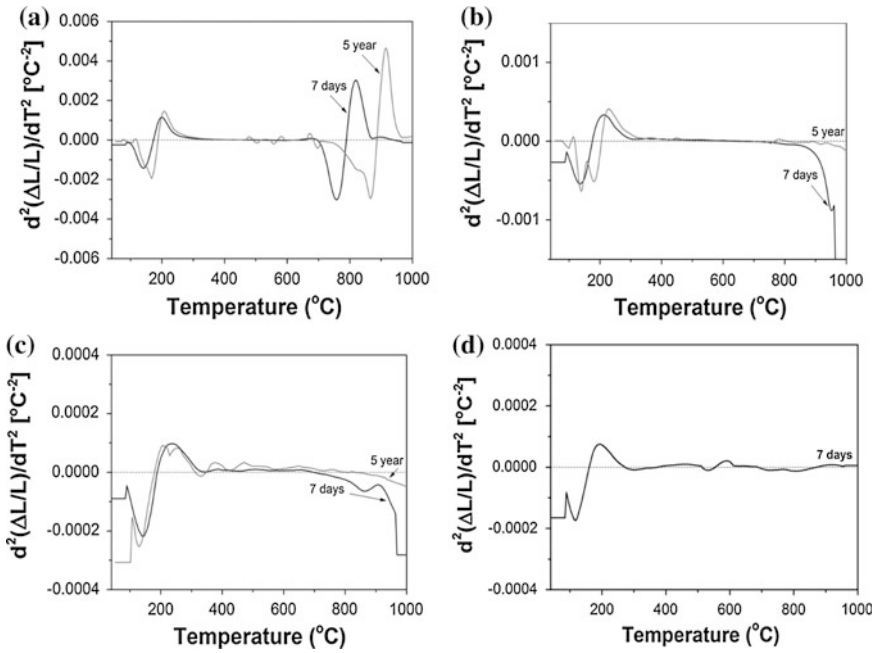

Fig. 3 Second derivative of the dilatometry curves of MK geopolymers formulated with a Si/Al ratio of 1.5, activated with **a** Na, **b** K, **c** Rb and **d** Cs silicate solutions, as a function of the curing time

densification of the geopolymer gel skeleton over the time of curing, as a consequence of pore refinement. There is a slight indication of an expansion phenomenon prior to the onset of shrinkage in this sample at 7 days and 5 years, just below 700 °C, which differs from the other samples studied. Conversely, in the K-based geopolymer (Fig. 3b) at early age initiation of shrinkage is observed above 800 °C, but almost no dimensional change is detectable in the mature sample. A similar effect is observed in the Rb-based geopolymer (Fig. 3c), which at early age showed slightly less shrinkage below 500 °C but more at temperatures between 600 and 700 °C, compared with the K-based formulation. Cs-based geopolymers only show dimensional changes below 300 °C (Fig. 3d), associated with the dehydration of loosely bonded water in the geopolymer gel, and are dimensionally stable from this temperature to above 1000 °C.

4 Conclusions

Production of metakaolin geopolymers using rubidium and cesium silicate solutions is feasible. All geopolymers studied are predominantly X-ray amorphous after 5 years of curing; however, in Rb-based and Cs-based geopolymers the formation

of additional aluminosilicate crystalline phases is taking place. The thermal stability of MK-geopolymers is influenced by the alkali cation present in the material, so that different thermal shrinkage profiles are observed when using different silicate solutions as activators. There seems to be a direct correlation between the alkali radius and the onset of the viscous sintering process identified in Na-geopolymers above 600 °C, so that geopolymers produced with Rb and Cs show negligible dimensional changes in the range of temperatures evaluated. This cannot solely be attributed to the alkali cation, and might be consequence of the combined effect of the higher ordering identified in the Rb and Cs geopolymers compared with Na and K geopolymers, which may retard the dehydration of the geopolymers upon heating; the reduced energy of hydration of larger alkali cations, favouring water removal at reduced temperatures from the hydration shell of alkali cations associated with aluminium; and the differences in the amount of remnant MK present in the samples, associated with different degrees of reaction. These results elucidate that small microstructural changes are taking place in MK-geopolymers, independent of the alkali cation, over an extended period of curing, demonstrating the high stability of appropriately formulated MK geopolymers upon aging.

Acknowledgments This study was sponsored by the Australian Research Council (ARC) through Discovery Project and Linkage Project Grants, including co-funding of the linkage project by Zeobond Pty Ltd. We thank David G. Brice and Dr Peter Duxson for sample synthesis, data collection, and discussions. The participation of J.L Provis and S.A. Bernal was supported by the University of Sheffield.

References

1. Duxson, P., Fernández-Jiménez, A., Provis, J.L., Lukey, G.C., Palomo, A., van Deventer, J.S. J.: J. Mater. Sci. **42**, 2917 (2007)
2. Provis, J.L., Lukey, G.C., van Deventer, J.S.J.: Chem. Mater. **17**, 3075 (2005)
3. Elimbi, A., Tchakoute, H.K., Njopwouo, D.: Constr. Build. Mater. **25**, 2805 (2011)
4. Rowles, M., O'Connor, B.: J. Mater. Chem. **13**, 1161 (2003)
5. Provis, J.L., Bernal, S.A.: Annu. Rev. Mater. Res. **44**, 299 (2014)
6. Xu, H., van Deventer, J.S.J.: Int. J. Miner. Proc. **59**, 247 (2000)
7. Xu, H., van Deventer, J.S.J.: Colloids Surf. A **216**, 27 (2003)
8. Swaddle, T.W., Salerno, J., Tregloan, P.A.: Chem. Soc. Rev. **23**, 319 (1994)
9. Bell, J.L., Sarin, P., Provis, J.L., et al.: Chem. Mater. **20**, 4768 (2008)
10. Berger, S., Frizon, F., Joussot-Dubien, C.: Adv. Appl. Ceram. **108**, 412 (2009)
11. Duxson, P., Lukey, G.C., van Deventer, J.S.J.: J. Non-Cryst. Solids **352**, 5541 (2006)
12. Duxson, P., Lukey, G.C., van Deventer, J.S.J.: J. Mater. Sci. **42**, 3044 (2007)
13. Provis, J.L., Yong, C.Z., Duxson, P., van Deventer, J.S.J.: Colloids Surf. A **336**, 57 (2009)
14. Van Riessen, A., W Rickard, J S. In: Provis, J.L., van Deventer, J.S.J. (eds) Geopolymers: structures, processing, properties and industrial applications woodhead, Cambridge (2009)

Development and Introduction of a Low Clinker, Low Carbon, Ternary Blend Cement in Cuba

Jose Fernando Martirena Hernandez and Karen Scrivener

Abstract This paper discusses the strategy and results of a collaborative work carried out between 2005–2012 by two research teams at the Center for Research and Development of Structures and Materials (CIDEM) from the Universidad Central de las Villas, Cuba and the Laboratory of Construction Materials, from the Ecole Polytechnique Federal de Lausanne, EPFL, Switzerland on the use of low grade clays as Supplementary Cementitious Materials, SCM. On a first phase the work focused on the assessment of the reactivity of a low grade clay with Kaolinite content under 40 %. The success of the first phase enable the teams to enter on a second phase, which addressed the formulation and further test of a ternary blend cement composed of clinker and a synergetic blend of calcined clays and limestone, with clinker content under 50 %. As a proof of concept, the Cuban cement industry favored the realization of an industrial trial where bulky amounts of the new cement were produced on experimental sites.

1 Introduction

Portland cement is one of the most frequently used materials in modern life and is today associated with the level of development of a country [1]. The amount of cement manufactured in 2010 was 3.3 billion tonne. If average cement content in concrete is assumed to be 350 kg/m^3, approximately 12 billion m^3 of concrete were produced in 2010, which is equivalent to approximately 1.5 m^3 of concrete per inhabitant of planet Earth. No other material compares to cement and concrete in terms of volume of production [2].

J.F.M. Hernandez (✉)
CIDEM, Universidad Central de las Villas, Santa Clara, Cuba
e-mail: fmartirena@ecosur.org

K. Scrivener
LMC-Ecole Polytechnique Fédéral de Lausanne, Écublens, Switzerland

K. Scrivener and A. Favier (eds.), *Calcined Clays for Sustainable Concrete*,
RILEM Bookseries 10, DOI 10.1007/978-94-017-9939-3_40

Because of the huge production of cement and concrete for the construction sector, approximately 10 % of the total anthropogenic emissions of CO_2 are related to concrete manufacture; 85 % of these emissions are produced during the manufacture of cement, that is, approximately 6–8 % of the world's CO_2 emissions [3]. Any minor change in the manufacturing procedure could have a huge impact on CO_2 released to the atmosphere.

A path to improving sustainability is the use of Supplementary Cementitious Materials, SCM as partial replacement for clinker. Calcined clays become a better choice for both industrialized and developing countries. Clays are evenly distributed throughout the earth. Clay deposits, though not-renewable, can be exploited within certain limits without inflicting a severe damage to the environment, and their availability exceeds that of any of the other SCMs known by far. Metakaolin (MK), that is, the activation of the mineral kaolinite at temperatures between 600–700 °C, is the main commercial application for calcined clays [4]. MK, however, is still a very expensive material, because its production is energy intensive and demands clay with a high degree of purity.

This paper presents the results of collaborative work carried out by two academic institutions; EPFL in Switzerland and UCLV at Cuba, focused on the use of calcined clays for the manufacture of sustainable binders.

2 Low Grade Calcined Clays as Pozzolans

A research team with Cuban and Swiss scientists has been assembled at EPFL, funded by a collaborative effort between the Swiss Development Foundation and the Swiss National Foundation. This team has worked in two phases, each funded separately by the SDC-SNF project funding scheme. The main objective of phase I (2005–2008) was to assess the possibility of producing MK-like materials using low grade clay, with kaolinite content under 40 %. This avoids the problem of the very high price of metakaolin from high purity clays.

The aim of the work was to assess the possibility of producing MK-like materials using low grade clay, with kaolinite content under 40 %. The first part of the work consisted in studies to understand the influence of the nature of the clayey structure on the pozzolanic potential of the calcined product. The decomposition of different clayey structures could be followed and it was concluded that the mineral kaolinite, in the range of 600 °C to 800 °C, presented the major losses in crystallinity and lack of short range order, increasing therefore its potential of interaction with calcium hydroxide when mixed with cement. The percentage of kaolinitic clay of a soil was thus a determining factor for its use as pozzolanic material to substitute cement [5].

A Cuban clayey soil from Manicaragua composed of a variety of minerals including quartz, feldspar and 3 types of clays (kaolinite, illite and montmorillonite) was studied. The kaolinite content of the soil was 17 %. In order to increase its pozzolanic potential, the clayey fraction of the soil was extracted by a sedimentation process and the kaolinite content of the clay obtained was 40 % [6].

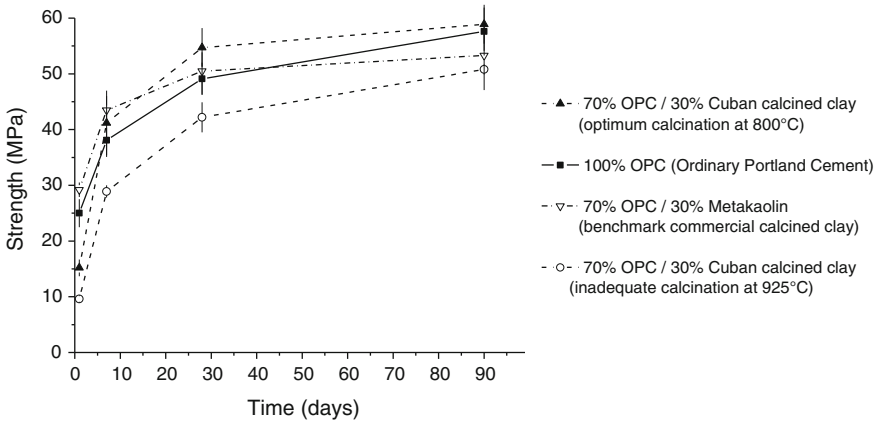

Fig. 1 Compressive strength development of Portland-calcined Cuban clays blends compared to standard Portland cement and Portland cement with highly active metakaolin

Characterization of the materials after calcination allowed us to identify an optimum temperature window, which was a compromise between loss of crystallinity and agglomeration of the clayey particles due to sintering phenomena. 800 °C was found to be the optimum activation temperature for both the soil and the clayey material.

The study of the interactions with cement was done by substituting 30 % of cement by calcined clays in the production of pastes and mortars. It was shown that a clay calcined at its optimum activation temperature had a high pozzolanic activity that was translated by a consumption of the calcium hydroxide produced by the cement during its hydration. This contributed to the final compressive strength of the materials (see Fig. 1) [5, 6].

The main conclusion is that kaolin-containing clayey soils, which are widely available, can be thermally activated to exhibit high pozzolanic activities in contact with cement. This allows reasonably high levels of substitution of cement in concrete by calcined clays without compromising the strength nor the durability of the building materials produced. Due to the lower embodied energy of these blends compared to ordinary concretes, these materials could represent a more ecological and economical alternative for rural and sub-urban communities in developing countries.

3 Ternary Blend Clinker-Calcined Clays-Limestone

The second phase of the project (2009–2012) focused on the investigation of the synergies between CCL and limestone, LS, to enhance the pozzolanic reaction and thus move the boundaries for clinker substitution further by producing a ternary

blend clinker-CCL-LS with much lower clinker content. This work was jointly done in Santa Clara and Lausanne. The new cement was coined as Low Carbon Cement, LC3.

There are already reports of such an approach for ternary Portland limestone blends with alumina rich pozzolans. [7, 8] and Moesgaard et al. [9] have worked in fly ash-limestone-Portland cement systems, and they have reported an increase of the mechanical properties caused by the synergy between the fly ash and limestone, which favors the formation of carboaluminate phases that provide a beneficial contribution of the performance of the system. [10] have worked on similar systems, and the synergy established between the Metakaolin and limestone, as well as its contribution to improving the mechanical properties of cementitious systems with high level of clinker substitution has been proven.

Based on this cementitious system, a mass of clinker can be replaced by the same mass of a mix of CCL/calcium carbonate having a 2:1 molar ratio, and yet form new hydration products capable of filling out the pore system in the matrix, thus contributing to improve strength. A prognosis based on thermodynamic modeling shows that up to 60 % of clinker can be substituted without decreasing the total volume of reaction products produced during cement hydration, thus the strength should not be compromised. The alumina phases are faster in reacting, thus the strength gain at early ages is not compromised. This cementitious system can move the boundaries of clinker substitution further without compromising performance compared to a normal OPC, as presented in Fig. 2 [10].

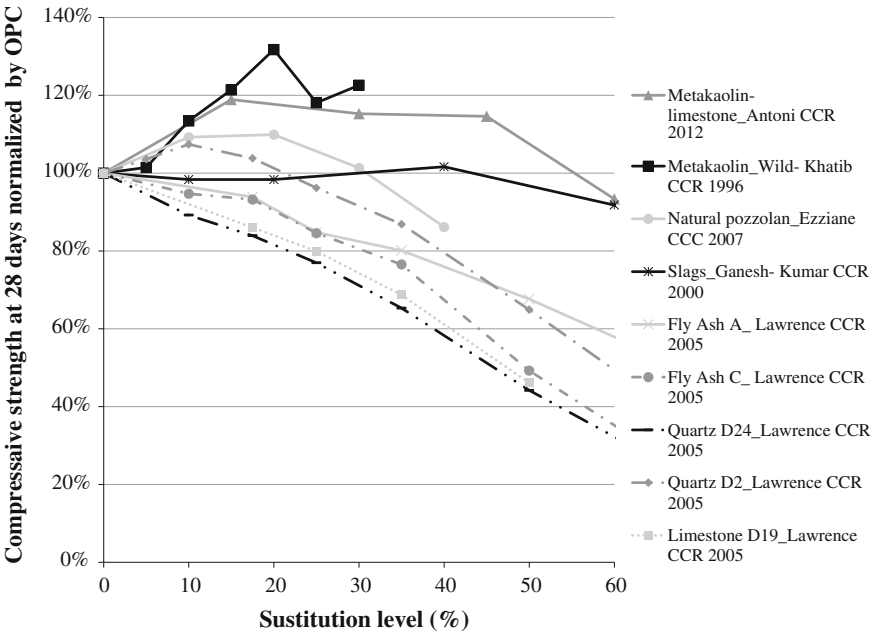

Fig. 2 comparison of 28d strength in different cementitious systems

LC3 is produced by using the ternary systems of clinker-calcined clays and limestone described above. Medium purity kaolinite clay has proven to be a good alternative to MK in this system, thus increasing the availability and reducing production cost of the cement. The LS introduced to the system is not calcined, thus no extra CO_2 is emitted to the environment.

LC3 cement proves to be far more efficient than any other binary pozzolanic blend. The new type of cement demands needs optimisation of the sulphate addition at all replacement levels. The replacement of cement by the blend of kaolinitic clay and limestone is associated with increasing reactivity of the aluminates phases, due to the aluminates content of the metakaolin. A correct sulphate level allows a good mechanical strength development by retarding sufficiently the aluminates peak to allow the main peak of the C3S hydration to occur [11].

4 Industrial Trial for the Production of LC3 in Cuba

The promising lab results prompted for an industrial trial for the production of bulky amounts of cement under real conditions. The Cuban cement industry designated the cement factory Siguaney for the industrial trial. The target ternary cement should have clinker content around 50 %. The trial included the calcination of 110 tonnes of CCL; mixing and homogenizing of the calcined material with LS in a 2:1 ratio; and co-grinding of the synergetic materials with clinker and gypsum.

For the trial, clay from the clay deposit Pontezuela was selected. The material is classified by the authors as a medium grade kaolinite clay, with an average content of kaolinite of 48.6 %. The clay was fed to the kiln and then heated to the 750 °C, temperature chosen as optimal for calcination of the material [4–6].

The pozzolanic reactivity of the calcined material was assessed through the compressive strength of standardized mortars, in which 30 % wt. of cement is replaced by the pozzolanic material. The reactivity of the material calcined in the rotatory kiln (average of batches) proved to be similar to that of the material calcined at the lab, thus indicating that the industrial calcination was successful.

Grinding was made under industrial conditions, by using a ball mill with a double chamber grinding system. In order to avoid high specific surface, it was decided to grind the material rather on the coarse side [12].

The final cement was characterized following the protocol established for blended cements in Cuban standards. Excess grinding of some softer materials through the interaction with other harder ingredients can be produced during the co-grinding process. This can have an influence on the grain size distribution of the cement, and it could eventually increase water demand of the mix. Results of the physical and mechanical tests are presented in Table 1.

Trial productions of several types of concrete were made using the LC3 produced at the industrial trial. Materials such as hollow concrete blocks having size 500 × 200 × 150 mm and 25 MPa precast concrete elements were made. Mix design was accredited by the laboratory of the National Enterprise for Applied Research, in

Table 1 Results of physical and mechanical test of the industrial low carbon cement

Material	Retained 4900 Sieve (%)	Consistency (%)	Setting time		Volume stability (mm)	Compressive strength (Mpa)		
			Initial (min)	Final (hr)		3d	7d	28d
LC3	12.0	25.0	135	2.9	0.3	11.0	17.5	30.3

Cuba, following the regulations of Cuban standards. All the materials produced met requirements of the Cuban standards [12].

A preliminary estimation of cost and CO_2 emission figures was made in order to compare LC3 with existing cements. Blended cements with clinker substitution up to 30 % enable reduction of approximately 15–20 % of the CO_2 emissions. LC3 produced in non-optimized conditions during industrial trial, reduces approximately 270 kg CO_2/tonnes in relation to OPC (P-35), this is approximately 31 %. Reduction in reference to traditional Cuban blended cement (PP-25) is in the range of 125 kg CO_2/tonne. P-35 and PP-25 are both regularly produced at cement plant Siguaney.

The introduction of LC3 brings about marginal cost reductions. Savings are associated with the lower firing temperatures of CCL, which reflect on direct energy costs. Estimates range around 15–18 % savings related to OPC currently produced under Cuban conditions.

5 Conclusions

The collaborative work carried out between EPFL and CIDEM in the period 2006–2012 has yielded a new strategy to meet environmental challenges in cement production, among them, the shift from traditional SCMs whose scarcity is proven to more abundant SCMs such as low-grade calcined clays, which prove a reasonably good reactivity even for very low kaolinite content. Further, moving clinker substitution boundaries further, to limits around 50 %, without compromising the performance of the cement produced, and finally, by proving the robustness of the production system through an industrial trial carried out under far from optimal conditions in Cuba for the production of LC3 and its use in common applications on the industry.

References

1. Schneider, M. et al.: Cement and concrete research sustainable cement production—present and future. Cem. Concr.Res., **41**(7), 642–650 (2011). Available at: http://dx.doi.org/10.1016/j.cemconres.2011.03.019
2. CEMBUREAU: Building a future, with cement & concrete. Adapting to climate change by planning sustainable construction (2010)

3. Habert, G. et al.: Cement and concrete research cement production technology improvement compared to factor 4 objectives. Cem. Concr. Res., **40**(5), 820–826 (2010). Available at: http://dx.doi.org/10.1016/j.cemconres.2009.09.031
4. Sabir, B., Wild, S., Bai, J.: Metakaolin and calcined clays as pozzolans for concrete: a review. Cem. Concr. Compos. **23**, 441–454 (2001)
5. Fernandez, R., Martirena, F., Scrivener, K.L.: The origin of the pozzolanic activity of calcined clay minerals: a comparison between kaolinite, illite and montmorillonite. Cem. Concr. Res. **41**(1), 113–122 (2011)
6. Alujas, A., Fernández, R., Quintana, R., Scrivener, K.L., Martirena, F.: Pozzolanic reactivity of low grade kaolinitic clays: influence of calcination temperature and impact of calcination products in OPC hydration. Appl. Clay Sci. **108**, 94–101 (2015)
7. De Weerdt, K., Haha, M.B., Le Saout, G., Kjellsen, K.O., Justnes, H., Lothenbach, B.: Hydration mechanisms of ternary Portland cements containing limestone powder and fly ash. Cem. Concr. Res., **41**(3), 279–291. Available at: http://dx.doi.org/10.1016/j.cemconres.2010.11.014
8. De Weerdt, K., Kjellsen, K.O. et al.: Synergy between fly ash and limestone powder in ternary cements. Cem. Concr. Compos., **33**(1), 30–38 (2011). Available at: http://dx.doi.org/10.1016/j.cemconcomp.2010.09.006
9. Moesgaard, M. et al.: Physical performances of blended cements containing calcium aluminosilicate glass powder and limestone. Cem. Concr. Res., **41**(3), 359–364 (2011). Available at: http://dx.doi.org/10.1016/j.cemconres.2010.12.005
10. Antoni, M. et al.: Cement substitution by a combination of metakaolin and limestone. Cem. Concr. Res., **42**(12), 1579–1589 (2012). Available at: http://linkinghub.elsevier.com/retrieve/pii/S0008884612002074. Accessed 18 Sept 2014
11. Andrés, L.V., Mathieu, G., Hernández, M., José F.; Scrivener, K.L.: Advances in cement research effect of fineness in clinker-calcined clays-limestone cements. Adv. Cem. Res. (2015)
12. Vizcaíno-Andrés, L.M., Sánchez-Berriel, S., Damas-Carrera, S., Pérez-Hernández, A., Scrivener, K.L., Martirena-Hernández, J.F.: Industrial trial to produce a low clinker, low carbon cement. Materiales de Construcción, **65**(317) (2015)

Influence of Calcination Temperature in the Pozzolanic Reactivity of a Low Grade Kaolinitic Clay

Adrián Alujas and J. Fernando Martirena

Abstract The influence of thermal activation temperature in the pozzolanic reactivity of low grade kaolinitic clay is assessed in this paper. The raw material, with approximately 40 % kaolinite and 40 % of 2:1 clay minerals, was calcined to temperatures ranging between 500–1000 °C. Mortars with a 30 % replacement of OPC by the clay calcined at 800 °C, a temperature representing the best compromise between structural disorder of the clay fraction and its specific surface, show values of compressive strength from seven days on similar or higher than the reference 100 % OPC mortars. Pozzolanic reactivity assessed by cumulative heat of lime-pozzolan pastes are in correspondence with these results. The increase in compressive strength with calcination temperature up to 800 °C could be associated to a more complete thermal activation of the multicomponent clay fraction. The experimental results indicate that low grade kaolinitic clay deposits with moderate contents of kaolinite constitute a potential source of high reactivity pozzolanic materials.

1 Introduction

Because of their relatively abundance and their proven pozzolanic properties once calcined under specific conditions, there is a growing interest in calcined clays as SCM,. Most of the studies on calcined clays focus on specific clay minerals, particularly kaolinite, which have shown the highest pozzolanic activity and the lower activation temperature [1–3]. Although the occurrence of kaolinite is common on

A. Alujas (✉)
Centro de Estudios de Química Aplicada, Universidad Central de Las Villas, Santa Clara, Cuba
e-mail: adrianad@uclv.edu.cu

J. Fernando Martirena
Centro de Investigación y Desarrollo de Estructuras y Materiales, Universidad Central de Las Villas, Santa Clara, Cuba

K. Scrivener and A. Favier (eds.), *Calcined Clays for Sustainable Concrete*, RILEM Bookseries 10, DOI 10.1007/978-94-017-9939-3_41

the earth crust, commercially usable high grade kaolin deposits are relatively few in number and find extensive application in several industrial sectors other than cement industry [4]. This reflects in a limited availability and relative high prices for metakaolin in comparison with other SCMs. However, clays highly often occur in nature as common clays, containing different clay and non-clay minerals. Thus, the potential to use these multicomponent clays as pozzolanic materials is of great interest. Of particular interest are low grade kaolinitic clay deposits, where relative large quantities of non-kaolinite clay and non-clay minerals limit their exploitation in traditional industrial applications of kaolinitic clays. Although the performance of calcined high grade kaolinitic clays is well documented in the literature, there are limited references on the thermal activation and pozzolanic reactivity of low grade kaolinitic clays, a topic that would be assessed in this paper.

2 Results and Discussion

2.1 Characterization of the Raw Material and Its Calcination Products

Clay used in this study was collected from a secondary clay deposit located at the province of Villa Clara, Cuba. After being dried and ground for 30 s in a disc mill, the raw material was calcined at temperatures ranging between 500 and 1000 °C for 60 min. The raw materials and their calcination products were chemically and mineralogically characterized by XRF, XRD, FTIR, and TGA-DTA. Particle Size Distribution (PSD) of the raw material and their calcined products were analyzed by laser granulometry, and the specific surface area was determined by BET-nitrogen adsorption analysis.

Kaolinite, illite and montmorillonite are identified as the main clay minerals by XRD (Fig. 1) whereas low amounts of quartz and feldspars are also present as companion minerals. The presence of kaolinite is also confirmed by FTIR analysis (Fig. 2), where it is identified by four absorption bands in the 3000–4000 cm^{-1} spectral region, corresponding to the asymmetric stretching vibrations of structural O-H groups [5]. The relatively high content of Fe_2O_3 (Table 1) in the sample is mainly related to the presence of iron oxyhydroxides.

The mass loss up to 250 °C shown in TGA curves (Fig. 3a) is due to the presence of water adsorbed on the surface and in the interlayer region of expandable clays, and could be associated to the presence of montmorillonite or poorly crystalline illite, whereas mass loss in the 250–350 °C range is assigned to the decomposition of iron oxyhydroxides. The dehydroxylation of clay minerals present in the raw material takes place between 350 and 900 °C. Up to temperatures close to 600 °C this effect is dominated by dehydroxylation of kaolinite, for which this dehydroxylation represents approximately 13.9 % loss by mass [6], and roughly represents 75 % of the total degree of dehydroxylation of the clay, as shown in Fig. 3b. At higher temperatures, the degree of dehydroxylation gradually

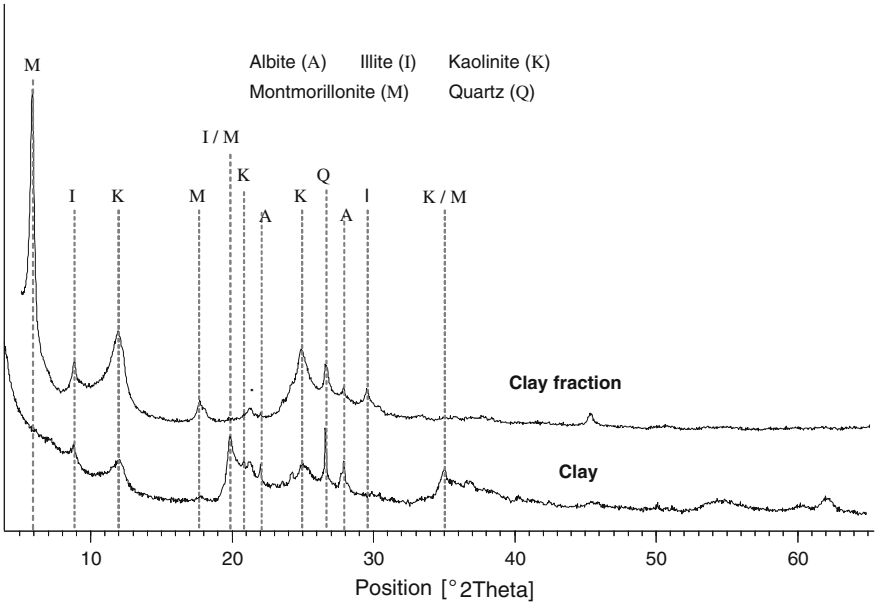

Fig. 1 XRD pattern of the clay and the clay fraction

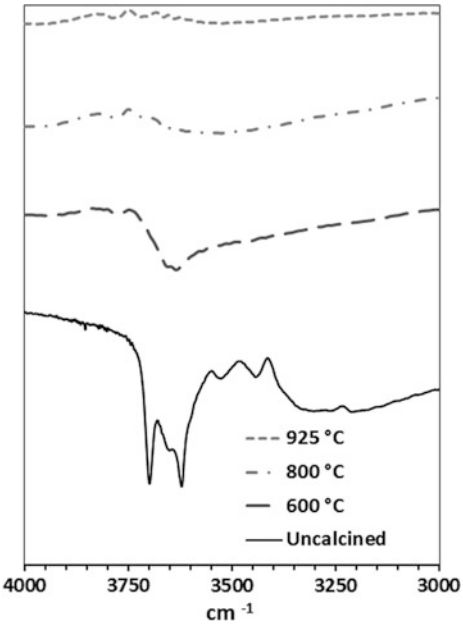

Fig. 2 FTIR spectra of the clay and its calcination products

Table 1 Chemical composition of the uncalcined clay

SiO_2	Al_2O_3	Fe_2O_3	CaO	MgO	SO_3	K_2O	Na_2O	Others	LOI
43.89	24.73	11.13	1.38	2.63	0.08	1.10	1.99	3.25	9.81

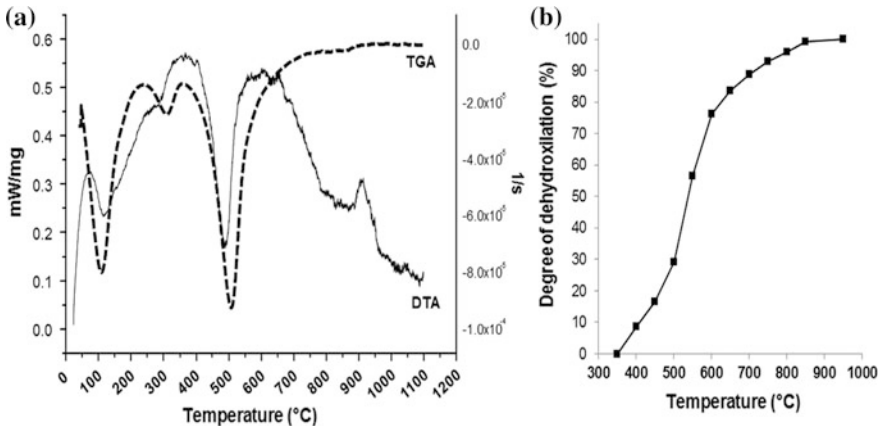

Fig. 3 TGA–DTA curves (**a**) and dehydroxylation degree (**b**) of the raw clay

increases up to temperatures close to 900 °C, where clay dehydroxylation is assumed to be completed. For the temperature range 600–900 °C, the mass loss is mainly assigned to the dehydroxylation of 2:1 clay minerals, for which it represents approximately only 5 % by mass [6]. The dehydroxylation temperature for montmorillonites typically ranges between 550–850 C, whereas for illite this effect could take place between 600–900 °C as a broad, low intensity peak, which increase overlapping with the thermal decomposition of other clay minerals [3]. By assignment of mass loss in the 350–600 °C temperature range to kaolinite [3, 6], the content of the clay mineral could be estimated approximately: kaolinite (40 %), 2:1 clay minerals (illite and montmorillonite) (40 %). The main sources of error on this estimation are due to potential isomorphic substitution in the clay structures, and to the overlap of the dehydroxylation temperature intervals.

XRD patterns for materials calcined in the 500–1000 °C range indicates the collapse of the basal and non-basal planes of kaolinite already at 500 °C. The collapse of the montmorillonite structure occurs around 800 °C, whereas the collapse of the illite structure and the detection of high temperature crystalline phases such as mullite and cristobalite are observed simultaneously around 900 °C. This is in good agreement with the DTA exothermal peak in the same range of temperatures (Fig. 3), typical for crystallization phenomena [1, 2, 7–9]. Therefore, 925 °C is considered as the high temperature limit for the thermal activation window of the studied clay. From this point on, structural disorder begins to decrease because of the onset of the recrystallization phenomena. The FTIR spectra show that absorption bands corresponding to kaolinite on the 3000–4000 cm^{-1} spectral region for

Table 2 Median diameter and specific surface of calcined clay

Calcination Temp. (°C)		500	600	700	800	850	925	1000	LOI
Sp. Surface (m^2/g)	40.76	42.38	43.81	35.63	32.09	4.95	1.03	0.39	9.81

samples calcined at 600 °C disappear, but a low intensity broad band, characteristic of dioctahedral montmorillonite [5] could still be detected, thus indicating that at this calcination temperature kaolinite could be considered as completely dehydroxylated and that montmorillonite structure is less severely affected.

The average particle size distribution gradually coarsens with calcination temperature up to 800 °C (Table 2), and for higher calcination temperatures this trend is rapidly accelerated, probably associated with sintering phenomena [10], as shown also by the decrease in specific surface. The slight increase on specific surface from 500 to 600 °C has been previously reported by He et al. [8] and it is attributed to the partial structural disorder of the kaolinite interlayer region that accompanies the dehydroxylation process.

2.2 Pozzolanic Reactivity of Calcined Clays

The pozzolanic activity of calcined clays was assessed by two methods: (1) Compressive strength in mortars made with a blend of OPC-pozzolan and (2) cumulated heat in lime-pozzolan pastes determined by Isothermal Calorimetry (IC). Mortar prisms were prepared following European Standards (EN) 196-1 at a water/solid ratio of 0.5. A type I OPC (42.5R) was used for the assessment of pozzolanic reactivity by compressive strength in OPC-pozzolan mortars. The substitution level of OPC by calcined clays was fixed to 30 % by mass, and 30 °C was chosen as the curing temperature to better simulate natural conditions in the Cuban tropical environment. To differentiate between the filler effect and the pozzolanic contribution of calcined clays in the blended systems, a ground quartz powder (Dv50 = 14.9 μm) was used for comparison, assuming that it would behave as a chemically inert material.

For the measurement of cumulative heat released by pozzolanic reaction using IC, lime–pozzolan pastes were prepared using a liquid/solid ratio of 0.8 and a calcium hydroxide/pozzolan ratio of 2/3. This ratio roughly corresponds to the portlandite/calcined clay ratio in a blended system were 30 % of OPC has been substituted by calcined clay, and still ensures enough availability of calcium hydroxide for the pozzolanic reaction. A 0.5 M NaOH was used instead of pure water, to accelerate the pozzolanic reaction by alkali dissolution of reactive phases. IC was conducted for 72 h at 30 °C, using a TAM AIR calorimeter.

Clays calcined at temperatures of 600 °C (high specific surface, practically complete dehydroxylation of kaolinite and incomplete decomposition of 2:1 clay minerals); 800 °C (partial decomposition of the clay fraction, best compromise

Table 3 Compressive strength in mortars (MPa)

	A-ref	A-66	A-86	A-96	A-filler
1 day	25.01	12.94	15.39	9.54	12.07
7 days	38.12	35.27	41.22	28.74	29.57
28 days	49.10	50.02	54.78	42.27	35.73
90 days	57.55	53.70	58.89	50.60	40.62

between structural disorder and specific surface); and 925 °C (total decomposition of the clay fraction, low specific surface, marks the onset of the recrystallization phenomena) were studied. Denomination of the different series are given by the letter A followed by a code representing the material used as OPC substitution: 66–600 °C calcined clay; 86–800 °C calcined clay; 96–925 °C calcined clay; Filler—Quartz filler. Reference series (100 % OPC) is denominated as A-Ref.

Compressive strengths (Table 3) at 1 day for all blended systems are considerably lower than for the OPC, because the amount of hydration products formed through the pozzolanic reaction did not yet compensate for the dilution effect. At early ages, the main contribution of SCMs to the hydration process is strongly related to the filler effect [11]. As the strength values are similar to the filler system, it can be concluded that at 1 day, all calcined clays behave predominantly as fillers. The pozzolanic reaction starts to become significant between 1 and 7 days, as can be observed by the evolution of compressive strength for mortars containing clays calcined at 600 and 800 °C from 7 days onwards. Clay calcined at 800 °C exhibits the highest contribution to the increase of compressive strength, with values for the A-86 series matching or exceeding those of the control series at all ages from 7 days onwards. This behavior suggests the presence of more reactive material in comparison with clay calcined at 600 °C, which should have been favored by its higher specific surface. Calcination temperatures close to 900 °C decrease the specific surface and represent the onset for structural reorganization of aluminosilicates, both factors that limit the pozzolanic reactivity, as could be observed from the low contribution to the compressive strength of the clay calcined at 925 °C. However, these values are higher than for the filler series from 28 days on, which indicates that even at this high calcination temperature there is still some contribution to the pozzolanic reaction.

The cumulative heat from isothermal calorimetry of the lime-pozzolan pastes at 1, 2 and 3 days are shown in Fig. 4. The cumulative heat released at different ages is assumed to be directly proportional to the degree of reaction and therefore to the pozzolanic reactivity of the tested materials. According to their cumulative heat values at all ages, the clay calcined at 800 °C shows the highest pozzolanic reactivity, followed by the raw material activated at 600 °C, whereas clay calcined at 925 °C exhibits the lowest pozzolanic reactivity. These results are in correspondence with the trend in compressive strength of the blended cement mortars.

Previous studies found that the structural disorder of kaolinite slightly increased in the 600–800 °C temperature range [3, 8]. However, the increase in structural disorder in this temperature range is minor compared to that caused by

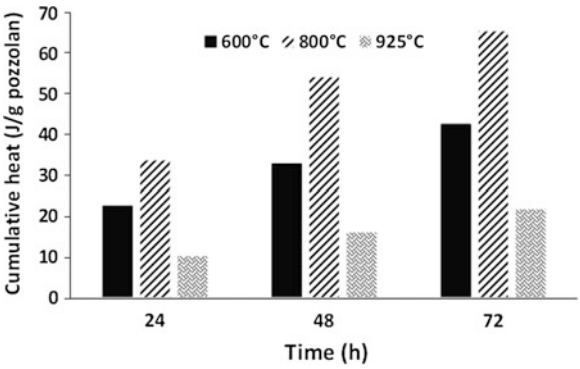

Fig. 4 Cumulative heat of lime-calcined clay pastes

dehydroxylation at lower temperatures [2, 8], while the structural disorder of montmorillonite, with an overall pozzolanic reactivity much lower than for kaolinite, increases around temperatures close to 800 °C, as previously shown by XRD and FTIR. Thus, the increase on pozzolanic reactivity with the increase of calcination temperature from 600 to 800 °C could be considered as the combined contribution of both kaolinite and 2:1 type clays.

3 Conclusions

Mortars with a 30 % replacement of OPC by the investigated low grade kaolinitic clay, containing approximately 40 % kaolinite and 40 % of 2:1 clay phases, calcined at 800 °C, show values of compressive strength from seven days on similar or higher than the reference 100 % OPC mortars. Pozzolanic reactivity assessed by cumulative heat of lime-pozzolan pastes are in correspondence with the trend in mortar`s compressive strength. The experimental results indicate that low grade kaolinitic clay deposits with moderate contents of kaolinite constitute a potential source of high reactivity pozzolanic materials.

The increase in compressive strength with calcination temperature up to 800 °C could be associated to a more complete thermal activation of the multicomponent clay fraction. The pozzolanic reactivity appears to be primarily driven by dehydroxylation of kaolinite at temperatures around 600 °C, but at higher temperatures contribution from thermally activated 2:1 clays should not been ruled out.

The increase of pozzolanic reactivity with the increase of activation temperature is limited not only by recrystallization that take place above 900 °C, but also by the sudden decrease of the specific surface that occurs between 800 and 900 °C. The impact of the partial substitution of OPC by calcined clays on blended system hydration is a combination of a filler effect at early ages, and the pozzolanic reaction of the calcined clays later on.

References

1. He, C., Makovicky, E., Osbæck, B.: Thermal stability and pozzolanic activity of raw and calcined mixed-layer mica / smectite. Appl. Clay Sci. **17**, 141–161 (2000)
2. He, C., Osbaeck, B., Makovicky, E.: Pozzolanic reactions of six principal clay minerals: activation, reactivity assessments and technological effects. Cem. Concr. Res. **25**(8), 1691–1702 (1995)
3. Fernández López, R., Martirena Fernández, J.F., Scrivener, K.: The origin of the pozzolanic activity of calcined clay minerals: a comparison between kaolinite, illite and montmorillonita. Cem. Concr. Res. **41**, 113–122 (2011)
4. Murray, H.H.: Traditional and new applications for kaolin, smectite, and palygorskite: a general overview. Appl. Clay Sci. **17**(5–6), 207–221 (2000)
5. Madejová, J.: FTIR techniques in clay mineral studies. Vib. Spectrosc. **31**, 1–10, 2003
6. Todor, D.N.: Thermal Analysis of Minerals. Abacuss Press, Kent, p. 256 (1976)
7. He, C., Makovicky, E., Osbaeck, B.: Thermal stability and pozzolanic activity of calcined illite. Appl. Clay Sci. **9**(5), 337–354 (1995)
8. He, C., Makovicky, E., Osbaeck, B.: Thermal stability and pozzolanic activity of calcined kaolin. Appl. Clay Sci. **9**(3), 165–187 (1994)
9. He, C., Makovicky, E., Osbaeck, B.: Thermal treatment and pozzolanic activity of Na- and Ca-montmorillonite. Appl. Clay Sci. **10**, 351–368 (1996)
10. Lee, V.-G., Yeh, T.-H.: Sintering effects on the development of mechanical properties of fired clay ceramics. Mater. Sci. Eng., A **485**(1–2), 5–13 (2008)
11. Cyr, M., Lawrence, P., Ringot, E.: Efficiency of mineral admixtures in mortars: quantification of the physical and chemical effects of fine admixtures in relation with compressive strength. Cem. Concr. Res. **36**(2), 264–277 (2006)

Pozzolanic Reactivity of Low Grade Kaolinitic Clays: Influence of Mineralogical Composition

Adrián Alujas, Roger S. Almenares, Sergio Betancourt and Carlos Leyva

Abstract The influence of chemical and mineralogical composition of five Cuban clays in the pozzolanic reactivity of its calcination products is studied in this research. Raw materials were chemically and mineralogically characterized by XRF, XRD and TGA. Pozzolanic reactivity of 800 °C calcination products was evaluated by heat released in chemically modified lime-pozzolan pastes, and by compressive strength in mortars with a 30 % substitution of OPC by calcined clays. Preliminary results shown that pozzolanic reactivity of clays calcined at temperatures that guarantees a complete dehydroxylation of the raw materials could be qualitatively assessed by its relative positions along the diagonal trend in an Al_2O_3–SiO_2–OH^- ternary plot, where pozzolanic reactivity is related to the percent of structural hydroxyl groups and the percent of Al_2O_3 in the raw material. Conducted pozzolanic reactivity test highlight the potential of kaolinite rich red clay soils as source for the obtaining of highly reactive pozzolanic materials.

1 Introduction

As clays seldom occur in nature as highly pure deposits but rather as common clays, there is a growing interest in the use of these multicomponent clays deposits as source of pozzolanic materials. Of particular interest are low grade kaolinitic clay deposits, where low to moderate contents of kaolinitic clays ensures pozzolanic reactivity of calcination products, but where relative large quantities of

A. Alujas (✉)
Centro de Estudios de Química Aplicada, Universidad Central de Las Villas, Santa Clara, Cuba
e-mail: adrianad@uclv.edu.cu

R.S. Almenares · C. Leyva
Instituto Superior Minero-Metalúrgico de Moa, Holguín, Cuba

S. Betancourt
Facultad de Construcciones, Universidad Central de Las Villas, Santa Clara, Cuba

K. Scrivener and A. Favier (eds.), *Calcined Clays for Sustainable Concrete*, RILEM Bookseries 10, DOI 10.1007/978-94-017-9939-3_42

non-kaolinitic clays and other companion minerals limit their industrial exploitation in traditional applications for kaolinite. In the obtaining of pozzolanic materials from these multicomponent clay deposits, the reactivity of calcination products will be determined by the combined contribution of each clay mineral present in the sample and how they are affected by thermal activation, unlike high grade clay deposits, where the development of pozzolanic reactivity will be dominated by the contribution of one clay mineral. Due to the mineralogical complexity of these multicomponent clayey materials, strategies are required that may include a comprehensive approach of the influence of the chemical and mineralogical composition of raw materials in the pozzolanic reactivity of its calcination products. This kind of tools will allow a better assessment of low grade kaolinitic clay deposits as potential source of pozzolanic materials. In this research, the influence of chemical and mineralogical composition of five Cuban clays in the pozzolanic reactivity of its calcination products is studied.

2 Results and Discussion

2.1 Characterization of the Raw Materials

Clay used in this study were collected by representative sampling of different clay deposits located at the central and eastern regions in Cuba. Selection was made based on its estimated reserves and its distance to cement plants, in order to guarantee future exploitation as source of pozzolanic material for the cement industry. A brief geological description of the clay deposits is presented in Table 1. Chemical and mineralogical composition of clay samples, as determined by XRF and XRD respectively, are presented in Tables 2 and 3. In most samples (CG, PZ, LL, LS) minerals from the kaolinite group are dominant among clay minerals, although low or moderate contents of 2:1 clays are also present. Besides quartz, iron oxyhydroxides are almost ubiquitous as companion minerals, as it is frequent in Cuban tropical environment, where kaolinitic clays are frequently associated with oxisols [1], a factor that limits the use of these raw materials for traditional application of kaolinitic clays, such as paper industry, white ceramics or production of white cement [2]. Only the CT sample presents no kaolinite content, with

Table 1 Geological description of the clay deposits

LL/ LS	Primary origin, associated to hydrothermal alteration of acid tuffs. Presence of lateritic soils. Predominance of minerals from the kaolinite group
CG	In situ weathering of gabbros. Weathering crust rich in kaolinitic clays and Fe and Al oxyhydroxides
PZ	Hydrothermal alteration of tuffs and intrusive rocks. Abundance of lateritic soils. Abundance of kaolinitic clays in the clay fraction. Presence of smectites
CT	Redeposited. Abundance of feldspars, quartz and calcite. Montmorillonitic clays

Table 2 Chemical composition of the clay samples

	SiO_2	Al_2O_3	Fe_2O_3	CaO	MgO	SO_3	K_2O	Na_2O	TiO_2	Others	LOI
CT	51.29	10.40	5.24	13.09	2.265	0.09	0.84	1.04	0.54	0.42	14.80
LL	61.40	18.86	9.61	0.07	0.15	0.02	0.90	0.26	0.62	0.37	7.80
LS	50.88	25.23	12.58	0.28	0.95	0.02	0.32	0.08	0.98	0.38	8.39
CG	39.87	27.95	10.88	0.05	0.36	0.13	0.09	0.13	0.54	5.51	14.44
PZ	41.45	25.61	18.10	0.09	0.68	1.36	0.47	0.12	0.33	0.64	11.54

Table 3 Mineralogical composition of the clay samples

	Kaolinite/ Halloysite	Montmorillonite/ Illite	Quartz/ Cristobalite	Haematite/ Gohetite	Calcite
CT		++	++		++
LL	++		++	+	
LS	+++	+	++	+	
PZ	+++	+	++	++	
CG	+++	+	+	+	

Table 4 Content of structural OH^- in the clay samples

	CT	CT (*)	LL	LS	CG	PZ
OH^- (%)	12.02	1.74	9.85	8.30	10.03	9.10

montmorillonite being identified as the main clay mineral. High CaO content for this sample is associated to the presence of calcite as companion mineral.

Percent of hydroxyl groups in the raw materials was determined through TGA by weight loss in the 350–850 °C range, an interval of temperature that covers the whole range of dehydroxylation temperature for clay minerals [3, 4]. The result was normalized by sample weight at 200 °C, to avoid interference of hydration water, a factor that may be influenced by sample storage conditions. Results for content of structural hydroxyl groups are reported in Table 4. For sample CT, a correction was needed to subtract the contribution of calcite decomposition in the studied temperature range, under the assumption that all the CaO content is assigned to calcite. Corrected value is reported as CT (*) in Table 4.

2.2 Assessment of Pozzolanic Reactivity of Calcined Clays

Clay samples were calcined at 800 °C for 60 min. This calcination temperature guarantees a complete dehydroxylation of the raw materials, as determined by TGA. Pozzolanic reactivity of calcined clays was assessed by compressive strength

in mortars made with a 30 % substitution of calcined clays of OPC-pozzolan and measurement of cumulated heat in lime-pozzolan pastes by Isothermal Calorimetry (IC). The purpose of Isothermal Calorimetry test is to quantify pozzolanic reaction of the calcined clays in a simplified model system that simulate the chemical environment of the cement paste, where the pozzolanic reaction could be measured without interference of clinker hydration reactions. Therefore, soluble alkalis and sulphate were added to reproduce the cement pore solution pH and form similar reaction products such as ettringite and AFm phases, and proportions were selected to provide excess of reactants in relation to pozzolanic material. Mix design includes a sulphate to calcined clay ratio of 0.15, an alkali to calcined clay ratio of 0.20 and a portlandite to calcined clay ratio of 3.0. A water to solid ratio of 1.2 was used in order to provide excess water for the hydration reactions and to obtain a suitable paste workability. A ground quartz powder was used for comparison, assuming that it would behave as a chemically inert material The cumulative heat released is assumed to be directly proportional to the degree of reaction and therefore to the pozzolanic reactivity of the tested materials. According to the results for this test (Fig. 1) pozzolanic reactivity of calcined clays follow the sequence: CG > PZ > LS ≫LL ⋙ CT.

For calcined clays with the highest pozzolanic reactivity (PZ, CG) mortars were prepared using a type I OPC at a water/solid ratio of 0.5, following European Standards (EN) 196-1. The substitution level of OPC by calcined clays was fixed to 30 % by mass. A reference series, with 100 % OPC was also prepared. Mortars bars were cured at 20 °C and tested for compressive strength at 3, 7 and 28 days. Values for compressive strength were similar or slightly higher for PZ series in comparison with reference OPC series, whereas for CG series values of compressive strength were higher in comparison with reference OPC series at all ages (Fig. 2). Results of this test confirms the higher pozzolanic reactivity of CG sample in comparison with PZ sample and highlight the potential of kaolinite rich red clay soils to be used as sources for the obtaining of highly reactive pozzolanic materials.

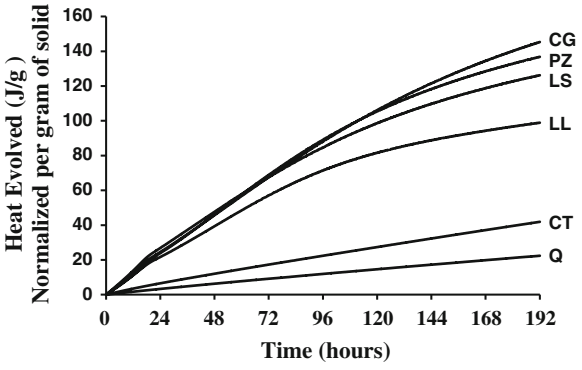

Fig. 1 Heat evolved normalized per gram of solid

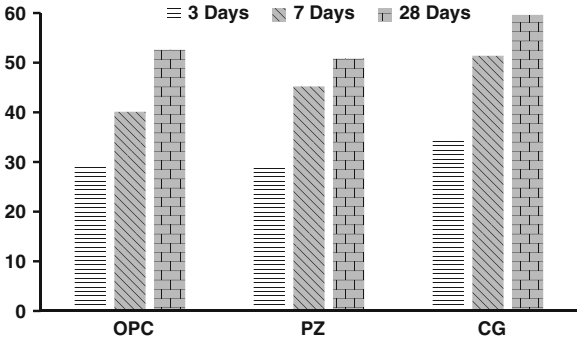

Fig. 2 Compressive strength of OPC-calcined clay mortars

2.3 *Influence of Mineralogical Composition on Pozzolanic Reactivity of Calcined Clays*

Pozzolanic reactivity of calcined clays depends on the content of potentially reactive material (directly related to Al_2O_3 and SiO_2 content) and the extent of structural disorder reached during thermal activation (directly related to the loss of hydroxyls groups). For low grade kaolinitic clays or for common clays, where pozzolanic reactivity could be considered as the combined contribution of all the clay minerals present in the sample, it is difficult to assigned the content of reactive phases or weight loss due to structural hydroxyls groups to one clay mineral in particular. Previous studies have shown that clay minerals from the kaolinite group (Al_2O_3 ~39.50 %; OH^- ~13.95 %) have the highest pozzolanic reactivity, whereas 2:1 clay minerals (Al_2O_3 ~28.50 %; OH^- ~5.00 %) exhibits only moderately high to low pozzolanic reactivity [3, 5, 6]. Then, it is reasonable to assume that even if the contribution of each clay mineral to pozzolanic reactivity could not be determined separately, the higher the overall Al_2O_3 and structural OH^- content in the raw material, the higher the potential pozzolanic reactivity of calcination products.

Contents of Al_2O_3, SiO_2 and structural OH^- of the studied clay samples (corrected value of % OH^- for CT sample) were charted in the ternary plot presented in Fig. 3. Lines 1:1 and 2:1 represent the path for increasing contents of 1:1 and 2:1 clay minerals respectively, as calculated from idealized formulas and assuming quartz as companion mineral. Under these assumptions, dotted lines in the diagram delimit the area assigned to clay minerals. However, this area should only be considered for reference purposes, as deviation from ideal behavior always arise due to the presence of isomorphic substitution in clay structure, the presence of alumina rich companion minerals or the minor contributions of other minerals to the weight loss in the analyzed temperature range.

The relative positions of clay samples along the trends pointed out by lines 1:1 (CG > PZ > LS ≫ LL) and 2:1 (CT(*)) are in good agreement with pozzolanic reactivity tests performed by Isothermal Calorimetry in lime-calcined clay pastes

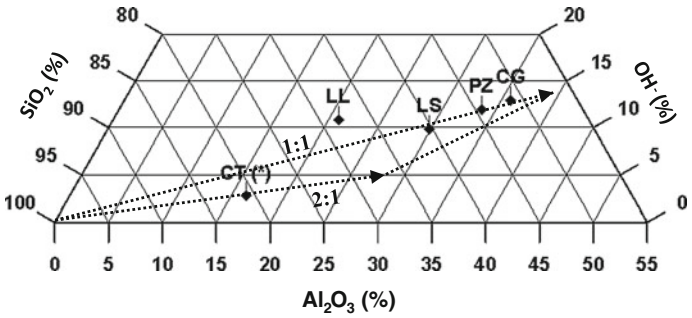

Fig. 3 Ternary plot Al_2O_3–SiO_2–OH^-

and by compressive strength in OPC-calcined clay mortars. The higher the position of the clay sample along the diagonal (increasing % of Al_2O_3 and OH^-), the higher the pozzolanic reactivity of its calcination products. Clay samples with high pozzolanic reactivity, where kaolinite is the dominant clay mineral, groups along line 1:1, whereas CT sample locates along line 2:1, in correspondence with its content of montmorillonitic clays and absence of 1:1 clay minerals in the clay fraction. According to the traditional approach, in which potential content of reactive material in clay samples is related uniquely to its content of structural hydroxyl groups, pozzolanic reactivity for LL sample (% OH^- = 9.85) should be higher than for LS sample (% OH^- = 8.30). This could be corrected in the ternary plot by also taking into account the chemical composition as an additional criterion, allowing a better correlation with results of pozzolanic reactivity tests.

3 Conclusions

For low grade kaolinitic clays, where pozzolanic reactivity could be considered as the combined contribution of all the clay minerals present in the sample, preliminary results shown that pozzolanic reactivity of calcination products is directly related to the percent of structural hydroxyl groups and the percent of Al_2O_3 in the raw material. Pozzolanic reactivity of clays calcined at temperatures that guarantees a complete dehydroxylation of the raw materials could be qualitatively assessed by its relative positions along the diagonal trend in an Al_2O_3–SiO_2–OH^- ternary plot. Results from pozzolanic reactivity test by compressive strength in mortars and released heat in lime-pozzolan pastes highlight the potential of kaolinite rich red clay soils as source for the obtaining of highly reactive pozzolanic materials.

Acknowledgments The authors would like to thanks the valuable collaboration of Francois Avet on the performance of lime-pozzolan reactivity tests, and the Laboratoires des Matériaux de Construction (LMC) of the École Polytechnique Fédérale de Lausanne (EPFL) for offering their facilities. The authors would also like to acknowledge to the Cuban Geological Services, for the technical support in clay deposits sampling.

References

1. Njila, T., et al.: An overview of non-nickeliferous weathering crusts in Eastern Cuba. Mineria y Geología **26**(2), 14–34 (2010)
2. Murray, H.H.: Traditional and new applications for kaolin, smectite, and palygorskite: a general overview. Appl. Clay Sci. **17**(5–6), 207–221 (2000)
3. Fernández López, R., Martirena Fernández, J.F., Scrivener, K.: The origin of the pozzolanic activity of calcined clay minerals: a comparison between kaolinite, illite and montmorillonita. Cem. Concr. Res. **41**, 113–122 (2011)
4. Habert, G., et al.: Clay content of argillites: influence on cement based mortars. Appl. Clay Sci. **43**(3–4), 322–330 (2009)
5. He, C., Makovicky, E., Osbæck, B.: Thermal stability and pozzolanic activity of raw and calcined mixed-layer mica/smectite. Appl. Clay Sci. **17**, 141–161 (2000)
6. He, C., Osbaeck, B., Makovicky, E.: Pozzolanic reactions of six principal clay minerals: activation, reactivity assessments and technological effects. Cem. Concr. Res. **25**(8), 1691–1702 (1995)

Industrial Manufacture of a Low-Clinker Blended Cement Using Low-Grade Calcined Clays and Limestone as SCM: The Cuban Experience

L. Vizcaíno, M. Antoni, A. Alujas, F. Martirena and K. Scrivener

Abstract The results of an industrial trial for the production and applications of a low-clinker blended cement—also called low carbon cement (LCC)—based on the system clinker-calcined clay-limestone are presented. A low-purity kaolinitic clay was calcined in a rotatory kiln and used in the manufacture of the ternary blended cement. The produced cement contains 50 % of clinker, 41 % of the combined addition calcined clay-limestone in a 2:1 proportion and gypsum. The ternary blend accomplish with the requirements of Cuban standards for blended cements although it exceed the allowed additions limit in 10 %. Concrete prefabricated elements made with the LCC under industrial conditions exhibit nice mechanical and permeability properties. It is estimated that the massive production of this type of cements may contribute to the reduction of CO_2 emission in more than 25 % related to daily practice.

1 Introduction

In the period 2000–2011 cement production was doubled to 3.6 billion tonnes [1, 2]. The increase of the demand has been founded on the development & growing of the so called "emergent economies", which need to build the infrastructure for the industrialization and urbanization in these countries.

Linked to the manufacture process of cement large amounts of CO_2 are released to the atmosphere. It is estimated that per each tonne of cement produced between 0.7–0.9 tonnes of CO_2 are released [3, 4]; these figures make cement industry

L. Vizcaíno (✉) · A. Alujas · F. Martirena
Centro de Investigación y Desarrollo de Estructuras y Materiales,
Universidad Central de Las Villas, Santa Clara, Cuba
e-mail: f.martirena@enet.cu

M. Antoni
Innovation, Product Technology, Holcim Technology Ltd, Holderbank, Switzerland

K. Scrivener
LMC, EPFL, Santa Clara, Cuba

K. Scrivener and A. Favier (eds.), *Calcined Clays for Sustainable Concrete*,
RILEM Bookseries 10, DOI 10.1007/978-94-017-9939-3_43

responsible of approximately 5–8 % of the global CO_2 emissions [5–7]. For 2050, demand is expected to raise to more than 5 billion tonnes [8–11], which may contribute to the increase of around 3 % of CO_2 emissions related to values reported in 2011 (calculated by the authors), if current conditions for production remain.

An established strategy for the reduction of CO_2 emissions during cement manufacture is the reduction of the amount of clinker used; for it is the main responsible of CO_2 emissions. This can be attained through the use of Supplementary Cementitious Materials (SCM) as clinker substitutes. However, when pozzolans are used; the substitution rate is around 35 %; which is not sufficient enough to drastically reduce the global carbon emissions associated with cement manufacture [12]. Further, the availability of suitable SCMs is limited and it is closely related with industrial development; which considerably affects developing countries [4]. The challenge for cement industry lays into increase clinker substitution levels to fulfil the expected demand of cement while a green profile is attained.

Use of limestone as SCM has become in a common practice in many countries, especially in Europe, although calcined kaolinite clays in the form of Metakaolin has proved to be a very effective pozzolan [13, 14]. A new ternary cementitious system has been developed by the authors of this paper that allows the increase of clinker substitution to 45 % without significantly influencing cement performance. The new system is based on the interaction of the aluminates supplied by calcined kaolinite clay and the carbonates from limestone; which enhances the pozzolanic reaction of the calcined clay; and thus enables a higher clinker substitution rate [15]. The CO_2 emissions associated to clinker are considerably reduced in the new system; and the $CaCO_3$ added to the system is not calcined; thus no extra CO_2 is not released to the atmosphere; this justifies the label "low carbon cement" (LCC) given to the cement.

Low grade kaolinite clay has proven to be a suitable alternative and its reserves are huge and better geographically distributed than pure kaolinite clay deposits currently used by the industry [16]. So, a calcined low grade kaolinite clay is used in the new system combined with limestone; both materials have higher availability than other SCMs.

This paper presents the results of an industrial trial carried out at a cement plant in Cuba for the production of the new cement at industrial scale. The performance of the ternary blend in the production of concrete under industrial conditions are also presented. Further, a preliminary environmental assessment of the production of the new cement was done, which included a comparison with cements produced industrially in Cuba.

2 Materials Characterization

For the industrial trial, clay from the Cuban deposit *Pontezuela*, was selected. The geology of the quarry results from the alteration of basic hydrothermal intrusive rocks and has an estimated average content of kaolinite of 48.5 % determined by

thermo gravimetric analysis (TGA). Clinker was produced at Siguaney cement factory in Cuba. Calcium sulfate and limestone originated also from Siguaney Cuba are used in the manufacture of plain Portland cement.

Chemical and mineralogical composition was assessed aided by X-Ray Fluorescence (XRF) and X-Ray Diffraction (XRD) using a Bruker AXS S4 Explorer spectrophotometer operating at a power of 1 kW and equipped with a Rh X-ray source while XRD measurements were carried out on powder with a Panalytical X'Pert Pro MPD diffractometer in a θ-θ configuration using CuKα source (λ = 1.54 Å) with a fixed divergence slit size of 0.5°. Samples were scanned on a rotating stage between 4 and 65 [°2θ] using an X'Celerator detector with a step size of 0.0167°2θ and a time per step of 30 s.

Results of chemical composition are presented in Table 1. XRD of the clayey material confirmed, besides kaolinite, the presence of companion mineral such a quartz, goethite and a non-identified 2:1 clay. The content of gypsum in the raw material to be used to produce the cement was determined by combining XRD and XRF. Bassanite ($CaSO_4 \cdot 0 \cdot 6H_2O$ was detected by XRD, with only minor traces of other calcium sulfates, this corresponds to around 71 % bassanite according to sulfur trioxide (SO_3) content by XRF; further, minor quantities of quartz, feldspar and carbonates were identified. Limestone used had 92 % of calcium carbonate ($CaCO_3$) as determined by thermogravimetric analysis (TGA), with minor amounts of quartz identified by XRD.

TGA on samples of about 50 mg of pieces crushed in an agate mortar were done with a Mettler-Toledo TGA/SDTA 851 balance using a 10 °C/min ramp from 30 to 900 °C under a 30 ml/min flow of N_2.

Table 1 Chemical composition of raw materials used

Oxides (%)	Clay sample 1	Clay sample 2	Clay sample 3	Clinker	Limestone	Gypsum
SiO_2	54.7	54.2	55.0	20.1	6.4	4.6
Al_2O_3	27.8	28.2	26.0	5.1	2.1	1.4
Fe_2O_3	12.1	12.3	13.4	4.8	1.2	1.4
CaO	1.7	1.7	1.8	66.6	88.9	36.1
MgO	0.9	0.9	1.0	1.2	0.7	2.3
SO_3	0.0	1.4	0.7	0.7	0.1	38.6
Na_2O	0.3	0.3	0.3	0.2	0.0	–
K_2O	1.5	1.6	1.6	0.6	0.2	0.4
TiO_2	0.8	0.8	0.8	0.2	0.1	0.2
P_2O_5	0.2	0.1	0.2	0.1	0.1	–
Mn_2O_3	0.0	0.0	0.0	0.1	0.0	–
Cr_2O_3	1.6	–	–	0.1	0.0	–
LOI	10.4	10.3	9.8	7.4	40.1	14.8
Humidity	3.5	6.1	2.9	0.1	0.1	3.9
Kaolinite	49.7	48.2	47.5	–	–	–

3 Procedures and Experimental Techniques

For clay calcination a wet process rotary kiln—regularly used for clinker production- was modified in order to calcine the material on dry conditions. The raw clay was fed to the kiln and heated to approximately 750 °C; temperature chosen as the optimal for *Pontezuela* clay based in previous laboratory results [17].

After the calcination 90 tonnes of calcined material were obtained and stored in five heaps. The quality of calcination was assessed through the dehydroxylation of the calcined clay by using TGA and the structural disorder followed by XRD. The pozzolanic reactivity of the calcined clay was assessed through the compressive strength of standardized mortars according to EN 196-1, in which 30 % wt. of cement is replaced by the pozzolanic material, following the protocol of Fernández and Antoni [15, 18]. Two reference series were prepared with 100 % of ordinary Portland cement (OPC) and cement with 30 % wt. pozzolanic material calcined under optimal conditions at the laboratory with a Naberthern oven LH30/14. The compressive strengths were measured at 3, 7, and 28 days.

Grinding was made under industrial conditions by using a ball mill with a double chamber grinding system. In order to avoid high specific surface, it was decided to grind the material rather on the coarse side. Excess grinding of some softer materials through the interaction with other harder ingredients can be produced during the co-grinding process. This can have an influence on the grain size distribution of the cement; and it could eventually increase water demand of the mix [19]. Gypsum was adjusted to optimize the reaction of the alumina phase [15], but the total SO_3 content was adjusted to fulfill cement standards. Finally; grinding parameters were set as: 10–12 % retained in the 90 μm sieve; specific surface measured by Blaine test between 4000–5000 cm^2/g and SO_3 up to 3.0 %. Grinding was completed in 8 h. Samples of the material were taken every approximately 30 min.

Final cement was characterized by determining its physical, mechanical and chemical properties according to Cuban standards for blended cements [20–24].

Batches of the cement produced were distributed among builders and building material manufacturers, and their use was strictly supervised by the technical team. Potential customers were asked to use the new experimental cement in the same proportions as they usually use the Portland cement.

The trial focused on two main cement applications: (i) manufacture of hollow concrete blocks having size 500 × 200 × 150 mm, produced on a semiautomated vibro-compacting machine; and (ii) manufacture of 25 MPa precast concrete elements at a prefabrication plant in Cuba. Table 2 presents mix proportions used for both applications. Mix design was accredited by the laboratory of the National Enterprise for Applied Research, in Cuba, following the regulations of Cuban standards [25–29].

A preliminary study to evaluate the durability of the concrete was performed on some precast concrete elements of 4 months old based on air permeability measurements. This is a non-destructive method that allows in a reliable and rapid way

Table 2 Mix proportions used in concrete manufacture

For 1 m^3	Mix proportion (kg)		Mix proportion (m^3)	
Materials	Hollow block 150 mm	Concrete 25 MPa	Hollow block 150 mm	Concrete 25 MPa
LCC	300	360	1	1
Sand "El Purio" quarry	654	–	1.8	–
Powder "Palenque" quarry	–	780	–	1.6
Aggregates 5–13 mm "El Purio" quarry	1302	–	3.5	–
Aggregates 19–10 mm "Palenque" quarry	–	1034	–	2.4
Water (L)	112	169	0.4	0.5
Superplasticizer Dynamon SX-32 (L)	–	4.0	–	–
w/c batch	0.4	0.5	–	–
w/c effective	0.2	0.4		–
Designed slump	0	12 ± 3 cm	0	12 ± 3 cm

to evaluate the quality of the concrete cover and this can be correlated to others durability properties such as carbonation rate and chloride ingress [30–32].

Air permeability test was done with a Permea-Torr equipment operating through the air contained in the concrete pores that flows from it to a double cell coupled to the element in vacuum conditions. The permeability of the concrete cover is expressed through the coefficient kT and is the result of no less than 3 measurements in different points [33, 34].

4 Results and Discussion

Figure 1 presents the weight loss versus temperature for each of the five heaps of calcined material evaluated. It is considered that the complete dehydroxylation is achieved when all OH—groups are released during calcination; and the peak associated with this in TGA disappears. All heaps have been completely dehydroxylated; thus indicating that the material has been fully activated.

XRD results presented in Fig. 2 confirms the structural disorder of the calcined material in comparison with the raw clay. The peaks associated to kaolinite are modified or removed although peak associated to quartz remains the same.

Figure 3 presents the results of compressive strength of standardized mortars at 3, 7 and 28 days. The reactivity of the material calcined in the rotary kiln (average of batches) proved to be similar to that of the material calcined at the lab (reference) and to Portland cement (OPC); thus indicating that the industrial calcination was successful.

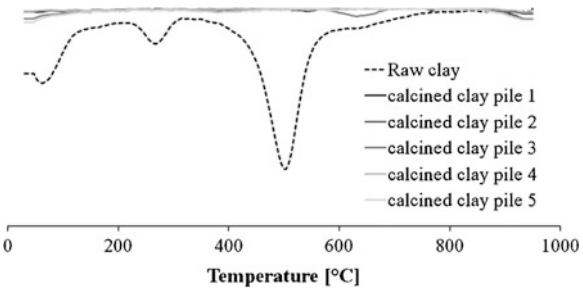

Fig. 1 TGA of different clay samples took after industrial calcination (pile 1–5) and raw clay used as a reference

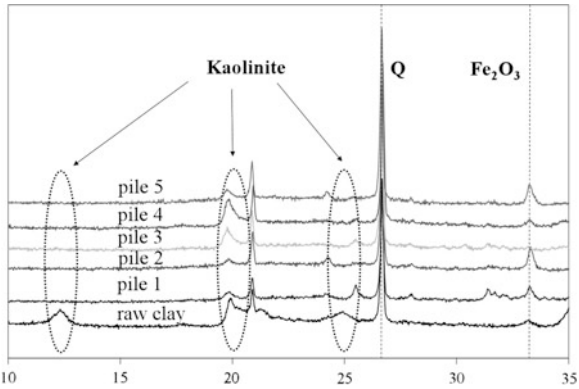

Fig. 2 X-Ray Diffraction pattern from 10 to 35 (2θº) of the different heaps of calcined material

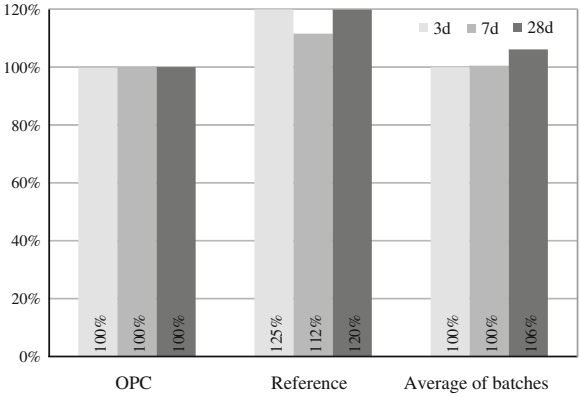

Fig. 3 Compressive strength of the cements prepared with 30 % wt. of calcined clay normalized to ordinary Portland cement

Results of the physical, chemical and mechanical tests performed on the blended cement produced are presented in Table 3, so the average proportion of the components.

Due to some technological issues during the industrial grinding, final SO_3 content exceed the optimal value determined previously in the laboratory. Fineness

Table 3 Summary of the chemical, physical and mechanical properties of the low carbon cement produced

Chemical composition	*Oxides composition [%]*									
	SiO_2	Al_2O_3	Fe_2O_3	CaO	MgO	SO_3	IR	LOI	CaO_{free}	Total
	27.3	4.6	4.6	49.8	1.3	3.7	12.6	7.1	0.9	98.4
	Average proportion of the components [%]									
	Clinker			Calcined clay/limestone		Gypsum				
	50.0			41.1		8.9				
Physical properties	Retained 90 μm sieve	Blaine test	Bulk density	Normal consistency	Initial setting	Final setting	Volume stability			
	%	cm^2/g	g/cm^3	%	Min.	Hours	mm			
	12.0	4190	2.9	25.0	135	2.9	0.3			
Mechanical properties	Compressive strength [MPa]									
	3 days	7 days	28 days							
	11.0	17.5	30.3							

expressed through the % of material retained in the 90 μm sieve although accomplish with the initial fixed parameters, is considered as coarse. Nevertheless, based in the compressive strength results the LCC classifies as a PZ-25 according to Cuban standards [20] despite it surpass the clinker substitution level allowed by the standards. Rheology behaves similar to the OPC usually produced in the factory.

10 938 hollow concrete blocks were produced under standard manufacturing conditions, with a 1:1 cement substitution by the new cement. The quality of the blocks was assessed through the Cuban standard NC 247:2010 (37 article). This standard requires fulfillment of compressive strength and sorptivity. Table 4 presents the results of the evaluation of concrete blocks made with the low carbon cement. The experimental blocks met the standard's requirements for compressive strength and sorptivity; thus indicating that the new cement can replace Portland cement in this kind of industrial application.

Several cubic meters of 25 MPa concrete were cast under standard manufacturing conditions, with a 1:1 cement substitution by the new cement. Quality of the precast elements produced was assessed aided by the Cuban standards (32–36 article). Table 5 presents the results of compressive strength of both the experimental and normal concretes cast for the trial. Both mixes exceed the 28 day strength prescribed, and again, no major differences in rheology were observed; thus indicating that the new cement can replace Portland cement in this kind of industrial application.

Table 4 Results of compressive strength and % absorption of concrete and hollow blocks made with LCC

Dimensions hollow blocks (mm)	Average compressive strength at 7 d (MPa)	Average compressive strength at 28 d (MPa)	Performance	Sorptivity (%)
500 × 200 × 150	3.3	5.9	2.0	5.6
Specification	4.0	5.0	–	≤10

Table 5 Results of compressive strength of concrete made for prefabricated elements with OPC and LCC

Material	Cement consumption (kg/m^3)	Average compressive strength (MPa)			Cement performance[a]
		3 days	7 days	28 days	
LCC-1 (slabs, sewage boxes)	360	–	21.0	31.4	0.9
LCC-2 (foundations)	360	–	18.5	30.8	0.9
LCC-3 (panels)	360	–	19.7	27.7	0.8
OPC (panels)	360	20.4	–	33.2	0.9

[a]Relation between the compressive strength obtained at 28 days in kg/cm^2 and the cement consumption

Table 6 Air permeability results of prefabricated concrete elements produced with LCC and OPC

Class	PK1	PK2	PK3	PK4	PK5
Classification gave by manufacturer					
kT (10^{-16} m^2)	<0.01	0.01–0.10	0.10–1.00	1.00–10.00	>10.00
Permeability	Very low	Low	Moderate	High	Very high
Measurements in prefabricated concrete elements					
LCC-1	–	0.08	–	–	–
	–	0.06	–	–	–
	–	–	0.23	–	–
Average			**0.12**		
OPC	–	–	0.12	–	–
	–	–	0.19	–	–
	–	–	0.10	–	–
Average			**0.14**		

The permeability coefficient measured in prefabricated concrete elements is presented in Table 6, so the rates of classification established by the Permea-Torr manufacturer. The concrete covers of the elements produced with both cements were all classified as moderate permeability, although LCC values are lower related to OPC. Taking into account that LCC has only 50 % of clinker content and that mix proportions used are not the result of an optimum design for this type of ternary blend, this results are considered as very positive.

4.1 Preliminary Assessment of the Environmental Impact of LCC Produced at Industrial Scale

Conventional blended cements with clinker substitution up to 30 % enable reduction of approximately 15–20 % of the CO_2 emissions. The new cement formulation presented in this paper enables to decrease clinker factor to 50 % without compromising performance; this represents a reduction of around 30 % of the CO_2 emissions associated to the cement manufacture; as Table 7 presents.

With the aim of shedding light on the viability, from the environmental viewpoint, of the LCC production at cement factory *Siguaney*, a preliminary assessment of the environmental impact was made by Vizcaíno et al. [19]. The low carbon cement produced in non-optimized conditions during industrial trial, reduces approximately 270 kg CO_2/tonnes in relation to OPC (P-35), this is approximately 31 %. Reduction in reference to traditional Cuban blended cement (PP-25) is in the range of 125 kg CO_2/tonne. P-35 and PP-25 are both regularly produced at cement plant *Siguaney*.

Figure 4 presents emissions and compressive strength at 28 days of LCC produced at the industrial trial, compared with reference values of cements P-35 and

Table 7 CO_2 emissions versus clinker factor in the cement production (calculated in reference [35])

Phases of the productive process	Unitary value (kg CO_2/t)	Clinker factor (%)		
		100	70	55
Raw materials calcination (CaO and MgO)	502.0	502.0	351.4	276.1
Fuel	320.0	320.0	224.0	176.0
Additions (calcined clay, limestone)	380.0	0.0	38.2	57.2
Grinding	100.0	100.0	100.0	100.0
Others	60.0	60.0	60.0	60.0
Total		**982.0**	**773.6**	**669.3**
Savings related to a clinker factor of 100 %		**100 %**	**79 %**	**68 %**

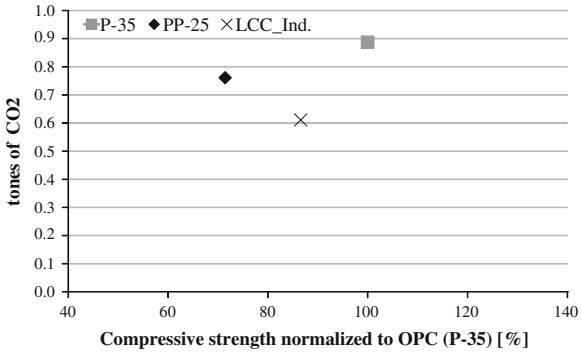

Fig. 4 Relation between emissions of CO_2/ton cement and associated compressive strength of P-35, PP-25 and LCC produced in industrial trial (calculated in reference [19])

PP-25. This illustrates the idea that LCC, despite its very low clinker content which leads to low carbon emissions, does not compromise performance of cement, even compared with other cements produced industrially at the cement plant.

5 Conclusions

– There are alternatives available to move the current boundaries of clinker substitution for the production of blended cements through the use of ternary systems based on clinker, calcined clays and limestone. The principle behind this proposal is the synergy between calcined clay and limestone, which allows increasing the reactivity of the SCMs and reduces clinker factor. This system is based on the use of low grade kaolinite clay, and only small changes should be made to the production process. Reserves of low and medium grade clay and limestone are much higher than any other SCM.

- The industrial trial to produce cement with a clinker factor of 50 % at the industrial scale has proven that the new system is very robust, while even in non-optimized conditions acceptable results have been achieved in terms of performance of the resulting material as cement, as well as in its applications in concrete.
- The new cementitious system could enable reduction on the emissions associated to the cement manufacture in the range of 25–35 % related to business as usual practice. This reduction is based on replacing clinker, which is the main CO_2 releaser, by a combination of materials whose emissions are negligible compared to clinker.

Acknowledgments The authors would like to thanks the financial support from the Suisse National Foundation (SNF) to this project and the Laboratoires des Matériaux de Construction (LMC) of the École Polytechnique Fédérale de Lausanne (EPFL) for offering their facilities. The authors would also like to acknowledge to the Cuban Ministry of Construction, especially to *Siguaney* cement factory, for all the technical and material support.

References

1. U.S.G.S.: Mineral commodity summaries. U.S. Geological Survey. http://minerals.usgs.gov/minerals/pubs/commodity/cement/ (2002)
2. U.S.G.S. Mineral commodity summaries, January 2013. U.S. Geological Survey. http://minerals.usgs.gov/minerals/pubs/commodity/cement/ (2013)
3. Gartner, E.: Industrially interesting approaches to "low-CO_2" cements. Cem. Concr. Res. **34** (9), 1489–1498 (2004)
4. Damtoft, J.S., et al.: Sustainable development and climate change initiatives. Cem. Concr. Res. **38**(2), 115–127 (2008)
5. WBCD—CSI: Guidelines for emissions monitoring and reporting in the cement industry. Emissions Monitoring and Reporting_Version 2.0. www.wbcsdcement.org, p. 40 (2013)
6. Flatt, R.J., Roussel, N., Cheeseman, C.R.: Concrete: an eco material that needs to be improved. J. Eur. Ceram. Soc. **32**, 2787–2798 (2012)
7. Müller, N., Harnisch, J.: A blueprint for a climate friendly cement industry. WWF, Lafarge Conservation Partnership. www.panda.org/climatesavers (2008)
8. John, V.M.: On the sustainability of the Concrete. UNEP J. Ind. Environ. **7** (2002)
9. Cembureau: Activity report, D/2011/5457/May, Editor. www.cembureau.eu (2010)
10. Olivier, J.G.J., Janssens-Maenhout, G., Peters, J.A.H.W. Trends in Global CO_2 Emissions; 2012 Report, p. 42 (2012). ISBN 978-92-79-25381-2
11. Taylor, M., Tam, C., Gielen, D.: Energy Efficiency and CO_2 Emissions from the Global Cement Industry in Energy Efficiency and CO_2 Emission Reduction Potentials and Policies in the Cement Industry. Energy Technology Policy Division International Energy Agency: IEA, Paris, p. 77 (2006)
12. Schneider, M., et al.: Sustainable cement production—present and future. Cem. Concr. Res. **41**(7), 642–650 (2011)
13. Tennis, P.D., Thomas, M.D.A., Weiss W.J.: State of the art report on use of limestone in cements at levels of up to 15 %, R.D. Information, Editor, p. 78. www.cement.org (2011)
14. Sabir, B.B., Wild, S., Bai, J.: Metakaolin and calcined clays as pozzolans for concrete: a review. Cement Concr. Compos. **23**(6), 441–454 (2001)

15. Antoni, M., et al.: Cement substitution by blends of metakaolin and limestone. Cem. Concr. Res. **42**(12), 1579–1589 (2012)
16. Fernández López, R.: Calcined Clayey Soils as a Potential Replacement for Cement in Developing Countries, in Faculté Sciences et Techniques de L'Ingeniur. École Polytechnique Federale de Lausanne: Lausanne, p. 178 (2009)
17. Vizcaíno Andrés, L.M.: Cemento de bajo carbono a partir del sistema cementicio ternario clínquer - arcilla calcinada - caliza, in Ingeniería Civil. Universidad Central Marta Abreu de Las Villas: Impreso en Cuba (2014)
18. Fernández, R., Martirena, F., Scrivener, K.: The origin of the pozzolanic activity of calcined clay minerals: a comparison between kaolinite, illite and montmorillonite. Cem. Concr. Res. **41**(1), 113–122 (2011)
19. Vizcaíno, L., et al.: Effect of fineness in clinker-calcined clays-limestone cements accepted for Advanced in Cement Research **27**(1), 1–11 (2015)
20. NC/CTN22, NC 96: 2011 Cemento con adición activa. Especificaciones.Oficina Nacional de Normalización Impreso en Cuba (2011)
21. NC/CTN22, NC 54-207: 2000 Cemento - Ensayos físico-mecánicos. Oficina Nacional de Normalización (NC): Impreso en Cuba 2000
22. NC/CTN22, NC 54-206:2000 Cemento - Análisis químico de arbitraje. Oficina Nacional de Normalización (NC): Impreso en Cuba (2000)
23. NC/CTN22, NC 524: 2007 Cemento hidráulico. Método de ensayo. Determinación de la consistencia normal y tiempos de fraguado por aguja Vicat. Oficina Nacional de Normalización (NC): Impreso en Cuba 2007
24. NC/CTN22, NC 506: 2007 Cemento hidráulico. Método de ensayo. Determinación de la resistencia mecánica. Oficina Nacional de Normalización (NC): Impreso en Cuba (2007)
25. NC/CTN37, NC ISO 1920-3: 2010. Ensayos de Hormigón – Parte 3: Elaboración y curado de Probetas de Ensayos. Oficina Nacional de Normalización (NC): Impreso en Cuba 2010
26. NC/CTN37, NC ISO 1920-2:2010 Ensayos al hormigón. Propiedades del hormigón fresco. Oficina Nacional de Normalización (NC): Impresa en Cuba 2010
27. NC/CTN37, NC 724:2009 Ensayos del Hormigón. Resistencia del Hormigón en estado endurecido. Oficina Nacional de Normalización (NC): Impreso en Cuba (2009)
28. NC/CTN37, NC ASTM C 1231/C 1231M: 2006 Hormigón. Refrentado de probetas cilíndricas utilizando placas no adheridas. Oficina Nacional de Normalización (NC): Impreso en Cuba (2006)
29. NC/CTN37, NC 167:2002 Hormigón Fresco. Toma de muestras. Oficina Nacional de Normalización (NC): Impreso en Cuba (2002)
30. RILEM-TC116-PCD: Permeability of concrete as a criterion of its durability. Final report TC 116 PCD: concrete durability—an approach towards performance testing. Mater. Struct. **32**, 163–173 (1999)
31. Torrent, R.J.: A two-chamber vacuum cell for measuring the coefficient of permeability to air of the concrete cover on site. Mater. Struct. **25**(150), 358–365 (1992)
32. Andrade, C., Gonzales-Gasca, C., Torrent, R.J.: Suitability of torrent permeability tester to measure air-permeability of covercrete. In: Durability of concrete. (ACI International), Barcelona, pp. 301–317 (2000)
33. Torrent, R.J.: Measures the air concrete and other porous materials. Swiss standard method SIA 262/1: 2013. User Manual Version M2S.2© M.A.S. Ltd, Editor (2014)
34. SIA, Norme Suisse SIA 262/1: 2013 Construction en béton - Spécifications complémentaires, in Annexe E, "Perméabilité à l'air dans les Structures" (German + French). Société suisse des ingénieurs, pp. 30–31 (2013)
35. Habert, G., et al.: Cement production technology improvement compared to factor 4 objectives. Cem. Concr. Res. **40**, 820–826 (2010)

Development of Low Cost Geopolymer from Calcined Sedimentary Clay

Anurat Poowancum and Suksun Horpibulsuk

Abstract Geopolymer, a low environmental impact material, is recently used as an alternative binder to Portland cement in concrete manufacturing because the geopolymer production is a low-energy-consuming process, and does not emit pollutants, especially carbon dioxide, which is the main cause of the global warming problem. Geopolymer is synthesized from variety kinds of raw materials/precursor such as fly ash, slag, and kaolinite clay. However, supplies of slag and fly ash are limited due to the large demand of cement. These are the driving forces for the need to seek for alternative precursor. Abundant Sedimentary Clay (SC) in Nakhon Ratchasima province, Thailand contains high amount of kaolin and is possibly used to develop a cost-effective and sustainable calcined precursor, which is the focus of this paper. The precursor was prepared by calcining SC at 600 °C for 1, 2 and 5 h. The precursor was mixed with the alkali activator solution, which is the mixture of sodium silicate (Na_2SiO_3) solution and sodium hydroxide (NaOH) solution to develop a SC-geopolymer binder. The ratios of Na_2SiO_3 to NaOH studied were 0.5, 1 and 1.5. The geopolymer pastes were cured at 60 °C for 7 days. The results show that 2 h-calcined SC and Na_2SiO_3 to NaOH ratio of 0.5 provides the highest strength of the SC-geopolymer paste. Its compressive strength is higher than that of the ordinary Portland cement.

1 Introduction

Nowadays, Portland Cement (PC) concrete is extensively used as a construction material, because it is more economical in comparison to metals and other materials. However, the manufacture of PC emits high quantities of carbon dioxide gas [1], which is the cause of the global warming problem. Recently, geopolymer has

A. Poowancum · S. Horpibulsuk (✉)
School of Ceramic Engineering, Faculty of Engineering, Suranaree University of Technology, Nakhon Ratchasima, Thailand
e-mail: suksun@g.sut.ac.th

K. Scrivener and A. Favier (eds.), *Calcined Clays for Sustainable Concrete*,
RILEM Bookseries 10, DOI 10.1007/978-94-017-9939-3_44

been the subject of intent study for use as an alternative cementing agent due to it is the environmental-friendly material [2]. Geopolymer is an inorganic polymer technology, and is synthesized by the aluminosilicate compound materials [3, 4]. Geopolymer production does not emit carbon dioxide gas, and is a low-energy-consuming process [2]. In addition, geopolymer can be synthesized from variety kinds of silica and alumina rich materials such as kaolinite clay, fly ash, and bottom ash.

Fly ash derived from coal-fired electricity generation provides the greatest opportunity for commercial utilization of geopolymer technology due to the plentiful worldwide raw material supply [5]. However, supplies of fly ash are limited due to the large demand of cement. These are the driving forces for the need to seek for alternative precursor. Sedimentary clay (SC) is a clay mineral, which was transformed from primary clay (kaolinite clay) by geological process. Although SC is impure, its advantages are low cost and worldwide available. Dan Kwian Clay (DKC) is abundant SC in Nakhon Ratchasima province, Thailand. DKC contains high amount of kaolinite and is possibly used as a raw material to develop a cost-effective and sustainable calcined precursor, which is the focus of this paper. Compressive strength, porosity and setting time of the calcined DKC-geopolymer are also examined and analyzed.

2 Experimental Procedure

DKC from Dan Kwian Village, Tambon Dan Kwian, Chok Chai district, Nakhon Ratchasima province, Thailand was oven dried at 150 °C for 24 h, then was milled by a disk mill and passed through sieve number 100 mesh. The DKC—powder was calcined at 600 °C for 1, 2, and 5 h to obtain the calcined DKC-powder. Sodium hydroxide (NaOH) pellets and distilled water were mixed to obtain a concentration of 8 M, and then allowed to cool down at a room temperature (27–30°C). Sodium silicate (Na_2SiO_3) solution was mixed with NaOH solution in the ratios of Na_2SiO_3 to NaOH were 0.5, 1 and 1.5 by volume to prepare the alkali activator solution. The mixed solution was stored for 24 h prior to use.

The calcined DKC-powder was mixed with the alkali activator solution by a mortar at a solid to liquid ratio of 2.0. The geopolymer paste was poured into a 50 mm × 50 mm × 50 mm steel mold and compacted as described in ASTM C109 [6]. The geopolymer samples along with the molds were then sealed with vinyl sheet to prevent moisture evaporation during curing at 60 °C for 7 days. Porosity and compressive strengths of all geopolymer samples were measured after 7 days of curing.

Chemical compositions of DKC were evaluated by X-ray fluorescence (XRF, HORIBA XGT-5200). X-ray diffraction (XRD, Bruker D5005) with CuK_α radiation was used for analyzing mineral compositions of DKC. Setting time of geopolymer pastes was examined according to ASTM C266 [7]. Porosity and compressive strength of the 7 days cured geopolymer were measured following ASTM C138 [8] and ASTM C109 [6], respectively.

3 Results and Discussion

The XRD diffractogram of DKC is presented in Fig. 1. Only XRD peaks of quartz and kaolinite are detected. Table 1 shows chemical compositions of DKC. Silica (SiO_2 = 73 wt%) and alumina (Al_2O_3 = 19 wt%) are the main compositions, which are the main required composition for a precursor. DKC is the sedimentary clay, which is transformed from feldspar and kaolinite clay by geological process [9]. Although, XRD peak of feldspar was not detected, Table 1 shows the feldspar existence, i.e., K_2O. Table 2 shows the mineral compositions of DKC, which were approximated from Table 1 by the rational mineralogical analysis method [10]. The main mineral compositions of DKC are 42.3 wt% kaolinite, 45.7 wt% quartz and 5.6 wt% feldspar. Table 2 shows that DKC is a useful raw material for a synthesis of the sustainable geopolymer, because, it is comprised of the geopolymer precursor (kaolinite) and the filler (quartz and feldspar).

Setting time relates to reactivity of the calcined precursor. Normally, the high reactivity calcined precursor has a short period of setting time. Figure 2 shows reactivity of the calcined-DKC is reduced when increasing the calcination time from 2 to 5 h. The setting time is 55 min for both 1 and 2 h of calcination while is 60 min for 5 h of calcination. The calcination is a process to manufacture metakaolin, which is amorphous phase and has high reactivity. It is a dehydroxylated form of kaolin, and is achieved by calcined kaolin. However, excessive calcination

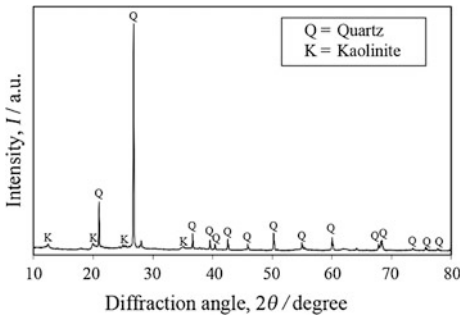

Fig. 1 X-ray diffraction (XRD) spectra of DKC

Table 1 XRF results of Dan kwian clay

Compositions	Weight%
SiO_2	72.95
Al_2O_3	18.76
K_2O	1.02
CaO	0.38
MgO	1.19
TiO_2	0.84
Fe_2O_3	4.72
Etc.	0.14

Table 2 Mineral compositions of Dan Kwian clay

Mineral	Content (wt%)
Kaolinite	42.3
Quartz	45.7
Feldspar	5.6

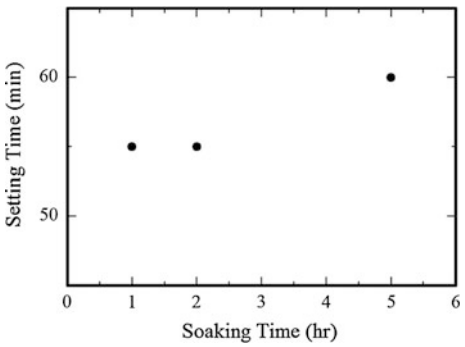

Fig. 2 Setting time of DKC-geopolymer calcined with different time

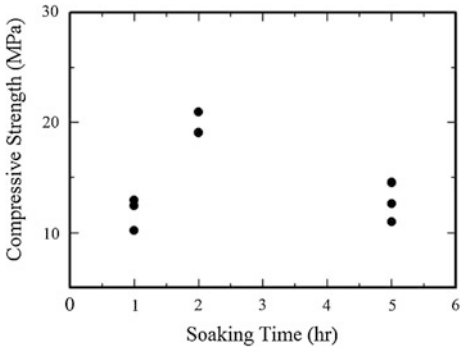

Fig. 3 Compressive strength of DKC-geopolymer calcined with different time

temperature and/or period of the calcination time changes an amorphous phase to a crystalline phase, which is a low reactivity phase. As such, the setting time of geopolymer paste increases to 60 min when DKC was calcined at 5 h. This increase in setting time is associated with a strength reduction of DKC-geopolymer as shown in Fig. 3.

Strength of DKC-geopolymer for DKC calcined for 5 h is lower than that for DKC calcined for 2 h. The lower strength indicates the lower reactivity of calcined-DKC for 5 h. The low strength of DKC-geopolymer for 1 h calcined DKC might be due to insufficient calcination time for the complete dehydroxylation process. In other words, the calcined DKC powder obtained is not in purely reactive phase (metakaolin) but also composed of non-reactive phase (kaolin). Reactive phase increases with increasing the calcination time from 1 to 2 h. Therefore, strength of DKC-geopolymer increases with increasing the calcination time from 1 to 2 h. Likewise, porosity of DKC-geopolymer for 2 h calcined DKC is lower than that of

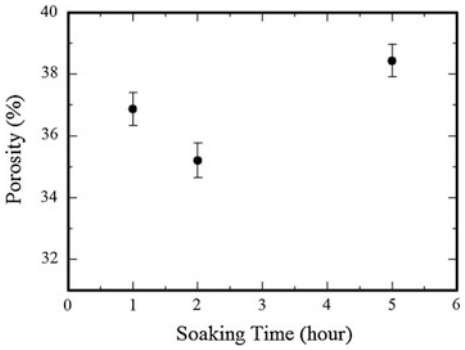

Fig. 4 Porosity of DKC-geopolymer calcined with different time

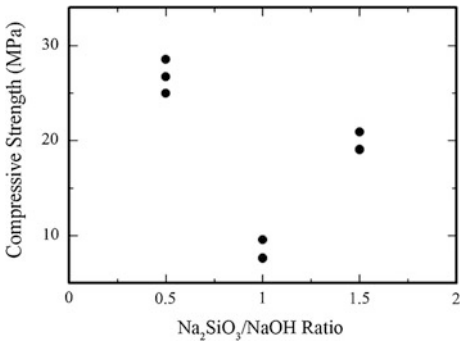

Fig. 5 Compressive strength of DKC-geopolymer calcined at 600 °C for 2 h in different ratio of Na_2SiO_3 to NaOH

DKC-geopolymer for 1 and 5 h, as illustrated in Fig. 4. The lower porosity is because the geopolymerization products (Sodium alumino silicate hydrate) filling the pore space and making the structure of geopolymer paste denser.

Role of NaOH and Na_2SiO_3 in geopolymerization process is the dissolvent and the binder, respectively. Figure 5 illustrates the effect of Na_2SiO_3 to NaOH (binder to dissolvent) ratios on strength of DKC-geopolymer. Strength of DKC-geopolymer reduces with increasing the Na_2SiO_3/NaOH ratio and the lowest value is found at Na_2SiO_3/NaOH ratio of 1.0. Beyond this ratio, the strength increase with increasing Na_2SiO_3/NaOH ratio. Although Na_2SiO_3 is required for the geopolymerization process, it may inhibit the geopolymerization process at the high Na_2SiO_3/NaOH ratio [11]. A Na_2SiO_3/NaOH ratio of 1.0 contains insufficient amount of both dissolvent and binder in comparison to the ratio of 0.5 (high dissolvent, low binder) and 1.5 (low dissolvent, high binder). As a result, the geopolymerization process lacks Al and Si ion to form geopolymer gel, and lacks binder for condensation process. The maximum strength is obtained at the Na_2SiO_3/NaOH ratio of 0.5, and is 27 MPa, which is higher than the minimum requirement of PC, i.e., 19 MPa [12].

Since NaOH is cheaper than Na_2SiO_3, low cost alkali activator solution could be achieved by using Na_2SiO_3 as small amount as possible. As such, the Na_2SiO_3/NaOH ratio of 0.5 benefits not only in term of engineering but also economic points of view. The research demonstrations that the high strength geopolymer could be synthesized from a low cost raw material and a low cost alkali activator solution.

4 Conclusions

Low cost and sustainable geopolymer alternative to Portland cement is developed by using Dan Kwian Clay (DKC) as a precursor in this research. DKC is a sedimentary clay whose mineral compositions are 42.3 wt% kaolinite, 45.7 wt% quartz, and 5.6 wt% feldspar. By using the optimum calcined condition (600 °C, 2 h) and the optimum alkali activator solution (Na_2SiO_3/NaOH ratio of 0.5), strength of DKC-geopolymer is higher than that of the minimum requirement of the Portland cement. Sufficient calcination time is required for obtaining the high reactivity calcined precursor. However, excessive calcination time reduces reactivity of the calcined precursor. Strength of geopolymer reduces with increasing the ratio of Na_2SiO_3/NaOH, due to the excess of Na_2SiO_3 inhibiting the geopolymerization process.

Acknowledgments This research was supported by the Suranaree University of Technology. The second author acknowledges the Thailand Research Fund under the TRF Senior Research Scholar program Grant No. RTA5680002.

References

1. Habert, G., de Lacaillerie, J.B.D.E., Roussel, N.: An environmental evaluation of geopolymer based concrete production: reviewing current research trends. J. Cleaner Prod. **19**(11), 1229–38 (2011)
2. Pacheco-Torgal, F., Abdollahnejad, Z., Miraldo, S., Baklouti, S., Ding, Y.: An overview on the potential of geopolymers for concrete infrastructure rehabilitation. Constr. Build. Mater. **36**, 1053–1058 (2012)
3. Komnitsas, K., Zaharaki, D.: Geopolymerisation: a review and prospects for the minerals industry. Miner. Eng. **20**(14), 1261–1277 (2007)
4. Zhang, L.: Production of bricks from waste materials—a review. Constr. Build. Mater. **47**, 643–655 (2013)
5. Mohapatra, R., Rao, J.R.: Some aspects of characterisation, utilisation and environmental effects of fly ash. J. Chem. Technol. Biotechnol. **76**(1), 9–26 (2001)
6. ASTM C109: Standard test method of compressive strength of hydraulic cement mortars (using 2-in. or [50 mm] cube specimens). Annual Book of ASTM Standard, vol. 04.01 (2002)
7. ASTM C266: Standard test method for time of setting of hydraulic-cement paste by Gillmore needles. Annual Book of ASTM Standard, vol. 04.01 (2013)
8. ASTM C138: Standard test method for density (unit weight), yield, and air content (gravimetric) of Concrete. Annual Book of ASTM Standard, vol. 04.02 (2011)
9. Ye, Y., Guanghai, S., Mengchu, Y., Yinuo, W., Zhaochong, Z., Anjie, H., Jiajing, Z.: Formation of a hydrothermal kaolinite deposit from rhyolitic tuff in Jiangxi, China. J. Earth Sci. **25**(3), 495–505 (2014)
10. Coelho, C., Roqueiro, N., Hotza, D.: Rational mineralogical analysis of ceramics. Mater. Lett. **52**, 394–398 (2002)
11. Liewa, Y.M., Kamarudina, H, Mustafa Al Bakria, A.M., Binhussainb, M., Luqmana, M., Khairul, N.I., Ruzaidia, C.M., Heaha, C.Y.: Influence of Solids-to-liquid and Activator Ratios on Calcined Kaolin Cement Powder. Physics Procedia. **22**, 312–317 (2011)
12. ASTM C150/C150 M: Standard specification for Portland Cement. Annual Book of ASTM Standard, vol. 04.01 (2012)

Hydrothermal Synthesis Products of CaO Metakaolin H_2O System at 90 °C

Mian Sun, Tao Sun, Weiwei Han, Guiming Wang and Mingjun Mei

Abstract In order to fully utilize the low-grade kaolin resources, the hydrothermal synthesis products of CaO-Metakaolin-H_2O system at 90 °C were studied. Starting from in-depth analysis of the hydration characteristics and mechanism of CaO-SiO_2-H_2O systems and basing on calculation of its Gibbs free energy at different temperature, the stable hydration products at different temperature or n(Ca)/n(Si) are identified. Meanwhile, 363 K (90 °C) has been designated as the hydrothermal temperature. The relationship between the extent of hydration and reaction time of three n(Ca)/n(Si) varieties was studied by the coordination of six curves subsequently. The analysed conclusion showed that their best mimic curves were Jander equation. It was calculation through the equation that their KJ value are 49.06×10^{-4}, 42.22×10^{-4} and 27.3×10^{-4} in each variety. According to the result of SEM, X-ray, the major hydration products of hydro-thermal synthesis were porous surface and semi-crystalline C-S-H (B), filament and network shape C-S-H (II), numerous cube and granule shaped $C_3AS_nH_{6-2n}$ encapsulated within C-S-H gel, a small quantity of C_4AH_{13} and C_2ASH_8.

1 Introduction

In recent decades, supplementary cementitious materials (SCMs), especially slag, fly ash and silica fume being well known as their pozzolanic activity, have been used to improve the performances of concrete capable of withstanding serious

M. Sun · T. Sun (✉) · G. Wang
State Key Laboratory of Silicate Materials for Architectures,
Wuhan University of Technology, Wuhan, China
e-mail: sunt@whut.edu.cn

W. Han
Key Laboratory of Roadway Bridge and Structure Engineering,
Wuhan University of Technology, Wuhan, China

M. Mei
Maoming Kaolin Science and Technology Company, Maoming, China

K. Scrivener and A. Favier (eds.), *Calcined Clays for Sustainable Concrete*,
RILEM Bookseries 10, DOI 10.1007/978-94-017-9939-3_45

environmental condition [1, 2]. Metakaolin (MK), a kind of pozzolanic SCM, is obtained by the calcination of kaolinitic clay at a temperature ranging from 500 to 850 °C [3]. Addition of MK not only causes the lower cost of concrete but did as silica fume and other SCMs in terms of improving workability, microstructure and mechanical strength as well as permeability, higher durability [4–7].

The effects of MK on performances of cement/concrete mainly resulted from the pozzolanic reaction between MK and $Ca(OH)_2$, which are affected by many factors, for example, the chemical composition of MK, MK/$Ca(OH)_2$ ratio and curing temperature, etc. [8].

Among different factors, curing temperature is the most important one because of the effects on the stability and transformation of the hydrates [9]. Silva and Glasser reported the phase development pattern of MK-$Ca(OH)_2$ system apparently changes with curing temperature ranging from 20 to 55 °C. At 55 °C, C_4AH_{13} and C_2ASH_8 are instable and gradually convert into C_3ASH_6 with time increase [10]. It's that easily accurate results calculation of hydration extent of MK is very important to get comprehensive understanding about the effect of curing temperature on performance of MK-$Ca(OH)_2$ system. Luke and Glasser [11] showed that EDTA solvent presented more advantages in dissolving residues which was the best method to study the pozzolanic activity of material. Meanwhile, Polwman and Cabrera [12] showed that the secondary pozzolanic reaction in pozzolana-cement or pozzolana-lime system was mainly affected by the diffusion rate, and the hydration process of MK-lime-H_2O system at 20 and 60 °C can be described with Jander kinetic model.

In order to fully utilize the low-grade kaolin resources, the hydration of CaO-MK-H_2O system at different temperature or n(Ca)/n(Si) ratio is carried out based on the Gibbs free energy (ΔG) under different temperature. Appropriate hydrothermal temperature is confirmed and a mathematical model is applied to calculate the reaction constant. Qualitative study of the hydrothermal synthesis products is followed by XRD, SEM and etc.

2 Experimental Program

2.1 Materials

MK used is obtained by the calcination of kaolin (massive, Maoming kaolinite Technology) powder that's grinded 20 min in ball mill at 750 ºC for 2 h. CaO and water used are analytically pure and deionized water, respectively (Table 1).

Table 1 Chemical composition of Kaolin and MK (%)

Composition	Al_2O_3	SiO_2	Fe_2O_3	CaO	TiO_2	SO_3	P_2O_5	Na_2O	K_2O	MgO	L.O.I
Kaolin	38.09	45.51	0.60	0.02	0.25	0.19	0.33	0.29	0.45	0.10	14.18
MK	44.58	53.27	0.70	0.02	0.29	0.22	0.39	0.34	0.53	0.13	–

2.2 Methods

Hydration extent of CaO-MK-H_2O is obtained by calculating the amount of unreacted MK by using EDTA as a solvent to dissolve any substances except for MK with double medium speed filter paper and G6 sand core funnel filtration o filtration. Meanwhile, two kinetic models-kinetic equation of Jander and Ginstling are also applied. On the other hand, X-ray diffraction (D/max-RB, RIGAKU, Japan) with scan rate of 10.00° per min, XRF fluorescence analyzer (PANzlytical, Netherlands) and JSM-5610LV SEM (JEOL, Japan) combined with Horiba 250 spectra and backscattered electron detector are separately performed to the analyses of the chemical composition, mineralogical composition and morphology of hydration products.

3 Results and Discussion

3.1 Hydrothermal Temperature and Hydration Extent

In Table 2, there are two hydration products no matter what the temperature is-C-S-H gel with complex structure and species and hydrated calcium aluminate or hydrated calcium silicate that its specie and structure are clear. Thus, for CaO-MK-H_2O system, hydrated calcium silicate crystals with similar n(Ca)/n(Si) ratio is regarded as a research object because of uncertain thermodynamic data of C-S-H with a state microcrystal.

Table 2 Main hydration products of CaO-MK-H_2O system at different temperature and time

Temperature	Time (d)	C_2ASH_8	C_4AH_{13}	Hydrogarnet	$Ca(OH)_2$	C-S-H
20	10	+	+		+	+
	90	+	Trace		+	+
	180	+	Trace		Trace	+
55	3		+	+	+	+
	28		Trace	+	+	+
	90		Trace	+	Trace	+
60	3	+	+	+	+	+
	5	+	+	+	+	+
	9	+	+	+	+	+

Table 3 Thermodynamic data of related compounds

Name	Composition	n(Ca)/n(Si)	Status	ΔG_f^0	$C_p = f(T)$		
				kj/mol	a	b × 10^3	c × 10^{-5}
Disclasite	$C_2SH_{1.17}$	2	crystal	−2480.69	41.4	22.4	−7.4
Afwillite	$C_3S_2H_3$	3/2	crystal	−4405.54	81.54	45.1	−14.67
Kilchoanite	$C_4S_3H_{1.5}$	4/3	crystal	−5639.61	87.95	3.95	−13.48
Xonotlite	C_6S_6H	1	crystal	−9453.33	132.25	65.2	−18.35
Tobermorite	$C_5S_6H_{5.5}$	5/6	crystal	−9880.31	110.6	189	–
Gyrolite	$C_2S_3H_{2.5}$	2/3	crystal	−4542.36	79.47	36.3	−17.55
Fiber Okenite	CS_2H_2	1/2	crystal	−2871.90	44.81	18.7	−10.35
Portlandite	$Ca(OH)_2$	–	crystal	−896.76	19.79	10.45	2.94
Glass	SiO_2	–	glassy	−848.60	13.38	3.68	−3.45
water	H_2O	–	liquid	−237.19	7.93	16.95	2.67

As for Table 3, it's known that when the n(Ca)/n(Si) ratio changes with some uncertain factors, ΔG is more suitable than equilibrium constant on determining the direction of reaction. Therefore, combined with the principle of composition calculation, ΔG can be calculated based on the following formula (1) when the temperature is separately 298, 333 and 363 K.

$$\begin{aligned}\Delta G_T &= \int_{298}^{t} \Delta C_p \mathrm{d}t - T - \int_{298}^{t} \frac{\Delta C_p}{t}\mathrm{d}t \\ &= \int_{298}^{t} (\Delta a + \Delta b T + \frac{\Delta c}{T^2})\mathrm{d}t - T \int_{298}^{t} \frac{\Delta a + \Delta b T + \frac{\Delta c}{T^2}}{t}\mathrm{d}t\end{aligned} \tag{1}$$

As the Fig. 1 depicted, the hydration product of CaO-SiO_2-H_2O system at 298 K is $C_2SH_{1.17}$ corresponding to the minimum ΔG, which means it's the most stable product. And $C_2SH_{1.17}$ will not changed with n(Ca)/n(Si) ratio. At 333 or 363 K, there is a most stable product-$C_2S_2H_3$ for 333 K or $C_4S_3H_{1.5}$ for 363 K, but they will change with the n(Ca)/n(Si) ratio-when the n(Ca)/n(Si) ratio decreases, its most stable product will be converted into other most stable product-$C_2S_2H_3 \rightarrow C_2S_3H_{2.5}$ for 333 K and $C_4S_3H_{1.5} \rightarrow C_2S_3H_{2.5}$ for 363 K.

In Fig. 2, the hydrated calcium silicate product may be located between the point A1 and A2 that its n(Ca)/n(Si) ratio change from 0.5 to 3.0, and the hydration products are C_2ASH_8(C1), C_3ASH_6(C2), C_3AH_6(C3) and C_4AH_{13}(C4). Considering the limited proportion of n(Ca)/n(Si) ratio in kaolin, the point of raw material ratio must be located at D1D2 straight line to get more hydration products-hydrated calcium silicate (aluminate). With the results of Murat M [8], the ratios of MK/CaO are 0.5(D1), 0.6(D2) and 0.8 that aims to get more about the influence of CaO on the hydration of CaO-MK-H_2O system. On the other hand, the minimum

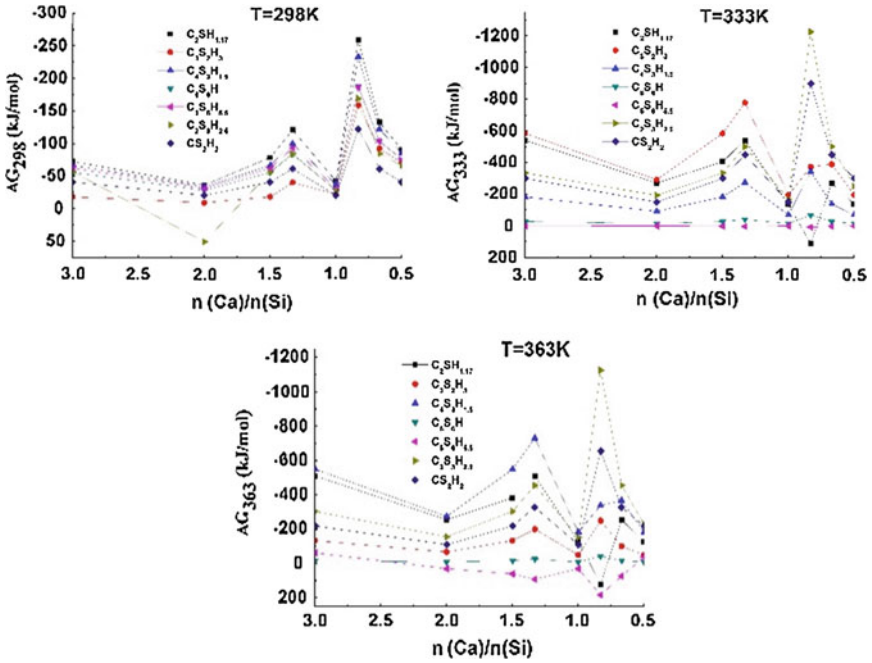

Fig. 1 ΔG with different n(Ca)/n(Si) ratio at 289, 333 and 363 K

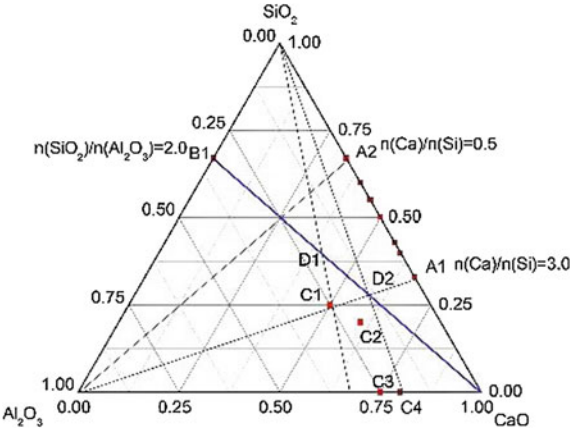

Fig. 2 Three-phase graph of CaO-SiO_2-Al_2O_3

point of n(Ca)/n(Si) ratio is D1(n(Ca)/n(Si) = 1.0) by the equal ration principle of concentration triangle. When the n(Ca)/n(Si) ratio is more than 1.0, the most stable product will not be change no matter what the temperature is 298 K or 333 K or 363 K, and the most stable product is $C_4S_3H_{1.5}$ (n(Ca)/n(Si) = 1.33) that is the minimum value at atmospheric when the temperature rises to 363 K. Therefore,

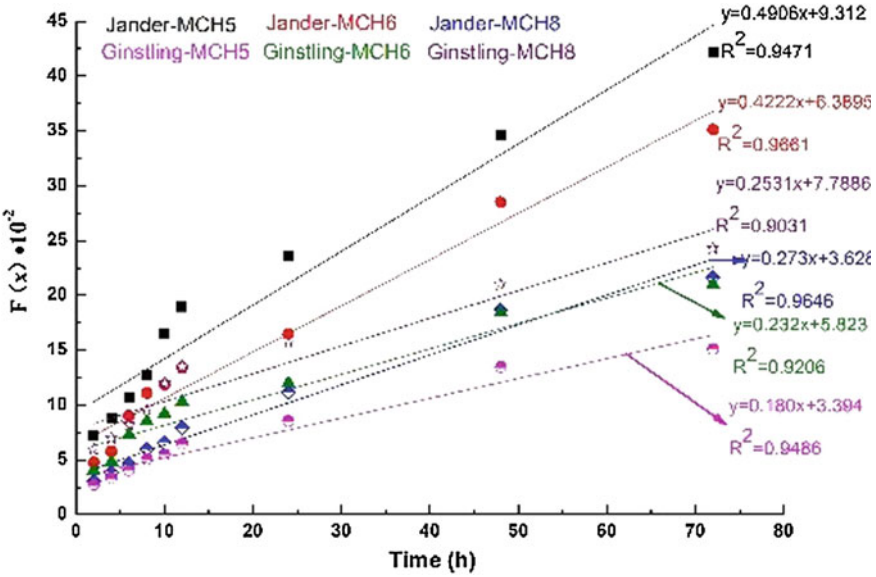

Fig. 3 Regression lines for six results

when the n(Ca)/n(Si) ratio decreases, 363 K(90 °C) is the most suitable hydrothermal temperature to get more hydrated calcium silicate (aluminate).

The pastes with water/solid ratios of 5(solid: MK/$Ca(OH)_2$ = 0.5, 0.6, 0.8, the mass of $Ca(OH)_2$ is converted from the mass of CaO) were obtained in terms of MCH5, MCH6 and MCH8. The hydration extent of MK in system was carried out at 90 °C in the equipment with the hydrothermal synthesis time of 2 h, 4 h, 6 h, 8 h, 10 h, 12 h, 24 h, 48 h and 72 h. Then, the sample is put into vacuum oven to dry at 105 °C for 48 h until constant weight.

The kinetic model that best fit the results at 90 °C is that of Jander for CaO-MK-H_2O system (Fig. 3). K_J of MCH5, MCH6 and MCH8 is separately calculated by Jander equation with the result of 49.06×10^{-4}, 42.22×10^{-4} and 27.3×10^{-4} that are bigger than 20.6×10^{-4} got by Cabrera [9] at 60 °C, which means the hydrothermal synthesis temperature makes a significant effect on hydrothermal synthesis rate. And, the hydration extent and hydration rate increase with n(Ca)/n(Si) ratio.

3.2 XRD and SEM

As for Fig. 4, the main hydration products are C_3AH_6(d = 0.231, d = 0.204), C_3ASH_4(d = 0.276, d = 0.329), C_4AH_{13}(d = 0.786, d = 0.398) and a few C_2ASH_8(1.268, d = 0.287), $CaCO_3$(d = 0.303, d = 0.209), α-SiO_2(d = 0.334, d = 0.425) and C-S-H(B) (d = 0.307, 2θ = 28.7°) that is not completely recognized

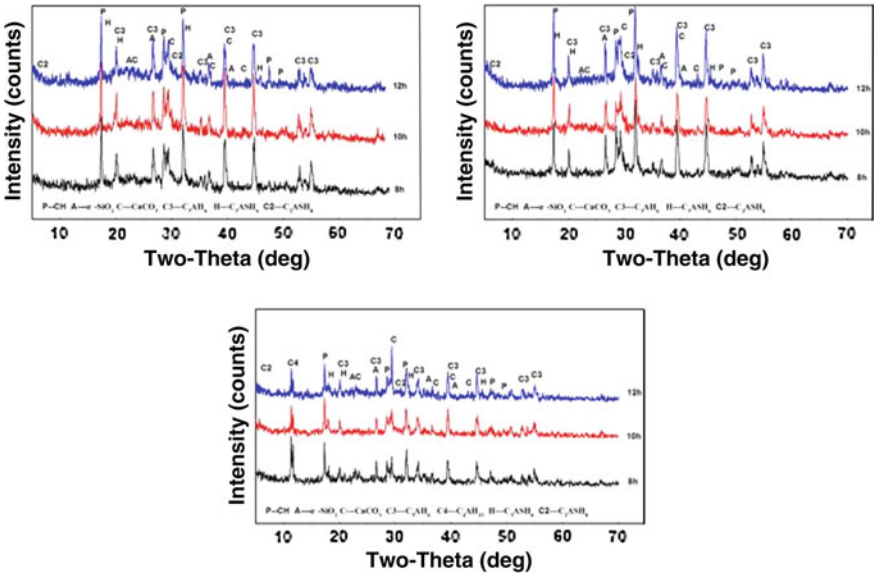

Fig. 4 XRD patterns of MCH5, MCH6 and MCH8

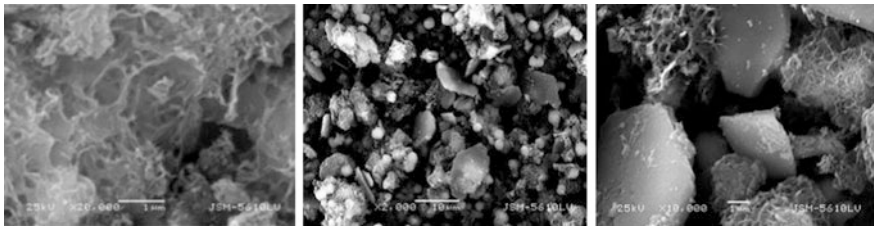

Fig. 5 SEM images of MCH6 for 8 h

because of its semi-crystalline state. And the intensity of hydration products increase with MK/CaO ratio providing that more insoluble hydration product generated with increasing dissolution rate of SiO_2 and Al_2O_3, which caused by higher concentration of Ca^{2+} and OH^- that resulted from the content of CaO increases.

In the SEM images (Fig. 5), there is a kind of hydration products with foil laminated structure and porous surface, which is semi-crystalline C-S-H(B). And there are numerous cube and granule $C_3AS_nH_{6-2n}$ shaped encapsulated with C-S-H gel and some $Ca(OH)_2$ crystals with hexagonal flake grow in capillary pores and get larger among C-S-H gel.

4 Conclusions

- The most suitable hydrothermal synthesis temperature is 363 K (90 °C), which is confirmed by the most stable hydration products of $CaO\text{-}SiO_2\text{-}Al_2O_3$ system obtained by ΔG based on the principle of composition calculation.
- Jander kinetic model is more suitable for hydration of $CaO\text{-}MK\text{-}H_2O$ system, and K_J decreases with increase of $MK/Ca(OH)_2$ ratio, KJ with $MK/Ca(OH)_2$ of 0.5, 0.6 and 0.8 at 90 °C is separately 49.06×10^{-4}, 42.22×10^{-4} and 27.3×10^{-4}, which is more higher than that of 60 °C. Meanwhile, higher hydrothermal synthesis temperature significantly improve the hydration of $CaO\text{-}MK\text{-}H_2O$ system.
- The hydrothermal synthesis products are porous surface and semi-crystalline C-S-H (B), numerous cube and granule shaped $C_3AS_nH_{6-2n}$ encapsulated within C-S-H gel, a small quantity of C_4AH_{13} and C_2ASH_8.

Acknowledgments This research is financially supported by YangFan Innovative & Entrepreneurial Research Team Project (No.201312C12) and National "Twelfth Five-Year" Plan for Science & Technology Support Development Program of China (Project 2014BAB15B01).

References

1. Duan, P., Shui, Z., et al.: Effects of metakaolin, silica fume and slag on pore structure, interfacial transition zone and compressive strength of concrete. Constr. Build. Mater. **44**, 1–6 (2013)
2. Cyr, M., Trinh, M., Husson, B., Casaux-Ginestet, G.: Effect of cement type on metakaolin efficiency. Cem. Concr. Res. **64**, 63–72 (2014)
3. He, Z., Qian, C., et al.: Nanoindentation characteristics of calcium hydroxidemetakaolin blended with sodium hydroxide solutions. J. Wuhan Univ. Technol. Mater. Sci. Ed. **29**(1), 185–189 (2014)
4. Ambroise, J., Maximillen et al.: Properties of metakaolin blended cements. Adv. Cem. Mater. **1**(4), 161–68 (1994)
5. Ramlochan, T., Thomas, M., Gruber, K.A.: The effect of metakaolin on alkali-silica reaction in concrete. Cem. Concr. Res. **30**(3), 339–344 (2000)
6. Guneyisi, E., Gesoglu, M., Karaoglu, S., Mermerdas, K.: Strength, permeability and shrinkage cracking of silica fume and metakaolin concretes. Constr. Build. Mater. **34**, 120–130 (2012)
7. Kim, H.S., Lee, S.H., Moon, H.Y.: Strength properties and durability aspects of high strength concrete using Corean metakaolin. Constr. Build. Mater. **21,** 1229–37 (2007)
8. Murat, M.: Hydration reaction and hardening of calcined clays and related minerals. I. Preliminary investigation on metakaolinite. Cem. Concr. Res. **13**(2)259–66 (1983)
9. Rojas, M.F., Cabrera, J.: The effect of temperature on the hydration rate and stability of the hydration phases of metakaolin-lime-water systems. Cem. Concr. Res. **32**133–38 (2002)
10. Silva, P.S., Glasser, F.P.: Phase relation in the system $CaO\text{-}Al_2O_3\text{-}SiO_2\text{-}H_2O$ relevant to metakaolin-calcium hydroxide hydration. Cem. Concr. Res. **23,** 627–39 (1993)
11. Luke, K., Glasser, F.P.: Selective dissolution of hydrated blast furnace slag cements. Cem. Concr. Res. **17**(2), 273–282 (1987)
12. Plowman, C., Cabrera, J.G.: The use of fly ash to improve the sulphate resistance of concrete. Waste Manage. **16**, 145–49 (1996)

Reactivity of Calcined Clay in Alite-Calcium Sulfoaluminate Cement Hydration

Natechanok Chitvoranund, Barbara Lothenbach, Sakprayut Sinthupinyo and Frank Winnefeld

Abstract Alite-calcium sulfoaluminate (ACSA) cement is a low energy cement which contains both alite (C_3S) and ye'elmite ($C_4A_3\$$). Blending of ACSA with calcined clay would be a possibility to further decrease the CO_2 balance of ACSA. Clay with 40–50 % kaolinite content was calcined in a static furnace at 750 °C for 30 min. The pozzolanic reaction of the calcined clay was studied using the reaction between calcite, portlandite and calcined clay under controlled pH conditions (in 0.1 and 0.3 M KOH solutions). The portlandite consumptions up to 7 days were characterized by thermogravimetric analysis (TGA) and used to determine the reaction degree of the calcined clay using thermodynamic modelling. Calcined clay showed a high reactivity during the first days. This initial high reactivity of the clay observed in the pozzolanity test agrees with the results of the ACSA-clay blends obtained by X-ray diffraction and thermogravimetric analysis, where significant portlandite consumption by added clay was observed during the first days of hydration. After 28 days the ACSA blends with 10 % calcined clay show a significant higher compressive strength than the plain ACSA.

1 Introduction

Portland cement production generates about 5–7 % of the total global carbon dioxide (CO_2) emission mainly from limestone calcination and use of primary fuels [1]. Thus alternative binders, such as special cements based on clinkers with a lower

N. Chitvoranund (✉) · S. Sinthupinyo
Siam Research and Innovation, 51 Moo 8, Tubkwang, Kaeng Khoi 18260, Saraburi, Thailand
e-mail: natechac@scg.co.th

B. Lothenbach · F. Winnefeld
Laboratory for Concrete and Construction Chemistry, Empa, Swiss Federal Laboratories for Materials Science and Technology, Überlandstrasse 129, 8600 Dübendorf, Switzerland

K. Scrivener and A. Favier (eds.), *Calcined Clays for Sustainable Concrete*, RILEM Bookseries 10, DOI 10.1007/978-94-017-9939-3_46

limestone content in the raw meal or cement-free alkali activated binders, have been developed.

Alite-calcium sulfoaluminate cement (ACSA) is one type of calcium sulfoaluminate cement produced at 1250–1300 °C. CO_2 emissions are reduced compared to Portland cement due to lower burning temperature and lower limestone content in the raw meal. The phase composition of ACSA clinker contains mainly alite co-existing with ye'elimite and some other phases such as belite, ferrite and anhydrite. Fluxing agents or some added dopants, such as CaF_2, MgO and CuO, are important to lower the formation temperature of alite, providing its coexistence with ye'elimite [2, 3].

The use of supplementary cementitious materials (SCMs) is another alternative way to lower the amount of CO_2 emissions by replacing a part of the clinker. Metakaolin is a pozzolanic material produced from the calcination of kaolinitic clay between 550–800 °C. It reacts with portlandite under the formation of hydration products, mainly calcium aluminum silicate hydrates (C-A-S-H) [4]. Calcined clays, such as metakaolin, can be used at a high level of clinker substitution due to their high pozzolanic activity [5].

The main idea of this study is to combine the two possibilities to lower CO_2 emissions, synthesizing a low energy cement and blending it with an SCM.

2 Materials and Methods

2.1 Materials

ACSA clinker was synthesized in a laboratory furnace at 1300 °C. The main phases of the clinker are alite (50 %), ye'elimite (10 %), belite, and ferrite. Calcined clay was produced from a source of kaolinitic clay containing 40–50 % of kaolinite located in the central part of Thailand. After the calcination process for 30 min at 750°C in a static furnace, kaolinite could not be identified by X-ray diffraction (XRD), and amorphous content increased instead.

ACSA cement was prepared by blending 95 mass% of ACSA clinker and 5 mass % of anhydrite. In the blended system 10 mass% of ACSA cement was replaced by calcined clay. Chemical (X-ray fluorescence analysis) and phase composition (XRD/Rietveld) of the raw materials used are shown in Table 1.

2.2 Pozzolanicity Test

The pozzolanic reactivity of the calcined clay was tested under controlled pH conditions in a mixture with calcite ($CaCO_3$) and portlandite ($Ca(OH)_2$) with a ratio portlandite-calcite-calcined clay of 6:1:2 by mass. The solid material was blended with KOH solution at a liquid to solid ratio of 1:1. Two concentrations of 0.1 and

Table 1 Chemical and phase composition of the raw materials (wt%)

	ACSA clinker	Anhydrite	Calcined clay		ACSA clinker		Anhydrite	Calcined clay
SiO_2	14.91	0.01	44.6	C_3S	48.3	C$	93.6	
Al_2O_3	9.64	0.06	33.16	(α + β) C_2S	11.8	Cc	1.7	
Fe_2O_3	4.22	0.02	14.77	γ-C_2S	2.2	CH_2	4.7	
CaO	61.61	40.7	1.31	C_4AF	12.9	SiO_2		0.8
MgO	0.78	0.01	0.76	$C_4A_3$$	9.6	KAS_3		1.7
SO_3	6.64	58.04	0.08	CaO (free)	1.5	NAS_3		1.1
Na_2O	0.12	0.03	0.38	C$	5	MA_2SH		4.7
K_2O	0.12	0.01	0.16	C_2A_2S	3.3	Fe_2O_3		5.7
TiO_2	0.62	0.01	2.34	$C_5S_2$$	2.6	TiO_2		1.2
LOI	1.08	1.07	1.85	CH	2.4	Amorphous		84.8

0.3 M KOH (referring to pH about 12.8 and 13.2, respectively) were applied, related to the range of pH values measured for ACSA pastes (the result of pore solution measurements will be reported elsewhere). The samples were cured under sealed conditions at 20 °C. Prior to analysis, hydration was stopped by solvent exchange using first isopropanol and then diethyl ether, followed by a gentle grinding of the stopped pastes in an agate mortar. Portlandite consumption up to 7 days was quantified by thermogravimetric analysis (TGA). By thermodynamic modelling using GEMS [6, 7] updated with the cement-specific database CEMDATA14 [8, 9], the amount of portlandite consumed was calculated depending on the amount of dissolved calcined clay, thus allowing to convert portlandite consumption to reaction degree of calcined clay.

2.3 Hydration Study

The hydration of plain ACSA cement and ACSA cement blended with clay was studied by XRD and TGA using a water to binder ratio of 0.485 at 20 °C. Sample preparation was performed as described in Sect. 2.2.

The change of the potential phase assemblage of hydrated ACSA clinker blended with 0–15 mass% of calcined clay was calculated by thermodynamic modelling, assuming complete hydration of the reactive phases.

2.4 Compressive Strength

Compressive strength of mortar cubes (50 mm × 50 mm × 50 mm) was determined after 1, 3, 7 and 28 days according to ASTM C109 M.

3 Results and Discussion

3.1 Pozzolanic Reactivity of the Calcined Clay

The two different concentrations of KOH solution were prepared to observe the effect of pH on pozzolanic reactivity of calcined clay. Figure 1 shows that portlandite content strongly decreases up to 7 days for both concentrations of KOH. In case of the sample with the higher pH, portlandite consumption proceeds faster. Figure 2 shows the reaction degree of the calcined clay calculated from portlandite consumption and thermodynamic modelling. The calcined clay shows a high reactivity in both pH environments, reaching reaction degrees of about 70 % after 7 days for 0.1 M KOH, and of about 90 % after 7 days for 0.3 M KOH.

3.2 Influence of Calcined Clay on Hydration and Strength Development of ACSA

The hydration products of plain ACSA and the clay-blended ACSA-as determined by XRD and TGA are similar for these two systems. The crystalline hydrate phases identified by XRD (Fig. 3a) after 91 days are mainly ettringite, monosulfate and portlandite. There seems to be slightly less portlandite and slightly more monosulfate in the sample containing clay compared to the plain ACSA. Similar results can be derived from TGA analysis (Fig. 3b).

Portlandite content of the two systems was determined by TGA. The consumption of portlandite in the ACSA system with calcined clay starts after 1 day of hydration (Fig. 4), confirming the results from the pozzolanic test.

Thermodynamic modelling agrees well with the experimental results. When adding calcined clay to ACSA (Fig. 5), ettringite and portlandite amounts decrease, and the quantities of monosulfate and C-S-H increase. The volume of hydrates

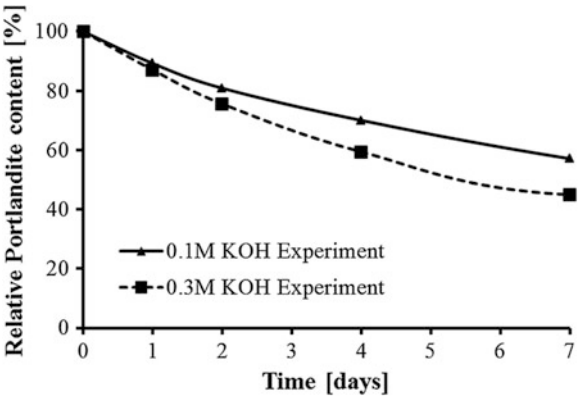

Fig. 1 Relative amount of portlandite referred to the dry starting material

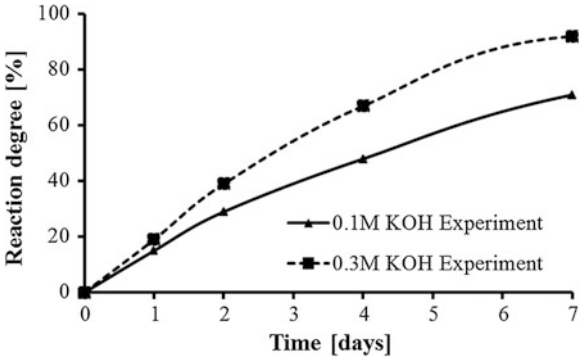

Fig. 2 Reaction degree of calcined clay with time derived from TGA and thermodynamic modelling

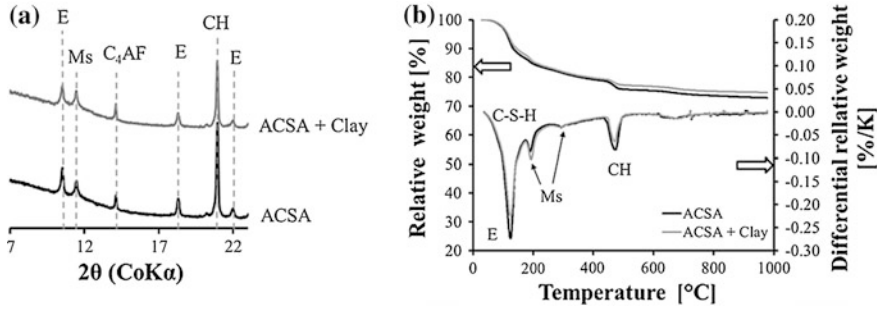

Fig. 3 **a** X-ray diffraction patterns and **b** thermogravimetric analysis of ACSA and ACSA + Clay after 91 days of hydration. E = ettringite, Ms = monosulfate, C_4AF = ferrate phase, CH = portlandite

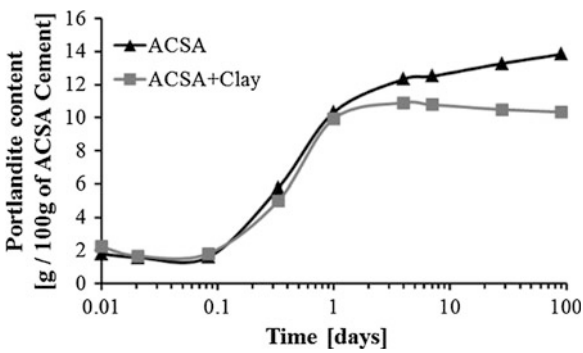

Fig. 4 Portlandite content in ACSA and ACSA with calcined clay up to 91 days of hydration. The data is normalized to unhydrated ACSA cement

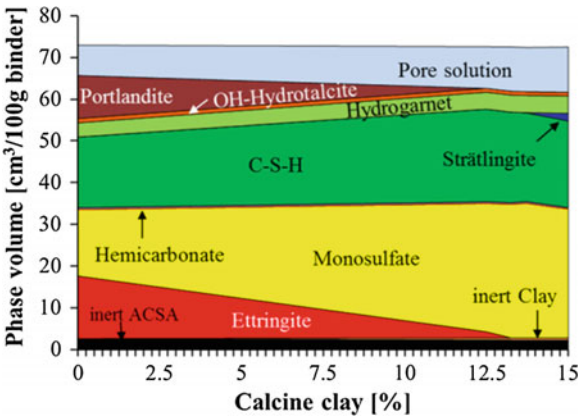

Fig. 5 Thermodynamic modelling of the phase assemblage of ACSA blended with 0–15 mass% calcined clay, assuming complete hydration of all reactive phases

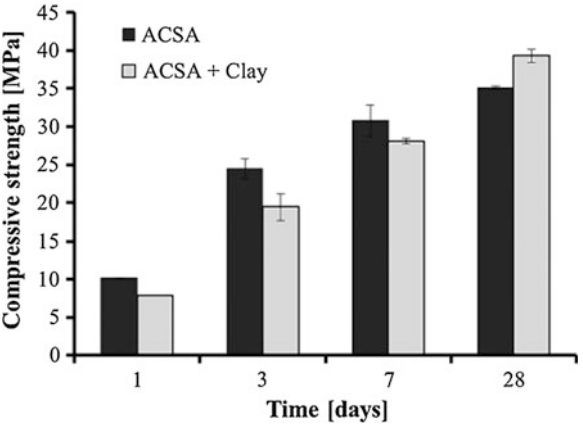

Fig. 6 Strength development of mortars based on ACSA and ACSA + calcined clay

increases up to a clay content of 12 mass%. Beyond about 14 mass% clay added, portlandite is calculated to disappear, and strätlingite occurs as stable hydrate phase.

Up to 7 days, the clay-blended system shows a lower compressive strength than the plain ACSA (Fig. 6). After 28 d, the sample blended with clay shows higher strength than the reference, corresponding to the higher volume of hydrate phases and the lower porosity developed in the blended system (Fig. 5).

4 Conclusions

- The reactivity of the calcined clay can be assessed by the proposed pozzolanic test. It increases with increasing pH.

- When blended with ACSA, the calcined clay shows as well a high pozzolanic reactivity. The clay addition decreases portlandite and ettringite contents and increases the amounts of C-S-H and monosulfate.
- ACSA blended with 10 % calcined clay shows a higher compressive strength after 28 days than the plain ACSA cement. This corresponds to an increase of the volume of hydrate phases and thus to a decreased porosity.

Acknowledgements The authors would like to thank Siam Cement Group (SCG) for financial support and Swiss Federal Laboratories for Materials Science and Technology (Empa), Laboratory for Concrete and Construction Chemistry for technical and facilities support.

References

1. Turner, L.K., Collins, F.G.: Carbondioxide equivalent (CO_2-e) emissions: a comparison between geopolymer and OPC cement concrete. Constr. Build. Mater. **43**, 125–130 (2013)
2. Altun, A.I.: Effect of CaF_2 and MgO on sintering of cement clinker. Cem. Concr. Res. **29**, 1847–1850 (1999)
3. Ma, S., et al.: Influence of CuO on the formation and coexistence of $3CaO.SiO_2$ and $3CaO.3Al_2O_3.CaSO_4$ minerals. Cem. Concr. Res. **36**, 1784–1787 (2006)
4. Tironi, A., et al.: Kaolinitic calcined clays - Portland cement system: Hydration and properties. Constr. Build. Mater. **64**, 215–221 (2014)
5. Tironi, A., et al.: Assessment of pozzolanic activity of different calcined clays. Cem. Concr. Compos. **37**, 319–327 (2014)
6. Wagner, T., Kulik, D.A., Hingerl, F.F., Dmytrieva, S.V.: 'GEM-Selektor geochemical modeling package: TSolMod library and data interface for multicomponent phase models'. Can. Mineral. **50**(5), 1173–1195 (2012)
7. Kulik, D.A., Wagner, T., Dmytrieva, S.V., Kosakowski, G., Hingerl, F.F., Chudnenko, K.V., Berner, U.: GEM-Selektor geochemical modeling package: revised algorithm and GEMS3 K numerical kernel for coupled simulation codes. Comput. Geosci. **17**(1), 1–24 (2013)
8. Matschei, T., Lothenbach, B., Glasser, F.: Thermodynamic properties of Portland cement hydrates in the system $CaO-Al_2O_3-SiO_2-CaSO_4-CaCO_3-H_2O$. Cem. Concr. Res. **37**(10), 1379–1410 (2007)
9. Lothenbach, B., Matschei, T., Möschner, G., Glasser, F.: Thermodynamic modelling of the effect of temperature on the hydration and porosity of Portland cement. Cem. Concr. Res. **38**(1), 1–18 (2008)

Primary Kaolin Waste as Pozzolanic Material in Dry Concrete: Mechanical Properties and Resistance to Attack by Sulphates

M.L.S. Rezende, J.W.B. Nascimento, G.A. Neves and H.C. Ferreira

Abstract This work reported to study the influence of metakaolin obtained from waste beneficiation of primary kaolin, the mechanical and durability properties of dry concretes for precast industry. The metakaolin was obtained by micronization of wastes and subsequent calcination at 800 °C for 2 h. Thermal and X-ray diffraction analyses were also carried out aiming at evaluating the consumption of calcium hydroxide by adding the material to be analysed. Was evaluated by replacing 10, 15 and 20 % by weight of cement in concretes with 12, 15 and 18 % of cement at 7, 14 and 28 days of age under ambient conditions. The substitution of 10 and 15 % by weight of cement by metakaolin in the concrete with 12 % of cement which provided, respectively, an increase of 12 and 6 % in compressive strength compared to concrete without metakaolin. The durability was evaluated by exposure to sulphates whose results showed that, for all traits, using 10 % of metacaulin promoted reduction of dimensional expansion. The results showed that the use of metakaolin obtained from waste in processing kaolin, can foster greater progress in resistance and durability in dry concrete from 28 days of cure.

Keywords Pozzolan · Tailings · Precast concrete

1 Introduction

The concrete used in precast industry has low water content which gives it the usual terminology of "dry concrete", being the air removal and compaction usually obtained by automated machines. Representing 20 % of world production of concrete [1], few studies have been published on the use of pozzolans in dry concrete.

M.L.S. Rezende (✉)
UAEP, CCT, Universidade Federal de Campina Grande, Campina Grande, Brazil
e-mail: luiza@uaep.ufcg.edu.br

J.W.B. Nascimento
UAEAg, CTRN, Universidade Federal de Campina Grande, Campina Grande, Brazil

G.A. Neves · H.C. Ferreira
UAEMat, CCT, Universidade Federal de Campina Grande, Campina Grande, Brazil

K. Scrivener and A. Favier (eds.), *Calcined Clays for Sustainable Concrete*,
RILEM Bookseries 10, DOI 10.1007/978-94-017-9939-3_47

The metakaolin is a pozzolan obtained by calcination kaolinitic clay but, despite the importance of purity of the clay to obtain highly reactive pozzolan [2, 3] researchers [4, 5] reported that metakaolin obtained from kaolinite clays with low ratio Al_2O_3/SiO_2 showed similar results compressive strength when used in partial replacement of Portland cement. In Borborema pegmatitic province (Paraiba–Brazil), the kaolin processing wastes are discarded in the open, in volume estimated by Rezende et al. [6] in two million cubic meters representing environmental risks, however, this residue afforded improvements in the properties of concrete and mortar in which was used as pozzolanic material [7–9]. Being also common in precast elements concrete the attack by sulfates [10] results in the formation of ettringite and thaumasite, expansive reaction that causes fissures and concrete's deterioration. The metakaolin showed to be effective in reducing the expansion in concrete immersed in sodium sulfate solution [11]. This document reports study conducted at the Federal University of Campina Grande on the use of metakaolin, obtained from kaolin waste in dry concrete being evaluated the mechanical properties and the durability by exposure to sulfates.

2 Materials and Methods

2.1 Cement

Table 1 presents the characteristics of the cement employed in this study.

2.2 Kaolin Waste

Were used wastes from first stage (coarse waste—CW, >250 μm) and second stage (thin waste—TW, >75 μm) of the kaolin's processing (Table 2). Table 3 provides the characteristics of metakaolin obtained from CW and TW (1:1) micronized and calcined at 800 °C for 2 h.

2.3 Mixtures

The aggregates was crushed granite (≤9.5 mm), quartzose sand and stone powder (37, 40 and 23 % respectively). In Table 4 are described the mixtures and the amount of binders.

Table 1 Characteristics and cement composition CPV ARI [12]

SO_3 (%)	3.37	Specific gravity: (g/ cm^3)	3.13
(CaO) livre (%)	2.16	B.E.T. (m^2/g)	6.81
Compressive strength at 7 days (MPa)			40.47

Table 2 Chemical composition of kaolin waste (CW and TW)

(%)	SiO_2	Al_2O_3	Fe_2O_3	K_2O	TiO_2	Na_2O	LOI	$SiO_2 + Al_2O_3 + Fe_2O_3$
CW	69.92	15.07	0.64	6.08	Traces	0.28	8.0	85.63
TW	51.07	32.54	0.90	5.55	0.11	–	9.6	84.51

Table 3 Metakaolin characteristics

D_{50} (μm)	9.45	B.E.T. (m^2/g)	25.95
Passing 45 μm (%)	3.13	Pozzolanicity index	95

2.4 Methodology

Cylindrical specimens (Ø 50 mm × 100 mm) were molded and kept at ambient conditions (23 °C and RH 83 %) for 7, 14 and 28 days and was evaluated the compressive strength at the end of each period and the results were compared to those without metakaolin. The reduction of $Ca(OH)_2$ caused by pozzolanic reaction was evaluated by thermogravimetric analysis. For the sulphates exposure's test, specimens (28 days of cure) were immersed in sodium sulphate solution (10 %) for 42 days and the dimensions measured every 7 days. The results were compared with specimens immersed in water for the same period.

3 Results and Discussion

3.1 Compressive Strength

Figure 1 shows the graphs of the evolution of compressive strength.

For the concrete with 18 % cement (Group A) there was a decrease in compressive strength with increasing replacement levels of the cement by metakaolin, reaching a reduction 28.9 for 20 % of metakaolin. For the concretes with 15 % (Group B) and 12 % (Group C) of cement, it appears that after 28 days of curing the reduction of resistance decreased to values on the order of 1 %, which was expected considering that the index of pozzolanic activity of metakaolin was less than 100 %.

In Table 5 are reported the values of compressive strength, hydration index (Hindex) and of pozzolanicity (Pindex), the latter obtained through thermal analysis [13].

The thermogravimetric analysis showed a reduction of calcium hydroxide and increase of hydrated products in relation to concrete without metakaolin, confirming the presence of pozzolanic reaction. However, for the mixture with 18 % of cement, the pozzolanic reaction was not enough to compensate for the replacement of cement by metakaolin.

Table 4 Mixtures evaluated

Mixture	A (18 % cement)				B (15 % cement)				C (12 % cement)			
	A0	A10	A15	A20	B0	B10	B15	B20	C0	C10	C15	C20
Cement	375	337	319	300	322	290	274	258	266	239	226	213
MK	0	38	56	75	0	32	48	64	0	27	40	53
W/(C + MK)	0.52	0.53	0.54	0.56	0.54	0.57	0.58	0.60	0.56	0.57	0.58	0.60

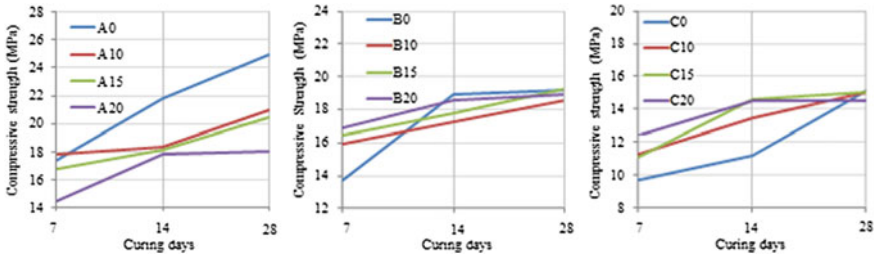

Fig. 1 Graphs of the evolution of compressive strength at 7, 14 and 28 curing days

Table 5 Compressive strength (CS), hydration (H_{index}) and pozzolanicity index (P_{index})

	Age (days)	A (18 % cement)				B (15 % cement)				C (12 % cement)			
		A0	A10	A15	A20	B0	B10	B15	B20	C0	C10	C15	C20
CS (MPa)	7	17	15	15	15	14	14	13	12	10	10	12	10
	14	20	19	17	16	17	15	15	12	11	12	13	12
	28	22	21	18	17	18	17	17	16	15	16	14	13
H_{index} (%)	7	78	85	89	81	71	74	79	81	71	74	76	76
	14	73	80	80	80	69	76	78	80	69	75	76	79
	28	75	79	80	76	73	78	79	81	70	74	74	79
P_{index} (%)	7		109	115	105		105	112	114		104	107	107
	14		109	110	109		110	113	115		108	110	114
	28		105	107	101		108	109	111		106	107	113

3.2 Sulfate Resistance

Figure 2 shows the results of dimensional variation after exposure to sodium sulphate.

Observing the Fig. 2 it turns that the use of metakaolin 10 % for all mixtures, promoted reducing the dimensional variation resultant of exposure to sodium sulphate in relation to the concrete without metakaolin, staying below 0.03 % maximum limit recommended by the ABCP (Brazilian Portland Cement Association).

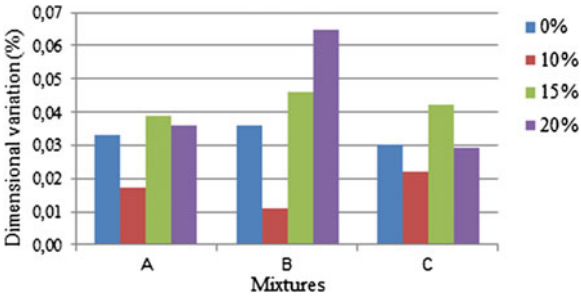

Fig. 2 Dimensional variation after exposure to sodium sulfate for 42 days

Fig. 3 Wear of the specimens due to intrusion of sulphates on the edges

The samples immersed in sodium sulphate solution at the end of the assay, exhibited little deterioration located at the edges formed by the side face and base due to the intrusion of sulphate in two adjacent faces (Fig. 3).

4 Conclusions

The residue kaolin of the Borborema region in the composition 1:1 (50 + 50 % grit thin stillage) after grinding and calcination at 800 °C for 2 h has characteristics that allows its use as a pozzolanic material;

The low moisture content of concrete for the production of hollow blocks for masonry, limits the use of metakaolin for concretes with lower cement percentage in its composition, wherein the water/cement ratio becomes greater;

Concretes with 12 % of cement and replacement of 10 % by weight of cement with metakaolin, presented increase of compression strength in relation the concrete without metakaolin;

The use of 10 % metakaolin promoted reduction in dimensional variation of all samples when exposed to sodium sulfate solution (10 %) for 42 days.

Acknowledgments The authors thank CNPq—Conselho Nacional de Desenvolvimento Científico e Tecnológico e a CAPES—Conselho de Aperfeiçoamento de Pessoal de Nível Superior for the financial support, the Kaolin Caiçara Ltda.—Ecuador/RN/Brazil for donating the waste and Ultrafine Technologies—Indaiatuba/SP/Brazil by micronization services.

References

1. Cassagnabère, F., Mouret, M., Escaidelas, G.: Broilliard. 'Use of flash metakaolin in a slip-forming concrete for the precast industry'. Mag. Concr. Res. **61**(10), 767–778 (2009)
2. Souza, P.S.L.: 'Verificação da influência do uso de metacaulim de alta reatividade nas propriedades mecânicas do concreto de alta resistência', Doutoramento em Engenharia Civil – Porto Alegre, RS: Universidade Federal do Rio Grande do Sul (2003)
3. Zampieri, V.A.: 'Mineralogia e mecanismos de ativação e reação das pozolanas de argilas calcinadas', Mestrado em Geociências – São Paulo, SP: Universidade de São Paulo (1989), 191 p
4. Cassagnabère, F., Mouret, M., Escaidelas, G., Broilliard, P., Bertrand, A.: Metakaolin a solution for the precast industry to limit the clinker content in concrete: mechanical aspects. Constr. Build. Mater. **24**, 1109–1118 (2010)
5. Siddique, R., Klaus, J.: Influence of metakaolin on the properties of mortar and concrete: a review. Appl. Clay Sci. **43**, 392–400 (2009)
6. Rezende, M.L.S., Menezes, R.R., Neves, G.A., Nascimento, J.W.B., Leal, A.F.: Utilização de resíduo de caulim em blocos de vedação. REM. Revista Escola de Minas **61**(3), 285–290 (2008)
7. Menezes, R.R., Neves, G.A., Souza, J., Melo, W.A., Ferreira, H.S., Ferreira, H.C.: Atividade pozolânica dos resíduos de caulim para uso em argamassas para alvenaria. Revista Brasileira de Engenharia Agrícola e Ambiental **13**(6), 795–801 (2009)
8. Barata, M.S., Angélica, R.S.: Caracterização dos resíduos cauliníticos das indústrias de mineração de caulim da Amazônia como matéria-prima para produção de pozolanas de alta reatividade. Cerâmica **58**, 36–42 (2012)
9. Rezende, M.L.S.: 'Resíduo de caulim primário como material pozolânico em concretos secos: propriedades físico-mecânicas e durabilidade', Doutoramento em Engenharia Agrícola – Campina Grande, PB: Universidade Federal de Campina Grande (2013)
10. Glasser, F.P., Marchand, J., Sanson, E.: Durability of concrete—degradation phenomenon involving detrimental chemical reactions. Cem. Concr. Res. **38**, 226–246 (2008)
11. Al-Akhras, N.M.: Durability of metakaolin concrete to sulphate attack. Cem. Concr. Res. **36**, 1727–1734 (2006)
12. ABNT - Associação Brasileira de Normas Técnicas 'Cimento Portland de alta resistência inicial' **NBR 5733 EB 2** (Rio de Janeiro, 1991)
13. Lima, P.R.L., Toledo Filho, R.D.: Uso de metacaulinita para incremento de compósitos à base de cimento reforçados com fibra de sisal. Ambiente Construído **8**(4), 7–19 (2008)

The Influence of Cavitation Treatment on Amorphization of Kaolinite in the Dispersion of the "Kaolin—$Na_2O \cdot nSiO_2 \cdot mH_2O$—NaOH—$H_2O$" Composition

P. Krivenko, S. Guziy and J. Abdullah Al Musa

Abstract The paper covers the results of study of cavitation treatment on amorphization of kaolinite n the alkaline aluminosilicate dispersions of the "Kaolin—$Na_2O \cdot nSiO_2 \cdot mH_2O$—NaOH—$H_2O$" composition. The purpose of the study was to establish a possibility to substitute metakaolin in these dispersions for kaolin. The results show that amorphization of the kaolinite in the field of dynamic cavitation takes place at relatively low temperatures (below 60 °C) resulting in the formation of the properties of these dispersions that are comparable to those of the metakaolin-based dispersions. Above this, rheological and technological properties of the alkaline aluminosilicate dispersions of the "Kaolin—$Na_2O \cdot nSiO_2 \cdot mH_2O$—NaOH—$H_2O$" composition such as viscosity, shelf life, adhesion to concrete, metal and wood have considerably improved.

1 Introduction

Traditionally, kaolin is the main raw material in the manufacture of technical ceramics. Product of his firing—metakaolin—is used an active mineral additives in concrete mixes and as a basis for the synthesis of geocements. To heating kaolin, the chemical reactions be going up to following scheme:

P. Krivenko (✉) · S. Guziy · J. Abdullah Al Musa
Scientific Research Institute for Binders and Materials,
Kiev National University of Civil Engineering and Architecture, Kiev, Ukraine
e-mail: pavlo.kryvenko@gmail.com

K. Scrivener and A. Favier (eds.), *Calcined Clays for Sustainable Concrete*,
RILEM Bookseries 10, DOI 10.1007/978-94-017-9939-3_48

$$2Al_2Si_2O_5(OH)_4 \xrightarrow{823-1073K} 2Al_2Si_2O_7 + 4H_2O$$
kaolin → metakaolin

$$2Al_2Si_2O_7 \xrightarrow{1198-1223K} Si_3Al_4O_{12} + SiO_2$$
spinel + amorphous (silicon spinel)

$$3Si_3Al_4O_{12} \xrightarrow{1323K} 2Si_2Al_6O_{13} + 5SiO_2$$
mullite + cristobalite

The above process of transition of kaolin in metakaolin enough energy intensive and prolonged in time. According to the thermal analysis, the activation energy of thermal degradation of kaolin in metakaolin is 24.146 J/mol K. To achieve a given value of the activation energy by conventional grinding devices is virtually impossible. We have suggested that the transition of kaolin in metakaolin, bypassing the stage of firing, it is necessary to create special conditions, namely kaolin dispersion can be activated in a highly alkaline medium at elevated pressures. Make this process possible with the help of cavitation devices [1–3].

The aim of this work is to study the effect of cavitation treatment for amorphization of kaolinite in the dispersion of the form "Kaolin—$Na_2O \cdot nSiO_2 \cdot mH_2O$—NaOH—$H_2O$".

2 Experimental

To investigate the process of transformation of metakaolin to kaolin in an alkaline medium using a dispersion containing kaolin type $Na_2O \cdot Al_2O_3 \cdot 6SiO_2 \cdot 20H_2O$. These dispersions were prepared by mixing in a conventional mixer such Hobart and hydrodynamic cavitator (Figs. 1 and 2).

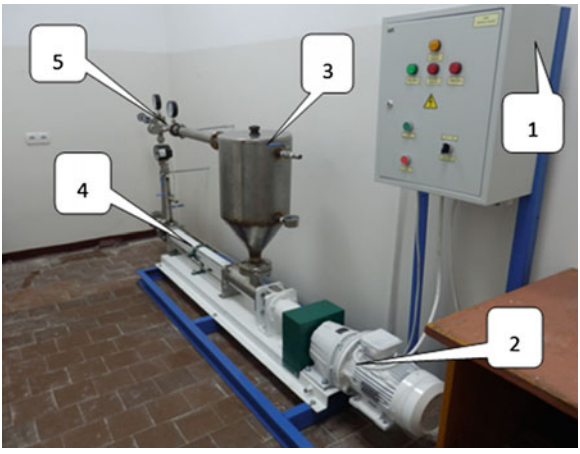

Fig. 1 Appearance hydrodynamic cavitator: *1*—control panel; *2*—motor-reducer; *3*—reactor; *4*—screw pump; *5*—homogenizer

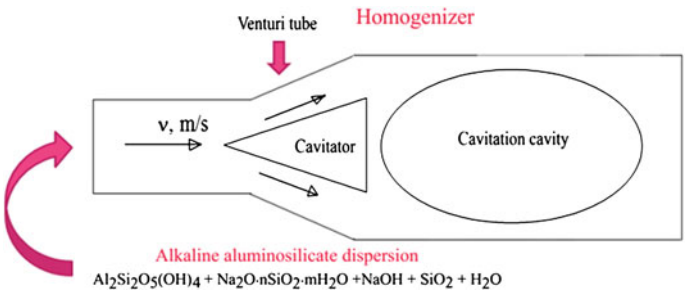

Fig. 2 Scheme homogenizer hydrodynamic cavitator

In the alkali treatment process of cavitation dispersions containing kaolin cavitation number was determined, changes in pressure and temperature, and activation energy of the process.

The number of activation was calculated according to the formula:

$$\chi = \frac{2(P - P_s)}{\rho v^2}, \tag{1}$$

where P—flow pressure, Pa; P_S—saturated vapor pressure, Pa; ρ—the density of the dispersion, kg/m^3; v—flow rate at the inlet nozzle, m/s.

Given the fact that the occurrence of cavitation is performed when the flow rate boundary $V = Vc$, under the condition of equality of pressure in the flow and the formation of vapor (saturated vapor gas) calculated activation energy of the process:

$$E = tg\varphi \cdot R \tag{2}$$

where $tg\varphi$—angle curve $p = f(t)$; R = 8.31, J/mol K—universal gas constant.

With the help of X-ray analysis was performed confirmation of transformation transition kaolin in metakaolin in dispersions studied [4, 5].

Viscosity of the dispersion process, the value of adhesion to various substrates and the viability of the dispersions was determined according to normative and technical documents in Ukraine.

3 Discussion of Results

Analysis of the data (Fig. 3) shows that the 3 min cavitation treatment of the kaolin dispersion at a pressure of 2 bar, a temperature of 308 K and a dispersion including cavitation X = 0.29 < 1 (cavitation film) processes occur dispersion of kaolinite particles in the alkaline dispersion. The activation energy of the process amounts to 16.311 J/mol K. The process of dispersion is carried out by cumulative exposure to

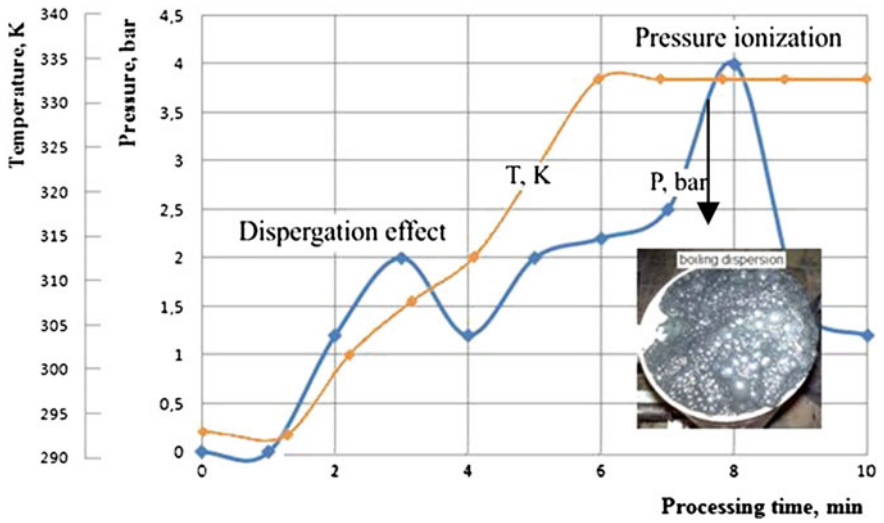

Fig. 3 Pressure and temperature changes in the alkaline aluminosilicate dispersion depending on the time of the cavitation process

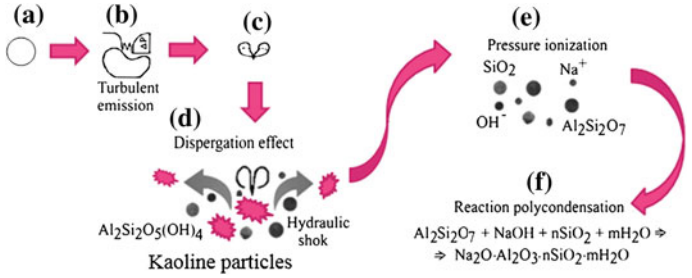

Fig. 4 Diagram of the amorfization of kaolin in metakaolin in alkaline dispersion in the fields of dynamic cavitation: **a** steam-gas bubble; **b**, **c**, **e** the transformation of steam bubbles; **d** hydrodynamic impact on kaolin particles (dispersion effect); **e** ionized components of the dispersion; **f** reaction polycondensation towards the formation of alkali aluminosilicate structures at the nanoscale

jets of solid particles at the moment of collapse of gas bubbles (Fig. 4a–d) with a rise in temperature of the dispersion from 293 to 308 K.

In the transition to the regime already super cavitation 6 min processing alkaline dispersion (cavitation number $X = 0.088 \ll 1$), there is growing pressure to 4 bar and temperatures up to 333 K. The activation energy of the process amounts to 24.146 J/mol K, which is achieved and during firing kaolinite. Under these process parameters indicated ionization protonation and dispersion components (Fig. 4e) to form active monomeric molecules of silicates and aluminosilicates.

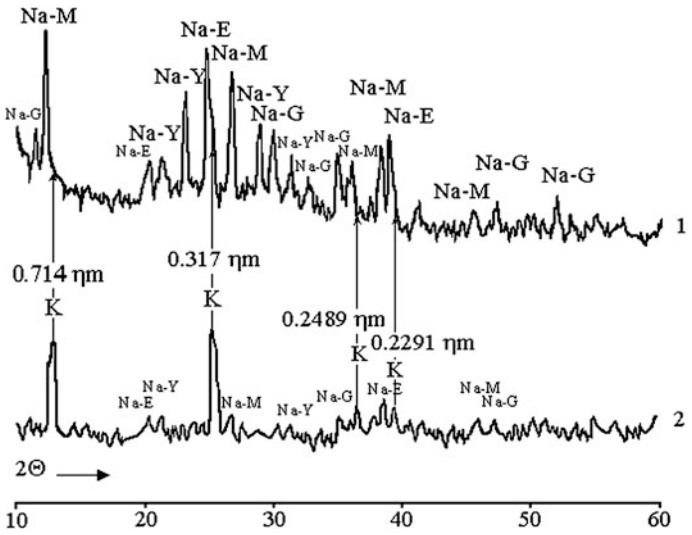

Fig. 5 X-ray images of hardening artificial stone based on alkali kaolin dispersions after cavitation (*1*) and the routine processing (*2*). Designations: *K*—kaolin; *Na-G*—heulandite; *Na-E*—chabazite; *Na-Y*—faujasite; *Na-M*—mordenite

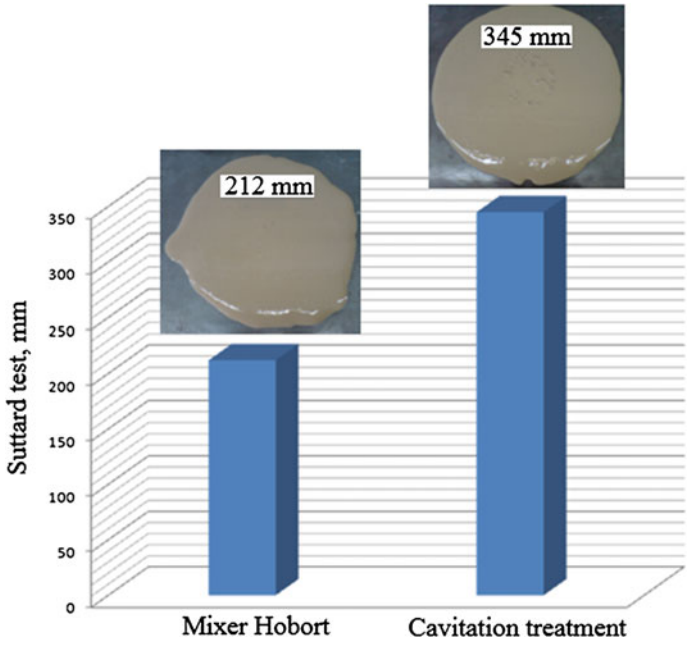

Fig. 6 Technological viscosity, mm, Suttard test

Table 1 Basic physical and mechanical properties of alkali aluminosilicate dispertions after cavitation treatment

Properties	Mixer hobart	Cavitation treatment
Preservation of alkaline aluminosilicate dispertions months (closed container)	1	24
Adhesion, MPa, to the substrate: Concrete Metal Wood	0.6–1.5 0.6–0.9 1.2–2.3	0.9–2.3 0.9–1.2 2.5–2.7

After completion of the cavitation treatment alkaline kaolin dispersion (Fig. 4f) the process of condensation components of the dispersion in the direction of the nucleation of zeolite similar structures at the nanoscale [6–9]. After cavitation treatment alkaline kaolin dispersion (Fig. 5 curve 1) in products of hardening are not fixed diffraction spikes kaolin (d = 0.714; 0.317; 0.2489; 0.2291 nm).

In alkaline kaolin, dispersion prepared by conventional means, in products marked hardening diffraction spikes characteristic kaolin (Fig. 5 curve 2).

Cavitation treatment alkaline kaolin dispersions their reduces technological viscosity 1.63 times (Fig. 6), shelf life by 24 times and adhesion to substrates, on average, 1.5 fold compared with those of alkaline dispersions of kaolin which are not subjected to cavitation treatment (Table 1).

4 Conclusions

Because of research, the possibility of amorphization of kaolin in metakaolin in alkaline dispersions, bypassing the stage of firing, due to the action of cavitation effects. These effects are justified dynamic action of the vapor phase, aimed at dispersant solids dispersion, changes in physical and chemical parameters of the liquid phase to form a dispersion of the active monomeric molecules of silicates and aluminosilicates, zeolites such embryos phases at the nanoscale. The process parameters to ensure the transformation of the following: a pressure of 4 bar, the temperature of 333 K, the processing time 6 min, the activation energy of 24,146 J/mol K.

Cavitation treatment of the kaolin dispersion alkaline process reduces the viscosity of 1.63 times, to increase shelf life by 24 times and adhesion to substrates, an average of 1.5 times as compared with those in the alkaline dispersion of the kaolin, which has not been subjected to cavitation treatment.

References

1. Fedotkin, I.M., Gulyi, I.S.: Cavitation: Cavitation Engineering, their use in the Industry (Theory, Calculations and Designs of Cavitation Devices), Part I. Poligrafknika Publish, Kiev (1997)
2. Fedotkin, I.M., Gulyi, I.S.: 2000: Cavitation: Cavitation Engineering, their use in the Industry (Theory, Calculations and Designs of Cavitation Devices), Part II. OKO JSC, Kiev (2000)
3. Vitenko, T.M.: Mechanism and kinetics of intensifying action of hydrodynamic cavitation in chemical and technological processes: Synopsis of the thesis… for Doc. of Sci. (Eng.), 36 p. 17 May 2008, Lvov (2008)
4. Gorshkov, V.S., Timashev, V.V., Savelyev, V.G.: Methods for Physical and Chemical Analysis of Binders. Vysshaya Shkola Publishing House, Moscow (manual) (1984)
5. Semushin, V.N.: X-ray Detector for Zeolites. Nauka Publish, Novosibirsk (1986)
6. Guziy, S.G.: Features of processes of structurization of binders compositions in the system "$xNa_2O{\cdot}yAl_2O_3{\cdot}nSiO_2{\cdot}mH_2O$. In: Proceedings of XII Symposium on Science and Research in the Silicate Chemistry, Chemistry of no Silicate Binders and Technology Application SILICHEM, pp. 35–41, Brno, Czech Republic
7. Guziy, S.G.: Research of a microstructure of an artificial stone of a binder composition in system $xNa_2OyAl_2O_3nSiO_2mH_2O$. In: Proceedings of the International Symposium on Non-traditional Cement and Concrete III, pp. 312–319, Brno, Czech Republic (2008)
8. Guziy, S.G., Terenchuk, S.A.: Research of physical properties of alkali aluminosilicate suspensions after cavitational treatment. NTU "KhPI" Scientific Journals. Collection of scientific papers. Special issue "Chemistry, chemical technology and environment", No. 65, pp. 119–126. NTU "KhPI", Kharkov (2010)
9. Kryvenko, P.V., Guziy, S.G., Abdullah Al Musa, J.: Effect of cavitational treatment on nanostructuring of alkali aluminosilicate dispersions. In: Proceedings of VI International Conference on Nano-Technology in Construction (NTC 2014), pp. 52–64, Cairo, Egypt

Role of Metakaolin on Lowering pH of the Alkali Activated Cement Concrete in Barrier Application

P. Krivenko, O. Petropavlovsky and E. Kavalerova

Abstract The paper covers the results of analysis of the known-in-the-art methods and techniques allowing to lower pH-values of a hardening cement stone used in immobilization of low and intermediate level wastes (cementation) or erection of engineering facilities for long-term disposal of these wastes. The best cement for this application is an alkali activated cement. Properties of the alkali activated slag cement with a modifying additive—metakaolin—added in a quantity of 10 % by mass are reported and discussed. The obtained results show that depending upon type and content of alkaline activator these properties can be tailored in a target direction. The addition of metakaolin was found to accelerate the process of free alkali binding resulted in the formation of insoluble compounds, thus lowering a pH-value of the resulted cement stone to the values of pH-index below 11. Moreover, the insoluble components that are formed and which are analogs to natural zeolites exhibit excellent physico-chemical properties and add high durability to barrier systems for which these cements are used.

1 Introduction

Current practice of nuclear waste management includes their conditioning and immobilization, for example, by cementation, and placement in special containers with following long-term disposal in engineered facilities.

Structures of the engineered facilities should be constructed in such a way that materials of which they are made would maintain their properties during a long-term period. For example, this period for low and intermediate level nuclear wastes with half-life of 30 and 29.1 years (Cs-137 and Sr-90 respectively) is 300 years [1].

Main types of near-surface disposal facilities for these wastes are represented in [1].

P. Krivenko (✉) · O. Petropavlovsky · E. Kavalerova
Scientific Research Institute for Binders and Materials, Kiev National University of Civil Engineering and Architecture, Kiev, Ukraine
e-mail: pavlo.kryvenko@gmail.com

K. Scrivener and A. Favier (eds.), *Calcined Clays for Sustainable Concrete*,
RILEM Bookseries 10, DOI 10.1007/978-94-017-9939-3_49

As it follows from [1], basic structural elements of a disposal facility are structures made from concrete and materials constituting sealing and hydro-insulating backfiller, selected chiefly from clay materials (bentonite clay). Stability of properties of these materials in time, as well as absence of influence of various factors on these properties as a result of inner genesis of these materials and impact of environment (temperature, humidity, aggressive exposure) are key factors determining reliability and safety of nuclear waste disposal [2].

Thus, stability of the engineered barrier systems is caused chiefly by chemical aspects, these are:

- interaction occurring between the products of concrete corrosion and a secondary barrier;
- durability of concrete;
- ability of secondary barriers to reliable localization of radioactive elements.

A majority of the applied design solutions of the near-surface nuclear waste storage facilities is based on the use of engineered anti-migration (engineered-geochemical) structures of secondary barriers made using bentonite clays.

According to the results reported in [3], the use of sodium bentonites as secondary barriers turned out to be highly effective with regard to sorption of radionuclides provided that the values of pH-index of environment did not exceed 11.5 [4].

A portland cement stone creates, upon contact with an aqueous medium, the values of pH-index higher than 12.5, thus affecting negatively efficiency of operational work of secondary barriers (bentonite clay).

That is why a choice of a proper cement type for concretes should be done in terms of required low value of pH-index of the cement stone (pH ≤ 11.5) [4] and high durability of the resulted concrete which can be achieved due to specific features of hydration products and high physico-mechanical properties.

Analyzing data on properties of various hydraulic binding materials suggested concluding that these requirements could be met with the help of the alkali activated slag cements [5–9], which in physico-chemical properties are superior to traditional cements. The lowering of pH of the alkali activated slag cement stone can be reached by introduction into the cement composition of an aluminosilicate additive which can bind free ions of Na (Na^+) [10].

The objective of the study was to determine the effect of metakaolin additive on changes in values of pH-index of the hardening alkali activated slag cement stone and its properties.

2 Experimental

The alkali activated slag cement with 10 % metakaolin additive by mass contained basic granulated blast-furnace slag with modulus of basicity (CaO + MgO/Al_2O_3 + SiO_2) = 1.09 and Portland cement clinker as major components.

The process of grinding in a laboratory ball mill filled with metallic balls was done until a fineness expressed by Blaine specific surface area of 430–450 m^2/kg was obtained.

The solutions of sodium metasilicate of densities 1050, 1100, and 1160 kg/m^3 (further, MS), as well as a solution of soda ash (further, SA) of density 1160 kg/m^3 were used as alkaline activators.

A standard sand meeting the EN 196-1 requirements was used as fine aggregate.

Preparation of test samples was done in accordance with the EN 196 requirements.

In measuring shrinkage deformations, a length of the samples aged 7 days was taken as an initial (basic) measurement, and the lengths of the samples aged 14, 28, 56 and 90 days were measured.

The measured shrinkage deformations were presented as percentage of the basic measurement.

Measurement of pH-index of the leachate was done using a pH-meter 150M with an accuracy to 0.05 units in accordance with the following procedure: 10 g of a powdered sample with particle size less than 0.2 mm was mixed with 100 ml distilled water and cured for 24 h at t = (20 ± 2) °C. A pH of the leachate was measured 3–5 min after the electrode system of the pH-meter was switched on automatic system of thermo-compensation was dipped. The pH-index of the cement was measured at standard-specified age (28 days) and at 91 days of water hardening. The changes in pH-index over time were studied in accordance with the ISO standard procedure (ISO 6961-82 "Long-term leach testing of solidified radioactive waste forms"), the leaching liquid (water) was exchanged after 1, 3, 7, 10, 14 and 21 days.

3 Discussion of Results

Analysing the obtained results shown in Table 1 suggested drawing the following conclusions:

- the amounts of liquid (alkaline activator solution or water) required for normal consistency of hydraulic cement paste of the alkali activated cement pastes were 30.4–35.0 % and 26.2–29.7 % respectively;
- all cement formulations under study have passed successfully test for soundness, that is no radial and visible cracks passing through the sample (open cracks) have been visualized on the samples that passed test (after boiling in water);
- initial setting times of the cements under study varied from 39 min to 1 h- 40 min;
- the alkali activated slag cements under study showed no any water bleeding.

Flowability of the cements under study and their physico-mechanical properties at ages of 1–91 days are given in Table 2.

Table 1 Compositions and properties of the alkali activated slag cements under study

No. of cement composition	Alkaline activator		Amount of liquid required for normal consistency (%)		Soundness test	Set times (h-min)	
	Type	ρ (g/cm^3)	Water (W/C)	Alkaline activator solution (AAS/slag)		Initial	Final
1	MS	1160	26.2	30.4	Passed	0–39	1–35
2	MS	1100	27.8	30.6	Passed	1–20	2–00
3	MS	1050	29.5	31.0	Passed	1–40	2–15
4	SA	1160	29.7	35.0	Passed	1–11	3–15

Table 2 Flowability and physico-mechanical properties of the alkali activated slag cements tested in mortar (cement:standard sand = 1:3)

No. of cement composition	Alkaline activator		AAS/C	Flow (mm)	Compressive/flexural strength (MPa)				
	Type	ρ (kg/m^3)			1 day	3 days	7 days	28 days	91 days
1	MS	1160	0.50	175	15.2/2.4	31.3/4.5	48.8/7.1	73.7/10.4	79.6/10.4
2	MS	1100	0.50	210	10.0/1.3	25.2/2.4	31.5/5.5	59.1/7.4	64.0/11.9
3	MS	1050	0.50	210	–	15.0/4.6	22.5/8.2	25.0/7.7	27.5/8.0
4	SA	1160	0.59	150	–	1.20/0.4	8.4/3.6	31.8/5.1	48.8/6.3

The obtained results suggested to show that at the AAS/C = 0.5 the required flowability of 160–220 mm (a flow value measured on a standard cone) can be achieved with the alkali activated slag cement compositions prepared with solutions of sodium metasilicate as alkaline activator. The alkali activated slag cement compositions with sodium ash even at the AAS/C = 0.59 did not show the required flowability and evidently might require a plasticizing agent to be added.

Shrinkage deformations of the cements under study are given in Fig. 1.

Analysing the effect of type of alkaline activator, a conclusion can be drawn that in this case the alkali activated slag cement formulations with soda ash showed the

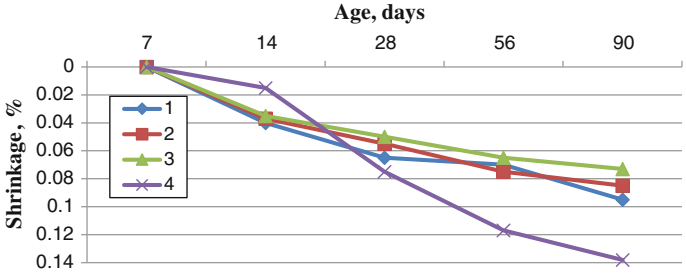

Fig. 1 Shrinkage deformations of the alkali activated slag cements under study (Nos. 1–4, Table 1)

Table 3 Coefficients of corrosion resistance of the cements under study

No. of cement composition	Alkaline activator		Coefficient of corrosion resistance after storage in below solutions after (month)			
	Type	ρ (kg/m^3)	Na_2SO_4 (5 %-concentration)		$MgSO_4$ (3 %-concentration)	
			1	3	1	3
1	MS	1160	1.13	1.22	1.12	1.07
2	MS	1100	1.39	1.09	1.18	1.50

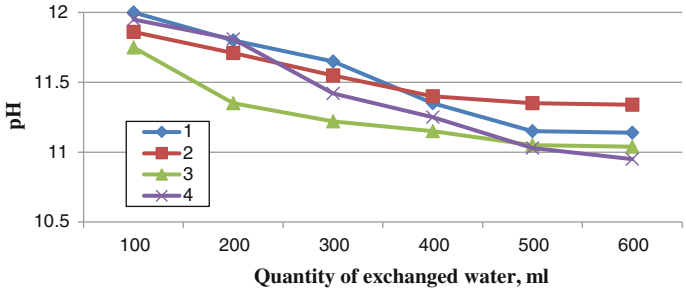

Fig. 2 The pH-index of the cements under study (Nos. 1–4) at 28 days

highest shrinkage. So, if deformations of the alkali activated slag cement formulations with sodium metasilicate (density = 1050–1160 g/cm^3) at 90 days were 0.064–0.105 %, those made with soda ash (density = 1160 g/cm^3)—0.124–0.136 %. Above all, as it follows from Fig. 3, the alkali activated slag cement formulations with sodium metasilicate showed a tendency to a faster stabilisation of shrinkage compared to that with soda ash.

By comparing the obtained data on shrinkage with those of portland *cements a conclusion was drawn that* the alkali activated slag cement formulations with sodium metasilicate (density = 1050–1100 kg/m^3) with shrinkage values in the range of 0.064–0.083 % fall within the range of shrinkage values of Portland cements with active mineral additives (blast-furnace slag cements, pozzolanic cements, etc.), these are: 0.04–0.09 %.

In order to study corrosion resistance, two cement compositions which showed maximal compressive strength (Nos. 1 and 2, Table 2) have been chosen. Characteristics of the alkali activated slag cements and corrosion resistance are given in Table 3.

The coefficient of corrosion resistance after storage for 1 month in a 5 %—Na_2SO_4 was 1.13–1.39, for 3 months—1.09–1.22; for 1 month in 3 %—$MgSO_4$—1.12–1.18, and after 3 months—1.07–1.50.

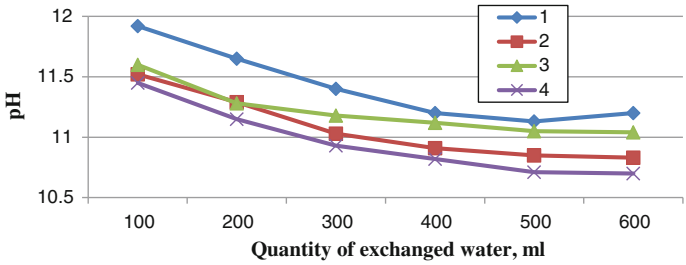

Fig. 3 The pH-index of the cements under study (Nos. 1–4) at 91 days

Leach test results of the alkali activated slag cement stone at a standard specified age of 28 days and through cracks after 91 days of hardening are given in Figs. 2 and 3.

As it follows from Fig. 2, at the standard age the pH-value of the alkali activated slag cement stone is below 11.5, what is required for low pH-cements.

The closer to the age of 91 days the more the values of pH-index tend to lower and even reached the pH-values below 11 (Fig. 3).

On the contrary to traditional hydraulic binding materials, the structure-forming phases of the alkali activated slag cements are represented by low basic calcium silicate hydrates, hydrogarnets, alkaline aluminosilicate hydrates of zeolite and mica structures, as well as alkaline-alkali earth compounds characteristic of low solubility and high stability in various environments [11].

The structure forming processes taking place in the alkali activated slag cements simulate in general features the processes of rock transformations that occur in nature.

A schematic representation of the processes of rock transformations and how the alkalis are bound within the cements with low pH-values is given below:

$$\text{kaolinite } (OH)_4Al_2(Si_2O_5) + 2\ NaOH \rightarrow \text{hydrosodalite } (Si_2O_4Al_2O_4 2Na)3H_2O$$

The metakaolin added to the composition of the alkali activated slag cement accelerates the above process [12].

As it follows from Figs. 2 and 3, the longer is the duration of hardening, the more Na^+-ions are bound by the metakaolin additive resulting in lowering a pH-index of the hardening alkali activated cement stone.

4 Conclusions

The addition of metakaolin to the composition of the alkali activated slag cements allows for to provide the required values of pH (below 11.5) at maintaining high technology-related and physico-mechanical properties, thus making these cements of special interest for disposal facilities for nuclear wastes.

References

1. Beckman, I.N.: Nuclear Industry. Course of lectures. Lecture No. 23. Final stage of nuclear fuel cycle, Moscow, Russian Federation (2005)
2. Sabodina, M.N., Kalmykov, S.N., Zakharova E.V.: Conceptual, technical solution on creation of engineered anti-migration barrier based on clays. Collection of Reports "Efficient Nature Management", Yaroslavl, Russian Federation (2006)
3. Khrushchov, D.P., Cherevko, I.A.: A system "environment—disposal facilities for toxic wastes": conditions for release and migration of toxic substances. Reports of the National Academy of Sciences of Ukraine, No. 3, pp. 131–133 (1999)
4. Kornilovich, B.U.: Structure and surface properties of mechano-chemically activated silicates and carbonates. Naukova Dumka Publish, Kiev (1992)
5. Johnston, R.M., Miller, H.G.: Hydrothermal stability of bentonite-based buffer materials. Whiteshell Nuclear Research Establishment Report AECL-8376. Atomic Energy Canada Ltd (1985)
6. Krivenko, P.: Alkaline cements: terminology, classification, aspects of durability. In: Proceedings of 10th International Congress on the Chemistry of Cement, Goeteborg, Sweden (1997)
7. Energy-saving technologies, use of industrial wastes in building materials and construction. Publications of II International Scientific-Practical Conference, Kiev, USSR (2004)
8. TU U V.2.7-16403272.006-98: Alkaline Binders for Special Use—Geocements. Specifications
9. Milestone, N.B.: Reactions in cement encapsulated nuclear wastes: need for toolbox of different cement types. Adv. Appl. Ceram. **105**(1), 13–20 (2006)
10. Krivenko, P., Cao, H., Weng, L., Kavalerova, E.: Mineralogical aspects of durable geocement matrix formation—role of alkali. Adv. Mat. Res. **1004–1005**, 1523–1530 (2014)
11. Глуховский В.Д. Грунтосилікатні вироби і конструкції. Київ, Будівельник
12. Krivenko, P., Drochytka, R., Gelevera, A., Kavalerova, E.: Mechanizm of preventing the alkali activated reaction in the alkali activated cements. Cement Concr. Compos. **45**, 157–165 (2014)

Protocol for Prediction of Durability of New Cements: Application to LC^3

Aneeta Mary Joseph, Vineet Shah and Shashank Bishnoi

Abstract As Ordinary Portland Cement has been the most widely used binder till 1990s, its long term behaviour in concrete is well understood. However, environmental concerns and resource availability has driven cement industry to move to use of supplementary cementitious materials and developing new binders with less environmental footprint and more utilisation of locally available resources. As more such cements suiting local needs get developed, it will be critical to rapidly understand the durability of concretes containing these blends so as to reduce the typical period required to standardise cements. Since durability related tests are, by definition, time-consuming, this paper suggests a framework that can be used to gain a faster prediction of the performance of these cements when subjected to different deterioration processes. The application of this framework to Limestone Calcined Clay Portland Cement is also described. This framework promises to significantly reduce the time required for the standardisation of new cements, saving precious resources in the process.

1 Introduction

The development of infrastructure is a key indicator of the development of a country, and globally as well. In India, around 8 % of GDP is spent on infrastructure [1]. Availability and cost of raw materials for construction has a colossal impact on the construction industry and thus, on the economy of the country. Concrete, being the most used construction material, has a critical role in the economic development. Among the constituents of concrete, i.e. coarse aggregate, fine aggregate (sand), cement and water, cement contributes the major share of environmental footprint and energy consumption. The annual production of cement at present in India is around 2.8 billion tonnes, which is expected to go up to around

A.M. Joseph (✉) · V. Shah · S. Bishnoi
Indian Institute of Technology Delhi, Delhi, India
e-mail: aneetamajo@gmail.com

K. Scrivener and A. Favier (eds.), *Calcined Clays for Sustainable Concrete*,
RILEM Bookseries 10, DOI 10.1007/978-94-017-9939-3_50

Table 1 Prediction of demand for cement [2]

Global Indices	2006	Baseline 2050 (low)	Baseline 2050 (high)	Roadmap 2050 (low demand)	Roadmap 2050 (high demand)
Clinker (%)	79	75	74	71	73
Alternate fuels (%)	3	4	4	37	37
Clinker (GJ/t)	4.2	3.5	3.5	3.3	3.2
Cement (kWh/t)	111	95	95	92	92
tCO_2/t cement	800	693	636	426	352
Global volumes					
Cement production (Mt)	2559	3657	4397	3657	4397
CO_2 emissions	2047	2337	2796	2052	2521

4 billion tonnes in next 3–4 decades. Despite this huge demand, the availability of raw materials is a question still unanswered (Table 1).

As per the data of Indian Bureau of Mines, presently estimated value of Limestone deposit in India suitable for cement production is around 10,622 million tonnes, and the present consumption of limestone is around 250 million tonnes per year [3]. So on an average, the limestone deposit would decline in around another 50 years. A look at the percentage of the elements in earth's crust suggest that the alternate for limestone availability crisis could be retorted by use of alternate mineral with more alumino-silicates. Also, there will be localised solutions, based on materials that are available in abundance locally (Fig. 1).

This emphasises the need for developing new technologies that increases the band width of raw materials, which ensures catering needs for a longer duration of time. The present protocol for durability testing demands much time for exposure of the specimens, and then testing. The structures built today are built for a period

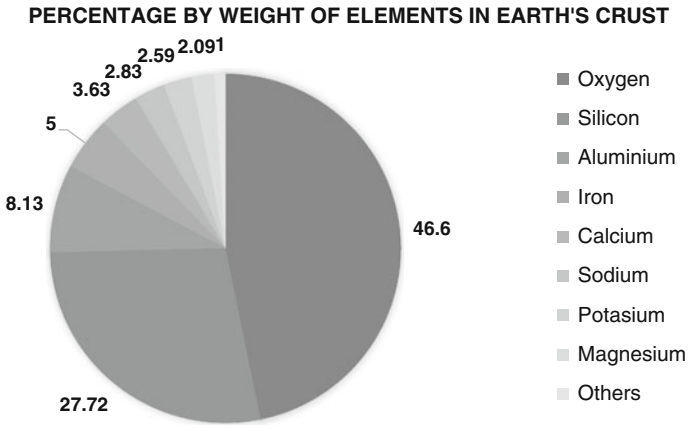

Fig. 1 Percentage of elements in earth's crust [4]

Table 2 Various technologies under consideration and their percentage saving in clinker

	Approximate percentage saving in clinker
Portland pozzolana cement	40
Portland slag cement	70
Portland limestone cement	15
Composite cement	60
Limestone calcined clay cement	50
Geopolymer cement	100

of average 50–100 years. Testing the cement in actual conditions for durability will take that long a time period. This causes huge delay in putting the cement into actual applications. This delay will effect in consumption of excess resources, CO_2 emission, and financial loss for cement industry, all of which could be avoided by timely application of new state of the art technologies.

The main alternate technologies available at present are shown in Table 2.

2 Durability

Durability of a cement is its capacity to resist the forces that causes its deterioration throughout its designed service life. The impact of durability on economy, safety and environmental point of view is very huge. Various processes that causes deterioration of concrete includes chemical routes such as corrosion (in reinforced concrete), alkali silica reaction, Freeze/Thaw effect, Sulphate attack, Acid attack etc. and physical routes such as abrasion, erosion, cavitation etc. Corrosion process is accelerated by both carbonation and chloride ingress. At each location, the deterioration mechanism will be different as the deterioration forces are different [5].

Corrosion is a major problem for reinforced concrete structures. Concrete is a material that is weak in tension. Steel reinforcements are added to improve its tensile strength, which also adds to the compressive strength of concrete. Corrosion of steel causes volume expansion and thus spalling of concrete from the surface. The bond between concrete and steel will be lost, the cross sectional area of steel decreases and thus causes reduction in load carrying capacity of the structure.

For Ordinary Portland Cements, $Ca(OH)_2$(Portlandite) is produced as a result of the hydraulic reaction. The pore solution, is thus alkaline due to presence of various hydroxides. This condition is favourable for stability of a passive film around the reinforcements, which is around a few nanometres thick [6]. Use of alternate raw materials in place of clinker poses the risk of production of less portlandite, and consumption of portlandite by supplementary cementitious materials, which makes the reinforcements more prone to corrosion. The major mechanisms which destroy the coating are carbonation and chloride attack.

The carbonation mechanism proceeds as follows. CO_2 from atmosphere will diffuse into the pores of concrete, will react with calcium hydroxide in solution and neutralise the alkalinity, reducing the pH. At low pH, the protective layer will disintegrate, exposing the underlying iron to electrochemical reaction.

3 New Protocol

To address the above mentioned complications, a new protocol for testing the durability with respect to carbonation is being suggested here. The process of carbonation in concrete follows the following steps [7]:

1. Diffusion of CO_2 through the gaseous part of the pores
2. Dissolution of CO_2 in water in the pores
3. Dissolution of $Ca(OH)_2$ in pore water
4. Reaction of $Ca(OH)_2$ and CO_2 in pore water
5. Reduction in pH
6. Initiation of corrosion (Fig. 2)

The diffusion of CO_2 through the gaseous part of pores will follow Fick's law. Since diffusion take place only through the gaseous part, diffusivity will depend on the relative humidity of atmosphere around. The diffused CO_2 will dissolve in pore water according to Henry's law. Then dissolved CO_2 and $Ca(OH)_2$ will react in pore solution, precipitating $CaCO_3$, thus decreasing pH of the solution. The initial amount of alkalinity in cement is a characteristic of the cement and degree of hydration. The pH starts decreasing once the reserve alkalinity maintained by $Ca(OH)_2$ gets consumed. Initiation of corrosion is assumed to happen when pH falls

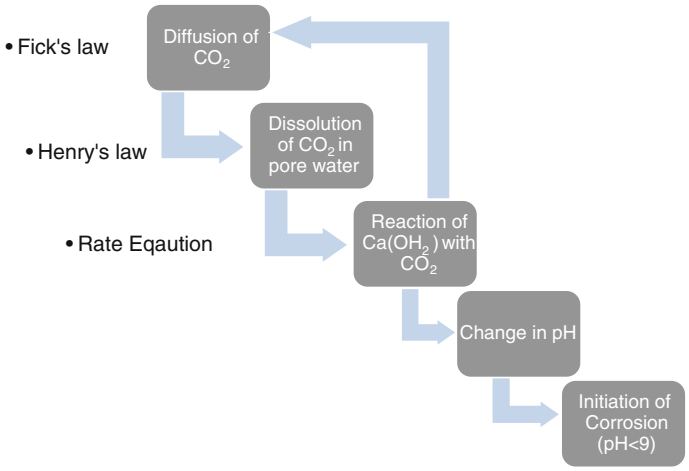

Fig. 2 Step by step illustration of initiation of corrosion

below 9, when the passivating layer around steel is not stable anymore. Thus, from the diffusivity, reserve alkalinity and rate of reaction, it will be feasible to predict the time required for all the alkalinity to get neutralised, and thus for initiation of corrosion.

3.1 Experimental Procedure for New Protocol

The main indicators that are tested in this protocol are mainly,

1. Diffusivity of CO_2
2. Hydration and carbonation products (Composition)
3. Total possible carbonation
4. pH change due to total carbonation
5. Rate of carbonation reaction

The chemical parameters that affect carbonation, i.e. composition (hydration products and carbonation products), pH change caused due to carbonation, total quantity of carbonation possible etc. can be deduced from accelerated tests in paste samples. Paste samples exposed to accelerated carbonation are characterised both pre and post carbonation to find the hydration products and carbonation products. X-ray diffraction technique (XRD) or Thermo Gravimetric Analysis (TGA) are the techniques applicable for characterisation. TGA will be mostly useful for quantifying the $CaCO_3$ produced, and portlandite initially present and consumed.

Diffusivity of CO_2 in the sample can be determined by Gas Permeability test on matured concrete samples. The value of diffusivity can be double checked using the pH change values from accelerated carbonation.

The reaction rate can be determined by simulating carbonation in natural conditions, since rate of reaction depends a lot on thermodynamic conditions, testing in natural conditions will be more apt (Fig. 3).

4 Applicability to Other Durability Problems

Most of the durability problems deals with diffusion of one or more reactive species to inside of the concrete, interaction with the constituents of concrete, and thus affects the integrity of microstructure as a whole. For e.g. Chloride attack deals with ingress of chloride ions from outside, and thus causes localised corrosion. The main steps of the attack are as follows.

1. Diffusion of chloride ions to inside of concrete.
2. Binding of chloride ions, either by physical adsorption on C-S-H, or by chemical binding with aluminate phases.

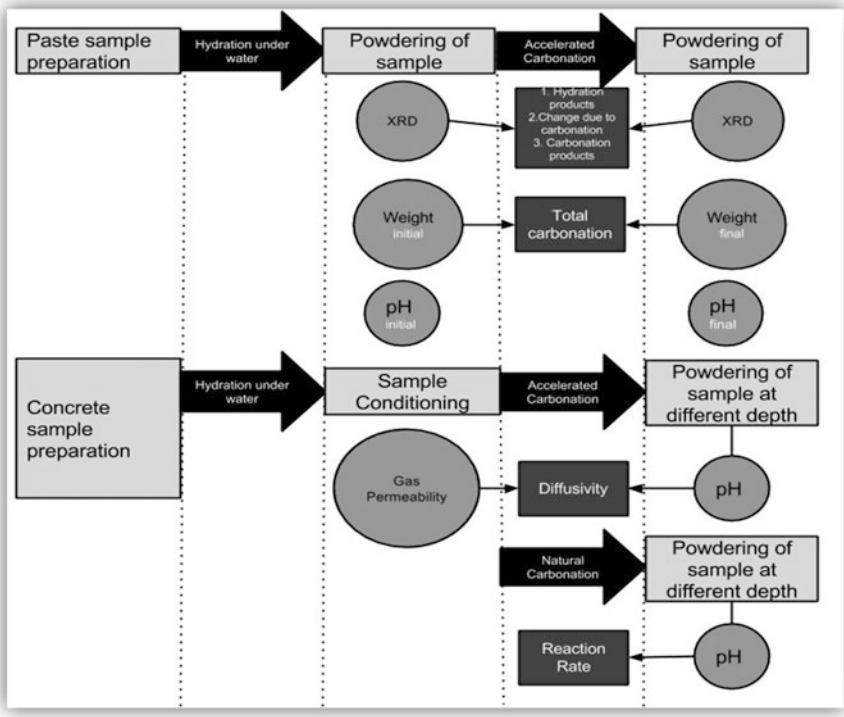

Fig. 3 Experimental procedure for new protocol for carbonation

3. The maximum tolerable level is reached at reinforcement level, when the chloride concentration reaches chloride threshold level. It is different for different pH. At higher pH, chloride threshold level will be higher and vice-versa.

External sulphate attack is caused by diffusion of sulphate ions from soil to inside of the concrete, reaction with calcium hydroxide and alumina phases of hydrated cement and thus causes spalling due to expansion. A tolerable threshold concentration for the external incoming species can be established for all these reactive species from previous experiences. Like the above proposed protocol is applied to carbonation, with minor modifications it can be applied for all these problems as well, since these are the main durability problems being faced in tropical climatic conditions.

5 Conclusions

The rising need for developing new technologies and putting them into application as soon as possible is well understood now. The major time consuming factor that affects timely application is durability testing, which can be accelerated by adopting

faster protocols as mentioned above, since most of them deals with a mechanism which involves ingress of a reactive species to the inside of concrete through pores, reaction with cementitious materials, till a point that can be tolerated for normal service.

References

1. I.B.E. Forum: www.ibef.org, January 2013 (Online). Available: http://www.ibef.org/download/Infrastructure-Sector-040213.pdf. Accessed Feb 2015
2. World Business Council for sustainable Development and International Energy Agency: Cement Technology Roadmap (2009)
3. I.B.o.M. Government of India: Indian Minerals Yearbook Part-II (2011)
4. Fleischer M.: Recent Estimates of the Abundances of Elements in the Earth's crust, Washington D.C. (1953)
5. Richardson, M.G.: Fundamentals of Durable Reinforced Concrete. CRC Press, Boca Raton (2003)
6. Bertolini, L., Elsener, B., Pedeferri P., Polder, R.: Corrosion of Steel in Concrete: Prevention, Diagnosis and Repair. Wiley–VCH Verlag GmbH & Co.KGaA (2003)
7. Papadakis, G.V., Vayenas, C.G., Fardis, M.N.: Fundamental modelling and experimental investigation of concrete carbonation. ACI Mater. J. (1991)

The Role of Calcined Clay Cement vis a vis Construction Practices in India and Their Effects on Sustainability

Arun C. Emmanuel, Anuj Parashar and Shashank Bishnoi

Abstract Being a fast growing developing nation, India has vast potential in the infrastructure and construction sector. One of the major challenges that the construction industry faces is the availability of construction materials. There's an urgent need to look at material consumption in the Indian construction sector and ways to optimize their use. For example, it has been observed that overdesign is one of the main causes of unnecessary consumption of natural resources as this leads to over use of materials. The quality and grade of cement being used in the concrete today also has an important role in the consumption of these resources. This paper studies the sources of inefficiencies in the usage of natural resources in the construction industry in India. It is seen that calcined clay can play an important role in improving these efficiencies. A look at the available resources emphasizes the need to diversify the products available according to location and applications.

Keywords Calcined clay · Sustainability · Resource consumption · Field applications

1 Introduction

It's no longer a notion that the global population is on the rise and, India is about to become the most populated country in the world. As populations rises, the pressure on earth's resources exponentially increases in various direct and indirect ways such as basic needs, energy, infrastructure development and transportation etc. In the case of non renewable resources; it leads to reduction in reserves, increase in cost. Use of non renewable resources such as fossil fuels which produce greenhouse gases, leads to environmental pollution and climate change. Sustainable development aims to practice lower/effective use of resources. As the time goes, sustainable development will no longer be a choice and it will be the only option for the entire

A.C. Emmanuel (✉) · A. Parashar · S. Bishnoi
Department of Civil Engineering, Indian Institute of Technology, Delhi, India
e-mail: aruncemmanuel@gmail.com

K. Scrivener and A. Favier (eds.), *Calcined Clays for Sustainable Concrete*,
RILEM Bookseries 10, DOI 10.1007/978-94-017-9939-3_51

world especially fast growing development nations such as India. As the country is expected to become the largest consumer of cement in near future by overtaking China, it is extremely important to look at the alternative methods of production and consumption of cement from the sustainability point of view.

2 Role and Future of Cement Industry in Indian Economy

In this 20th century era, it is clearly visible that India is the fastest growing economy; the Government, different sectors are working progressively to accommodate this change in future. Infrastructure and construction sectors have always been an indicator of growth and development to a country's economy. By looking at India's existing and future potential for development in these sectors, the cement industry is expected to gain maximum benefit. At present, Indian Cement Industry stands second behind China, and accounts for 8 % of the total global production. Still, the per capita consumption of cement stands low at 190 kg where as the average global figure is about 450 kg [1]. Cement industry and its growth always stand as a measure of growth in infrastructure and construction industry directly, which leads to an indicator to the economic growth. It has a direct relationship with GDP of the country.

The usage of cement in various sectors also needs to be considered. It is further observed that more than half of the total consumption is for the housing sector followed by infrastructure development. In view of soaring rate of urbanization, and various programs announced by government of India to accelerate the expansion of housing and infrastructure projects such as special economic zones, the cement sector in India holds potential for further growth. In addition to this, authorities are looking into feasibility of cement for the construction of all new road projects instead of bitumen as it is more durable, cheaper and easier to maintain throughout service life of roads. Consumption of cement by various sectors in India is shown (Fig. 1).

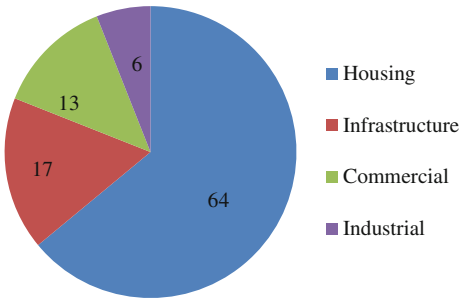

Fig. 1 Cement consumption by various sectors in India (in percentage) [2]

3 Hurdles of Cement Industry: Indian Construction Practice

Construction is second largest employment sector in India next to agriculture. A large percentage of this labour force belongs to unskilled category. Moreover the industry is highly fragmented in nature. Proper construction management practices are still not employed by a larger portion of the construction industry particularly the small firms in rural areas. Therefore it can be acknowledged that construction delays are most common, and wastage of materials are very high in the country. Moreover, lack of knowledge and deficiency of adequate quality control during material production, design and construction of concrete structures often leads to overdesign of structures and wastage of good quality materials. It is widely seen that utilization of higher grade cements for ordinary purpose such as masonry works, where it might not be necessary.

As far as Indian cement industry is concerned, numerous barriers need to be overcome so as to meet the demand without compromising on quality and cost. One such hurdle is the availability of good quality raw materials such as limestone. The existing limestone reserves are expected to last another 20 to 30 years at the current rate of cement production. This can lead to a potential scenario in which India has already depleted the good quality limestone available at time when country requires it the most.

Cement industry is a major consumer of electricity. Availability of stable and continuous power supply is very important. The scarcity and lack of reliability of Government owned power supply demands construction of power generation units in the cement plant. Coal has been the main resource for the power generation in the cement. The recent times, the good quality coal is being diverted for electricity generation from thermal power plants, which leads to shortage and high prices. In addition, the recent government regulations for coal blocks allocation makes accessibility of this non renewable fuel even more difficult. The lack of supply of adequate quality and quantity of coal, forces cement plants to use either alternate fuels such as petcoke or imported coal, which increases the cost of production.

Cement plants normally situated near to the mines particularly limestone mines in India. This result in the concentration of cement plants at a few areas which are mineral rich, due to which the industry becomes highly freight depended even within the country. The Indian railway has been the most used freighter for cement. However, the lack of infrastructure, irregular delivery and continuous changes in policies makes the Railways an unreliable partner for the cement industry.

4 Environmental Effect of Cement Industry: Indian Scenario

The cement industry is one of the most significant sources of greenhouse gases. The sector is responsible for about 7 % of the total anthropogenic CO_2 emissions worldwide [1]. This percentage is going to increase as the cement production is expected to grow at high rate. Various measures have been proposed globally to reduce the environmental impact of cement, out of which the most important is substitution of clinker in OPC commonly as PPC or blended cement. In India, being one of the major consumers of cement, lot of initiatives have been taken from the government as well as the cement companies. Currently the Portland Pozzolana Cement (PPC) holds the major share of the total production (65 %), followed by Ordinary Portland Cement (OPC) (24 %) and Portland Slag Cement (PSC) (8 %) [1]. The usage of blended cement is expected to reduce the problem of waste disposal, improve energy efficiency and reduce carbon footprint. As coal is the major source of power in India, Fly ash which is a by-product from thermal power generation is widely used material in PPC. Lack of availability of good quality fly ash in close proximity prevents extensive use of fly ash in many cement manufacturing units. Also, transportation of fly ash over long distances drastically reduces the significance of sustainability and economic feasibility of fly ash in cement. It is to be considered that Government is keen on research and development of alternate power resources such as solar, nuclear, wind and geothermal. This could reduce contribution of electricity from thermal power plants significantly, leading to drastic reduction of fly-ash availability in future. Also, as per the Indian standard, replacement factor for fly ash is just 35 % [3], mainly due to reduction in performance of concrete at higher replacement level. Ground granulated blast furnace slag seems to be a good option, but the total production of slag from Iron industry in the country is very low when compared to the demand for slag.

5 Calcined Clay Cement: A Brief Overview

The recent research in Cuba, Switzerland and India has shown that clinker substitution up to 50 % is possible by using a mixture of calcined clay and limestone and it can give almost same or better result in terms of OPC or PPC [4]. This blended cement had produced in industrial scale recently in India to study the feasibility and constraints of industrial scale production using available technology. The quality of clay and limestone used in pilot study and trial industrial scale production were considerably low with respect to which normally used in OPC/PPC production. This composition of raw materials used for initial research and pilot production is shown (Fig. 2).

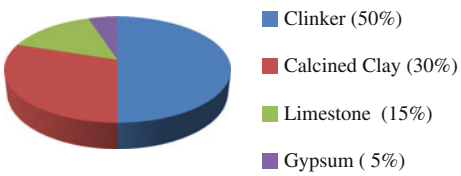

Fig. 2 Composition of limestone calcined clay cement [5]

6 Sustainability Potential of Calcined Clay Cements in India

Being a binder which is still being researched, further studies need to carried out to study the feasibility of extended usage of Limestone calcined clay cement in India. The following paragraphs describe the possible answers for the queries regarding the sustainability threshold of limestone calcined clay based cements in India.

Based on the initial studies it is found that 50 % clinker substitution is possible in calcined clay based cements. In this way, CO_2 emissions due to clinkerization can be substantially reduced.

It was found observed that lower grade clay seems to be softer than typical clays which are used in OPC production, leading to energy and time saving during grinding. This needs to be verified with the help of further studies. The very fine nature of calcined clay could help achieving a higher production output of this ternary cement by using the same facilities during grinding.

As the low quality clay is bound towards the upper layers of clay mines, the resource and fuel usage during excavation can reduced. Most of the existing clay mines uses low quality overburden clays either for backfilling of the exhausted mines or dumping which leads to extra cost.

The temperature required for calcination of clay is found to be in the range of 700 °C–900 °C, which is substantially low when compared with the temperature required for the production of clinker i.e. 1400 °C. The exact calculation of energy saving need further studies.

The reduction in quality requirement of raw materials such as clay and limestone could lead to exploration of new mines which ultimately leads to decentralization of cement units across the country. Further the overall freight cost can be reduced which may lead to reduction in cement price.

It is also observed that practice of using higher grade cement where a lower grade is sufficient, is common in India. For example; manufacturing of concrete blocks, cement mortar for brick wall construction, low cost housing, low rise buildings and construction in rural areas. This might be because of practical difficulty to produce various grades of cement from the same plant by using same quality of material and production parameters. This type of wastage can be reduced by blending calcined clay cements from a locally available plant and using good quality clinker from a large scale plant.

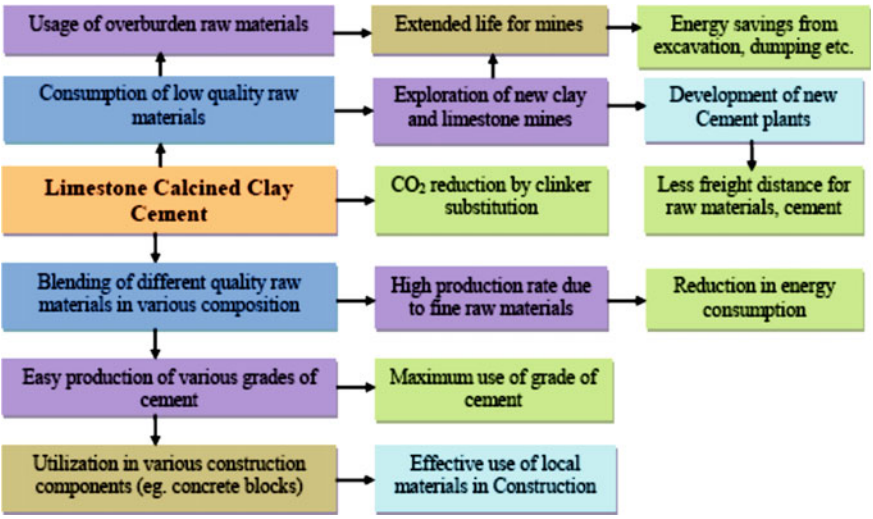

Fig. 3 Flow chart of possible sustainability benefit from calcined clay cement

The sustainability potential of calcined clay has been summarized with the help of flow chart given Fig. 3.

7 Discussions

Complete mapping of suitable raw material is necessary to estimate the sustainability value of the new product. A detailed investigation on its economic feasibility is also necessary. Further, knowledge transfer and workshops for various stake holders such as cement companies, suppliers and consumers may be required to encourage the early uptake of this low carbon binding material. Inclusion of 'green cement' in green building rating systems can motivate the use of this product. The production of low carbon calcined clay cement may even allow cement companies to make considerable sums of money through carbon trading under the Kyoto protocol. Active participation from the Government particularly for certification and formulation of standards for the new binder is crucial to implement calcined clay based cements in market.

References

1. Technology Roadmap: Low carbon technology for Indian cement industry. International energy agency In: 95th report on performance of cement industry, Department of Commerce, Government of India (2012)
2. IS 3812(Part 1):2003-Pulvarized Fuel Specification, For use as Pozzolana in cement, cement mortar and concrete
3. Scrivener, K.L.: Options for the future of cement. Indian Concr. J. **88**(7), 11–21 (2014)
4. Bishnoi, S., Maity, S., Malik, A., Joseph, S., Krishnan, S.: Pilot scale manufacture of limestone calcined clay cement; the Indian experience. Indian Concr. J. **88**(6), 22–28 (2014)
5. Indian Bureau of Mines: Government of India, 'Indian minerals yearbook (Part-II) (2011)

Testing of Suitability of Supplementary Materials Mixed in Ternary Cements

Anuj Parashar, Sreejith Krishnan and Shashank Bishnoi

Abstract As the market for cement has slowly moved from Portland cements towards pozzolanic cements and continues to move towards ternary cements, the tests for cements and the components blended in them remain largely unchanged. While it is recognised that certain mineral additives, e.g. limestone, do not meet the traditional definition of pozzolanic materials, the amount of processing and testing conditions play an important role in the measured reactivity of other additives. In addition, the current testing methods are unable to take the interaction of different components and their effects on the overall properties of cements into account. This paper reviews the methods currently available for the characterisation of materials and their suitability for application to ternary cements. Possible modifications to these tests, in order to take the cements of future into account are suggested. The inclusion of test methods to ascertain the suitability of the materials mixed in the cements is also suggested.

Keywords Calcined clay · Pozzolanicity · Reactivity methods

1 Introduction

One of the most important binders in the construction industry for concrete is ordinary Portland cement (OPC), which is nearly 200 years old now. Due to its economy, versatility, and since it is a well-understood material for concrete manufacturer, its popularity and growth is still ongoing. Though OPC has many positive points, its production causes a major environmental footprint, i.e. CO_2 emission. Approximately 0.9 tonne of CO_2 is produced for every 1 tonne of production of cement and around 5 % of global CO_2 emission is only due to the cement production [1]. So, that is one of the reasons why cement industries are looking

A. Parashar (✉) · S. Krishnan · S. Bishnoi
Department of Civil Engineering, Indian Institute of Technology, Delhi, India
e-mail: anuj_parashar12@yahoo.co.in

K. Scrivener and A. Favier (eds.), *Calcined Clays for Sustainable Concrete*,
RILEM Bookseries 10, DOI 10.1007/978-94-017-9939-3_52

forward for other alternatives i.e. supplementary cementing materials (SCM) to reduce overall emission. SCMs are also well known for high strength, durability, and high resistance to sulphate attack, reduced energy consumption etc. [2].

Most of the pozzolanic materials are either waste materials from other industries, or made with less energy consumption and emitting less CO_2 in comparison with OPC. Fly ash and slag are the examples of industrial waste; whereas calcined clay is produced separately to be added in cement formation. Few benefits of using calcined clay are better quality control, easy alternative to other SCMs and consistent quality. As in case of fly ash and slag, quality can vary from one plant to another because they are totally waste for the industry and they didn't take care of their quality. Some basic properties are explained below with the help of Fig. 1.

This concept of adding single SCM with OPC is also known as Pozzolanic Portland cements (PPC) in India. PPCs are well understood and standardized in almost all countries. In India itself, three main types of PPCs Indian Standards are available which allows a maximum replacement of 35 % fly ash, 25 % clay and 70 % of slag. Now a days, concept of ternary blended cements (TBC) is also in trend. In this type of blended cement, we can reduce our clinker content up to 50 % and rest of 50 % can be any two SCMs with gypsum. ASTM standard

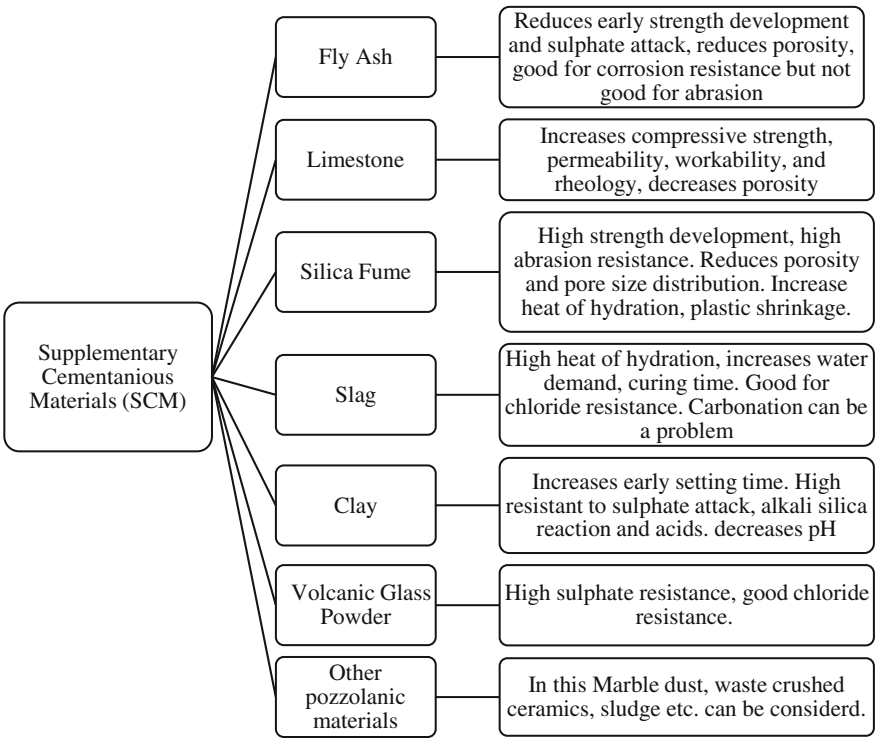

Fig. 1 Some SCM's with their properties

C595/C595 M defines ternary blended cement as "blended hydraulic cement consisting of Portland cement mixed with either slag cement, pozzolanic material, or limestone". European code EN 197/1, 2002 and Canadian code CAN/CSAA23.2 2000 has also standardized TBC. Brazil code EB-2138/91 standard defines two types of ternary cement as CPII-E and CPII-Z. Mexico recently standardized composite cement in NMX C-414-0/99.

In India, bureau of Indian standards (BIS) is working on composite cement. The main concern for the development of TBC in cement industry is the reactivity of SCMs. Their reactivity plays an important role in the cement hydration. This is also known as synergic effect. On the basis of material quality, synergic effects can very from 7 days age to 28 days. It can be due to chemical as well as physical effects [3].

For calcined clay this synergic effect is different from other SCMs, because it contains Al_2O_3, which also reacts in the presence of Limestone and produce monocarboaluminate [4]. This phenomenon also changes the definition of limestone from filler to SCM, because generally limestone acts as filler in secondary cement phase.

2 Pozzolanicity or Pozzolanic Activity

Pozzolanicity means, "measurement of the degree at which lime (CH) react with pozzolanic material to form calcium silicate hydrate (CSH)" or in other words it is an index of degree of lime pozzolan reaction" [5]. Simply it is the efficiency of pozzolanic material which is contributed for improving strength and durability properties. Pozzolanicity is complex problem to calculate because it depends on numerous factors such as, fineness, chemical composition, silica content, quality of lime with which a pozzolanic material is reacting, impurities, atmospheric conditions, method of formation, calcination temperature for clay, impurities etc. [5]. A fast and reliable method for all SCM's is not found yet [2].

There are various methods to find out pozzolanicity that are differentiated by different authors in different ways. Test methods can be classified on the basis of physical, chemical, or visual observation, or direct or indirect method of study. Some of them are well known and standardized also, but still there is no single method to be applicable on all SCM's. This study will help in differentiating test methods on the basis of their application on calcined clays.

3 Methods to Find Pozzolanicity/Reactivity of Scm's

Test methods are classified as direct and indirect tests. Direct methods, which mainly focuses on the CH consumption from the paste due to pozzolanic reaction such as X-Ray Diffraction, Thermo Gravimetry Analysis, microscopy, some titration methods such as Chapelle test, Frattini test etc., secondly indirect test method

such as, strength activity index, lime reactivity or lime combination test, uncombined lime test calorimetry, electric conductivity etc. [6]. This study will discuss the best suitable test methods for calcined clay and also suggest some modification that can be applied for their application in field of TBC.

3.1 Direct Test Methods

3.1.1 Chapelle's Test

This method is purely designed for the study of calcium hydroxide consumed in the pozzolanic reactivity of metakaolin (MK). It is always better to use this test for calcined clay then lime reactivity test [7]. This method is standardized in French standard NF P18-513. As per the procedure, 1-gm of MK is mixed with 2-gm of CaO and 250 ml of water. Then the mix is heated for 16 h at a temperature of 900 C. finally the hydrated paste is titrated with 0.1 N HCl. Finally result is expressed as mg of $Ca(OH)_2$ consumed per gm of MK.

As studied by some authors, high temperature affects the kinetics of reaction, which alternately affects the nature of hydration product formed. An alternative to this test method was developed by in Garcia et al. [8] in which, test is performed for longer duration at lower temperature i.e. at 400 C for 90 days. But another problem with this modified method is time.

3.1.2 Modification Suggested

By reducing the temperature of the reaction and increasing the time for dilution using stirrer can modify this method. Best suitable time can be found out for the same yield in two different time and temperatures. Also, this will not disturb the kinetics of the reaction.

3.1.3 Frattini Test

This is standardized in British standard BS EN 196-5:1995 and is used for measuring pozzolanicity of pozzolanic cements. Basic concept of this test is to measure the quantity of CH consumed, in aqueous solution that is in contact with the hydration product. A saturated solution of CH is required. If the concentration of CH ions is lower than saturation concentration, then it is considered as positive. Tironio et al. [8] use this method for study of pozzolanic activity of different calcined clay. They suggest SAI and Frattini test as most accurate method for testing calcined clay.

3.1.4 Modification Suggested

This method assumes that, no other source of Ca^{2+} is present in the system, but due to leaching of calcium from examining material can affect the result. This method can be adopted for ternary blends in which limestone is to be used. Initially OH^- and Ca^{2+} ions can be found from the MK reaction can be found by calculating. Then further can be added and then allowed to react for some time. Finally the free carbonates can be calculated using titration method.

3.2 Indirect Test Methods

3.2.1 Lime Reactivity

This method is standardized in India ([9] methods of test for pozzolanic materials). This test measures the rate of development in compressive strength due to reaction in between lime and pozzolanic material. For this purpose mortar cubes are cast in a ratio of 1:2 M: 9 (lime: pozzolan: standard sand) where M is ratio of specific gravity of pozzolana and specific gravity of lime (i.e. CH). Main problem with this test is regarding workability of mortar, because water demand of some pozzolanic materials such as calcined clay, rice husk ash. High water demand cause low compressive strength. Some admixture can be used for fixing the w/c ratio at its optimum value.

Test based on the compressive strength (Indirect methods) always gives results on the basis of total efficiency of the mineral addition and do not give any information about its potential on chemical reactivity [10]. Due to uncertainty in test results of lime reactivity for flash calcined kaolinite, S. Salvador suggests to perform different test method to check reactivity. He tried later with Chapelle test in which, w/c ratio is not a concern at all.

3.2.2 Modification Suggested

However, it is not feasible to rely on indirect test, but sometimes cement and concrete industry are only concerned primarily on strength, especially in developing countries. This test method can be modified with several attempts on different quantities. As explained earlier, 1:2 M: 9 can be used as same but the value of pozzolanic material can be changed according to the application of that, such as PPC or TBC. For TBC an example is shown below.

Suppose metakaolin (MK) is used with lime stone in ratio of 2:1

$$\mathrm{M} = \frac{\text{Specific gravity of two pozzolanic material in there mass or volume ratios}}{\text{Specific gravity of CH}}$$

$$M = \frac{\text{Specific gravity of MK} \times 0.66 + \text{Specific gravity of lime stone} \times 0.33}{\text{Specific gravity of CH}}$$

In such a way, the synergy effect of MK and LS together can be found out easily.

Strength Activity Index (ASTM C 311)
As per ASTM C311 "Standard test method for sampling and testing fly ash or natural pozzolans for use in Portland cement concrete" 20 % of mass replacement of pozzolanic material is made with Portland cement. Some authors suggest some modification in this test method. Pourkhorshidi et al. suggests that, an identical w/b ratio is to be adopted on mortar with 20 % natural pozzolan replacement. Whereas Bentz et al. suggest that the replacement should be made by volume, not by mass [10]. Another author find that, 90 days strength depends on content of clay mineral, rather then type of mineral because in long term curing, the reaction will be equilibrated [8].

3.2.3 Modification Suggested

The basic concept used in the present test is same as Indian Standard method for lime reactivity, so same approach can be applied but with a slight modification. Also if w/b ratio is above 0.55 then it can also be adjusted using a plasticizer because clay can absorb more water at initial stage. Unnecessary water can affect the final strength result.

Isothermal Conduction Calorimetry
There are different types of calorimetry methods, but Isothermal conduction calorimetry is the most accurate. Small amount of sample mixed with lime or cements can be use to study. Mainly rise in temperature due to hydration of paste is studied. But this method is not well suitable for calculating for some low reactive pozzolans in which rise in temperature can be very less or low [11]. For cements, it works better.

3.2.4 Modification Suggested

Modification suggested for this method can be divided into two steps. In first step, increase in temperature for TBC paste can be measured, and then in second step, paste of MK with calcium hydroxide can be analysed. The water/powder ratio should be kept constant for both the pastes. By subtracting first value from the second can give an idea of the rate of reaction of MK and limestone based cement.

Adiabatic calorimetry can also be used for this purpose. For comparing clays of different origins with different calcinations temperatures can be studied at fix w/c ratio and then effect of LS can also be studied in the combination. This method can give an idea of good reactive material.

4 Conclusions

- This paper summarises the existing methods for testing pozzolanicity of different SCM's and TBC's. This study can help in selecting a suitable method for specific material. Following conclusions are made on the basis of review.
- Titration methods, Chapelle,s test and Frattini test are found most accurate and efficient for calcined clays. They can be modified for the future purposes of calcined clay in TBC.
- SAI and lime reactivity are not suitable for materials which are hydrophilic in nature. But by adding some admixture to the paste, test can be modified and also the quantities can be adjusted on the basis of their synergy effect.
- Frattini test can be best suitable for comparing reactivity of two different clays.
- It is always better to use two or three methods to confirm the reactivity, as single method acceptable for all materials is not developed yet.

References

1. Juenger, M.C.G., Winnefeld, F., Provis, J.L., Ideker, J.H.: Advances in alternative cementitious binders. Cem. Concr. Res. **41**, 1232–1243 (2011)
2. Mertens, G., Snellings, R., Van. Balen, K., BicerSimsir, B., Verlooy, P., Elsen, J.: Pozzolanic reactions of common natural zeolites with lime and parameters affecting their reactivity. Cem. Concr. Res. **39**, 233–240 (2009)
3. Radlinski, M., Olek, Jan: Investigation into the synergistic effects in ternary cementitious systems containing portland cement, fly ash and silica fume. Cement Concr. Compos. **34**, 451–459 (2012)
4. Antoni, M., Rossen, J., Martirena, F., Scrivener, K.: Cement substitution by a combination of metakaolin and limestone. Cem. Concr. Res. **42**, 1579–1589 (2012). doi:10.1016/j.cemconres.2012.09.006
5. Mostafa, N.Y., El-Hemaly, S.A.S., Al-Wakeel, E.I., El-Korashy, S.A., Brown, P.W.: Characterization and evaluation of the pozzolanic activity of Egyptian industrial by-products I: Silica fume and dealuminated kaolin. Cem. Concr. Res. **31**, 467–474 (2001)
6. Donatello, S., Freeman-Pask, A., Tyrer, M., Cheeseman, C.R.: Effect of milling and acid washing on the pozzolanic activity of incinerator sewage sludge ash. Cement Concr. Compos. **32**, 54–61 (2010)
7. Salvador, S.: Pozzolanic properties of flash calcined kaolinite: a comparative study with soak-calcinedproducts. Cem. Concr. Res. **25**(1), 102–112 (1995)
8. García, R., Vigil, R., Vegas, I., Frías, M., et al.: The pozzolanic properties of paper sludge waste. Constr. Build. Mater. **22**, 1484−1490 (2008)

9. Tironi, A., Trezza, M.A., Scian, A.N., Irassar, E.F.: Assessment of pozzolanic activity of different calcined clays comparison of test methods to assess pozzolanic activity. Cement Concr. Compos. **37**, 319–327 (2013)
10. IS: 1727 Indian Standard - Methods of Test for Pozzolanic Materials. Indian (1967)
11. Aubert, J.E., Segui, P., Husson, B., Measson, M.: A method developed to quantify lime and gypsum consumed by mineral additions. Cement Concr. Compos. **34**, 874–880 (2012)
12. McCarter, W.J., Tran, D.: Monitoring pozzolanic activity by direct activation with calcium hydroxide. Constr. Build. Mater. **10**(3), 179–184 (1996)

Compatibility of Superplasticizers with Limestone-Metakaolin Blended Cementitious System

Behnaz H. Zaribaf, Burak Uzal and Kimberley Kurtis

Abstract This study investigates the performance of polycarboxylate ether (PCE), polymelamine sulfonate (PMS), sodium lignosulfonate and naphthalene formaldehyde condensate (PNS) superplasticizers (SPs) with ASTM C595 Type IL cement (with up to 15% calcium carbonate) combined with 10 and 30 % metakaolin (MK) substitutions by mass. The required dosage of each SP for 10 % and 30 % MK substitutions were determined based on mini slump test to establish equivalent paste flow. At these dosage rates, the effects of SPs on setting time, hydration kinetics, and strength development were measured. Life cycle assessment (LCA) was carried out on different cement compositions used in this study to evaluate the greenhouse gas emissions and embodied energy of limestone-metakaolin blended cement with SP addition. While MK substitution decreases the workability of samples and shortens the setting time, this study shows that adequate dosages of a compatible type of SP can be used to compensate for these effects. Of the SPs examined, PCE and PMS are found to be more compatible, compared to PNS and sodium lignosulfonate, with limestone-metakaolin blended cements.

1 Introduction

Replacing a fraction of portland cement with of metakaolin (MK) helps to reduce the clinker fraction and consequently decreases the associated greenhouse gas emissions and embodied energy of concrete [1]. Metakaolin replacement can improve compressive strength at earlier ages than other supplementary cementitious

B.H. Zaribaf (✉) · K. Kurtis
School of Civil and Environmental Engineering, Georgia Institute of Technology, 790 Atlantic Dr., Atlanta, GA 30332-0355, USA
e-mail: Behnaz@gatech.edu

B. Uzal
Department of Civil Engineering, Abdullah Gul University, Sumer Campus, 38080 Kayseri, Turkey

K. Scrivener and A. Favier (eds.), *Calcined Clays for Sustainable Concrete*, RILEM Bookseries 10, DOI 10.1007/978-94-017-9939-3_53

materials (SCMs). Additionally, permeability of concrete decreased with metakaolin substitution that can improve the concrete durability [2].

Extending the use of MK and using it combined with ASTM C595 Type IL cement (Type IL-MK cement) can potentially further contribute to sustainability, by reducing the clinker fraction in concrete [3]. However, decreases in concrete workability can be problematic, as the fraction of metakaolin increased, particularly with limestone cements that have greater fineness.

In practice, several different types of superplasticizers can be used to improve concrete mixture workability. However, the compatibility and dosing of the various types of commercially available superplasticizers (SP) with Type IL-MK cement has not been well examined. This study examined four common superplasticizer types—polycarboxylate ether (PCE), polynaphthalene sulfonate (PNS), lignosulfonate (LS) and polymelamine sulfonate (PMS)—in Type IL-MK cement. After establishing dosage rates, which produce equivalent flow characteristics, time to set, hydration kinetics and strength development are assessed. Finally, life cycle analysis is performed to better understand the influence of binder composition and superplasticizer use on sustainability.

2 Materials and Methods

Pastes were produced from ASTM C595 Type IL hydraulic cement (Argos, Calera, AL) and metakaolin (OPTIPOZZ, Burgess Pigment Company, Sandersville, GA); compositional data and particle size distributions are given in Table 1 and Fig. 1, respectively. For mortars, natural sand (Vulcan Materials, Lithia Springs, GA) with fineness modulus of 3.04 and absorption capacity of 0.42 % was used. Four commercially available superplasticizers (SPs), polycarboxylate ether (PCE),

Table 1 Chemical composition of the cementious materials

Component (%)	Type IL cement	MK
SiO_2	17.13	51.4
Al_2O_3	4.16	44.8
Fe_2O_3	2.86	0.42
CaO	62.05	–
MgO	3.12	–
Na_2O	0.07	–
K_2O	0.48	–
Na_2O_e	0.38	–
TiO_2	0.26	1.46
SO_3	3.31	–
S/A ratio	0.8	–
LOI	6.33	1.05
Free CaO	0.56	–

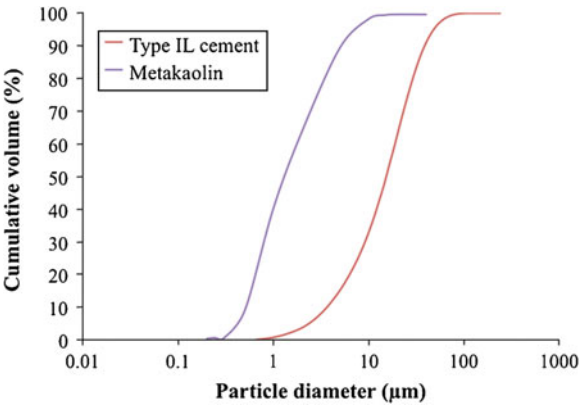

Fig. 1 Particle size distributions of type IL cement and metakaolin

sodium lignosulfonate and naphthalene formaldehyde condensates (PNS) and polymelamine sulfonate (PMS) were obtained from two different producers (Grace, BASF). All the SPs are liquid, except PMS that was received and used as powder.

Pastes were produced at water-to-binder (w/b) of 0.40 with 10 % (MK10) and 30 % (MK30) cement substitutions by mass. For similar workability as paste, mortars were produced at w/b of 0.50 and sand-to-cement ratio of 2.75, at the same MK rates of use as the pastes.

Mini slump tests were carried out on pastes containing MK10 or MK30 and each type of superplasticizer, where dosages were adjusted to achieve 12 cm flow as a target [4]. Flow tests were performed on a broader range of paste compositions—with 10, 20, 30, and 40 % MK substitutions—to assess the trend between metakaolin substations and each superplasticizer dosage.

After establishing dosage rates required producing equivalent flow in each binder system with each SP type, isothermal calorimetry (TAM Air calorimeter, TA Instruments) was conducted on fresh paste samples at 25 °C, according to ASTM C1679 [5]. Time to set of mortar samples with Type IL-MK cement cement was measured by the Vicat test, ASTM C191 [6]. Compressive strength, ASTM C109 [7], was measured at 1, 3, 7, and 28 days on 2 inch (50 mm) mortar cubes prepared at w/b of 0.50. Mortar cubes were cured in limewater at 23 ºC. Life cycle assessment (LCA) was conducted using SimaPro 7.1 software (USLCI and BUWAL 250 database) [8].

3 Results and Discussion

3.1 Flowability

Flowability of paste samples was measured using mini slump cone with Type IL-MK cement to assess the effect of metakaolin on flowability of Type IL-MK cement pastes [9]. Four superplasticizer chemistries—PCE, PMS, sodium lignosulfonate and

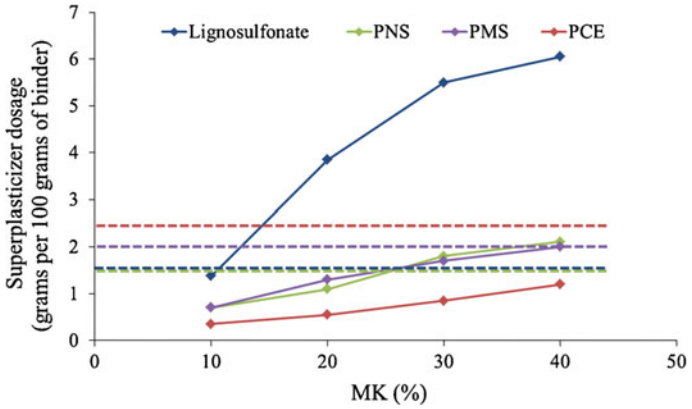

Fig. 2 Superplasticizer dosage required for pastes containing varying metakaolin levels in order to achieve flow comparable to control paste (no metakaolin)

PNS—were tested and the required dosage of each superplasticizer determined for pastes containing 10, 20, 30 to 40% metakaolin substitutions to achieve flow comparable to the control Type IL cement (no metakaolin). (These pastes denote MK10, MK20, etc.) All the superplasticizers used were in liquid form except PMS that was in powder form and dissolved in water before mixing. Figure 2 shows the required dosages of each superplasticizer expressed as the solid content of each superplasticizer for 100 g of binder (cement + metakaolin). The dashed lines show the maximum allowable level of each superplasticizer provided by the manufacturers. The results indicate that several types of superplasticizers, specifically the lignosulfonate and PNS, required significantly higher dosage than the maximum recommended dosage to achieve flow values comparable to the control samples. Use of superplasticizers at such high dosage rates may produce undesirable behavior including set retardation or false set; the latter is primarily found with lignosulfonate.

3.2 Cement Hydration

The early hydration behavior up to 40 h after mixing of Type IL-MK blended cement with water was studied with isothermal calorimetry. Paste samples with 30 % metakaolin were tested with different types of SPs at the dosages determined by the mini slump test to compare the effect of superplasticizers on the hydration of the paste mixtures. Paste samples with 30 % MK and lignosulfonate were not workable enough for testing.

Figure 3 shows that MK30 samples with no SP exhibit a lower cumulative heat of hydration and a slightly accelerated hydration compared to the control sample (no MK), while adding any of the SPs adjusted the rate of heat evolution and increased the cumulative heat released. Samples with PCE showed the highest peak

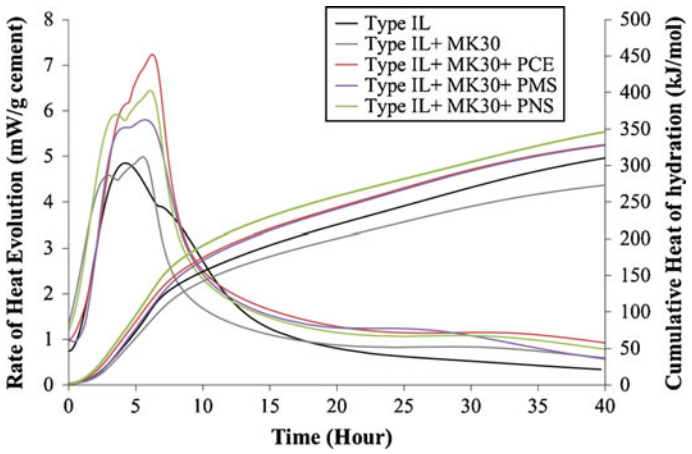

Fig. 3 Isothermal calorimetry results for type IL cement and 30 % MK and each of the four types of superplasticizers

rate of heat evolution while the cumulative heats of hydration were similar for all three types of SPs, and still higher than control sample with no MK.

3.3 Time to Set

The effect of metakaolin substitution on initial and final setting times of mortar samples was assessed by Vicat test. The initial and final setting time of mortar samples (w/b = 0.5) MK10 and MK30 are shown in Fig. 3. In general, metakaolin substitution shortens the initial and final setting time of samples; however, with appropriate dosage of superplasticizer, setting time can be adjusted to be similar to the control cement (i.e., no metakaolin).

The initial and final setting time of MK10 and MK30 mortar samples with each type of superplasticizer with the dosage determined by the mini slump test, is shown in Fig. 4. The results show that metakaolin mortars with no SP has a shorter final set while PMS, PNS and PCE increased the final set time of samples to be similar to the control samples. Lignosulfonate slightly lengthen the setting time of MK10 sample but MK30 sample with lignosulfonate was not sufficiently workable to measure the setting time. The retardation effect of PCE was observed for samples with MK30.

In addition to varying the chemistry of SP used, two procedures of adding PMS powder to cement (PMS (S)) and adding PMS to water (PMS (L)) were tested. It can be seen that the setting time results are very consistent. Based on setting time and calorimetry data, PCE was determined to be an effective SP and was chosen for further testing with MK10 and MK30.

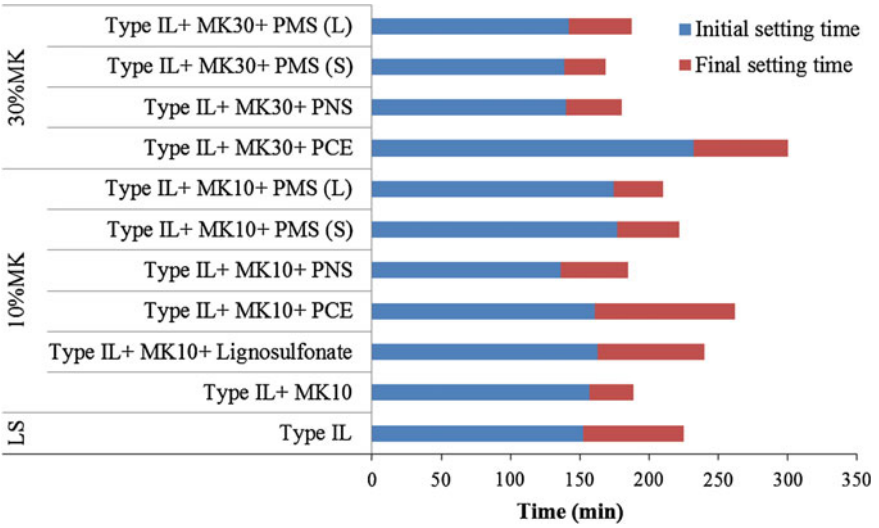

Fig. 4 Setting time data for limestone cement mortar samples with metakaolin substitution of 30 % and each type of superplasticizers

3.4 Compressive Strength

The compressive strength of samples with 10 and 30 % metakaolin with PCE was measured at 1, 3, 7, and 28 days of age. Figure 5 show that mortar samples with 10 and 30 % metakaolin have 40 and 20 % higher compressive strength at early age (1 day) compared to control sample (no MK). Higher compressive strength (30–40 %) was also observed for 7 day and 21 day samples.

3.5 Environmental Impacts

Life cycle assessment (LCA) was conducted to compare the embodied energy and greenhouse gas (GHG) emissions associated with ordinary (ASTM C150 Type I) and Type IL cement with 0, 10 and 30 % metakaolin substitution rates [8]. Data in Fig. 6 show use of Type IL cement saves up to 15 % in GHG emissions and embodied energy. Moreover, limestone cement with 10 and 30 % MK replacements can save up to 20 and 32 % of the GHG emissions and 17 and 22 % of the embodied energy associated with cement portion in concrete mixtures.

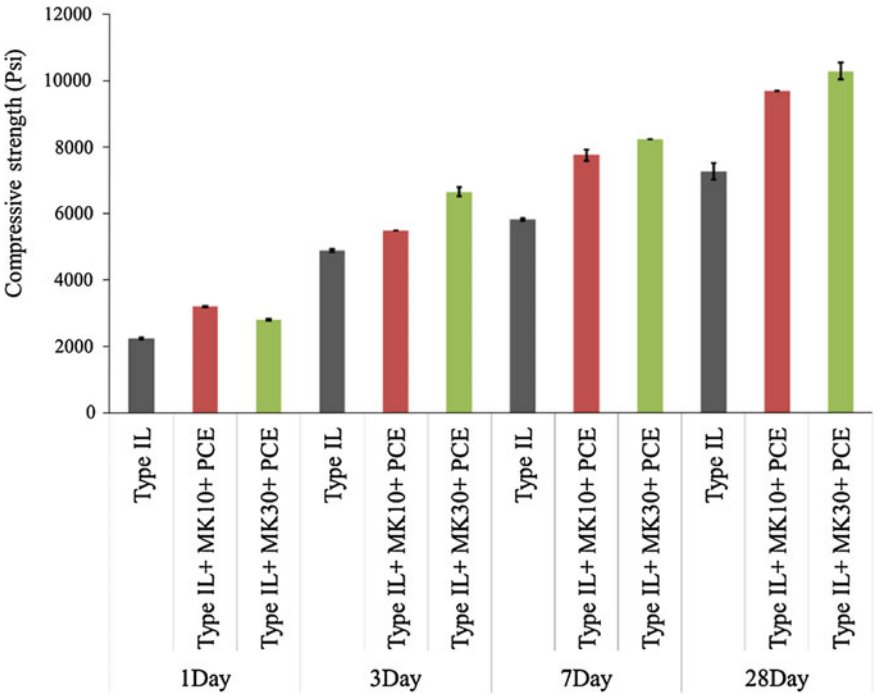

Fig. 5 Compressive strengths of mortars with limestone cement and 10 and 30 % MK and PCE superplasticizer (w/b = 0.50)

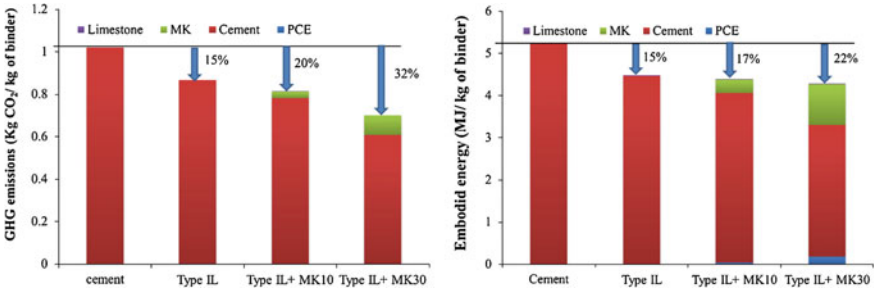

Fig. 6 Life cycle assessment of cements with metakaolin substitutions of 10 and 30 %

4 Conclusions

This study shows that PMS and PCE are the most compatible SPs for Type IL-MK cement. MK inclusion accelerates the hydration of cement and shortens the setting time, while addition of compatible SP can increase the setting time and adjust the hydration rate. Finally, compressive strengths of specimen increased with MK

substitutions (10 % and 30 %) and PCE as a superplasticizer. Further, LCA study showed that MK replacements can reduce the GHG emissions and embodied energy associated with cement portion in concrete mixtures, even when increased SP dosages necessary for workability are considered.

Acknowledgments The support of Burgess Pigment Company is kindly acknowledged.

References

1. Juenger, M.C.G., Winnefeld, F., Provis, J.L., Ideker, J.H.: Advances in alternative cementitious binders. Cem. Concr. Res. **41**(12), 1232–1243 (2011)
2. Boddy, A., Hooton, R.D., Gruber, K.A.: Long-term testing of the chloride-penetration resistance of concrete containing high-reactivity metakaolin. Cem. Concr. Res. **31**(5), 759–765 (2001)
3. ASTM C595-14: Standard specification for blended hydraulic cements. ASTM International, West Conshohocken (2014)
4. Kantro, D.: Influence of Water-reducing Admixtures on Properties of Cement Paste: A Miniature Slump Test. Portland Cement Association, Portland (1982)
5. ASTM C1679-14: Standard practice for measuring hydration kinetics of hydraulic cementitious mixtures using isothermal calorimetry. ASTM International, West Conshohocken (2014)
6. ASTM C191-13: Standard test methods for time of setting of hydraulic cement by Vicat Needle. ASTM International, West Conshohocken (2013)
7. ASTM C109: Standard test method for compressive strength of hydraulic cement mortars (using 2-in. or [50-mm] cube specimens). ASTM International, West Conshohocken (2013)
8. Priensma, R.: SimaPro database manual: the BUWAL 250 library. P. Consultants, Amersfoort (2004)
9. Kantro, D. (ed.) Influence of Water-reducing Admixtures on Properties of Cement Paste: A Miniature Slump Test. Portland Cement Association, Portland (1982)

Field Application of Limestone-Calcined Clay Cement in India

Soumen Maity, Shashank Bishnoi and Arun Kumar

Abstract A majority of the commercial cement production in India is based on substitution of clinker by pozzolanic materials in the form of fly ash from thermal power plants or blast furnace slag. The present study investigates the field application of a new type of ternary blend using limestone, calcined clay and clinker with small amount of gypsum. Four different blends were manufactured under pilot scale. Two different calcined china clay was used; one with a high kaolinite content and the other with a very low kaolinite content but high iron oxide phases giving a white and red colour to the respective blends. Two different limestone with varied quality was also used. Various types of alternate building materials were produced with these four blends for roofing, walling and flooring applications. Comparative study was undertaken with Ordinary Portland and Pozzolan Portland cement locally available. It was found that with a 30 % clinker replacement by high kaolinite calcined china clay the building materials show a higher strength compared to those manufactured with normal available cement. Even the low kaolinite content clay show comparative quality with 30 % replacement. No effect on productivity of the various types of building materials were observed. A two storied demonstration building has also been constructed entirely from the new blended cements. It was concluded that it is possible to replace 30 % or even more clinker by calcined clays to produce acceptable quality building materials.

S. Maity (✉) · A. Kumar
Technology and Action for Rural Advancement, New Delhi, India
e-mail: smaity@devalt.org

S. Bishnoi
Indian Institute of Technology Delhi, New Delhi, India

K. Scrivener and A. Favier (eds.), *Calcined Clays for Sustainable Concrete*,
RILEM Bookseries 10, DOI 10.1007/978-94-017-9939-3_54

1 Introduction

1.1 The Indian Cement Industry

The construction sector is one of the fastest growing sector in India contributing to 22 % of the total CO_2 emissions in India. With an average growth rate of 7% it is also one of the fastest growing sectors [1]. Within the construction industry, cement sector ranks second only to the steel in terms of revenue and forms the backbone of any shelter and infrastructure initiatives catering to all classes of life. With increasing development, increased construction activity will lead to higher use of cement and resultant concrete.

India is one of the largest cement producers in the world second only to China. The country has an installed capacity of 300 million tonnes (2011) which is slated to rise to 600 million tonnes by 2020 [2]. It is also one of the most efficient in the world operating totally on dry manufacturing process. However since the production of clinker relies totally on limestone, it produces around 137 million tonnes of carbon dioxide (as of 2010) which is approximately 7 % of the total man made CO_2 emissions of the country [3]. Apart for environmental emissions the industry also uses quite a substantial amount of natural resources, majority of which are in the form of limestone and coal. The cement industry also uses a substantial amount of thermal power plant waste in the form of fly ash to produce Portland pozzolana cement. By the year 2010-2011 this figure was around 45 million tonnes and around 10 million tonnes of blast furnace slag replacing clinker [2].

The resources of making the cement are finite. With increasing depletion of natural resources raw materials are becoming increasingly scarce which will affect the production of cement in the future. To optimize the use of natural resources, supplementary cementitious materials (SCM's) are a viable alternative [4–7]. India uses a substantial amount of fly ash as SCM's. However the substitution of fly ash is limited to 30 % since these materials reduces the early age mechanical properties.

The present study looks at the manufacture of a limestone-calcined clay cement reducing the clinker in base cement production to 50 % appropriately termed as a low carbon cement (LCC) due to additional savings in resources used, energy saved and CO_2 reduced.

2 Experimental

2.1 Selection of Raw Materials

The raw materials used for the production of low carbon cement (LCC) were calcined china clay, limestone, gypsum and clinker. Two types of china clay was procured from commercial mines in Birbhum district, West Bengal, India and calcined under static conditions at a temperature of 800 °C. Temperature for

calcination was determined by thermogravimetric analysis. Chemical composition of the china clay used are given in Table 1. XRD analysis of both the varieties of raw and calcined china clay are given in Fig. 1.

Table 1 Chemical analysis of China clay B1 and B3 from Birbhum, West Bengal

Chemical constituents	China clay B1 (~60 % kaolin content)	China clay B3 (~40 % kaolin content)
SiO_2	43.30	55.78
Al_2O_3	36.35	17.46
Fe_2O_3	2.56	8.89
CaO	0.46	4.84
MgO	0.27	0.59
Na_2O	0.13	0.12
K_2O	0.08	1.93
TiO_2	2.56	0.46
LOI	13.94	9.49

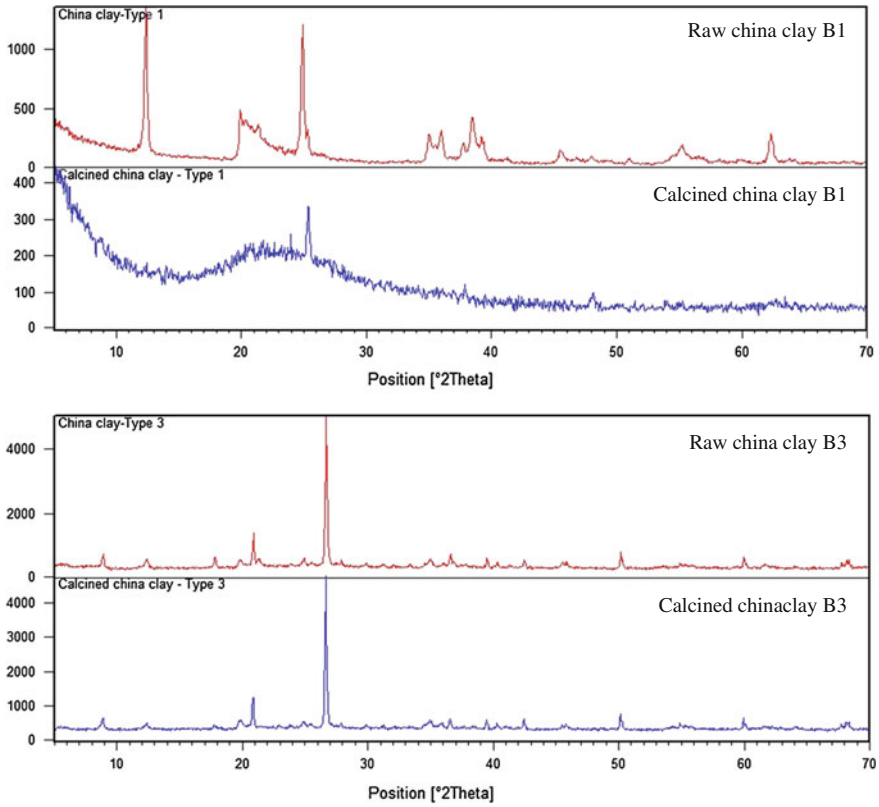

Fig. 1 XRD analysis of raw and calcined China clay B1 and B3

Table 2 Chemical analysis of limestone used in the pilot production

Parameter	Limestone A	Limestone B
LOI	37.04	35.10
SiO_2	14.04	18.20
R_2O_3	3.10	1.10
CaO	36.29	42.84
MgO	8.71	1.08

Limestone used in the pilot production of LCC was procured from commercial companies. Chemical analysis of both the varieties of limestone is given in Table 2.

Gypsum used was in the form of chemical gypsum from fertilizer companies. Clinker was also procured from a commercial cement company (Ambuja Cements, Bhatapara, Chattisgarh).

2.2 Composition Used

Four different blends were prepared using the combinations of china clay and limestone. They are given in Table 3.

2.3 Production of Building Materials and Their Use in Demonstration Building

Various types of alternate and low carbon building materials were produced for the building. All the building materials used are typical of building products usually used in Bundelkhand, Central India. For roofing, planks and joist system was used in the ground floor roof for load bearing purposes. These are usually made of reinforced cement concrete (RCC). In the roof of the first floor micro concrete roofing tiles were used. Walls were made of hollow concrete blocks. RCC door and window frames were used in the doors and windows. Various other flooring materials e.g. paving blocks, kerb stones were used in the exterior areas of the building.

Table 3 Low carbon cement blends used in the experimentation

Minerals used	Blend composition (% by weight)			
	LCCA	LCCB	LCCC	LCCD
China clay B1	30	30		
China clay B3			30	30
Limestone A	15		15	
Limestone B		15		15
Clinker	50	50	50	50
Gypsum	5	5	5	5

During production of the building materials, care was taken not to disturb the actual process and composition commercially followed. Water-to-cement ratio was also not changed. Thus during production only the normal cement was replaced by LCC. Quality of the LCC based building products were compared with products available in the market.

The demonstration building was a two storied structure build entirely of materials produced from LCC. LCC was also used in foundation, columns and beams to see the immediate and long term effect on reinforced cement concrete application.

3 Results and Discussion

3.1 Building Material Properties

Compositions used in production of the building materials are given in Table 4.

In normal construction, sand is used for production of building materials along with aggregates. However in the building materials used in the demonstration LCC building, sand was completely replaced with waste stone dust produced from stone quarries. No drastic reduction in compressive strength was found compared to normal PPC. This shows that quite a substantial amount of wastes can also be used in building materials made from LCC. Thus the behaviour and compatibility of LCC with unconventional materials are similar to normal PPC.

During production of Micro Concrete Roofing (MCR) tiles no change in production properties were noticed. The production parameters of vibration time are given in Fig. 2. Quality of MCR tiles produced are given in Fig. 3. It is observed that compared to normal PPC used in production, there is no change in production parameters of MCR tiles with various blends of LCC except LCCB. With LCCB, a low water: cement ratio of 0.475, was not possible to produce tiles under commercial conditions. Tiles made with all the blends gave a higher strength compared

Table 4 Composition of building materials used in the demo LCC building

Building material	Composition (parts by weight)		
	LCC	Stone dust waste	Aggregate (6 mm)
Micro concrete roofing tiles	1	1.5	1.5
Plans and joists	1	2	4
Hollow concrete blocks	1	3	3
Solid concrete blocks	1	2	2
RCC door and window frame	1	1	2
Paving blocks	1	3	6
Kerb stones	1	4	6

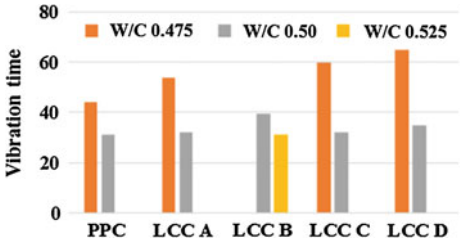

Fig. 2 Vibration time of MCR tiles

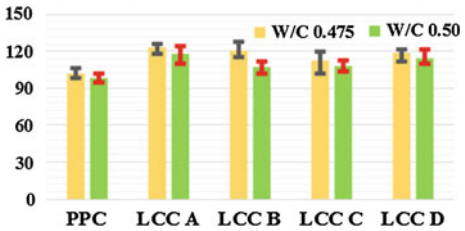

Fig. 3 Quality of MCR tiles

to normal PPC. Thus in case of MCR tile production, even a poor raw material quality blend e.g. LCCD does not have any appreciable effect on the strength.

Product quality development and analysis results for all kinds of building materials show that all grades of LCC blends have an equal or better strength compared to normal PPC blends.

Photographs of intermediate stage of construction and finished building is given in Fig. 4. In this building, the application of various types of building material can be seen.

Fig. 4 Various stages in construction of demo building

4 Conclusions

From the above study it was concluded that a new ternary blend of calcined clay, limestone, clinker manufactured with Indian raw materials can be beneficially used as a general purpose cement thereby reducing the clinker factor to 0.50. This is quite substantial compared to the presently used fly ash based PPC. Market standard quality building materials can also be produced with this cement without any effect on mechanical properties. However quality of the ternary blended cement is dependent on the metakaolin content. Although no effect on limestone was seen, more studies needs to be undertaken before any definitive conclusion can be drawn. Calculation of waste and CO_2 emissions from the demonstration building shows that a judicious use of industrial wastes and LCC in building materials can help in use of 1.72 kg of waste per m^2. A combined use of alternate building material and LCC can help in a reduction of CO_2 emissions by 0.5 kg per m^2 of floor area.

Acknowledgments The authors are indebted to Swiss Agency for Development and Cooperation, Government of Switzerland for supporting this research on low carbon cement. Sincere thanks to Prof. Karen Scrivener, EPFL, Switzerland for her never ending technical guidance and motivation during the entire period of work. Last, but not the lease our sincere thanks to Dr. Anjan K Chatterjee for his constant guidance, motivation and valuable suggestions during the entire course of work.

References

1. Indian Construction Industry: Construction industry development council (2006)
2. Existing and Potential Technologies for Carbon Emissions Reductions in the Indian Cement Industry: Cement sustainability initiative, world business council for sustainable development (2012)
3. Technology Roadmap, Low Carbon Technology for the Indian Cement Industry: World business council for sustainable development (2012)
4. Antoni, M., Rossen, J., Martirena, F., Scrivener, K.: Cement substitution by a combination of metakaolin and limestone. Cem. Concr. Res. **42**, 1579–1589 (2012)
5. He, C., Osbaeck, B., Makovicky, E.: Pozzolanic reactions of six principal clay minerals: activation, reactivity assessments and technological effects. Cem. Concr. Res. **25**(8), 1691–1702 (1995)
6. Murat, M., Comel, C.: Hydration reaction and hardening of calcined clays and related minerals III. Influence of calcination process of kaolinite on mechanical strengths of hardened metakaolinite. Cem. Concr. Res. **13**(5), 631–637 (1983)
7. Sabir, B.B., Wild, S., Bai, J.: Metakaolin and calcined clays as pozzolans for concrete: a review. Cem. Concr. Compos. **23**(6), 441–454 (2001)

Raw Material Mapping in Selected Areas of Rajasthan and West Bengal and Their Suitability for Use in Low Carbon Cement Production

Soumen Maity and Shashank Bishnoi

Abstract Low carbon cement is a ternary blended Portland cement with clinker factor as low as 0.40. It uses the synergetic hydration of clinker, calcined clay and crushed limestone to achieve comparable properties of commercial cements. One of the major components of low carbon cement is calcined china clay having a kaolinite content as low as 20 %. The present report discusses the availability of required clays in two surveyed areas of Rajasthan and West Bengal. Characterization of clays have been performed through various techniques and their suitability established from thermo-gravimetric analysis supplemented by mineral and chemical composition. Medium grade china clay (40-60 % kaolinite) is abundantly available in Rajasthan, whereas very high grade (60-80 % kaolinite) is commercially available in West Bengal. It was difficult to get low grade china clay under commercial terms and conditions although it is dumped as wastes in and around mine areas. All the various grades of china clay were found to be suitable for use in low carbon cement by replacing clinker.

1 Introduction

1.1 Low Carbon Cement (LCC)

With increasing affluence and development, there has been a spurt in infrastructural activities across the world. Most of the concentration of construction activities are in the developing countries e.g. China, India, Brazil, Russia and South Africa. The demand of infrastructural needs is also expected to increase the demand of cement which is expected to double by 2050. Almost 80 % of this demand is projected from the developing countries [1]. In the world, the main ingredients of cement are clay,

S. Maity (✉)
Technology and Action for Rural Advancement, New Delhi, India
e-mail: smaity@devalt.org

S. Bishnoi
Indian Institute of Technology Delhi, New Delhi, India

K. Scrivener and A. Favier (eds.), *Calcined Clays for Sustainable Concrete*,
RILEM Bookseries 10, DOI 10.1007/978-94-017-9939-3_55

limestone, gypsum and coal. Coal is used to produce clinker from a combination of limestone and clay. These materials are abundant in the earth's crust and available across regions. Thus cement can be produced anywhere and everywhere.

The resources of making the cement are finite within the earth. With increasing depletion of natural resources raw materials are becoming increasingly scarce which will affect the production of finished goods e.g. cement in the future. Thus to optimize the use of local materials, the need to look at supplementary cementitious materials (SCM's). The low carbon cement looks at SCM's to replace clinker in cement production [2]. The SCM's proposed in the new blends are combinations of china clay materials containing a kaolinite beyond 20%. Thus the proposed cement compositions are a combination of calcined kaolinitic clays, clinker, limestone and gypsum.

1.2 Raw Materials for Production of LCC

It has been widely known that the basic components of Portland cement are clinker and gypsum. Additionally clinker is produced through a combination of clay and limestone. In India to reduce the clinker factor supplementary cementitious materials e.g. fly ash and blast furnace slag are commonly used. In fact a majority of the cement produced in India is PPC or Portland Pozzolana Cement made up of atleast 25 % substitution of clinker by fly ash. However above a threshold substitution of about 30 %, these materials reduce the mechanical properties, particularly at early age [3]. On the other hand fly ash and blast furnace slag are limited to local availability retarding their widespread use. Consequently, alternative sources of SCM's such as calcined clays are of interest. These are widely available in the earth's crust and can easily be dehydroxilated at temperatures ranging between 700–800 °C to produce metakaolin [4, 5]. Metakaolin demonstrates excellent pozzolanic properties [6] and is one of the major raw materials of producing LCC.

Limestone is also an important raw material for use in production of cement. It has been shown that 45 % of substitution by 30 % metakaolin and 15 % of limestone gives better mechanical properties at 7 and 28 days that the 100 % Portland Cement reference. Results show that calcium carbonate reacts with alumina from the metakaolin, forming supplementary AFm phases and stabilizing ettringite [3]. It has also been shown that gypsum addition should be carefully balanced when using calcined clays because it considerably influences the early age strength by controlling the rapid reaction of aluminates.

In this study we map the availability of china clays in two areas to find its suitability in LCC use. This is expected to give us a broad idea on the possible availability of required quality of clay.

2 Availability of Raw Materials in India

2.1 China Clay

China clay resources in the country as per UNFC system as on 2010 have been calculated at 2,705 million tonnes [7]. The resources are spread over a number of states of which Kerala holds about 25 %, followed by West Bengal and Rajasthan (16 % each) and Odisha and Karnataka (10 % each). Out of total resources, about 22 % or 608 million tonnes fall under ceramic/pottery grade, 4 % are classified under chemical, paper and cement grades and about 73 % or 1,980 million tonnes resources fall under mixed grade, others, unclassified and not-known categories.

2.2 Limestone

1. The total resources of limestone of all categories and grades as per UNFC system as on 2010 are estimated at 184,935 million tonnes. Karnataka is the leading state having 28 % of the total resources followed by Andhra Pradesh (20%), Rajasthan (12 %), Gujarat (11 %), Meghalaya (9 %) and Chhattisgarh (5 %). Grade wise, cement grade has leading share of about 69% followed by other grades [8].
2. Andhra Pradesh was the leading producing state accounting for (21 %) of the total production of limestone, followed by Rajasthan (19 %), Madhya Pradesh (13 %), Gujarat (9 %), Tamil Nadu, Karnataka and Chhattisgarh (8 % each), Maharashtra and Himachal Pradesh (4 % each) and the remaining 6 % was contributed by Meghalaya, Uttar Pradesh, Odisha, Jharkhand, Kerala, Bihar, Assam and Jammu & Kashmir.

2.3 Gypsum

As per UNFC system, the total resources of mineral gypsum in India as on 2010 were estimated at 1,286 million tonnes [9]. By States, Rajasthan alone accounts for 82 % resources and Jammu & Kashmir 14 % resources. The remaining 4 % resources are in Tamil Nadu, Gujarat, Himachal Pradesh, Karnataka, Uttarakhand, Andhra Pradesh and Madhya Pradesh.

3 Experimental

3.1 Selection of Raw Materials

For the production of low carbon cement, china clay was brought from Rajasthan initially. However due to logistics reasons additional china clay was sourced from West Bengal. Experimentation was done with both high and low quality kaolinitic clay. Limestone was procured from the commercial market similar to clinker. Two types of limestone were used for the experimentation as per the details given below in Table 1.

Chemical gypsum used in the experimentation was procured from the commercial market.

3.2 Characterization Techniques Used

Most of the samples were procured in powdered form. Samples collected as lumps were reduced to smaller sizes, mixed thoroughly and sampled for testing through the coning and quartering method. X-ray diffraction of powder china clay were done in a Pan-Analytical diffractometer fitted with PW 1830 goniometer operating with CuKα radiation through a Ni filter. Scanning was done at a speed of 2^{o}/min for a 2θ range of 10^{o} to 70^{o}. The phases were identified by JCPDS numbers ICDD-PDF2 data base. Thermo-Gravimetric analysis (TGA) was performed by Perkin Elmer (Pyris Diamond) thermal analyser using α-alumina powder as reference material. Raw china clays were crushed and finally grounded to ~75μ. TGA measurements were performed by heating about 8 mg powder sample at a heating rate of 10 °C/min in a nitrogen atmosphere.

Table 1 Chemical analysis of limestone used in the experimentation

Parameter	Limestone A	Limestone B
LOI	37.04	35.10
SiO_2	14.04	18.20
R_2O_3	3.10	1.10
CaO	36.29	42.84
MgO	8.71	1.08

4 Results and Discussion

4.1 Rajasthan China Clay

8 different samples were collected from Bhilwara, Bikaner and Merta Road in Rajasthan based on the ease of availability and the quality of china clay. Results of TGA analysis to determine the quality of clay are given in Table 2.

From all the thermal and mineralogical analysis it was concluded that sample K1 and K8 fulfils the criteria of 60 % and 40 % kaolinite.

Despite the availability of a workable grade of china clay, the logistics of low carbon cement did not work out in Rajasthan. The project needed calcined clay, and there were no commercial calciners willing to undertake a low quantity calcination and of an impure variety china clay. Low purity china clay would contaminate their existing china clay facilities and thus hamper regular production. Thus raw materials in West Bengal were additionally mapped from Birbhum district since it is the area where maximum china clay occurrences have been prospected and being mined and static calcination facilities were available.

From the surveyed areas in Birbhum, three different types of clays were selected. Two clays were of commercial grade with no visual difference. As per supplier feedback, china clay B1 was of high grade (60 % alumina) priced between Rs. 2100 and Rs. 1600 based on mesh size. China clay B2 was of medium grade with an approximate alumina content of 40 %. It was rather difficult to get a china clay of poor quality since it is dumped and have no buyers. Price of the clay was Rs. 300 per tonne mainly due to high loading and unloading charges. The B3 clay was impure in nature, since visibly it was red in colour due to presence of high iron oxide content.

Chemical analysis of china clay B1 and B3 are given in Table 3.

Chemical analysis shows the presence of high iron oxide in the overburden clay giving its presumable red colour. Moreover with a low alumina content, the clay was confirmed to be of low kaolinite purity.

Four different blends were prepared using the combinations of china clay and limestone. They are given in Table 4.

Table 2 Thermo Gravimetric data of mapping samples in Rajasthan

Sample ID	% Weight loss (RT—200 °C)	% Weight loss (temp. range given)
K1	1.17	9.78 (200–700 °C)
K2	2.31	10.46 (200–600 °C)
K3	1.55	9.34 (200–700 °C)
K4	1.61	9.78 (200–800 °C)
K5	0.90	9.22 (200–700 °C)
K6	0.83	7.64 (200–600 °C)
K7	0.89	9.10 (200–800 °C)
K8	0.05	5.07 (200–850 °C)

Table 3 Chemical analysis of china clay B1 and B3 from Birbhum, West Bengal

Chemical constituents	China clay B1 (~60 % kaolin content)	China clay B3 (~40 % kaolin content)
SiO_2	43.30	55.78
Al_2O_3	36.35	17.46
Fe_2O_3	2.56	8.89
CaO	0.46	4.84
MgO	0.27	0.59
Na_2O	0.13	0.12
K_2O	0.08	1.93
TiO_2	2.56	0.46
LOI	13.94	9.49

Table 4 Low carbon cement blends used in the experimentation

Minerals used	Blend composition (% by weight)			
	LC3A	LC3B	LC3C	LC3D
China clay B1	30	30		
China clay B3			30	30
Limestone A	15		15	
Limestone B		15		15
Clinker	50	50	50	50
Gypsum	5	5	5	5

Results of mortar strength of the four different blends are given in Fig. 1.

It is seen from the strength of the mortar cubes tested that the LC3A and LC3B blends shows even higher strengths compared to Portland Cement made with the same clinker. Even with a very impure china clay commercially termed as over-burden, acceptable strength can be achieved.

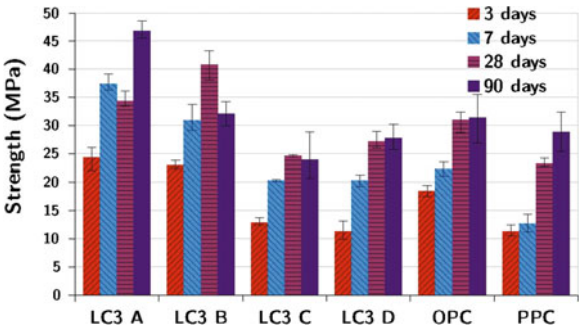

Fig. 1 Mortar strengths of various compositions

5 Conclusions

From the above preliminary mapping study it was found that various types and qualities of china clay are available in both Rajasthan and West Bengal. China clay occurrences in Rajasthan are not of very high quality. The Al_2O_3 content in all the clay samples varies between 24–32 % by weight. On the other hand, very high grade china clay with an Al_2O_3 content ranging between 35–40 % are commercially available in West Bengal. During the entire mapping exercise it was extremely difficult to get a steady source of low kaolin china clay. In mines these are usually dumped and not used. These are classified as mines overburden and rejects.

It has been shown that even with a low grade china clay and low grade limestone combination a good quality general purpose cement can be produced.

Acknowledgments The authors are indebted to Swiss Agency for Development and Cooperation, Government of Switzerland for supporting this research on low carbon cement. Sincere thanks to Prof. Karen Scrivener, EPFL, Switzerland for her never ending technical guidance and motivation during the entire period of work. The authors are deeply grateful to A.K. Tiwari and Dr. K. Suresh for their kind support in testing the samples at Aditya Birla Science and Technology Centre, Mumbai. Last, but not the lease our sincere thanks to Dr. Anjan K Chatterjee for his constant guidance, motivation and valuable suggestions during the entire course of work.

References

1. http://www.cembureau.eu/about-cement/key-facts-figures CEMBUREAU Report (2010)
2. Scrivener, K., Fernando Martirena, J., Antoni, M.: Tackling social housing through the commercial use of low clinker cementitious systems. Innovations on the use of calcined clay as supplementary cementitious material, EPFL, Lausanne, Switzerland, 29–31 May 2012
3. Antoni, M., Rossen, J., Martirena, F., Scrivener, K.: Cement substitution by a combination of metakaolin and limestone. Cem. Concr. Res. **42**, 1579–1589 (2012)
4. He, C., Osbaeck, B., Makovicky, E.: Pozzolanic reactions of six principal clay minerals: activation, reactivity assessments and technological effects. Cem. Concr. Res. **25**(8), 1691–1702 (1995)
5. Murat, M., Comel, C.: Hydration reaction and hardening of calcined clays and related minerals III. Influence of calcination process of kaolinite on mechanical strengths of hardened metakaolinite. Cem. Concr. Res. **13**(5), 631–637 (1983)
6. Sabir, B.B., Wild, S., Bai, J.: Metakaolin and calcined clays as pozzolans for concrete: a review. Cem. Concr. Compos. **23**(6), 441–454 (2001)
7. Indian Minerals Yearbook 2012—Part III: Mineral Reviews. Kaolin, ball clay, other clays and shale, 51st edn. Indian Bureau of Mines (2014)
8. Indian Minerals Yearbook 2012—Part III: Mineral Reviews. Limestone and other calcareous minerals, 51st edn. Indian Bureau of Mines (2014)
9. Indian Minerals Yearbook 2012—Part III: Mineral Reviews. Gypsum, 51st edn. Indian Bureau of Mines (2014)

Suitability of Raw Materials in Gujarat for Production of Low Carbon Cement

Palas K. Haldar and Soumen Maity

Abstract The state of Gujarat has quite a substantial amount of kaolinitic clays found uniformly distributed across the state. Most of the clays are surface outcrops with varied quality. They are used for ceramic, paper, textile and cement industries. The present study explores the use of calcined kaolinitic clays, limestone and clinker available in Gujarat for the production of pozzolanic cement. For production of the cement; clinker and limestone were procured from an existing cement production unit. Both the raw materials showed acceptable properties as per Indian cement industry standards. For the experimentation commercial grade gypsum was used with very low levels of P_2O_5. Various types of china clay were collected from Kutch area of Gujarat. These china clays were analysed in terms of kaolinite content and other mineral phases. Calcination experiments conducted in a static calciner showed optimum calcination between 700 and 800 °C with maximum reactivity. Various pilot blends in the lab showed encouraging results in terms of 3, 7, 14 and 28 days strength. It was concluded that the state of Gujarat has quite varied quality of china clay suitable for production of alternate cementitious blends.

1 Introduction

China clay or kaolin is formed by weathering of feldspars which mainly consists of Kaolinite ($Al_2O_3 \cdot 2SiO_2 \cdot 2H_2O$), associated with other clay minerals. Kaolin is commercially valued for its whiteness and fine particle size which distinguishes it from other clays. Other physical characteristics that influence commercial utility include brightness, glossiness, abrasiveness and viscosity. Crude china clay is usually used in cement industry and processed china clay in ceramic, paint, paper, pigment industries etc.

P.K. Haldar (✉) · S. Maity
Technology and Action for Rural Advancement, New Delhi, India
e-mail: pkhaldar@devalt.org

K. Scrivener and A. Favier (eds.), *Calcined Clays for Sustainable Concrete*,
RILEM Bookseries 10, DOI 10.1007/978-94-017-9939-3_56

Gujarat was the lead producing state of kaolin accounting for 48 % of the total kaolin production in India in 2011-2012. Total reserve of china clay in Gujarat was 112 million tonnes in 2009-10 [1].

It has been widely known that the basic components of ordinary Portland cement are clinker and gypsum. Additionally clinker is produced through a combination of limestone and minor amounts of clay. In India to reduce clinker factor, supplementary cementitious materials (SCM's) e.g. fly ash and blast furnace slag are commonly used. In fact a majority of the cement produced in India is PPC or Portland Pozzolana cement made up of at least 25 % substitution of clinker by fly ash. However above the threshold substitution of about 30 %, these materials reduce the mechanical strength of mortar particular at early age [2]. On the other hand fly ash and blast furnace slag are limited to local availability, retarding their widespread use. Consequently, alternative sources of SCM's such as calcined clays are of interest [3, 4]. These are widely available in the earth's crust and can easily be dehydroxylated at temperatures ranging between 700–800 °C to produce metakaolin [5, 6]. Metakaolin demonstrates excellent pozzolanic properties [7] and is one of the major raw materials of producing a low carbon cement.

Limestone is also an important raw material for use in production of cement. Fine limestone is commonly added to cement and it is established that limestone additions up to around 5 % can react with cement and enhance most properties [8]. It has been shown that 45 % of substitution by 30 % metakaolin and 15 % of limestone gives comparable mechanical properties at 7 and 28 days to that of the 100 % Portland cement reference. Results show that calcium carbonate reacts with alumina from the metakaolin, forming supplementary AFm phases and stabilizing ettringite [2]. It has also been shown that gypsum addition should be carefully balanced when using calcined clays because it considerably influences the early strength by controlling the rapid reaction of aluminates. In this study low grade kaolinitic clay was collected from Kutch region of Gujarat and studied to find their suitability in low carbon cement (LC^3) application.

2 Experimental

Clay samples were initially collected from five different locations of Kutch, western region of Gujarat in India. Reasons for selecting this region as a source of clay sampling were:

- Availability of wide ranges of china clay
- Maximum reserve of china clay
- Better communication through road and sea
- Availability of rotary calcination and other clay processing facility

Chemical composition of the china clay was determined by X-Ray Fluorescence (XRF) method. Mineralogical phases were identified by X Ray Diffraction (XRD) with X'Pert Pro diffractogram system. Scanning was done at a speed of 2°/min for a

2θ ranging from 0° to 70°. The phases were identified by JCPDS, ICDD-PDF2 data base. % wt. loss of clay sample was measured by thermo gravimetric analysis (TGA). From the weight loss measurement, % kaolinite content of the clay sample was calculated. Calcination of china clay was done by static method using a temperature controlled muffle furnace. Temperature of calcination was determined through the TGA analysis. Amount of released heat during hydration reactions were determined by isothermal calorimetric study. LC^3 blend was formulated by using a standard composition of 50 % clinker, 30 % calcined clay, 15 % limestone and 5 % gypsum. Compressive strength of the mortar cubes was measured by standard compression testing device.

3 Results and Discussion

3.1 Analysis of Clay

Results of chemical composition of raw clay as determined by XRF technique is summarised in Table 1. Clay 5 shows the highest alumina and lowest silica content with Titania content more than 4 %. It contains iron oxide less than 1.5 %. Clay 3 and Clay 4 show almost comparable alumina content in the range of 21 % to 23 % with lower iron oxide (<1 %) and titania (<2 %) content. On the other hand Clay 2 shows alumina content in the range of 25 % which is higher than that of all other clays except Clay 5. Since the iron content is very high, thus this type of clay is not generally used for any ceramic applications. All the clays were collected within a radius of 10 km. Within this short distance the variation in clay quality is only due to change in geology of formation of the clays.

Figure 1 shows the TGA plots of the various clays indicating corresponding weight loss due to de-hydroxylation of the raw clay. Kaolinite content of the china clay has been calculated using molecular formula. Results are given in Table 2. Based on higher alumina content and % kaolinite content, Clay 5, 2 and 4 were selected for further calcination studies.

Mineralogical phases were obtained from XRD analysis. XRD patterns of Clay 5, 2 and 4 are compared in Fig. 2. Major peaks (2θ) at 12.3° & 24.9° indicate the presence of Kaolinite (K) in all clays whereas peaks at 20.8° & 26.5° are due

Table 1 Chemical composition of sampled china clays

Sample	SiO_2	Al_2O_3	Fe_2O_3	CaO	MgO	TiO_2	K_2O	Na_2O	LOI
Clay1	63.52	20.52	4.99	0.10	0.11	1.44	0.22	0.12	8.97
Clay2	58.43	24.95	5.08	0.09	0.19	1.41	0.215	0.05	9.58
Clay3	68.82	21.45	0.86	0.09	0.12	1.25	0.07	0.22	7.26
Clay4	66.77	22.89	0.49	0.03	0.09	1.29	0.25	0.15	8.09
Clay5	41.10	37.13	1.39	0.10	0.14	4.67	0.09	0.47	14.37

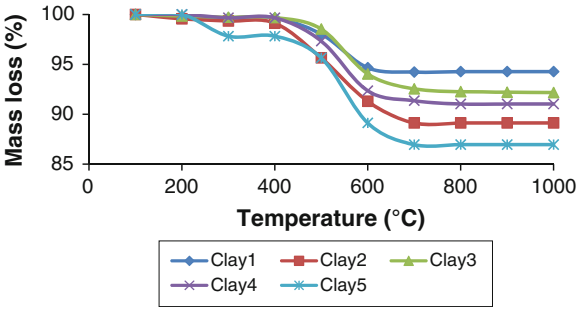

Fig. 1 TGA plots of various clays

Table 2 % Kaolinite content of clays

Parameters	Clay1	Clay2	Clay3	Clay4	Clay5
Weight loss (%)	5.2	7.9	6.3	6.9	9.9
Al_2O_3 content (%)	20.52	24.95	21.45	22.89	37.13
Kaolinite content (%)	38	57	45	50	71

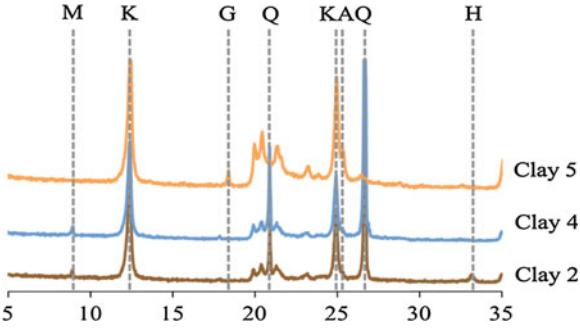

Fig. 2 XRD analysis of raw china clay

presence of Quartz (Q). From the XRD it is evident that Kaolinite and Quartz are the major phases present in all the raw clays. Other minor peaks are due to presence of Muscovite (8.9°), Anatase (25.4°), and Haematite (33.35°). Clay 5 gives a prominent peak at 18.4° indicating the presence of Gibbsite.

3.2 Calcination Analysis of China Clay

Calcination of the various types of China clay was done in a static muffle furnace. Results of TGA of raw and lab calcined clays are given in Fig. 3 showing that all the different clay types were completely calcined between 700 °C to 800 °C. Thus

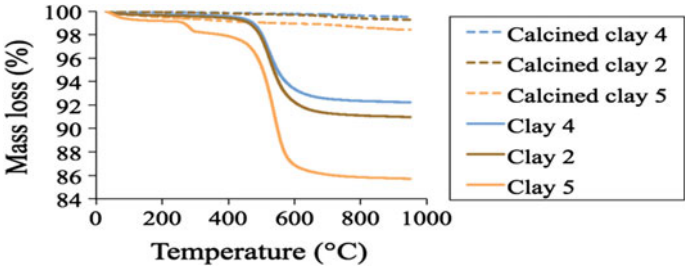

Fig. 3 TGA of raw and calcined clays

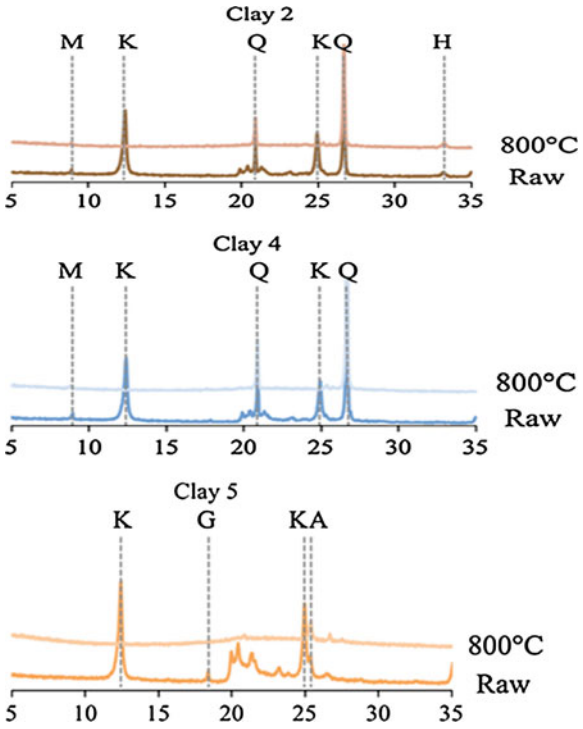

Fig. 4 Comparative XRD analysis of raw and calcined china clay

the calcination temperature was optimised at 800 °C for better effectivity and efficiency. XRD analysis (Fig. 4) of the calcined clays at 800 °C ensured complete de-hydroxilation since no kaolinite peak was observed. Additionally absence of any spinel or mullite peaks confirmed the efficiency of calcination process and temperature.

3.3 Analysis of Cement Blend

With the various types of calcined clays blended cements were produced of composition 50 % clinker, 30 % calcined clay, 15 % limestone 5 % gypsum. Reactivity of the blends made from various types of china clay was measured through isothermal calorimetric studies (Fig. 5). Highest amount of heat is released from the blend with calcined Clay 5 indicating highest pozzolanic reactivity. Calcined Clay 2 is slightly more reactive than Clay 4 due to increased kaolinite content.

Figure 6 illustrates the development of mortar compressive strength of the respective cement blends compared to Portland cement prepared from the same clinker. Blends containing Clay 4 shows relatively lower strength than others which is in agreement to lower kaolinite content. Cements made with Clay 2 and Clay 5 have almost similar strength though the pozzolanic reactivity of Clay 5 is higher than Clay 2. From the comparative strength analysis, it is inferred that though kaolinite content is a key indicator of the quality of the china clay for preparation of ternary blends, but there are other factors like specific surface area, microstructure, and relative miscibility in the blend which play important roles in developing strength. OPC shows the highest compressive strength resulting from higher degree of homogeneity and fineness.

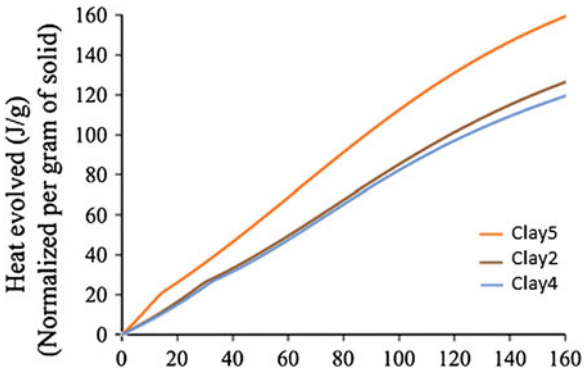

Fig. 5 Reactivity of calcined China clays

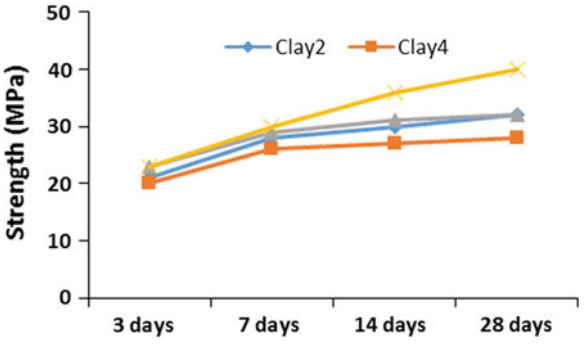

Fig. 6 Compressive strength of mortars of low carbon cement blends

4 Conclusions

Good quality china clay is abundant in Gujarat, Western part of India. Optimum calcination temperatures of these types of china clay is around 800 °C. Higher calcination temperatures might result into formation of crystalline phases. With all types of calcined china clay a good quality ternary blended cement can be formed. The quality of the cement depends not only on the kaolinite content but is influenced by the presence of additional phases. Apart from chemical composition of calcined china clay, properties of blended cement depends on the specific surface area and the uniformity of mixes. It is concluded that low quality china clay which are not used for ceramic or refractory applications can be used optimally into production of a comparable quality general purpose cement.

Acknowledgments The authors are indebted to Swiss Agency for Development and Cooperation, Government of Switzerland for supporting this research on low carbon cement. Sincere thanks to Prof. Karen Scrivener, EPFL, Switzerland for her never ending technical guidance, analysis of samples and motivation during the entire period of work. Thanks are also due to IIT Delhi for testing and analysis of samples. Our sincere thanks to Dr. Anjan K Chatterjee for his constant guidance, motivation and valuable suggestions during the entire course of work.

References

1. Indian Minerals Yearbook 2012, part III: Mineral Reviews, 51 edn. Indian Bureau of Mines, Nagpur (2014)
2. Antoni, M., Rossen, J., Martirena, F., Scrivener, K.: Cement substitution by a combination of metakaolin and limestone. Cem. Concr. Res. **42**, 1579–1589 (2012)
3. Badogiannis, E., Kakali, G., Tsivilis, S.: Metakaolin as supplementary cementitious material: optimization of kaolin to metakaolin conversion. J. Therm. Anal. Calorim. **81**, 457–462 (2005)
4. Scrivener, K., Fernando, J., Martirena, F. and Antoni, M.: Tackling social housing through the commercial use of low clinker cementitious systems. In: Innovations on the use of calcined clay as supplementary cementitious material (2012)
5. He, C., Osbaeck, B., Makovicky, E.: Pozzolanic reactions of six principal clay minerals: activation, reactivity assessments and technological effects. Cem. Concr. Res. **25**(8), 1691–1702 (1995)
6. Kakali, G., Perraki, T., Tsivilis, S., Badogiannis, E.: Thermal treatment of kaolin: the effect of mineralogy on the pozzolanic activity. Appl. Clay Sci. **20**, 73–80 (2001)
7. Murat, M., Comel, C.: Hydration reaction and hardening of calcined clays and related minerals III. Influence of calcination process of kaolinite on mechanical strengths of hardened metakaolinite. Cem. Concr. Res. **13**(5), 631–637 (1983)
8. Souza, P.S.L., Dal Molin, D.C.C.: Viability of using calcined clays, from industrial by-products, as pozzolans of high reactivity. Cem. Concr. Res. **35**(10), 1993–1998 (2005)

Effects of Metakaolin on Nanomechanical Properties of Cement Paste

Salim Barbhuiya and PengLoy Chow

Abstract Metakaolin (MK) is a pozzolanic material, which is a dehydroxylated form of the clay mineral kaolinite. It is obtained by calcination of kaolinite clay at a temperature between 500 °C and 800 °C. In cement matrix, MK reacts with Ca $(OH)_2$, to produce calcium silicate hydrate (CSH) gel. MK also contains alumina that reacts with $Ca(OH)_2$ to produce additional alumina-containing phases, including C_4AH_{13}, C_2ASH_8 and C_3AH_6. This research aims to provide a better understanding of the effects of MK on the nanomechanical properties of the main phases present within the cement paste. Two different mixes were prepared, one control mix and the other one with 10 % MK (by cement weight). A constant water-binder ratio of 0.4 was used for both the mixes. Fraction volumes determined from nanoindentation testing show an increase in the amounts of high-density CSH at the cost of low-density CSH gel in cement pastes containing 10 % MK.

1 Introduction

In recent years the use of metakaolin (MK) in concrete has received considerable interest. MK is used as a supplementary cementitious material mainly because of its pozzolanic properties [1–4]. It is a thermally activated alumino-silicate material obtained by calcining kaolin clay within the temperature range 650–800 °C [5]. An important difference between MK and other pozzolans is that MK is a primary product, while others are either secondary products or by-products. Thus, MK can be produced with a controlled process to achieve the desired properties. The use of MK is reported to increase the strength of concrete especially during the early ages of hydration [6, 7].

S. Barbhuiya (✉) · P. Chow
Department of Civil Engineering, Curtin University,
GPO Box U1987, Perth, WA 6845, Australia
e-mail: salim.barbhuiya@curtin.edu.au

K. Scrivener and A. Favier (eds.), *Calcined Clays for Sustainable Concrete*,
RILEM Bookseries 10, DOI 10.1007/978-94-017-9939-3_57

Nanoindentation is a reliable technique to quantitatively determine the local nanomechanical properties [8]. By establishing contact between a substrate (sample) and an indenter with known properties and geometry, elastic and hardness values of the substrate can be evaluated. Due to the heterogeneity of cementitious composites, so-called "grid" indentation method, also called the statistical nanoindentation method (SNI), can be used to make the experiment more reliable [9, 10]. Extensive research is reported in the literature concerning different properties of cement paste, mortar and concrete containing MK, such as pozzolanic reaction, compressive and flexural strength and shrinkage cracking. However, limited information is available on the effect of MK on the nanomechanical properties of cement paste. Therefore, this research was conducted in order to have a better understanding of the nanomechanical properties cement paste containing using nanoindentation techniques.

2 Experimental Programme

2.1 Materials

Commercial Swan General Purpose Portland cement (Type GP) was used to cast the cement paste. The chemical composition and physical properties of cement and MK used in this study are reported in Table 1. Two different mixes were prepared, one control mix and the other one with 10 % MK (by cement weight). A constant water-binder ratio of 0.4 was used for both the mixes.

2.2 Sample Preparation

Small samples were obtained by initially cutting cement cube samples using a tile cutter into 10 × 10 × 50 mm sticks. The cement sticks were then cut using a Precision

Table 1 Chemical composition and physical properties of cement and MK used

Parameters	PC	MK
SiO_2 (%)	21.41	52.10
Al_2O_3 (%)	5.11	41.00
Fe_2O_3 (%)	2.61	4.30
CaO (%)	61.50	0.09
MgO (%)	1.78	1.36
SO_3 (%)	3.03	–
Na_2O (%)	0.33	0.01
K_2O (%)	0.61	0.62
P_2O_5 (%)	0.16	–
Loss on ignition (%)	2.58	0.50
Specific gravity	3.18	2.63
Specific surface area (m^2/kg)	352	12,000

Saw down to smaller 10 × 10 × 10 mm samples. The samples were then placed into moulds and cast into epoxy resin. Initial grinding and polishing of samples were performed using silicon carbide papers of reducing gradation 52, 35, 22 and 15 μm to expose the surface of the cement. Following the exposure of the cement surface, samples were impregnated using red-pigmented epoxy resin to provide structural support to the fragile porous cement matrix, which can otherwise be easily damaged during indentation. Once impregnated, samples were put through a final stage of grinding and polishing using reducing carbide papers of 52, 35, 22, 15 μm and diamond suspensions of reducing gradations 9, 6, 3 and 1 μm and 0.05 μm on a polishing cloth. Samples were then mounted onto sample disks, placed into samples trays and installed into the indenter ready for nanoindentation tests.

2.3 Nanoindentation

Nanoindentation, also known as instrumented or depth sensing indentation, involves the application of a controlled load to the surface of a material to induce local surface deformation. Mechanical properties such as reduced elastic modulus and hardness can be calculated using well-established equations based on elastic contact theory [11]. During the test, load and displacement are continuously monitored, resulting in a load-displacement curve, as shown in Fig. 1a. The interaction between the tip of the indenter and the specimen during the indentation process is illustrated in Fig. 1b.

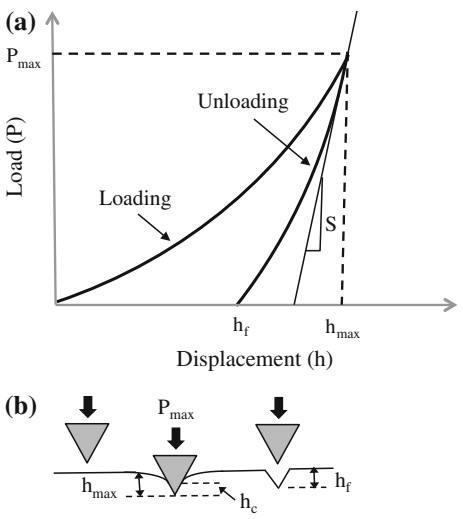

Fig. 1 Typical load-displacement curve

The contact stiffness S defined as the slope at the beginning of the unloading curve, is given by:

$$S = \frac{dP}{dh} \tag{1}$$

where P is the indentation load and h is the indentation depth for the determination of the slope. The initial portion of the unloading curve is fitted by a power law:

$$S = \frac{2\beta}{\sqrt{\pi}} \left(\frac{1}{E_r}\right)^{-1} \sqrt{A_c} \tag{2}$$

where E_r is the reduced modulus of the indentation contact, A_c is the contact area of the indenter and β is a constant for the indenter geometry. E_r is related to the elastic modulus of the sample (E) and the elastic modulus of the indenter (E_i) by the following equation:

$$\frac{1}{E_r} = \frac{1 - v^2}{E} + \frac{1 - v_i^2}{E_i} \tag{3}$$

where v is the Poisson's ratio of the test sample and v_i is the Poisson's ratio of the indenter. For the Berkovich indenter, the E_i and v_i are 1140 GPa and 0.07 respectively [12]. Consequently, the reduced elastic modulus, E_r, can be defined as:

$$E_r = \frac{\sqrt{\pi}}{2\beta} \frac{S}{\sqrt{A_c}} \tag{4}$$

If the indenter is considered to be much stiffer than the probed material, the hardness is defined by:

$$H = \frac{P_{\max}}{A_c} \tag{5}$$

where $P_{\max}$ is the peak achieved loading force.

The nanoindentation apparatus used in this study was an Agilent Nano Indenter® G200 fitted with a Berkovich indenter tip. The calibrated contact area function was derived from indentation tests conducted previously on a fused quartz standard specimen. In this study, all testing was programmed in such a way that the loading started when the indenter came into contact with the test surface and the load maintained for 30 s at the pre-specified maximum value before unloading. The unloading data for the lower indentation depth (i.e. h_p = 300–400 nm) was used to determine the reduced modulus and hardness values of the indentation point. Information on the mechanical properties was obtained from a matrix of a minimum of 320 indents on the surface for cement composite samples. The selected indent spacing was 20 μm. Grid indentation technique was used to ensure that a

representative set of data was collected for the samples. The selected method of grid indentation was 4 × 10 indents per area. On each sample this was repeated 8 times for a total of up to 320 indentation tests per sample. Each test area was selected by manual inspection using the indenters built in microscope. The experimental data (i.e. modulus and hardness values) were then statistically analysed to produce a frequency histogram.

3 Results and Discussion

The experimental frequency distributions of the indentation modulus for cement paste with and without MK are shown in Figs. 2 and 3 respectively. Figures 4 and 5 show the indentation hardness for reference cement paste with and without MK. The C-S-H and other phases present in a cement paste sample are expected to have

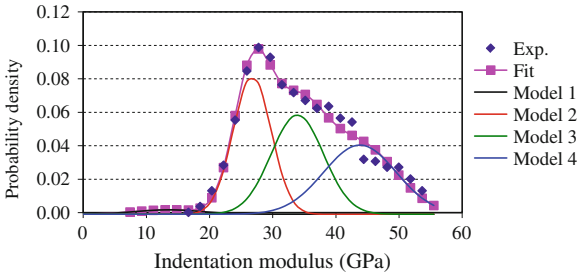

Fig. 2 Frequency plots for indentation modulus for cement paste without MK

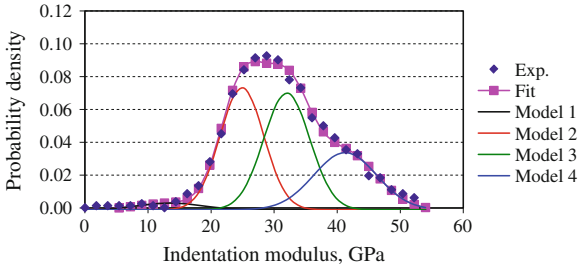

Fig. 3 Frequency plots for indentation modulus for cement paste with 10 % MK

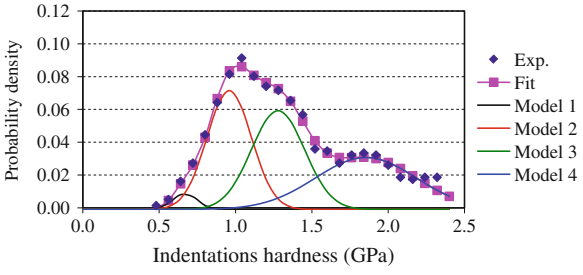

Fig. 4 Frequency plots for indentation hardness for cement paste without MK

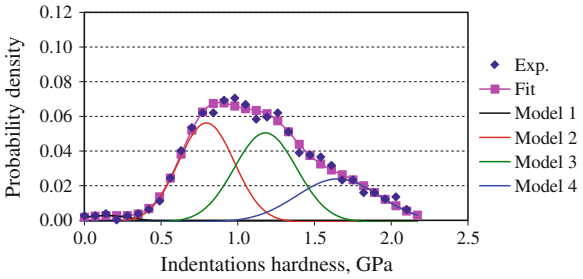

Fig. 5 Frequency plots for indentation hardness for cement paste with 10 % MK

a unique set of modulus and hardness. All the distributions in Figs. 2, 3, 4 and 5 show a similar trend. In most of the data the modulus values ranged between 10 to 50 GPa (Figs. 2 and 3), while the hardness values ranged between 0.15 to 2.30 GPa (Figs. 4 and 5). This is in agreement with the results reported by other researchers. The *E* and *H* values extracted from the model fits for the individual hydrate phases identified from these figures are summarised in Table 2.

The lowest characteristic modulus–hardness phase in Figs. 2–5 has a modulus of *E* between 13.55 GPa and 16.55 GPa and a hardness value between 0.14 and 0.67 GPa. These very low properties can be attributed to the material regions dominated by capillary pores and termed as loosely packed C-S-H or LP-CSH. The second peak in the frequency plots is attributed to a low-density C-S-H (LD-CSH) phase. The *E* values of LD-CSH obtained in this study ranges from 24.90 ± 3.46 GPa to 26.75 ± 3.00, while H values ranges from 0.80 ± 0.18 GPa to 0.96 ± 0.15 GPa. These values are slightly higher than the reported values by other researchers (E = 18.2 ± 4.2 GPa, H = 0.45 ± 0.14 GPa by Constantinides and Ulm [13],

Table 2 *E* and *H* values extracted from model fits for the individual hydrate phase

Mix	Phases identified	*E* (GPa) (Mean ± SD)	*H* (GPa) (Mean ± SD)	Volume fraction (%)
Cement paste without MK	LP-CSH (Model 1)	13.55 ± 5.31	0.67 ± 0.08	1.9
	LD-CSH (Model 2)	26.75 ± 3.00	0.96 ± 0.15	33.2
	HD-CSH (Model 3)	33.90 ± 4.15	1.28 ± 0.17	33.0
	CH (Model 4)	43.80 ± 5.76	1.85 ± 0.33	31.9
Cement paste with 10 % MK	LP-CSH (Model 1)	13.50 ± 5.00	0.14 ± 0.18	2.8
	LD-CSH (Model 2)	24.90 ± 3.46	0.80 ± 0.18	36.3
	HD-CSH (Model 3)	32.01 ± 3.64	1.18 ± 0.20	36.5
	CH (Model 4)	41.22 ± 4.98	1.65 ± 0.27	24.4

E = 20.0 ± 2.0 GPa, H = 0.80 ± 0.2 GPa by Acker [14], E = 2.34 ± 3.4 GPa and H = 0.73 ± 0.15 GPa by Zhu et al. [15]. The third peak in the frequency plots is attributed to a high density C-S-H (HD-CSH) phase.

The values of E for HD-CSH in this study ranges from 32.01 ± 3.64 GPa to 33.90 ± 4.15 GPa, which are in excellent agreement with the E values reported by Constantinides and Ulm [13] (29.1 ± 4.0 GPa), Acker [14] (31.0 ± 4.0 GPa) and Zhu et al. [15] (31.4 ± 2.1 GPa). The H for HD-CSH (1.18 ± 0.2 GPa to 1.28 ± 0.17 GPa) is slightly higher than the values reported by Constantinides and Ulm [13] (0.83 ± 0.18 GPa) and Acker [14] (0.90 ± 0.3 GPa). However, this matches well with the values reported by Zhu et al. [15] (1.27 ± 0.18 GPa). The fourth peak in the frequency plots is attributed to the portlandite crystals dispersed in the cement paste matrix. Previous reported indentation properties for portlandite are E = 40.3 ± 4.2 GPa, H = 1.31 ± 0.23 GPa [16] and E = 36 ± 3 GPa, H = 1.35 ± 0.5 GPa [14], which are in excellent agreement with the values obtained in this study (E = 41.27 ± 4.98 GPa to 43.80 ± 5.76 GPa, H = 1.65 ± 0.27 GPa to 1.85 ± 0.33 GPa).

4 Conclusions

There was a reduction in the volume fraction of $Ca(OH)_2$ in samples containing metakaolin. The volume fraction of $Ca(OH)_2$ in sample without metakaolin was 31.9 %, whereas in samples containing 10 % metakaolin it was 24.4 %. Metakaolin does not change the average values of the hardness and modulus of elasticity of any of the phases of C-S-H gel. However, it modifies their relative proportions. The use of 10 % metakaolin in cement paste was found to modify the relative proportions of the two phases of C-S-H gel, promoting the formation of LD-CSH and HD-CSH.

References

1. Wild, S., Khatib, J.M., Jones, A.: Relative strength, pozzolanic activity and hydration in superplasticised metakaolin concrete. Cem. Concr. Res. **26**(10), 1537–1544 (1996)
2. Coleman, N.J., Page, C.L.: Aspects of the pore solution chemistry of hydrated cement pastes containing MK. Cem. Concr. Res. **27**(1), 147–154 (1997)
3. Frias, M., Cabrera, J.: Pore size distribution and degree of hydration of metakaolin-cement pastes. Cem. Concr. Res. **30**(40), 561–569 (2000)
4. Asbridge, A.S., Page, C.L., Page, M.M.: Effects of metakaolin, water/binder ratio and interfacial zones on the micro hardness of cement mortars. Cem. Concr. Res. **32**(9), 1365–1369 (2002)
5. Sabir, B.B., Wild, S., Bai, J.: Metakaolin and calcined clay as pozzolans for concrete: a review. Cem. Concr. Comp. **16**(1), 441–454 (2001)
6. Zhang, M.H., Malhotra, V.M.: Characteristics of a thermally activated alumino-silicate pozzolanic material and its use in concrete. Cem. Concr. Res. **25**, 1713–1725 (1995)
7. Curcio, F., DeAngelis, B.A., Pagliolico, S.: Metakaolin as a pozzolanic microfiler for high-performance mortars. Cem. Concr. Res. **28**(6), 803–809 (1996)

8. Mondal, P., Shah, S.P., Marks, L.D.: A reliable technique to determine the local mechanical properties at the nano-scale for cementitious materials. Cem. Concr. Res. **37**(2), 1440–1444 (2007)
9. Sorelli, L., Constantinides, G., Ulm, F.J., Toutlemonde, F.: The nano-mechanical signature of ultra high performance concrete by statistical nanoindentation techniques. Cem. Concr. Res. **38**(12), 1447–1456 (2008)
10. Vandamme, M., Ulm, F.J., Fonollosa, P.: Nanogranular packing of C-S-H at substochiometric conditions. Cem. Concr. Res. **40**(1), 14–26 (2010)
11. Fischer-Cripps, A.C.: Critical review of analysis and interpretation of nanoindentation test data. Surf Coat. Technol. **200**(14-15), 4153–4165 (2006)
12. Shokrieh, M.M., Hosseinkhani, M.R., Naimi-Jamal, M.R., Tourani, H.: Nanoindentation and nanoscratch investigations on graphene-based nanocomposites. Polym. Test. **32**, 45–51 (2013)
13. Constantinides, G., Ulm, F.-J.: The nanogranular nature of C-S-H. J. Mech. Phys. Solids **55** (1), 64–90 (2007)
14. Acker, P.: Micromechanical analysis of creep and shrinkage mechanisms. In: Ulm, F.J., Bazant, Z.P., Wittmann, F.H. (eds.) Creep, shrinkage and durability mechanics of concrete and other quasi-brittle materials. Elsevier, Cambridge (2001)
15. Zhu, W., Huges, J.J., Bicanic, N., Pearce, C.J.: Nanoindentation mapping of mechanical properties of cement paste and natural rocks. Mater. Charact. **58**, 1189–1198 (2007)
16. Constantinides, G., Ulm, F.-J.: The effect of two types of C-S-H on the elasticity of cement-based materials: results from nanoindentation and micromechanical modelling. Cem Concr Res **34**(1), 67–80 (2004)

Meta-Kaolin for High Performance Concrete

Sui Tongbo, Wang Bin, Zhang Lijun and Cheng Zhifeng

Abstract Natural Kaolinite was calcined under different temperatures and the reactivity, performance and hydration of the resultant meta-kaolin when added into Portland cement were evaluated as a comparison with silica fume addition into Portland cement. Both of the comparison results of cement and concrete indicate that both meta-kaolin calcined at suitable temperature and silica fume almost exhibit the same performance in terms of workability, strength development and durability and that it is technically feasible to use meta-kaolin as replacement of silica fume.

Keywords Meta-kaolin · Silica fume · Cement and concrete performance

1 Introduction

Concrete is the most extensively used construction material in the world. It is only second to water as the most heavily consumed substance [1]. The majority of the binding materials used in concrete are based on Portland cement clinker produced through an energy-intensive process. In addition, the process produces a large amount of greenhouse gas emissions, mostly CO_2 due to the decomposition of calcium carbonate and the sintering of clinker. In order to reduce energy consumption, CO_2 emission and increase production while reducing the cost, supplementary cementitious materials (SCM) and blending materials such as meta-kaolin (MK), silica fume (SF), natural pozzolan, fly ash and limestone etc. have been increasingly used as clinker replacement for cement production and as cement replacement for concrete production.

Considering the situation of the local unavailability and depleting of high quality SCMs, meta-kaolin in recent years has been intensively studied for these purposes

S. Tongbo (✉) · W. Bin · Z. Lijun · C. Zhifeng
Sinoma Research Institute, Sinoma International Engineering Co. Ltd,
Chaoyang District, Beijing 100102, People's Republic of China
e-mail: suitongbo@sinoma.com.cn

K. Scrivener and A. Favier (eds.), *Calcined Clays for Sustainable Concrete*,
RILEM Bookseries 10, DOI 10.1007/978-94-017-9939-3_58

because of its high pozzolanic properties [2–5]. Unlike other pozzolans, it is a primary product, not a secondary product, which is formed by the dehydroxylation of kaolin upon heating in the temperature range of 700–800 °C [6, 7]. Metakaolin when reacting with $Ca(OH)_2$, produces C-S-H gel and alumina containing phases, including C_4AH_{13},C_2ASH_8, and C_3AH_6 [8, 9]. Extensive research is reported in the literature concerning different properties of MK-containing paste and concrete, particularly high-strength, high-performance concrete with improved durability, such as porosity, pore size distribution, pozzolanic reaction, compressive strength and durability [3, 10, 11].

Brooks and Johari reported that compressive strength increased with the increase in the metakaolin content [12]. Similar results were also reported by Li and Ding where concrete achieved the highest compressive strength with 10 % MK content [13].

The incorporation of metakaolin in concrete led to significant increase of resistance to chloride penetration. Gruber et al. reported that the use of 8 % and 12 % high-reactivity metakaolin (HRM) significantly lowered the chloride ion diffusion coefficient of concrete [14]. Parande et al. deduced that up to 15 % replacement with metakaolin in ordinary Portland cement showed good corrosion resistance property, water absorption and resistivity in concrete [15].

China has abundant kaolin mines in multiple regions. This study tried to use different types of clay to develop MK calcined under varying temperatures as high quality SCMs by investigating the performance and reaction mechanism of mortar and concrete mixtures containing such MK. Comparison tests were made to compare MK with market-available silica fume (SF) in terms of mortar and concrete workability, compressive strength, corrosion resistance, and dry shrinkage compared with SF.

2 Experimental Program

2.1 Materials

Ordinary Portland cement and silica fume were used for all of the mortar and concrete mixtures. Chemical and physical characteristics of them are shown in Tables 1 and 2, respectively. The 6 kinds of kaolin used in this investigation were delivered from 3 provinces of China and the chemical composition was presented in Table 3.

Table 1 Chemical composition of PC and SF

	Chemical analysis (%)						
	SiO_2	Al_2O_3	Fe_2O_3	CaO	MgO	SO_3	LOI
Cement	23.03	5.11	3.34	63.33	2.06	2.33	1.21
SF	92.80	2.04	0.52	0.45	0.58	/	2.01

Table 2 Physical performance of cement

	Blaine (m^2/kg)	Setting time (h:min)		Bending/compressive strength (MPa)		
		Initial	Final	3d	7d	28d
Cement	355	2:23	3:14	4.6/28.4	6.6/43.1	8.3/61.6

Table 3 Chemical composition of kaolin

No.	Chemical analysis (%)						
	SiO_2	Al_2O_3	Fe_2O_3	CaO	MgO	SO_3	LOI
A	47.29	36.34	0.85	0.10	0.49	0.83	13.56
B	51.96	30.14	2.37	0.25	0.52	4.46	13.58
C	41.78	38.79	1.99	0.72	0.90	0.71	14.18
D	39.18	26.51	5.13	1.08	0.26	0.92	18.16
E	47.16	34.50	1.06	0.24	0.56	0.93	14.28
F	57.38	24.40	1.67	0.84	0.47	0.79	13.21

2.2 Test Methods

2.2.1 Mortar

Compressive and flexural strength Three prismatic specimens with dimensions of 40 × 40 × 160 mm were made by molding and standard curing, with w/cm ratios of 0.44 and sand/cm ratios of 2.5. Bending strength and compression were measured after 3, 7 and 28 days (according to Chinese standard GB 177).

Corrosion resistance: Mortar prisms of dimensions 40 × 40 × 160 mm were cast in metallic moulds and demoulded after 24 h. 9 prisms were made for one mix, while one third were curing in clean water, one third in 3 % Na_2SO_4 solution and the other 3 in 5 % $MgCl_2$ solution. The curing of specimens lasted for 28 days in a controlled temperature of 20 ± 2 °C and then the flexural strength were tested.

Dry shrinkage: The drying shrinkage for each specimen was measured using three 25 × 25 × 280 mm prisms as ASTM C 596 procedure.

2.2.2 Concrete

Natural sand and 25 mm maximum size stone were used as fine and coarse aggregates, respectively. The coarse and fine aggregates each had a specific gravity of 2.65 and 2.70. The calcium lignosulphonate (CLS) and polynaphthalene sulphonate (UNF-5) as water reducer were used to adjust the flowability of the mixtures. The compressive strength was tested according to the Chinese standard GBJ 81 on the three 150 × 150 × 150 mm specimens with a 2000 kN hydraulic testing device.

3 Results and Discussions

3.1 Reaction Mechanism

3.1.1 Calcination Temperature

Hydration reaction of MK depends upon the level of reactivity, which in turn depends upon the thermal and physical reaction process. Chinese kaolin-A was thermally treated in lab furnace at different temperature for 2 h and then cooled down in air to produce metakaolin. The burning temperature and physical performance of cement mixtures with 10 % MK used as SCM are given in Table 4. It shows that thermal activation has an important influence on the reactivity of MK and 10 % replacement in cement can increase mortar strength effectively from 61.6 MPa to 82.9 MPa. The best burning temperature as can be seen is between 700 and 800 °C.

3.1.2 Calcination Time

Suitable during temperature and duration of calcination by dehydroxylation leads to the breaking down or partial break down of the structure and the formation of a transition phase with high reactivity. As can be seen in Table 5, the suitable burning time at the same temperature of 750 °C for MK-A has been proved by compressive strength test to be no longer than 2 h. Further extending the burning time does not make any better result in terms of technical performance and economical cost.

3.1.3 Types of MK

Three kinds of Kaolinite with different content of the sum of SiO_2 and Al_2O_3 were tested as the same experiment as above (750 °C, 2 h). As expected from the result in

Table 4 Compressive strength of cement with MK-A from different calcination temperature

No.	Calcination temperature (°C)	Compressive Strength (MPa)		
		3d	7d	28d
Control	/	28.4	43.1	61.6
A1	650	30.4	45.8	75.2
A2	700	31.5	46.4	79.3
A3	750	32.4	48.8	82.9
A4	800	33.0	51.0	79.0
A5	850	30.9	47.8	76.3
A6	900	32.9	46.8	76.1
A7	950	30.3	45.8	73.2

Table 5 Compressive strength of cement with MK-A from different calcination time

No.	calcination temperature (°C)	Calcination time (h)	Compressive strength (MPa)		
			3d	7d	28d
Control	/		28.4	43.1	61.6
A31	750	2	30.4	47.8	82.9
A32	750	4	32.0	47.8	78.3
A33	750	6	31.6	47.3	76.7

10 % of cement replacement with MK-A

Table 6 Compressive strength of cement with MK of different chemical composition

No.	SiO_2 (%)	Al_2O_3 (%)	$SiO_2 + Al_2O_3$ (%)	Compressive strength (MPa)		
				3d	7d	28d
Control	/			28.4	43.1	61.6
A	47.29	36.34	83.63	30.4	47.8	82.9
C	41.78	38.79	80.57	30.9	47.8	77.9
D	39.18	26.51	65.69	29.1	43.7	68.9

10 % of cement replacement with MK

Table 6, the 28-day compressive strength for MK-containing mortars is higher than control sample. It can also be found that the strength seems to be higher with the sum of SiO_2 and Al_2O_3 increases. MK sample A therefore has the highest reactivity compared with others and was adopted to conduct the performance evaluation test compared with silica fume.

3.2 Cement Performance with MK Replacement

3.2.1 Physical Performance

Physical performance of different dosage of MK and SF replacement in cement were shown in Table 7. For mortar compressive strength, replacement of cement by MK up to 15 % dosage increases the compressive strength during the 3 days and 28 days. This is the same as with SF. Moreover, MK has a better impact on the strength of 28 days with 15 % of dosage. Both MK and SF have a similar effect on water demand, flow, and setting time, i.e., the increase of replacement dosage leads to an increase in water demand and a decrease in both the setting time and mortar flow. The suitable dosage of MK replacement in cement is between 10 and 15 %.

Table 7 Physical property of cement with addition of MK and SF

No.	Dosage (%)	Water demand (%)	Setting time (h: min)		Mortar flow (mm)	Compressive strength (MPa)		
			Initial	Final		3d	7d	28d
Control	0	26.7	4:05	6:24	144	28.4	43.1	61.6
MK-1	5	28.0	3:55	5:29	136	29.4	45.7	70.1
MK-2	10	30.0	3:01	4:37	128	30.1	45.3	71.2
MK-3	15	32.0	2:40	4:19	122	29.8	46.4	76.0
MK-4	20	34.0	1:38	3:13	113	30.5	49.2	72.8
SF-1	5	26.0	3:42	5:17	135	31.4	48.0	71.1
SF-2	10	27.5	3:10	4:41	119	33.4	47.2	72.5
SF-3	15	29.0	2:42	4:01	115	31.8	44.8	70.2
SF-4	20	35.0	1:45	3:19	107	29.3	39.7	61.6

3.2.2 Corrosion Resistance

The effect of meta-kaolin on the resistivity of sodium sulfate and magnesium chloride corrosion of Portland cement mortars was also studied. 15 % metakaolin was used as partial replacement for Portland cement (Table 8). Results showed that the residual bending strength of PC + MK is evidently higher than control PC, which indicates that meta-kaolin can better increase the chemical resistance of such mortars.

3.2.3 Dry Shrinkage

Dry shrinkage results for mortar mixtures containing 0, 5, 10, and to 15 % of MK were summarized in Table 9. In one aspect, water/cement ratio has to be increased

Table 8 Performance of corrosion resistance of MK cement

No.	28d (Flexural, MPa/%)		
	Water	3 % Na_2SO_4	5 % $MgCl_2$
PC	11.8/100	10.8/92	9.0/76
PC + 15 %MK	12.9/100	13.9/108	12.0/93

10 × 10 × 40 mm prismatic specimen

Table 9 Dry shrinkage of MK + PC of different dosage

No.	W/C	Dosage (%)	Flow (mm)	Dry shrinkage (%)				
				7 d	14 d	28 d	2 m	3 m
Ds1	0.44	0	139	0.006	0.049	0.085	0.090	0.092
Ds2	0.45	5	139	0.008	0.052	0.089	0.093	0.104
Ds3	0.46	10	139	0.007	0.061	0.095	0.096	0.114
Ds4	0.47	15	138	0.006	0.059	0.091	0.101	0.110

with the increase of MK dosage as a result to control the same mortar flow rate. Slight increase in the dry shrinkage of MK containing mortars was also found.

3.3 Concrete Performance of MK Replacement of Cement Compared with SF

3.3.1 Workability of Fresh Pastes with MK and SF

Two kinds of water reducers, CLS and UNF-5 were used to adjust the flowability of fresh pastes containing different percentages of MK and SF. The mixture workability is presented in Table 10. As seen from the table, the addition of MK or SF increases demand for water, that therefore results in a decrease in flow spread at the same w/cm ratios. However, the spread of fresh pastes with the addition of MK appears to have higher flowability that with SF at the same dosage respectively, regardless of CLS and UNF-5.

3.3.2 Workability of Concrete with MK and SF

Initial and after 90 min slump for each of the concrete mixtures are summarized in Table 11. MK concrete demonstrates a similar decrease of slump with SF concrete when comparing with the control as well as when increasing the percentages of replacement. Considerably better workability was found for MK concrete both at initial and after 90 min than SF concrete at the same cement replacement.

3.3.3 Performance Comparison of Concrete with Addition of MK and SF

The results of the compressive strength tests are shown in Table 12 and Fig. 1, where each value is the average of three measurements. It can be seen that both MK

Table 10 Fresh pastes spread with MK-PC and SF-PC

WR		CLS	UNF-5
WR dosage (%)		0.20	0.70
W/C		0.35	0.29
Spread (mm)	0	202	240
	5 %MK	197	237
	5 %SF	189	233
	10 %MK	181	234
	10 %SF	174	225
	15 %MK	161	215
	15 %SF	151	206

Table 11 Concrete workability with MK or SF as admixtures

Addictive		Cem. + SCMs	W/C	SP		Initial slump (cm)	Slump after 90 min (cm)
No.	Dosage (%)	(kg/m^3)		Type	Dosage (%)		
Control	0	385	0.42	UNF-5	1	22.3	18.6
MK-1	5	385	0.42	UNF-5	1	21.6	16.7
MK-2	10	385	0.42	UNF-5	1	20.0	15.1
MK-3	15	385	0.42	UNF-5	1	16.9	8.0
SF-1	5	385	0.42	UNF-5	1	21.2	16.0
SF-2	10	385	0.42	UNF-5	1	19.4	14.1
SF-3	15	385	0.42	UNF-5	1	15.1	5.5

Table 12 Performance comparison of concrete with addition of MK and SF

No.	Mixture	Dosage (%)	W/C	Slump (cm)	Compressive (MPa)		
					3 d	7 d	28 d
Control	1:1.90:2.84	0	0.42	21	39.6	52.3	63.5
MK-1	1:1.90:2.84	5	0.42	22	40.4	58.2	69.3
MK-2	1:1.90:2.84	10	0.42	22	38.9	56.7	69.9
MK-3	1:1.90:2.84	15	0.43	18	37.8	53.9	70.9
SF-1	1:1.90:2.84	5	0.41	22	40.3	56.0	71.9
SF-2	1:1.90:2.84	10	0.41	21	39.2	53.3	71.2
SF-3	1:1.90:2.84	15	0.42	16	36.3	52.2	67.6

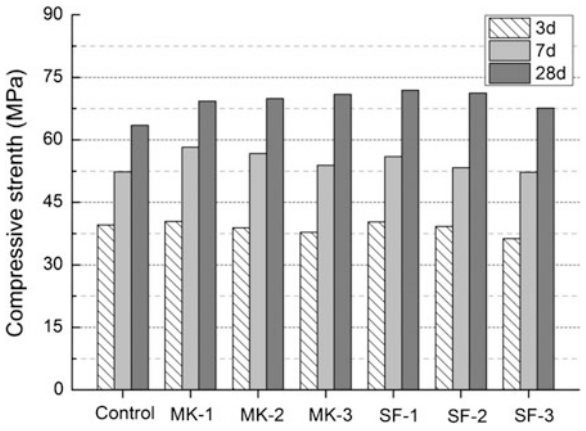

Fig. 1 Compressive strength of concrete with addition of MK and SF

and SF perform almost the same in terms of strength development of concrete. Both mixtures containing 5 % to 15 % MK and SF had higher compressive strengths than the control at tested ages of 7 and 28 days and the same level of 3-day strength at

Table 13 Performance comparison of concrete with addition of MK and SF combined with PFA

No.	W/(Cem + SCMs)	Cement (kg/m^3)	Addictive and dosage (kg/m^3)			Water (kg/m^3)	SP (C × %)	Slump (cm)	Compressive (MPa)			
			Pfa-I	MK	SF				3 d	7 d	28 d	90 d
MKP-1	0.32	360	130	25	–	165	1.0	23.0	55.4	60.1	72.1	90.2
MKP-2	0.30	376	134	27	–	160	1.1	22.5	59.3	63.2	76.0	93.9
MKP-3	0.28	385	137	28	–	155	1.2	23.0	62.5	67.9	83.3	97.1
MKP-4	0.26	393	142	28	–	145	1.4	23.5	66.8	72.5	93.7	101.1
MKP-5	0.24	406	145	30	–	140	1.5	21.5	72.1	76.3	96.7	107.2
SFP-1	0.32	360	130	–	25	165	1.0	22.5	57.1	61.0	72.4	90.7
SFP-2	0.30	376	134	–	27	160	1.1	23.0	60.7	64.1	77.1	94.1
SFP-3	0.28	385	137	–	28	155	1.2	23.0	63.1	69.1	83.9	98.0
SFP-4	0.26	393	142	–	28	145	1.4	23.5	65.1	74.1	94.3	101.3
SFP-5	0.24	406	145	–	30	140	1.5	21.5	72.4	77.1	96.8	111.3

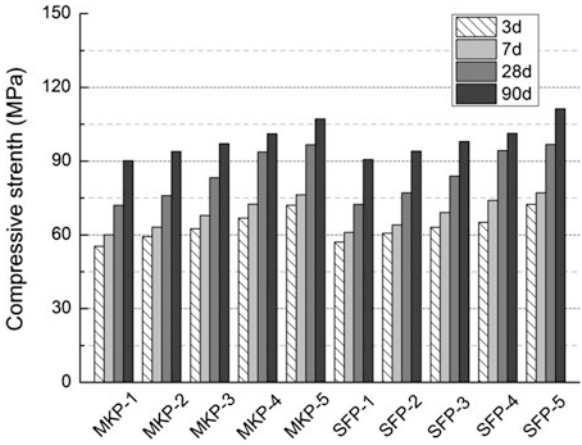

Fig. 2 Compressive strength of concrete with addition of MK and SF combined with PFA

lower dosage of 5–10 %. While mixtures with addition of 15 % of MK and SF had lower 3-day strength mainly due to the increase of water demands in maintaining the same level of workability of concrete.

3.3.4 Performance of Concrete with Addition of MK and SF Combined with PFA

To compensate the slump decrease with the addition of MK and SF in concrete, PFA was combined with MK and SF. The performance of concrete specimens with varying dosage of MK and SF combined with PFA are shown in Table 13. High workability of the fresh concrete mixtures can be obtained with the combination with PFA and superplasticizer. Figure 2 shows the strength development of the various concrete mixes with ages. Each data set for compressive strength at 3, 7, 28, and 90 days is also the average of three test results as above. Again it can be seen that both MK and SF-contacting concrete mixtures had almost the same strength at corresponding ages, which indicates the technical feasibility of substituting SF with MK.

4 Conclusions

1. The reactivity of MK results mainly from the chemical composition (mostly $A1_2O_3$ and SiO_2) and calcination temperature. The higher content of $A1_2O_3$ + SiO_2 in MK seems to be more reactive, and the optimal calcination temperature ranges from 700 °C to 800 °C.
2. MK shows high reactivity and can not only remarkably improve the strength of cement and concrete, but also enhance the chemical resistance performance. The optimum replacement of cement with MK is 10 % considering both the workability and strength development.

3. MK and SF-contacting concrete mixtures had almost the same strength development under the same replacement dosage at corresponding ages, which indicates the technical feasibility of substituting SF with MK.

References

1. Sabir, B.B., Wild, S., Bai, J.: Metakaolin and calcined clays as Pozzolans for concrete: a review. Cem. Concr. Compos. **23**(6), 441–454 (2001)
2. Wild, S., Khabit, J.M., Jones, A.: Relative strength pozzolanic activity and cement hydration in uperplasticised metakaolin concrete. Cem. Concr. Res. **26**(10), 1537–1544 (1996)
3. Coleman, N.J., Page, C.L.: Aspects of the pore solution chemistry of hydrated cement pastes containing MK. Cem. Concr. Res. **27**(1), 147–154 (1997)
4. Frias, M., Cabrera, J.: Pore size distribution and degree of hydration of metakaolin–cement pastes. Cem. Concr. Res. **30**(4), 561–569 (2000)
5. Asbridge, A.H., Page, C.L., Page, M.M.: Effects of metakaolin, water/binder ratio and interfacial transition zones on the microhardness of cement mortars. Cem. Concr. Res. **32**(9), 1365–1369 (2002)
6. Klimesch, D.S., Ray, A.: Use of the second-derivative differential thermal curve in the evaluation of cement–quartz pastes with metakaolin addition autoclaved at 180 °C. Thermochim. Acta **307**(2), 167–176 (1997)
7. Klimesch, D.S., Ray, A.: Autoclaved cement–quartz pastes with metakaolin additions. Adv. Cem. Based Mater. **7**(3), 109–118 (1998)
8. Changling, H., Osbaeck, B., Makovicky, E.: Pozzolanic reaction of six principal clay minerals: activation reactivity assessments and technological effects. Cem. Concr. Res. **25**(8), 1691–1702 (1995)
9. Zhang, M.H., Malhotra, V.M.: Characteristics of a thermally activated aluminosilicate pozzolanic material and its use in concrete. Cem. Concr. Res. **25**(8), 1713–1725 (1995)
10. Khatib, J.M., Wild, S.: Pore size distribution of metakaolin paste. Cem. Concr. Res. **26**, 1545–1553 (1996)
11. Curcio, F., DeAngelis, B.A.: Dilatant behavior of superplasticized cement pastes containing metakaolin. Cem. Concr. Res. **28**(5), 629–634 (1998)
12. Brooks, J.J., Johari, M.M.A.: Effect of metakaolin on creep and shrinkage of concrete. Cem. Concr. Compos. **23**(6), 495–502 (2001)
13. Li, Z., Ding, Z.: Property improvement of Portland cement by incorporating with metakaolin and slag. Cem. Concr. Res. **33**(40), 579–584 (2003)
14. Gruber, K.A., Ramlochan, T., Boddy, A., Hooton, R.D., Thomas, M.D.A.: Increasing concrete durability with high-reactivity metakaolin. Cem. Concr. Compos. **23**(6), 479–484 (2001)
15. Parande, A.K., Ramesh Babu, B., Karthik, M.A., Kumaar, K.K., Palaniswamy, N.: Study on strength and corrosion performance for steel embedded in metakaolin blended concrete/mortar. Constr. Build. Mater. **22**(3), 127–134 (2008)

Clay Activation and Color Modification in Reducing Calcination Process: Development in Lab and Industrial Scale

Fabiano F. Chotoli, Valdecir A. Quarcioni, Sérgio S. Lima, Joaquim C. Ferreira and Guilherme M. Ferreira

Abstract Calcined clays have been used in pozzolanic portland cement manufacturing in Brazil for many years. However, their color imposes commercial limitation when cements show reddish or pinkish hues. This work presents two case studies consisting of reducing process calcination of two clays by reducing process in: electric static furnace to obtain maximum temperature (700–1000 °C) and burning time (5–20 min) conditions, as a function of color and pozzolanic reactivity, and; rotary kiln for both laboratorial and industrial scales. Chemical (XRF, TGA/DTA), mineralogical (XRD), physical-mechanical (compressive strength), pozzolanic reactivity (Chapelle´s method and Strength Activity Index) and color test (colorimeter spectrometer using CIE color system standard) were applied in clays and pozzolanic cements characterization. Results show satisfactory performance of grayish pozzolanic cements, and indicate an alternative process to obtain calcined clays according to cements specifications.

1 Introduction

Clay calcination can modify its properties and favor its application as pozzolanic material, depending on the chemical and mineralogical composition. As example, there are kaolinite and illite clays that produce metakaolinite and other metastable structures when calcined between 600 °C and 1000 °C.

However, the application of reddish and pinkish clays is not well accepted due to non-conventional Portland cement color. In Brazilian construction materials retail

F.F. Chotoli · V.A. Quarcioni (✉) · S.S. Lima
Instituto de Pesquisas Tecnológicas Do Estado de São Paulo (IPT) - Laboratório de Materiais de Construção Civil, São Paulo, Brazil
e-mail: quarciva@ipt.br

F.F. Chotoli
e-mail: fchotoli@ipt.br

J.C. Ferreira · G.M. Ferreira
Dynamis Mecânica Aplicada, São Paulo, Brazil

K. Scrivener and A. Favier (eds.), *Calcined Clays for Sustainable Concrete*, RILEM Bookseries 10, DOI 10.1007/978-94-017-9939-3_59

market, reddish and pinkish cements are misjudged as low quality cement. Due to this misjudgment, changes in clay color can be an alternative to allow its application in cement industry.

Color hue variations in clays are a result of inorganic impurities due to changes in oxidation state of chemical elements as iron, titanium and manganese commonly present in clay minerals, which can directly affect their color properties [1, 2]. Iron impurities researches in kaolin showed that it can be present as "structural iron" (part of kaolinite structure or accessory minerals), and "free iron" as oxides, hydroxides, carbonates, sulfides and others. Researchers [3] described three possible forms of Fe^{2+} occurrence in clay minerals: structural iron, complexed iron, as hydroxyl groups, on the surface and associated iron by ionic changes at siloxane basal surfaces. Iron position within clay mineral structure is very important and can define reactivity. Other researches [4] associate directly the titanium and iron oxides content to colorimetric parameters and chromaticity of red, and correlates a* and b* CIE parameters to free and structural iron content in clay. Thereby, iron in "structural" form associated to titanium has a more deleterious (reddish) effect in color properties.

To attend the purpose of work, clays were calcined in laboratory, pilot and industrial scales, under reducing conditions, aiming at both color change from reddish/pinkish to grayish and increase of pozzolanic reactivity. The clays samples were analyzed in order to verify color, chemical, mineralogical and physical-mechanical characteristics, according to technical and normative specifications.

2 Experimental Study

2.1 Materials

Two clays, petroleum coke and Ordinary Portland Cements (analogous to Cement I in EN 197-1:2000) were used in this study. Clays were dried in stove at 105 °C and after were grinded in a disks mill to 0.150 mm. The coke was grinded in a disks mill and sieved to obtain material between 0.850 mm and 0.300 mm.

2.2 Static Furnace Calcination, Laboratorial Scale (Clays 1 and 2)

Two mixes of clays containing 10 % addition of coke were prepared and homogenized manually (20 g). Portions of these mixture were calcined in electric static furnace, in a covered platinum crucible for 20 min, at different temperatures (700 °C to 1000 °C), to obtain ideal temperature through pozzolanic activity by Chapelle's method. Based on these pozzolanic activity results, clay and coke mix were calcined for 5, 10, 15 and 20 min. All samples were removed from the static

furnace and air cooled quickly to avoid excessive oxidation. The grayish color hue was the criteria for selecting the best conditions for pilot and industrial calcinations, regardless Chapelle's results.

2.3 Pilot Scale Rotary Kiln Calcination, Laboratorial Scale (Clay 1)

Mix of clays containing 30 % addition of coke were prepared and homogenized in a rotary shaker (30 rpm) for 1 h. An electric rotative pilot scale rotary kiln [5] was required in order to produce enough clay to compressive strength tests. Calcined clay and residual coke were separated through a 0.180 mm sieve. After calcined clay-coke separation, magnetic fraction was removed from calcined clay employing a magnet. The fractions obtained were weighed in order to calculate their percentages. Non-magnetic calcined clay was ground in ball mill to 0.075 mm and reserved to tests.

2.4 Calcination in Countercurrent Rotary Kiln, Industrial Scale (Clay 2)

The industrial tests were carried out in a plant designed by Dynamis in 2009 to produce calcined clay for Cimento Planalto (CIPLAN), located at the Federal District in Brazil. The pozzolan activation line has a countercurrent rotary kiln of Ø3.0 m × L = 52 m with a nominal production capacity of 600 metric tons per day. The raw material was loaded into a hopper and fed at the kiln gas outlet through a belt conveyor. The calcined clay was cooled by a rotary cooler (that also preheats the combustion air) and the de-dusting was done by high efficiency cyclones and a bag-house filter. The combustion system burns 100 % grinded petroleum coke.

During the tests, the clay feeding rate of the kiln was 25.870 kg/h, the reduction agent (petroleum coke) feeding rate was 800 kg/h and the combustion system was supplied with 1.610 kg/h of pulverized petcoke. The kiln speed drive was set to 2 rpm and the exhaust gas had a temperature of 122 °C. The raw feed had a moisture of 20.2 % and a LOI of 10.35 %.

2.5 Methods Characterization

X-ray diffraction (XRD) was applied for mineralogical composition analysis. Samples were manually pressed into a 27 mm diameter sample holder and performed in a Rigaku Windmax 1000 X-Ray powder Diffractometer, in a rotating

sample stage, employing CuKα radiation, 40 kV, 20 mA, step size of 0,02° 2θ, time per step of 2 s, 1° divergence slit. The minerals identification and phases quantification by Rietveld method was performed in X-Pert HighScore version 3.0d(3.0.4) and based on standard diffraction data provided by ICDD (International Center For Diffraction Data). The chemical composition was characterized by X-Ray Fluorescence (XRF) using a Panalytical Minipal Cement and fused beads were produced in Claisse M4 fusion machine. A TA Instruments TGA/DSC SDT 2960 was used for thermogravimetric measurements, with a heating rate of 10 °C/min from room temperature to 1000 °C. A argon flux was used in the heating chamber. The color parameters "L *", "a *" and "b *" were measured using a spectrocolorimeter model "Color Guide Sphere d/8" spin, manufactured by Byk Gardner, with standard observer D65 and opening angle 10. The measurements were investigated according international agreements colors CIELAB-CIE [6].

Two mixes of non-magnetic calcined clays and cement type I were used to produce CEM II/B-P for compressive strength tests according Brazilian Standard NBR 11578:1997 (analogous to European Standards EN 197-1:2000 and EN 196-1: 2005).

According AFNOR Standard NF P 18-513, Chapelle's method is an accelerated method for direct determination of the lime consumption by the pozzolan. In this test, a mixture of 2 g of CaO and 1 g of pozzolan was placed in a plastic Erlenmeyer with 250 ml of boiled deionized water, and set in a bath at 90 ºC during 16 h. The fixed or consumed lime by pozzolan is calculated by the difference between the added and the free lime in suspension, valued by basic-acid titration.

2.6 Results and Discussion

The results obtained from XRF (Table 1) and XRD (Table 2) show presence of typical compounds on natural clays such as kaolinite and illite. The presence of those minerals were confirmed by thermal analysis where kaolinite exhibited endothermic peak at 450 °C–600 °C due to the dehydration effect, followed by an exothermic peak associated with nucleation of mullite, while illites exhibit endothermic effects at 100–200 °C, 500–650 °C, and around 900 °C, and an exothermic peak immediately following the third endothermic peak. Hematite and goethite contributes to reddish (for Clay 1) and pinkish (for Clay 2) clay's color when calcined in oxidant atmosphere. XRD pattern of calcined clays (with coke; 950 °C; 20 min) showed occurrence of kaolinite decomposition and probable formation of metakaolin as non-crystalline phase. The presence of kaolinite in the calcined Clay 2 (Table 2) could be associated to slightly coarse clay grain size when added in industrial rotary kiln. Pozzolanic activity and visual final color demonstrated that 800 °C were satisfactory burning temperature to Clays 1 and 2, respectively (Fig. 1), in static furnace condition. Gray color was obtained until 10 min regarding the time of reaction, but color reversion was observed in samples surface when contacts air inside the furnace. It was observed a tendency of reddish or pinkish

Table 1 Chemical analysis results of clays, in mass%

Components	Clay 1	Clay 2	Components	Clay 1	Clay 2
LOI	13.9	14.5	MgO	0.08	0.18
SiO_2	40.6	43.0	K_2O	0.48	0.33
Al_2O_3	32.5	35.4	Mn_2O_3	0.07	–
Fe_2O_3	11.8	3.83	TiO_2	1.51	1.57
CaO	0.02	0.06	P_2O_5	0.06	0.05

Table 2 Mineralogical composition data of clays, identified by XRD

Compound name	Chemical formula	Clay 1	Clay 2	Calcined Clay 1	Calcined Clay 2
Kaolinite	$Al_2Si_2O_5(OH)_4$	75	83	–	1
Illite	$KAl_2(Si_3Al)O_{10}(OH)_2$	2	8	–	–
Quartz	SiO_2	6	4	6	5
Hematite	Fe_2O_3	8	<1	–	–
Goethite	$Fe^{3+}O(OH)$	7	3	–	–
Gibbsite	$Al(OH)_3$	1	<1	–	–
Anatase	TiO_2	3	2	2	<1
Rutile	TiO_2	–	–	1	<1
Mullite	$Al_2(Al_{2.8}Si_{1.2})O_{9.6}$	–	–	–	<1
Muscovite	$(K,H_3O)Al_2(Si, Al)_4O_{10}(OH)_2$	4	<1	4	<1
Iron	Fe	–	–	<1	–
Amorphous or non-crystalline phase		Low		87	94

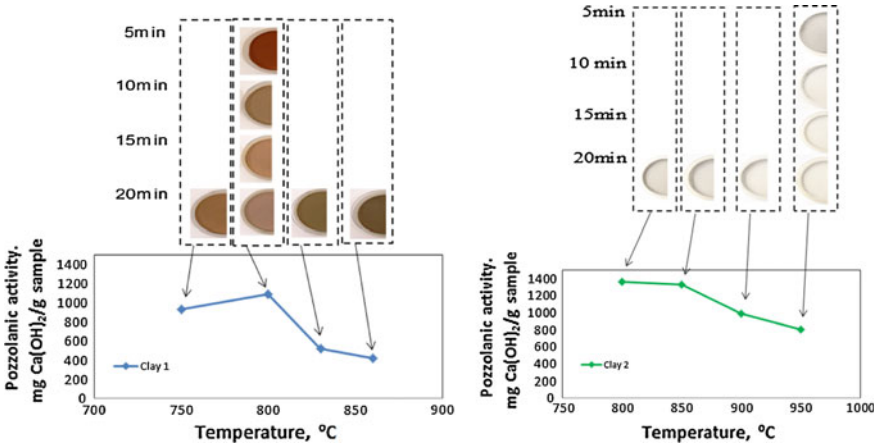

Fig. 1 Pozzolanic activity and color results for calcined clays on electric static furnace

color to vanish and the arising of grayish hues when burning time and maximum temperature increases.

Based on obtained results at electric static furnace mixtures of clays and coke, were applied the following tests: mix of Clay 1 and coke calcined in a pilot scale rotary kiln at 800 °C, and; mix of Clay 2 and coke calcined in an industrial rotary kiln between 850 and 950 °C, although 800 °C is the suitable burning temperature. The temperature interval is a furnace pre-fixed kiln condition, which could not be modified. In conformity with European Standard EN 197-1:2000, compressive strengths results of cements at 3, 7 and 28 days define cement as CEM II/B-P 42,5 N (Table 3). Both clays showed Strength Activity Index (SAI) ≥ 75 % (analogous to European Standards EN 197-1:2000) and negligible formation of magnetic fraction.

The XRD analysis showed changes in the mineralogical composition of calcined clays, absence of hematite and goethite (Table 2). This phenomenon directly reflects the cements final color. The disappearance of kaolinite as well a decrease in illite content, indicates that mineralogical transformation has occurred, which influences directly to the pozzolanic activity (Table 3). The amount of $Ca(OH)_2$ consumed was higher than 700 mg/g of pozzolan, which could be considered satisfactory to a pozzolanic material according AFNOR Standard NF P 18-513. The presence of TiO_2 contributed to clays darkening. According to instrumental color analysis, *in natura* clays strongly tends to red and highly positive a* index (Table 4). However, the calcined clays in reducing atmosphere and respective cements presented the tendency to darker hues, with smaller values in the a * and b * coordinates. Calcination in reducing atmosphere suggests the reduction of iron oxide without formation of metallic Fe, and allows obtaining cements with the desirable grayish hues. Complementary, in order to better understand the pozzolanic activity of calcined clays submitted to reducing calcination process, it is recommend to continue this study by microstructural point of view, applying SEM-EDS, NMR ^{27}Al and ^{29}Si nuclei and other techniques [7, 8] for explain the possible Al and/or Si replacement by Fe.

Table 3 Calcined clays tests results

Parameters	Calcined clay 1	Calcined clay 2
	Pilot	Industrial
Coke fraction, %	13	0
Non-magnetic calcined clay fraction, %	87	100
Magnetic calcined clay fraction, %	< 1	0
Coke consumed, in relation to calcined clay, %	15.0	11.7
Pozzolanic activity, mg $Ca(OH)_2$/g clay	1095	835
Compressive strength, MPa 3d		
7d		
28d	23.1	37.8
	34.1	49.5
	44.3	59.6

Table 4 Color coordinates results and respective visual appearance

Lab	Color coordinates			
	OPC Cement	Clay 1 *in natura*, dried and milled	Non-magnetic pilot calcined fraction Clay 1	Non-magnetic calcined Clay 1 + OPC Cement
L*	58.8	40.4	40.5	50.5
a*	1.1	21.0	−0.1	0.8
b*	10.5	23.4	−0.6	6.4
Color				
Lab	OPC Cement	Clay 2 *in natura*, dried and milled	Non-magnetic industrial calcined fraction Clay 2	Non-magnetic calcined Clay 2 + OPC Cement
L*	59.4	70.8	65.3	61.7
a*	1.4	9.2	4.3	1.8
b*	8.8	20.4	7.5	8.2
Color				

3 Conclusions

- The laboratorial and industrial reducing calcination process allowed obtaining desired grayish pozzolanic materials to Portland cement, and presents a solution for the application of originally reddish or pinkish clays.
- Evaluation of cements color stability, produced with color transformed calcined clays, is recommended, focusing the durability and performance of pozzolanic cements.
- The fuel consumption of the industrial scale process, when applying the color change technique, was slightly higher than the recorded at conventional operation. Despite of this, the kiln industry condition could be optimized by decreasing burning temperature for increasing performance of the calcined clay.

References

1. Gámiz, E., et al.: Relationships between chemico-mineralogical composition and color properties in selected natural and calcined Spanish kaolins. Appl. Clay Sci. **28**, 269–282 (2005)
2. Chandrasekhar, S., Ramaswamy, S.: Iron minerals and their influence on the optical properties of two Indian kaolins. Appl. Clay Sci. **33**, 269–277 (2006)
3. Hofstetter, T.B., et al.: Reactivity of Fe(II) species associated with clay minerals. Environ. Sci. Technol. **37**, 519–528 (2003)
4. Chandrasekhar, S., Ramaswamy, S.: Influence of mineral impurities on the properties of kaolin and its thermally treated products. Appl. Clay Sci. **21**, 133–142 (2002)

5. Castanho, M.P., Chotoli, F.F., Costa, R.G.: Forno Rotativo Tubular Laboratorial—Estudo de Perfil Térmico. In: Enqualab. São Paulo (2008). (http://www.vertent.net/remesp/enqualab2008/cdrom/pdf/TT036.pdf)
6. CIE System L*a*b* by L'ECLAIRAGE INTERNATIONAL COMMISSION in 1976
7. DE Souza, C.M., Garcia, E., Jäger, C.H., Quarcioni, V.A., Greiser, S.: Evaluation of pozzolanic reactivity of calcined kaolinite. In: 5th International Conference Non Traditional Cement and Concrete, 2014, Brno. Non-Traditional Cement & Concrete V, vol. 1, pp. 225–228. Brno: NOVPRESS (2014)
8. Fernandez, R., Martirena, F., Scrivener, K.L.: The origin of the pozzolanic activity of calcined clay minerals: a comparison between kaolinite, illite and montmorillonite. Cem. Concr. Res. **41**, 113–122 (2011)

Experimental Study on Evolution of Pore Structure of Cementitious Pastes Using Different Techniques

D. Yuvaraj and Manu Santhanam

Abstract Hydration of cement results in the formation of pores, which are mostly interconnected. Supplementary cementitious materials (SCM) lead to a reduction in the interconnectivity of the pores, as well as alter the pore size distribution. An assessment of the performance of alternative cements incorporating SCMs should therefore necessarily include a study of the pore structure characteristics. In the recent times, there has been a renewed interest in calcined clay based SCMs for cement concrete, because of the large reserves of such materials. Further, the use of limestone in a ternary combination with cement and calcined clay gives rise to a new chemistry that can be successfully used to produce high quality cementing materials for concrete. The work reported in this paper is part of a larger project that investigates the potential for limestone – calcined clay based cementitious binders in concrete. This paper describes an experimental investigation of the pore structure of different binder systems using mercury intrusion porosimetry and electrical conductivity measurements. The parameters investigated include total porosity, pore size distribution, and threshold diameter of pores. The cementitious systems include: (i) ordinary Portland cement (OPC), (ii) Portland pozzolana cement (PPC–i.e. OPC with 30 % Fly Ash Type F), (iii) Limestone Calcined Clay Cement (LC3).

1 Introduction

Global cement consumption is predicted to nearly double in the upcoming decades, and is already putting a huge burden on the available natural resources. Supplementary cementitious materials (SCM) are therefore a major necessity today. Binary blends of cement with fly ash, slag, or silica fume have been shown to cause significant enhancement in strength and durability performance of concrete [1–3]. Among SCMs, calcined clay is perhaps the best suited to reduce the problem of

D. Yuvaraj (✉) · M. Santhanam
Department of Civil Engineering, IIT Madras, Chennai, India
e-mail: dyuvarj@gmail.com

K. Scrivener and A. Favier (eds.), *Calcined Clays for Sustainable Concrete*,
RILEM Bookseries 10, DOI 10.1007/978-94-017-9939-3_60

shortage of limestone resources for cement production, because of its vast reserves [4]. Calcined clay has also shown potential to be an efficient substitute for clinker in large amounts (up to 40–50 %) when used in conjunction in limestone. Besides the pozzolanic reaction, the interaction of calcined clay with limestone in the presence of lime leads to the formation of other hydrate phases that cause an improvement in the hardened properties of the blend [5].

This paper discusses the evolution of porosity and pore structure in the ternary blended system of cement, limestone and calcined clay, at different stages of hydration. In addition, the hydration characteristics are also monitored in the system to understand the synergy due to limestone and calcined clay combination.

2 Materials

Ordinary Portland cement (OPC) from a single batching plant was used for the study. The limestone – calcined clay cement (LCCC) was produced in the lab scale using a ball mill. Limestone was ground to cement fineness (approximately 300 m^2/kg) in the ball mill, and OPC, Calcined clay and limestone were mixed in the ratio of 55:30:15 in the ball mill for 10 min to produce a uniform blend. The particle size distribution of the OPC and the lab scale LCCC are shown in Fig. 1.

The physical properties of the OPC and LCCC determined in accordance with IS 4031 [ref] are presented in Table 1.

Pastes were prepared with 0.35 water to cement ratio. Specimens of 10 mm × 10 mm × 50 mm were cast. At 4, 7 and 28 days of hydration, small chunks were broken from the specimens and stored in acetone to stop hydration by solvent exchange method. After 3 days, the samples were removed from acetone and were stored dry under vacuum until testing.

The pore structure of the OPC and LCCC paste specimens was periodically assessed using a mercury intrusion porosimeter. The LCCC system was also examined for its heat evolution characteristics using semi-adiabatic calorimetry. Further, X-ray diffraction (XRD) was also performed to establish the mineralogical differences in the OPC and LCCC systems.

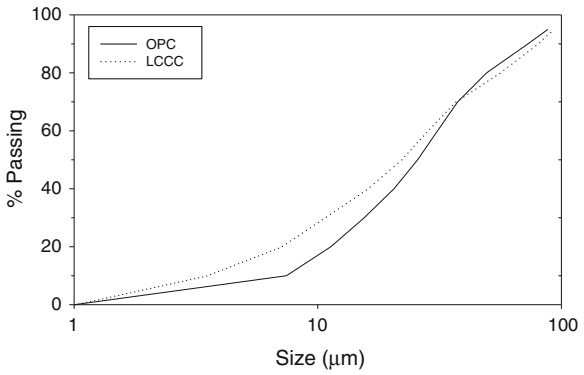

Fig. 1 Particle size distribution of OPC and LCCC

Table 1 Physical characteristics of OPC and LCCC

Physical characteristics	OPC	LCCC
Specific gravity	3.16	2.96
Consistency	30 %	37 %
Initial setting time	126 min	145 min
Final setting time	165 min	270 min

3 Results

The results from the study will be discussed in detail in the presentation.

References

1. Aponte, D.F., Barra, M., Vàzquez, E.: Durability and cementing efficiency of fly ash in concretes. Constr. Build. Mater. **30**, 537–546 (2012)
2. Uysal, M., Akyuncu, V.: Durability performance of concrete incorporating Class F and Class C fly ashes. Constr. Build. Mater. **34**, 170–178 (2012)
3. Dhanya, B.S., Santhanam, M., Nithish Bharath Kumar, B.: Durability performance of slag as a supplementary cementing material. In: International congress on durability of concrete, New Delhi, December 2014
4. Scrivener K.L.: Options for future of cement. The Indian Concr. J. 11–21 (2014)
5. Antoni, M., Rossen, J., Martirena, F., Scrivener, K.L.: Cement substitution by a combination of metakaolin and limestone. Cem. Concr. Res. **42**(12), 1579–1589 (2012)

Various Durability Aspects of Calcined Kaolin-Blended Portland Cement Pastes and Concretes

M. Saillio, V. Baroghel-Bouny and S. Pradelle

Abstract The use of calcined clay, in the form of metakaolin (MK), as a pozzolanic constituent for concrete has received considerable attention in recent years, due to the lower CO_2 emission of this supplementary cementitious material compared to the production of a classic portland cement. Furthermore, concretes incorporating MK show some improve durability properties. In this paper, the durability of concretes and cement pastes with MK as partial replacement of cement (10 and 25 %) has been investigated in comparison with CEM-I materials one. Water porosity, chloride migration and diffusion, electrical resistivity and natural and accelerated carbonation tests have been performed. In addition, microstructural study is performed to better understand the results on the durability indicators. The cement pastes microstructure was characterized not only by usual techniques such as mercury intrusion porosimetry, XRD and TGA-DTA, but also by ^{29}Si and ^{27}Al NMR spectroscopy. For example, Friedel's salt (chemical binding) has been quantified by ^{27}Al NMR spectroscopy and XRD on cement paste. In addition, the progress of the durability properties for various water curing times has been investigated. Results show an evolution of the properties, as a function of the cement replacement degree by MK, such replacement increases durability against chloride penetration but decreases resistance to carbonation. The aluminate phases equilibrium is modified in concrete with metakaolin in comparison with a CEM-I one. Both chemical and physical chloride binding increases with MK replacement. In addition, since portlandite quantity decreases in cement materials with MK, these materials are less resistant to carbonation process for a same exposure condition (time and CO_2 concentration).

Keywords Concrete · Metakaolin · Durability · ^{29}Si and ^{27}Al NMR spectroscopy

M. Saillio (✉) · V. Baroghel-Bouny · S. Pradelle
IFSTTAR, 14-20 bd Newton, 77447 Marne la Vallée, France
e-mail: mickael.saillio@ifsttar.fr

M. Saillio
BOUYGUES-TP, 1 rue Guynemer, 78114 Magny les Hameaux, France

K. Scrivener and A. Favier (eds.), *Calcined Clays for Sustainable Concrete*,
RILEM Bookseries 10, DOI 10.1007/978-94-017-9939-3_61

1 Introduction

Supplementary cementitious materials (SCMs) are included into concrete to substitute part of cement in order to reduce the carbon footprint. SCMs are mainly pozzolanic materials including industry waste such as ground granulated blast slag and fly ash. Metakaolin (MK) is known for having similar effects to improve strength and durability of concrete [1–4]. Metakaolin is produced by calcining kaolin at 650–800 °C and is mainly amorphous [4]. MK needs aqueous calcium hydroxide produced during clinker hydration to form C-S-H or C-S, Al-H gels [5]. In addition, MK induces a filler effect to the mixture [6].

This study focuses on the durability indicators of MK cement materials such as water porosity, apparent chloride diffusion coefficient ($D_{app,Cl}$), electrical resistivity. The resistance to the carbonation process (in replacement of gaz permeability as durability indicator) and chloride binding isotherms (CBIs) are also evaluated. In addition, microstructural study (XRD, thermal analyses and NMR) is performed to better understand the results on the durability indicators.

2 Experimental

Various concretes were mixed with the same clinker and granular squeleton using siliceous aggregates. The main constituents of the clinker are given in Table 1. The binder content is 300 kg/m^3 and the water to binder ratio (w/b is equal to 0.53 for all the mixtures. Studied binders are CEM I (OPC with 97 % clinker), CEM I + 10 % MK denoted CEM I MK(10 %) and CEM I + 25 % MK denoted CEM I MK(25 %). The partial replacement of CEM I by MK in binders is called here MK degree. Cement pastes with the same binders were also prepared with w/b equal to 0.50.

Many water-curing times are chosen (7, 28, 90, 180 and 365 days) in order to take into account the evolution of the microstructure as a function of the age. Sound samples (i.e. non-carbonated) will be denoted “reference” in the paper.

Various durability tests are performed on these concretes and pastes: water porosity, chloride migration and diffusion [7], electrical resistivity [8] and natural and accelerated carbonation tests [9]. In addition, chloride binding isotherms (CBIs) are obtained by equilibrium method [10]. Finally, microstructure is characterized by mercury intrusion porosimetry (MIP) [7], XRD [10], TGA-DTA [9] and ^{29}Si and ^{27}Al nuclear magnetic resonance magical angle spinning spectroscopy (NMR MAS) [10].

Table 1 Chemical composition of the cement and SCM tested (%) and mineralogical composition of the CEM I from BOGUE calculation (%)

	CaO	SiO_2	Fe_2O_3	Al_2O_3	TiO_2	MgO	Na_2O	K_2O	MnO	SO_3	C_3S	C_2S	C_3A	C_4AF
CEM I	62.53	19.54	2.90	4.98	0.30	0.84	0.30	0.82	0.09	2.97	51.23	28.32	9.90	8.81
MK	0.00	66.29	4.29	21.30	1.12	0.25	0.84	0.49	0.00	0.08				

3 Results and Discussion

3.1 Compressive Strength and Durability Indicators

At the young age (see Fig. 1), CEM I MK(10 %) concrete has a higher compressive strength than others concretes (an increase of 50 % in comparison of CEM I concrete) which is consistent with previous studies [11]. MK concretes reach theirs stabilization value within 28 day. The high reactivity of MK at young age is related to their aluminate phases and their high surface area. MK pozzolanic reactions consume portlandite and produce C-S-H and C-S,Al-H denser [12]. Furthermore, MK also plays an accelerator on hydration of C_3S by the nucleating effect due to the increase of fines in a cementitious matrix [6]. The filler effect could have an impact in increasing the compactness of concrete, and thus improving the mechanical properties [1]. However, at the long term, the maximum compressive strength of MK concrete (65 MPa) is still lower than the CEM I concrete (80 MPa). A MK degree of 25 % in binder improves slightly the strength properties at early age compared to CEM I concrete; it seems that there is an optimum in terms of the MK degree. This optimum (between 10 and 25 %) is also being studied to establish a European standard. In France, it is the new standard issued in March 2010, the NF P 18-513 that governs this type of addition.

Water porosity of CEM I MK(25 %) concrete decrease slightly (see Fig. 2 in left) in comparison to CEM I one, but the measurement uncertainties (not figured here) are relatively close. For cement pastes, the tendency is clearer: CEM I MK (25 %) porosity is very low porosity compared to CEM I one and evolve to less porosity with water-curing time in concordance with other results [12]. Here, cement paste porosity is a negative linear function of MK degree (see Fig. 2) confirmed by two methods (water porosity and MIP) for each water-curing time.

Less porosity has consequences on other durability properties such as chloride diffusion. Indeed, it appears in Fig. 3 that chloride apparent coefficient ($D_{app,Cl}$) of MK concretes decrease compared to CEM I one. These results obtained by migration tests are similar to those obtained by diffusion tests (respectively 12; 7

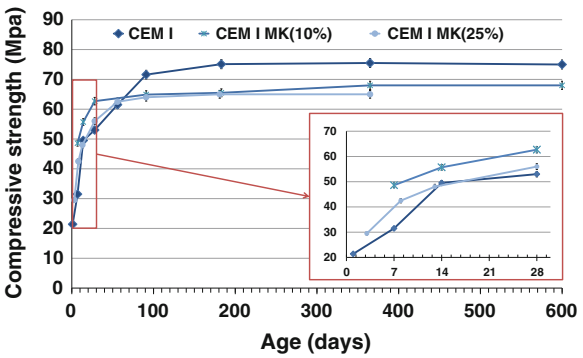

Fig. 1 Compressive strength of concretes in function of water-curing time

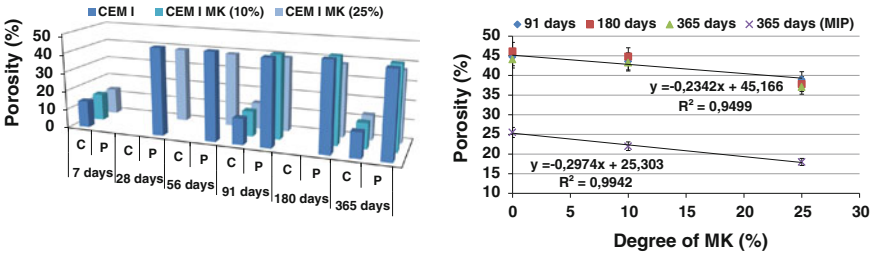

Fig. 2 Water porosity of paste (P) and concrete (C) in function of water-curing time. In *right*, comparison between water porosity and porosity obtained by MIP for cement pastes

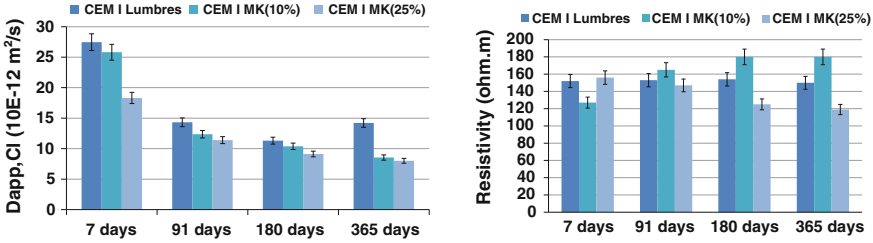

Fig. 3 Chloride apparent coefficients (in *left*) obtained by chloride migration and resistivity (in *right*) of concretes in function of water-curing time

and 1.10E-12 m^2/s for respectively CEM I, CEM I MK(10 %) and CEM I MK (25 %). Nevertheless, the observed differences are larger in these tests for MK cementitious materials. For example, a factor 5 is reached for $D_{app,Cl}$ of CEM I MK (25 %) obtained by migration and diffusion tests. In general, it is considered [7] that $D_{app,\ Cl}$ obtained by the migration depends only on the porous network. Indeed, during the migration test, interactions (between chloride and cementitious matrix) are very weak and can be often neglected. In contrast, $D_{app,\ Cl}$ from diffusion tests depends in part on these interactions and also the porous network which explain why $D_{app,\ Cl}$ obtained by the migration are higher to $D_{app,\ Cl}$ obtained by diffusion tests. Consequently, CEM I MK(25 %) seems to have a higher capacity for chloride binding which is confirmed by CBIs presented in Fig. 4. There is also linear relationship between chloride binding and MK content.

Resistivity tests show contrasted results (see Fig. 3 in right) in opposite to some other studies [2]. Here, it seems that CEM I MK(10 %) concrete has the best resistivity for 365 days of water curing time.

For cement pastes, portlandite amounts decrease when MK degree increases (see Fig. 5 in left) because it is only produced by the clinker and CEM I MK(25 %) contains less clinker than CEM I (dilution effect). In addition, the pozzolanic reactions in MK pastes consume portlandite. In order to separate the effect of the dilution and the consumption of portlandite due to pozzolanic reactions, the mass proportion of portlandite compared to the clinker is calculated. It is 22 % for CEM I

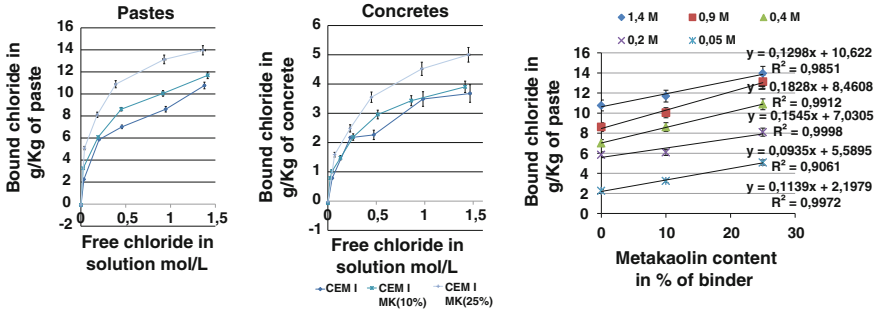

Fig. 4 Concretes and cement pastes CBIs (in *left*) and chloride binding of cement pastes in function of MK content (in *right*) obtained by equilibrium method

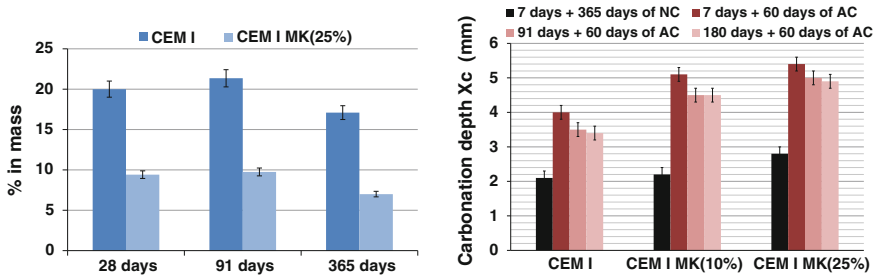

Fig. 5 % in mass of portlandite (in *left*) in cement pastes and carbonation depth (in *right*) measured by phenolphthalein tests on concretes after various water-curing times and natural (NC) or accelerated carbonation (AC) (1.5 % CO_2, 65 % RH and T = 20 °C)

and 14 % for CEM I MK(25 %). Therefore, large amounts of portlandite are consumed by pozzolanic reactions in these materials. The main consequence is that MK cementitious materials are less resistant than CEM I ones against a same carbonation treatment (see Fig. 5) confirming results [4].

3.2 Microstructure

Pore size distribution of cement pastes obtained by MIP is presented in Fig. 6. The main peak of the distribution decreases whereas MK degree increases. It can due to the filler effect [6]. Additionally, C-S,Al-H denser forms inside the porous during the pozzolanic reactions. This can explain the better results of CEM I MK(25 %) $D_{app,\,Cl}$ obtained by migration compared to CEM I one (see Fig. 3).

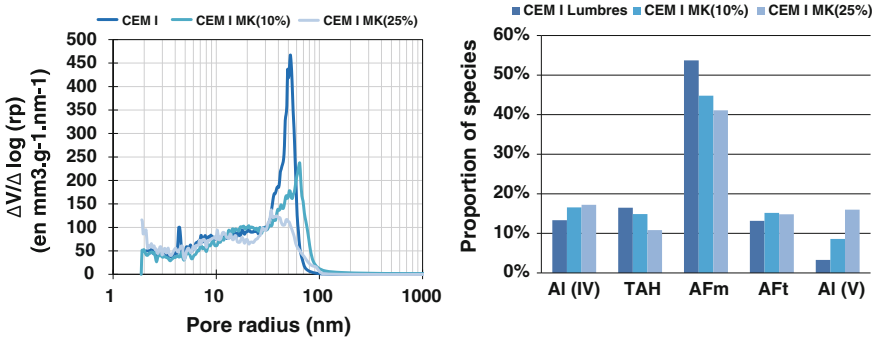

Fig. 6 Pore size distribution obtained by MIP (in *left*) and proportion of Al species obtained by ^{27}Al MAS NMR (in *right*). Al(IV) aluminum substituted for silicon in C-S-H chains and residual anhydrous cement. Al(V) aluminum substituted for calcium in the C-S-H interlayers or present in non-hydrated phases or in MK. TAH : amorphous/disordered aluminum hydroxide or a calcium aluminate hydrate

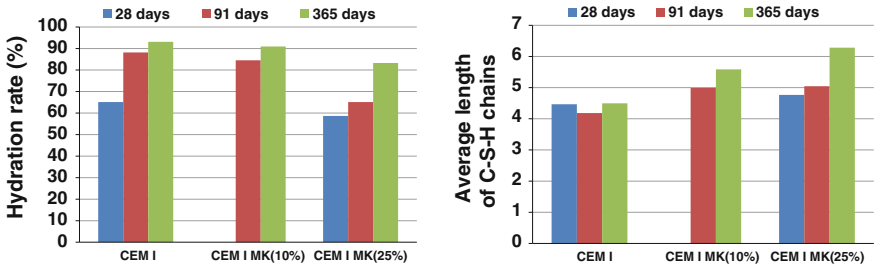

Fig. 7 Hydration rate (in *left*) and average length of C-S-H chains obtained by ^{29}Si MAS NMR for various water-curing time

Equilibrium of aluminates phases in cement pastes is presented in Fig. 6. There are more AFt phases (respectively less AFm phases) in MK cement pastes than in CEM I. Furthermore, MK cement pastes contains more Al(IV) and Al(V) due to residual MK but also to Al incorporated in C-S-H during pozzolanic reactions.

The hydration rate obtained by ^{29}Si NMR (ref) is presented in Fig. 7. For each water-curing time, hydration rate of MK cement pastes stays inferior to CEM I one. By combination of microstructural techniques (DRX, TGA and NMR), the anhydrous phases remaining are evaluated at 8 % in mass in CEM I MK(25 %) after one year of water-curing, against 3 % in CEM I.

Average length of C-S-H chains (obtained by ^{29}Si NMR,) presented in Fig. 7 is longer in MK cement pastes than CEM I. It appears that C-S-H chains polymerise in MK cement pastes. It is probably due to the presence of Al substituted to Si in C-S-H from pozzolanic reactions of MK.

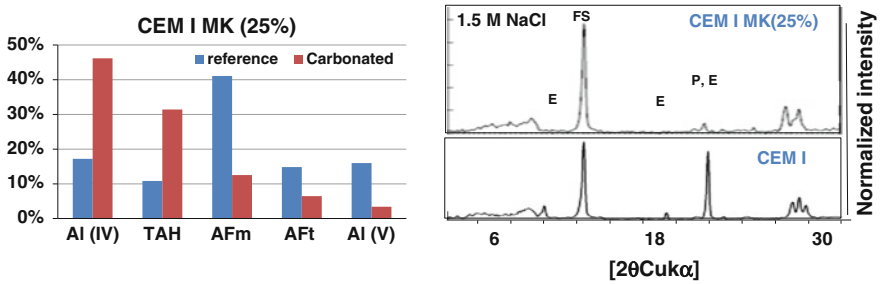

Fig. 8 Proportion of Al species obtained by ^{27}Al MAS NMR (in *left*) and diffractogramms (in *right*) of crushed pastes in contact of NaCl solution (1.5 M). E ettringite, FS Friedel's salt, P portlandite

The microstructure has been investigated after exposure to chloride or after carbonation and only the most remarking results are presented here.

Concerning carbonation, a partial treatment (3 days 1.5 % CO_2 and 65 %RH) was applied on crushed pastes. Almost no difference is observed for CEM I before and after the carbonation treatment. In opposite, after carbonation, CEM I MK (25 %) shows a lower portlandite amount (5 % instead of 8 %), a new equilibrium of aluminate phase (see Fig. 8), a higher decalcification (C/S is 0.5 instead 0.9) and polymerisation of C-S-H chains. Consequently, for a same carbonation treatment (condition exposure and duration), MK cementitious materials are less resistant to carbonation than CEM I confirming the results presented in Sect. 3.1 and the modification of aluminate phase equilibrium and C-S-H decreases the binding capacities as reported in [10].

Concerning chloride ingress, crushed pastes were put in contact to various NaCl solutions then analysed by ^{27}Al NMR and XRD. For a same NaCl concentration of the solution (see Fig. 8), CEM I MK(25 %) produces more Friedel's salt than CEM I and physical binding (accessed by combination of NMR and CBIs results) is also higher confirming results presented in Sect. 3.1. More binding means more resistant to chloride ingress for MK cementitious materials for example in marine environment. However, in case of a multiple aggression, such as carbonation then chloride ingress, MK cementitious materials lose this advantage.

4 Conclusions

In term of durability properties, MK concretes exhibit advantages compared to CEM I concretes. A decrease in porosity is recorded and the apparent coefficient of chloride ion diffusion. However, their lower Portlandite content makes them more sensitive to carbonation. Water porosity and chloride binding clearly evolve (according to a linear trend) with MK content of the binder within the range studied (0–25 %).

Further investigation of the microstructure yields a better understanding of these advantages and disadvantages concerning carbonation and chloride ingress. The finer pore network and the largest capacity to bind chlorides improves $D_{app, Cl}$ compared to CEM I materials. Consequently, MK cement materials can be used in marine environment. However, compared to CEM I mixture, their lower Portlandite amount increases carbonation progress which results in a rearrangement of the aluminate phases and a decalcification/polymerization of C-S-H (which both decreases chloride binding). In presence of CO_2 or in case of multiple aggression (carbonation and chloride environment), the use of MK cement materials has to be limited.

Acknowledgments Authors are grateful to G.Platret and B.Duchesne from IFSTTAR (France) for XRD and TGA/DTG investigations, to J.B.D'Espinose de Lacaillerie from ESPCI (France) for NMR MAS experiments and P.Gégout and F.Barberon from Bouygues-TP (France) for providing concretes and cement pastes.

References

1. Badogiannis, E., Papadakis, V.G., Chaniotakis, E., Tsivilis, S.: Exploitation of poor Greek kaolins: strength development of metakaolin concrete and evaluation by means of k-value. Cem. Concr. Res. **34**(6), 1035–1041 (2004)
2. Ramezanianpour, A.A., Jovein, H.B.: Influence of metakaolin as supplementary cementing material on strength and durability of concretes. Constr. Build. Mater. **30**, 470–479 (2012)
3. Hong-Sam, K., Sang-Ho, L., Han-Young, M.: Strength properties and durability aspects of high strength concrete using Korean metakaolin. Constr. Build. Mater. **21**(6), 1229–1237 (2007)
4. San Nicolas, R., Escadeillas, G., Cyr, M.: Performance-based approach to durability of concrete containing flash-calcined metakaolin as cement replacement. Constr. Build. Mater. **55** (31), 313–322 (2014)
5. Janotka, I., Puertas, F., Palacios, M., Kuliffayova, M., Varga, C.: Metakaolin sand–blended-cement pastes: rheology, hydration process and mechanical properties. Constr. Build. Mater. **24**(5), 791–802 (2010)
6. Kadri, E.H., Kenai, S., Ezziane, K., Siddique, R., De Schutter, G.: Influence of metakaolin and silica fume on the heat of hydration and compressive strength development of mortar. Appl. Clay Sci. **53**(4), 704–708 (2011)
7. Baroghel-Bouny, V., Kinomura, K., Thiery, M., Moscardelli, S.: Easy assessment of durability indicators for service life prediction or quality control of concretes with high volumes of supplementary cementitious materials. Cement Concr. Compos. **33**(8), 832–847 (2011)
8. Andrade, C., Prieto, M., Tanner, P., Tavares, F., D'Andrea, R.: Testing and modelling chloride penetration into concrete. Constr. Build. Mater. **39**, 9–18 (2013)
9. Vilain, G., Thiery, M., Platret, G.: Measurement methods of carbonation profiles in concrete: thermogravimetry, chemical analysis and gammadensimetry. Cem. Concr. Res. **37**(8), 1182–1192 (2007)
10. Saillio, M., Baroghel-Bouny, V., Barberon, F.: Chloride binding in sound and carbonated cementitious materials with various types of binder. Constr. Build. Mater. **68**(15), 82–91 (2014)
11. Palomo, A., Grutzeck, M.W., Blanco, M.T.: Alkali-activated fly ashes: a cement for the future. Cem. Concr. Res. **29**, 1323–1329 (1999)
12. Badogiannis, E.: The effect of metakaolin on concrete properties. In: Challenges of Concrete Construction, Proceeding of an International Congress, Dunde, pp. 81–89 (2002)

Economic Implications of Limestone Clinker Calcined Clay Cement (LC^3) in India

Shiju Joseph, Aneeta Mary Joseph and Shashank Bishnoi

Abstract Limestone Clinker Calcined Clay Cement (LC^3) is a recently developed cement with a low clinker factor in which clinker is partially replaced by calcined clay, limestone and gypsum. This article presents a preliminary analysis of the economy of Limestone Calcined Clay Cement in India. The production cost of LC^3 is compared with that of ordinary Portland cement (OPC) and Portland pozzolanic cement (PPC) on various cement plants and grinding units. While the results are encouraging, they demonstrate the subjectivity of economics of producing new cement blends. While it is found that LC^3 is significantly economical compared to OPC, it was found to be economical with respect to PPC as well in many scenarios. At the level of concrete, even blends made using higher quality kaolinitic clays could be more economical.

1 Introduction

Limestone Clinker Calcined Clay Cement (LC^3) is a recently developed cement blend which contains 40–50 % clinker content, 30–40 % calcined clay, 15–20 % limestone and 4–7 % gypsum [1]. This blend having synergy between all the ingredient materials is thus showing better performance in terms of strength compared to other conventionally used cement blends.

This paper studies the economic feasibility of LC^3 in India. India being second largest consumer and producer of cement, with abundant amount of fly ash available it would be interesting to study the economic feasibility of LC^3 in India. LC^3 cement turning out to be economical in India does mean a lot to other countries like Brazil which has very large reserves of kaolinitic clay.

S. Joseph (✉)
KU Leuven, Leuven, Belgium
e-mail: shiju.joseph@student.kuleuven.be

A.M. Joseph · S. Bishnoi
Indian Institute of Technology, Delhi, India

K. Scrivener and A. Favier (eds.), *Calcined Clays for Sustainable Concrete*,
RILEM Bookseries 10, DOI 10.1007/978-94-017-9939-3_62

This study aims at comparing the production cost of LC^3 cement with that of Ordinary Portland Cement (OPC) and Pozzolanic Portland Cement (PPC), PPC being blend of OPC with fly ash. The different factors affecting the economy of LC^3 is also on the scope of this study, and all these factors are based on actual data from Indian Cement Industry.

2 Data and Assumptions Used for the Present Study

1. The assumptions used in this studied are briefed. The cost of materials used in this study was provided by Dalmia Cements and Bansal cements.
2. The composition of OPC is fixed at 95 % clinker and 5 % gypsum, PPC as 60 % clinker, 35 % fly ash and 5 % gypsum and LC^3 as 50 % clinker, 30 % calcined clay, 15 % low grade limestone and 5 % gypsum.
3. Weight loss occurring by calcination of clay is assumed to be 18 %.
4. The electricity requirement for production of clinker and calcination of clay are assumed to be same, and the fuel requirement for calcination of clay is assumed to be 50 % of that required for clinkering.
5. The electricity requirement for grinding could be lower for LC^3 than PPC and OPC, as calcined clay being one of the major raw material, need not be ground, and even if needed, a basic grinding would suffice for better performance by inter-grinding.
6. In a large scale dedicated production unit for LC^3, a separate grinding unit could be assigned for better efficiency of plant. The electricity requirement in this study for calcination has also been made on the conservative side by assuming it to be same as that required for clinkering, while it would be most probably less.
7. The limestone is assumed to be near by the plant which would be transported by a belt conveyor and other clinkering materials such as iron and alumina base fluxes, gypsum and coal are at a distance of 50, 200 and 500 kilometres respectively. In this analysis, the mode of transportation is selected as road.

3 Analysis

3.1 Comparison of Cost of Production of OPC, PPC and LC^3 in a Cement Plant

Comparison of cost of production of OPC, PPC and LC^3 is shown in the Fig. 1. All the costs are calculated in Indian Rupees (Rs.). It is assumed that the source of fly ash and clay is 100 km away from the cement plant and they have been transported by road. It is seen that, under assumed conditions, LC^3 and PPC is more economically sustainable than OPC. The reduction is primarily due to two factors,

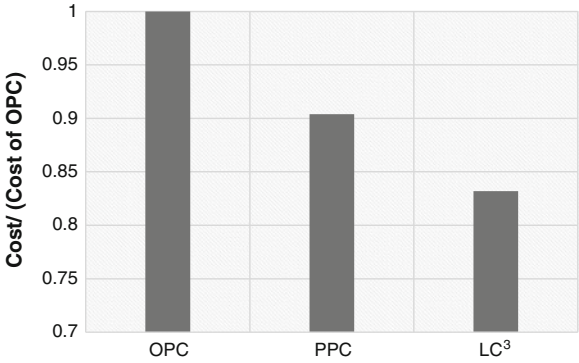

Fig. 1 Comparison of production cost of PPC and LC^3 with OPC

(i) low clinker factor and (ii) less fuel and electricity requirement for calcination of clay compared to that for production of clinker. The assumed cost of fly ash is Rs. 800/ton. Since the cost of fly ash is variable, it shall not be directly inferred from the graph that LC^3 is more economical that PPC.

3.2 Comparison Between the Production Cost of PPC and LC^3

One of the main variable that affects the production cost of PPC is the cost of fly ash available in India which varies from location to location depending on the availability and quality. In this analysis the cost variable of fly ash is coupled with the distance between the source of fly ash and clay from the cement plant. The results has been summarized in Fig. 2. The source of fly ash which is mainly from the thermal power plant could be far away from the cement plants as cement plants would be more concentrating on selecting a site near the limestone deposits. It can be inferred from the analysis that depending on the source of fly ash and clay, cost of fly ash, both could be more economical than other in select conditions.

In this analysis, the mode of transportation is selected as road. It must be noted that there is an added advantage of clay over fly ash, for the possibility of transporting clay to the cement plant in train which would be a much cheaper mode of transportation compared to road. Most already existing cement plants have a railway line connecting to the plant for the transportation of coal. Due to the environmental hazards posed by fly ash, it is currently not possible to be transported by rail.

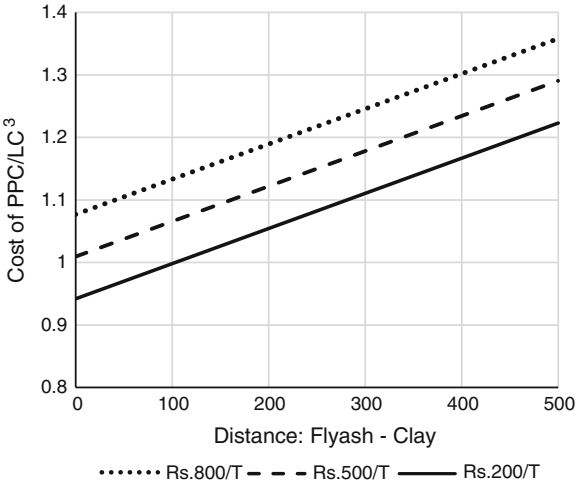

Fig. 2 Cost comparison between PPC and LC3 with variable cost of fly ash and variable distance of source of fly ash and clay from the cement plant

3.3 Effect of Clinker Factor of LC^3 on the Economy Between LC^3 and PPC

In this scenario, the effect of clinker factor of LC^3 is compared with different replacement values of fly ash. For this particular analysis, the cost of fly ash is assumed to be Rs. 500/T and both the source of fly ash and clay is at equal distance. The possible clinker factor of LC^3 is still not fixed as researches are going on and it would depend on lot of factors from availability of suitable raw materials and the required grade of cement and the recommendations from the standard committee. But Fig. 3 is an indicator of possible savings this technology could make. But from the preliminary research (EPFL and India), it could be said that a clinker factor of up to 40 % is achievable for this cement.

The amount of replacement of clinker by fly ash for PPC also depends on the quality of fly ash. Most fly ashes which are available in India is of inferior quality as it is primarily considered as a waste material and proper care is not taken. Quality of fly ashes could be improved upon processing but would result in higher cost.

Figure 4 indicates savings in LC^3 technology compared to PPC, especially when the clinker factor of LC^3 could be made low.

4 Normalized Cost for Concrete

The study on economy of cement will not be complete, unless it is compared with concrete as cement is mostly used in concrete. In the pilot studies in India [citation], 10 tons each of 4 different blends was produced.

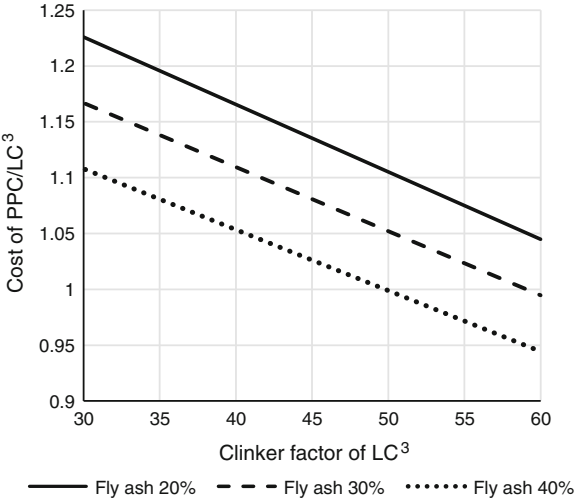

Fig. 3 Effect of clinker factor of LCC on the production cost ratio of PPC and LCC for different fly ash replacement values

Concrete cubes of 15 × 15 × 15 cm was casted and tested at 28 days for different water to cement ratio. And the water to cement ratio at which it gives 35 MPa mean strength has been selected to compare the normalized cost for concrete. The raw mix composition of different blends of LC^3, OPC and PPC are given in Table 1. And the water to cement ratios at which the blends give a strength of 35 Mpa has been recorded in Table 2. LC^3 A and B is having a strength that is higher than 35 Mpa at 0.5 water to cement ratio. But still, that value is chosen to be on the conservative side. LC^3 C and LC^3 D is using a very low grade clay with kaolinite content around 20 %. Still they are getting comparable strengths with OPC and better strength than PPC with 30 % fly ash replacement (Fig. 4; Tables 1 and 2).

In the analysis for the economy it is assumed that the good quality clay is having 4 times cost than that of the lower quality. It could be seen that all LC^3 blends are cheaper than OPC and PPC for production of concrete.

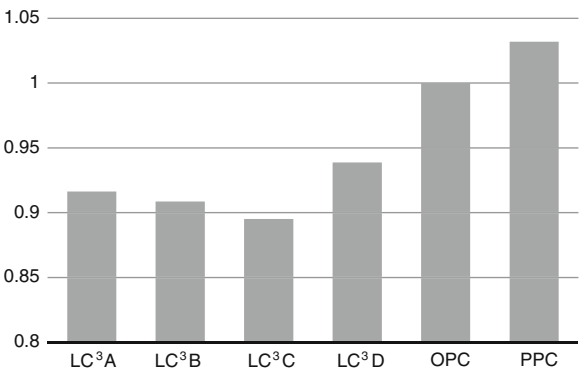

Fig. 4 Amount of cement required for a mean strength of 35 MPa with respect to amount of OPC required for the same

Table 1 Raw mix composition of different cement blends used for study

	LC^3 A	LC^3 B	LC^3 C	LC^3 D	OPC	PPC
Clinker	50 %	50 %	50 %	50 %	95 %	65 %
Fly ash	–	–	–	–	–	30 %
Calcined Clay	30 %, High grade	30 %, High grade	30 %, Low grade	30 %, Low grade	–	–
Limestone	15 %, High grade	15 %, Low grade	15 %, High grade	15 %, Low grade	–	–
Gypsum	5 %	5 %	5 %	5 %	5 %	5 %

Table 2 W/C ratio for different blends for 35 MPa mean strength [1]

	LC^3 A	LC^3 B	LC^3 C	LC^3 D	OPC	PPC
w/c ratio	0.5	0.5	0.45	0.425	0.475	0.41

5 Economy for a Grinding Unit

In the case of a grinding unit the case is different. The main cost over there is the cost of clinker which would be as much as double the production cost (at production unit) after including transportation costs etc. And the next most influential factor for the economy would be the cost of calcined clay. Unlike a cement plant, a grinding unit may not be able to acquire clay mines and mine themselves. And the calcination could be also done in some other place and the mode of calcination could be different and the cost of calcination could also vary on the type of calcination used. For grinding units, and for normal costs of calcination, LC^3 is found more economical over PPC because of the lower clinker factor of the former to the latter.

6 Factors to Be Included in Future Study

The factors which are not included in the study and which would be crucial would be the sustainability of cement plant due to the better usage of limestone deposits, increased capacity of the current cement plants and which in turn compensating the future demands, savings from carbon credit [2], marketing or selling cost etc.

7 Conclusions

The initial study on the economy of Limestone Calcined Clay Cement in the Indian market seems to be very positive. Thus implies that LC^3 is suitable for India. More study has to be conducted to verify the outcomes and for more realistic ideas and to

know about the economy on a localised scale. The inferences from this study (under specified assumptions) is summarised below:

- LC^3 is economical than OPC
- LC^3 is economical than PPC under several circumstances
- When clay is more locally available
- When suitable fly ash is not available locally or the cost of suitable fly ash is high
- When high replacement of clinker is possible with LC^3

Acknowledgments The authors express their deep gratitude towards Swiss Agency of Development and Corporation (SDC) for funding this research, Ultratech Cement for guiding about the cement plant production, Dalmia Cement and Bansal Cement for providing the different associated cost.

References

1. Bishnoi, S., Maity, S., Malik, A., Joseph, S., Krishnan, S.: Pilot scale manufacture of limestone calcined clay cement: the Indian experience. Indian Concr. J. **88**(6), 22–28 (2014)
2. Imbabi, M.S., Carrigan, C., McKenna, S.: Trends and developments in green cement and concrete technology. Int. J. Sustain. Built Environ. **1**, 194–216 (2012)

Fresh and Mechanical Properties of High Strength Self Compacting Concrete Using Metakaolin

S.N. Manu and P. Dinakar

Abstract Concrete is probably the most consumed construction material in the world. However, environmental concerns both in terms of damage caused by the extraction of raw material and carbon dioxide emission during cement manufacture have brought pressures to reduce cement consumption by the use of supplementary cementing materials (SCM). Metakaolin is a SCM, which has a significant potential for the production of High Strength Concrete (HSC) and Self-Compacting Concrete (SCC). Because of the lower processing temperature compared to cement clinker, use of metakaolin can contribute to sustainability through energy savings, as well as reductions in greenhouse gas emissions. The present study evaluates the fresh and mechanical properties of high strength self-compacting concrete developed using metakaolin. SCC having a strength category of 80, 100, 120 MPa developed a with metakaolin replacement percentages of 7.5, 15, and 22.5 % respectively. All the SCCs developed using metakaolin exhibited good fresh properties. It has been observed that SCC with metakaolin having powder content 550 kg/m^3 is sufficient to produce 120 MPa. At higher replacement level of metakaolin, it was also observed that the autogeneous shrinkage reduced considerably. All these evidences justifies that metakaolin is potential material for the development of high strength self-compacting concrete.

Keywords HSC · SCC · Metakaolin

1 Introduction

Development of self-compacting concrete (SCC) is one of the significant development in the area of concrete technology. On the other hand high strength concrete is the most desirable structural component for many infrastructure projects. It can be manufactured by most concrete plants due to the availability of a variety of

S.N. Manu · P. Dinakar (✉)
School of Infrastructure, IIT Bhubaneswar, Bhubaneswar, India
e-mail: pdinakar@iitbbs.ac.in

K. Scrivener and A. Favier (eds.), *Calcined Clays for Sustainable Concrete*,
RILEM Bookseries 10, DOI 10.1007/978-94-017-9939-3_63

additives such as silica fume, metakaolin and superplasticizers. The combination of high strength with self compacting property offers potential benefits to the construction industry.

Metakaolin (MK) is a supplementary cementing material (SCM) that has sufficient potential for the production of high-strength and high-performance concretes, if appropriately designed. Metakaolin differs from the most commonly used SCM, such as fly ash, slag and silica fume, in that it is not a by-product. It is manufactured under controlled conditions by thermally activating purified kaolinite clay within a specific temperature range (650–900 °C) [1]. There are very few studies reported on the development of SCC using metakaolin. The effect of MK on the rheological properties and strength development on SCC was studied earlier [2]. Based on the investigation it was found that as the metakaolin content increases in SCC mixture the corresponding 28 day compressive strength, the rheological parameters (plastic viscosity and yield stress) and also the demand of superplasticizer increases [2]. In the present investigation the effect of metakaolin on the development of high strength SCCs has been attempted by adopting a specific mix design methodology and the fresh and the mechanical properties of the same have also been determined.

2 Experimental Program

2.1 Materials

The materials used throughout the experiment were Ordinary Portland cement and the metakaolin meet the requirements mentioned in IS: 12269 (53 grade) and ASTM C618 respectively. Crushed granite with maximum nominal size of 20 mm and good quality well-graded river sand of maximum size 4.75 mm were used as coarse and fine aggregates, respectively. Poly-carboxylate ether (PCE) based chemical admixture was used as superplasticizer.

2.2 Mix Proportions & Test Methods

The mix details of various SCCs developed in the present study is given in Table 1. The mix design methodology followed in the present study was developed by Dinakar and Manu [3] based upon the efficiency concept. Three strength categories 80, 100 and 120 MPa of normal vibrated and self-compacting concretes were developed. In the case of SCCs, metakaolin replacements were taken as 7.5, 15 and 22.5 % respectively. It was also ensured that all the SCCs mixes satisfied the regulations given in EFNARC guidelines [4]. The fresh properties of the SCCs were determined by slump flow, V- funnel and L-Box blocking ratio, and the mechanical properties by compressive strength, split tensile strength, elastic modulus and autogeneous shrinkage.

Table 1 Mix details of the concretes developed

Name	TCM kg/m^3	MK (%)	Cement (c) kg/m^3	Total Aggregate, kg/m^3	Water kg/m^3	w/(c + k_{28}*m)	SP (%)	VMA (%)
NC80	516	0	516	1031	160	0.31	0.40	0
SCC80	550	7.5	508.75	1075	221	0.31	0.90	0.10
NC100	596	0	596	998	155	0.26	0.60	0
SCC100	550	15	467.5	1113	197	0.26	1.25	0.05
NC120	681	0	681	964	150	0.22	0.90	0
SCC120	550	22.5	426.2	1156	170	0.22	1.45	0.05

TCM Total Cementitious Materials Content (Powder Content), *MK* Metakolin, *SP* Super plasticizer, *VMA* Viscosity Modifying Agent, *NC* Normal Concrete, *SCC* Self Compacting Concrete, k_{28} efficiency of metakaolin at 28 days, *m* metakaolin content

3 Results and Discussions

3.1 Fresh Properties

The fresh properties results are presented in Table 2. From the results it was observed that, increase in the metakaolin replacement content influences many of the properties of fresh concrete. It was observed that as the metakaolin content increases the slump flow also increases correspondingly, this may be due to the liquefying and dispersive action of the superplasticizer [5]. The higher T_{500}, V-funnel times and L-Box ratios indicates that the addition of metakaolin improves the viscosity of the mix. In other words it significantly improves the cohesiveness of the mix. All the normal vibrated concretes had a design slump of more than 100 mm.

3.2 Compressive Strength

The results of compressive strength test are included in Table 3 and the strength gain rate of all the concretes with age are illustrated in Fig. 1. The result shows except NC 120 all the normal vibrated concretes have obtained their design strengths. SCC 120 attained its design strength only at 90 days. It was also observed that up to third day all the normal vibrated concretes show comparatively higher results than the corresponding metakaolin SCC, but from seventh day onwards all

Table 2 Fresh properties of the developed mixes

Mix	T_{500} (s)	Slump flow (mm)	V funnel time (s)	L-Box ratio
SCC 80	3.34	605	12.06	0.87
SCC 100	6.31	625	37.59	0.81
SCC 120	9.91	670	58	0.78

Table 3 Hardened properties of the developed mixes

Mix	28 day Compressive strength (MPa)	90 day Compressive strength (MPa)	Tensile strength (MPa)	E- Modulus (GPa)
SCC 80	94.1	101.2	4.65	41.04
SCC 100	105.8	112.2	4.69	43.95
SCC 120	107.5	121.2	5.16	53.48
NC 80	88.9	97.7	4.66	45.53
NC 100	103.2	109.5	4.77	51.58
NC 120	101.5	111.6	5.22	56.16

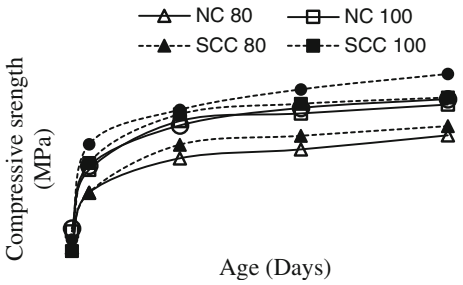

Fig. 1 Strength gaining behaviour

the high reactive metakaolin SCCs surpassed the NCs. From 28th day onwards significant improvements were observed in the case of SCCs. By comparing the 56th and 90th day compressive strength it is clear that the strength gain rate in normal vibrated concretes is less than the metakaolin SCC. This may be due to the secondary pozzolanic reaction which contributes towards the strength improvement. The most significant finding of this investigation is that to obtain 111.6 MPa compressive strength, normal vibrated concrete required a powder content of 681 kg/m^3, whereas in the case of SCC a powder content of 550 kg/m^3 is sufficient to produce 120 MPa. These results justify the effective use of metakaolin in the development of high strength SCCs.

3.3 Tensile Strength

The results show that in general tensile strength is lower in SCC than the NC (Table 3). Generally aggregate-paste interlocking has a great influence on the tensile strength than compressive strength of concretes. The use of PCE based superplasticizers or higher fines content may significantly affect the bond behaviour. Roncero and Gettu [6] pointed out that large calcium hydroxide (CH) crystals and ettringite will be formed when PCE based superplasticizers were used. These large CH crystals weaken the aggregate–paste transition zone and, as a result, decrease the

concrete's tensile strength. As far as the influence of fines content is concerned, increasing the volume of fines will obviously increases the specific surface area of the aggregates thereby increasing the aggregate-paste transition zone, which is the weakest phase of concrete. Similar findings were also observed previously in SCCs by Parra et al. [7].

3.4 Modulus of Elasticity

From the elastic modulus results it was observed that, there is a slight tendency for the SCCs to show a somewhat lower modulus of elasticity (Table 3), than the normal vibrated concretes. These results also agree with Felekoglu et al. [8], who also concluded that differences between the SCC and NC was below 5 %, in the tests carried out to determine the modulus of elasticity of two types of concretes. In the present investigation normal vibrated concretes exhibited 9.87 %, 7.04 %, and 4.76 % greater modulus of elasticities than that of SCCs for 80, 100 and 120 MPa mixes. Also, according to the nano-indentation tests carried out by Zhu and Bartos [9], the aggregate–paste transition zone is also denser and stiffer in SCCs. The lower stiffness of SCCs' can only be explained by the more amount of paste and paste's deformability is higher than that of the aggregates [8].

3.5 Autogenous Shrinkage

The average autogenous shrinkage strains of SCCs and normal concretes are shown in Fig. 2. From the figure it can be seen that there is an increase in shrinkage strains in all the concretes. It was observed that the final shrinkage of SCC 80 and NC 80 are almost same, may be because of the same cement contents employed in the mixes. However, 100 and 120 grade SCCs showed lesser shrinkages than the corresponding normal concretes. This may be probably due to the reduction in the cement contents of the corresponding mixes, i.e., SCC 100 and 120 contains

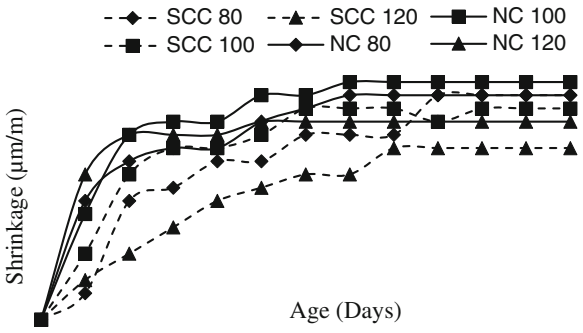

Fig. 2 Shrinkage characteristics of all concretes

467.5 and 426.2 kg/m^3 of cement whereas NC 100 and 120 contains 596 and 681 kg/m^3 of cement respectively. By comparing the normal concrete shrinkage behaviour it was observed that NC 120 showed lesser shrinkage than NC 100. This could be due to the effect of superplasticizer and low water binder ratios. When a large amount of superplasticizer is used, the hydration is significantly delayed, thereby providing a delay in autogenous shrinkage [10]. Also during this time a formation of more rigid structure of hydrated cement paste will occur at this low water binder ratio.

4 Conclusions

This study was carried out to evaluate the fresh and hardened properties of SCC containing MK with different replacement levels. The following conclusions can be made from the obtained results:

- It is possible to develop high strength self-compacting metakaolin concretes of strengths ranging from 80 to 120 MPa, at various replacement levels ranging from 7.5 to 22.5 %.
- The increase in metakaolin content in SCC increases the viscosity of the mix.
- Tensile strength and the modulus of elasticity are lesser for SCC compared to the corresponding normal vibrated concrete.
- Using metakaolin there is a reduction in autogeneous shrinkage.

References

1. Dinakar, P.: High reactive metakaolin for high strength and high performance concrete. Indian Concr. J. **85**(4), 28–34 (2011)
2. Hassan AAA, Lachemi M, Hossain KMA(2010) Effect of metakaolin on the rheology of self-consolidating concrete. In: Design, Production and Placement of Self-Consolidating Concrete. Rilem Bookseries, vol 1(3), pp. 103–112
3. Dinakar, P., Manu, S.N.: Concrete mix design for high strength self-compacting concrete using metakaolin. Mater. Des. **60**, 661–668 (2014)
4. Self Compacting Concrete European Project Group. The European Guidelines for Self-Compacting Concrete. (2005). BIBM, CEMBUREAU, EFCA, EFNARC and ERMCO, http://www.efnarc.org, 27 Jan 2014
5. Safiuddin, M., West, J.S., Soudki, K.A.: Flowing ability of self-consolidating concrete and its binder paste and mortar components incorporating rice husk ash. Can J Civil Eng **37**, 401–412 (2010)
6. Roncero, J., Gettu, R.: Influencia de los superplastificantes en la microestructura de la pasta hidratada y en el comportamiento diferido de los morteros de cemento. Cemento Hormigon **832**, 12–28 (2002)
7. Parra, C., Valcuende, M., Gomez, F.: Splitting tensile strength and modulus of elasticity of self- compacting concrete. Constr. Build. Mater. **25**, 201–207 (2011)

8. Felekoglu, B., Turkel, S., Baradan, B.: Effect of water/cement ratio on the fresh and hardened properties of self-compacting concrete. Build Environ **42**(4), 1795–1802 (2007)
9. Zhu, W., Bartos, P.J.M: Microstructure and properties of interfacial transition zone in SCC. In: Yu, Z., Shi, C., Khayat, K.H., Xie, Y.(eds.). Proceedings of First International Symposium on Design Performance and use of Self Consolidating Concrete, RILEM Publications S.A.R.L., Changsha, pp. 319–27 (2005)
10. Termkhajornkita, P., Nawaa, T., Nakaib, M., Saito, T.: Effect of fly ash on autogenous shrinkage. Cem. Concr. Res. **35**, 473–482 (2005)

Effective Clinker Replacement Using SCM in Low Clinker Cements

Sreejith Krishnan, Arun C. Emmanuel and Shashank Bishnoi

Abstract Supplementary cementing materials (SCM) are being widely used for partial clinker replacement. The hydration of cement results in the production of portlandite which in turn reacts with the SCM to produce C-S-H. A combination of SCM and other mineral additives is being used in new ternary and quaternary blends having very low clinker factors. Other similar reactions producing more complex hydration products are known to occur in composite cements. Although sustainability concerns require that clinker factors and the grade of SCM used to be as low as possible, it is the composition of the clinker and the other components that will govern optimal proportions that would lead to highest degrees of hydration possible. While sufficient quantities of hydration products that react with SCM may not be produced at very low clinker factors, the reactive fraction in an SCM may be too low to allow high clinker replacement. This paper studies the case of Limestone Calcined Clay Portland Cement (LC^3) to understand how the clinker and SCM compositions would affect the possible replacement levels. It is demonstrated how a scientific approach can be used for the optimal design of low clinker cements.

1 Introduction

The rapid urbanization and infrastructure development undertaken by developing nations has resulted in a huge increase in cement consumption. The cement demand is set increase nearly four fold of the current demand by the year 2050 [1]. Cement industry is one of the major sources of man made carbon dioxide emissions with around 0.815 tonne of carbon dioxide emitted per tonne of cement produced. The present challenge is to find sustainable solutions that can reduce the carbon

S. Krishnan (✉) · A.C. Emmanuel · S. Bishnoi
Indian Institute of Technology, Hauz Khaz, New Delhi 110016, India
e-mail: sree1111@gmail.com

K. Scrivener and A. Favier (eds.), *Calcined Clays for Sustainable Concrete*,
RILEM Bookseries 10, DOI 10.1007/978-94-017-9939-3_64

footprint of the cement industry without compromising the developmental needs of the nations. Many techniques have been proposed to improve the environmental friendliness of the cement industry such as Alternate Fuel and Raw materials (AFR), Waste Heat Recovery (WHR), improved thermal & electrical efficiency and clinker substitution. Out of the above mentioned methods, clinker substitution seems to be most promising.

Clinker substitution involves replacing a part of clinker with mineral additives known as Supplementary Cementing Materials (SCM). These mineral additives such as fly ash, calcined clay, ground granulated blast furnace slag etc are pozzolanic in nature. These SCM contain reactive silica (S) which can react with the portlandite (CH) produced from the hydration of cement to form calcium silicate hydrate (CSH) [2].

$$C_3S + 5.3H \rightarrow C_{1.7} - S - H_4 + 1.3CH \quad (1)$$

$$C_2S + 4.3H \rightarrow C_{1.7} - S - H_4 + 0.3CH \quad (2)$$

$$S(\text{Pozzolana}) + 1.5CH + 2.8H \rightarrow C_{1.5} - S - H_{3.9} \quad (3)$$

2 Low Clinker Cements

Clinker replacement up to 35 % is possible using single SCM beyond which arises many practical difficulties. While it is possible to replace up to 70 % of clinker using GGBS, the availability of slag is an issue. Fly ash which is one of the most abundant SCM available is a slow acting pozzolan. The strength gain due to addition of fly ash occurs mostly at later ages [3]. On the other hand, metakaolin is a fast acting pozzolan but adversely affects the workability of the paste due to high fineness [4]. Studies have shown that the addition of limestone in ordinary Portland cement improves the strength and rheological properties due to filler effect. Limestone was believed to be acting as inert filler in the Portland cement system. However recent studies have revealed that a small quantity of limestone does in fact react with the aluminate phase present in the clinker to form carboaluminate phases which can improve the properties of the cement matrix [5].

Low clinker factors can be achieved using ternary cements in which a clinker is replaced by a combination of SCM. These combinations can be optimized so as to improve the desirable properties like strength, workability and durability. In this study, one such novel cement blend called Limestone Calcined Clay Cement (LC^3) in which clinker is replaced with a combination of calcined clay (metakaolin) and limestone is further investigated (Fig. 1).

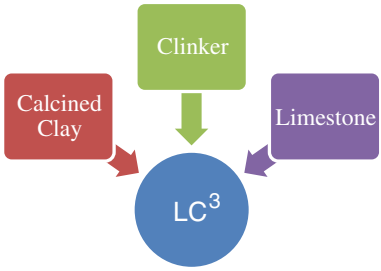

Fig. 1 Synergy in LC^3 system

3 Optimization of LC^3 System

As the pozzolanic reaction depends upon the amount of portlandite produced by hydration reaction of cement, it is critical to estimate the quantity of portlandite produced in the system for the optimal composition design for LC^3. The clinker phases can be calculated with the help of modified Bogue equations, using the oxide composition obtained from chemical analysis of clinker. Clinkers with higher alite content will be more suitable for the production of low clinker factor cements due to the higher quantity of calcium hydroxide produced. The theoretical maximum of portlandite available can be estimated from the Eqs. (1) and (2) and verified experimentally with the help of Thermo-Gravimetric Analysis (TGA) and X-Ray Diffraction (XRD). It is also important to keep in mind that the rate of hydration depends upon various parameters such as fineness, water/cement ratio used etc. The LC^3 tries to take advantage of the formation of carboaluminate in the system so as to improve properties of the cement matrix. Hence it is essential to understand the reaction stoichiometry of formation of carboaluminate phase. One mole of calcium carbonate can react with one mole of metakaolin to produce one mole of monocarboaluminate phase. This reaction takes place in the presence of excess calcium ions in aqueous solution [6].

$$A + CaCO_3 + 3CH + H \rightarrow C_3A \cdot CaCO_3 \cdot H_{12} \quad (4)$$

Formation of monocarboaluminate phase is known to stabilize the ettringite phase. This results in the reduction of monosulpate phase in the LC^3 system as compared to conventional Portland cement system [7]. In order to better understand these reactions and reaction kinetics, it beneficial to simulate them using laboratory grade reagents. The volume efficiency is defined as the volume of product formed when a unit volume of cement reacted. Volume efficiency can be determined by calculating the specific gravity of the reactants and products formed. The porosity is also an indicator of the volume efficiency which can be measured for a given

cement paste using Mercury Intrusion Porosimetry (MIP). The porosity can then used for making strength predictions.

The carboaluminate formation can be investigated with the help of modified lime reactivity test. The lime reactivity test, as specified in the Indian Standard 1727 – 1967, measures the strength of mortar cubes cast with mixing $Ca(OH)_2$, pozzolan and standard sand. The specimens are cured at 90–100 % relative humidity at 50 °C and tested after 10 days. However, compressive strength may not be the best metric for characterization of the pozzolan. The test can be modified by casting paste samples instead of mortar cubes while maintaining the same curing conditions. The pozzolan used will be a combination of metakaolin and limestone. The paste can then be characterised using TGA and XRD to estimate the quantity of carboaluminate phases (decomposes beyond 60 °C) [8] and portlandite left at various ages. The lime – pozzolan rate of reaction can be estimated with the help of isothermal calorimetry which measures the total heat released. Thermodynamic modelling can help in identification of products formed by minimizing the Gibbs energy of the system (Fig. 2).

Incompatibilities between constituent materials could be a potential problem. The presence of certain impurities can affect the rate of hydration and reaction products formed, which can result in loss of strength at later ages. This can be detected by measuring the total heat produced during the hydration of cement paste coupled with an XRD analysis for the phases formed. Gypsum plays an important role in high aluminate cements such as LC^3. Lack of sufficient sulphate content will result in flash setting whereas too much sulphate can poison the aluminates. Therefore it is essential to optimize the sulphate content present in the system. An easy way to do this would be to conduct isothermal calorimetry on pastes with varying gypsum content. The ideal sulphate content can be calculated from the location and intensity of the aluminate hydration peak of the isothermal calorimetric curve.

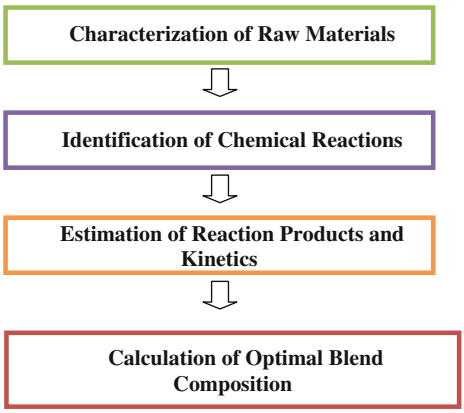

Fig. 2 Base framework for LC^3 optimization

4 Conclusions

As the global focus shift towards sustainability along with lack of raw materials, it has become essential to identify innovative solutions to ensure that cement industry is not left behind. Low clinker cements can be a potential solution to help the cement industry to innovate further. Development of a scientific framework for designing such cements will help in extracting maximum potential from such systems. A scientific method of design for developing adequate knowledge base can help in optimizing the cement composition and the prediction of properties of similar systems. Another advantage is that incompatibilities between constituent raw materials can be identified at an early stage. This can significantly reduce the time required for the cement to make the transition from laboratory to the field. One such framework for the design of low clinker cements has been presented in this study. While this study is focussed on Limestone Calcined Clay Clinker cement (LC^3), the frame work can be utilized for the design of similar cements containing other supplementary cementing materials.

References

1. Technology Roadmap, Low-Carbon Technology for Indian Cement Industry: Conference Proceedings—International Energy Agency (2012)
2. Taylor, H.F.W.: Cement Chemistry, 2nd edn. Thomas Telford, London (1997)
3. Lothenbach, B., Scrievener, K., Hooton, R.D.: Supplementary cementitious materials. Cem. Concr. Res. **41**, 1244–1256 (2011)
4. Ramezanianpour, A.A., Jovein, H.B.: Influence of metakaolin as supplementary cementing material on the strength and durability of the concretes. Constr. Build. Mater. **30**, 470–479 (2012)
5. Bonavetti, V.L., Rahhal, V.F., Irassar, E.F.: Studies of carboaluminate formation in limestone blended cement. Cem. Concr. Res. **31**, 853–859 (2001)
6. Antoni, M., Martinera, F., Scrievner, K.: Cement Substitution by a combination of metakaolin and limestone. Cem. Concr. Res. **42**, 1579–1589 (2012)
7. Lothenbach, B., Saout, G.L., Galluci, E., Scrievner, K.: Influence of limestone on hydration of cement. Cem. Concr. Res. **38**, 848–860 (2008)
8. Indian Standard 1727–1967: Methods of test for pozzolanic materials. Bureau of Indian Standard

Durability Characteristics of Sustainable Low Clinker Cements: A Review

Vineet Shah, Aneeta Mary Joseph and Shashank Bishnoi

Abstract Cement is an important industrial product for economic development. Global consumption of cement is predicted to continue to grow from current level of 450 kg per capita with escalation in economic growth of world. Cement production is an energy intensive industry and the industry is facing major challenges in terms of the air pollutants produced during production along with that amount of energy resources invested in the production process and consumption of natural resources. Use of low clinker cement can ensure to provide sustainable explanation to minimize the total environmental impact. Use of various supplementary cementitious materials as clinker replacement is being carried out since past 70 years. In order to mitigate the long term impacts on structures built using such binders, the durability study is of utmost importance. In this paper a comparative study of various low clinker cements consisting of fly-ash, slag, calcined clay, limestone and their subsequent effect on durability is reviewed.

Keywords Supplementary cementitious materials · Clinker replacement · Durability · Ternary cement · Metakaolin

1 Introduction

Economic and demographic growth of the place is fundamentally associated to the type of infrastructure it possesses. Different building materials steel, wood, cement, concrete, bricks etc. are being used to meet the infrastructure demand. Global consumption of cement is predicted to continue to grow from current level of 450 kg per capita with escalation in economic growth of world. Cement industry contributes 5-8 % of global CO_2 emission of world and with the increase in demand of cement contribution of cement industry in environmental pollution is set to rise.

V. Shah (✉) · A.M. Joseph · S. Bishnoi
Department of Civil Engineering, Indian Institute of Technology, Delhi, India
e-mail: vineet.shah9@gmail.com

K. Scrivener and A. Favier (eds.), *Calcined Clays for Sustainable Concrete*,
RILEM Bookseries 10, DOI 10.1007/978-94-017-9939-3_65

Use of by-products or industrial wastes possessing pozzolanic properties like slag, calcined clay, fly-ash, rice husk, silica fume etc. by cement industry is known now from a long time, it can be seen as one of the development alternatives towards a sustainable material. Portland slag cement, Portland fly-ash cement, Portland limestone cement are examples of blended cements which are already standardized. Use of supplementary cementitious materials (SCMs) helps to refine the pore diameter, improves durability performance of concrete [1]. Binary blended cements have got associated limitations with it, low hydraulic activity of blended cements leads to increase in setting time, low early age strength, use of admixtures, increased curing period [1]. Methods like using finer SCMs after further grinding and chemical activation being implemented in order to proliferate the reactivity of SCMs during early age but they are not effective to the required level [2]. Incorporating one SCMs for certain specific durability performance may lead to attenuated performance of other durability parameters [2].

Development of composite cements, with Portland cement along with two different SCMs has been increased in past two decades. Using two different SCMs at the same time will help to compensate shortcoming of each other, and also has a twofold effect of higher packing density and microstructure densification [2, 3]. Ternary blends containing combinations of fly-ash/silica-fume, slag/silica-fume, slag/fly-ash, limestone/fly-ash, limestone/slag with Portland cement are already reported.

Metakaolin obtained from calcining clay has received sizeable interest in recent years as a pozzolanic material. On heating, the long range ordered structure of kaolin gets breakdown. About 14 % of water is lost from kaolin when heated till the temperature of 900 °C, resulting from this dehydroxylation and disorder generating a highly reactive amorphous aluminosilicate phase, metakaolin. Various studies has been carried out using metakaolin as pozzolanic material.

Primary reason for the use of metakaolin as cement replacement is its wide availability and durability improvement. In order to mitigate the long term impacts on structures built using such binders, the durability study is of utmost importance. In this paper a comparative study of various low clinker cements and their subsequent effect on durability is reviewed as information pertaining to these blends is comparatively scare. In the article, composite cements having clinker content of 40 to 60 percent with two different types of SCMs are studied. Accumulative study of some of the factors affecting durability of the low clinker cement is discussed in the article.

2 Chloride Penetration/Migration

Corrosion of steel in reinforced concrete is one of the most common reason for deterioration of concrete. Reinforcement corrosion is related to the diffusion of chloride ions in concrete because of difference in concentration. Ahmed et al. [4] carried out tests on different binary and ternary cements containing OPC, fly-ash, slag and silica fume to evaluate permeability of chloride ions in concrete. Charge passed in ternary blend of fly-ash and silica fume is lower than the charge passed

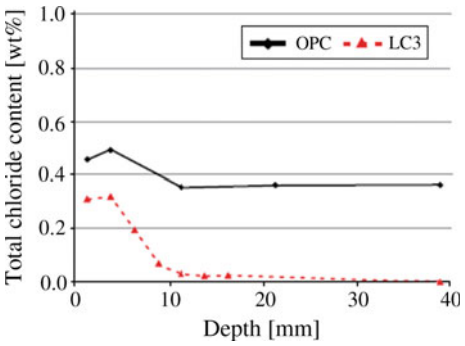

Fig. 1 Chloride profile after 2 years of ponding in 0.5 M NaCl solution [8]

through fly-ash binary blend signifying importance of ternary blend of fly-ash. The ternary blend of slag and silica fume also showed reduction in charge passed as compared to the control blend of OPC and respective binary blends of slag. The results infer that addition of silica fume in binary blends contributes to reduce the chloride ion permeability of concrete. Nehdi et al. [5] replaced 50 % OPC with 25 % fly-ash and 25 % slag. The charge passed through the concrete reduced as compared to the reference OPC. However, the percentage reduction of charge passed with his blends were less as compared to Ahmed et al. results which replaced 60 % clinker with slag and silica fume.

Similar results were reported by Ali et al. [6] on concurrent use of different amount of slag and silica fume (30-50 % replacement) with OPC. Simultaneous use of silica fume and slag resulted in substantial decrease of the charge passed through concrete in RCPT. Thomas et al. [7] showed that concrete with ternary blend of fly-ash and silica fume has lower chloride diffusivity and enhanced the resistance than concrete containing either silica fume or fly-ash.

The chloride profile of LC^3 cement in which 30 % clinker is replaced by calcined clay and 15 % by limestone, after 2 years of ponding in sodium chloride solution, is better as compared to OPC implying that the resistance to penetration of chloride ions is pretty good [8] as shown in Fig. 1. Kim et al. [9] reported increase in resistance against chloride penetration on replacing 20 % OPC with metakaolin because of continued pozzolanic reaction resulting decrease in porosity.

3 Carbonation

The reaction of calcium hydroxide in concrete with carbon dioxide present in the atmosphere leads to formation of calcium carbonate and water. Due to carbonation, pH of concrete gets reduced possessing risk of corrosion of steel embedded in concrete. Cementitious combinations comprising of 0-40 % fly-ash and 0-15 % silica fume were incorporated in study conducted by khan et al. [10]. Carbonation results of such blends shows that with increase in fly-ash proportion in the blend the carbonation increase whilst increase in proportion of silica fume demonstrated

insignificant increase in carbonation depth. Daria presented influence of high calcium fly ash (HCFA) in blended cements on carbonation resistance of structure. He also adopted composition similar to the work of Nehdi et al. [5]. The carbonation tests were carried out at CO_2 concentration of 1 % and relative humidity of 60 % for different exposure age. The composite blend comprising of slag and fly-ash showed the greatest depth of carbonation. The carbonation depth increased with higher clinker substitution in consistent with the work of other researchers.

Espion et al. carried out work to validate the composition of new ternary cements comprising of clinker, limestone and slag, the clinker percentage in the blends was varied from 18-60 % and were tested for durability and mechanical performance. Carbonation study of ternary cement was carried out by exposing specimens at CO_2 concentration of 1 % and relative humidity of 60 %. Blend comprising of 34 % slag and 6 % limestone showed carbonation depth similar to that of control mixes whereas further reduction in clinker content lead to greater carbonation depth.

Antoni [11] also worked on similar type of substitution in his ternary binder. Instead of slag he used calcined clay for replacement of OPC along with limestone having ratio of 2:1. The results of natural carbonation does not show noteworthy difference between the blends as the exposure time was not long enough. Whilst accelerated carbonation at 3 % CO_2 concentration showed deepest carbonation ingress for ternary blend and lowest for OPC. For the similar blend work carried out by Joseph [12] shows carbonating depth obtained for such a blend is 3-5 times more. Increase in carbonation depth of 100-370 % was observed by Kim et al. [9] on replacing 20 % OPC with metakaolin. Bai et al. [13] exposed concrete specimens at 4 % CO_2 concentration and 65 % relative humidity containing metakaolin and fly-ash. The carbonation depth increases with increasing substitution by fly-ash and by systematically substituting fly-ash with metakaolin decrease in carbaontion depth was obtained till a certain optimum level as shown in Fig. 2. With increase in

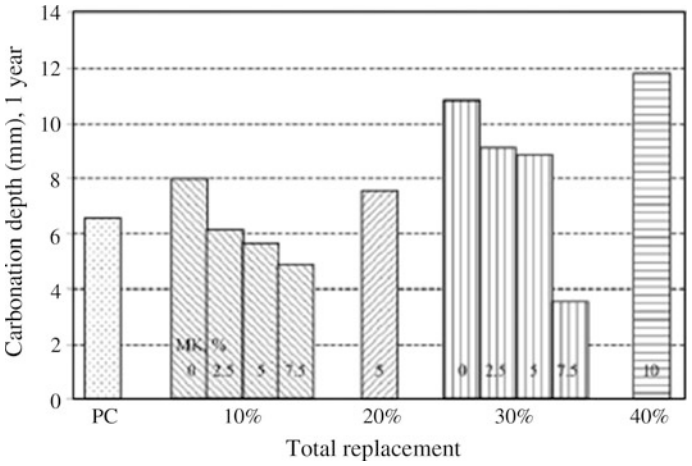

Fig. 2 Carbonation depth of blend containing OPC, fly-ash and metakaolin at 10, 20, 30, 40 % cement replacement [14]

replacement level by pozzolanas calcium hydroxide from the system gets consumed at faster rate and the amount of reserve alkalinity necessary for protection of reinforcement reduces down quickly.

4 Sulfate Attack

Sulfate attack is caused by sulfate ions present either internally in the system or due to penetration form external source. Sulfate ions react with tri-calcium aluminate or calcium hydroxide present in the system resulting in the formation of ettringite or gypsum which occupies larger volume as compared to reactants leading into disintegration of concrete. Sulfate ions in presence of carbonate, react with calcium silicate hydrate (CSH) to form thaumasite leading to severe weakening of concrete strength as CSH is getting consumed which is the binding agent in concrete. Portland limestone cement with up to 15 percent inter-ground limestone is approved in Canadian standards. Performance of ternary cement in sulfate exposure condition was carried out by Hooton et al. [14] by replacing 50 % of Portland limestone cement with slag. On addition of slag the expansion of specimens in the sodium sulfate solution was well within the range whereas blends of Portland limestone cement showed a greater expansion making it inappropriate to use in sulfate environment. Portland limestone cement with 50 % slag replacement showed better performance at low temperatures at which thaumasite is formed in presence of carbonates and sulfate as compared to 30 % replacement with slag. Expansion due to sulfate exposure reported by Ghrici et al. [15] in limestone and fly ash ternary blends were found similar to the expansion observed with only fly-ash. Similar results were reported by Espion the change in length for the blends containing slag and limestone was insignificant whereas specimens made from OPC showed notable change in length after one year immersion of specimens in sodium sulfate solution.

The ternary blend comprising of metakaolin/fly-ash, marble dust and OPC was subjected to sulfate attack under magnesium sulfate solution. The ratio of metakaolin/fly-ash to marble dust was 2:1, 50 % of OPC was replaced by SCMs. After 60 days of exposure in sulfate solution blends comprising of metakaolin got deteriorated to an extent that change in length was not measured, whereas blends with fly-ash showed expansion within the limit [16]. Ivan et al. [17] reported evidence of gel like substance in cubes containing metakaolin content as low as 7 % at 5 °C implying association of alkali carbonate reaction. Use of SCMs leads to reduction and discretization of pores reducing the penetration rate of sulfate ions. The alumina content of mineral admixtures influences the performance of cement in sulfate environment.

5 Alkali Silica Reaction

Alkali-Silica Reaction (ASR) occurs in concrete on reaction of reactive amorphous silica and hydroxyl ions present in alkaline nature of concrete. The reaction results in formation of ASR gel which swells as it absorbs water leading to spalling and loss of strength of concrete because of expansive pressure exerted inside the material. Robert et al. [18] studied the influence of fly-ash and metakaolin to mitigate expansion caused by ASR. Blends having OPC replaced by 25 % fly-ash and 5-8 % with two different types of metakaolin were used. The results of accelerated mortar bar test and concrete prism test infers that ternary blend cement does not provide any extra benefit to mitigate ASR over blend containing only metakaolin. Reduction in expansion is mixture of behavior of fly ash and metakaolin rather than superposition of individual binders.

Hooton [14] Portland limestone cement under alkali environment showed average change in length greater than the limit specified but on replacement with slag the average change in length was well within the limits. The ternary cement showed less expansion as compared to OPC. Expansion in concrete due to alkali silica reaction was completely eliminated when OPC was replaced with 15 % metakaolin as reported by Sabir et al. [19]. Favier et al. [20] found that ternary blend of limestone and calcined clay with 50 % OPC replacement showed the ASR is mitigated by use of such blend, however they are skeptical about the performance of the same blend in long term as the limestone present in the system also consume alumina which is the most important parameter in controlling ASR.

6 Conclusions

- By using combinations of mineral admixtures substantial chloride resistance can be achieved and performs better than binary cement. Calcined clay reduces the chloride penetration resistance because of chloride binding capacity and intrinsic diffusivity. Calcined clay in coalition with carbonate mineral admixtures can help in further increasing the resistance because of formation of carboaluminates and other hydration products.
- Carbonation tend to increase after certain maximum replacement level of OPC with mineral admixtures. Calcined clay shows greater depth of carbonation at all the replacement levels as compared to OPC when used either of binary or ternary cement blends.
- ASR is mitigate to a large extent by incorporating SCMs as OPC replacement. Metakaolin with 20-25 % in cement has seen to perform well, metakaolin consumes freely available CH and and CH/SiO_2 (active) and hence help in dipping formation of swelling gel.

- Due to synergic effect of different materials in composite cements the sulfate resistance of the cement increases. Use of combination slag, limestone, fly-ash as clinker replacement shows better durability against sulfate, whilst blends of calcined clay and limestone seems to get deteriorate in sulfate environment further studies on such blends is required.
- Packing density plays a significant role to improve properties of concrete. With wide range of particles among various binder component will help in improving the packing density which will reduce the voids in concrete hence enhancing durability and also creating synergic effect between different constituents. Optimizing calcined clay can help to achieve required performance with its finer particle size distribution.

References

1. Mehta, P.K., Monteiro, P.J.M.: Concrete: Structure, Properties, and Materials. Prentice Hall, New Jersey (1993)
2. Tongsheng, Z., Xiangyang, L., Jiangxiong, W., Qijun, Y.: Influence of preparation method on the performance of ternary blended cements. Cem. Concr. Compos. **52**, 18–26 (2014)
3. Deepa, A.S., Verma, A.K., Prakash, K.B.: 'The need of ternary blended concrete' Indian. J. Appl. Res. **2**, 80–81 (2012)
4. Ahmed, M.S., Kayali, O., Anderson, W.: Chloride penetration in binary and ternary blended cement concretes as measured by two different rapid methods. Cem. Concr. Compos. **30**, 576–582 (2008)
5. Nehdi, M., Pardhan, M., Koshowski, S.: Durability of self consolidating incorporating high volume replacement composite cements. Cem. Concr. Res. **34**, 2103–2221 (2004)
6. Ali, R.B., Hamed, Z., Mohamad, M.M.: Mechanical and durability properties of ternary concretes containing silica fume and low reactivity blast furnace slag. Cem. Concr. Compos. **34**, 663–670 (2012)
7. Thomas, M.D.A., Shehata, M.H., Shashiprakah, S.G., Hopkins, D.S., Cail, K.: Use of ternary cementitious systems containing silica fume and fly-ash in concrete. Cem. Concr. Res. **29**, 1207–1214 (1999)
8. Scrivener, K.L.: Options for the future of cement. Indian Concr. J. **88**, 11–21 (2014)
9. Kim, H.S., Lee, S.H., Moon, Y.H.: Strength properties and durability aspects of high strenth concrete using Korean metakaolin. Constr. Build. Mater. **21**, 1229–1237 (2007)
10. Khan, M.I., Lynsdale, C.J.: Strength, permeability, and carbonation of high-performance concrete. Cem. Concr. Res. **32**, 123–131 (2002)
11. Antoni, M.: Investigation of cement substitution by blends of calcined clays and limestone. PhD Thesis, ÉcolePolytechniqueFédérale De Lausanne (2013)
12. Joseph, A.M.: Investigation and modeling of durability of LC3 cement with respect to Initiation of corrosion. M.S. (R) thesis, Indian Institute of Technology, Delhi (2015)
13. Bai, J., Wild, S., Sabir, B.B.: Sorptivity and strength of air-cured and water-cured PC-PFA-MK concrete and the influence of binder composition on carbonation depth. Cem. Concr. Res. **32**, 1813–1821 (2002)
14. Hooton, R.D., Ramezanianpour, A., Schutz, U.: Decreasing the clinker component in cementing materials: Performance of Portland-Limestone Cements in Concrete in Combination with Supplementary Cementing Materials Concrete Sustainability Conference, pp. 1–15 (2010)

15. Ghrici, M., Kenai, S., Said-Mansour, M.: Mechanical properties and durability of mortar and concrete containing natural pozzolana and limestone blended cements. Cement Concr. Compos. **29**, 542–549 (2007)
16. Shah, V.: Feasibility study of ternary cement containing clinker, fly-ash and marble dust. Master's thesis, Indian Institute of Technology, Delhi (2014)
17. Ivan, S., Stan, W., Edward, M.: The resistance of Metakaolin (MK) Portland Cement (PC) concrete to the Thaumasite-type of Sulfate Attack (TSA) programme of research and preliminary results. Cement Concr. Compos. **25**, 931–938 (2003)
18. Robert, D.M., Amal, R.J., Victor, Y.G., Kimberly, E.K.: Assessment of binary and ternary blends of metakaolin and class C fly ash for alkali silica reaction mitigation in concrete. Cement Concr. Res. **40**, 1664–1672 (2010)
19. Sabir, B.B., Wild, S., Bai, J.: Metakaolin and calcined clays as pozzolans for concrete: a review. Cement Concr. Compos. **23**, 441–454 (2001)
20. Favier, R.A., Dunant, F.C., Scrivener, K.L.: Alkali–silica reaction mitigating properties of ternary blended cement with calcined clay and limestone. International Congress on Durability of Concrete, New Delhi (2010)

Calcined Shale as Low Cost Supplementary Cementitious Material

Saamiya Seraj, Rachel Cano, Raissa P. Ferron and Maria C.G. Juenger

Abstract Despite the various benefits of using metakaolin as a supplementary cementitious material (SCM), the high price of metakaolin limits its use in concrete to premium applications. However there are other sedimentary minerals, such as calcined shale, that may be able to fill the need for low cost, abundant SCMs in concrete construction. The study presented here investigated a low cost calcined shale, sourced from a lightweight aggregate producer, and compared its performance as an SCM to that of a commercially available metakaolin. The effect of both SCMs on compressive strength, resistance to alkali silica reaction and mixture workability were evaluated. Results show that, other than early age compressive strength, the performance of calcined shale in cementitious mixtures is comparable to that of metakaolin. Differences in behavior of the SCMs are discussed in the context of their chemical and physical properties.

Keywords Alternative SCMs · Natural pozzolans · Calcined clay · Metakaolin · Shale

1 Introduction

The benefits of metakaolin as a supplementary cementitious material (SCM) in terms of improving concrete strength and durability have been established in previous literature [1–4]. However, due to limited sources and a high demand of pure kaolinite from industries other than concrete, the price of metakaolin is very high. While the use of metakaolin as an SCM can become prohibitive due to its cost, there are other calcined sedimentary minerals that may be able to fill the need for low cost, abundant SCMs in concrete construction. Clay shale (referred to as shale

S. Seraj · R.P. Ferron · M.C.G. Juenger (✉)
University of Texas at Austin, Austin, USA
e-mail: mjuenger@mail.utexas.edu

R. Cano
Texas Department of Transportation, Houston, USA

K. Scrivener and A. Favier (eds.), *Calcined Clays for Sustainable Concrete*,
RILEM Bookseries 10, DOI 10.1007/978-94-017-9939-3_66

elsewhere in this paper), a fine grained sedimentary rock formed from the compaction of clay minerals and other particulate debris [5, 6], can be one such promising, low cost SCM when calcined. Although previous research on the use of calcined shale as an SCM is limited, results from past studies are encouraging [7–9] and showed that the 28 day compressive strengths of specimens with calcined shale as a cement replacement were similar to those of control specimens made with only cement. The main motivation of the study presented here was to further investigate calcined shale as a low cost SCM and to compare its performance in terms of mortar compressive strength, resistance to alkali silica reaction (ASR) and mixture workability to that of the more well-known metakaolin SCM.

2 Materials and Methods

The calcined shale used for this paper, referred to as "Shale-T," was sourced from a lightweight aggregate producer in Texas, USA, and cost approximately $50/ton. The fine shale aggregate was crushed in the laboratory using Bico Inc. UA V-Belt Drive Pulverizer and passed through a No. 200 sieve (75 µm opening) before use. The metakaolin used, referred to as "Metakaolin-D," is a commercially available SCM, sourced from Missouri/Indiana, USA, with an approximate cost of $325/ton. Metakaolin-D is not a high reactivity metakaolin intended for silica fume replacement, but is marketed for general SCM use. Both SCMs passed the ASTM C 618 [10] criteria for Class N pozzolans. The X-ray florescence (XRF)-determined oxide compositions are shown in Table 1, along with moisture content (MC), loss on ignition (LOI) and median particle size (d_{50}). The cement used for all the mixtures was an ASTM C 150 [11] Type I portland cement from Texas, USA. The sand used for all mortar mixtures, except for those testing resistance to ASR, was standard graded sand from Ottawa in Illinois, USA. A sand containing quartz and chert from Texas, USA that has been shown to be reactive in previous literature

Table 1 Characteristics of the SCMs

	Metakaolin-D	Shale-T
SiO_2 (%)	51.66	65.43
Al_2O_3 (%)	35.23	14.55
Fe_2O_3 (%)	1.98	5.72
CaO (%)	0.57	2.44
MgO (%)	0.45	2.30
SO_3 (%)	0.06	0.39
Na_2O (%)	0.1	1.14
K_2O (%)	1.42	2.88
MC (%)	0.87	0.29
LOI (%)	1.04	0.36
d_{50} (µm)	17	23

[12] was used in the ASR mortar mixtures. This reactive fine aggregate was re-graded in the laboratory to meet the requirements of ASTM C 1567 [13].

The compressive strength tests on mortar cubes were carried out following the instructions of ASTM C 109 [14] except that the water to cementitious material ratio (w/cm) was fixed at 0.5. The SCM replacement dosage used for the compressive strength test samples was 20 % by mass of cement. Resistance to ASR was evaluated using the accelerated mortar bar test method from ASTM C 1567 [13]. The initial SCM replacement dosage for the ASTM C 1567 [13] mortar bars was also 20 % by mass of cement. However, depending upon the results of the test, the SCM percentage was increased or decreased, to find the minimum SCM replacement dosage at which expansions were kept below the 0.1 % limit of ASTM C 1567 [13]. Mixture workability of cementitious pastes with SCM replacement dosages of 20 % and a w/cm of 0.45 was assessed using an MCR 301 Anton Paar rotational rheometer. A cup and bob measurement system geometry with a 1.0 mm gap was used. Before the test, the pastes were mixed mechanically for 2 min at 1000 rpm. The mixed sample was then added to the cup and pre-sheared for 4 min at a shear rate of 50 s^{-1}, followed by 30 s of rest. Then, the shear rate was gradually increased from 10 s^{-1} to 50 s^{-1} and brought back down to 10 s^{-1} in increments of 10 s^{-1}. The shear rate was held constant for 3 min after each increment to ensure that equilibrium had been reached. Data from the equilibrium range of each shear rate were used to plot a rheological flow curve, from which the viscosity and yield stress of the mixture were determined by fitting the Bingham model, which defines the slope of the linear trend line to be the viscosity and the y-axis intercept to be the yield stress [15]. Control samples, without any SCMs, were also prepared for each test.

3 Results and Discussion

3.1 Compressive Strength

Figure 1 shows the average compressive strength of the control, Shale-T and Metakaolin-D mortar cubes. From Fig. 1, it can be seen that both the metakaolin and shale-containing mortar cubes had lower strengths than the control at 1 and 3 days. However, within 7 days, the strength of the Metakaolin-D mortar was comparable to that of the control, and by 28 days it surpassed the strength of control by approximately 22 %. The Shale-T mortar, on the other hand, gained strength at a slower rate than the Metakaolin-D mortar, achieving only 90 % of the control strength by 28 days. However, by 90 days, the Shale-T mortar reached a compressive strength comparable to that of the control. Despite the slower rate of strength gain for the Shale-T mortar, at 90 days the difference in strength between the Shale-T and Metakaolin-D mortar was only 10 %.

The difference in the early age strength between the Shale-T and Metakaolin-D mortar is most likely due to differences in their particle size. The smaller particle size of Metakaolin-D, compared to that of Shale-T, might have led to a greater

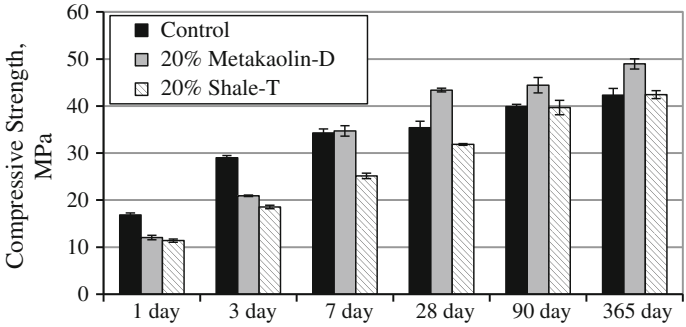

Fig. 1 Compressive strength of mortar cubes

enhancement of nucleation and growth of the cement hydration products and higher dissolution rate of the Metakaolin-D. Additionally, previous research has linked the early reactivity of metakaolin to the transformation of aluminum in the clay structure during calcination [1]. More research looking at the role of alumina in shale and metakaolin needs to be done to understand whether the differences in alumina content between the two SCMs could account for their early age strength difference.

3.2 Resistance to ASR

Figure 2 shows the results of the accelerated mortar bar test, which requires the average expansion of the mortar bars to be below 0.1 % at 14 days, to prove "low risk of deleterious expansion" from ASR [13]. The error for all 14 day expansions was less than 0.01 %. From Fig. 2, it can be seen that Metakaolin-D is very effective at mitigating expansions from ASR. At a replacement dosage of 20 %, the expansion of the metakaolin mortar bar was only 0.02 %. Although decreasing the metakaolin replacement dosage to 15 % produced a higher expansion of 0.06 %,

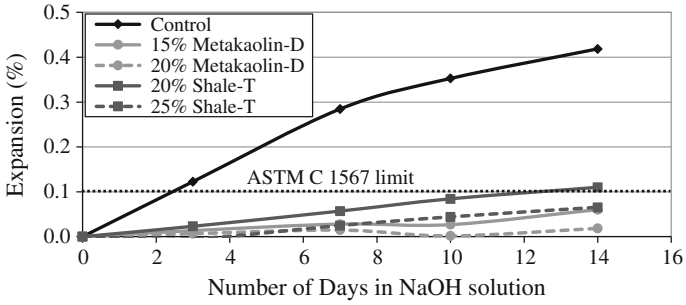

Fig. 2 Expansion of mortar bars in ASTM C 1567 ASR test

the expansion was still well below the 0.1 % limit. The Shale-T mortar, on the other hand, had expansions higher than the 0.1 % limit when used at a replacement dosage of 20 %. However, when the dosage was increased to 25 %, the expansion of the Shale-T mortar bars was below the 0.1 % limit. The more pronounced ability of Metakaolin-D to mitigate ASR compared to Shale-T may be related to its higher alumina content, which can slow down the dissolution of reactive aggregates [16].

3.3 Mixture Workability

Figure 3 shows the rheology flow curve of the cementitious pastes, while Table 2 shows the average Bingham yield stress and viscosity of the pastes and the range of the data from duplicate tests. Out of the three mixtures tested, the 20 % Shale-T paste displayed the lowest viscosity and yield stress, indicating that the addition of Shale-T to a concrete mixture would increase flow and lead to higher slump values. On the other hand, the 20 % Metakaolin-D paste had both a higher viscosity and a higher yield stress than the control paste, which indicates that the addition of Metakaolin-D to concrete will result in a mixture with reduced flow and lower slump values. The difference in the rheological properties between the metakaolin and the shale-containing pastes can be partially attributed to differences in their particle size. Since particles need to be fully coated with water to flow easily, materials with a smaller particle size (and consequently a higher surface area) often require more water than materials with a larger particle size to achieve the same

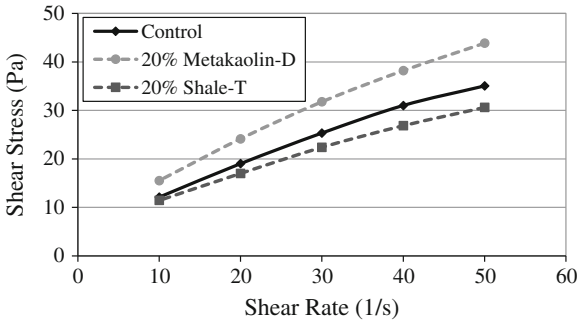

Fig. 3 Rheological flow curves of cementitious pastes

Table 2 Average Bingham yield stress and viscosity of mixtures

Mixture name	Yield stress (Pa)	Viscosity (Pa · s)
Control	7.78 ± 0.64	0.56 ± 0.01
20 % Metakaolin-D	10.08 ± 0.60	0.70 ± 0.01
20 % Shale-T	7.21 ± 0.01	0.48 ± 0.00

level of workability [15]. Additionally, previous researchers have attributed the decreased viscosity of shale mixtures to the smooth texture of shale particles, as observed in SEM images [7, 17].

4 Conclusions

The results of this paper show that the use of calcined shale as an SCM improves mixture workability and durability in terms of resistance to expansions from ASR. Additionally, the results show that, although the use of shale does not contribute to high early strength as in the case of metakaolin, in the long run the difference in strength between the metakaolin and shale-containing mortars is minimal. Therefore, if high early strength is not a requirement, then the use of shale can be a viable low cost alternative to metakaolin.

Acknowledgments The authors wish to acknowledge the Texas Department of Transportation (TxDOT) for funding this research. The authors also wish to thank Cliff Coward from TxDOT, and Victoria Valdez for help with the data collection of this project.

References

1. Fernandez, R., Martirena, F., Scrivener, K.L.: The origin of the Pozzolanic activity of calcined clay minerals: a comparison between kaolinite, illite and montmorillonite. Cem. Concr. Res. **41**, 113–122 (2011)
2. Ramlochan, T., Thomas, M., Gruber, K.A.: The effect of metakaolin on alkali—silica reaction in concrete. Cem. Concr. Res. **30**, 339–344 (2000)
3. Zhang, M.H., Malhotra, V.M.: Characteristics of a thermally activated alumino-silicate Pozzolanic material and its use in concrete. Cem. Concr. Res. **25**, 1713–1725 (1995)
4. Ambroise, J., Murat, M., Pera, J.: Hydration reaction and hardening of calcined clays and related minerals. V. Extension of the research and general conclusions. Cem. Concr. Res. **15**, 261–268 (1985)
5. Snellings, R., Mertens, G., Elsen, J.: Supplementary cementitious materials. Rev. Mineral. Geochem. **74**, 211–278 (2012)
6. Cook D.J.: Calcined clay, shale and other soils. Cem. Replace. Mater. 40–72 (1986)
7. Ramsburg, P., Neal, R.E.: The use of a natural Pozzolan to enhance the properties of self—consolidating concrete. In: Proceedings of the First North American Conference on the Design and Use of Self-Consolidating Concrete, Northwestern University, Evanston (2002)
8. Khanna, R.L., Puri, M.L.: The use of calcined shale as pozzuolana in mass concrete. Indian Concr. J. 257–263 (1957)
9. Mielenz, R.C., Witte, L.P., Glantz O.J.: Effect of calcination on natural Pozzolana. In: Symposium on Use of Pozzolanic Materials in Mortars and Concretes, vol. 99, pp. 43–91, ASTM International STP (1950)
10. ASTM C 618. Standard Specification for Coal Fly Ash and Raw or Calcined Natural Pozzolan for Use in Concrete. ASTM International, West Conshohocken (2012)
11. ASTM C 150. Standard Specification for Portland Cement. ASTM International, West Conshohocken (2011)

12. Ideker, J.H., Bentivegna, A.F., Folliard, K.J., Juenger, M.C.G.: Do current laboratory test methods accurately predict alkali-silica reactivity. ACI Mater. J. **109**(4), 395–402 (2012)
13. ASTM C 1567. Standard Test Method for Determining the Potential Alkali-Silica Reactivity of Combinations of Cementitious Materials and Aggregate (Accelerated Mortar-Bar Method). ASTM International, West Conshohocken (2013)
14. ASTM C 109. Standard Test Method for Compressive Strength of Hydraulic Cement Mortars (Using 2-in. or [50-mm] Cube Specimens). ASTM International, West Conshohocken (2011)
15. Mindess, S., Young, J.F., Darwin, D.: Concrete, 2nd edn. Pearson Education, New Jersey (2002)
16. Chappex, T., Scrivener, K.: The influence of aluminium on the dissolution of amorphous silica and its relation to alkali silica reaction. Cem. Concr. Res. **42**, 1645–1649 (2012)
17. Seraj, S.: Evaluating natural Pozzolans for use as alternative supplementary cementitious materials in concrete. Doctoral dissertation, UT Austin (2014)

Development of a New Rapid, Relevant and Reliable (R^3) Testing Method to Evaluate the Pozzolanic Reactivity of Calcined Clays

F. Avet, R. Snellings, A. Alujas and K. Scrivener

Abstract This paper introduces a new rapid, relevant and reliable (R^3) test to characterize the pozzolanic reactivity of calcined clays. This test uses isothermal calorimetry to evaluate the reactivity by monitoring the heat release in portlandite/calcined clay/limestone model systems. Once the mix design was adjusted, a wide range of calcined clays was investigated. Tests were first run at 20 °C. Good correlations were found between the heat release at 6 days and the compressive strength results on mortar blends containing calcined clays and limestone. Another series of tests were carried out at 40 °C, enabling the isothermal calorimetry test duration to be reduced from 6 to 1 day, while keeping good correlations with strength results.

1 Introduction

The use of calcined clays as clinker substitute is a promising approach in order to decrease the economic and environmental costs of cement production, thanks to their wide availability and their high reactivity as pozzolanic material. Among the different kinds of clays, kaolinitic clays show the highest pozzolanic potential after calcination [1]. The calcination of kaolinite leads to the formation of the highly-reactive metakaolin phase, which then reacts during hydration to form C-A-S-H and in some cases, strätlingite [2]. To reach even higher clinker substitution levels, a coupled substitution with limestone can be used. The advantage of combining calcined clay and limestone is the enhancement of limestone reaction thanks to the

F. Avet (✉) · K. Scrivener
Laboratory of Construction Materials, IMX, EPFL, Lausanne 1015, Switzerland
e-mail: francois.avet@epfl.ch

R. Snellings
Sustainable Materials Management, VITO, 2400 Mol, Belgium

A. Alujas
CIDEM-UCLV, Universidad Las Villas, Santa Clara, Cuba

K. Scrivener and A. Favier (eds.), *Calcined Clays for Sustainable Concrete*,
RILEM Bookseries 10, DOI 10.1007/978-94-017-9939-3_67

aluminate provided by the metakaolin. This synergetic effect of calcined clay and limestone leads to the increase of the volume of hydrates formed. The feasibility of substituting half of cement by a combination of high-grade calcined clay and limestone has been demonstrated [3], but high-grade-kaolinitic clays are too expensive to be massively used in cement production. Therefore, a method to evaluate widely-available lower grade clays was investigated.

Several tests have been proposed to evaluate the pozzolanic reactivity of Supplementary Cementitious Materials. These tests are mostly based on portlandite consumption [4, 5]. However, they do not generally correlate accurately the mechanical properties of blended systems. This paper introduces a new rapid, relevant and reliable (R^3) method to evaluate the pozzolanic reactivity by monitoring the heat release during the pozzolanic reaction in portlandite/calcined clay/limestone mixes. This test was applied to a wide range of calcined clays and results were correlated to compressive strength results of mortars.

2 Materials and Methods

Seven different kaolinitic clays from various places around the world were used in this work. Their kaolinite content was determined by Thermogravimetric Analysis (TGA) from the water loss during kaolinite dehydroxylation. Since some calcined clays were not received completely calcined, the calcined kaolinite content was defined as the difference of the kaolinite content before and after calcination, as shown in Eq. 1.

$$\%\ \text{calcined kaolinite} = \%\ \text{kaolinite}_{\text{rawclay}} - \%\ \text{kaolinite}_{\text{calcinedclay}} \quad (1)$$

The physico-chemical properties of calcined clays are described in Table 1. The properties of clinker and limestone used for the mortar compressive strength tests are also described.

The results obtained on simplified systems of portlandite/calcined clay/limestone were compared to strength results of mortars. The different systems used for mortar testing are summarized in Table 2. Plain PC system was used as reference. Two

Table 1 Physico-chemical properties of calcined clays, clinker and limestone

Calcined clay	1	2	3	4	5	6	7	8	Clinker	Lime-stone
Origin of clay	NAm	SAs	SAm	SeAs	NAm	SAm	SAs	Quartz		
Calcined kaolinite (%)	95	79.4	66.2	50.8	38.9	35.0	17.0	0	–	–
D_{50} (µm)	5.1	5.3	4.0	10.9	8.5	23.5	5.9	11.2	8.4	7.2
Specific surface (m^2/g)	9.6	15.3	12.9	45.7	23.1	18.5	18.7	1.2	0.9	1.8

Origin of calcined clays *NAm* North America; *SAm* South America; *SAs* South Asia; *SeAs* Southeast Asia

Table 2 Composition of PC, PPC30 and LC^3-50 systems

	Clinker	Calcined clay	Limestone	Gypsum
PC	95	0	0	5
PPC30	65	30	0	5
LC^3-50	50	30	15	5

substitution levels were used: PPC30 refers to systems with 30 % of clinker substitution by calcined clays and LC^3-50 corresponds to systems containing 50 % of clinker and a combination of 30 % of calcined clay and 15 % of limestone and 5 % gypsum. Mortar bars were cast and tested mechanically according to EN 196-1 at 1, 3, 7, 28 and 90 days.

For the R^3 pozzolanic test, mixes containing portlandite and calcined clay were cast and the results of the tests were correlated to the strengths of PPC30 systems. Limestone was added to the mix for comparison with LC^3-50 blends strengths. The calcined clay to limestone ratio was fixed to 2:1 for the R^3 test. In order to reproduce similar reaction environment as in cement system, K_2O and SO_3 to calcined clay ratios were adjusted to 1/12 and 1/18 by mass, respectively. Moreover, the portlandite to calcined clay ratio was adjusted to 3/1 by mass in order not to run out of portlandite during the test. A water to solid ratio of 1.2 was used for all systems to ensure suitable workability and to provide excess water to the system for the reaction to keep occurring. The mix design was then applied to the different calcined clays, first at 20 °C. Then, 40 °C experiments were run in order get even quicker indication of calcined clay reactivity.

3 Results and Discussion

3.1 Strength Results

The compressive strength results for PPC30 and LC^3-50 are plotted as function of the calcined kaolinite content of calcined clay, as shown in Fig. 1. Dotted horizontal lines indicate the PC strengths at the different ages. Equivalent strengths to PC are obtained for blends containing only 40 % of calcined kaolinite from 7 days onwards. Thus, the use of low-grade clays still enables to get good results. Moreover, for each age, the strength linearly increases with the calcined kaolinite content of calcined clays. This demonstrates that the calcined kaolinite content is the dominant parameter determining the compressive strength results. Moreover, close strength values of PPC30 and LC^3-50 blends are obtained, especially at late age. The decrease of clinker content for LC^3-50 blends is thus compensated by the synergetic effect of calcined clay and limestone.

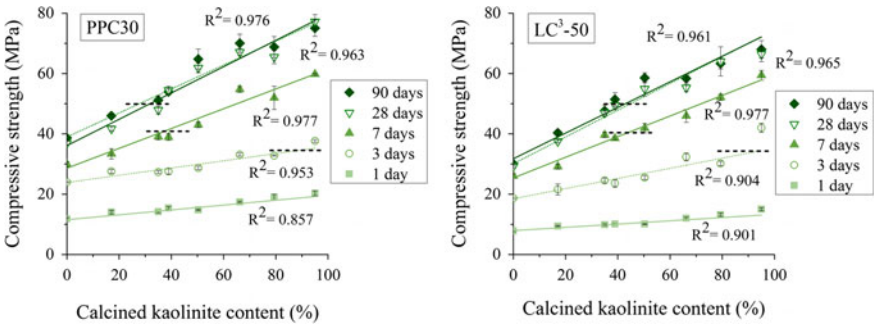

Fig. 1 Influence of the calcined kaolinite content on compressive strength results for PPC30 (*left*) and LC^3-50 (*right*) blends. *Dotted lines* indicate the PC strengths

3.2 R^3 Test Results at 20 °C

The cumulative heat normalized per gram of solid is shown in Fig. 2 for systems without and with limestone. The heat release globally increases with the calcined kaolinite content. The heat value at 6 days was chosen for the correlation to strength results, since the reaction stabilizes at this age. Figure 3 shows the correlations obtained are linear. Thus, the R^3 test is a valid way of characterizing the reactivity of calcined clays, since there is a globally good agreement with strength results.

3.3 Impact of Temperature

The increase of temperature from 20 °C to 40 °C of the isothermal calorimeter clearly accelerates the pozzolanic reaction, as shown in Fig. 4. The heat values after only 1 day at 40 °C are globally close to the heat values at 6 days at 20 °C. Thus,

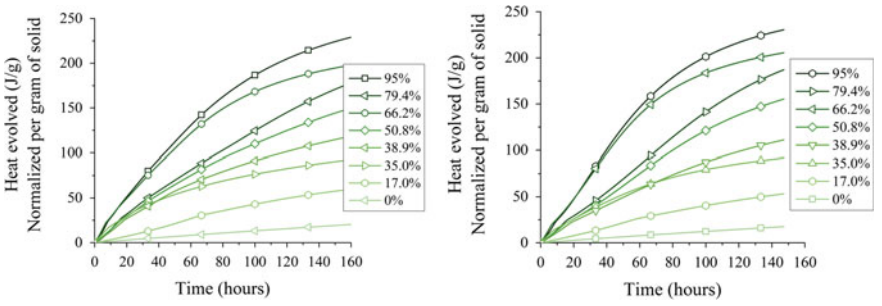

Fig. 2 Cumulative heat release of portlandite/calcined clay mixes without (*left*) and with (*right*) limestone at 20 °C

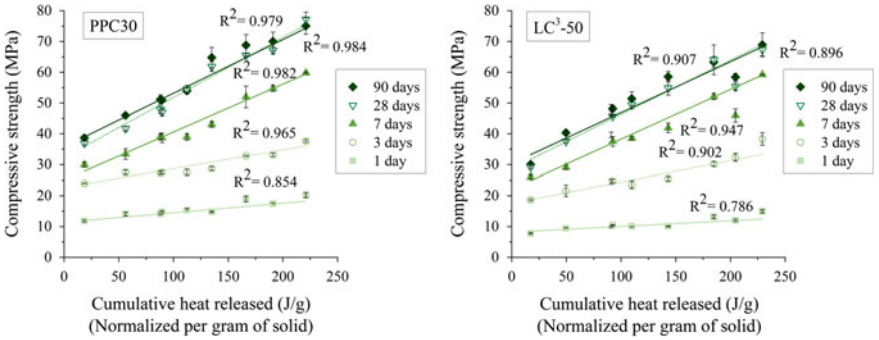

Fig. 3 Correlations of mortar compressive strength with the heat values at 6 days at 20 °C of portlandite/calcined clay mixes. PPC30 and LC^3-50 strengths are respectively compared with heat values of mixes without (*left*) and with (*right*) limestone

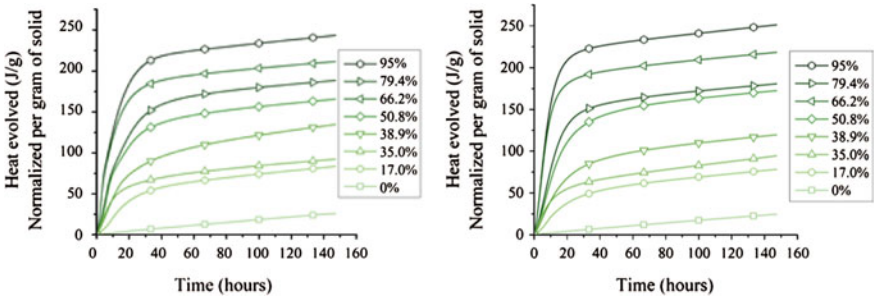

Fig. 4 Cumulative heat release of portlandite/calcined clay mixes without (*left*) and with (*right*) limestone at 40 °C

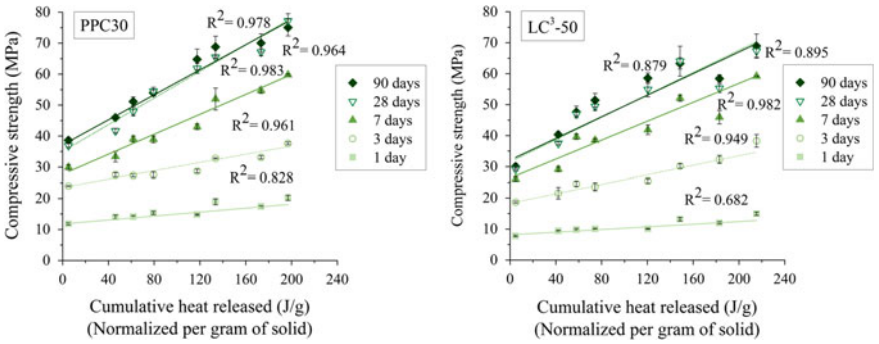

Fig. 5 Correlations of mortar compressive strength with the heat values at 6 days at 20 °C of portlandite/calcined clay mixes. PPC30 and LC^3-50 strengths are respectively compared with heat values of mixes without (*left*) and with (*right*) limestone

the correlation to compressive strength results was based on the 1-day heat values. Similar good linear correlations are found with strength results, as shown in Fig. 5. Thus, reliable indication on the reactivity of calcined clays can be obtained after only 1 day of testing.

4 Conclusions

This new R^3 pozzolanic test permits to get reliable indication of clay reactivity after 6 days of testing at 20 °C. For portlandite/calcined clay mixes without and with limestone, the heat release is linearly correlated to the compressive strengths of PPC30 and LC^3-50 blends. The test duration can even be reduced to 1 day by increasing the temperature of isothermal calorimetry to 40 °C. Correlations to compressive strength results are not significantly affected by this temperature increase.

Acknowledgments F. Avet and R. Snellings respectively acknowledge financial support by the Swiss Agency for Development and Cooperation (SDC) and the European Community under FP7-Marie Curie IEF grant 298337.

References

1. Fernandez, R., Martirena, F., Scrivener, K.L.: The origin of the pozzolanic activity of calcined clay minerals: a comparison between kaolinite, illite and montmorillonite. Cem. Concr. Res. **41** (1), 113–122 (2011)
2. Silva, P.S.d., Glasser, F.P.: Hydration of cements based on metakaolin: thermochemistry. Adv. Cem. Res. **3**, 167–177 (1990)
3. Antoni, M., et al.: Cement substitution by a combination of metakaolin and limestone. Cem. Concr. Res. **42**(12), 1579–1589 (2012)
4. Donatello, S., Tyrer, M., Cheeseman, C.R.: Comparison of test methods to assess pozzolanic activity. Cem. Concr. Compos. **32**(2), 121–127 (2010)
5. Tironi, A., et al.: Assessment of pozzolanic activity of different calcined clays. Cement Concr. Compos. **37**, 319–327 (2013)

Investigation of Ternary Mixes Made of Clinker Limestone and Slag or Metakaolin: Importance of Reactive Alumina and Silica Content

M. Antoni, L. Baquerizo and T. Matschei

Abstract Ternary cements made of clinker, limestone and metakaolin present a high potential to be used as general-use cement with decreased associated CO_2 emissions and embodied energy. In this article a systematic investigation of the synergies in the ternary system containing up to 50 % limestone, metakaolin or slag was done following a DoE approach. Flow results and compressive strengths at 2, 7 and 28 days are reported as well as phase assemblage as obtained by Rietveld refinement. The results in the ternary system are compared with results that have been obtained with slag and limestone and the respective contributions of carboaluminates hydrates and C-A-S-H gel are assessed. The contribution of the reactive aluminates from the SCMs is decisive for 7 day strength, while strength at 28 days seems to be more dependent on the reactive silicate fraction. At early age (2 days), compressive strength depends more on the fineness of the mineral addition.

Keywords Metakaolin · Limestone · Slag · Synergy · Carboaluminates · Kinetics

1 Introduction

Cement is the most produced man-made material and its demand keeps increasing. Yet cement manufacturing accounts for approximately 5–8 % of man-made CO_2 emissions worldwide. Most of the required energy and emissions are related to clinker production. It explains the strong trend in the cement industry to reduce clinker factor and develop novel low binder concrete. The ongoing development of new standards such as the EN 197-1 CEM II-C class in Europe or the ASTM C595 2014 in the US is further enhancing this trend. Several recent publications [1–3] show that blends made of clinker; limestone and calcined clay may be promising

M. Antoni (✉) · L. Baquerizo · T. Matschei
Innovation, Product Technology, Holcim Technology Ltd, Im Schachen, 5113 Holderbank, Switzerland
e-mail: mathieu.antoni@holcim.com

K. Scrivener and A. Favier (eds.), *Calcined Clays for Sustainable Concrete*,
RILEM Bookseries 10, DOI 10.1007/978-94-017-9939-3_68

candidates that can help to further decrease the clinker content and the associated CO_2 emissions of the cement industry.

It has been shown that one advantage of calcined clays and its use in combination with limestone over other common SCMs is its fast kinetics of reaction; compressive strengths in the same range than OPC were obtained already at 7 days for clinker factors a low as 55 % [1] while other SCMs generally contribute to late strength mainly visible at 28 or even 90 days only.

2 Materials and Methods

A CEM I 42.5 R PC has been used as reference cement. High purity limestone, LL class and as well as high purity commercial metakaolin were used. In addition, a ground granulated blast furnace slag (GGBFS) with an average European composition has also been investigated for comparison. It has an amorphous content above 95 % and contains 9.9 % Al_2O_3. XRF, Blaine values as well as Rietveld analysis of the OPC are given in the Table 1. Note that OPC contains non negligible amount of calcite and dolomite on his own.

Mortar bars were cast according to EN 196-1 procedure, at constant water/binder ratio of 0,5. Standard sand was used in all mortar mixes. A DoE approach has been used in order to screen the full range of compositions covering both the CEM II-B and the CEM II-C range with clinker replacement up to 50 % and strengths have been statistically analysed in order to find out the best quadratic regression model that fits the strength variation within the ternary system. 13 and 23 different samples have been cast for the metakaolin and the slag cases respectively.

Table 1 XRF and Blaine values of raw materials (left) and Rietveld of OPC

Method	OPC	Limestone	Metakaolin	Slag	Phase	OPC
L.o.i.	1.4	41.8	0.7	−0.8	Alite	69.2
SiO_2	19.7	2.6	52.0	37.8	Belite	5.3
Al_2O_3	4.7	1.0	44.8	9.9	Aluminates	4.7
Fe_2O_3	3.1	0.5	0.4	0.4	Ferrite	10.2
CaO	63.8	52.9	0.1	39.5	Gypsum	2.9
MgO	2.0	0.5	<0.01	9.1	Hemihydrate	0.9
SO_3	3.0	0.0	<0.02	3.2	Anhydrite	0.2
K_2O	1.1	0.1	0.2	0.8	Calcite	1.7
Na_2O	0.1	0.0	0.2	0.2	Periclase	0.5
TiO_2	0.3	0.1	1.5	0.8	Arcanite	1.7
Mn_2O_3	0.0	0.0	<0.01	0.2	Free lime	<0.5
SrO	0.1	0.0	0.0	0.1	Portlandite	0.9
Total	99.7	99.6	100.0	101.1	Quartz	0.5
Blaine (cm^2/g)	2900	6500	>10,000	3900	Dolomite	0.7

The flow behaviour was monitored by applying 15 shocks on an EN 196 based shock table. For the mixtures with metakaolin, a constant flow was maintained by addition of PCE based superplasticizer. Up to 2 wt% had to be used for the blend with 50 % clinker and 50 % metakaolin. No extra sulfate was added to the binder than the one originally present in the OPC. Compressive strengths at 2, 7 and 28 days are reported here.

The investigation of phase assemblages was done on selected ground paste samples, cast at water/binder ratio of 0.4. Samples with 35 % cement substitution have been studied, and half of the SCM content has been systematically replaced by limestone in order to compare the system 35 % SCM-65 % OPC with the ternary system 17.5 % SCM-65 % OPC-17.5 % limestone. At 1, 2, 7 and 28 days, hydration was stopped by carefully grinding 10 g of paste sample with 12 g isopropanol in an agate mortar. Isopropanol was later removed by drying in a ventilated oven at 40 °C during 90 min. The evolution of the phase assemblage was then obtained by combining XRD and Rietveld analysis with TGA data.

3 Results

3.1 Flow Results

The addition of very fine metakaolin required superplasticizer addition in order to maintain acceptable flow behaviour. The flow obtained for the several mixes are given in Fig. 1. Up to 2 wt% of superplasticizer was required to obtain sufficient flow for the mix with 50 % metakaolin and 50 % OPC, and the superplasticizer required to maintain constant seems to linearly vary with the metakaolin addition.

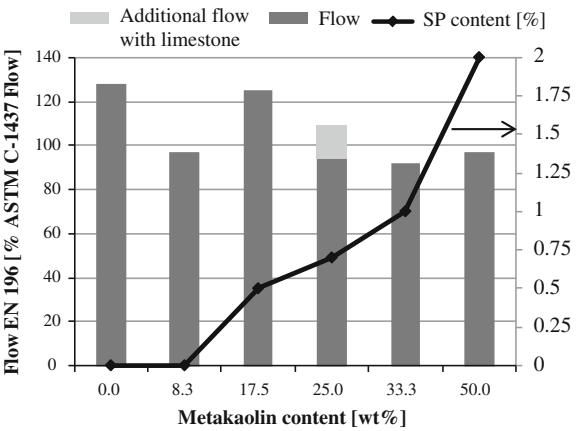

Fig. 1 Flow value in percent of the ASTM C-1437 minicone test and superplasticizer addition as a function of the metakaolin content

It is important to note that for constant metakaolin and superplasticizer content, replacement of OPC by limestone has a positive impact on flow.

3.2 *Compressive Strengths in the Ternary System Clinker-Metakaolin-Limestone*

The contour plot analysis from the statistical analysis of the compressive strengths at 2, 7 and 28 days are given in Fig. 2. The compressive strength at 2 days in the ternary diagram is mostly governed by the OPC content, and the more the replacement of OPC by either metakaolin or limestone, the less the strength. In ternary mixes, metakaolin contributes slightly more than limestone to early strength at 2 days.

At 7 days, the strength optimum is reached for a composition of about 25 % metakaolin and 75 % OPC. But a strong synergy can be observed and for 25 % metakaolin, 15 % limestone and 60 % OPC which means a further replacement of 15 % OPC by 15 % limestone would be possible while the strength only marginally decreases. Similarly, at constant clinker factor of 50 %, the strength optimum lies for combined addition of 30 % metakaolin and 20 % limestone. At 28 days, the synergy can also be observed. The overall optimum also approximately lies for the composition of 25 % metakaolin and 75 % OPC. Limestone contribution is still tangible but tends to decrease in comparison with 7 days; at constant clinker factor of 50 %, the strength optimum lies for combined addition of 40 % metakaolin and 10 % limestone, If we compare strength at given clinker factor it can be seen that except for 2 days a significant proportion of metakaolin can be replaced by limestone without a negative impact on compressive strength, while at the same time the workability/water demand of the ternary mixes will significantly improve.

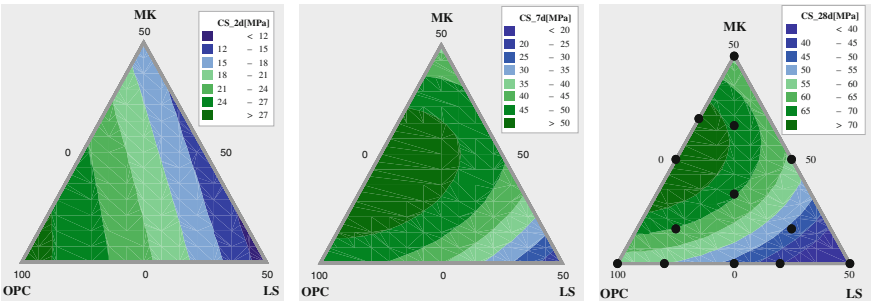

Fig. 2 Contour plots analyses with strength isolines in the ternary diagram OPC-MK-LS at 2 days (*left*), 7 days (*middle*) and 28 days (*right*) in the ternary diagram 100 % OPC (*bottom left*); 50 % OPC-50 % MK (*top*); 50 % OPC-50 % limestone (*bottom right*). The *black dots* represent the compositions that have been experimentally evaluated

3.3 Phase Assemblage in the Ternary System Clinker-Metakaolin-Limestone

The phase assemblages as determined by XRD, Rietveld refinement together with TGA is given in Fig. 3 for the system 65 % OPC + 35 % metakaolin (left) and for the system 65 % OPC, 17.5 % limestone and 17.5 % metakaolin (right). In the system with 35 % metakaolin, ettringite forms at 1 day and tends to later decrease while monosulfate forms from 2 days on. From 7 days significant amounts of strätlingite were observed and its amount further increases with time. Portlandite amount reaches its maximum at 1 day, stays relatively constant until 7 days and is consumed later on. Total amount of amorphous content (including metakaolin) logically increases considerably with time and the formation of C-A-S-H gel.

In the system with 17.5 % metakaolin and 17.5 % limestone, ettringite is already present at 1 day and remains constant with time. In addition, carboaluminates also form in increasing amount from 1 day too; and monosulfate is absent, according to thermodynamic predictions [4]. Calcite content decreases from 17.5 to 14.4 % with time. It is further interesting to see that there is apparently a competition for reactive aluminates amongst different AFm phases. While in the binary system significant amounts of strätlingite formed, this phase was not observed in limestone blended systems, where carboaluminates formed instead. Additional mass balance calculations are underway to further understand the consequences of these phase changes.

Alite consumption and more generally the degree of reaction of Portland cement is slightly enhanced in the system with limestone in comparison with the system with 35 % metakaolin. The totally bound chemical water content increased at all ages in presence of limestone compared with the binary system with 35 % metakaolin, further highlighting the synergistic behaviour between metakaolin and limestone.

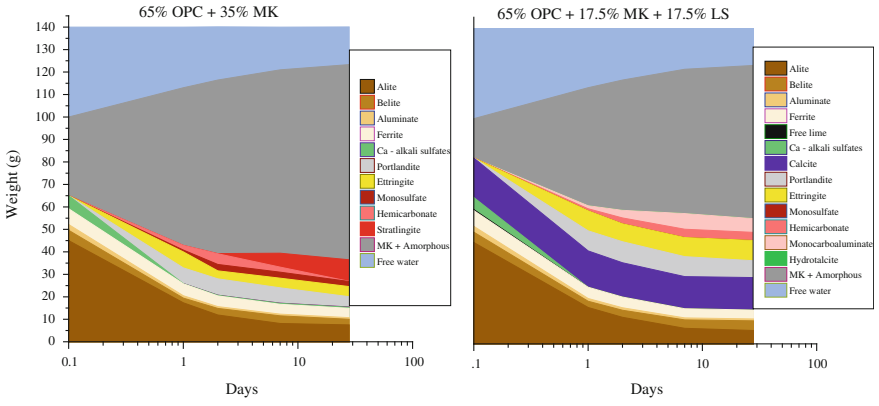

Fig. 3 Phase diagrams obtained by XRD-rietveld-TGA for the system 65 % OPC-35 %MK (*left*) and 65 % OPC-17.5 %MK-17.5 % (*right*) as a function of time

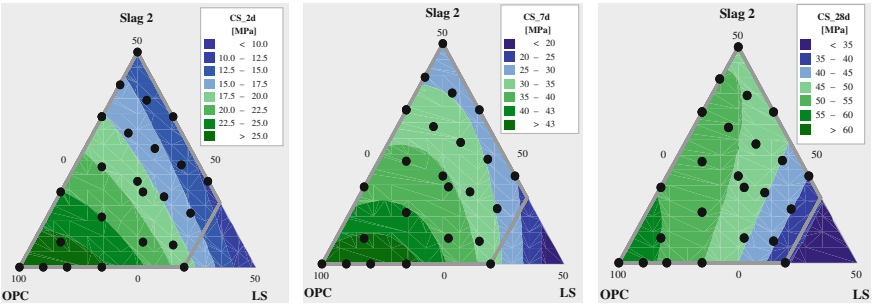

Fig. 4 Strength isolines in the ternary diagram OPC-Slag-LS at 2 days (*left*), 7 days (*middle*) and 28 days (*right*) for up to 50 % replacement

3.4 Ternary System Clinker-Slag-Limestone

The compressive strengths at 2, 7 and 28 days in the ternary system clinker-slag-limestone for the slag are presented in the Fig. 4. At 2 days, slag is mostly diluting the OPC and strength decreases with increasing OPC substitution. A strength improvement can be observed for low amounts of limestone (around 5 %) as commonly known. In general at constant clinker factor the ternary systems incl. limestone and slag have a very similar or even slightly improved early strength compared to OPC-slag systems.

As shown in Fig. 2 (middle) the synergy of the combined addition of limestone and slags is strongest at 7 days. Ternary blends containing both slags and limestone have systematically higher strengths that blends with only slags or only limestone. At 28 days however, the synergy with limestone is reduced and strength tends to decrease with increasing limestone contents. Nevertheless at a given clinker factor acceptable strengths can be also achieved for ternary cements, depending on the required 28 days strength values.

3.5 Phase Assemblage in the Ternary System Clinker-Slag-Limestone

The phase assemblages as determined by XRD, Rietveld refinement together with TGA is given in Fig. 5 for the system 65 % OPC + 35 % slag (left) and for the system 65 % OPC, 17.5 % limestone and 17.5 % slag (right). In the system with 35 % slag, ettringite forms at 1 day and tends to later decrease with tiny amount of monosulfate forming from 2 days on. Note that due to its low crystallinity it is likely that part of monosulfate is included in the amorphous content. Similarly, hydrotalcite could not be quantified as its peaks overlap with carboaluminate peaks. Portlandite amount increases until 7 days and is almost constant from 7 up to

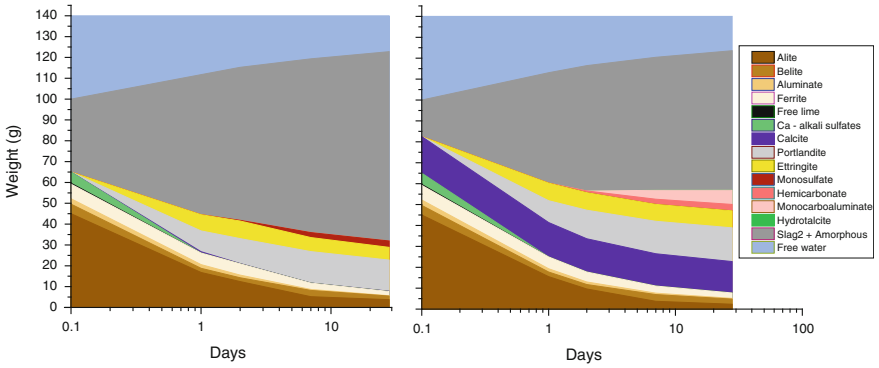

Fig. 5 Phase diagrams obtained by XRD-Rietveld-TGA for the system 65 % OPC-35 % Slag (*left*) and 65 % OPC-17.5 % Slag-17.5 % (*right*) as a function of time

28 days in both systems. Total amount of amorphous content (including slag) logically increases considerably with time and the formation of C-A-S-H gel.

In the system with 17.5 % slag and 17.5 % limestone, ettringite is already present at 1 day and remains constant with time. In addition, carboaluminates also form in increasing amount from 2 days. Calcite content decreases from 17.5 to 15 % with time. Alite consumption and more generally the degree of reaction of Portland cement are slightly enhanced in the system with limestone in comparison with the system with 35 % slag. The totally bound chemical water content increased at all ages (the maximum is observed at 7 days and tends to level off at 28 days) in presence of limestone compared with the binary system with 35 % slag, further highlighting the synergistic behaviour between slag and limestone.

3.6 Elements of Comparison of the Limestone Synergy with Metakaolin or Slag

Several differences arise from the comparison between the metakaolin and slags examples. At early age metakaolin performs better than limestone while slag brings about the same contribution than limestone or tends to be slightly worse. This can be mainly related to the higher fineness of metakaolin compared with limestone and slag. It is also interesting to see that in term of absolute strength metakaolin and metakaolin-limestone outperforms the slags & slags-limestone blending at all ages (for instance the mix with 20 % limestone and 10 % metakaolin still outperforms any of the compositions from the slags-limestone system at 28 days), even if the fineness/physical contribution cannot be distinguished from the chemical contribution and keeping in mind that such a blend is irrelevant to the market considering its poor workability and economical unfeasibility. There is a clear correlation between the strong increase in the total content of ettringite and AFm phases at

7 days and the improved synergetic strength in the combined SCM-limestone system for both slags and metakaolin when compared to the blends without limestone.

But there is a significant difference between the slag—and the metakaolin-limestone ternary blend with limestone is their strength evolution between 7 and 28 days. While in ternary systems with metakaolin, the synergistic effect with limestone can be still clearly observed also at 28 days, in system with slags 28 days strength more or less linearly decreases with increasing limestone contents. The phase assemblages are obviously different; with metakaolin the high Al content fosters strätlingite precipitation while C-A-S-H and hydrotalcite to a minor extent probably plays a more important role with slag. The combined addition of limestone tends to create more similar phase assemblages; strätlingite does not precipitate anymore for metakaolin case, C-A-S-H, ettringite and carboaluminates being the main hydrates phases with either metakaolin or slag. This should be supported in the future by further analysis to discriminate the non-reacted metakaolin or slag fraction from the C-A-S-H gel fraction and obtain degree of reaction of the SCMs.

4 Conclusions

Ternary blends with limestone and alumina-siliceous SCMs are generally a very interesting option to further reduce the carbon footprint of the cement industry. However as shown in this article the knowledge of synergistic as well as application limiting interactions between the different SCM's is very important to further optimise these binders. For example high additions of metakaolin decrease workability dramatically and therefore require high amounts of superplasticizers to obtain useful flows. But a combined addition of limestone and metakaolin improves the picture significantly and we expect further improvement with mixes of industrially relevant calcined clays and limestone blends. The mechanical properties in ternary systems with clinker factors as low as 50 % show that both tested alumina-siliceous SCM's present very interesting synergy potential with limestone. Metakaolin shows the best potential compared with slag, where synergy is mostly relevant at 7 days. The respective contributions of AFm, AFt and C-(A)-S-H gel were assessed with Rietveld analysis. In both systems (slag and metakaolin) most significant strength synergies were observed at 7 days coinciding with the main formation of carboaluminates in the system. At 28 days strength seems more dependent on the reactive silicate fraction, and the additional formation of C-(A)-S-H, while at early ages compressive strength depends more on the fineness of the replacement materials. With the knowledge obtained in parameter studies as presented here, we can tailor-make cementitious products fulfilling customer requirements. An open field that needs more study is of course the durability behaviour of multiple blends especially at clinker factors below 35 % which are beyond current standard practices in Europe.

References

1. Antoni, M., Rossen, J., Martirena, F., Scrivener, K.: Cement substitution by a combination of metakaolin and limestone. Cem. Concr. Res. **42**, 1579–1589 (2012). doi:10.1016/j.cemconres.2012.09.006
2. Beuntner, N., Rapp, K., Thienel, K.-C.: Efficiency of calcined clay in cementitious systems. Presented at the American Concrete Institute, ACI Special Publication, pp. 413–424 (2012)
3. Danner, T., Justnes H, Ostnor T.: Calcined marl as a pozzolan for sustainable development of the cement and concrete industry. ACI Special Publication 289 (2012). doi:10.14359/51684275
4. Matschei, T., Lothenbach, B., Glasser, F.P.: The role of calcium carbonate in cement hydration. Cem. Concr. Res. **37**, 551–558 (2007). doi:10.1016/j.cemconres.2006.10.013

Using of Libyan Calcined Clay in Concrete

Abdelsalam M. Akasha

Abstract Strong and durable concrete structures might be the common target for structural designer. Many cementitious materials have been used in the recent years to improve the strength and durability of concrete structures. One of those cementitious materials was the natural pozzolan (calcined clay). Clay acts as one of the main raw materials available in different countries. Libya is one of those countries which possess large amounts of clay deposits, especially in the south area. The utilisation of calcined clay, in the form of metakaolin (MK), as a pozzolanic material for mortar and concrete has received considerable attention recently. This interest is part of the widely spread attention directed towards the utilisation of wastes and industrial by-products in order to minimise Portland cement consumption. Another reason is that mortar and concrete, which contain pozzolanic materials, exhibit considerable enhancement in strength and durability properties. The main goal of the present research is to investigate the effect of using Libyan pozzolanic materials in the form of MK on the compressive strength.

Keywords Metakaolin · Calcined clay · Pozzolana concrete

1 Introduction

An extensive research work has been carried out in the past years by the Libyan industrial research center on the natural raw materials in the south region of Libya. The investigation shows that there are many raw materials that can be used in the building material industry, one of that materials was natural pozzolan (kaolinite) [1]. From that point we start thinking to carry out a wide range investigation for the possibility of using the kaolinite in the form of metakaolinite as replacement cement material in concrete. Metakaolinite is obtained by heating kaolinite at 700–850 °C. It is a poorly crystalline transition phase which behaves as highly reactive artificial

A.M. Akasha (✉)
Department of Civil Engineering, Sebha University, Sebha, Libya
e-mail: confcivil@yahoo.com

K. Scrivener and A. Favier (eds.), *Calcined Clays for Sustainable Concrete*,
RILEM Bookseries 10, DOI 10.1007/978-94-017-9939-3_69

Table 1 Location of clays

Symbol of site	Location	Clay mineral (%)
A	10 km from Sebha	Kaolinite 95, Quartz 5
B	10 km from Temenhint_Sebha	Kaolinite 50, Quartz 50
C	Alafya_Brack	Kaolinite 54, Quartz 46
D	Agar_Wadi Shatti	Kaolinite 90, Quartz, Illite
E	Tarout_Wadi Shatti	Kaolinite 30, Quartz 70

pozzolan. Nowadays, the properties of calcined clays are widely discussed in cement literature for their pozzolanic properties. Metakaolinite reacts with calcium hydroxide and water to yield hydrated compounds of Ca and Al silicates. Pozzolanic activity of metakaolinite is related to the cristallinity of the original kaolinite. Pozzolana is a siliceous material which whilst itself possesses no cementitious properties, either processed or unprocessed and in finely divided form, reacts in the presence of water with lime at normal temperatures to form compounds of low solubility having cementitious properties. Pozzolanas may be natural or artificial, When mixed with cement the silica of the pozzolana combines with the free lime released during the hydration. Silicas of amorphous from react with lime readily compared to those of crystalline form and this constitutes the difference between active pozzolanas and materials of similar chemical composition which exhibit little pozzolanic activity. It is commonly thought that lime-silica reaction is the main or the only one that takes place, but recent information indicates that alumina and iron if present also take part in the chemical reaction [2]. This paper deals with the influence of south Libya metakaolin as partially replacement of ordinary Portland cement on the compressive strength of concrete mortar, for that reason, calcined clay from five different places in the south of Libya, the clays were collected as shown in Table 1 and Fig. 1. The calcined clay produce from these places were grinding to pass 150 micrometer sieve and calcined at 800 °C for 2 h. The effect of addition calcined clays 10, 15, 20 % as partially replacement of Portland cement was investigated by various tests.

2 Materials and Methods

The materials that used in this investigation were as follows:

- *Cement*: The Portland cement type I have been obtained from Alburg manufactory (Ziliten). The type I Portland cement used in this study complies with the specifications defined by the ASTM C150 standard and Libyan standard specifications 340/97.
- *Fine Aggregate*: The standard sand is silica sand, composed almost entirely of naturally rounded grains of nearly pure quartz, used for preparing mortars for mechanical tests. The sand that used in making test specimens for mechanical

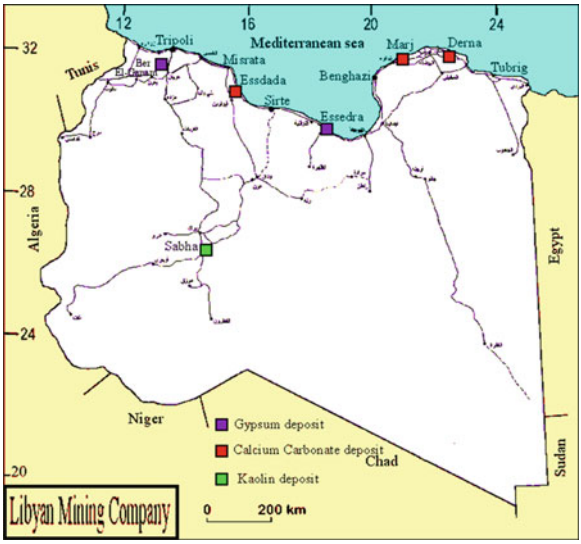

Fig. 1 Kaolin clay deposits in Libya

tests was natural silica sand from Zellaf desert 30 km from Brack city. The grade of original sand was out of the grade limits of ASTM C778-03, to conform to the requirements for standard sand, it was modified. The graded Sand was used for compressive strength test according to ASTM C109-03.

- *Clays*: Five clay soils as shown in Table 1 were brought from different sites at Sebha and Brack cities regions, the Clay minerals proportion was obtained by XRD (X-Ray Diffraction Method). The samples were excavated with shovels from the sides of natural slopes. They were generally dry with blocky structure and in order to perform laboratory tests the samples were crushed to the size of 0.25–0.5 in. and calcined at 800 ºC for a period of 2.0 h to produce fired clay bricks. The chemical analysis results of the selected samples are shown in Table 2 (Figs. 2 and 3).

2.1 Mix Proportion

Three different proportions of blended cement paste and mortar mixes were prepared. For each type OPC replacing with three different amount of calcined clay in dry condition, the mixtures were thoroughly homogenized and kept in polythene bottles until the test.

Table 2 Chemical analysis of studied samples

	Sebha (A)	Temenhint (B)	Alafya ('C)	Agar (D)	Tarout (E)
SiO_2	82.75	67.39	56.73	53.41	54.52
TiO_2	0.52	1.43	1.05	1.25	1.30
Al_2O_3	10.65	22.16	20.73	30.07	24.89
Fe_2O_3	0.89	0.99	8.90	2.10	2.50
Mn_3O_4	0.03	0.02	0.05	0.02	0.03
MgO	0.20	0.14	0.55	0.20	0.29
CaO	<0.004	<0.004	0.01	0.05	0.58
Na_2O	0.25	0.01	0.09	<0.009	0.83
K_2O	0.53	0.34	2.76	1.35	1.14
P_2O_5	0.15	0.04	0.16	0.12	0.50
SO_3	0.03	0.02	0.09	0.04	0.51
V_2O_5	0.01	0.02	0.04	0.02	0.03
Cr_2O_3	0.02	0.03	0.02	0.03	0.03
SrO	0.02	0.01	0.02	0.02	0.03
ZrO_2	0.06	0.07	0.05	0.04	0.05
BaO	<0.006	<0.006	0.04	0.02	0.02
NiO	<0.002	<0.002	<0.002	<0.002	<0.002
CuO	<0.002	0.00	0.01	0.01	0.00
ZnO	<0.001	<0.001	0.02	0.00	0.00
PbO	0.02	0.02	0.02	0.02	0.01
HfO_2	0.01	<0.004	0.01	0.00	0.01
SiO_2	82.75	67.39	56.73	53.41	54.52

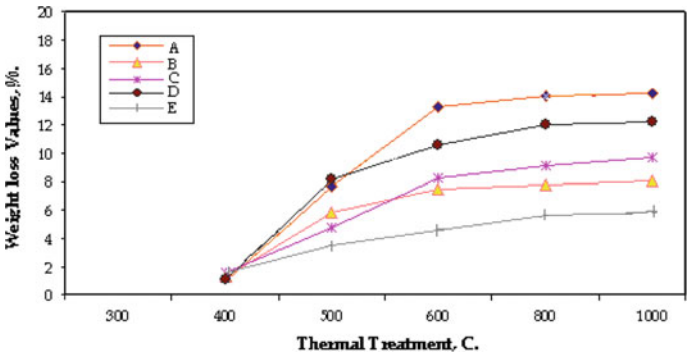

Fig. 2 Weight loss of samples

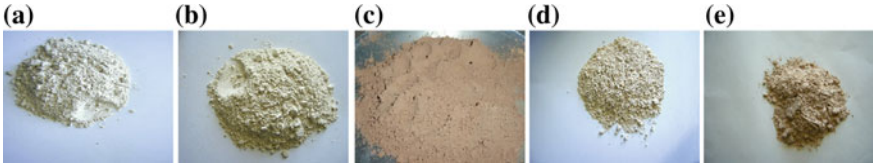

Fig. 3 Calcined clay

2.2 Compressive Strength

The control mixture was prepared with w/c ratio equal to 0.459, cement: standard graded sand equal to 1:2.75. The mortar mix were prepared using ELE (UK) Automatic Mortar Mixer in accordance with ASTM C 305-99. Fifty-millimeter cubes were cast in two equal layers and compacted as per ASTM C109 After 24 h of initial curing in a moist room (23 ± 2 °C) with relative humidity not less than 95 %, the specimens were demoulded and cured in water until the age of testing. For all blended cement mixes The water/blended cement ratio (w/bc) was maintained constant.

3 Results

The average compressive and relative compressive strength of the mortar cubes after 3, 7, 28 days of mixing was shown in Fig. 4a, b.

The relative compressive strength (RS) at the different curing times for MK mortar is plotted in Fig. 4b. The RS is the strength of MK mortar divided by the strength of the control (i.e. 0 % MK) at the same curing time. At 3 and 7 days of curing AII mortar seems to be slightly reduce the compressive strength resulting in RS value of less than one. However, beyond 7 days of curing, the RS of AII mortar increases and reaches a maximum at 28 days of curing. The optimum percentage of MK that results in higher strength is around 10 %. BI and BIII mortars seem to increase the compressive strength resulting in RS value of more than one for most curing time and reaches a maximum in BI except at 7 days where compressive strength of BIII mortar less than control. Moreover the maximum contribution of BI occurs at 90 days of curing where more than 18 % increase in strength is obtained. CI and CII mortars seem to increase the compressive strength resulting in RS value of more than one for most curing time and reaches a maximum in CII except at 10 days where compressive strength of CI mortar less than control. Moreover the maximum contribution of CII occurs at 3 and 90 days of curing where more than 20 and 12 % increase in strength is obtained. DI and DII mortars seem to increase the compressive strength resulting in RS value of more than one most curing time and reaches a maximum in DI, except at 7 days where compressive strength of DII mortar less than control. Moreover the maximum contribution of DI occurs at 3 and

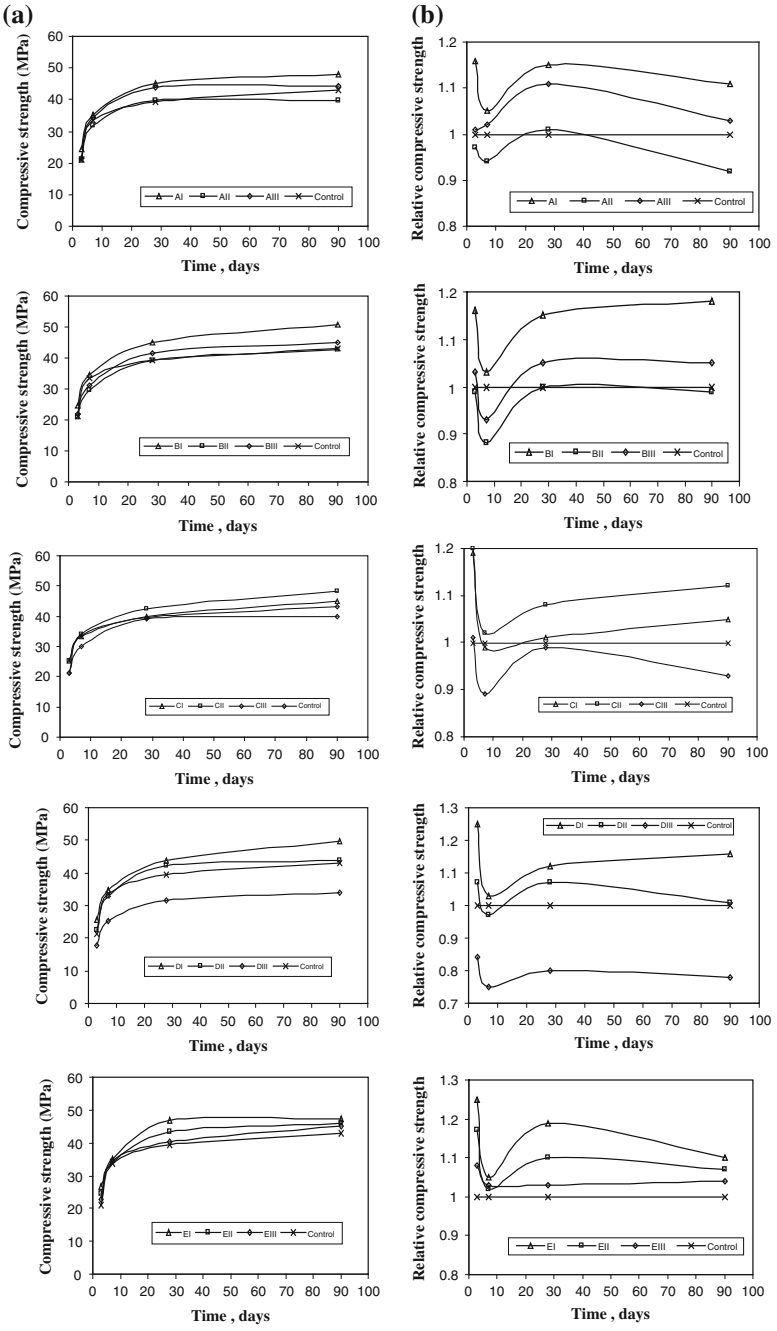

Fig. 4 Compressive and relative compressive strength

90 days of curing where more than 25 and 15 % increase in strength is obtained. At all time of curing all E mortars seems to increase the compressive strength resulting in RS value of more than one and reaches a maximum in EI. Moreover the maximum contribution of EI occurs at 3 and 28 days of curing where more than 25 and 18 % increase in strength is obtained (i.e. RS > 1.25 and >1.18) due to pozzolanic reaction. The optimum percentage of MK that results in higher strength is around 10 %.

4 Conclusion

This paper present the results for the effect of south Libya MK replacement of cement on the concrete mortar compressive strength. Based on the results obtained from this study, the following conclusion may be drown:

1. The using metakaolin material effectively improving the compressive strength, for example the compressive of AI and DI mortar has been increased by 11 and 16 % respectively, and all replacement level of C and B mortar samples were improved the strength, specially BI and BII.
2. In all samples the optimum percentage of MK that results in higher strength is around 10 %, except C sample where the optimum percentage was 15 %.

References

1. Akasha, A.M., Soib, M.M., Abdulsalam, H.M.: Utilization of some deposited clay in South Libya as a pozzolanic material. 7th International Congress, Concrete: Constructions Sustainable Option 4–6 September 2007 Dundee, Scotland, UK
2. Akasha, A.M., Abdussalam, H.M.: Utilization of some locally pozzolanic materials as blended cement. Second Conference of Engineering Structures and Building Materials, Musrata, pp 69–75, 21–21 November (2006)

Part II
Abstracts

Physical, Mineralogical and Chemical Characterization of Venezuelan Kaolins for Use as Calcined Clays in Cement and Concrete

Fuentes Irania, Martínez Francis, Reátegui Katya and Bastos Vannesa

Abstract The use of calcined clays as a pozzolanic material for mortar and concrete has received considerable attention in recent years. This interest has focused on the chemical composition and reactivity for use as a pozzolanic material, and its major contribution is recognized in enhanced mechanical strength, reduced permeability and chemical durability. Different studies have concluded that pozzolanic behavior depends on calcination temperature and surface area. It is also related to the original kaolinite crystallinity and the quantity and nature of the partners, such as quartz, rutile or feldspar minerals.

This work concerns the characterization of two Venezuelan kaolinitic clays: A1 obtained from a primary deposit was developed in situ, and A2 obtained from a sedimentary deposit. For both clays were determined the loss on ignition (LOI), specific gravity, surface area and particle size distribution; mineralogy was studied by X-ray diffraction (XRD) and a binocular microscope. Chemical analyzes were performed by the technique of X-ray fluorescence (XRF) and inductively coupled plasma atomic emission spectroscopy (ICP-AES). The results indicate that kaolin A1 is chemically constituted by 56.4 % SiO_2, 22.70 % Al_2O_3, 1.10 % (Fe_2O_3 and TiO_2) and 1.62 % (CaO + MgO + Na_2O + K_2O), while the kaolin A2 is chemically constituted by 58.13 % SiO_2, 27.17 % Al_2O_3, 2.05 % (Fe_2O_3 and TiO_2) and 0.37 % (CaO + MgO + Na_2O + K_2O), and has a mineral composition consisting mainly kaolinite, quartz, and minor amounts of heavy minerals such as ilmenite, zircon and magnetite.

The kaolin A1 consist of 56.38 % in silt-clay size minerals with high crystallinity and angularity, also, the main mineral phase is kaolinite and less abundants quartz and illite. Whilst the 43.62 % of kaolin sample, have a particle size between silt and sand, where quartz is the predominant mineral phase and as accessory minerals

F. Irania · M. Francis · R. Katya
Instituto de Ciencias de la Tierra, Universidad Central de Venezuela, Caracas, Venezuela

B. Vannesa (✉)
Instituto de Tecnología Venezolana para el Petróleo (INTEVEP), Los Teques, Venezuela
e-mail: bastosv@pdvsa.com

K. Scrivener and A. Favier (eds.), *Calcined Clays for Sustainable Concrete*,
RILEM Bookseries 10, DOI 10.1007/978-94-017-9939-3_70

zircon, hematite and magnetite has been found. While the kaolin A2 consist of 72.1 % in silt-clay size minerals.

The morphological aspect of clays was observed by Scanning Electron Microscopy (SEM). It can be observed that A1-clay shows the typical micro-structure of kaolinite, consisting of pseudo- hexagonal plates. A2-clay classified as disordered structure, a fine particle size, an irregular kaolinite forms and very small flakes the microstructure has presented.

The kaolin deposit (A1) was developed in situ, because have no evidence of transport, in addition, the presence of secondary minerals as kaolinite (with a high crystallinity), together with quartz (highly angulated in veins) in smaller fractions to 0.045 mm, leads to infer that the origin of deposit was due to hydrothermal alteration.

The high surface area of the sieved fraction of kaolin A2 may infer a low crystallinity kaolinite. The high sphericity of quartz grains and rounded edges of the heavy minerals and the presence of lamination and cross-bedding of the deposit may be inferred transport of sediments rich in kaolinite that were transported from their original source and subsequently deposited in the area. Accordingly with the felsic composition of the clay and its relationship with local geology, it is believed that Parguaza Rapakivi granite is the main source of these sediments.

Pozzolanic Potential of the Calcined Clay-Lime System

Sofie Hollanders, Özlem Cizer and Jan Elsen

Abstract This study investigates the potential use of calcined clays from a mineralogical point of view by linking the characteristics of the untreated clays to the pozzolanic activity of the calcined clays. Since it is of key importance to understand the origin of the pozzolanic activity and to determine the main parameters that influence the pozzolanic activity, pure reference clays have been used to avoid interference of impurities.

Seven reference clays, 4 kaolinitic and 3 smectitic clays, were purified and thermally treated in order to estimate their pozzolanic potential in cementitious materials. The clays were calcined in a fixed-bed electrical furnace at temperatures ranging between 500 °C and 900 °C. Both raw and calcined clays were characterized by XRD, XRF, FTIR and BET techniques. Their pozzolanic activity was evaluated using thermogravimetry (TGA) on clay-lime pastes after 3, 7, 14, 28, 56 and 90 days.

The results indicate that all kaolinitic clays are highly active at a broad range of firing temperatures (500–900 °C), that is influenced by the degree of ordering of the kaolinite clay. The smectitic clays possess a more clear optimal firing temperature at 800 °C for montmorillonite and 700 °C for hectorite. The degree of ordering and thereby the specific surface area of kaolinitic clay, only influences the pozzolanic activity of the sample at the early stage of the reaction. After 28 days high, medium and low ordered kaolinites have consumed a similar amount of portlandite. Ca-rich smectites are proven to be somewhat more reactive than Na-rich smectite and hectorite, however, even at 800 °C, its activity is only mediocre compared to kaolinite. The activity of the smectitic clays might be influenced by the present cation or/and the difference in specific surface area.

S. Hollanders (✉) · J. Elsen
Division Geology, Department of Earth and Environmental Sciences,
University of Leuven, Celestijnenlaan, 200E, 3001 Louvain, Belgium
e-mail: Sofie.Hollanders@ees.kuleuven.be

Ö. Cizer
Building Materials and Building Technology, Department of Civil Engineering,
University of Leuven, Kasteelpark Arenberg, 44, 3001 Louvain, Belgium

K. Scrivener and A. Favier (eds.), *Calcined Clays for Sustainable Concrete*,
RILEM Bookseries 10, DOI 10.1007/978-94-017-9939-3_71

Effect of Metakaolin on the Drying Shrinkage Behaviour of Portland Cement Pastes

Duyou Lu, Jingwang Luo and Zhongzi Xu

Abstract In order to explore the mechanism of the effect of the metakaolin (MK) on the drying shrinkage of cementitious materials, the drying shrinkage and mass loss of Portland cement pastes with various MK contents (0, 5 %, 10 %, 15 %) and different maturities (pre-cured in water for 3 d and 28 d, respectively), were investigated by drying at 20 °C and 55 % relative humidity. The composition and microstructure of cement pastes were determined by thermal analysis and mercury intrusion porosimetry. Results show that the effect of MK on the drying shrinkage of cement pastes is closely related to the MK content and maturity of the pastes. The late-age drying shrinkage of cement pastes with different maturities decreased with the increase of MK contents. However, the effect on the early age drying shrinkage depended on the maturity of paste. The MK increased slightly the early age drying shrinkage of the paste pre-cured for 3 d, and decreased the early age shrinkage of the paste pre-cured for 28 d. The drying shrinkage of cement paste was proportional to its mass loss and the mechanism of water loss and its relation with the drying shrinkage varied. The decrease of drying shrinkage of blended cement paste with the MK was due to the result of less and slower evaporation of water in the MK blended cement paste with low porosity and refined pores structure by the micro-filler effect, nuclear effect and/or pozzolanic reaction of the MK.

D. Lu (✉) · J. Luo · Z. Xu
College of Materials Science and Engineering, Nanjing Tech University, 210009 Nanjing, China
e-mail: duyoulu@njtech.edu.cn

K. Scrivener and A. Favier (eds.), *Calcined Clays for Sustainable Concrete*, RILEM Bookseries 10, DOI 10.1007/978-94-017-9939-3_72

BIND-AMOR: Reuse of Dredged Sediments as Supplementary Cementitious Materials

Liesbeth Horckmans, Ruben Snellings, Peter Nielsen, Philippe Dierckx, Joris Dockx, Jos Vandekeybus, Özlem Cizer, Lucie Vandewalle, Koen Van Balen and Lea Lindequist Kohler

Abstract In the Port of Antwerp, 500.000 tonnes dry matter base (DM) of sediments need to be dredged each year to ensure the navigability of the waterways. Traditionally, these maintenance dredged sediments were disposed in settling ponds or underwater cells. However, due to near exhaustion of the existing storage capacity as well as the limited availability of new storage sites, an alternative, sustainable solution needed to be developed. Between 2008 and 2011, the state-of-the-art treatment and storage facility **AMORAS** was realised by the Flemish Government represented by the Department of Mobility and Public Works (MOW), division Maritime Access. Since 2011, the AMORAS-installation treats up to 600.000 ton DM of sediments annually by mechanical dewatering with membrane filter presses. Pre-treatment steps include sand separation (63 μm cut-off hydrocyclones) and lime addition to enhance flocculation. The produced fine grained (< 63 μm) filter cakes have a dry matter content of minimally 60 %, resulting in a significant volume decrease of the sediments as well as physical properties suitable for storage in an onsite landfill. To increase the operational lifetime of the storage facility, reuse of the non-contaminated filter cakes was considered. A strict separation between highly and marginally contaminated sediments is maintained throughout the process. Furthermore, the sediments are homogenized in different

L. Horckmans (✉) · R. Snellings · P. Nielsen · P. Dierckx
VITO (Flemish Institute for Technological Research), Materials Technology, Boeretang 200, 2400 Mol, Belgium
e-mail: liesbeth.horckmans@vito.be

J. Dockx · J. Vandekeybus
Division Maritime Access (AMT), Flemish Government, Department for Mobility and Public Works (MOW), Tavernierkaai 3, 2000 Antwerp, Belgium

Ö. Cizer · L. Vandewalle · K. Van Balen
Civil Engineering Department, Building Materials and Building Technology Division, KU Leuven, Kasteelpark Arenberg 40 Bus 2448, 3001 Heverlee, Belgium

L.L. Kohler
FLSmidth a/S, Vigerslev Allé 77, 2500 Valby, Denmark

K. Scrivener and A. Favier (eds.), *Calcined Clays for Sustainable Concrete*, RILEM Bookseries 10, DOI 10.1007/978-94-017-9939-3_73

steps, resulting in a continuous supply of homogeneous filter cakes with a good environmental quality. As such, the fine fraction filter cakes of AMORAS are uniquely suited for valorisation.

In the ongoing **BIND-AMOR** project, the potential of the filter cakes for the production of supplementary cementitious materials (SCMs) is investigated. The project is executed under the authority of the Flemish Government (MOW) by VITO (Flemish Institute for Technological Research), KU Leuven and FLSmidth.

In a first stage, material characterisation and feasibility tests were carried out to evaluate the suitability for SCM production by thermal activation. Calcination of the filter cakes was performed by static box furnace heating as well as by the flash calcination technique developed by FLSmidth. Initial results were very promising with 35 % cement replacement level delivering no significant 28 day compressive strength decrease compared to the reference system. This demonstrates the enhancement of the pozzolanic activity of the filter cakes after calcination treatment despite the low kaolinite content. In the second stage of the project, efforts will be focused on better understanding the rate and mechanism of the hydration reactions and on the identification of the mineral components that contribute to the pozzolanic activity and filler effect. In addition, the optimisation of the binder formulation and upscaling of the calcination process will be investigated.

Influence of Mineral Impurities on the Pozzolanic Reactivity of Metakoalin

Sofie Hollanders, Özlem Cizer and Jan Elsen

Abstract In nature, kaolinite deposits are rarely completely pure. In addition to the mineral kaolinite other clay minerals such as smectites and illites, but also non-clay minerals such as quartz, feldspar, calcite and muscovite are often present in the clay. These less pure clays are economically interesting to be used as SCM, however the impurities might have an effect on the pozzolanic activity or/and the calcinations process. Therefore this study will investigate how these impurities effect the pozzolanic reactivity of the calcined clay and whether the optimal firing temperature change due to the presence of the impurities.

Artificial mixtures of kaolinite and various percentages (15, 30, 45 and 60 %) of six different impurities, quartz, calcite, feldspar, muscovite, smectite and illite, were prepared and calcined in a fixed-bed electrical furnace at different temperatures in the range between 500 and 900 °C. After calcinations the mixtures will be characterized by XRD, FTIR and BET techniques. Their pozzolanic activity will be evaluated with thermogravimetry (TGA) on calcined clay-lime pastes after 3, 7, 14, 28, 56 and 90 days. The changes in pozzolanic activity will then be correlated to the percentage of the impurities in order to find systematic differences.

S. Hollanders (✉) · J. Elsen
Division Geology, Department of Earth and Environmental Sciences,
University of Leuven, Celestijnenlaan 200E, 3001 Louvain, Belgium
e-mail: Sofie.Hollanders@ees.kuleuven.be

Ö. Cizer
Building Materials and Building Technology, Department of Civil Engineering,
University of Leuven, Kasteelpark Arenberg 44, 3001 Louvain, Belgium

K. Scrivener and A. Favier (eds.), *Calcined Clays for Sustainable Concrete*,
RILEM Bookseries 10, DOI 10.1007/978-94-017-9939-3_74

Fresh Properties of Limestone Calcined Clay Cement (LC^3) Pastes

Sendhil Vigneshwar and Prakash Nanthagopalan

Abstract The fresh properties of concrete have a significant influence on the strength and durability of concrete. The flow properties of the cementitious paste have a predominant effect on the fresh properties of concrete. The present investigation focused on evaluating the flow properties of the cementitious pastes prepared from lime stone calcined clay (LC^3) with different water cement ratio (0.30, 0.35, 0.40, 0.45) with optimised dosage of three generation water reducers (namely Ligno based, SNF and PCE based) at different time period (5, 30, 60 & 120 min.). Further, the setting time of the cementitious pastes was also determined for all the combinations. The fresh properties of Ordinary Portland Cement pastes and Portland Pozzolana Cement pastes was also analysed and compared with LC^3 pastes.

S. Vigneshwar · P. Nanthagopalan (✉)
Department of Civil Engineering, IIT Bombay, Bombay, India
e-mail: prakashn@iitb.ac.in

K. Scrivener and A. Favier (eds.), *Calcined Clays for Sustainable Concrete*,
RILEM Bookseries 10, DOI 10.1007/978-94-017-9939-3_75

Alkali Silica Reaction Mitigating Properties of Ternary Blended Cement with Calcined Clay and Limestone

Aurélie R. Favier, Cyrille F. Dunant and Karen L. Scrivener

Abstract Supplementary cementitious materials (SCMs) are widely used in concrete either in blended cements or added separately in the concrete mixer. SCMs such as calcined clays, slags or fly ashes are widely used to partially substitute plain Portland cement (PC). A particurlarly promising blend is a blend with a high level of substitution by widely available SCMs such low grade calcined clay and limestone. The use of such materials, where no additional clinkering process is involved leads to a significant reduction in CO_2 emissions per ton of material. Further, blended systems have numerous well established benefits in terms of durability. ASR is the most important such issue not related to reinforcing steel. Prevention of this phenomenon is critical as sources of non-reactive aggregates are increasingly scarce. The most economical path to ASR resistant concrete is through ternary blends. Since the reaction occurs between alkalis in pore solution and reactive silica, most mitigation methods rely on lowering the alkalinity of the solution through Supplementary Cementitious Materials (SCMs). The effectiveness of SCMs in mitigating ASR is attributable to pore refinement, alkali binding by secondary hydration due to replacing part of the Portland cement, but mainly to the inhibition of silica dissolution when Al ions provided by the SCM are present in the solution. Due to yet uncommon usage in the field, the performances and mechanisms which underlie the properties of such blends are still not wholly understood. In this study, we demonstrate the performance of blends with high level of replacement (reaching 50 %) of cement with limestone and calcined clay. The use of these two SCMs at such high level of replacement promise improvement of the resistance to expansion compared to PC in environmentally friendly blends.

A.R. Favier (✉) · C.F. Dunant · K.L. Scrivener
EPFL-STI-IMX LMC, Station12, 1015 Lausanne, Switzerland
e-mail: aurelie.favier@epfl.ch

K. Scrivener and A. Favier (eds.), *Calcined Clays for Sustainable Concrete*,
RILEM Bookseries 10, DOI 10.1007/978-94-017-9939-3_76

Autogenous Shrinkage of Limestone and Calcined Clay Cements

J. Ston and K. Scrivener

Abstract Reducing the clinker factor is a target with increasing priority in cement industry, as a solution to lower greenhouse gases emissions and increasing cement production. Replacing a fraction of the clinker from the kiln with supplementary cementitious materials (SCMs) has proven efficient for many decades. Calcined clays are good candidates for SCMs, as the raw material can be found in many parts of the world, especially developing countries. Limestone and calcined clay ternary cements show a great potential as building material and mechanical properties close to OPC. On the other hand, little is known about the shrinkage behavior of such systems. Assessing this phenomenon is of prime importance for the elaboration of blends bound to be used for building purposes, as those mixes are controlled by strict standards in each country. Therefore, the mechanisms causing autogenous strain in such systems need to be understood. Ternary blends, such as Portland cement with blast furnace slag and limestone, tend to have a different strength development than OPC, therefore modifying their response to internal stresses caused by self-dessication, among other phenomena. However, no precise study on shrinkage behavior of limestone and calcined clay systems has been reported yet. Autogenous shrinkage measurements were done according to the actual standards and compared to OPC. In addition, clays with different grades of kaolinite were tested. Kaolinite is transformed into reactive metakaolin by the calcination process. Therefore, the impact of impurities or other phases, in particular expanding clays such as smectite, is studied.

J. Ston (✉) · K. Scrivener
Laboratory of Construction Materials, École Polytechnique Fédérale de Lausanne,
1015 Lausanne, Switzerland
e-mail: julien.ston@epfl.ch

K. Scrivener and A. Favier (eds.), *Calcined Clays for Sustainable Concrete*,
RILEM Bookseries 10, DOI 10.1007/978-94-017-9939-3_77

Sustainable Benefits of a Low Carbon Cement Based Building

Kriti Nagrath and Soumen Maity

Abstract The current trends of production and consumption are unsustainable in terms of environmental emissions and resource use. With current trends of energy application, the emission and resource use will increase nearly two-fold by 2050, creating an increased stress on the global resource base. Thus the only option is to create and promote low carbon and resource efficient technologies without compromising on the cost of goods produced and financial viability. As per WBSCD, by 2010 the cement industry in India alone contributed to 7 % of the total CO_2 emissions of the country. Realizing this the Indian cement industry has embarked on an ambitious roadmap of reducing it by 50 % within 2050. Despite this improvement, still the emissions will rise from current (2010) 137 $MtCO_2$ to around 468 $MtCO_2$ by 2050. The present initiative explores the role of a new type of developed low carbon cement in reducing CO_2 emissions and natural resource use. The cement is based on a ternary blend of calcined clay-limestone-clinker. Building made out of this low carbon cement and its associated building materials indicates a preliminary saving of 0.46 kg CO_2 per square meter and 1.55 kg wastes per square meter. Considering the fact that India has a current shortage of 1.2 billion square meter of rural and urban housing which is increasing by 10 % per year, the potential of CO_2 and resource saving from sustainable construction is quite high considering only the housing sector.

K. Nagrath (✉)
Development Alternatives, New Delhi, India
e-mail: knagrath@devalt.org

S. Maity
Technology and Action for Rural Advancement, New Delhi, India

K. Scrivener and A. Favier (eds.), *Calcined Clays for Sustainable Concrete*,
RILEM Bookseries 10, DOI 10.1007/978-94-017-9939-3_78

CO_2 Abatement During Production of Low Carbon Cement

Bhaskar Dutta and Soumen Maity

Abstract In order to reduce the Greenhouse Gas (GHG) emissions from the cement industry, the percentage of clinker in cement blends can be reduced by using various other materials, such as calcined clay, low grade (dolomitic/siliceous) limestone, which are often available at the cement manufacturing site itself. The present study focuses on direct or indirect impacts on CO_2 emission by reducing the use of high temperature clinker by low grade limestone during the production of low carbon cement. Implementing raw material substitution is fairly simple technically and requires comparable capital investments but the application is subject to the availability of the substituting materials. They offer opportunities to significantly reduce CO_2 emissions arising from cement production. The production of limestone calcined clay cement has strong positive environmental credentials. It has substantial potential of CO_2 abatement which is mainly achieved due to conserving fast depleting cement grade limestone reserves, utilizing unused low grade limestone not suitable for conventional cement manufacturing and reducing energy consumption, leading to emission reductions during finished grinding (low grade limestone being softer to grind compared to clinker).

B. Dutta (✉)
Development Alternatives, New Delhi, India
e-mail: bdutta@devalt.org

S. Maity
Technology and Action for Rural Advancement, New Delhi, India

K. Scrivener and A. Favier (eds.), *Calcined Clays for Sustainable Concrete*,
RILEM Bookseries 10, DOI 10.1007/978-94-017-9939-3_79

Role of Blended Cement in Reducing Energy Consumption

Bhaskar Dutta and Soumen Maity

Abstract The cement industry has long recognized that the cost of energy can be significant, varying between 25 and 35 % of total direct costs. Consequently, the industry is continuously investigating and adopting more energy-efficient technologies to improve its profitability and competitiveness. In particular, plants have moved steadily away from less energy-efficient wet process kilns toward the more fuel-efficient dry process kilns. The industry has achieved additional energy efficiency gains by using pre heaters and pre calciners. These technologies have helped the industry reduce its energy consumption per tonne of cement by 30 %. Since these processes has attained its maximum outreach, the present study focuses on role of blended cement in reducing energy consumption during the cement manufacturing process. This has been achieved primarily due to adaptation of significant steps which was not being practiced during the production of conventional cement. Firstly as the use of even inferior quality of limestone can be used, it will save huge amount fossil fuels, which otherwise had been used during transportation of superior quality of limestone from large distances. Additionally since the limestone will not undergo through clinkerization, it will save enormous amount of energy. It is also being found that this blended cement uses calcined clay at lower temperature, and hence will be able to save huge amount of energy.

B. Dutta (✉)
Development Alternatives, New Delhi, India
e-mail: bdutta@devalt.org

S. Maity
Technology and Action for Rural Advancement, New Delhi, India

K. Scrivener and A. Favier (eds.), *Calcined Clays for Sustainable Concrete*,
RILEM Bookseries 10, DOI 10.1007/978-94-017-9939-3_80

Investigation of Sulphate Attack on Limestone-Calcined Clay Cement Mortars

Fathima Suma and Manu Santhanam

Abstract Calcined clay, especially in combination with limestone powder, is emerging as an excellent supplementary cementitious material. While a number of studies have reported on the pozzolanic performance of calcined clay blended cements, a detailed investigation on the durability characteristics is not available in the existing literature. In this context, the resistance of calcined clay blended cements against sulphate attack needs to be comprehensively studied to understand its potential for use in sulphate rich environments. This paper reports an experimental investigation on cementitious mortars that are subjected to (i) continuous immersion and (ii) alternate wetting and drying, in highly concentrated sodium sulphate solutions, with a methodology based loosely on ASTM C1012. The length change and flexural strengths are monitored periodically to get an assessment of the degree of damage. The cementitious systems considered in the study are: (i) OPC, (ii) OPC with 30 % fly ash, and (iii) Limestone calcined clay cement (LC3). The alterations in microstructure are studied using X-ray diffraction and thermal analysis. The work reported in this paper is part of a larger project that investigates the potential for limestone—calcined clay based cementitious binders in concrete.

F. Suma (✉) · M. Santhanam
Department of Civil Engineering, IIT Madras, Chennai, India
e-mail: fathima.suma.m@gmail.com

K. Scrivener and A. Favier (eds.), *Calcined Clays for Sustainable Concrete*,
RILEM Bookseries 10, DOI 10.1007/978-94-017-9939-3_81

Experimental Study of the Flow Behaviour of Superplasticized Pastes with Cement-Calcined Clay-Limestone Blends

B. Karmugil and Ravindra Gettu

Abstract The superplasticizer demand and evolution of flow in cement pastes with time are significantly affected by the mineral admixtures. It is well known that there could be compatibility issues that arise due to the addition of higher dosages of mineral admixtures. Further, superplasticizers that function satisfactorily in portland cement pastes may not provide good performance in pastes with blended cements. It is, therefore, necessary to study the flow behaviour of pastes with new blends of cement. This paper describes an experimental investigation of the variation of the Marsh cone flow time with superplasticizer dosage in cementitious systems that include: (i) ordinary portland cement (OPC), (ii) portland pozzolana cement (PPC —i.e. OPC with 25 % Fly Ash Type F), (iii) Calcined Clay—Limestone—Cement ternary blends. The superplasticizer demand and the evolution of the flow will be discussed.

B. Karmugil · R. Gettu (✉)
Department of Civil Engineering, IIT Madras, Chennai, India
e-mail: gettu@iitm.ac.in

K. Scrivener and A. Favier (eds.), *Calcined Clays for Sustainable Concrete*,
RILEM Bookseries 10, DOI 10.1007/978-94-017-9939-3_82

Hydration Properties of Cement Pastes with Recycled Demolition Waste from Clay Bricks and Concrete

Thiago Melo Grabois, Guilherme Chagas Cordeiro and Romildo Dias Toledo Filho

Abstract The crushing of concrete and masonry to produce recycled aggregates for concretes produces a significant amount of fine powder usually rejected. This work aims to investigate how the heterogeneities inclusion—fine powder from different sources of recycled construction and demolition waste (CDW)—affects the hydration process of cement pastes. The powder used to produce the cement pastes derives from two types of clay bricks (face and hollow) typically adopted in building constructions and a laboratory concrete beam crushed to generate recycled aggregates. Fine particles (lower than 75 μm) were separated for use as supplementary cementitious materials substituting 10 % of cement. Isothermal conduction calorimetry and thermogravimetric analysis were the techniques employed to evaluate the pastes hydration. The results presented signs of pozzolanic activity by the brick powder waste even with higher particles than Portland cement. The concrete powder waste did not presents relevant reactivity.

T.M. Grabois (✉) · R.D. Toledo Filho
Programa de Engenharia Civil, COPPE/Universidade Federal do Rio de Janeiro, Av. Brigadeiro Trompovski S/N, Centro de Tecnologia, Bloco I-2000, Sala 216, 21941-970 Rio de Janeiro, RJ, Brazil
e-mail: thiagomgrabois@coc.ufrj.br

G.C. Cordeiro
Laboratório de Engenharia Civil, Universidade Estadual do Norte Fluminense Darcy Ribeiro, Av. Alberto Lamego, 2000, Parque Califórnia, 28013-602 Campos dos Goytacazes, RJ, Brazil

K. Scrivener and A. Favier (eds.), *Calcined Clays for Sustainable Concrete*, RILEM Bookseries 10, DOI 10.1007/978-94-017-9939-3_83

Calcined Natural Clays: Performance Evaluation as Cementitious Material

Nikola Mikanovic, Michael Hoffeins, Diego Rosani and Inga Hauschildt

Abstract This study was done to evaluate technical feasibility of using unrefined, relatively low quality clay materials for the production of industrial pozzolan based on calcined clay. The ultimate objective is to provide a greater degree of flexibility regarding the range of cementitious materials that can be incorporated in cement. In the first part of the study, a wide variety of clay material samples containing different clay types and amounts have been received to evaluate their suitability for calcined clay production. These samples were examined visually and by X-Ray Fluorescence (XRF) and X-Ray Diffraction (XRD). The most interesting samples were calcined under controlled laboratory conditions and their performance evaluated in cement paste and mortar. The test results clearly showed that highly reactive pozzolan can be produced from unrefined clays and its performance is related to chemical and mineralogical composition of the raw material. The influence of calcination conditions on performance of the calcined natural clays has been investigated in the second part of the study. For this purpose, four previously investigated clay materials have been selected and calcined under different conditions (temperature, residential time). The calcined clay samples were examined by XRD and their performance again evaluated in cement paste and mortar. When mixture of clay minerals is present, the optimal calcination temperature can be sometimes hard to identify as the compromise has to be made between compressive strength development and water demand. This is especially true for raw materials containing swellable clays. The optimal conditions for calcining the mixtures of various clay minerals are discussed in the light of existing guidelines for calcination of pure clay minerals and results of our study.

N. Mikanovic (✉) · M. Hoffeins · D. Rosani · I. Hauschildt
HeidelbergCement Technology Center GmbH, Leimen, Germany
e-mail: Nikola.Mikanovic@htc-gmbh.com

K. Scrivener and A. Favier (eds.), *Calcined Clays for Sustainable Concrete*,
RILEM Bookseries 10, DOI 10.1007/978-94-017-9939-3_84

Rheology of Limestone Calcined Clays Cement Pastes. A Comparative Approach with Pure Portland Cement Pastes

Lukas Gebbard, Blandine Feneuil, Marta Palacios and Nicolas Roussel

Abstract In this work, we measure and compare the rheological behavior of suspensions of limestone calcined clays cement paste and pure Portland cement pastes at the same solid volume fraction. The limestone calcined clays cement pastes are prepared with two different calcined clays. We first focus on the influence of clay particles on the suspensions yield stress and viscosity in steady flows and we discuss the influence of these particles on both interaction forces and packing properties. We then study the effect of adsorbing polymer addition on these three systems and analyze our results in terms of polymer adsorption or depletion. We finally measure the evolutions of the rheological properties at rest and conclude on the effect of clay particles on early structuration/nucleation features of these suspensions.

L. Gebbard · M. Palacios · N. Roussel (✉)
Institut für Baustoffe (IfB), ETH Zürich, Zürich, Switzerland
e-mail: dr.nicolas.roussel@gmail.com

B. Feneuil · N. Roussel
Université Paris Est, IFSTTAR, Laboratoire Navier, Marne la Vallée, France

K. Scrivener and A. Favier (eds.), *Calcined Clays for Sustainable Concrete*,
RILEM Bookseries 10, DOI 10.1007/978-94-017-9939-3_85

Chloride-Induced Corrosion Rates of Steel Embedded in Mortar with Ordinary Portland and Limestone Calcined Clay Cements (OPC and LC3)

Sripriya Rengaraju and Radhakrishna G. Pillai

Abstract Chloride induced corrosion is a serious deterioration mechanism in concrete structures. Corrosion rate is an important parameter required to estimate the service life, especially propagation life, of concrete structures. The corrosion rate of the embedded steel significantly depends on the properties of the surrounding concrete and cementitious systems. The thermo-mechanically-treated (TMT) steel is widely used in Indian construction. However, literature provides very limited information on corrosion rates of TMT steel embedded in concrete with Ordinary Portland Cement (OPC) and Limestone Calcined Clay Cement (LC3). This makes it difficult to quantify and compare the service life of such systems. This paper presents experimental results on the corrosion rates of TMT steel embedded in mortar (w/c = 0.5) with OPC and LC3. Each test specimen (lollipop type) consisted of an 8 mm diameter steel rod embedded in a 100 mm long mortar cylinder with a 10 mm cover. To accelerate the corrosion studies, chlorides were premixed to the mixing water/mortar. Four levels of premixed chloride content (i.e., 0, 3, 6, and 9 % NaCl) were used. A total of 40 lollipop specimens with 5 replicas for each variable combination were prepared. Corrosion rates were measured using Linear Polarization Resistance (LPR) technique and were monitored for a period of 2 months. Comparison of the corrosion rates and propagation periods for the steel embedded in systems with OPC and LC3 are presented.

S. Rengaraju · R.G. Pillai (✉)
Department of Civil Engineering, Indian Institute of Technology Madras, Chennai, India
e-mail: pillai@iitm.ac.in

K. Scrivener and A. Favier (eds.), *Calcined Clays for Sustainable Concrete*,
RILEM Bookseries 10, DOI 10.1007/978-94-017-9939-3_86